R-07-55

Hydrochemistry in surface water and shallow groundwater

Site descriptive modelling SDM-Site Forsmark

Mats Tröjbom, Mopelikan

Björn Söderbäck, Svensk Kärnbränslehantering AB

Per-Olof Johansson, Artesia Grundvattenkonsult AB

October 2007

Svensk Kärnbränslehantering AB
Swedish Nuclear Fuel
and Waste Management Co
Box 5864
SE-102 40 Stockholm Sweden
Tel 08-459 84 00
+46 8 459 84 00
Fax 08-661 57 19
+46 8 661 57 19

ISSN 1402-3091
SKB Rapport R-07-55

Hydrochemistry in surface water and shallow groundwater

Site descriptive modelling SDM-Site Forsmark

Mats Tröjbom, Mopelikan

Björn Söderbäck, Svensk Kärnbränslehantering AB

Per-Olof Johansson, Artesia Grundvattenkonsult AB

October 2007

Keywords: Surface water, Shallow groundwater, Hydrochemistry, Integrated evaluation, Precipitation, Regolith, Sediment, Chemical analyses, Chemical composition, Field measurements, Water composition, Major constituents, Minor constituents, Dissolved ions, Trace elements, Nutrient salts, Nutrients, Isotope, Forsmark.

A pdf version of this document can be downloaded from www.skb.se.

Preface

This work has been conducted for SKB within the framework of SurfaceNet, the group working with the site description and modelling of surface systems, with the purpose of evaluating hydrochemical issues with specific bearing on the surface system. The main part of the work has been done by Mats Tröjbom (Mopelikan) and Björn Söderbäck (Svensk Kärnbränslehantering AB), with assistance of Per-Olof Johansson (Artesia Grundvattenkonsult AB). Eva-Lena Tullborg (Terralogica AB) and Bill Wallin (Geokema) have also contributed with support and valuable comments during the work. The following persons have contributed with many relevant comments during the internal review of the report (listed in alphabetical order).

Sten Berglund (Svensk Kärnbränslehantering AB)

Anna Hedenström (SGU)

Sven Follin (SF Geologic AB)

Marcus Laaksoharju (Geopoint AB)

Regina Lindborg (Stockholm University)

Gustav Sohlenius (SGU)

Mats Åström (University of Kalmar)

Abstract

With a mathematical/statistical approach, a large number of visualisations and models reflect the hydrochemistry in the Forsmark area, with the intention to give an understanding of important processes and factors that affect the hydrochemistry in the surface systems. In order to widen the perspective, all data from the Forsmark 2.2 stage including observations from different levels of the bedrock, as well as hydrological measurements and characterisations of the Quaternary deposits, have been included in the analyses. The purpose of this report is to give a general understanding of the site and to explain observed overall patterns as well as anomalies, and, ultimately, to present a conceptual model that explains the present hydrochemistry in the surface system in the light of the past. The report may also function as a basis for further evaluation and testing of scenarios, and may be regarded as an intermediate step between raw data compilations from the vast Sicada database and specialised expert models.

The flat topography and the recent withdrawal of the Baltic Sea due to the isostatic land-uplift are two important factors determining the hydrochemistry in the Forsmark area. Marine remnants in the Quaternary deposits, as well as modern sea water intrusions, are therefore strongly influencing the hydrochemistry, especially in areas at low altitude close to the coast. Large-scale marine gradients in the surface system are consistent with the conceptual model that describes the hydrochemical evolution in a paleo-hydrologic perspective.

The Forsmark area is covered by glacial remnants, mostly in the form of a till layer, which was deposited during the Weichselian glaciation and deglaciation. When the ice cover retreated about 11,000 years ago, these deposits were exposed on the sea floor. This till layer is characterized by a rich content of calcite, originating from the sedimentary bedrock of Gävlebukten about 100 km north of Forsmark. The dissolution of this mineral has a central role in the forming of today's hydrochemistry in surface systems, and probably also on the composition of the dilute, non-brackish, groundwater in the upper parts of the fractured bedrock. The rich supply of calcium and the high alkalinity affects the structure of the whole ecosystem, for example by forming the oligotrophic hardwater lakes which are characteristic for the area.

One major issue in the report is if there can be found any indications on deep groundwater discharge in the surface system. According to observations in surface water and shallow groundwater, and to the hydrological/hydrochemical conceptual model, there is probably no ongoing deep discharge into the freshwater surface system. In restricted areas there are, however, indications that relict marine remnants, which also includes deep saline signatures, prevail in the groundwater at relatively shallow depths in the Quaternary deposits, but not reach the surface due to the downwards directed groundwater flow pattern that generally prevail in the area. This hydrochemical pattern could according to the conceptual model probably be explained by influence from marine remnants formed under a previous hydrological regime and these signatures are preserved because of stagnant conditions in some areas.

Sammanfattning

Med en matematisk/statistisk utgångspunkt beskrivs i den här rapporten hydrokemin i Forsmarksområdet med ett stort antal visualiseringar och modeller av olika komplexitet, med avsikten att spegla de viktigaste faktorerna som styr hydrokemin i ytsystemet. För att bredda perspektivet har också samtliga data från olika nivåer i berget inkluderats i analysen, liksom hydrologiska mätdata och karaktäriseringar av de kvartära avlagringarna. Syftet med denna rapport är dels att ge en generell förståelse för platsen och att förklara storskaliga mönster och anomalier, dels att presentera en konceptuell modell som beskriver dagens hydrokemi i ytsystemet med utgångspunkt från den paleo-hydrologiska utvecklingen. Rapporten, som kan betraktas som ett mellansteg mellan sammanställningar av rådata från databasen Sicada och specialiserade expertmodeller, kan också utgöra en bas för fortsatta utvärderingar av scenarion och alternativa hypoteser.

Den flacka topografin och den pågående landhöjningen är två faktorer som har stor inverkan på hydrokemin i Forsmark. Hela Forsmarksområdet har relativt nyligen stigit upp ur Östersjön, och marina lämningar i de kvartära avlagringarna, liksom återkommande havsvatteninträngningar i modern tid, påverkar därför hydrokemin i stor utsträckning, i synnerhet i de lågt liggande områdena närmast kusten. De storskaliga marina gradienter som syns i ytsystemet överrensstämmer med den konceptuella modellen som beskriver hydrokemin i paleo-hydrologiskt perspektiv.

Forsmarksområdet är täckt av glaciala lämningar, främst i form av ett moränlager som bildades under Weichseltidens glaciationer och avsmältningar. När istäcket slutgiltigt drog sig tillbaka för cirka 11 000 år sedan blev dessa lämningar frilagda på havsbotten. Moränlagret karaktäriseras av ett stort kalcitinnehåll som härrör från den sedimentära bergrunden i Gävlebukten cirka 100 km norr om Forsmark. Vittringen av detta mineral har en central roll för dagens hydrokemi i ytsystemet, liksom troligen också för det utspädda, söta grundvattnet i den övre delen av det uppspruckna berget. Den rikliga förekomsten av kalcium och den höga alkaliniteten påverkar hela strukturen hos ekosystemen, till exempel genom de för området typiska kalkoligotrofa sjöarna.

En viktig frågeställning i rapporten är frågan om det finns några tecken på utflöde av djupt grundvatten i de ytliga systemen. Det finns dock inga observationer i ytvatten eller i ytligt grundvatten som indikerar ett pågående utflöde av djupt grundvatten i det söta ytsystemet, och detta stöds också av den hydrologiska/hydrokemiska konceptuella modellen. Däremot finns det indikationer på att relikt marina lämningar, som även inkluderar djupsalina jonsignaturer, återfinns i grundvattnet på ganska måttligt djup i de kvartära avlagringarna, men att dessa sannolikt inte når ytan på grund av den nedåtriktade grundvattenflöde som generellt sett råder i området. Detta hydrokemiska mönster kan enligt den konceptuella modellen sannolikt förklaras av relikt marina lämningar som bildades under ett tidigare hydrologiskt strömningsmönster och dessa signaturer har bevarats på grund av de stagnanta förhållanden som råder i vissa områden.

Extended Summary

With a mathematical/statistical approach, a large number of visualisations and models reflect the hydrochemistry in the Forsmark area, with the intention to give an understanding of important processes and factors that affect the hydrochemistry in the surface systems. In order to widen the perspective, all data from the Forsmark 2.2 stage including observations from different levels of the bedrock, as well as hydrological measurements and characterisations of the Quaternary deposits (QD), have been included in the analyses. The purpose of this report is to give a general understanding of the site and to explain observed overall patterns as well as anomalies, and, ultimately, to present a conceptual model that explains the present hydrochemistry in the surface system in the light of the past.

One major concern in the report is if there are any indications deep groundwater discharge in the surface system. According to observations in surface water and shallow groundwater, there is probably no ongoing deep discharge into the freshwater surface system. This finding is in accordance with the hydrological/hydrochemical conceptual model of the Forsmark area, developed in the last chapter of the report

Important prerequisites forming the hydrochemistry in the surface systems

The flat topography and the recent withdrawal of the Baltic Sea due to the isostatic land-uplift are two important factors determining the hydrochemistry in the Forsmark area. Marine remnants in the Quaternary deposits, as well as modern sea water intrusions, are therefore strongly influencing the hydrochemistry, especially in areas at low altitude close to the coast.

The Forsmark area is covered by glacial remnants, mostly in the form of a till layer, which was deposited during the Weichselian glaciation and deglaciation. When the ice cover retreated about 11,000 years ago these deposits were exposed on the sea floor. This till layer is characterized by a rich content of calcite, originating from the sedimentary bedrock of Gävlebukten about 100 km north of Forsmark, and it has a central role in the forming of today's hydrochemistry in surface systems, and probably also on the composition of the dilute groundwater in the upper parts of the bedrock. The rich supply of calcium and high alkalinity affects the structure of the whole ecosystem, for example by forming the oligotrophic hardwater lakes which are characteristic for the area.

In samples from the upper parts of the bedrock extending down to depths of several hundred metres, as well as in some shallow groundwater sampling points, a brackish groundwater type with a clear relict marine signature prevail. Major ions in these groundwaters seem to originate mainly from a marine source but, at least to some extent, also from a deeper saline source. The isotope signatures of the water (i.e. ^{2}H, ^{18}O) also show a clear evaporation signature, which reflects the marine (Littorina) origin of the solvent. However, the relict marine groundwater differs in isotopic composition from the present-day sea water in the Baltic, which may be interpreted as influence of meteoric recharge during a period of cold climate.

Conceptual hydrochemical model with paleo-hydrologic perspective

The development of the hydrochemistry in the Forsmark area since the latest deglaciation 11,000 years ago is outlined in a conceptual model (cf Chapter 8). This model describes a generalised hydrological picture, in combination with hydrochemical processes important for the interpretation of past and present hydrological patterns in the surface system and in groundwater in the upper parts of the bedrock:

The period from deglaciation until onset of the Littorina Sea

Shortly after the deglaciation (c 9,000 BC), the groundwater in the fractured bedrock consisted of a mixture of glacial water, old meteoric water and deep saline groundwater originating from the previous glacial period and earlier interglacials. After the withdrawal of the ice cover, glacial (Quaternary) deposits were exposed at the bottom of the freshwater lake which was formed by the melting glaciers. In the Forsmark area, these deposits also contained large amounts of limestone. During this period, when the Forsmark area was covered by the non-saline water of the Ancylus Lake (c 9,000–7,500 BC), there was probably little exchange of water and elements through the Quaternary deposits due to the lack of hydrological driving forces.

The Forsmark area covered by Littorina Sea water

When the Forsmark area was covered by the brackish Littorina Sea with increasing salinity (c 7,500–3,000 BC), the difference in density between Littorina Sea water and the mixture of glacial meltwater, old meteoric and deep saline groundwater in the bedrock gave prerequisites for a density turnover, which may have infiltrated sea water through the bottom sediments and the minerogenic Quaternary deposits. If there were suitable conditions, organic sediments accumulated onto the sea floor during the Littorina period and gave prerequisites for altered redox conditions within the deposits due to oxygen consumption by microbial decomposition of organic matter. The lowered redox conditions gave in turn prerequisites for anoxic reactions to take place within the sediments/deposits. If there was a density-driven flow pattern from the Littorina Sea through the Quaternary deposits, mobilised Mn^{2+}, as well as SO_4 with a microbial altered ^{34}S-isotopic signature, may have been transferred with the relict marine groundwater into the upper parts of the bedrock.

The resulting mixing of Littorina Sea water and the primordial groundwater mixture gave the groundwater in the fractured bedrock a distinct marine signature regarding ions as Na, Cl and Mg, as well as a typical marine evaporation signature of the water (the solvent). Additionally, infiltration through the sediments may have altered the isotopic composition of the marine SO_4 and may have also have added significant amounts of Mn^{2+} originating from the marine environment to the groundwater in the fractured bedrock.

The Forsmark area covered by Baltic Sea water

When the Forsmark area was still covered by Baltic Sea water after the Littorina salinity maximum (c 3,000–0 BC), there was no driving force transporting ions and water from the less saline sea water to the heavier, more saline groundwater in the bedrock. On the contrary, there was a possible discharge of groundwater from the fractured bedrock upwards through the Quaternary deposits, driven by the topographical gradient near the coast. This flow regime may have transported the Littorina-dominated groundwater from the fractured bedrock, as well as any residual ion signature of the primordial groundwater mixture of the bedrock, into the Quaternary deposits.

The Forsmark area emerging from the sea

From around 0 BC until present date, when parts of the Forsmark area have emerged from the sea due to the isostatic uplift, the conditions in the Quaternary deposits (QD) are significantly altered. Recharge of meteoric water leads to a completely new flow pattern compared to the conditions prevailing when the area was submerged under sea water. This new situation results in local discharge in streams and lakes, as well as recharge through the QD down to the upper parts of the fractured bedrock. The widespread and horizontally extended fracture systems, which are characteristic for the upper parts of the bedrock in the Forsmark area, effectively channel the recharging groundwater, as well as any potential discharge from deeper levels, to discharge points near or below the Baltic Sea.

The effective recharge into the lower parts of the QD and further down into the upper parts of the bedrock is probably low, due to the low permeability of the till. This probably leads to a slow washout of marine remnants from the time submerged under the Baltic Sea, and in areas with supposed low turnover, e.g. areas covered by clay layers with low permeable, relict marine ion signatures should be more pronounced in the shallow groundwater. In some shallow groundwater objects (e.g. in the area of Lake Gällsboträsket), characterised by relict marine signatures regarding the composition of major constituents, sulphur isotope signatures and elevated concentrations of Mn^{2+} are observed, similar to what is observed in the relict marine groundwater in the bedrock. This pattern could, according to the conceptual model, be explained by influence from stagnant marine remnants formed under a previous hydrological regime and are preserved because of the stagnant conditions in these areas.

Aeration of the deposits by meteoric recharge and supply of organic carbon to the Quaternary deposits due to the development of a biologically active layer give prerequisites for drastic alterations of the hydrochemical conditions in the shallow groundwater. Oxidation of sulphide minerals leads to high concentrations of SO_4, especially in discharge from clayey organic sediments. Increased supply of H^+ ions, mostly derived from decomposition of biogenic carbon or oxidation of sulphide minerals, is the ultimate driving force for weathering reactions that take place in the QD or bedrock.

The QD in the Forsmark area are characterised by especially high contents of calcite ($CaCO_3$), which in combination with rich supply of H^+ from organic carbon leads to an extensive dissolution of calcite in the till. Calcite dissolution releases large amounts of Ca^{2+} and HCO_3^- ions into the shallow groundwater system. Some Ca^{2+} are discharged into streams and lakes through the local hydrological recharge/discharge patterns, and contribute to the forming of the Ca-rich oligotrophic hardwater lakes which are characteristic for the Forsmark area. The rich supply of Ca^{2+} ions is also an important prerequisite and driving force for an extensive cation exchange that seem to take place in the Quaternary deposits, where Na^+ and other cations, released by e.g. weathering of rock minerals, exchange with Ca^{2+} and get into the solution. Groundwater with long residence time, e.g. groundwater that reaches down to the upper parts of the bedrock, may be considerably depleted in Ca^{2+} but enriched in e.g. Na^+, and shows therefore a more "mature" signature than groundwater found at more shallow depths.

Conclusions concerning observations in the Forsmark area in relation to the conceptual model

The ongoing uplift after the latest glaciation, in combination with remnants from the past, are factors that have great impact on the present surface hydrochemistry observed in the Forsmark area. Large-scale marine gradients in the surface system are consistent with the conceptual model described above and with the paleo-hydrological history; areas recently emerged from the Baltic Sea show stronger marine influences compared to areas located at higher altitude. Discharge from Lake Eckarfjärden, located at c 5 m absolute elevation (RT90) contain low concentrations marine ions, whereas Lake Gällsboträsket, which was more recently separated from the Baltic and now is located at c 2 m elevation, still show significantly elevated concentrations of e.g. Na and Cl in discharge. At a smaller scale, for example in the area of Lake Bolundsfjärden, which was covered by the Baltic Sea less than hundred years ago, there are marine gradients among shallow groundwater sampling points, probably reflecting different stages of washout of marine remnants by meteoric recharge.

In shallow groundwater in the Quaternary deposits below the lakes, more or less stagnant conditions have preserved relict marine signatures, even at relatively shallow depths. These signatures, which are generally found in the groundwater of the bedrock down to several hundred metres depth, reflects a trapped relict marine groundwater which may have entered the deposits from below when the area was covered by the Baltic Sea, according to the conceptual

model. The possible presence of deep saline influences (shield brine) at these locations are difficult to explain without a vertical discharge gradient at any time during the paleo-hydrological history, especially as there are no hydrological indications of any deep discharge at present date (however, cf reservation in Section 8.2.4).

The marine signature in the soil tubes located in the Quaternary deposits below the lakes shows, similar to the marine influence in the discharge from the lakes, a topographical gradient which probably reflects the time for influence from meteoric recharge. There are, however, exceptions from this general trend, which reflects the importance of the local recharge/discharge patterns. The presence of low permeable deposits as clay, such is the case for Lake Gällsboträsket, may be an important prerequisite governing the local recharge/discharge patterns at these settings.

Conclusions on deep discharge in the surface system

According to an evaluation of a large number of elements, where differences in concentration between deep groundwater types and surface water was compared to the reporting limits in surface water, the content of major elements are probably most suitable for detecting deep groundwater discharge in the surface system.

By a multivariate approach the relative composition of major elements in the surface system was compared to the signatures found in the groundwater of the bedrock. According to the here developed *ion source model* (cf Sections 3.2 and 4.3), deep groundwater signatures are evident in shallow groundwater at a few locations. These signatures are most probably explained by relict remnants, not yet flushed out from the Quaternary deposits, according to the conceptual model and the present hydrological flow patterns. There is no clear indication of deep groundwater discharge into the freshwater surface system according to hydrochemical measurements in streams and lakes. In the ion source model there is, however, a weak tendency of influence from a deep signature in outlet of Lake Gällsboträsket, compared to the downstream sampling site. This could be explained by ongoing washout of relict marine groundwater and deep saline remnants trapped in the Quaternary deposits.

One shallow groundwater sampling point (the soil tube SFM0025), located in Quaternary deposits below the present Baltic Sea, contains brackish groundwater diluted with meteoric recharge, but show, according to the *ion source model*, possible influence from a deep saline ion signature. Perhaps the situation outlined in the conceptual model when the Forsmark area was covered by the Baltic Sea is applicable on this soil tube; meteoric recharge from the land nearby, mix with relict marine groundwater, which in turn show possible influence from a deep saline signature representing an (ongoing) deep discharge component.

The only remaining potential source for supply of present deep saline groundwater components into the fresh surface system is man-induced artificial “discharge” in brackish groundwater wells. Two private wells drilled in the bedrock in the Forsmark area, as well as many of the percussion drilled boreholes in the SKB site investigation, show very clear relict marine and possibly also deep saline signatures.

Contents

1 Introduction 15
1.1.1 This report 16
1.1.2 Objectives 17
1.1.3 Definitions of water types 17
1.1.4 Chemical abbreviations used in the text 18

2 Background and methods 19
2.1 The Forsmark area 19
2.2 Data used in this report 22
2.2.1 Compilation of hydrochemical parameters 22
2.2.2 Overview of sampling sites and sampled objects 23
2.2.3 Hydrochemical data from surface systems 24
2.2.4 Hydrochemical data from the bedrock 25
2.2.5 Correction for flushing water content in KFM-data 27
2.3 Statistical methods and visualisation techniques 28
2.3.1 Statistical handling of data 28
2.3.2 Handling of values below reporting limits 29
2.3.3 Representation of isotope measurements 29
2.3.4 Cross plots (scatter plots) 29
2.3.5 Piper plots 30
2.3.6 Projection plots 30
2.3.7 Cross sections and profiles 30
2.3.8 3D-scatterplots and 3D-interpolated data 30
2.3.9 Multivariate analysis and visualisation 31
2.3.10 Principal component analysis (PCA) 31
2.3.11 Partial least squares modelling (PLS) 31
2.3.12 Coding and labelling in figures 32
2.3.13 Marking of trendlines and scenarios in figures 32

3 Hydrochemical overview of the Forsmark area 33
3.1 Traditional water type classifications 33
3.1.1 Ludwig-Langelier plot 33
3.1.2 Piper plot 34
3.2 Exploring sources of dissolved ions 34
3.2.1 Summary of methodology 35
3.2.2 Calibration of the ion source reference model 36
3.2.3 Projection of surface data – the ion source model 38
3.2.4 Interpretation of the ion source model 39
3.2.5 Spatial visualisation and validation of the ion source model 41
3.2.6 Validation of the ion source model by independent parameters 43
3.2.7 Comparisons with results of the M3 mixing modell 45
3.3 Exploring the origin of water – the solvent 47
3.3.1 Global and local meteoric water lines 47
3.3.2 The water origin model 49
3.3.3 Detailed evaluation of four lakes in the Forsmark area 54
3.9 Exploring concentration trends and mixtures 54
3.4.1 The mixing model – version 1 54
3.4.2 The mixing model – version 2 56
3.4.3 Interpretation of the mixing model 58

3.5 Estimations of groundwater residence time 60
3.5.1 Estimating groundwater residence time by the ^{3}H activity 61
3.5.2 Estimating groundwater residence time by the ^{14}C activity 62
3.5.3 Groundwater residence time – summary with a shallow perspective 66

4 Detailed chemical evaluations 69
4.1 Origin and fate of selected elements 69
4.1.1 Tracing marine influences (marine ions, Mg, Na, Cl, Br) 69
4.1.2 On the origin of sulphur 74
4.1.3 On the origin of calcium 78
4.1.4 On the origin of carbon 83
4.2 Tracing chemical reactions and processes 89
4.2.1 Cation exchange in the Quaternary deposits 89
4.2.2 Redox processes 92
4.2.3 Microbially mediated processes 92
4.3 Tracing deep groundwater signatures in the shallow system 95
4.3.1 Reporting limits and dilution constraints 95
4.3.2 Possible deep signatures in shallow objects 95

5 Integrated evaluation of hydrochemical and hydrological data in the surface system 99
5.1 Evaluation of observed hydrochemistry in relation to hydrological recharge/discharge characteristics 99
5.1.1 Correlation analysis by Principal Component Analysis 99
5.1.2 Evaluation of relationships between the groundwater temperature and hydrological parameters 103
5.1.3 Comparisons of recharge/discharge classifications 106
5.1.4 Conclusions – recharge/discharge characteristics 110
5.2 Evaluation of concentrations and water flow 110
5.2.1 Conclusions – concentrations and water flow 117
5.3 Estimation of mass transports in Forsmark watercourses 118
5.3.1 Evaluation of discharge measurements used for transport estimations 119
5.3.2 Extrapolation of discharge time series 122
5.3.3 Description of hydrochemical data used for transport estimations 124
5.3.4 Compilation of transports, areal specific transports and flow weighted concentrations 125
5.3.5 Visualisation of area-specific transports 126
5.3.6 Estimated transports of trace elements 130

6 Evaluation of hydrochemistry on catchment scale 135
6.1 Catchment model VBX-VI 135
6.1.1 Hydrological network and water balance 135
6.1.2 Mathematical description of the VBX-VI model 137
6.1.3 Distributed land characteristics and prerequisites for retention 138
6.1.4 Model setup, calibration and validation 139
6.2 Mass balance scenarios 140
6.2.1 Mass balance for chloride (Cl) 141
6.2.2 Mass balance for sodium (Na) 145
6.2.3 Mass balance for potassium (K) 148
6.2.4 Mass balance for calcium (Ca) 151
6.2.5 Mass balance for magnesium (Mg) 153
6.2.6 Mass balance for sulphate (SO_4) 156
6.2.7 Mass balance for bicarbonate (HCO_3) 159
6.2.8 Mass balance for total organic carbon (TOC) 162
6.2.9 Mass balance for total nitrogen (Tot-N) 165

6.2.10 Mass balance for total phosphorus (Tot-P) 168
6.2.11 Mass balance for total silicon (Si) 172
6.2.12 Mass balance for strontium (Sr) 174
6.3 Summary and conclusions of catchment modelling 176

7 Integrated hydrochemical evaluation of selected objects and subareas 181
7.1 Identification of subareas of special interest 181
7.2 Bolundsfjärden subarea 182
7.3 Gällsboträsket subarea 185
7.4 Eckarfjärden subarea 190
7.5 Fiskarfjärden subarea 193
7.6 Subarea Norra Bassängen 195
7.7 Subarea Bredviken 200
7.8 Soil tubes located below sea water 202

8 A conceptual model for the hydrochemistry in surface systems in the Forsmark area 205
8.1 Important prerequisites forming the hydrochemistry in the surface systems 205
8.2 Conceptual model with paleo-hydrologic perspective 206
8.2.1 The period from deglaciation until onset of the Littorina stage 206
8.2.2 The Forsmark area covered by Littorina Sea water 207
8.2.3 The Forsmark area covered by Baltic Sea water 208
8.2.4 The Forsmark area emerging from the sea 208
8.3 Conclusions concerning observations in the Forsmark area in relation to the conceptual model 212

9 References 215

Appendix A Time-series and mean values of major constituents in all sampling points

Appendix B Compilations of hydrological data

Appendix C Evaluation of correlations among hydrological parameters

Appendix D Spatial distribution of regolith, land-use and vegetation classifications

Appendix E Compilation of mass-transports

Appendix F Detailed results from mass-balance calculations

Appendix G Compilation of number of hydrochemical observations

Appendix H Compilation of hydrochemical data

Appendix I Time-series and mean values of major constituents in all sampling points

1 Introduction

The Swedish Nuclear Fuel and Waste management Co (SKB) have been conducting site investigations at two sites, Oskarshamn and Forsmark, with the objective of siting a geological repository for spent nuclear fuel. The site investigations were initiated in 2002 and finalised in 2007. The results from the investigations are used as a basic input to the site descriptive modelling. A Site Descriptive Model (SDM) is an integrated description of the site and its regional setting, covering the current state of the geosphere and the biosphere, as well as ongoing natural processes of importance for long-term safety. The SDM shall summarise the current state of knowledge of the site, and provide parameters and models to be used in further analyses within Safety Assessment, Repository Design and Environmental Impact Assessment.

The site investigation programme involves extensive studies of the surface ecosystem as well as of the bedrock, in order to provide a detailed characterisation of the site (see /SKB 2001/ for a description of the general execution programme). The strategy which is adopted by SKB for developing a descriptive ecosystem model based on site data, is described in /Löfgren and Lindborg 2003/. The site investigation in the Forsmark area involves many disciplines, as outlined in Figure 1-1 which describes the current preliminary hierarchical report structure behind the SDM-Site main report. The present report is a level-III reference report which focuses on chemistry in the surface system, but also includes data and conclusions from the fields of geology, hydrogeology and hydrogeochemistry.

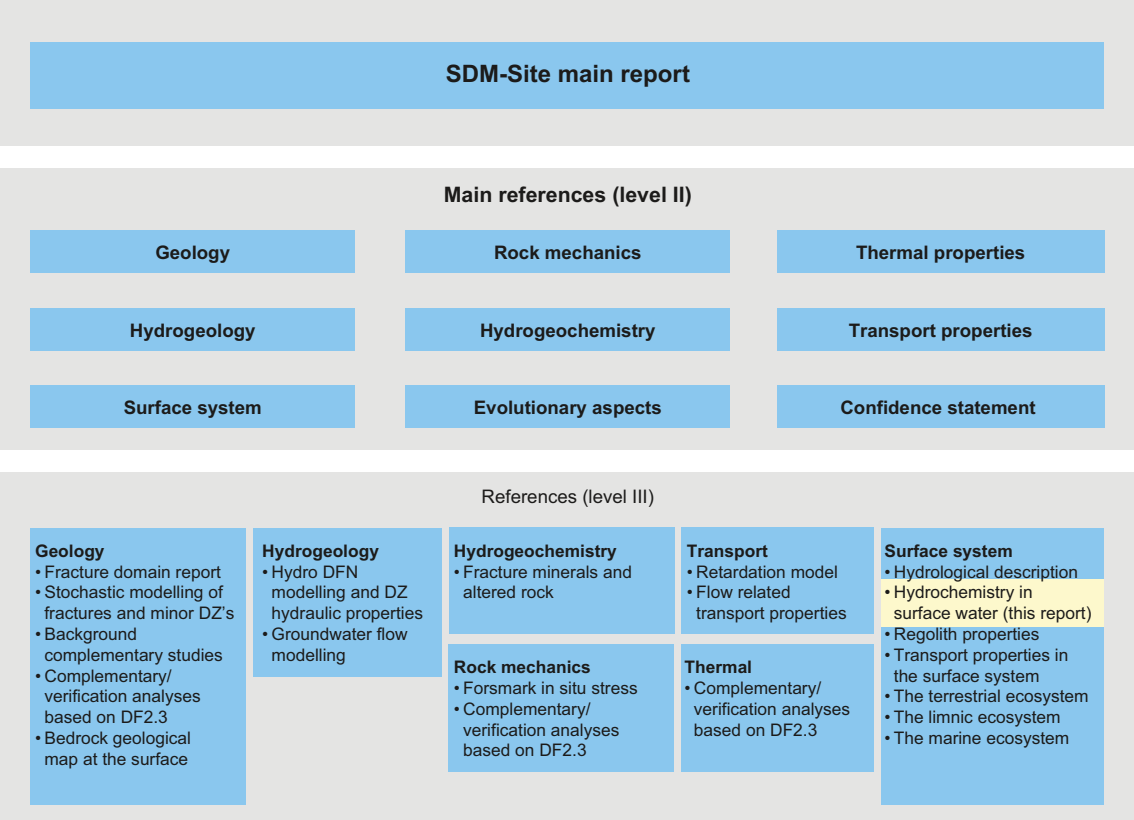

Figure 1-1. *The hierarchical report structure (preliminary) of references behind the SDM-Site main report.*

1.1.1 This report

This report focus on the surface system and is an evaluation of hydrochemical data from surface water and shallow groundwater in relation to observations from deep groundwater, based on data from the Forsmark 2.2 'datafreeze' (data available in the SKB Sicada database in June 2006). It is also an attempt to couple hydrochemical data with observations from other disciplines, e.g. hydrological measurements and distribution of different categories of regolith.

According to Figure 1-2, most shallow groundwater observations reflect the first 10 metres from the ground surface to the upper fractured parts of the bedrock. Deep bedrock hydrochemistry, with the main purpose of describing the conditions at the planned repository depth, primarily focus on depths below c 150 metres, leaving an intermediate zone of approximately 150 metres where the areas of interest overlap. Some objects attributed to the surface system such as private wells, reach this intermediate zone as well.

In order to understand the characteristics of the objects that reach the intermediate zone, deeper observations from the bedrock are included in all models as a reference. There is no ambition in this report to add interpretations of the deep hydrochemistry beside the interpretations made by the ChemNet hydrochemistry group /SKB 2005b, 2006/. Comments on patterns regarding these deep levels are mainly added as a service to the reader in order to convey a wider, integrated picture.

Focus in this report is to answer fundamental questions regarding the origin and fate of elements, and to identify important processes operating within the Forsmark area, rather than to give an overall description of the hydrochemical sampling programme. A complete, element-wise statistical compilation of all hydrochemical data from surface systems in the Forsmark area was conducted in /Sonesten 2005/ and in /Tröjbom and Söderbäck 2006/.

The report contains a large number of visualisations and models. However, due to the enormous amount of possible element combinations, and to the multitude of chemical processes that may influence the hydrochemistry at the site, all possible questions could not be evaluated. Accordingly, the report focus on a limited number of questions that may be regarded as important for an overall understanding of the hydrochemistry at the site, but certainly there are

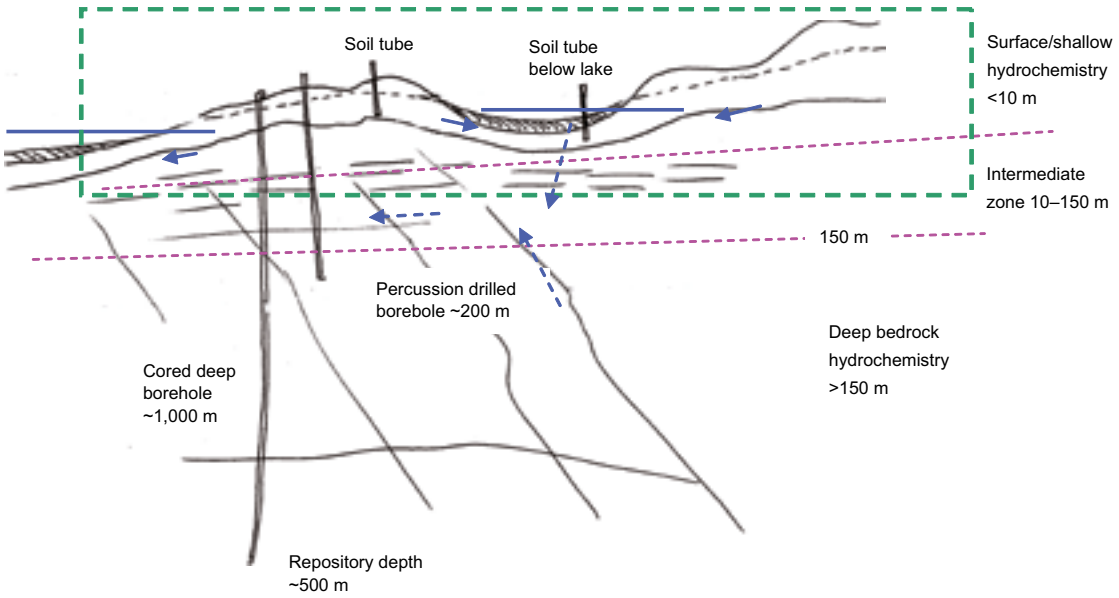

Figure 1-2. *Schematic profile of the Forsmark area identifying the area of interest focused on in this report, the surface and shallow hydrochemistry, and the approximate demarcations towards other disciplines and fields of responsibility.*

potentially important patterns and questions that remains unexplored. The report may therefore function as a basis for further evaluation and testing of scenarios, and may be regarded as an intermediate step between raw data compilations from the vast Sicada database and specialised expert models.

1.1.2 Objectives

The overall objective of this report is to contribute to the understanding of the surface system in the Forsmark area by adding an integrated perspective including deeper hydrochemical observations from the bedrock and data from other disciplines, e.g. regolith category distributions and hydrological measurements, as well as multi-element analyses considering combinations of elements and isotopes. In the last chapter of the report, important conclusions from the many visualisations and models are used to develop a conceptual model with the objective to explain the present hydrochemistry in surface systems in the light of the past.

Some more specific objects, each of them relating to one or several chapters in the report, are:

- To give an unbiased reflection of the data by using a mathematical/statistical approach (Chapters 3 and 6).
- To explain the overall hydrochemical patterns in the Forsmark area in terms of water origin (Chapter 3), sources and sinks for different elements (Chapters 4 and 6), and chemical reactions and processes (Chapter 4).
- To explain the hydrochemistry of anomalous objects in the Forsmark area, e.g. observations of shallow groundwater below lakes (Chapter 7).
- To identify potential areas for surface discharge of deep groundwater from the bedrock (Chapter 3 and 7).
- To quantify mass flows in the surface system (Chapters 5 and 6).

1.1.3 Definitions of water types

In this section a few important concepts regarding water types used in the report are defined. Three main water types representing different depth levels are defined below (cf Figure 1-2):

- *Surface water* denotes fresh or brackish water sampled in lakes, streams and in the Baltic Sea.
- *Shallow groundwater* denotes groundwater in the overburden sampled in soil tubes (In other SKB reports these are sometimes called soil pipes or groundwater monitoring wells in Quaternary deposits), or private wells.
- *Groundwater denotes* water sampled in the bedrock, e.g. in percussion drilled or cored boreholes, and in drilled private wells.
- *Deep (saline) groundwater,* which refers to groundwater originating from greater depths in the bedrock, is a subset of the "groundwater" type above. This water type also includes brine (alternatively shield brine), which is a designation of the highly saline groundwater present at great depths in the granitic Scandinavian shield.

Within the ChemNet reporting (e.g. /SKB2005b/), the use of 'end-members' is an important concept describing the composition of a number of ideal water types. Observed water composition in samples from the site is interpreted as mixtures of the different end-members. An end-member is defined by the absolute concentrations of the constituents and consequently reflects a very specific water type, e.g. the Baltic Sea at a specific point and time. The end-members used in the Forsmark 2.2 reporting stage are listed in Table 1-1 (Laaksoharju (ed.) in prep.).

Table 1-1. Compilation of end-members used in the Forsmark 2.2 modelling stage /Laaksoharju (ed.) in prep./.

End-member	Comment	Na mg/L	K mg/L	Ca mg/L	Mg mg/L	HCO_3 mg/L	Cl mg/L	SO_4 mg/L	Br mg/L	δ^2H ‰SMOW	^3H TU	$\delta^{18}O$ ‰SMOW
Brine	SGKLX02	8,200	45.5	19,300	2.12	14.1	47,200	10		–44.9		–8.9
Littorina Sea		3,674	134	151	448	92.5	6,500	890		–37.8		–4.7
Dilute Granitic GW	HFM09	274	5.6	41.1	7.5	466	181	85.1	0.572	–80.6	12.1	–11.1
Glacial		0.17	0.4	0.18	0.1	0.12	0.5	0.5		–158		–21
Meteoric	Average	0.4	0.29	0.24	0.1	12.2	0.23	1.4		–80		–10.5
Baltic		1,960	95	93.7	234	90	3,760	325		–53.3		–5.9

1.1.4 Chemical abbreviations used in the text

In order to achieve a compact presentation, elements, compounds and isotopes are usually referred in text and figures through chemical notation. Abbreviations used in the report are listed and explained in Table 1-2 below.

Table 1-2. Compilation of chemical abbreviations used in the report.

Abbreviation	Description	Abbreviation	Description
Ba	Barium	Mg	Magnesium
Br	Brome (bromide)	N	Nitrogen
^{12}C	Stable carbon isotope	Na	Sodium
^{13}C	Stable carbon isotope	N_{tot}	Total nitrogen
^{14}C	Radioactive carbon isotope	NH_4	Ammonium (nitrogen)
Ca	Calcium	NO_3	Nitrate (nitrogen)
Cl	Chlorine (chloride)	^{18}O	Stable oxygen isotope
CO_2	Carbon dioxide	P	Phosphorus
DIC	Dissolved inorganic carbon	pH	Hydrogen ion activity
DOC	Dissolved organic carbon	PO_4	Phosphate (phosphorus)
Eu	Europium	P_{tot}	Total phosphorus
F	Fluor (fluoride)	REE	Rare earth elements
Fe	Iron	^{222}Rn	Radioactive radon isotope
^2H	Deuterium (stable hydrogen isotope)	S	Sulphur
^3H	Tritium (radioactive hydrogen isotope)	^{34}S	Stable sulphur isotope
HCO_3	Bicarbonate	S^{2-}	Sulphide
I	Iodine (iodide)	Si	Silicon
K	Potassium	SO_4	Sulphate
La	Lanthanum (rare earth element)	Sr	Strontium
Li	Lithium	^{87}Sr	Radioactive strontium isotope
Mn	Manganese	TOC	Total organic carbon

2 Background and methods

2.1 The Forsmark area

The Forsmark site is located in north-eastern part of Uppsala County within the municipality of Östhammar, about 170 km north of Stockholm (Figure 2-2). The candidate area for the repository is located along the shoreline of Öregrundsgrepen and it extends from the Forsmark nuclear power plant in the northwest and towards the bay Kallrigafjärden in the southeast (Figure 2-1). The candidate area for the repository is approximately 6 km long and 2 km wide. The north-western part of the candidate area has been selected as the target area for continued site investigations /SKB 2005a/.

Different aspects of the Forsmark area have been described in a large number of reports from different disciplines, and it is out of the scope of this report to give a résumé of all these models. Instead, a selection of important background reports is compiled in Table 2-1, together with references to the preliminary site descriptions of the 1.2 stage. This report is based on data from the Forsmark 2.2 'datafreeze'. When available, preliminary results from the Forsmark 2.2 and 2.3 stages have been taken into consideration in the present evaluation, e.g. hydrological conceptual models and paleo-historical descriptions /Follin et al. 2007a/.

Figure 2-1. *Overview of the Forsmark area seen from the Baltic Sea towards south.*

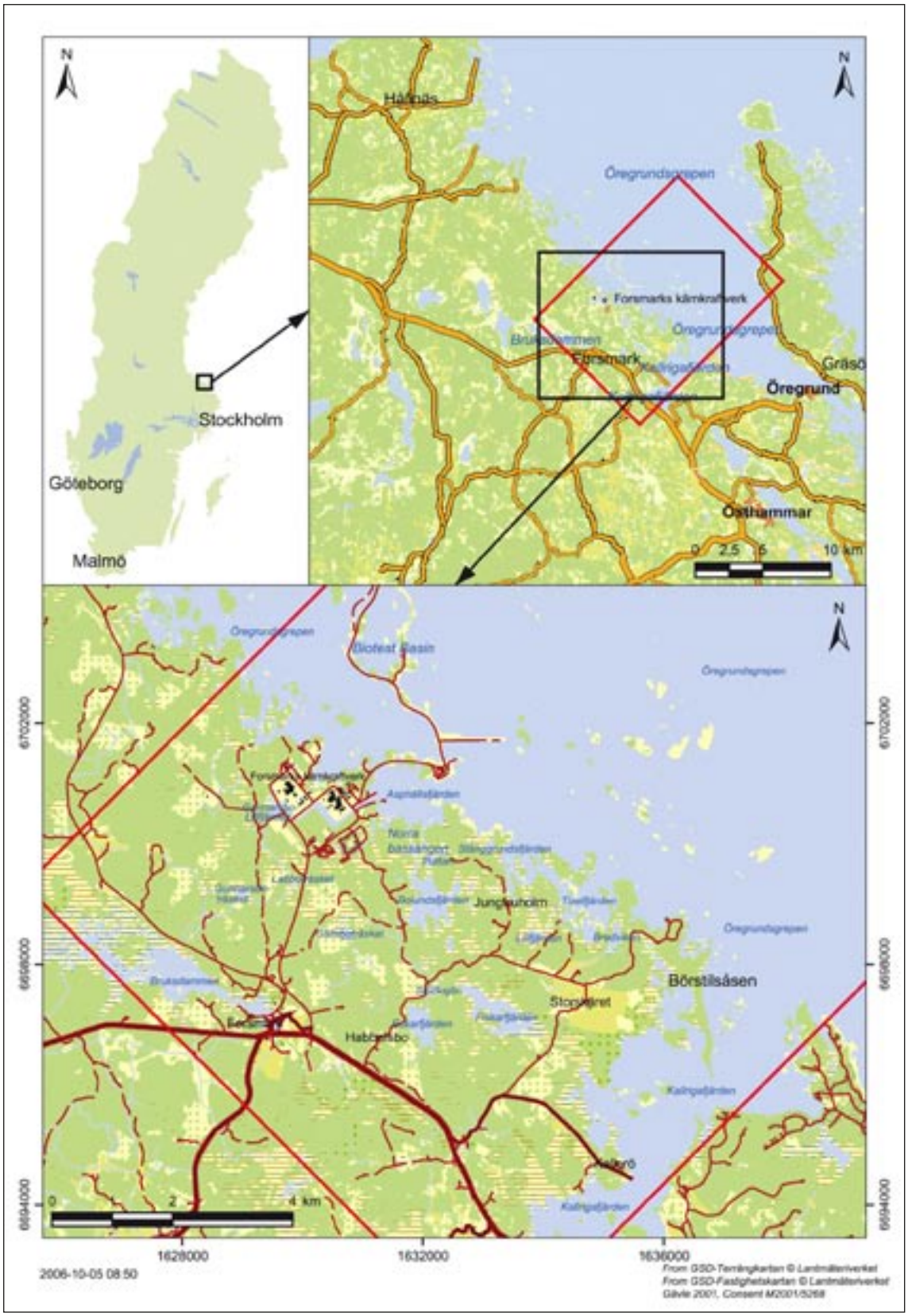

Figure 2-2. *The location of the Forsmark site, where the detailed map includes the geographical names used throughout this report, except for the names of some minor lakes in the area. The red rectangle shows the Forsmark regional model area.*

Table 2-1. Compilation of previous surface hydrochemistry reports and a selection of other reports containing descriptions of the Forsmark area.

	SKB Report	Reference
Preliminary site descriptions		
Preliminary site description Forsmark area – version 1.2.	R-05-18	/SKB 2005c/
Description of surface systems. Preliminary site description Forsmark area – version 1.2	R-05-03	/Lindborg et al. 2005/
Hydrochemical evaluations (surface water and shallow groundwater)		
Chemical characteristics of surface systems in the Forsmark area	R-06-19	/Tröjbom and Söderbäck 2006/
Chemical characteristics of surface waters in the Forsmark area.	R-05-41	/Sonesten 2005/
Forsmark site investigations – Sampling and analyses – Results from sampling in the Forsmark area, March 2002 to March 03.	P-03-27	/Nilsson et al. 2003/
The limnic ecosystems at Forsmark and Laxemar. Site descriptive modelling – SDM-Site.	R-08-XX	/Nordén et al. in prep/
Sampling and analyses of near surface groundwaters	P-05-171	/Nilsson and Borgiel 2005a/
Sampling and analyses of surface waters. Results from sampling in the Forsmark area, March 2004 to June 2005.	P-05-274	/Nilsson and Borgiel 2005b/
Sampling and analyses of groundwater in percussion drilled boreholes and shallow monitoring wells at drillsite DS1.	P-03-47	/Nilsson 2003a/
Sampling and analyses of groundwater in percussion drilled boreholes and shallow monitoring wells at drillsite DS2	P-03-48	/Nilsson 2003b/
Sampling and analyses of groundwater in percussion drilled boreholes at drillsite DS3. Results from the percussion boreholes HFM06 and HFM08.	P-03-49	/Nilsson 2003c/
Hydrogeochemical evaluations		
Hydrogeochemical evaluation. Preliminary site description Forsmark area – version 1.2.	R-05-17	/SKB 2005b/
Hydrogeochemical evaluation of the Forsmark site, modelling stage 2.1 – issue report.	R-06-69	/SKB 2006/
Hydrogeochemical evaluation. Forsmark area – version 2.3	R-08-XX	/Laaksoharju (ed.) in prep./
Hydrology and hydrogeology		
Description of climate, surface hydrology, and near-surface hydrogeology. Forsmark 1.2.	R-05-06	/Johansson et al. 2005/
Analysis of meteorological data, surface water level data and groundwater level data.	P-05-152	/Juston and Johansson 2005/
Analysis of meteorological, hydrological and hydrogeological monitoring data	R-06-49	/Juston et. al. 2006/
Recharge and discharge of near-surface groundwater in Forsmark. Comparison of classification methods	R-07-08	/Werner et al. 2007/
Updated strategy and test of new concepts for groundwater flow modelling in Forsmark in preparation of site descriptive modelling stage 2.2	R-07-20	/Follin et al. 2007a/
Geology		
Mapping of unconsolidated Quaternary deposits 2002–2003. Map description.	R-04-39	/Sohlenius et al. 2004/
Properties of the regolith at Forsmark. Site descriptive modelling – SDM-Site.	R-08-XX	/Hedenström and Sohlenius, in prep./
Depth and stratigraphy of regolith, Site description Forsmark.	R-08-XX	/Nyman et al. in prep./
Site descriptive modelling Forsmark, stage 2.2. A fracture domain concept as a basis for the statistical modelling of fractures and minor deformation zones, and interdisciplinary coordination.	R-07-15	/Olofsson et al. 2007/

2.2 Data used in this report

This report is based on hydrochemical data from the Forsmark 'datafreeze 2.2', which cover observations from March 2002 to June 2006. In this section, the dataset is briefly presented. More detailed descriptions of data from surface water and shallow groundwater is found in /Tröjbom and Söderbäck 2006/ and in /Sonesten 2005/. Information about deeper boreholes are compiled in ChemNet hydrogeochemical evaluations /SKB 2005b/. See compilation in Table 2-1 for further references.

2.2.1 Compilation of hydrochemical parameters

A large number of hydrochemical parameters are measured within the different sampling campaigns in the Forsmark area. The parameters may be grouped into a number of categories, based on the sampling interval of each parameter. In Table 2-2, parameter categories used in evaluations in this report are listed, together with a representative element for each group. The total number of observations of these representative elements in different objects are listed in appendix.

In Section 5.1.1 a number of aggregated parameters, derived from e.g. chemical and hydrological site data from soil tubes, are correlated to a field estimated recharge-discharge characteristics for each soil tube. These parameters, which are listed in Table 2-3, either represent mean values or the variability around the mean value, expressed as the coefficient of variation or the standard deviation. The variability of concentration parameters that may attain zero, but not negative values, is expressed as the coefficient of variation, CV, which reflect the relative dispersion from the mean, whereas the standard deviation is used for most other parameters. Soil tubes with less than three observations were excluded in the analysis in Section 5.1.1 as no measure of variability could be estimated for these objects.

The semi-quantitative recharge-discharge parameter, RDPO, is based on a hydrological field classification according to Table 2-4. Five discrete classes ranging from recharge to discharge are coded to form the semi-quantitative parameter ranging from 1 to 5. This parameter is further evaluated in relation to a large number of hydrological and physical parameters in Appendix C and in /Werner et al. 2007/.

Table 2-2. Listing of different parameter categories and representative parameters.

Representative parameter	Other parameters in category
pH	Conductivity
Cl	Na, K, Ca, Mg, HCO_3 SO_4
Sr	Li, I, F, Br
Si	SiO_2
Fe	Mn
S^2	O_2
Tot-N	NH_4-N, NO_{23}-N, tot-P, PO_4-P, TOC, DIC
DOC	
^{2}H	^{3}H, ^{18}O
^{13}C	
^{14}C	
^{34}S	
^{87}Sr	^{10}B, ^{37}Cl
Cu	Zn, Pb, Cd, Cr, Al, Ni, Hg, Co, V
La	Sc, Rb, Y, Zr, Mo, In, Sb, Cs, Ba, Hf, Tl, Ce, Pr, Nd, Sm, Eu, Gd, Tb, Dy, Ho, Er, Tm, Yb, Lu
U	Th
^{222}Rn	^{226}Ra, ^{238}U, ^{235}U, ^{234}U, ^{232}Th, ^{230}Th

Table 2-3. A selection of hydrochemical parameters measured in soil tubes, which in Section 5.1.1 are correlated to a field estimated hydrological parameter that describe recharge-discharge characteristic in each soil tube. The suffix "cv" denotes the coefficient of variation and "ss" the standard deviation.

	Aggregated parameter abbreviation	
Original parameter	**Variability**	**Mean value**
Bicarbonate	HCO3_cv*	
Chloride	Cl_cv*	Cl*
Conductivity (field)	Cond_cv*	–
Deuterium	D_ss*	–
DOC	DOC_cv*	DOC*
Groundwater level	GWL_ss*	GWL*
ORP (field)	ORP_ss*	ORP*
Oxygen	Ox_ss*	Ox*
Oxygen-18	O18_ss*	O18*
pH (field)	pH_ss*	–
Radon-222	–	Rn222*
Sulphate	SO4_cv*	SO4
Temperature	Temp_ss*	Temp*
Tritium	Tr_ss*	Tr*

Table 2-4. Explanation of the hydrological classification parameter RDPO. Most soil tubes in the Forsmark area are classified as class 1 or 5. See also Appendix C for further evaluations of this parameter.

Field classification (categorical variable)	RDPO (semi-quantitative variable)
Recharge	1
Probable recharge	2
Varying	3
Probable discharge	4
Discharge	5

2.2.2 Overview of sampling sites and sampled objects

Hydrochemical sampling is conducted in a number of different object types represented by a unique id-code in the SKB Sicada database. A three letter prefix and a serial number identify each object shown in Figure 2-3, e.g. SFM0001 is the soil tube with serial number 1. There are water samples from five different object types:

- Surface water samples (PFM) – precipitation, lake, stream and sea water.
- Private wells and springs (PFM) – drilled or dug wells and natural springs either representing shallow groundwater in the overburden or groundwater in the bedrock.
- Soil tubes (SFM) – groundwater monitoring wells drilled in the overburden, usually not extending more than 10 metres deep. The representative sampling depth corresponds to the location of the intake screen, usually the last meter of the soil tube.
- Percussion drilled boreholes (HFM) – boreholes drilled in the bedrock, usually extending to a depth of approximately 200 metres, sometimes sectioned by packers.
- Cored boreholes (KFM) – core drilled boreholes, usually extending towards a depth of 1,000 metres, and sectioned at several levels with packers.

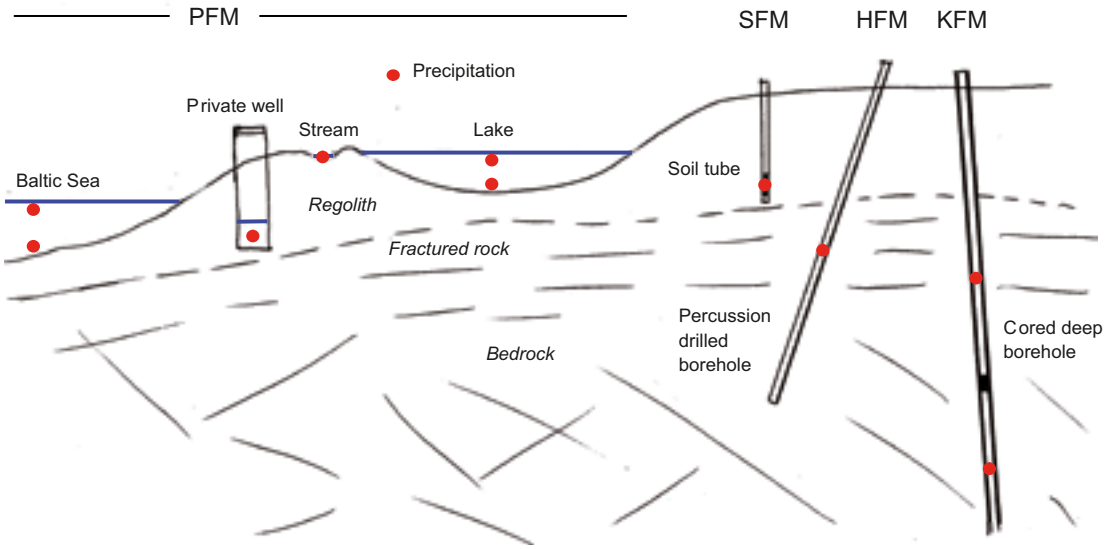

Figure 2-3. *Schematic picture showing the different object types which are sampled for hydrochemistry in the Forsmark area. The red dots denote the representative sampling level.*

Surface water sampling is conducted in all larger lakes within the Forsmark area, in the major (but still rather small) streams and at four locations in the Baltic Sea, according to Figure 2-5. The locations of private wells and the single natural spring are also included into this figure, together with the surface water divides that form the sub-catchments of the Forsmark area. A comprehensive summary of the hydrochemistry in all freshwater sampling points is given in /Sonesten 2005/ and in /Tröjbom and Söderbäck 2006/.

Cored boreholes are clustered at 'drill sites', surrounded by percussion drilled boreholes used for flushing water supply (cf Table 2-5) and monitoring purposes, as shown in Figure 2-6. Soil tubes are also localised around the drill sites for environmental monitoring purposes. There are also a relatively large number of soil tubes and percussion drilled boreholes located outside drill sites for monitoring and characterisation purposes. Many soil tubes and percussion drilled wells are mainly used for hydrological monitoring of groundwater levels and hydrological characterisations e.g. through pumping and so called 'slug tests', and in only a about half of the soil tubes have hydrochemical sampling been carried out.

Physical and hydrological information about soil tubes is compiled in Appendix B (Table 1-2), whereas information about private wells are found in /Ludvigson 2002/. Cored boreholes are described and evaluated in detail in /SKB 2005b/, and some depth information and hydrochemical data from percussion drilled boreholes are compiled in appendix.

In the 3D-view in Figure 2-4, the extensions of the deep cored boreholes are shown from a point west of the Forsmark model area.

2.2.3 Hydrochemical data from surface systems

Hydrochemical data from surface systems (precipitation, streaming water, lake water, sea water, shallow groundwater in soil tubes and private wells) are based on the Forsmark 2.2 datafreeze, covering the 4-year period from July 2002 to June 2006. Due to revisions of the monitoring programme and different extensions of sampling campaigns, there is a large variation in representativity and available number of samples from different objects. Samples with large charge balance errors have also been omitted in accordance with the ChemNet 2.2 representativity evaluation /Laaksoharju (ed.) in prep./.

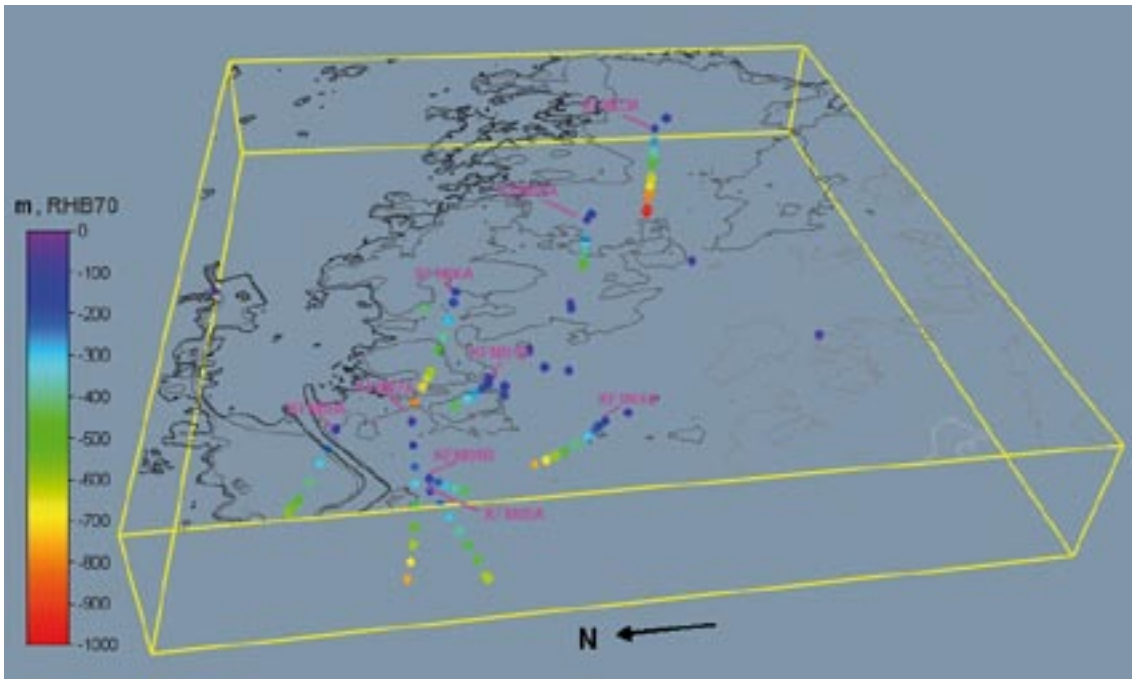

Figure 2-4. *3D-view of the Forsmark area seen from west. All hydrochemical observations below 100 metres vertical depth (both HFM and KFM) are marked by a colour code representing the absolute depth of the sampling level (m, RHB70). Dark lines mark the coast and lighter shaded lines indicate the topography.*

An overview of all available samples from the surface system is compiled in Appendix G. A statistical compilation of mean values is found in Appendix H, and time series including all available samples per object are shown in Appendix I. The geographical locations are revealed in Figures 2-5 and 2-6.

2.2.4 Hydrochemical data from the bedrock

Hydrochemical data of groundwater sampled from different types of boreholes in the bedrock are based on the Forsmark 2.2 datafreeze covering the period to June 2006. These data are mainly included in the visualisations and analyses in this report as a reference to shallow observations. Three different data selections of hydrochemical data from the bedrock are used:

A) All available data with acceptable charge balance and measurements, for the KFM-samples, of flushing water content. This set of data is used for calibration.

B) All samples from selection A, but with samples exhibiting unreliable depth information deselected, e.g. ‘tube samples’ and ‘drilling samples’.

C) ChemNet representative samples. Expert selection of single samples representing groundwater hydrochemistry with satisfactory height accuracy, stable redox conditions, acceptable charge balance and probable isotope values, according to the Forsmark 2.2 representativity check /Laaksoharju (ed.) in prep./.

Data set C is used in most visualisations and models throughout this report in order to harmonise with the hydrogeochemical reporting of deeper groundwater data. In some visualisations dataset B is used to reflect the greater variability of a larger number of samples, at the expense of slightly more unreliable depth information.

Figure 2-5. *Surface water sampling points and private wells in the Forsmark area.*

Figure 2-6. *Boreholes and soil tubes in the Forsmark area.*

An overview of all available groundwater samples from the bedrock is compiled in Appendix G. This compilation is based on data selection A (see bullet list above), and ChemNet representative samples are selected from depth levels marked in bold. A statistical compilation of mean values are found in Appendix H, and time series including all available samples per object are shown in Appendix I. The geographical locations of the objects are shown in Figures 2-5 and 2-6.

2.2.5 Correction for flushing water content in KFM-data

Flushing water used during drilling of the cored boreholes is labelled with uranine. If the composition of the flushing water source is known, it is theoretically possible to correct the measurements and recalculate the original composition. Percussion drilled boreholes are used as flushing water wells, and the approximate chemical composition of this water is documented by the hydrochemical sampling. The correction is complicated by the facts that:

- Element concentrations in percussion boreholes are not constant.
- Non uranine labelled surface water may contaminate during drilling and pumping.
- The altered chemical environment due to supply of flushing water may induce reactions, which influence the chemical composition measured in the groundwater of the bedrock.

Despite these drawbacks, a coarse recalculation has been conducted to correct for the influence from mixing with flushing water in the cored boreholes. Since the composition of flushing water varies much between different wells – from fresh to brackish – it is assumed that the correction leads to a more representative water composition, at least regarding conservative elements such as most major ions and some isotopes, e.g. ^{2}H, ^{3}H and ^{18}O.

The correction is based on the average composition of the flushing water wells used, according to the compilation in Table 2-5 (only samples with satisfactory charge balance were used). A simple linear binary mixing model was used.

Table 2-5. Compilation of flushing water wells (HFM) used during drilling of cored boreholes (KFM).

Cored borehole	Flushing water well	Cored borehole	Flushing water well
KFM01A	HFM01	KFM08A	HFM22
KFM01B	HFM01	KFM08B	HFM22
KFM01C	HFM01	KFM08C	HFM22
KFM01D	HFM01	KFM08D	HFM22
KFM02A	HFM05	KFM09A	FKA tap*
KFM03A	HFM06	KFM09B	FKA tap*
KFM03B	HFM06	KFM10A	HFM24
KFM04A	HFM10	KFM11A	HFM33
KFM05A	HFM13	KFM12A	HFM36
KFM06A	HFM05	KFM90A	FKA tap*
KFM06B	HFM05	KFM90B	FKA tap*
KFM06B	HFM05	KFM90C	FKA tap*
KFM06C	HFM05	KFM90D	FKA tap*
KFM07A	HFM21	KFM90E	FKA tap*
KFM07B	HFM21	KFM90F	FKA tap*
KFM07C	HFM21		

* Composition of FKA tap: Na 23, K 1.1, Ca 30, Mg 1.9, HCO_3 71, Cl 6.4, SO_4 64, pH 7.9, ^{2}H: –66, ^{18}O: –7.2, ^{3}H: 11.3.

The result of the flushing water correction may be concluded from Figure 2-7, where original and corrected values for Cl and HCO_3 are shown. Most Cl measurements increase after correction due to the dilution effect of the flushing water, whereas HCO_3 on the contrary generally decrease and the resulting negative concentrations make the non conservative behaviour of this ion evident (no negative values occur after correction for any other ions). Only a few of samples from data selection B show slightly negative HCO_3-values after correction, and the representative selection C is not corrected due to the low flushing water content in these selected samples.

The flushing water correction have no influence on the major part of the visualisations and results in this report, as most are based on data selection C for which no flushing correction was made. Points in the few visualisations based on data selection B are only slightly altered and the overall picture and conclusions are unchanged if the correction is deselected. The rationale for including the flushing water correction in this report is to give a conception of to what extent this contamination may affect observed concentrations.

2.3 Statistical methods and visualisation techniques

In this section statistical methods and visualisation techniques used in this report are described. Symbols and labels included in the figures to facilitate interpretations are also explained.

2.3.1 Statistical handling of data

The large sets of data described in Section 2.2 are handled by statistical methods in order to simplify visualisations. In most figures the arithmetic mean is used to get a single value representing all samples from a specific object or depth level, and in only a few plots individual samples are included to reflect the dispersion of the whole dataset. According to the compilations in Sections 2.2.3 and 2.2.4, these mean values are based on a varying number of samples depending on object type and sampling campaign.

A set of aggregated parameters is used in Section 5.1.1 to explore correlations to hydrological parameters (cf Section 2.2.1). These parameters either represent arithmetic mean values or measures of dispersion as standard deviation or the coefficient of variation. Standard deviation,

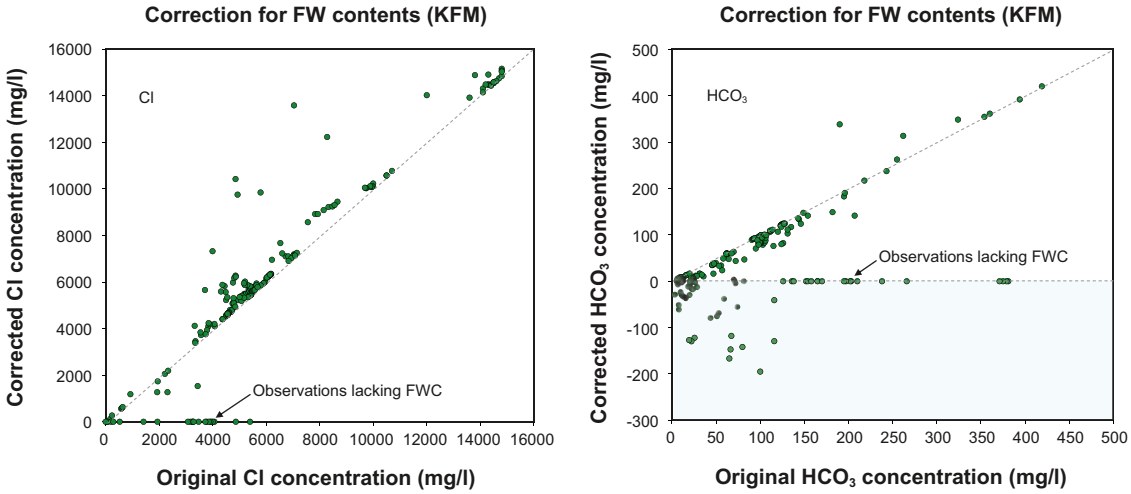

Figure 2-7. *The result of the flushing water correction (FWC) of measurements from cored boreholes. Original (horizontal axis) and corrected (vertical axis) Cl concentrations to the left and correspondingly for HCO_3 to the right. All available data from cored boreholes in the Forsmark area are included in these plots.*

which is expressed in the same unit as the measurements, is used for parameters as temperature and isotope deviations, whereas the coefficient of variation is used for concentration data that may attain zero values (the coefficient of variation is unit less and describes the relative dispersion around the mean value).

2.3.2 Handling of values below reporting limits

Measurements of all elements have reporting limits that reflect the accuracy of the analytical method used. There may also be a variation in the reporting limit for a specific element depending on changes in analytical methods or laboratories engaged. Environmental factors, e.g. salinity, may also influence the reporting limits. In all statistical calculations, values below reporting limits were set to a value equivalent to half of the reporting limit. When different reporting limits occur for a single object, the highest limit is shown in statistics and figures.

2.3.3 Representation of isotope measurements

Isotope measurements are usually expressed as relative deviations from an international standard according to the oxygen isotope example in Equation 1. International standards from /Clark and Fritz 1997/ are compiled in Table 2-6.

Equation 1. Example showing the calculation of the oxygen isotopic deviation from the international reference. The usually very small deviation is multiplied with 1,000 and therefore expressed in per mille (‰).

$$\delta\,^{18}O_{sample} = \left(\frac{(^{18}O/^{16}O)_{sample} - (^{18}O/^{16}O)_{reference}}{(^{18}O/^{16}O)_{reference}} \right) \cdot 1000 \ \text{(‰ SMOW)}$$

Isotope measurements of ^{2}H and ^{18}O in precipitation from a wide range of climatic regions follow a general relationship called the the Global Meteoric Water Line (GMWL – see Equation 2). Local precipitation measurements form Local Meteoric Water Lines (LMWL), that diverge slightly from GMWL due to of factors varying from place to place. Isotope measurements of groundwater or surface water may be related to GMWL or LMWL, and significant deviations from these lines may reflect processes influencing the water cycle, e.g. evaporation.

Equation 2. The Global Meteoric Water Line /Clark and Fritz 1997/, originally derived from /Rozaniski et al. 1993/.

$\delta^{2}H = 8.17(\pm 0.07)\delta^{18}O + 11.27(\pm 0.65)$ ‰ VSMOW

2.3.4 Cross plots (scatter plots)

Combinations of variables are visualised in standard cross plots of two axes. To facilitate interpretations regarding specific issues the original variables are sometimes transformed in order to focus into the range of interest. Logarithmic scales on one or two axes are used for the same purpose (cf Section 2.3.12 and 0 for descriptions of labels and trendlines).

Time series consisting of discrete measurements are shown as points connected by lines to facilitate interpretations, although these lines may not represent the actual trajectories between these points.

2.3.5 Piper plots

The Piper plot is a specialised plot for water classification. Compositional data (the relative molar amounts) of cations and anions are plotted into the ternary (triangular) coordinate systems, which as a second step are projected into the central prism. This methodology may be seen as a dimension-reducing technique that reduce the original seven major constituents (7 dimensions) into a two dimensional visualisation (the central prism), where dominating ions may be distinguished.

2.3.6 Projection plots

The here called 'projection plot' is used to visualise how a third parameter relate to two parameters in a two-dimensional scatter-plot. The magnitude of the third parameter is shown by a colour code representing a varying number of discrete classes. This type of plot visualises 3 parameters at the same time, corresponding to 3 dimensions.

2.3.7 Cross sections and profiles

In Section 7, cross sections of the 3-dimensional soil layer model /Nyman et al. in prep./ are used visualise how hydrochemical sampling points relate to various spatial information. Profiles in these cross sections were created in ArcGis 9.1 by the plug-in /EZ profiler 2007/.

2.3.8 3D-scatterplots and 3D-interpolated data

To show the variation of parameters in the 3-dimensional space, 3D-visualisations are used. The 3-dimensional scatter plot show the location of the sample in 3D-space in combination with the parameter value as a colour coded point.

As a complement to the 3-dimensional scatter plot, a number of measurements representing different 3D-locations may be visualised as an interpolated volume enclosing observations of similar values. The benefit of this type of representation is that the spatial distribution may be easier to grasp compared to the 3D-scatterplot, by using colour coded surfaces and shading techniques. The disadvantage is that the interpolation, which is based on fixed voxel elements (the 2D counterpart is called pixel), implies assumptions regarding the conditions between the observations.

Interpolated presentations in this report uses the 'inverse distance' interpolation method with anisotropy (5,000x, 5,000y, 1,000x), and a distance exponent of 4 /Voxler 2006/. This means that points in the same plane have greater influence on a interpolated voxel value than points from levels above or below, and that the nearest points have much greater influence than more distant points.

Table 2-6. Compilation of international isotope standards of isotopes used in this report. From /Clark and Fritz 1997/.

Isotope ratio	International reference	Reference ratio
$^{2}H/^{1}H$	VSMOW	$1.5575 \cdot 10^{-4}$
$^{11}B/^{10}B$	NBS 951	4.404362
$^{13}C/^{12}C$	VPDB	$1.1237 \cdot 10^{-2}$
$^{18}O/^{16}O$	VSMOW	$2.0052 \cdot 10^{-3}$
$^{34}S/^{32}S$	CDT	$4.5005 \cdot 10^{-2}$
$^{37}Cl/^{35}Cl$	SMOC	0.324
$^{87}Sr/^{86}Sr$	Absolute ratio measured	–

It should be held in mind that the interpolated representation of a dataset is heavily dependent on the spatial representativity of the included points and the chosen interpolation method. The interpolated representation of a fractured media as rock may therefore be inadequate at a local scale, but relevant at a larger scale.

2.3.9 Multivariate analysis and visualisation

Multivariate statistical methods are dimension reducing techniques used for extracting relevant information from large datasets that contain many parallel measurements (many parameters). These powerful methods are suitable for finding underlying factors affecting many parameters at the same time, factors which may be the ultimate explanation we are looking for.

Our limitation to imagine more than three or four dimensions at the same time restricts our ability to grasp large datasets of 10 or 100 dimensions (parameters). In short, multivariate analyses may be seen as methods that explore projections (shadows) of multidimensional objects plotted into coordinate systems of several orthogonal axes (each parameter on each axis), and by studying these two-dimensional projections conclusions may be drawn about the multidimensional object we are not able to imagine. The metaphysic nature of multivariate analysis is a necessary a consequence of our limited mind.

2.3.10 Principal component analysis (PCA)

A principal component analysis (PCA) is based on a correlation or covariance matrix and may be seen as a graphical tool to interpret the correlation structure among both variables and observations. In this report all PCA-models are based on a standard Pearson correlation matrix, which could be questioned if some of the variables show skewed distributions. Due to the explorative character of the analysis this simplified approach was, however, thought to facilitate the interpretations of the models. The results of the PCA analysis are visualised as loading- and score plots:

- In the *loading plot* the relationships among the variables are revealed. Each variable is projected onto the so called principal components, which can be seen as latent factors influencing several variables to a varying degree. If a variable show close connection to a principal component, it is in the loading plot located far from origin in the direction of that component. Variables that plot close to each other are correlated, whereas variables located on opposite sides of the origin are negatively correlated. Variables located near the origin show little correlation to the selected principal components, and therefore little can be said about the correlation structure among these variables. The principal components may have a real meaning, for example a climatic factor, or may just represent a linear combination of unknown factors.
- The *score plot* reveals relationships among the observations. The score plot is a complement to the loading plot in the sense that observations located in a specific region of the score plot show high values for variables located in the corresponding region of the loading plot.

2.3.11 Partial least squares modelling (PLS)

Partial Least Squares Regression modelling (PLS) is a multivariate method closely related to PCA. This technique may be seen as two PCA:s, one representing the explanatory parameters (X-space), and one representing the explained parameter(s), the Y-space. The principal components in both ‘spaces’ are rotated in order to achieve maximal correlation between these structures. Besides the use for fitting empirical explanatory models, PLS plots may be similar to PCA plots be used in explorative analysis of correlation structures among parameters.

2.3.12 Coding and labelling in figures

The different object types are in all plots throughout the report consequently marked by a unique symbol and colour according to Table 2-7. Individual observations are also labelled by an identification code to facilitate detailed analysis of the patterns among individual objects and different depth levels. This code contains a "label code" (cf Table 2-7) of the object type followed by an identification number of the Sicada variable IDCODE, and finally the absolute depth in RHB70. The depth code corresponds to the midpoint of the section (KFM), the main supply level (HFM), the midpoint of the intake screen (SFM) or the sampling depth (surface water – PFM). To the surface water samples, a suffix is also added to indicate whether the sample represents surface (S) or bottom (B) water in the lake or at sea. In private wells, the depth code corresponds to the absolute elevation of the midpoint of the drilled borehole or dug well. The soil tube with IDCODE "SFM0023", where the midpoint of the intake screen is located at 4 metres depth below Lake Bolundsfjärden, is for example labelled S23-4 in all figures.

2.3.13 Marking of trendlines and scenarios in figures

In many figures, hypothetical trendlines or scenarios have been added to facilitate interpretations and descriptions in the report. It should be held in mind that these scenarios are more or less probable. The use of non-linear scales on the axes, isotope ratios and parameter transformations leads to curved mixing lines which are visualised by the hypothetical binary mixing lines. Several types of lines are included in the figures, and they are consequently displayed according to the following:

- Hypothetical trendlines: – bold dashed pink line.
- Model line – bold dashed orange line.
- Mixing lines showing hypothetical binary mixing trends between specific objects: thin dashed pink line. These lines are not always probable and the purpose is to explore the borders of the conservative mixing hypothesis and to show the curvature of mixing lines in non-linear plots.
- The flow direction of surface water: thin dashed green arrow. These arrows connects surface water objects downstream the major catchments.
- Hypothetical depth trend from surface towards depth: black dotted arrow.

Table 2-7. Different objects are marked by a unique symbol/colour in the plots throughout the report. KFM = cored boreholes, HFM = percussion drilled boreholes, SFM = soil tubes, "Lake" and "Stream" are freshwater surface samples (PFM) and "Sea" brackish water samples from the Baltic (PFM). Reference samples of different types are marked as a black dot.

Object type	IDCODE prefix in Sicada database	Label code	Symbol
Cored borehole	KFM	K	●
Percussion drilled borehole	HFM	H	♦
Soil tube	SFM	S	■
Private well	PFM	PP	■x
Lake	PFM	PL	●
Stream	PFM	PW	○
Sea	PFM	PO	■x
Reference	–	–	●

3 Hydrochemical overview of the Forsmark area

The purpose with this part of the report is to visualise hydrochemical data in order to identify important patterns and to raise relevant questions concerning, for example, the origin and fate of water or dissolved elements, as well as effects of various processes.

3.1 Traditional water type classifications

Traditionally, different water bodies are classified in water types based on the (relative) chemical composition of major elements. Different plots are used for this purpose, for example the Ludwig-Langelier diagram and the ternary Piper diagram. The resulting classifications tell which cations and anions that dominates in a sample. Trends along flow paths may be identified in the diagrams and, based on generalised assumptions, conclusions of the evolution of water types may be drawn. However, these assumptions are primarily applicable on larger aquifers and flow systems, and the flat and small-scale topography characterising the Forsmark area, which results in very short flow-paths, may lead to pitfalls if these classifications are not interpreted cautiously.

3.1.1 Ludwig-Langelier plot

Ludwig-Langelier plots visualise the relative proportions of the major cations on the horizontal axes, and proportions of the anions on the vertical axes. Observations located in the lower left corner are dominated by Ca^{2+} and HCO_3^-, usually representing a relatively young groundwater. Observations in the opposite corner is dominated by cations as Na^+ and K^+, and anions as Cl^- and SO_4^{2-}, usually representing an older, developed groundwater, sometimes with possible marine influences (Figure 3-1).

The surface water flow path from the small inlet to Lake Eckarfjärden (PW71) to Lake Norra Bassängen (PL97S) near the outlet in the Baltic, show a clear trend from Ca-HCO_3-types at higher topographical levels to Na-Cl types close to the Baltic (Figure 3-1). This gradient probably reflects a gradually increasing marine influence, both by leakage from marine relics in the sediments and by saltwater intrusions in the lakes at lower levels. The relatively recent withdrawal of the sea due to the ongoing land uplift since the last glaciation gives prerequisites for rich marine relics.

Most of the shallow groundwater observations from soil tubes follow the main trend of the surface water, marked by the green arrows, indicating that they represent a gradient from undeveloped Ca-HCO_3 types to brackish Na-Cl types. From this pattern it can be concluded that mixing with marine ions is a major process influencing the shallow groundwater in the area. At higher topographical levels (recharge areas), the supply of Ca^{2+} and HCO_3^- from dissolution of the calcite-rich overburden is an important factor influencing the groundwater composition, leading to dominating Ca-HCO_3 groundwater types.

A few soil tubes located in the vicinity of Lake Eckarfjärden (S17 and S18) deviate from this main trend by showing enrichments of Na+K at the expense of Ca+Mg, probably an effect of cation exchange processes. As calcium is the dominating cation in the outlet of Lake Eckarfjärden, the observed Na+K enrichment seems to be a local phenomenon comprising only a marginal fraction of the discharging groundwater in the area.

The groundwater in the bedrock represented by cored (KFM) and percussion drilled (HFM) boreholes deviate substantially from the general mixing trend shown by most superficial samples. The deeper levels show large enrichments of Ca+Mg and Cl+SO_4, whereas some of the percussion drilled boreholes show a Na-HCO_3 type, similar to some shallow groundwater samples.

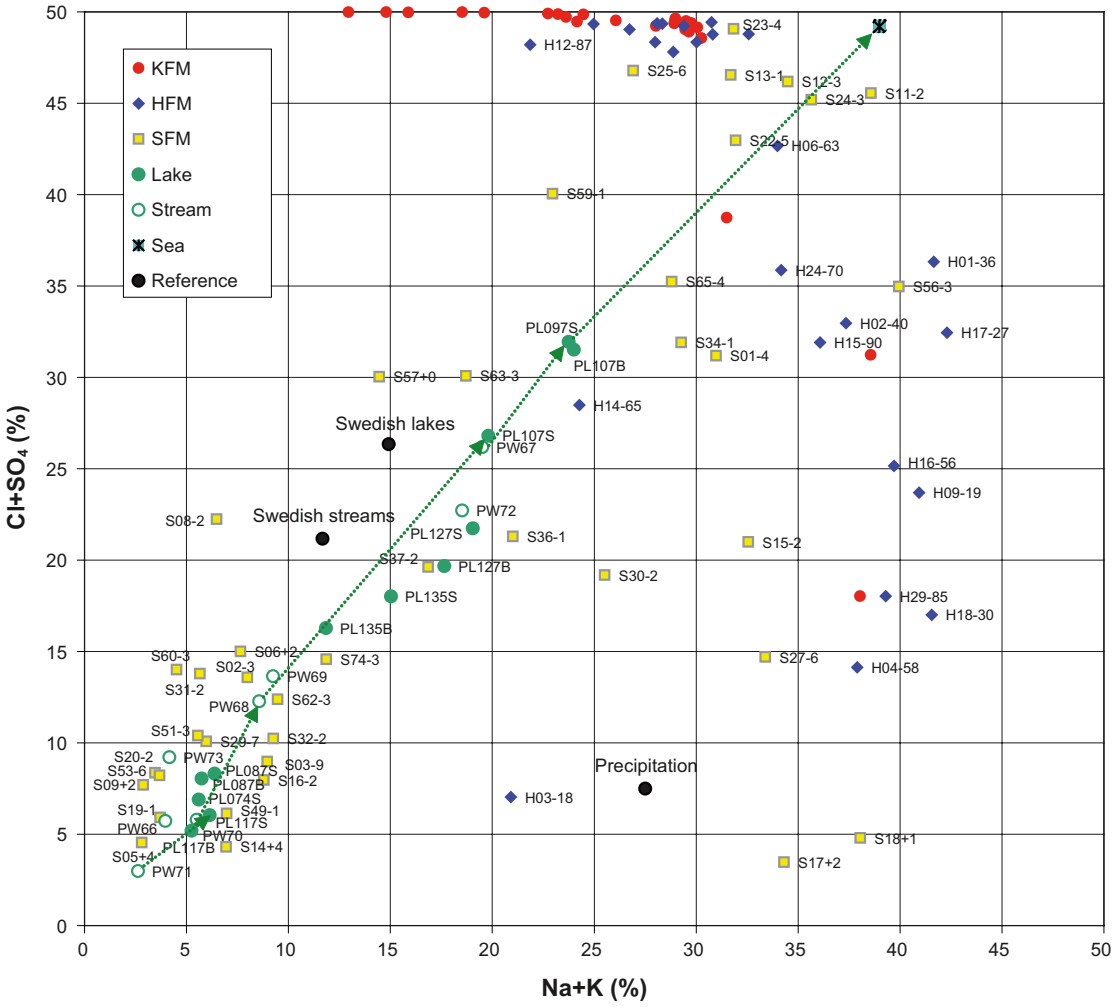

Figure 3-1. *Ludwig-Langelier plot of all Forsmark data. Mean values of representative dataset (cf Section 2.2.4). See Sections 2.3.12 and 2.3.13 for an explanation of labels and trendlines in the figure. The relative amounts on the axes are calculated according following formulas: Na+K(%) = 50×([Na]+[K])/([Na]+[K]+2[Mg]+2[Ca]), Cl+SO$_4$(%) = 50×([Cl]+2[SO$_4$])/(Cl)+2[SO4]+[HCO3]).*

3.1.2 Piper plot

A Piper plot is another, slightly more complex tool to visualise the relative fractions of the major ions (Figure 3-2). The lower ternary plots show the relative proportions of cations (Ca^{2+}, Mg^{2+}, Na^{+}+K^{+}) and anions (Cl^{-}, HCO_3^{-}, SO_4^{2-}), respectively. The prism, in which the ternary plots are projected, corresponds to the Langelier-Ludwig plot, turned 45 degrees clockwise.

The Piper plot adds little information besides the Ludwig-Langelier plot. In superficial waters this is mainly an effect of the mixing between two dominating water types (Ca-HCO_3 and Na-Cl). However, in some of the cored boreholes (KFM) an additional pattern may be distinguished, with a trend towards the Ca-Cl water type. These samples also show very low magnesium and sulphate content compared to the general mixing trend previously described.

3.2 Exploring sources of dissolved ions

Dissolved ions in the water are either supplied through mixing between different so called end-members (cf Section 1.1.3), e.g. sea water or brine, or formed (or removed) in situ as a result of chemical reactions with the rock matrix, the overburden, organic material or dissolved gases.

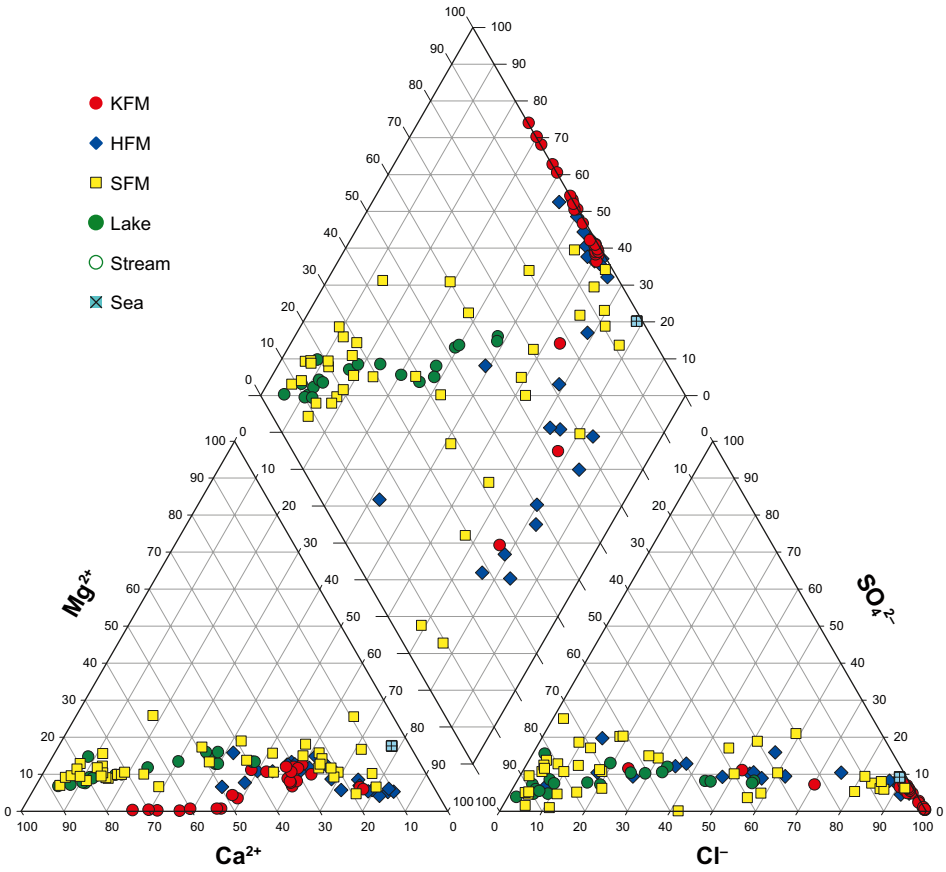

Figure 3-2. *Piper plot of all Forsmark data based on mean values of the representative dataset C (cf Section 2.2.4). See Section 2.3.5 for an explanation of this type of plot.*

The time-scale or, with other words, the water residence time determines which processes that are dominating within a specific water body.

By a multivariate approach, the main patterns in the chemical composition of surface water and groundwater in the Forsmark area was summarized in a PCA-model. Different trends (directions) in the model may be interpreted as different sources of ions contributing to the observed chemical composition among the observations.

The *ion source model* is based on data describing the relative molar amounts of major ions, similar to the previous classification plots. The resulting PCA-model can be viewed as a classification model optimised in separating the groundwater types found in the bedrock, in contrast to the previous "classical" classification plots which are convenient in separating dilute waters, but not effective in separating the more concentrated groundwater types in the bedrock.

One main application of the ion source model is to explore similarities between deep groundwater types and observations in shallow groundwater, and thereby possibly detect signatures of discharging deep groundwater.

3.2.1 Summary of methodology

In order to identify the main hydrochemical variation patterns in the bedrock and to establish a reference model, a common principal components analysis (PCA) was applied on relative compositional hydrochemical data from percussion boreholes and cored boreholes in the Forsmark area. The reason for using data only from boreholes during the calibration step was to optimize

the model for separating the groundwater types found in the bedrock. The use of relative compositional data cancels dilution effects and results in a model emphasising similarities in relative composition, regardless of the dilution by e.g. meteoric or glacial water.

The "calibrated" ion source model was then applied on the shallow groundwater and surface water data, revealing similarities in hydrochemical composition between shallow observations and the main variation patterns found in the groundwater of the bedrock (i.e. compositional data from surface water and shallow groundwater are projected onto the ion source model). The PCA-model was also validated in three steps:

1) A spatial validation where the spatial distribution of the observations, classified into four coarse classes, is explored.
2) A comparison with patterns shown by other, independent variables.
3) A comparison with the results of the multivariate mixing model M3 (cf /Laaksoharju et al. 1999, Gomez et al. 2006/).

Finally, the patterns in the model are interpreted in terms of water types and possible ion sources, the latter representing either the hydrochemical composition of end-members or the composition revealed by reactions, e.g. calcite dissolution. Similarities in chemical composition among observations from the surface system as well as from deeper objects in the bedrock may be explored in the visualisations of the model.

3.2.2 Calibration of the ion source reference model

The ion source reference model, which is based on relative compositional data from percussion drilled boreholes and cored boreholes, describes the major compositional patterns of the groundwater in the bedrock. A standard principal component analysis was used to condensate the patterns of 11 major and minor constituents into two components comprising 83% of the total variation.

The reference dataset used contains as much data as possible from cored boreholes (KFM) and percussion drilled boreholes (HFM) under the conditions of acceptable charge balance (± 5%) and, for cored boreholes, that information of flushing water content was available for the samples from the (dataset A, cf Section 2.2.4). A rationale for including data with uncertain depth information (e.g. tube samples and samples obtained during drilling) is that they all consist of water mixtures from the Forsmark area and therefore contribute to the overall variation in the model. Data from cored boreholes was corrected for flushing water content by a linear mixing model based on the average chemical composition of the wells used (cf 2.2.5).

Relative chemical composition, expressed as the relative molar abundance, was calculated for cations and anions separately. The calculations were based on the average concentration per object and depth level of all major ions (Na, K, Mg, Ca, Cl, SO_4, HCO_3) and a few trace elements (Li, Sr, F, Br). The PCA-model based on two principal components comprises about 83% of the total variation in chemical composition among the bedrock groundwater samples (PC1 67%, PC2 16%). This model condensate the major variation pattern among 11 variables (the use of closed compositional data seize two degrees of freedom, leaving 9 independent variables to the PCA) into two latent variables, the principal components. There may be theoretical objections against the application of a standard PCA on compositional data /e.g. Aitchison and Greenacre 2002/, although this procedure is commonly used in literature. The use of alternative techniques, e.g. log-contrasts, to circumvent these possible constraints was however deselected in favour of a more transparent approach.

In Figure 3-3 (upper panel), the PCA-model is visualised in score- and a loading-plots (cf 2.3.10 for explanation). The major variation (67%) is shown by the first component (PC1, vertical direction), whereas the second component (PC2, horizontal direction) catch a weaker pattern corresponding to 16% of the total variation. The enclosed loading plot show to what extent different variables contribute to the two first principal components. A labelled version of the ion source reference model is found in Appendix A.

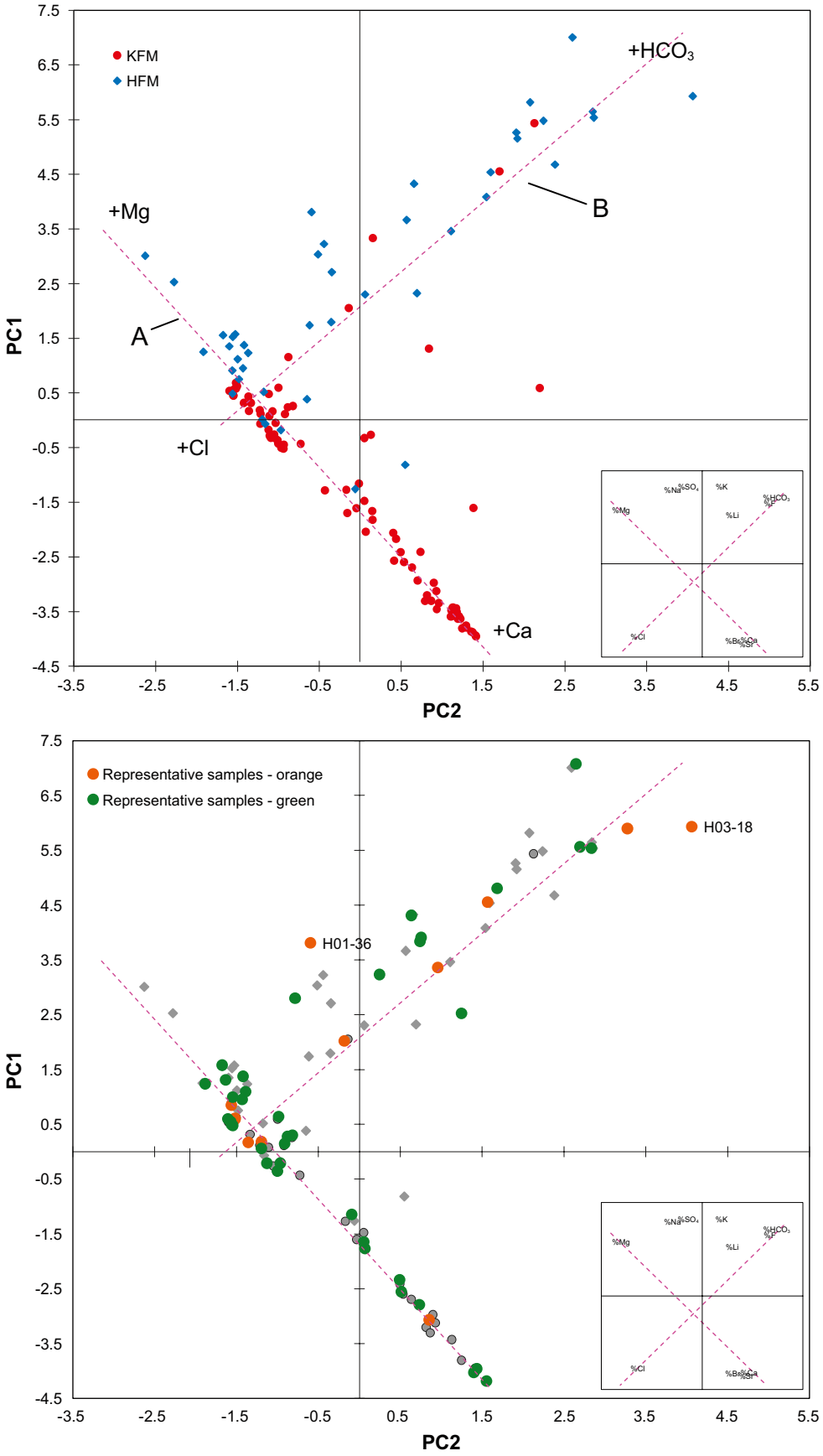

Figure 3-3. *The upper score plot shows how the observations of the calibration dataset A are related to the main variation pattern of the ion source reference model. The lower score plot shows instead the representative samples of dataset C (colour coded) and dataset B (grey marks). The insets show the corresponding loading plots.*

There are two main trends in the PCA-model denoted “A” and “B” in Figure 3-3. The major difference in composition among observations plotting along trend “A” is shown by Mg in the upper left and Ca, Sr and Br in the lower right. The major difference along trend “B” is shown by Cl in the lower left and HCO_3 and F in the upper right. A few parameters, Na, K, and SO_4, show a weaker association to both trends, which reflects the mixed origin of these ions.

Most observations from percussion boreholes plot along trend “B”, whereas deeper observations from cored boreholes predominantly plot along trend “A”. There is a cluster in the intersection between these trendlines, where observations from both percussion and cored boreholes plot (see Appendix A for labelling of individual observations).

For an orientation, the lower panel in Figure 3-3 shows the expert selected, representative samples (dataset C, cf Section 2.2.4) and dataset B projected onto the ion source reference model (orange colour indicates the most representative samples). These samples, and especially the orange ones, follow the major trends.

3.2.3 Projection of surface data – the ion source model

In order to explore similarities among different parts of the surface system and the observed hydrochemistry in groundwater of the bedrock, observations from shallow groundwater sampled in soil tubes and private wells, surface waters from streams, lakes and the Baltic Sea, were projected onto the ion source reference model described in Section 3.2.2.

In the visualisations of the *ion source model* a slightly different selection of bedrock groundwater data is shown than during the calibration phase of the reference model in previous section. The reason for this is that some of the samples from cored boreholes were sampled by techniques that represent mixtures with more or less uncertain depth information, leading a distorted picture when trends among individual depth sections are evaluated. All further visualisations are therefore based on dataset B, where all “tube samplings” and “drilling samples” from the cored boreholes have been omitted (cf Section 2.2.4).

In Figure 3-4, observations from the surface system have been projected onto the ion source reference model, together with bedrock groundwater data of selection B. This combination of data projected onto the ion source reference model is referred to as the *ion source model*. All individual objects have been individually labelled according to the principles described in Section 2.3.12.

Most of the observations from the surface system plot in the upper half of Figure 3-4. This indicates that water in the surface system for the most part differs considerably from the deeper samples (represented by the cored boreholes, KFM). It should be noted that all conclusions about similarities and dissimilarities in composition refer to the main variation patterns of the major elements, and sometimes adjacent observations may differ in a direction perpendicular to the paper plane.

Many soil tubes (SFM) plot along trendline B and therefore show resemblance to the chemical composition found in many of the percussion boreholes (HFM). There are also soil tubes as well as private wells that plot near trendline A. A group of soil tubes and surface waters from the upstream parts of the catchments form a separate group denoted “C”, to the right in Figure 3-4. The chemical composition in this group differs from all groundwater types found in the bedrock. Observations in lakes and streams show a gradient ranging from group “C” to Baltic Sea water in the left part of the figure.

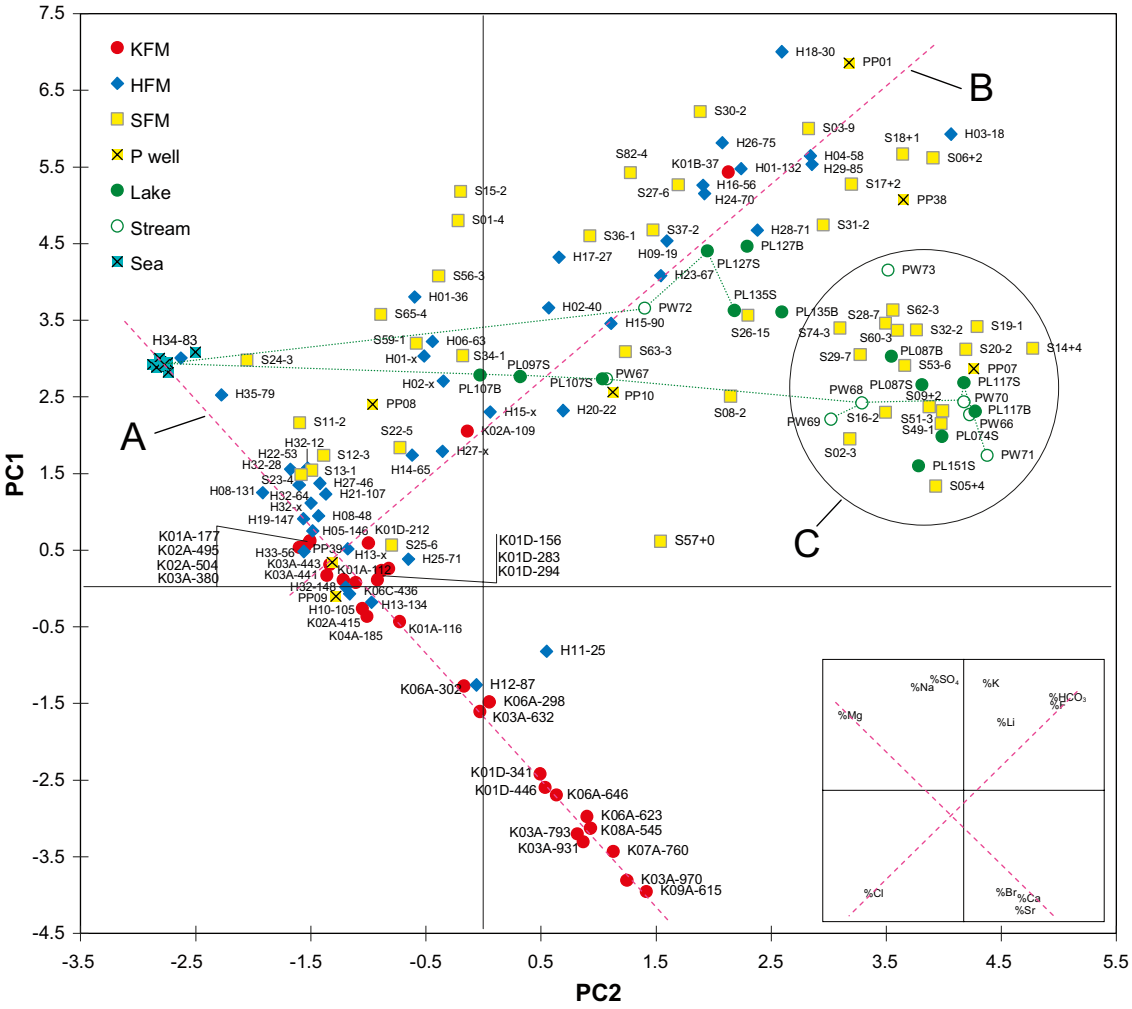

Figure 3-4. *The ion source model. The PCA score plot (cf description in Section 2.3.10) shows how the different groundwater and surface water objects relate to each other regarding the chemical composition of major elements. Labelling of individual objects is explained in Section 2.3.12.*

3.2.4 Interpretation of the ion source model

Trends formed by the observations in the *ion source model* may be interpreted as pointing in the direction of theoretical ion sources. Intermediate locations are assumed to constitute mixtures of ions from different sources. Possible ion sources (bold) as well as different potential groundwater types (italic) are marked in Figure 3-5.

To generalise, the four major ion sources influencing the groundwater in the Forsmark area are 1) supply of marine ions, 2) supply of shield brine, and 3) weathering of local minerals and 4) supply of bicarbonate of atmospheric biogenic CO_2 origin. In surface waters, calcite dissolution is an additional ion source, supplying mainly Ca and HCO_3.

Five major groundwater types may be identified in Figure 3-5 according to the encircled groups of observations. It should be noted, however, that any classification in some way is an artefact, as most observations belong to continuous gradients between theoretical end-members. The following water types are introduced in order to facilitate the interpretations (cf ChemNet end-members listed in Section 1.1.3 and the definitions of water types in Section 1.1.3).

- *Modern sea water.*
- *Relict marine groundwater* (mostly of Littorina origin).

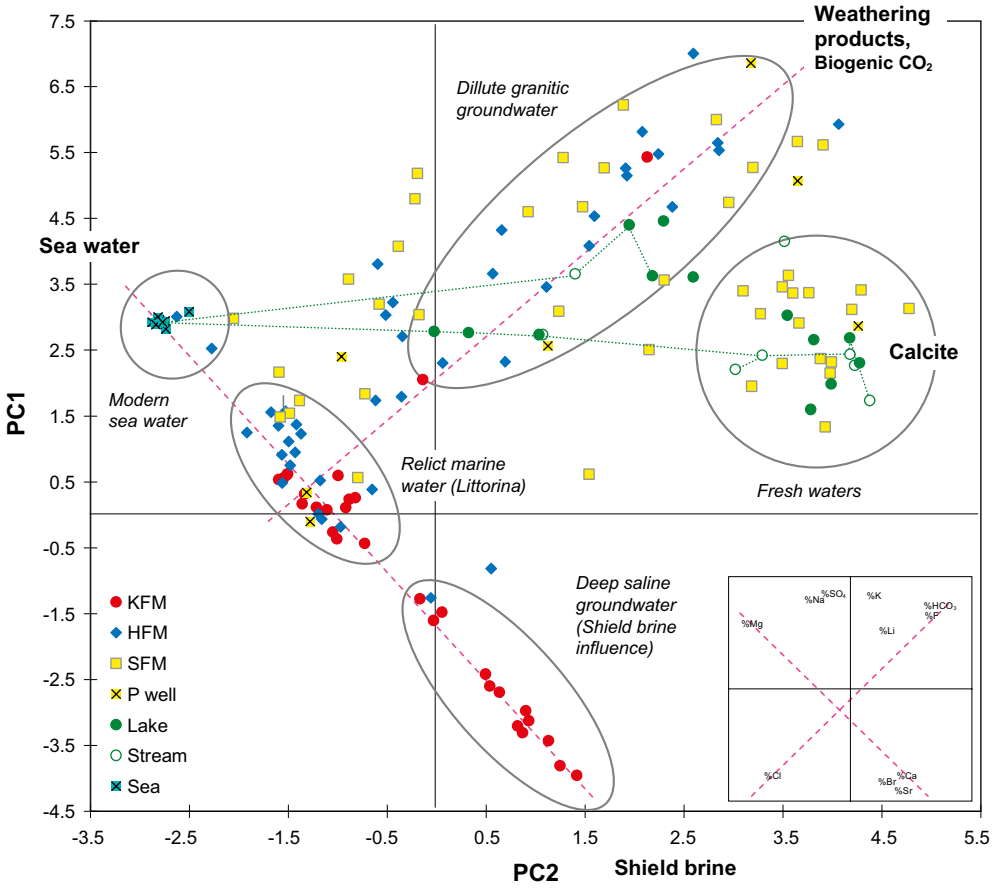

Figure 3-5. *The ion source model, with different possible ion sources marked in bold. Possible groundwater types are marked in italic. See Figure 3-4 for labels of individual objects and depth levels.*

- *Deep saline groundwater* significantly influenced by shield brine (shield brine is a highly saline groundwater present at great depths in the granitic environment of the Scandinavian shield).
- *Dilute granitic groundwater* is of meteoric origin, significantly altered by processes within the Quaternary deposits. According to a late agreement between the ChemNet and HydroNet expert groups, this water type will in the future be denoted *"altered meteoric groundwater"*. Due to lack of time, the old designation is kept within this report.
- *Freshwaters* include both surface water and shallow groundwater, showing "immature" ion signatures influenced from biogenic CO_2 and calcite dissolution.

The most apparent gradient is shown by a large number of observations ranging from *modern sea water* to the *deep saline groundwater* clearly influenced from shield brine. Most of the observations along this gradient are groundwater samples from the bedrock (percussion drilled boreholes, HFM, and cored boreholes, KFM). A few shallow observations in soil tubes and private wells also plot along this gradient.

The ground water type denoted *relict marine water* is located on the intersection between the major gradients pointing at sea water, shield brine and weathering. The intermediate location of this group may be interpreted as if the ingoing ions mainly are a product of mixing of these major ion sources, i.e. relict sea water, mixed with shield brine and with a relatively small influence from local weathering products. Alternatively, the shift from the modern ion composition of sea water could to some extent be explained as altered marine water due to chemical reactions within the bedrock (E-L Tullborg, pers. comm.).

Dilute granitic groundwater shows a large spread, which probably reflects the great variety of processes influencing these waters, e.g. variations in mineralogy, mixing with modern or relict

marine components, cation exchange reactions as well as influence from biogenic CO_2 and calcite dissolution (cf Section 4.2.1).

Freshwaters in the upstream part of catchments show influence from biogenic CO_2 and the calcite rich overburden in the Forsmark area (the location of this group in the projection indicates a concomitant supply of Ca and HCO_3 due to calcite dissolution driven by H^+ of biogenic CO_2 origin). Most lakes in the area are characterised as oligotrophic hardwater lakes /Brunberg and Blomquist 2000/, reflecting the impact of Ca on processes in the surface system. Many soil tubes also plot into this group, likely due to influence from calcite /Tröjbom and Söderbäck 2006/. The origin of calcium is further evaluated in Section 4.1.3.

As a coincidence or a causal relationship, the ion source model coincides with the geographical cross-section from land to sea and from depth to surface, according to Figure 3-6. No broad conclusions should be drawn from this picture, but there is a clear connection to the hydrological conceptual model for the Forsmark area /Follin et al. 2007a/ (cf spatial validation in Section 3.2.5). According to this model there are few or no examples of binary mixing between the shallow water types (dilute granitic groundwater and freshwaters) and deep saline waters with shield brine influence.

3.2.5 Spatial visualisation and validation of the ion source model

The ion source model was validated in three steps. Firstly, a spatial validation was performed, where the distribution of the observations was visualised in three dimensions. Secondly, the modelling results, which are based solely on the major constituents, were compared with a number of independent parameters. Finally, the results were compared with the results of the multivariate mixing model M3.

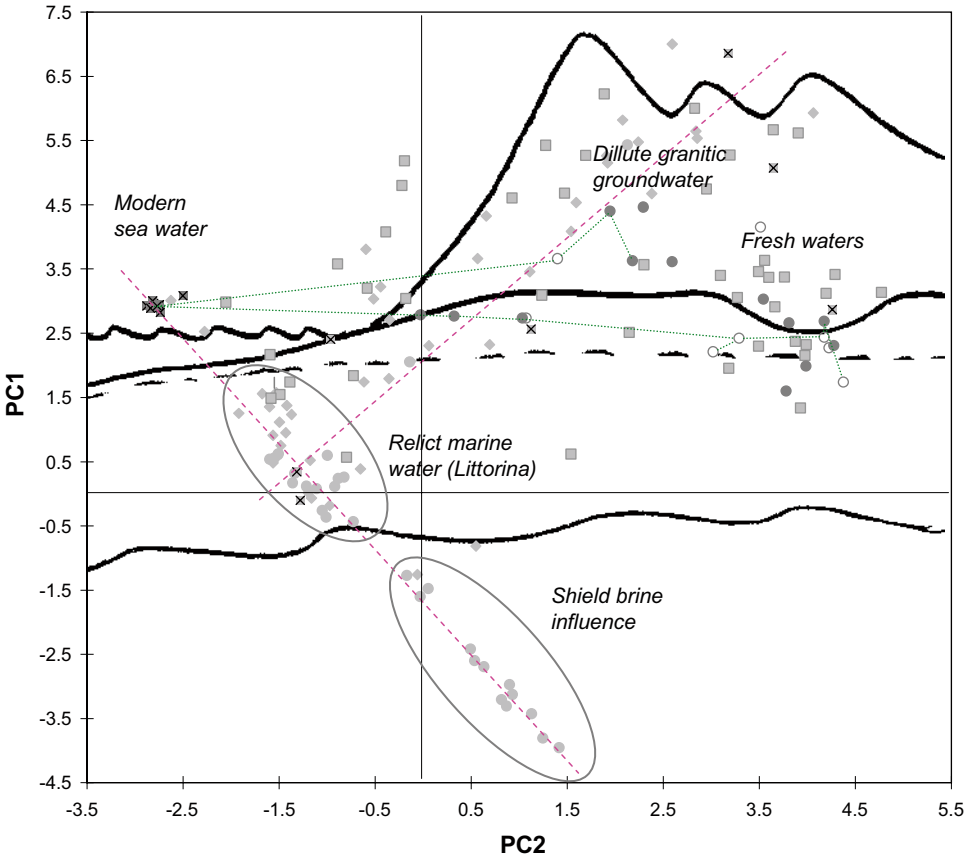

Figure 3-6. *Comparison of the ion source model (background) and a schematic geographical cross-section from land to see and from depth to surface.*

To explore if the main pattern and interpretation of the PCA-model corresponds to a plausible distribution in three dimensions, the observations were roughly classified into four groups according to Figure 3-7. For groundwater, only samples of dataset B (cf Section 2.2.4), i.e. observations with reasonably accurate depth information, were included in the spatial visualisation/validation (SFM, HFM, KFM, cf Section 2.2.2).

The spatial distribution of each class is visualised in Figure 3-8 as interpolated 3D-volumes, in order to facilitate interpretations (cf Section 2.3.8 for a description of the interpolation method). It should be noted that the 3D-visualisations is a tool to visualise available data, and the visualisations do not necessarily represent the situation of the real world of the fractured bedrock. The overall picture is greatly influenced by lack of spatial representativity and no proper boundary values due to the localisation of the boreholes or soil tubes, which means that data has to be spatially extrapolated. Moreover, the selected interpolation method strongly influence on the final outcome of the 3D-modell. Despite these reservations, the 3D-model gives a rough picture of how the observations relate in three dimensions.

In Figure 3-8, the spatial distributions of the four classes are visualised as coloured surfaces enclosing the observations belonging to each class. The yellow box comprises a rock volume vertically extended to a depth of 1,000 metres, and with a horizontal extent approximately corresponding to the local model area.

All observations classified as C_1 are located close to the ground surface. Class C_2, approximately corresponding to *dilute granitic groundwater* (cf Figure 3-5), reach slightly deeper levels. Class C_3, approximately corresponding to waters with marine influence show a vertical extent ranging from shallow levels to about 500 metres depth. Almost all observations belonging to class C_4, approximately corresponding to groundwater with significant shield brine influence, are located at a vertical depth of 500 metres or lower. There are two major exceptions from this pattern: the percussion drilled boreholes HFM11 and HFM12 located at the Eckarfjärden deformation zone show deep saline signatures (shield brine) at depths shallower than 100 metres. There is also an example within the tectonic lens /cf SKB 2005c/ shown by KFM01D, where the deep signature reach shallower levels of approximately 300–400 metres vertical depth. This interpolated lilac volume is disguised by a yellow surface in the visualisation as marked by a dashed line in the lower panel of Figure 3-8 (cf Figure 3-1).

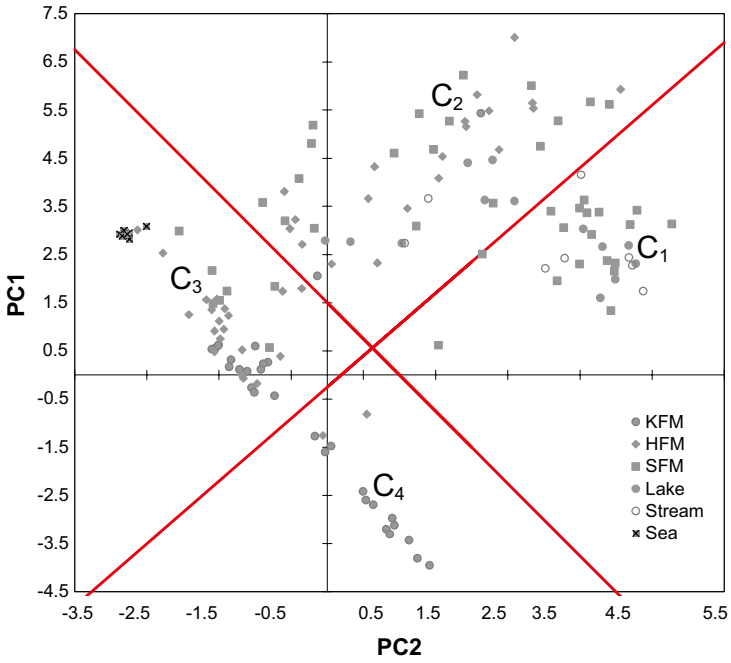

Figure 3-7. *The coarse classification of observations in the ion source model into four classes, C_1 to C_4.*

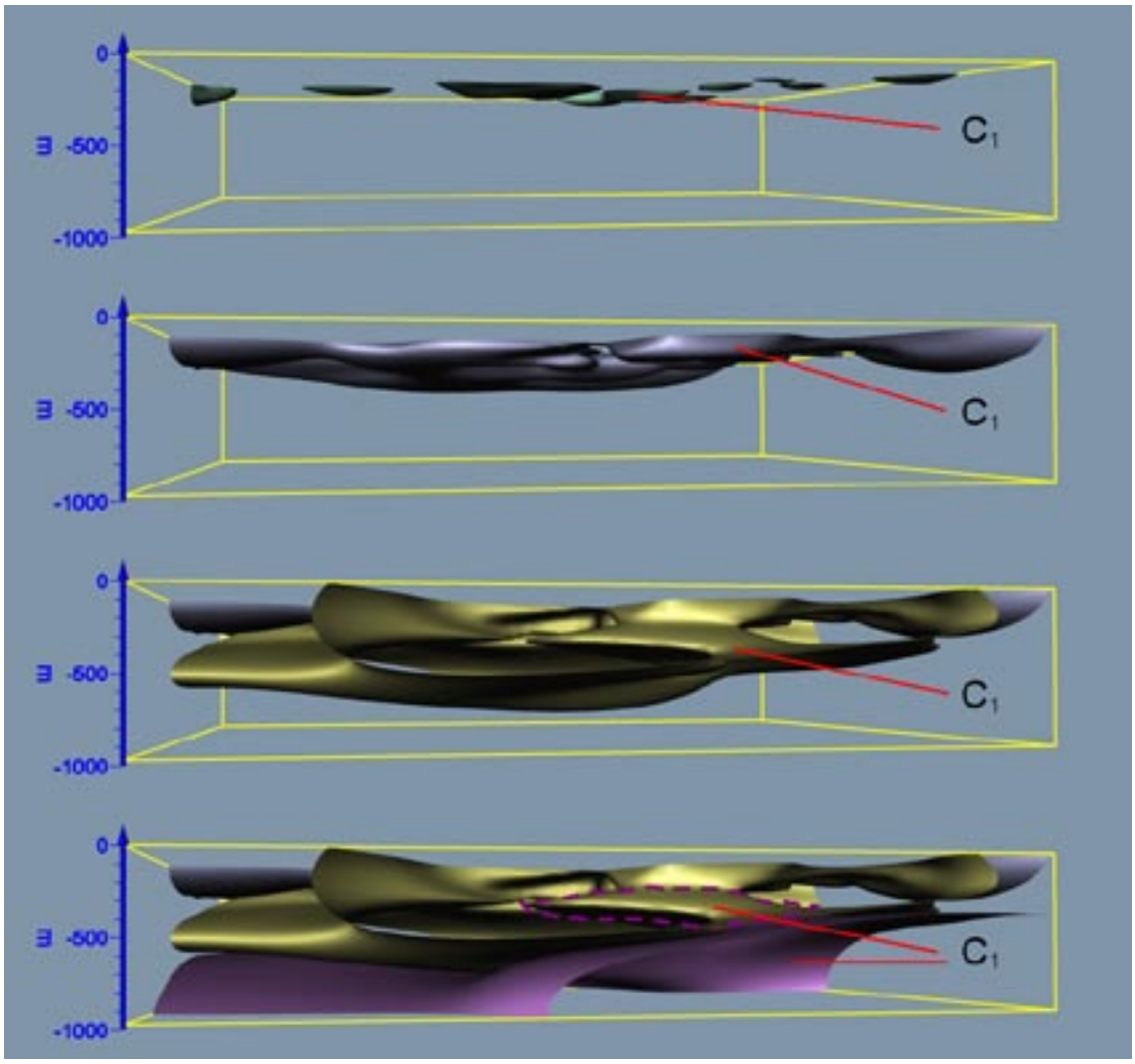

Figure 3-8. *Spatial distribution of the four classes defined in Figure 3-7. The view is seen from north, from a point below the Baltic Sea. The yellow box comprises a rock volume vertically extended to a depth of 1,000 metres, and with a horizontal extent approximately corresponding to the model area (cf Figure 2-2). According to dashed line in the lower panel, there is a portion of the lilac volume which is extending to shallower levels inside the yellow volume.*

In conclusion: the four different water type classes C_1 to C_4 show a plausible distribution in space, indicating that the hydrochemical discrimination into different groups by the ion source model probably reflects large scale structures in the bedrock.

3.2.6 Validation of the ion source model by independent parameters

Parameters as ^{3}H, $\delta^{18}O$, ^{2}H-excess and to some degree the absolute concentration of chloride may contain information on the sources of dissolved ions that is not used in the *ion source model*. By comparing the results of the model with the patterns shown by these parameters they may contribute to the understanding – a validation. Below, these parameters are projected onto the projection of the ion source model in Figure 3-9 (cf Figure 3-4). All parameters have been corrected for flushing water content according to the procedure described in Section 2.2.5.

When the selected parameters are projected onto the score plot of the ion source model (Figure 3-9) the following conclusions can be drawn:

- ^{3}H shows a scattered picture in the upper part of the plot, reflecting a clear influence from modern waters in these relatively shallow waters. The deeper waters with relict marine and shield brine influence (cf Figure 3-5), are as expected almost ^{3}H-free.
- $\delta^{18}O$ reflects the environment from which the water originate (cf Section 3.3). The scattered picture found in the upper half of the plot may reflect seasonal bias due to limited representativity in objects with few samples, in combination with effects of evaporation in lakes. The gradually lower values found in the "shield brine tail" probably reflects mixing with glacial water.
- The ^{2}H-excess parameter is a combined measure that reflects the deviation from the global meteoric water line (cf Section 3.3). ^{2}H deficiency may indicate that the water has undergone evaporation in a lake or sea (e.g. in the relict marine cluster), whereas excess may be an indication on shield brine influence (e.g. in the shield brine influenced tail).
- The concentration of chloride also shows an expected pattern, where the highest values are found towards depth in the "tail" influenced by shield brine.

The 3D-model in Figure 3-10 indicates that the highest chloride concentrations as well as the lowest $\delta^{18}O$ values are found within (below) the lilac volume, in turn indicating that this part of the rock corresponds to the tail of the ion source model influenced by shield brine. The distribution of ^{3}H also supports the interpretation of the ion source model.

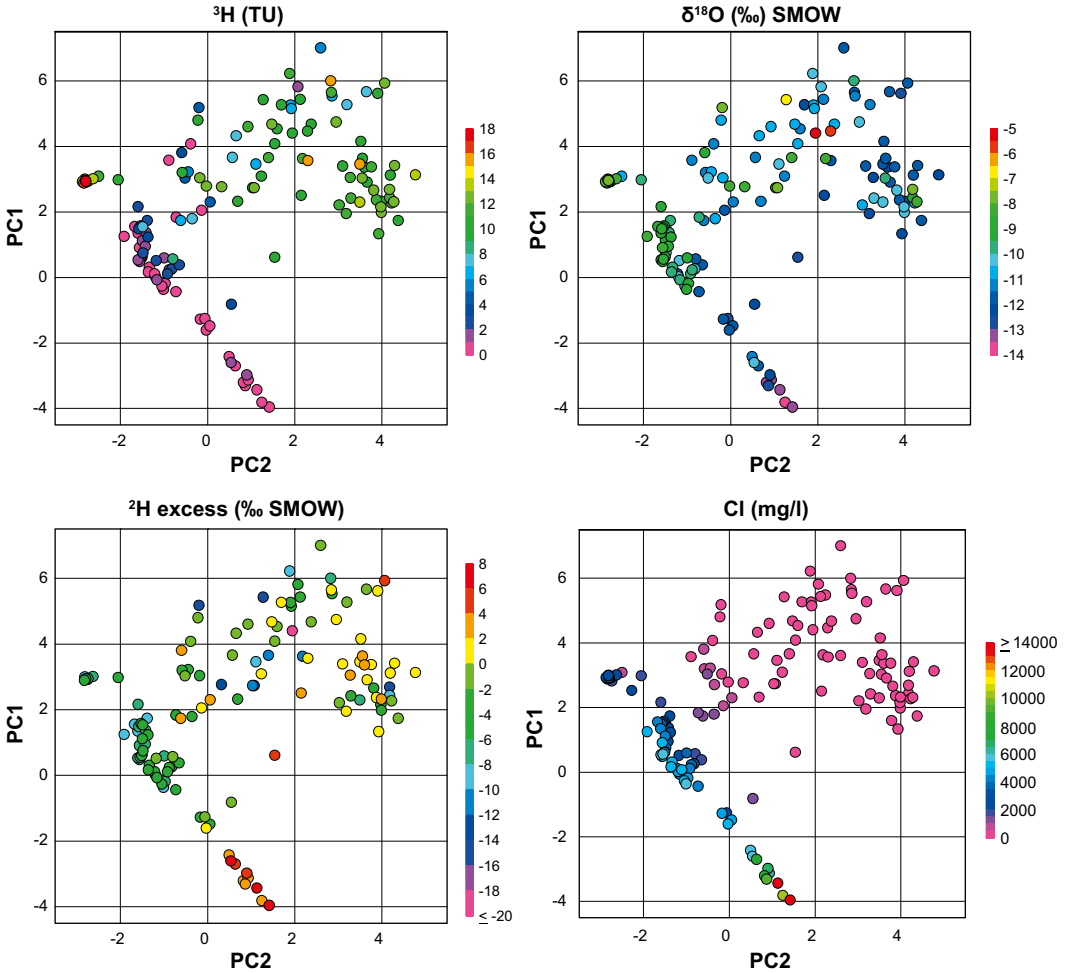

Figure 3-9. *^{3}H, $\delta^{18}O$, ^{2}H-excess and Cl projected onto the score plot of the ion source model. The first three parameters are fully independent of this model, whereas the concentration of chloride is included in the calculation of the relative compositional data on which the ion source model is based.*

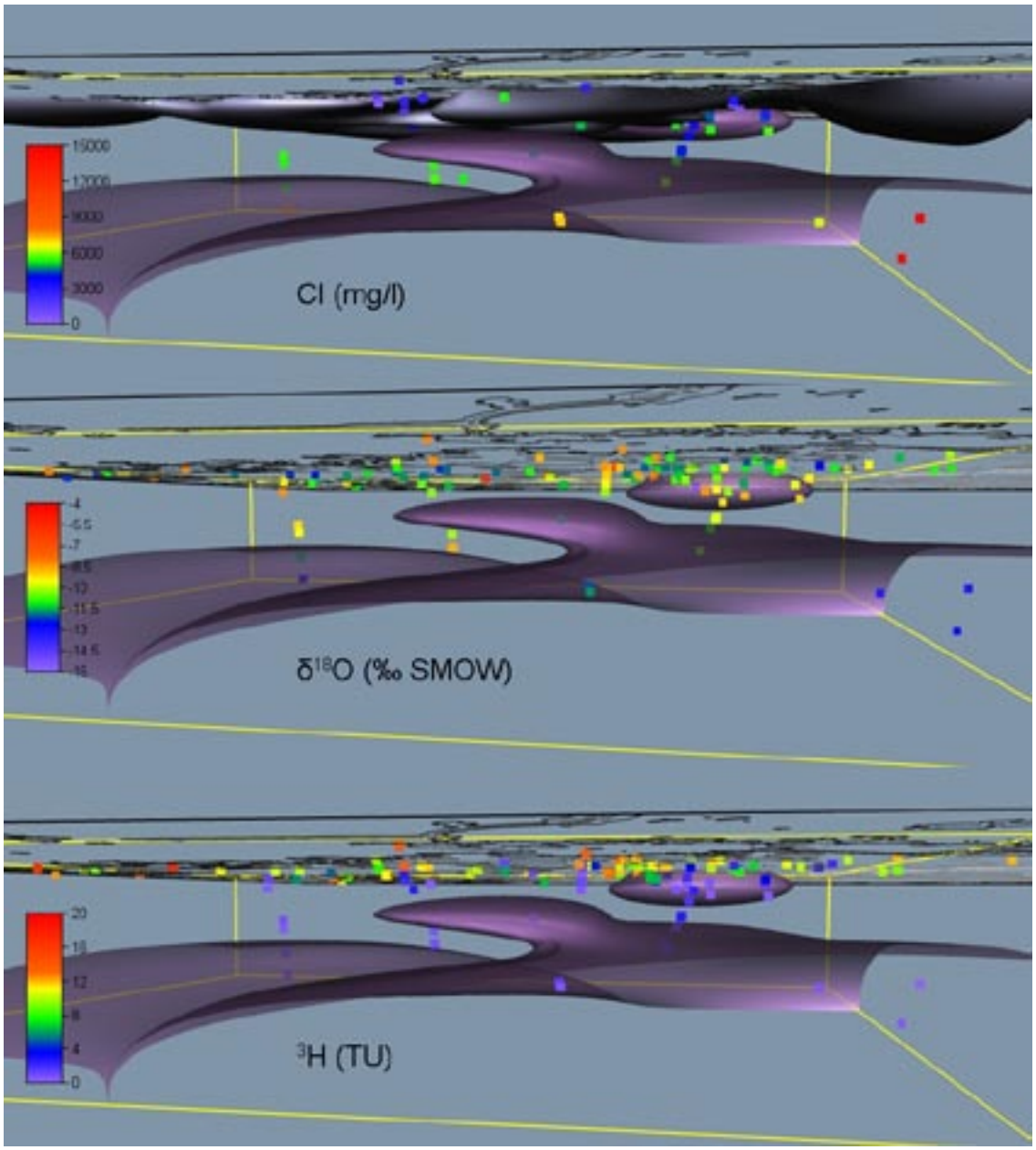

Figure 3-10. *3D-views seen from a point below Baltic Sea, north of the Forsmark area. The coloured volume encloses observations of class C_4 (shield brine influence according to the ion source model). Data from dataset B, with values corrected for flushing water content, are used in all three panels. The upper panel shows Cl concentrations, the middle panel $\delta^{18}O$ and the lower panel the ^3H-activity.*

3.2.7 Comparisons with results of the M3 mixing modell

In this section, the ion source model is compared to the results of the multivariate mixing model M3. These mixing calculations reflect the theoretical mixing proportions of the four pre-selected end-members; brine, Littorina Sea water, dilute granitic groundwater and glacial water. The M3-mixing model is thoroughly described in /Gómez et al. 2006/ and the mixing calculations presented here are based on datafreeze 2.2 /Laaksoharju (ed.) in prep./.

In Figure 3-11, the volumetric mixing proportions of each end-member are projected onto the ion source model. The models are consistent in the respect that the highest proportion of brine according to M3 is found in the shield brine tail of the ion source model, and the highest proportion of the Littorina end-member is found in the relict marine cluster. Also the dilute

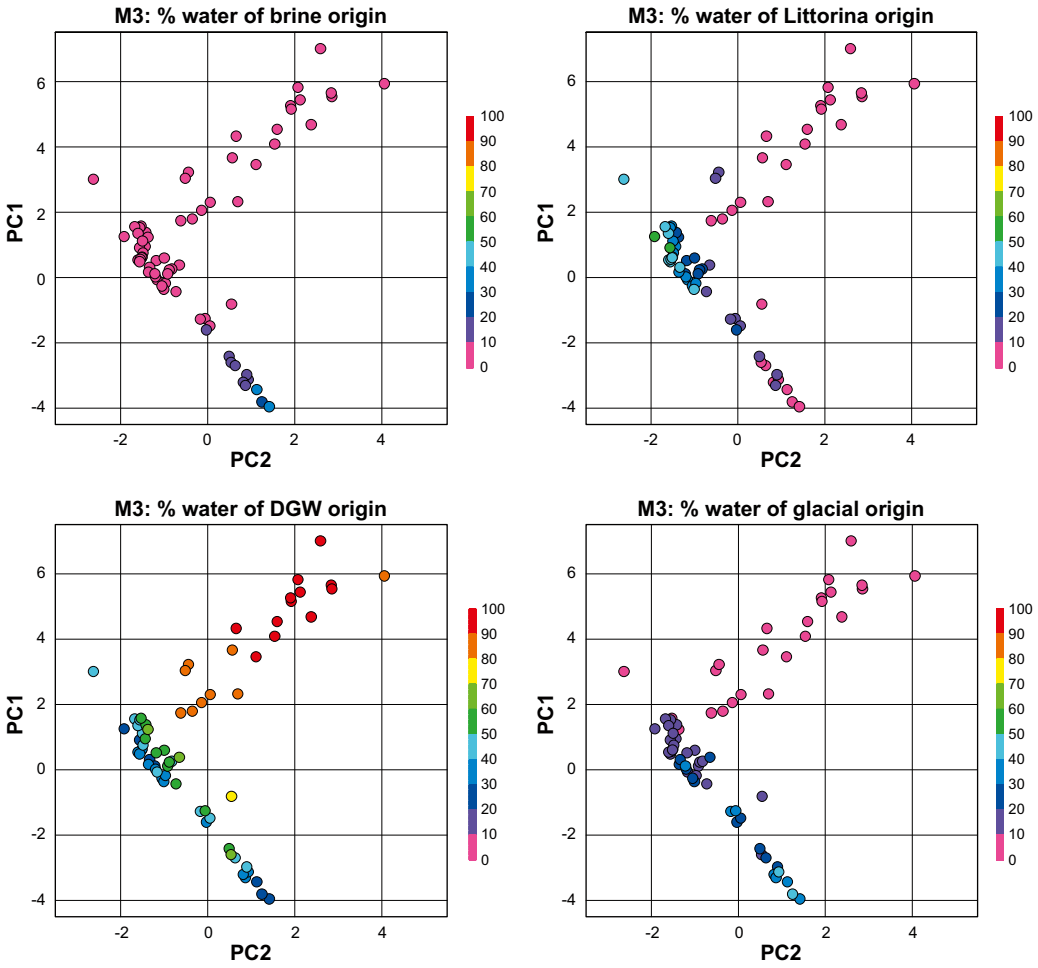

Figure 3-11. *The volumetric mixing proportions of each end-member, calculated by the multivariate mixing model M3, projected onto the score plot of the ion source model (cf Section 3.2.3, DGW = dilute granitic groundwater).*

granitic groundwater (DGW) end-member coincides in the two models. The glacial end-member contributes only to a minor extent to the supply of ions and is therefore not explicitly detected as an ion source in the ion source model.

When the fractions of chloride that originates from each of the end-members are calculated from the mixing proportions of the multivariate mixing model M3 and the theoretical concentrations of the end-members, the picture is radically changed (Figure 3-12).

The M3 model and the ion source model show, however, concordant results: both models indicates that samples classified into the *relict marine cluster* (cf Figure 3-5) contain an ion mixture of approximately equal amounts of Cl from marine and shield brine sources. As this mixture is also detected in some soil tubes and private wells, this may be an indication of shallow existence of a deep component including shield brine. Chloride originating from the end-members dilute granitic groundwater and glacial water contribute to a lesser extent to the chloride found in the deeper parts of the bedrock.

It should be noted that this calculation may violate the tolerance of the M3 model and may therefore lead in unreliable results when the volumetric proportions fall below 10%. This is especially the case for brine, where the original concentrations of the end-member is very high.

To summarize, there are no obvious contradictions between the ion source model and the M3 mixing model. Some results of the M3 model are in some respect contrary to the results of the

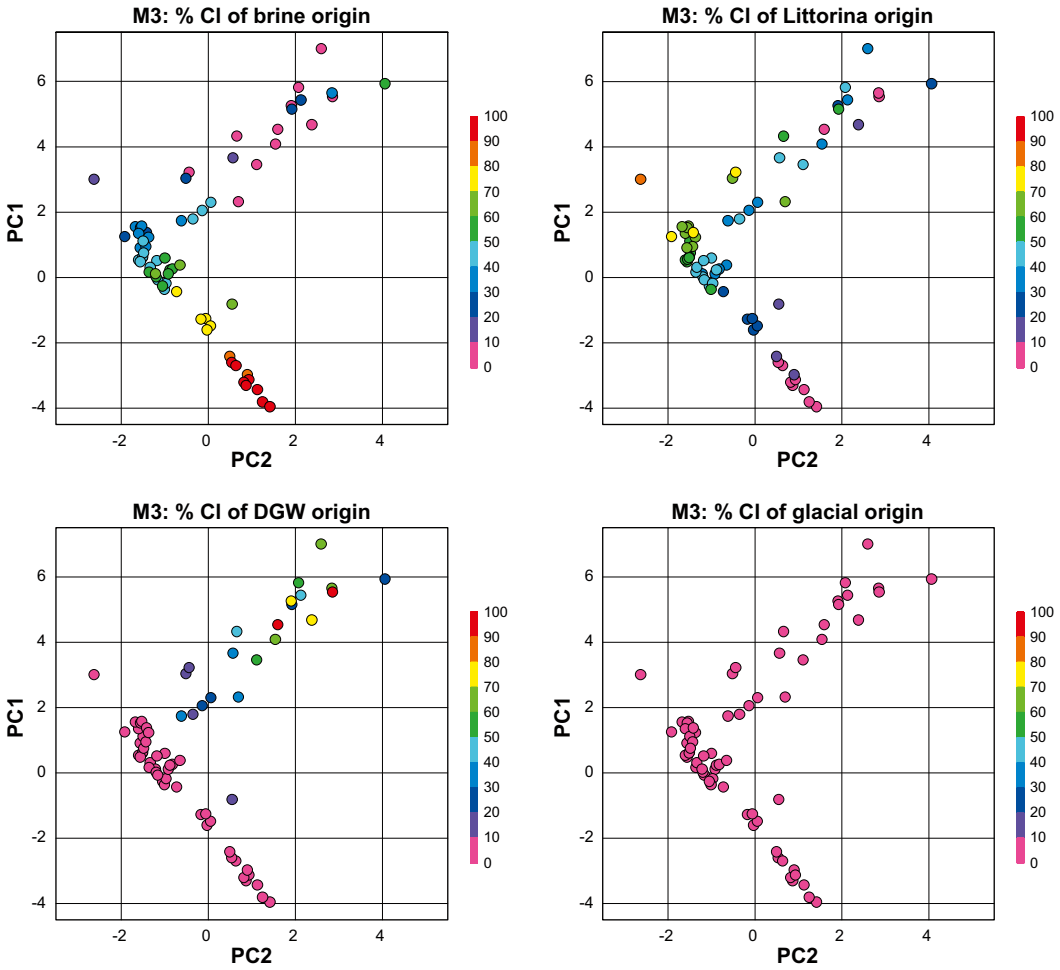

Figure 3-12. *The mass-fraction of chloride that originates from each end-member, calculated from the mixing proportions of the multivariate M3 mixing model and the theoretical chloride concentrations of the end-members, projected onto the score plot of the ion source model (cf Section 3.2.3).*

ion source model, for example the existence of dilute granitic groundwater at all depth levels (cf DGW in Figure 3-11, lower left panel), including the deepest KFM borehole sections with a clear signature of shield brine.

3.3 Exploring the origin of water – the solvent

This section deals with the origin of water, the solvent, reflected by the isotopes ^{2}H and ^{18}O, contrary to previous Section 3.2 where the origin of major ions (e.g. Ca, Mg, Na, K, Cl, SO_4 and HCO_3) was explored. Section 3.4 deals with the situation when ions meet water and form a concentration.

3.3.1 Global and local meteoric water lines

The origin of water may be traced from stable or radiogenic isotopes of the elements that form the water molecule: hydrogen and oxygen. The relation between the stable isotopes ^{2}H and ^{18}O varies depending on different processes influencing the water cycle /Clark and Fritz 1997/. The fraction of ^{2}H and ^{18}O, as well as the activity of the radiogenic ^{3}H isotope, are routinely measured in the SKB site investigations.

Globally, the relationship between ^{2}H and ^{18}O plots along the so called *global meteoric water line*, GMWL (cf Section 2.3.3). Due to different local conditions, the local precipitation deviates more or less from the global water line. All observations including ^{2}H and ^{18}O measurements from the Forsmark area are plotted in Figure 3-13, along with the GMWL.

The local meteoric water line for the Forsmark area was fitted to the 25 observations in precipitation by least squares regression. LMWL deviates slightly from GMWL by the equation of $\delta^{2}H = 7.2\ \delta^{18}O + 0.24$ (cf GMWL in Section 2.3.3).

Many observations from surface waters deviate from the LMWL due to fractionation by evaporation. Observations from Lake Eckarfjärden and Lake Bolundsfjärden form coinciding trend lines, probably originating from a point corresponding to the average composition in precipitation. Observations from sea water show a similar deviation.

The relative location along the evaporation line (based on the average composition in each lake) can be assumed to reflect the water retention time (i.e. the proportion between lake volume and catchment area). Consequently, the largest lakes in the Forsmark area, Eckarfjärden (PL117) and Bolundsfjärden (PL107), plot far from the LMWL, whereas very small lakes with large catchments, e.g. Labboträsket (PL074) and Gunnarsbo-Lillfjärden (PL087), plot close to the LMWL (Figure 3-14). Observations from Lake Fiskarfjärden (PL127 and PL135) also indicate a rather long retention time, but the picture is unclear as the average composition of this lake is based on fewer observations, sampled at two different locations in the lake.

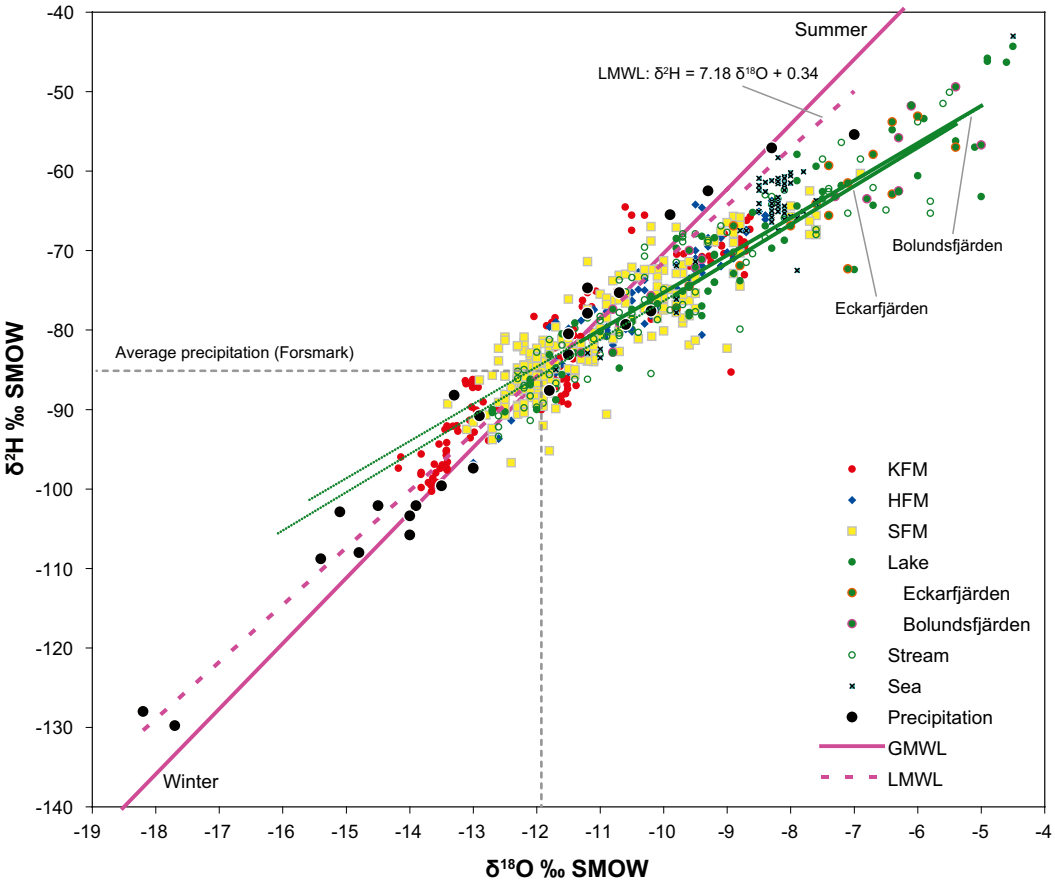

Figure 3-13. *All individual observations including ^{2}H and ^{18}O measurements from the Forsmark area, plotted together with the global meteoric water line, GMWL. The local meteoric water line, LMWL, based on all observations in precipitation, is also included. The average composition in precipitation is estimated from the intersection between LMWL and the evaporation trends of the lakes, which coincide with the mean composition of a cluster of soil tubes that are centred on the LMWL.*

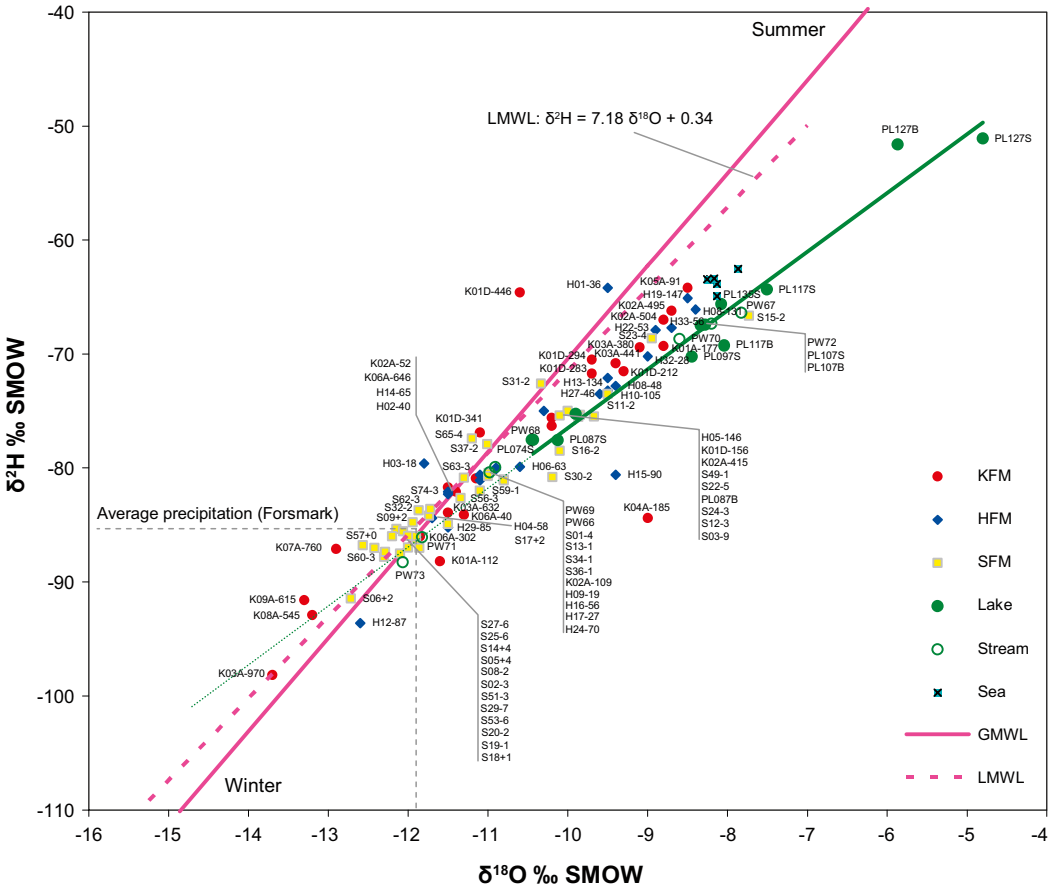

Figure 3-14. *Mean values per object for ^{2}H and ^{18}O, plotted together with the global and local meteoric water lines (GMWL and LMWL, respectively). Only bedrock samples from dataset C are included (cf Section 2.2.4). The green line indicates the 'evaporation line', based on mean values per lake.*

Most soil tubes plot in a cluster centred on the LMWL, indicating that the water composition in shallow groundwater reflects the local average precipitation. A few soil tubes plot along the evaporation trend (e.g. S11, S12, S23 and S15), which indicates an influence of either sea water or a fresh surface water component. Observations from the bedrock (HFM, KFM) show a more scattered picture, indicating a more complex origin of the water found at deeper levels. There are examples of percussion boreholes as well as cored boreholes that plot in the lower left region of the LMWL, probably reflecting water components of glacial origin. Many of the shallower observations in the bedrock coincide with the evaporation trend, and may thus indicate water components of (relict) marine origin, e.g. Littorina seawater. The fact that some of the soil tubes also plot in this region of the figure indicates that also these objects may be influenced by relict marine seawater. Deviations from the meteoric water lines are further explored in Section 3.3.2.

3.3.2 The water origin model

Due to the close correlation between $\delta^{2}H$ and $\delta^{18}O$, most points line up along LMWL. This means that the standard cross plot is less suitable for exploring deviations from the meteoric water lines. In order to facilitate interpretations of this type of deviation, the ^{2}H-excess was calculated (i.e. the deviation from the GMWL, here defined as $^{2}H_{excess} = \delta^{2}H - 8.2 \times \delta^{18}O - 11.3$). In Figure 3-15, the $^{2}H_{excess}$ parameter is projected onto the ion source model (cf Section 3.2.3) in order to facilitate comparisons among groundwater types identified by the composition of major ions.

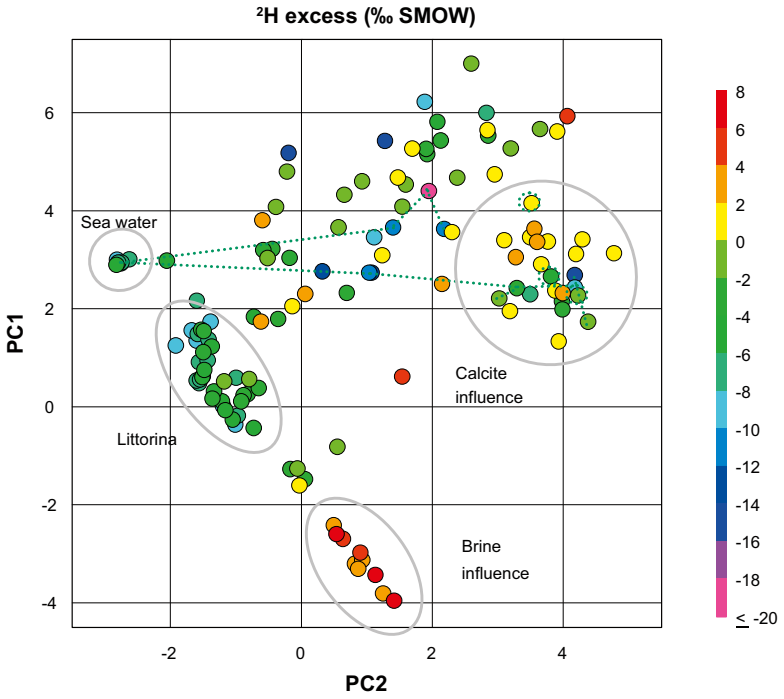

Figure 3-15. *The ^{2}H-excess parameter projected onto the ion source model (cf Section 3.2.3). $^{2}H_{excess}$, which is defined by the equation $^{2}H_{excess} = \delta^{2}H - 8.2 \times \delta^{18}O - 11.3$, represents the vertical deviation from the GMWL. Data from the bedrock comprise dataset B (cf Section 2.2.4) corrected for flushing water content according to the procedure described in Section 2.2.5. The green dashed line mark the flow-path of the surface water from the Lake Eckarfjärden catchment on the right side to the Baltic Sea to the left (only surface samples from lakes are shown in this figure).*

In order to make deviations from GMWL more visible, ^{2}H and ^{18}O may also be transformed and projected into a coordinate system where one axis coincides with the GMWL and the other represent the perpendicular deviation from the GMWL. This type of plot enlarges the area of interest by rotating the coordinate system displayed by the blue coloured box in Figure 3-16. In this figure is also the literature value of Canadian Shield brine marked /Clark and Fritz 1997/.

Two versions of the transformed GMWL-plot, *the water origin model*, are shown in Figure 3-17. Data from shallow groundwater and surface water (soil tubes, private wells and surface waters) are equal in both versions, but the reference data from the bedrock differ between the two versions; in the upper plot, only ”representative” individual samples of dataset C is selected, i.e. a conservative selection. The lower plot is based on dataset B, which includes both a few more depth levels from the cored boreholes and more observations from percussion boreholes. These data are also corrected for flushing water content (cf Section 2.2.5). When several samples per object and depth level were available, the composition is in both versions represented by mean values.

The patterns that appear in *the water origin model* presented in Figure 3-17 may be affected by a number of uncertainties. The spread around LMWL shown by the soil tubes in the encircled “modern meteoric cluster” may represent a rough estimate of the accuracy of the ^{2}H and ^{18}O measurements. Contamination by flushing water during drilling, and uncontrolled mixing due to shortcuts through fractures, will contribute to uncertainties in the model. In the lower plot of Figure 3-17, the bias due to mixing with uranine labelled flushing water in samples from the cored boreholes is roughly compensated for (cf Section 2.2.5), and this may give a more correct picture.

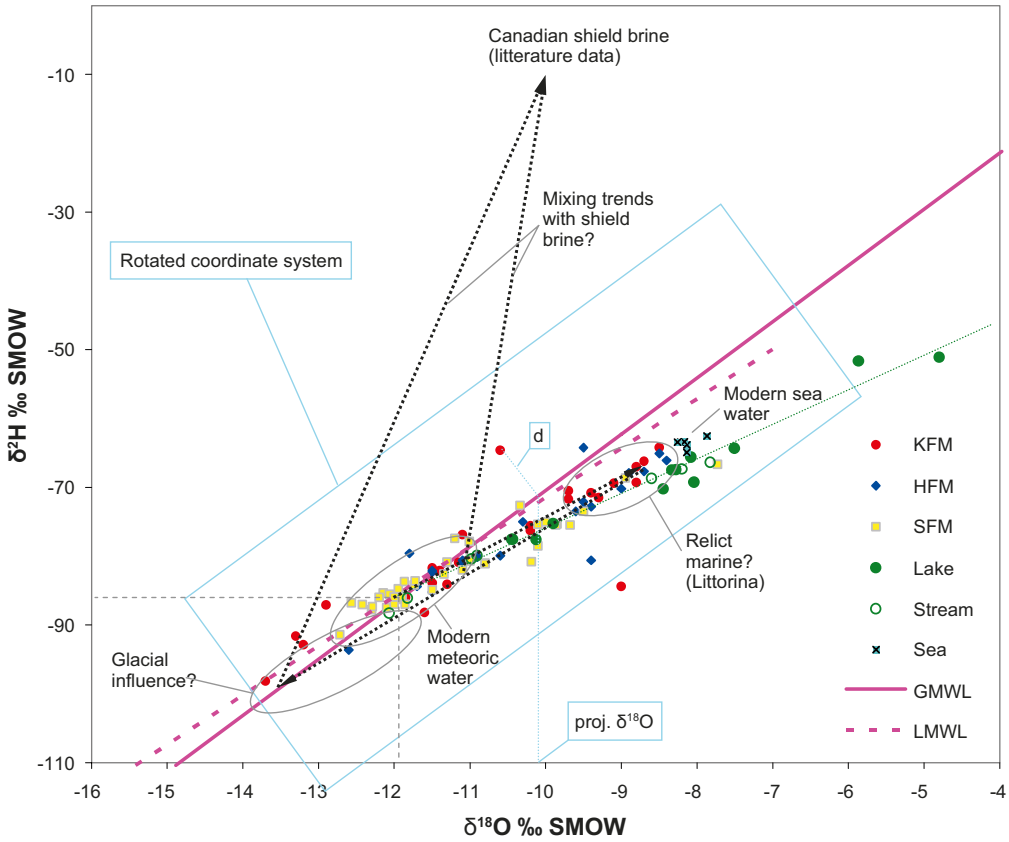

Figure 3-16. *Schematic figure showing the principles behind the rotated coordinate systems used in Figure 3-17. The perpendicular deviation from GMWL is marked by a "d", and the $\delta^{18}O$-value corresponding to a point perpendicularly projected on the GMWL is marked "proj. $\delta^{18}O$". A hypothetical mixing trend towards depth, from meteoric waters to the literature value of Canadian Shield brine, is marked by dashed black lines.*

Different possible water types, as well as hypothetical mixing lines, have been marked in Figure 3-17. The mixing lines form a hypothesis of the evolution towards depth from modern meteoric water in the surface system to water influenced by shield brine in samples from the deeper parts.

It should be noted that adjacent objects in the plots (i.e. objects with a similar composition of ^{2}H and ^{18}O) may belong to completely different water regimes, which may be separated by ^{3}H or other parameters. The overlap between the cluster consisting of soil tubes with modern meteoric water, and the deeper sections of the cored boreholes influenced by shield brine, is an example of two vertically separated water regimes that show similar ^{2}H and ^{18}O signatures. Another example is a mixture between relict marine and glacial components that mat be interpreted as meteoric water. When chloride, lithium and the Ca/Sr ratio is projected onto the pattern of Figure 3-17, the difference between these groups is apparent (see Figure 3-18).

The hypothesis formed by the dashed mixing lines indicates that the shallow meteoric water mix with an underlying water body of principally marine origin (i.e. there is a clear evaporation signature close to modern sea water). Further down, the mixture dominated by the marine signature is gradually influenced by an increasing glacial signature, marked by the near horizontal arrow pointing leftwards. At greater depths, the glacial signature is shifted towards a possible shield brine signature characterised by high deuterium excess (cf literature value of Canadian Shield brine in Figure 3-16). Alternatively, a possible explanation to this shift could, at least to some extent, be due to an input of enriched ^{2}H originating from oxidation of methane.

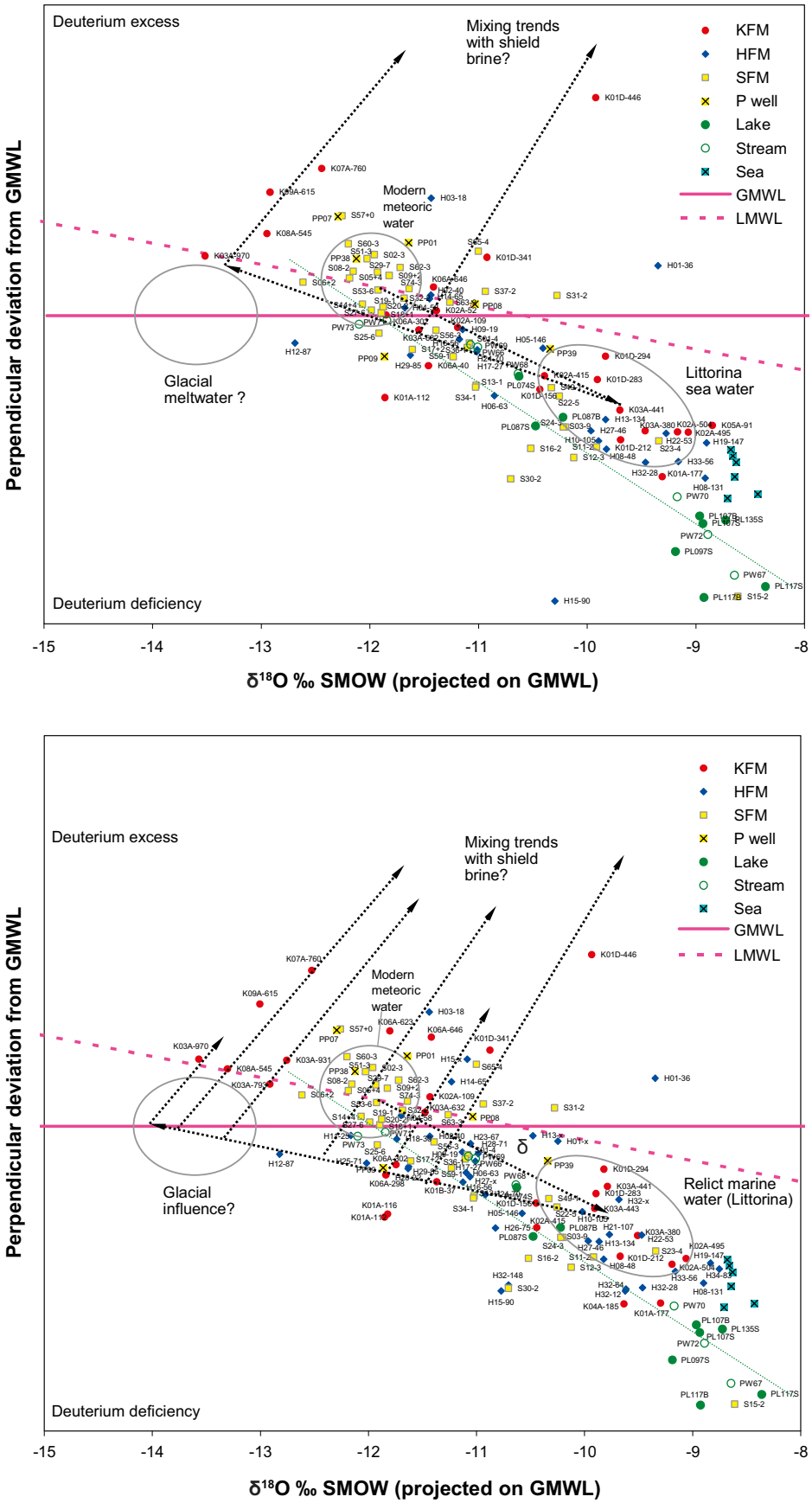

Figure 3-17. *A transformation of the traditional GMWL plot (see explanation in Figure 3-16). Data from the bedrock in the upper plot is based on dataset C, representative data (cf Section 2.2.4) and the lower plot is based on dataset B (values corrected for flushing water content). See text for an explanation of the hypothetical mixing lines.*

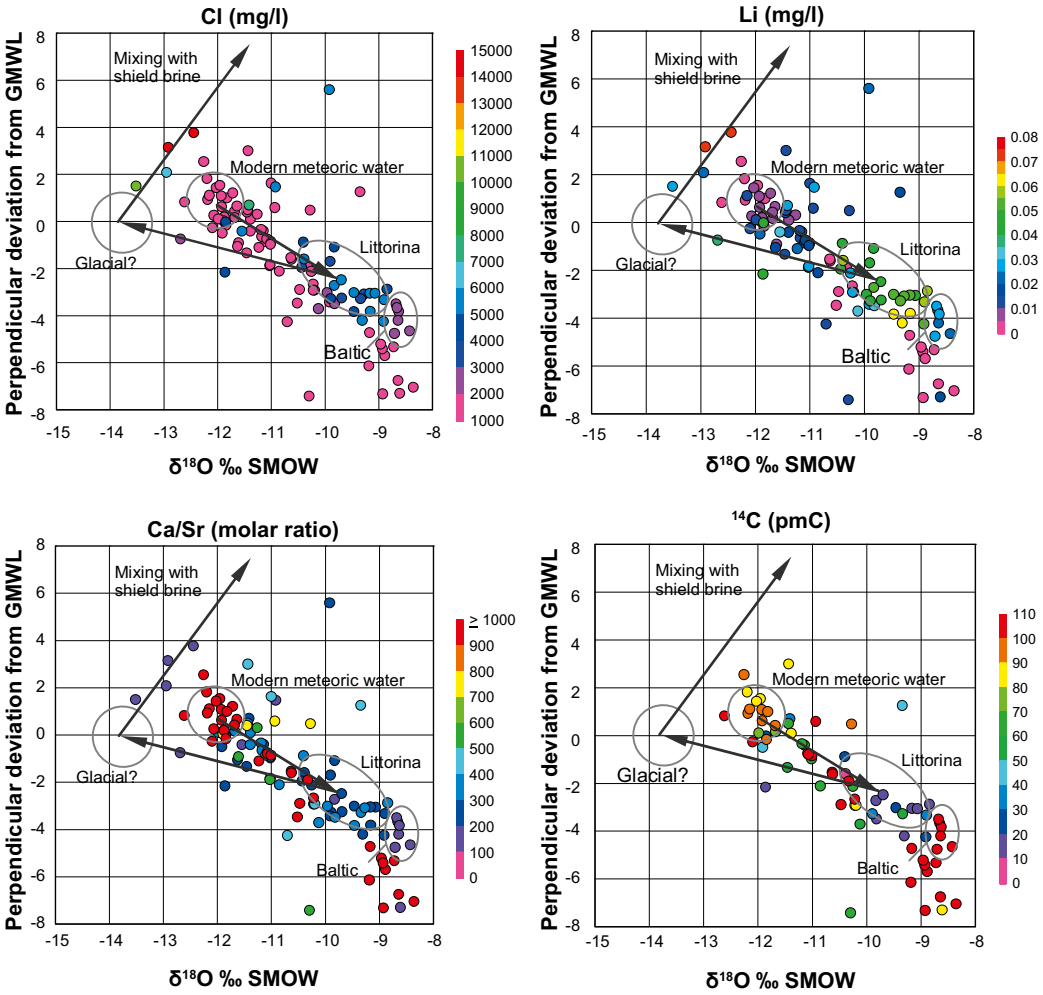

Figure 3-18. *Concentrations of Cl, Li, the Ca/Sr ratio and ^{14}C activity, projected on the pattern of the lower plot in Figure 3-17. Concentrations are not corrected for flushing water content.*

The multitude of hypothetical mixing lines towards shield brine suggests that the water component possibly influenced by shield brine mix with different water types (i.e. the possible mixing trend towards shield brine intersects the relict marine – glacial mixing line at different sections). This gradient of mixing lines may reflect a structural phenomenon, probably related to differing conditions in the lens, in the surrounding rock and in the fracture zones. The rightmost mixing lines probably reflects the conditions in the lens (e.g. KFM01D) and the lines to the left the fracture zones (e.g. KFM03A, KFM07A, KFM08A, KFM09A).

An implication of this interpretation is that the relict marine component, which only to some extent is influenced by glacial water, mix with the deep saline (shield brine) component at shallower depths inside the lens than outside, which may indicate rather stagnant conditions, less influenced by glacial flushing. It has been proposed by /Laaksoharju (ed.) in prep./ that this stagnant water represent an *old meteoric* water type, rather than a marine – glacial mixture. The presence of the glacial signature in the fracture zones, even at greater depths, probably reflects the deep penetration of glacial water in the fractured rock due to the flushing during glaciations (cf conceptual model in Section 8.2).

A few shallow objects contain water with dominantly (relict) marine origin, e.g. S11, S12, and S23. The private well PFM0009 probably also contain relict marine water, possibly with a higher proportion of a glacial component. Two percussion boreholes located at the Eckarfjärden deformation zone (HFM11, 12) show significant glacial influence, possibly mixed with a meteoric component which is indicated by the low ionic strength.

3.3.3 Detailed evaluation of four lakes in the Forsmark area

In this section, the isotopic signatures in water from four soil tubes located below lakes are explored in detail. Individual observations in the soil tubes are compared with observations in the overlying surface water, as well as with adjacent soil tubes and percussion boreholes. The composition of modern sea water is included in all figures as a reference.

Samples from soil tubes below the four lakes show rather dissimilar patterns in the relation between ^{2}H and ^{18}O. This may indicate that water found in the soil tubes below the different lakes have different origins. The periodical samplings in each soil tube show little variation, indicating rather stable conditions with little influence from the seasonal fluctuations of ^{2}H and ^{18}O. When evaluating these patterns it should be held in mind that contamination by surface waters during installation of the soil tubes may influence the measurements.

The evaporation signature (cf Figure 3-14) in lake water should be more pronounced the longer residence time of a lake is. Isotopic composition in the surface water of Lake Eckarfjärden shows a clear evaporation signature. Observations from the soil tube SFM0015, located in till below the sediments in Lake Eckarfjärden, show small fluctuations and a mean value centred at the range observed in lake water. This may be an indication that the water in the soil tube originates from the lake, or alternatively has a marine origin (the position of sea water in Figure 3-13 coincides with that of SFM0015). However, the chloride concentration in SFM0015 of about 300 mg/L contradicts the latter explanation. Soil tubes and percussion boreholes close to the lake deviate from SFM0015 by showing mainly meteoric signatures. Accordingly, the lake water signatures observed in SFM0015 may indicate that Lake Eckarfjärden and its near surroundings may serve as a recharge area. According to hydrological pressure head measurements in soil tubes below and around Lake Eckarfjärden, recharge conditions may prevail during dry periods (e.g. during the summers of 2003 and 2006), but that discharge conditions prevail most of the time /Werner et al. 2007/.

The isotopic composition in Lake Bolundsfjärden shows a similar pattern to that in Lake Eckarfjärden, indicating similar conditions. Contrary to the situation in Lake Eckarfjärden, the high chloride concentrations in the soil tube SFM0023 (4,000 mg/L) support the hypothesis of marine origin of the shallow groundwater, instead of recharging lake water. The nearby percussion borehole HFM32 indicates a similar composition even at deeper levels in this area, see Figure 3-19.

SFM0022, located below Lake Fiskarfjärden show a signature different from both the surface water and sea water, indicating a dominating meteoric origin. Lake Gällsboträsket differs from the other studied lakes by showing a weaker evaporation signature. This is most probable an effect of the short residence time in this small lake. The signature found in SFM0012 is similar to the signature of SFM0023, but with a slightly stronger influence of meteoric or surface water.

3.4 Exploring concentration trends and mixtures

A concentration is the amount of dissolved ions (or other compounds) per unit volume of water. When either ions or water are supplied (or removed) the concentration is altered. The concentration/mixing model described in this section may be seen as the product of the previous models describing the origin of ions and the origin of water. This model is also a complement to the other models as it provides information on the absolute contents of ions and may reveal possible mixing trends of different water types.

3.4.1 The mixing model – version 1

Similar to procedure described for the *ion source model* in Section 3.2, a standard principal component analysis, PCA, (cf Section 2.3.10) was applied on dataset A (i.e. only flushing water corrected data from the bedrock was selected, cf Section 2.2.4), but with the difference

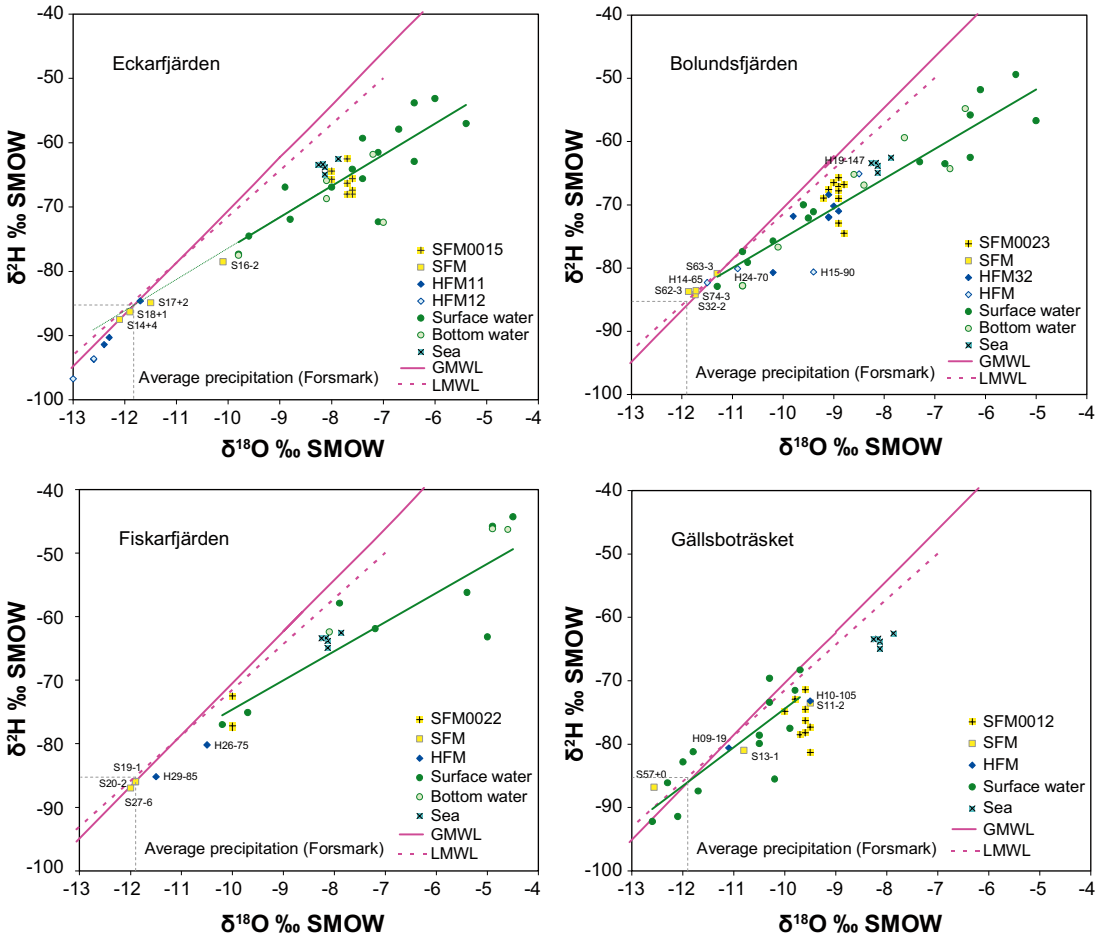

Figure 3-19. *Detailed explorations of the isotopic signatures (^{2}H and ^{18}O) in lake water and soil tubes below Lake Eckarfjärden, Bolundsfjärden, Fiskarfjärden and Gällsboträsket.*

that the calibration was conducted on absolute concentrations of major elements rather than relative compositional data. The two first principal components comprise about 81% of the total variation of the bedrock groundwater data (PC1 50%, PC2 31%). As a second step, flushing water corrected data from dataset B, as well as surface water and shallow groundwater data was projected onto the PCA-model, forming the *mixing model* in Figure 3-20.

The first component (vertical direction in Figure 3-20) reflects the contrast between Cl and HCO_3 (see cut-in loading plot, cf explanation in Section 2.3.10). This gradient range from nearly Cl-free, HCO_3-dominated surface waters, to the Cl-rich deep groundwater influenced by shield brine. Modern and relict marine groundwater forms an intermediate group with respect to Cl. Several cations (Ca, Na, Li and Sr) and anions (Br) follow this chloride pattern with higher concentrations at deeper levels.

The second component (horizontal direction in Figure 3-20) distinguishes groundwater of marine origin from water from the surface system as well as from deeper groundwater types. The strongest influence on this component is shown by marine ions as Mg, K and SO_4.

Visualisations based on the *mixing model* may be similar to the multivariate mixing model M3 /Gómez et al. 2006/, as the models share data and are based on similar statistical techniques. There are, however, important differences: while the mixing model is based solely on concentrations, the M3 mixing model also include isotope data reflecting the origin of water, which may lead to different appearance of the 2D visualisations depending on the rotation in hyperspace and which components are selected.

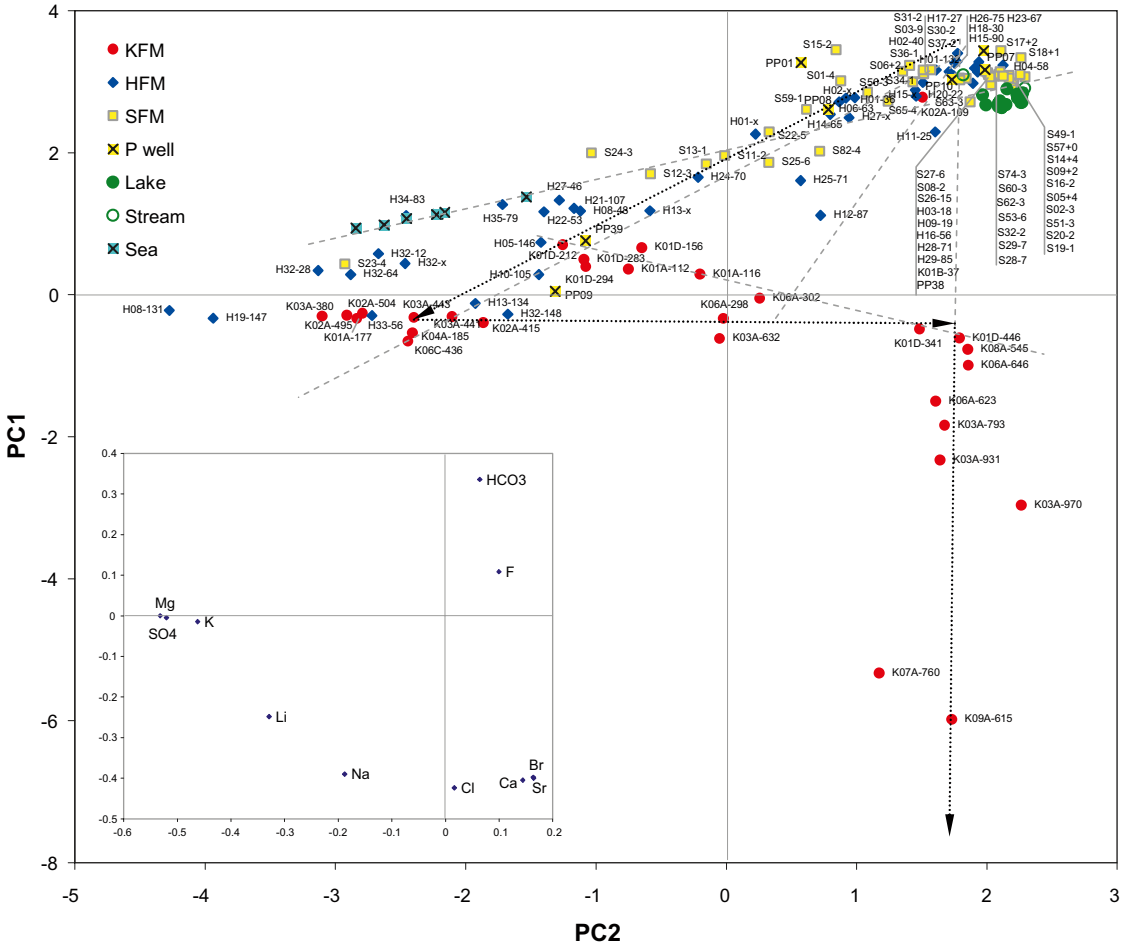

Figure 3-20. *The multivariate mixing model version 1 reflecting the main variation patterns among major elements (Na, K, Mg, Ca, Sr, Li, Cl, SO_4, HCO_3, Br, F). The first two components comprise 81% of the total variation (PC1 50%, PC2 31%). Dashed lines show hypothetical mixing trends and dotted arrows the hypothetical general groundwater evolution towards depth.*

3.4.2 The mixing model – version 2

The first version of the mixing model includes the non-conservative parameters HCO_3 and SO_4. Measurements of HCO_3 show a higher degree of uncertainty due to e.g. degassing during sampling, whereas SO_4 is influenced by various redox reactions. An alternative mixing model with these parameters excluded is shown in the upper panel of Figure 3-21. The calibration procedure followed the same scheme as was outlined for version 1, but with the following parameters included: Na, K, Mg, Ca, Sr, Li, Cl and Br.

The two first principal components of the version 2 model comprises as much as 92% of the total variation of the bedrock groundwater data (PC1 61%, PC2 31%), compared to 81% in the version 1 model. This marked improvement, together with an unchanged major pattern, implies that the deselected parameters HCO_3 and SO_4 mainly add "noise" and have minor importance for the overall pattern of the mixing model. These parameters are however valuable in other contexts, e.g. in evaluating the importance of calcite dissolution in shallow waters and tracing microbial sulphate reduction.

In the lower panel of Figure 3-20, the mixing model version 2 is compared to the end-members identified by the M3 methodology /Gómez et al. 2006/. Both end-members of marine origin, Littorina Sea Water (labelled M3-Li) and Baltic Sea Water (M3-Bal), plot on the marine mixing line MX1. The brine end-member, sampled in the deepest cored borehole in the Laxemar area, plots in the prolongation of the mixing line MX3. End-members of weaker ionic strength, i.e.

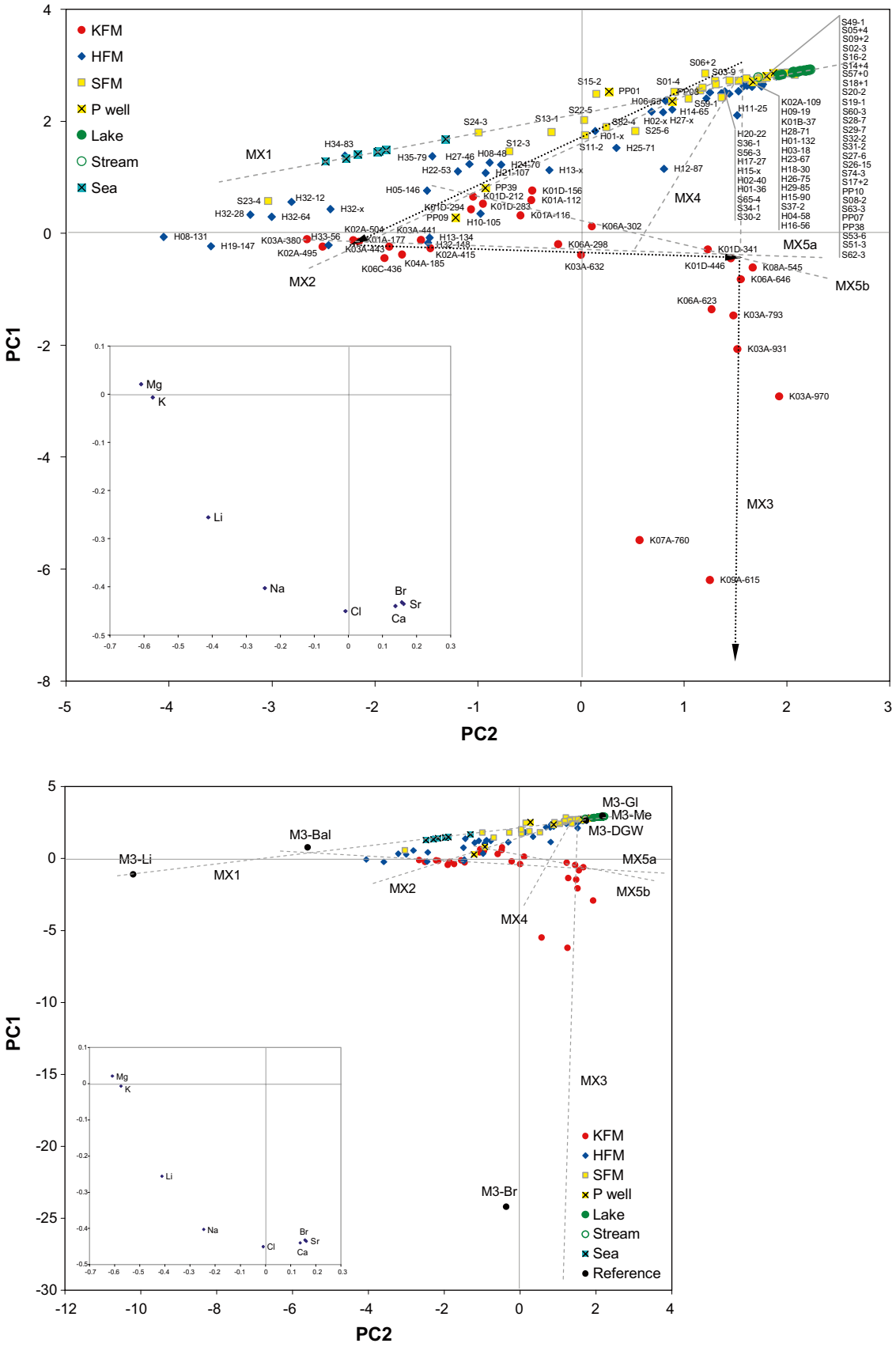

Figure 3-21. *The multivariate mixing model version 2, reflecting the main variation patterns among selected major elements (Na, K, Mg, Ca, Sr, Li, Cl, Br). The first two components comprise 92% of the total variation (PC1 61%, PC2 31%). In the overview (lower panel), M3 end-members have been introduced for comparison.*

dilute granitic groundwater (M3-DGW), glacial water (M3-Gl) and meteoric water (M3-Met), all plot in the "weak corner", together with most waters from the surface system (soil tubes and fresh surface water).

The relative positions of the end-members from the M3 model and the patterns of the mixing model are concordant, which is expected as they are based on the same data. The introduction of the M3 end-members may first of all be seen as an orientation of the relation between the two models.

3.4.3 Interpretation of the mixing model

An interpretation of the *mixing model* version 2 is shown in Figure 3-22. Hypothetical water types, also identified in the previous visualisations, are encircled in the figure, together with mixing lines showing hypothetical mixing scenarios. Patterns in the model may also reflect processes which have altered the water composition, e.g. ion exchange. The interpretation below assumes that mixing is the main process forming the water types in the Forsmark area.

There are six major hypothetical water types marked in the plot: 1) Modern seawater in the Forsmark area, 2) a pre-modern saline sea water (e.g. Littorina), 3) groundwater significantly influenced by relict seawater, 4) dilute granitic groundwater (DGW), 5) fresh surface water and 6) deep saline groundwater significantly influenced by shield brine. Seven mixing lines, denoted MX1 to MX7, mark the hypothetical evolution between different water types (MX1 to MX3 are relatively intuitive, whereas MX4 to MX7 are more speculative).

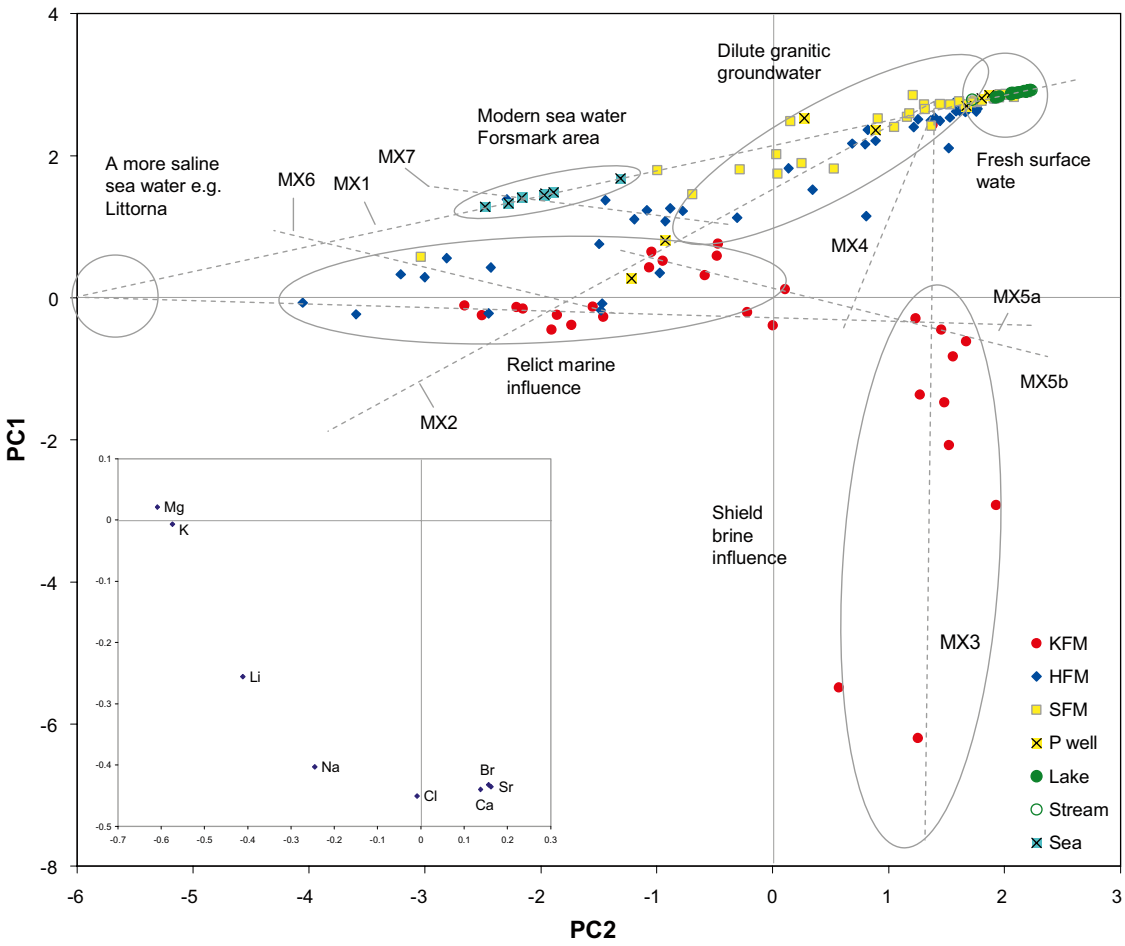

Figure 3-22. *Interpretation of the mixing model (cf Figure 3-21, version 2). Hypothetical groundwater types are encircled, and hypothetical mixing trends are marked by dashed lines.*

- Mixing line MX1, indicate a gradient ranging from fresh surface waters to present sea water in the Forsmark area. In the prolongation of this *marine trend*, more saline sea water, e.g. Littorina, plots.
- MX2 may represent a gradient ranging from fresh surface waters of low ionic strength to a groundwater significantly influenced by relict sea water. Many percussion boreholes and a few soil tubes plot along this line, indicating a varying degree of relict marine influence.
- MX3 is a hypothetical line which connects a few deep saline observations influenced by shield brine. In the approximate prolongation of this mixing line (see Figure 3-21), the deepest and most saline cored borehole in the Laxemar area plots. When this hypothetical line is extended upwards, this line meets the cluster representing waters of low ionic strength (dilute granitic groundwater, glacial and meteoric water).
- MX4 is a hypothetical line explaining the chemical composition in two percussion boreholes located at the Eckarfjärden deformation zone (HFM11 and HFM12). MX4 may represent mixing between dilute freshwater and a groundwater component significantly influenced by shield brine.
- The horizontal trend MX5a is ranging from groundwater with typical marine signatures towards deep saline groundwater significantly influenced by shield brine. Observations along this almost horizontal trend line show a nearly constant Cl concentration (and ion strength), but a major cation shift from Mg, K and Na on the left side to Ca on the right side. The observed pattern may be explained by an equilibrium process where marine influenced groundwater have reached density equilibrium with a deeper groundwater type /cf SKB 2006/.
- MX5b is an alternative to MX5a starting from a point on MX2 that corresponds to a slightly more diluted relict marine groundwater. This hypothetical trend line connects observations from KFM01D and KFM06A, located on MX2, with the upper section of MX3. A possible explanation to the pattern is that different slopes of MX5 reflect a structural phenomena, perhaps a (gradual) difference between the lens /Olofsson et al. 2007/ and the surrounding rock and fracture zones. Both KFM01D and KFM06A are located within the lens, in contrast to e.g. KFM03A and KFM04A that plot along MX5a.
- MX6 reflects a hypothetical trend displayed by the percussion borehole HFM32, located below Lake Bolundsfjärden. Also the soil tube SFM0023, located in till below the sediments of the same lake, plot along this line. This line intersects with the marine mixing line, MX1, at a point where ion concentrations are slightly higher than in the present brackish water in the Forsmark area.
- MX7 is a hypothetical mixing line connecting a number of percussion drilled boreholes with the cluster containing samples from modern sea water. This line emanate from MX2 at a composition corresponding to a diluted, relict marine influenced groundwater. For example HFM22, which may be hydraulically connected to the Baltic plots along MX7 /Juston et al. 2006/.

The general pattern identified in the *mixing model* probably reflects the groundwater evolution towards depth. Alternative paths shown by trend lines MX5a and MX5b may indicate a difference in groundwater evolution between the inside and outside of the tectonic lens, presumably an effect of structural differences in the rock. The broken appearance of the trend line MX3 may reflect the effects of glacial flushing, followed by intrusion of a marine component until density equilibrium with the remaining saline groundwater.

Most objects in the surface system, as soil tubes, private wells and surface water, plot near the mixing line between fresh surface water and modern sea water (MX1). There are, however, a few objects that plot near mixing line MX2, possibly indicating influence from relict marine groundwater and to some extent also deep saline groundwater (shield brine):

- Three of these objects (SFM0011, 12, 13) are located in the vicinity of Lake Gällsboträsket. Two private wells (PFM009 and PFM0039), both located very close to the Baltic coastline, show a significant relict marine signature similar to many of the percussion drilled boreholes that plot along MX2.
- Two soil tubes, SFM0024 and SFM0025, located in the Baltic Sea very close to the coast, represents groundwater in the till below sea sediments. Both of these soil tubes show a marine signature in their chemical composition, but they differ with respect to the marine origin. SFM0024 show a concentration very close to the present Baltic Sea water, whereas SFM0025 display relict marine influences.
- SFM0023, located in till below the sediments of Lake Bolundsfjärden, show a highly deviating pattern compared to most objects in the Forsmark area. However, the upper sections of the percussion drilled borehole HFM32, located very close to SFM0023, show a similar pattern. Most of the major ions in these two objects probably originate from a sea water slightly more saline than present Baltic Sea, with some additional influence from deeper signatures.
- Most of the percussion boreholes plot along MX2. However, HFM11and HFM12 deviate from this pattern by showing a slight attraction to the "deep saline pole" with possible shield brine influence. These boreholes, which are located close to each other at the Eckarfjärden deformation zone, may therefore show a possible indication of deep groundwater relatively close to the surface.

3.5 Estimations of groundwater residence time

Groundwater residence time may be estimated from the activity and decay of several radioactive isotopes. Depending on the half-life of the isotope, different time-scales are revealed. Examples of radioactive isotopes used for groundwater dating are ^{3}H, ^{14}C and ^{36}Cl, with half-lives of 12.4, 5,730, and 301,000 years respectively /Clark and Fritz 1997/.

Groundwater residence time estimations by ^{3}H and ^{14}C are problematical due to the difficulties in specifying initial conditions and in quantifying the influencing processes. The abundance in the atmosphere of these three isotopes was during the fifties and sixties heavily influenced by the nuclear bomb tests, and maximum activities during this period increased several orders of magnitude, compared to the normal atmospheric activity. Dilution of ^{14}C by ^{14}C-free carbon derived from calcite dissolution may lead to an overestimation of the groundwater residence time if all dissolved carbon is presumed to originate from the primordial groundwater

The many unknown factors may consequently lead to many possible interpretations of the observed patterns, and it should also be held in mind that estimations of groundwater residence time by ^{14}C reflect the age of the dissolved carbon, rather than the actual groundwater residence time. Scenarios based on different correction methods may nevertheless give an indication of possible average carbon age ranges. Figure 3-23, where ^{3}H is plotted versus ^{14}C, is a clear illustration of the difficulties associated to age dating by using these isotopes: despite the very different time-scales represented by these parameters, where ^{3}H refers to years and ^{14}C to thousands of years, a quick look may mistakenly identify a linear relationship. This pattern most probably reflects mixing of different sources of carbon, where calcite dissolution plays an important role.

The varying ^{3}H-activities observed in many shallow objects may also be an indication of contamination, a complicating fact that must be held in mind when ^{3}H and ^{14}C data are interpreted. Nuclear power plants have been recognized to emit both ^{3}H and ^{14}C to the surroundings. Some observations of ^{3}H in the Forsmark area, especially one sample in sea water exceeding 19 TU, may be an indication of emissions from the power plant. ^{3}H activities up to 100 TU have also been reported in the cooling water outlet from the power plants (A-C Nilsson, pers. comm.).

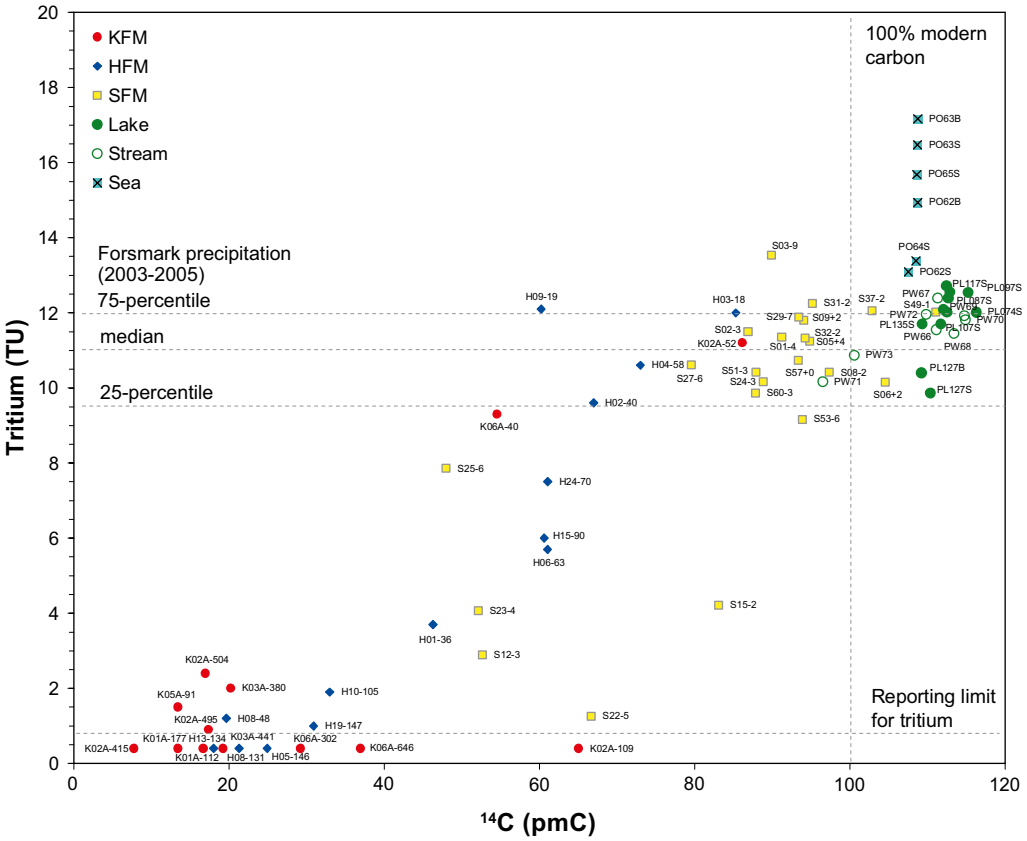

Figure 3-23. *Activities of ^{3}H versus ^{14}C. This picture most of all illustrates the difficulties addressed to age dating with these isotopes, as the axes represent very different time-scales (^{3}H years and ^{14}C thousands of years). See text for further comments.*

Most observations from fresh surface water show, however, activities close to the regional background, probably indicating that emissions from the power plant only contribute to a minor extent to the activities measured in the surface system. If ^{3}H measurements in precipitation from the Forsmark area are compared to reference measurements from Sjötorp in the central parts of southern Sweden, it is not yet possible to determine if there is a significant difference between these stations based on the time-series in Figure 3-24. The tropospheric CO_2 background of ^{14}C was about 110 pmC around year 2000 (ChemNet, pers. comm. originally from Cook et al. 2005), compared to the median in fresh surface water in the Forsmark area of 112 pmC during 2003–2005.

With all these reservations and difficulties in mind, ^{3}H and ^{14}C are used in this the following sections for a rough estimation of groundwater residence times.

3.5.1 Estimating groundwater residence time by the ^{3}H activity

As a consequence of the half-life of about 12.4 years and a detection limit of 1 TU (tritium unit), the maximum time-span estimated by decay of natural ^{3}H levels (about 12 TU) is limited to about 50 years. Since the bomb-peak lies about 50 years back in time, any quantitative estimations of groundwater residence time are precluded and only qualitative interpretations can be made, for example according to the proposal by /Clark and Fritz 1997/ in Table 3-1. This classification may, however, be ambiguous as there are many theoretical combinations of modern, sub-modern and recharge from the sixties that may result in ^{3}H activities in the range between the reporting limit of 0.8 TU and the modern recharge of about 12 TU. ^{3}H is mainly suitable for discriminating between modern and sub-modern groundwater /SKB 2005b/.

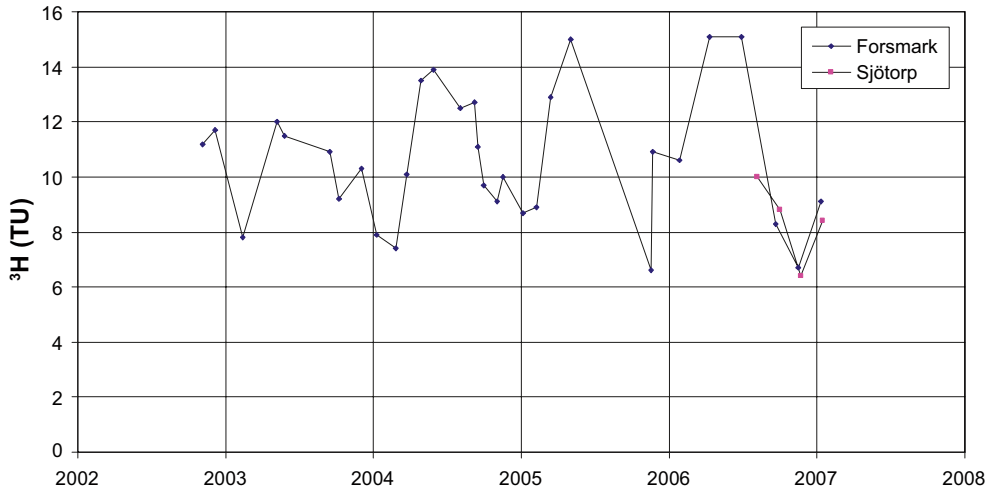

Figure 3-24. *^{3}H-activities in precipitation from the Forsmark area compared to the reference Sjötorp located in the central parts of southern Sweden (Västergötland), at least 200 km from the nearest nuclear power plant.*

Table 3-1. Qualitative estimations of groundwater residence time based on ^{3}H activities. From /Clark and Fritz 1997/. It should be noted that these interpretations could be ambiguous as there are many theoretical combinations of modern, sub-modern and recharge from the sixties that may result in ^{3}H activities in the range between 0.8 TU and 15 TU.

^{3}H activity	Estimated groundwater residence time
< 0.8 TU	Sub-modern – recharged prior to 1952
0.8 to ~4	Mixture between sub-modern and recent recharge
5 to 15	Modern (< 5 to 10 yr)
15 to 30	Some “bomb” ^{3}H present (or contamination from nuclear power plants)
> 30	Considerable component of recharge from 1960s or 1970s

To visualise ^{3}H activities in different water types in the Forsmark area, these are projected onto the ion source model (cf Section 3.2.3) in Figure 3-25. Most of the observations from the surface system in the upper half of the figure show ^{3}H activities between 8 to 14 TU, reflecting the modern origin. This range is centred on the average activity measured in precipitation (about 11 TU in the Forsmark area). Shallow observations with activities exceeding 16 TU are probably influenced by the nuclear power plant nearby. Deeper groundwater, characterised by relict marine and shield brine influence, are practically ^{3}H-free, indicating a sub-modern origin. The classification scheme in Table 3-1 is applied on shallow groundwater samples in Table 5-3 with the purpose of comparing several groundwater classification methods. According to this classification, which is based on minimum ^{3}H values per soil tube, SFM0010, 12, 15, 22, 53 and 56 contain groundwater of sub-modern origin (cf statistical compilation in /Tröjbom and Söderbäck 2006/).

3.5.2 Estimating groundwater residence time by the ^{14}C activity

Estimations based on the ^{14}C activity reflect the age of dissolved carbon rather than the actual retention time of the groundwater. Besides the radioactive decay that is used to calculate the groundwater residence time there are several factors that may influence the measured ^{14}C-activities and therefore diminish the possibilities to make an accurate estimation, e.g. uncertain initial ^{14}C activities and processes influencing the carbon pool (cf Section 3.5 for a discussion about uncertainties)

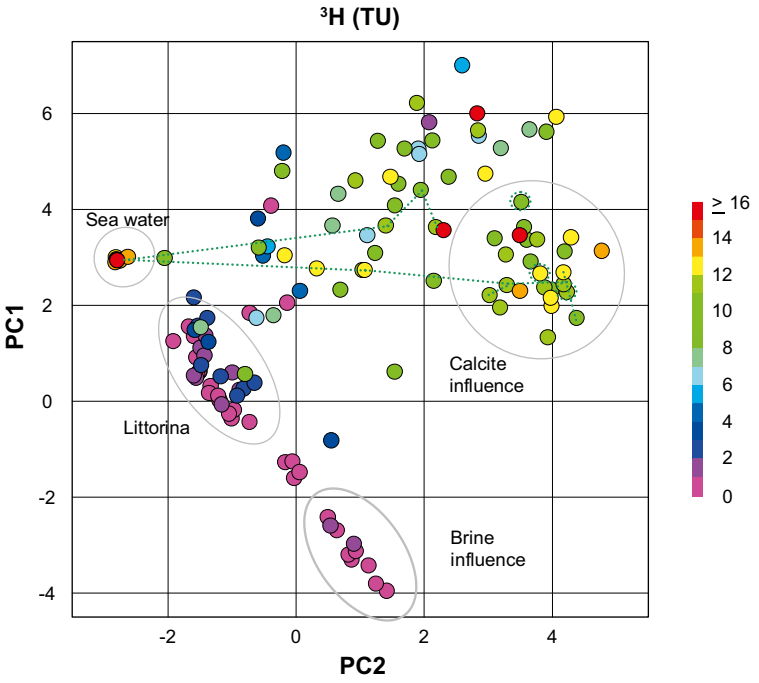

Figure 3-25. *^{3}H activities projected onto the ion source model (cf Section 3.2.3). Average ^{3}H activities of dataset B (cf Section 2.2.4). Observations from cored boreholes are corrected for flushing water content.*

Supply of zero-activity carbon from calcite dissolution lowers the measured ^{14}C-activity, which may lead to an overestimation of the groundwater residence time if all dissolved carbon is presumed to originate from the primordial groundwater. Other processes and sources may also complicate the ^{14}C dating by influencing the ^{14}C activity, e.g. matrix diffusion, sulphate reduction, incorporation of geogenic CO_2 and methanogenesis /Clark and Fritz 1997/. However, in the shallow waters of the Forsmark area, calcite dissolution is probably the most important process due to the calcite rich overburden.

There are several methods used to correct for the effects of calcite dissolution on the measured ^{14}C activity. Concomitant measurements of the $^{13}C/^{12}C$ isotope ratio give a possibility to correct ^{14}C-age for the effect of calcite dissolution, if the ^{13}C content of the calcite is known. A correction, based on a method described by /Fritz and Clark 1997/, was applied on shallow groundwater data from soil tubes in Figure 3-26. This correction was based on following assumptions: $^{13}C/^{12}C$ isotope ratio (denoted $\delta^{13}C$), in $HCO_{3(aq)}$ in soil –15.5‰ PDB, and in calcite 0‰ PDB, and initial ^{14}C activity 110 pmC (cf alternative results based on further corrections and other initial conditions listed in Table 3-2).

The high groundwater residence times indicated by the uncorrected dating in the encircled cluster in Figure 3-26 may be fully explained by calcite dissolution, as the centre of the cluster moved towards zero age after correction. There is, however, a large spread of the encircled green cluster of ± 2,000 years, reflecting uncertainties due to measurement precision and perhaps also other processes affecting the $^{13}C/^{12}C$ isotope ratio. A few soil tubes are overcompensated by the ^{13}C correction, leading to highly negative ages, indicating invalid initial assumptions, differing groundwater origin or other processes than calcite dissolution operating.

When all data including ^{13}C and ^{14}C measurements from the Forsmark area are plotted in Figure 3-27, a few trends are revealed (dashed pink lines). Supportive, generic data are shown by dashed grey lines. Both the ^{14}C-activity and $\delta^{13}C$ are assumed to be zero in limestone (calcite). $\delta^{13}C$ in air is –7 ‰ PDB, and $\delta^{13}C$ in soil DIC, mainly dissolved HCO_3 derived from biogenic CO_2 (–23 ‰ PDB), is –15.5 ‰ PDB at pH 7.25 /Clark and Fritz 1997/. In Section 4.1.4 this figure is further interpreted regarding the origin of carbon.

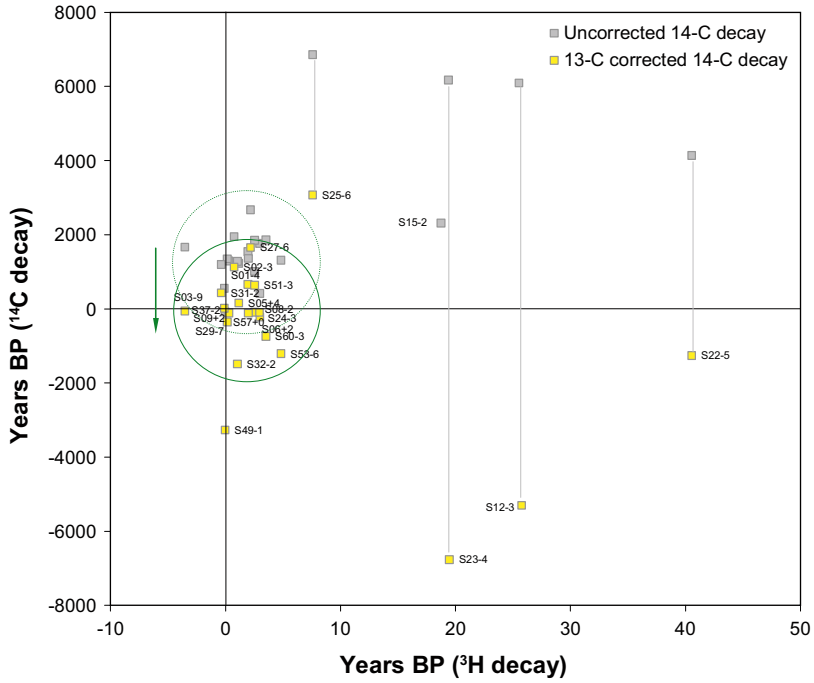

Figure 3-26. *The effects of ^{13}C correction on groundwater residence time datings based on ^{14}C activities. Data from soil tubes in the Forsmark area. Grey marks (and the dashed green circle) represent uncorrected ages, and yellow marks (and the solid green circle) represent the ^{13}C corrected ^{14}C-age. Grey lines underline the effects of the correction on a selection of observations which also show lowered ^{3}H-activities. It was not relevant to calculate a corrected ^{14}C-value for S15-2 because of the anomalous positive ^{13}C-values.*

Table 3-2. Mean carbon age estimated for selected objects by different correction methods: Non-corrected ^{14}C-decay (^{14}C-decay), correction for varying initial activities ($^{14}C_0$-corr) and ^{13}C-correction for dilution by calcite dissolution (^{13}C-corr) in combination with varying initial activities. Objects in the table refer to labels shown in Figure 3-27, cf Section 2.3.12 for explanation of nomenclature.

Object	Idcode	^{14}C-decay	^{14}C-decay $^{14}C_0$-corr	^{14}C-decay $^{14}C_0$-corr ^{13}C-corr
S27-6	SFM0027	1,845	1,891	486
H15-90	HFM15	4,086	4,204	1,255
S25-6	SFM0025	6,068	6,249	1,939
H01-36	HFM01	6,366	6,637	2,915
H10-105	HFM10	9,168	9,560	4,253
H05-146	HFM05	11,460	11,928	5,094
Relict marine cluster	–	14,176	14,784	6,676
Point ”E”	–	15,683	16,112	4,651

The ^{13}C-correction model (Equation 3) used in Figure 3-17 is marked as an orange dashed line in Figure 3-27; points plotting along this line may be fully explained by calcite dissolution if the model assumptions are valid. This model is however oversimplified as initial atmospheric ^{14}C-activities have not been constant through time. There are evidence based on dendro-chronological age and U/Th age, that the ^{14}C-activity have declined from as much as 140–160 pmC 35,000 years ago to the pre-modern value of 100 pmC according to /Clark and Fritz 1997/ and references therein.

Equation 3. Upper – Relationship describing the carbon age at time t, based on the measured ^{14}C activity ($a_t{}^{14}C$), the initial ^{14}C activity ($a_0{}^{14}C$) and the dilution factor q. Lower – Calcite correction model to describing the dilution factor q due to calcite dissolution, based on the measured ^{13}C content in the sample ($\delta^{13}C_{DIC}$), in recharge ($\delta^{13}C_{rech}$) and in calcite ($\delta^{13}C_{carb}$). From /Clark and Fritz 1997/.

$$t = -8267 \cdot \ln\left(\frac{a_t{}^{14}C}{q \cdot a_0{}^{14}C}\right) \text{ (years)}$$

$$q = \frac{\delta^{13}C_{DIC} - \delta^{13}C_{carb}}{\delta^{13}C_{rech} - \delta^{13}C_{carb}}$$

In order to explore how varying initial activities affect the estimated average carbon-age, a simple linear model based on this information (Equation 4) was used to iterate solutions that represent ^{14}C decay in combination with varying initial $^{14}C_0$-activities according to this model. The multitude of possible ^{13}C-correction models, where one is represented by the orange dashed CX2 line, span within the green surface (lines) in Figure 3-27.

Equation 4. Linear model giving the estimated initial ^{14}C activity at a specific age (t_0).

$$a_0{}^{14}C = \frac{40\,t_0}{35{,}000} + 100 \text{ (pmC)}$$

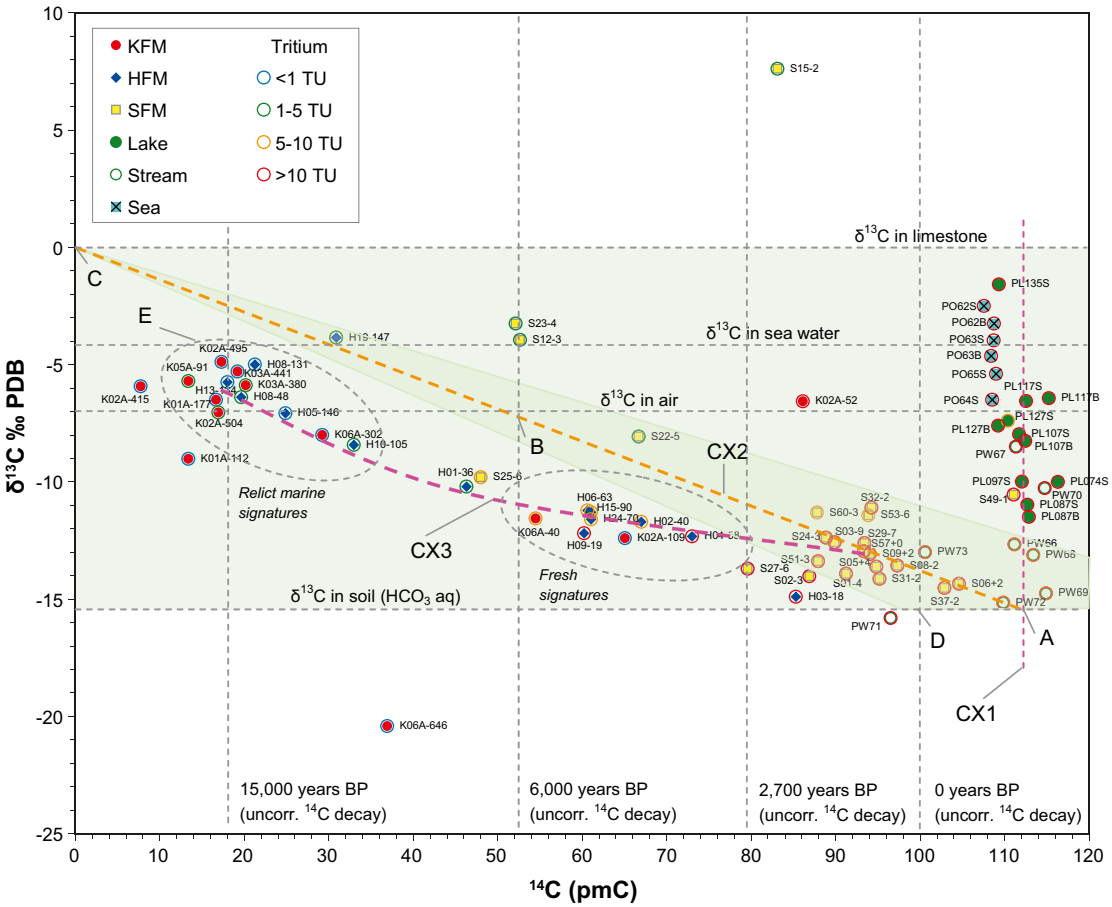

Figure 3-27. *Cross-plot of $\delta^{13}C$ versus ^{14}C-activity. Tritium (^3H) activities are shown by a coloured circle. Pink dashed lines represent hypothetical trend lines, the orange line the ^{13}C-correction model, grey lines represent supportive data (see text). Based on data selection C, cf Section 2.2.4. Explanation of labels, symbols and lines cf Sections 2.3.12. and 2.3.13. See further explanations in Figure 4-15 in the section dealing with carbon, which is identical to the figure above but includes additional information.*

The results of the iterative solutions, in combination with estimations based on uncorrected ^{14}C-decay, are summarised in Table 3-2 for selected objects. It should be noted that the main purpose of these estimations is to explore the limits of estimated carbon age depending on different assumptions and correction techniques, and no general conclusions on which estimations are most correct can be made.

From Table 3-2 it can be concluded that the average carbon age of the relict marine sea water (denoted *relict marine signatures/cluster* in Figure 3-27), depending on the correction model used, ranges from 6,700 to 15,000 years BP.

Two shallow groundwater wells that plot among deeper observations of percussion and core drilled boreholes are included in Table 3-2. SFM0027, which is the deepest soil tube located under the particularly thick sediments near Lake Fiskarfjärden, shows an average carbon age of 500–2,000 years. SFM0025, located in till below sea sediments in Kallrigafjärden, shows an average carbon age ranging from 2,000 to 6,000 years. This soil tube also deviates regarding other parameters by showing the strongest deep water signatures among the soil tubes (cf Sections 3.2.3 and 3.3.2).

3.5.3 Groundwater residence time – summary with a shallow perspective

Generally, there are many difficulties connected to the estimation of groundwater residence time with the radiogenic isotopes ^{3}H and ^{14}C, as described in the beginning of Section 3.5. Nevertheless, with these difficulties in mind, these estimations may give a range of possible groundwater residence times or average carbon ages that in combination with other supporting information, may contribute to the understanding of the site.

Most of the shallow groundwater sampling points (soil tubes) probably contain groundwater of recent origin according to the high ^{3}H-activities measured. Many of these objects, however, show slightly lowered ^{14}C-activities, probably not as a consequence of ^{14}C-decay reflecting high groundwater residence time, but due to supply of "dead" carbon from calcite dissolution. A few soil tubes which display isotopic signatures that may indicate increased groundwater residence time (carbon age) are discussed in the bullet list below:

- SFM0025, located in till below sediments in Kallrigafjärden, contains water with slightly lowered ^{3}H-activities compared to the present atmospheric background activity (observations range from 5–15 TU), indicating water of a mostly recent origin. ^{14}C dating of DIC (HCO_3 constant about 200 mg/L in all measurements) results in a contradictory average carbon-age ranging from 2,000 to 6,000 years. This soil tube also deviates regarding other parameters by showing the strongest deep groundwater water signatures among the soil tubes (cf Sections 3.2.3 and 3.3.2).
- SFM0027 shows compared to SFM0025, only a minor deviation in hydrochemical composition from most other soil tubes. Average carbon age in this shallow groundwater range from about 500 to 2,000 years depending on correction method. On the contrary, ^{3}H-activities that range from 9–12 TU in this soil tube indicate that modern meteoric recharge dominates. The location of the intake screen of this soil tube at 7 metres depth in very thick sediments of silty till, may explain a supposed long retention time of groundwater at this site. SFM0026 located very close nearby was drilled in least 16 metres thick sediments /Werner et al. 2007/.
- SFM0012 and SFM0023 show relatively low ^{14}C-activities in combination with (mostly) low ^{3}H-activities and a ^{13}C isotopic composition corresponding to sea water. Accordingly, these soil tubes may represent a relict marine sea water of about 6,000 year's uncorrected average carbon age. This conclusion, based on carbon only, is to some extent contradicted by the presence of high calcium concentrations, perhaps an indication that calcite dissolution is present in the till and that the uncorrected residence time may have been overestimated. As an alternative hypothesis, the observed carbon isotope signatures may have been formed by mixing between modern and relict sea water according to the hypothetical mixing line in Figure 4-15.

- SFM0015, located in till below the sediments of Lake Eckarfjärden shows a slightly lowered ^{14}C-activity in combination with an exceedingly enriched $\delta^{13}C$ isotopic composition. Such high $\delta^{13}C$ value is probable an indication of methanogenesis, a conclusion supported by high contents of DOC, NH_4-N and Ba, and low contents of SO_4 and NO_3. A concomitant low calcium concentration in SFM0015 may here indicate that calcite dissolution play a minor role. The estimated non-corrected average carbon age of 1,500 years suggests that the carbon source is rather old, and one possible source could be organic matter in sediments (cf Section 3.3.3 dealing with the origin of water in this soil tube). The low ^{3}H-activity in this groundwater also support a sub-modern origin of this groundwater.

4 Detailed chemical evaluations

The aim of this chapter is to provide detailed visualisations that complement the preceding chapter "Hydrochemical overview of the Forsmark area" with the purpose of answering questions relevant for the Forsmark area. The sections are dealing with the origin and fate of selected elements, tracing of geochemical reactions and, finally, summarising possible indications of deep groundwater signatures in the shallow system.

4.1 Origin and fate of selected elements

Dissolved elements at the Forsmark site originate either from solid or gaseous phases, transformed at the site by reactions, or have been transported to the site in dissolved form. Reversely, elements may be lost to the atmosphere or to the geosphere by the formation of solids. In this section focus is laid on marine ions, sulphur, calcium and carbon.

4.1.1 Tracing marine influences (marine ions, Mg, Na, Cl, Br)

The recent withdrawal of the Baltic Sea due to the ongoing isostatic uplift, gives rich prerequisites for influences from relict marine constituents in the Forsmark area. The flat terrain and presence of lakes close to the sea level also lead to recurring marine influences in the freshwater system during episodes of high sea water level /SKB 2005c/.

The major constituents in sea water, based on the molar contributions, are Cl, Na, Mg and SO_4. In Figure 4-1, the molar composition and concentrations of the major constituents are shown for the sea water sampling site Forslingens grund in the Forsmark area.

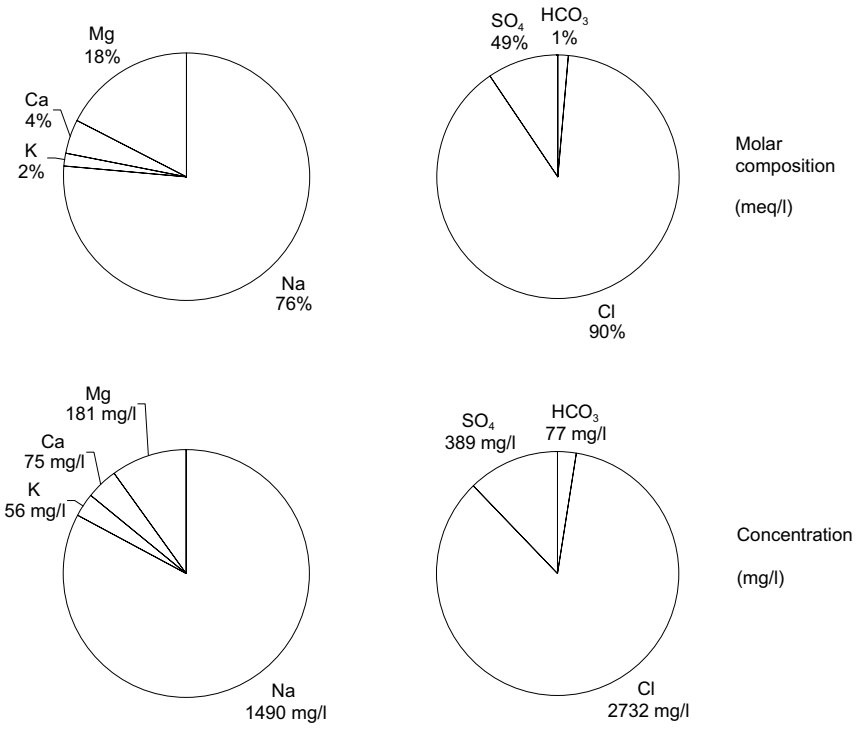

Figure 4-1. *Major ions in sea water measured in surface water at Forslingens grund (PFM000062) in the Forsmark area. Cations to the left and anions to the right. The upper figures represent the molar fractions (meq/L), and the lower the concentrations.*

As stated in the water type classification in Section 3.1.1, both shallow groundwater in soil tubes and surface water in lakes show clear marine influences. According to the reference models in previous chapter (see Chapter 3), also groundwater in the bedrock show marine signatures, from percussion drilled boreholes at less than 100 metres depth, to about 400 metres depth in core drilled boreholes. Most marine signatures in the bedrock probably reflect marine relics from the Littorina Sea stage and possibly also older marine remnants from preceding interglacials /SKB 2005b/.

The correlation between Na and Cl is explored in Figure 4-2. In the upper plot there is a clear general trend where Na correlates with Cl, and many points plot along the molar ratio trend of sea water. Points above (left) of this molar ratio trend indicate supply of Na, e.g. by weathering reactions or cation exchange. Deviations below this line may instead indicate supply of Cl, e.g. from shield brine. There is however deviations from this trend which are emphasised in the plot in the lower panel (Cl versus Na/Cl).

The hypothetical mixing trend (pink dashed lines) between the dilute freshwater of PW71 (the inlet to Lake Eckarfjärden) to the left and sea water to the right coincide with the evolution trend downstream the major catchment (green dashed line). Many shallow samples in soil tubes also follow this trend, indicating that mixing with marine components probably is an important ion source in these objects (e.g. SFM0024, 34, 59, 63 and 65). An explanation to the elevated levels of marine ions in the lower parts of the catchment is clearly demonstrated in Figure 4-3. At scarce occasions, sea water intrusions supply marine ions to all lakes located close to the sea level (e.g. Lake Norra Bassängen, Lake Bolundsfjärden, and Lake Fiskarfjärden).

Intrusions were evident in both 2002 and 2005 when the Cl concentrations rose to high values. In 2005, concomitant sea level measurements revealed a simultaneous peak during the Gudrun storm that hit Sweden in January /Juston at al. 2006/. After a saltwater intrusion, which first influence the bottom water, the supplied sea water is mixed with the whole water body, followed by a gradual decrease due to supply of freshwater from the catchment. When the two events are compared, the rate of the gradual decline in Cl is approximately constant, indicating that the dilution rate is determined mainly by the catchment size. During the years 2003 and 2004, which were unaffected by sea water intrusions, there was also a cyclical variation in Cl concentration. This probably reflects the annual water balance, with increasing concentrations during low-flow periods (cf Section 5.2).

At slightly higher topographical levels, unreachable for modern sea water intrusions, marine remnants in sediments and sea spray may be the sources supplying Cl to these dilute waters, which usually not exceed 30 mg/L of Cl. The Na excess (compared to sea water) evident in most dilute waters, probably reflects additional supply of Na from weathering and cation exchange reactions. As may be expected, this Na-fraction is most pronounced in ion-weak waters, and is gradually masked by mixing with marine Na in the downstream parts of the catchments.

In the upper panel of Figure 4-2 there is an interesting trend, NX1, that follow the hypothetical mixing line between S17+2 and H06-63. A group of percussion boreholes show Na excess similar to many soil tubes, but with significantly higher Na concentrations. A possible explanation to the Na excess can be cation exchange that takes place in the Quaternary deposits, driven by the high calcium levels which are caused by calcite dissolution in the Quaternary deposits (cf Section 4.1.3). Among the shallow objects, SFM0027, located below thick sediments in the vicinity of Lake Fiskarfjärden is most associated to this trend.

Most deep observations plot below the molar ratio of sea water in Figure 4-2, along the mixing trend towards the molar ratio of Laxemar deep saline groundwater (which shows a strong shield brine signature). This deviation below the sea water ratio may be interpreted as mixing of Na depleted deep saline groundwater (showing significant shield brine influence), with less depleted saline waters. This pattern is probably not reflecting ion exchange.

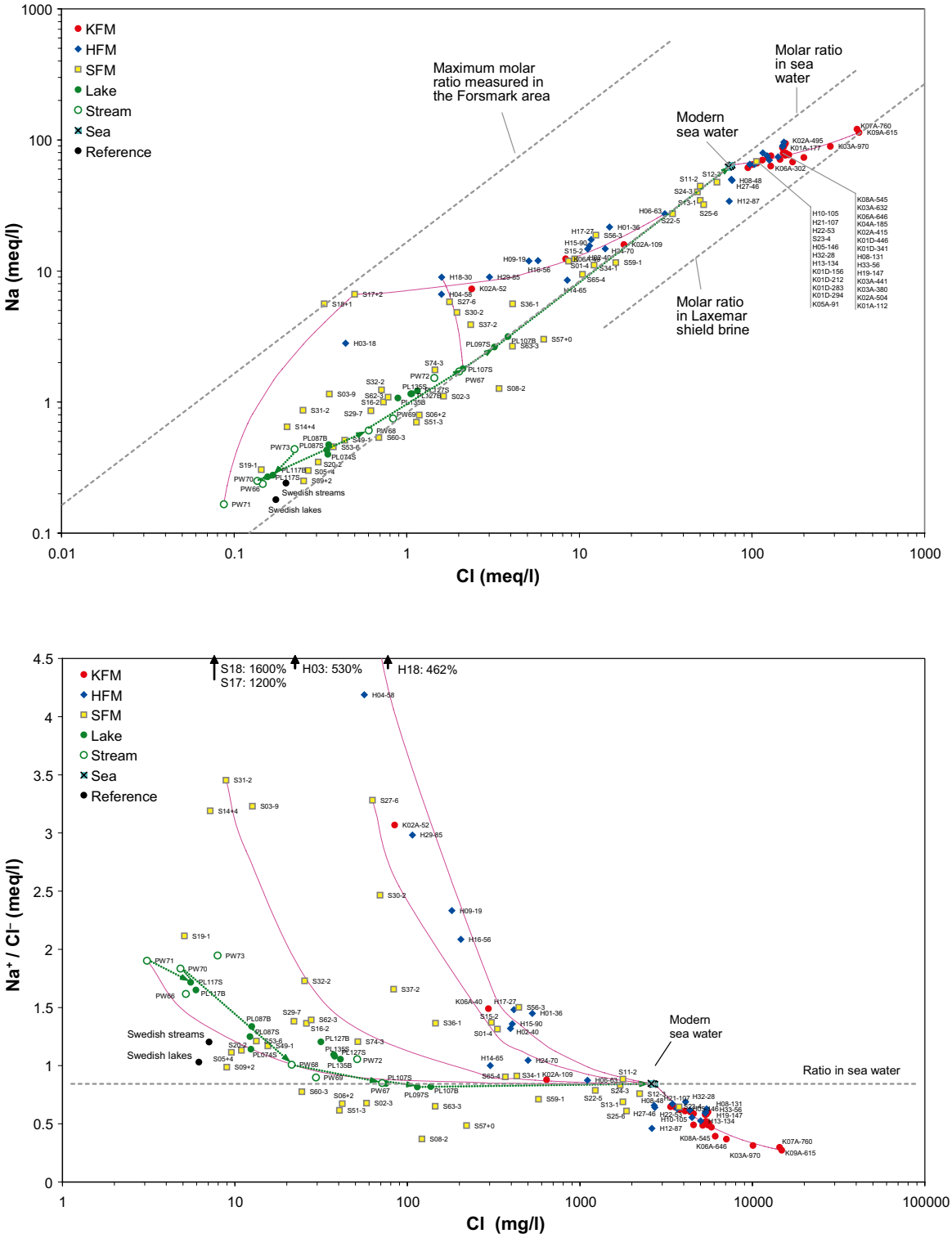

Figure 4-2. *Relationship between Na and Cl in surface water and groundwater in the Forsmark area. Upper: molar content of Na versus Cl. Lower: Na/Cl ratio (based on meq/L) versus Cl concentration (mg/L). Note that the Cl-scales differ between the plots. Dataset C, cf Section 2.2.4. Explanation of labels, symbols and lines cf Sections 2.3.12 and 2.3.13.*

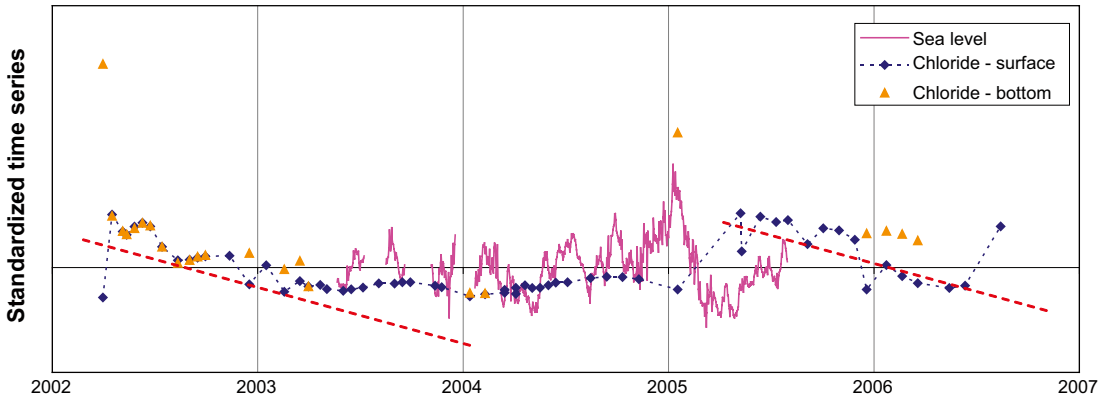

Figure 4-3. *Chloride concentrations in Lake Bolundsfjärden during the period 2002–2007, together with measurements of the sea level in the Baltic Sea. Red dashed lines mark the gradual decrease in Cl concentration due to dilution by supply of freshwater from the catchment.*

According to the *ion source model* in Section 3.2, the maximum discrimination between modern sea water and shield brine should be revealed by Mg and Br. In Figure 4-4, where the ratio of these elements is plotted against the Cl concentration, there is a clear discrimination between shallow and deeper objects. The horizontally extended cluster below the sea water ratio probably reflects the mixture of relict marine and shield brine contributions.

Sources of Mg and Br can also be explored in a log-log plot, where observations with the same molar ratio plot along straight lines (Figure 4-5). Two clear sources of Mg and Br are evident: sea water and shield brine, marked as grey dashed lines. The third source, which is more difficult to define, is mainly affecting surface water and shallow groundwater in the Forsmark area. A possible third Mg source may be dissolution of Mg bearing calcite (cf Section 4.1.3 dealing with the origin of Ca).

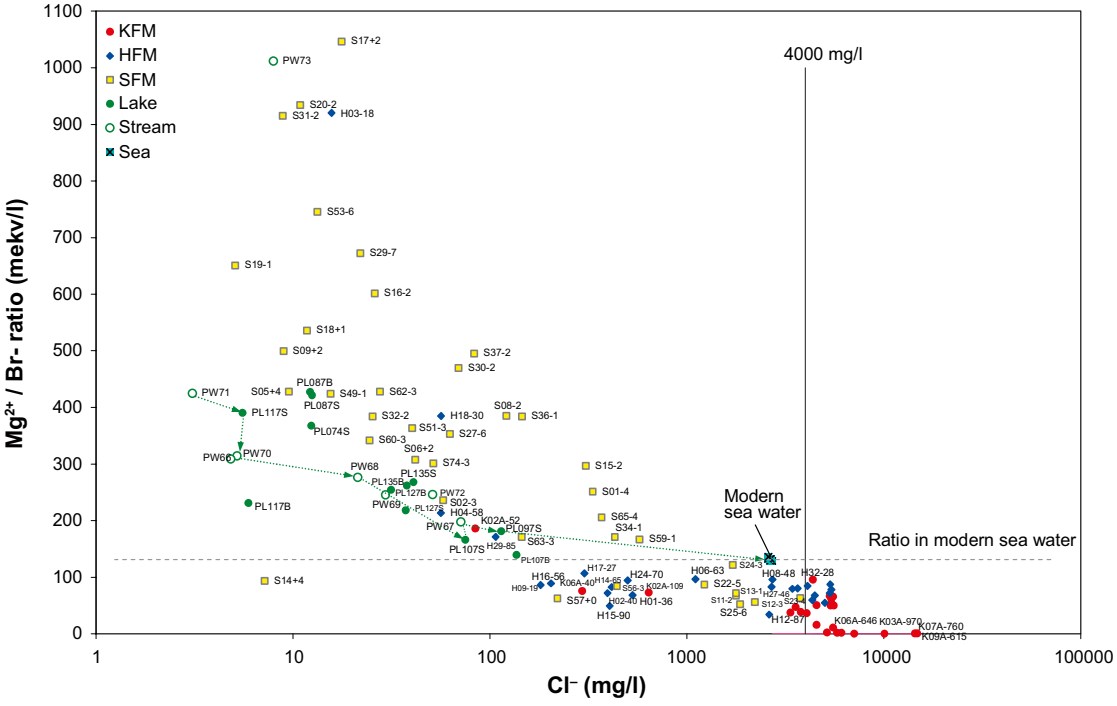

Figure 4-4. *Mg/Br ratio (based on meq/L) versus Cl concentration (mg/L) in water samples from the Forsmark area. The figure is based on data selection C, cf Section 2.2.4. For explanation of labels, symbols and lines, cf Sections 2.3.12 and 2.3.13. The limited precision in the Br analysis may contribute to the scattered picture among shallow objects.*

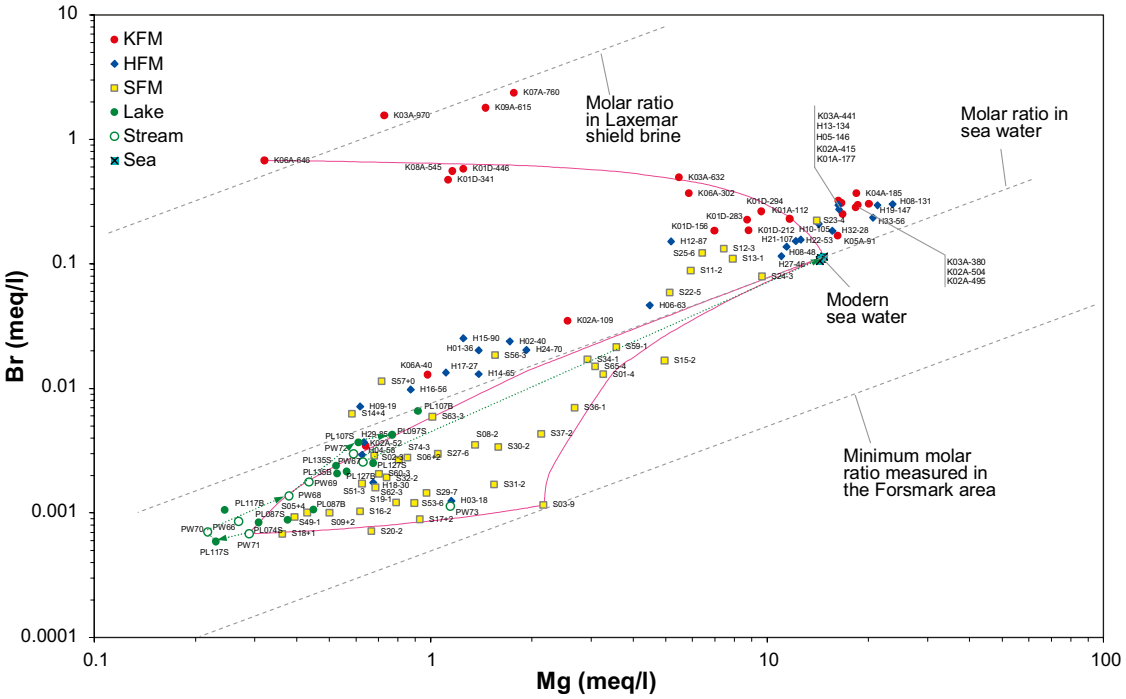

Figure 4-5. *Br versus Mg in water samples from the Forsmark area. Note the logarithmic scales on both axes. Grey dashed lines mark constant Br/Mg ratios. Based on data selection C, cf Section 2.2.4. For explanation of labels, symbols and lines, cf Sections 2.3.12. and 2.3.13.*

In surface water, the downstream trend in the catchments, indicated by green arrows, follows the hypothetical mixing trend between a dilute, Ca-rich water, and modern sea water. Supply from the marine source is consequently dominating in these waters. In shallow groundwater (soil tubes) a larger fraction of Mg probably originates from calcite in the Quaternary deposits, as these observations plot towards the Mg source associated to the limestone. The Mg content in all shallow samples may be explained by the marine and calcite sources.

Observations from the bedrock differ significantly from the shallow samples, by showing a higher Mg/Br ratio, even higher than modern sea water. The KFM borehole data probably imply a mixing between saline waters of possibly marine origin with deep saline groundwater with less marine origin. At deeper levels represented by KFM boreholes, observations follow a hypothetical mixing line until a distinct turn probably marks the evolution towards shield brine. Observations that plot along this upper trend show equal Mg/Br ratios, but a different degree of dilution.

A consequence of Mg not being a conservative element, the observed Mg/Br ratios may to some extent also be attributed to reactions involving Mg rather than mixing processes. In the Forsmark area, however, most variation in Mg concentrations in the bedrock seem to be a consequence of mixing, a fact that is used in the calibration of the geohydrological models.

The major conclusions regarding marine influences are summarised in the bullet list below:

- Shallow groundwater in soil tubes and surface water in lakes show clear marine influences in the Forsmark area. This may be attributed to the recent withdrawal of the Baltic Sea due to the ongoing isostatic uplift, which gives rich prerequisites for marine influences.
- In lakes close to the sea level sea water intrusions were evident in both 2002 and 2005 when Cl concentrations rose to high values in e.g. Lake Bolundsfjärden. These occasions coincided with episodes of especially high sea level. In between these events there was a gradual decline in Cl, at a constant rate, reflecting the dilution by freshwater from the catchment. During the years 2003 and 2004, which were unaffected by sea water intrusions, there was also a smaller cyclical variation in Cl concentration. This probably reflects the annual water balance, with increasing concentrations during low-flow periods.

- The Na excess (compared to Cl in sea water) evident in most dilute waters, probably reflects additional supply of Na from weathering and cation exchange reactions. As may be expected, this Na-fraction is most pronounced in ion-weak waters, and is gradually masked by mixing with marine Na in the downstream parts of the catchments.
- A group of percussion boreholes show Na excess similar to many soil tubes, but with significantly higher Na concentrations. A possible explanation to the Na excess can be cation exchange that takes place in the Quaternary deposits during recharge to the bedrock, driven by the high calcium levels which are caused by calcite dissolution in the Quaternary deposits.
- Also groundwater in the bedrock show marine signatures, from percussion drilled boreholes at less than 100 metres depth, to about 400 metres depth in core drilled boreholes. These signatures probably reflect marine relics from the Littorina Sea stage and possibly also older marine remnants from preceding interglacials.

4.1.2 On the origin of sulphur

Sulphur in groundwater and surface water may originate from many different sources: relict and modern marine sulphate, sulphur deposition originating from e.g. fossil fuels and dissolution of sulphur-bearing minerals as pyrite and gypsum. Moreover, in agricultural areas fertilizers may be a possible sulphur source.

Alternative sulphur sources may be distinguished by the use of sulphur isotopes in combination with other major constituents that covariate with sulphur, e.g. Cl from marine sources. Different processes may influence the isotopic composition of sulphur in different directions. Microbial SO_4 reduction may be traced in the remaining SO_4 pool by enrichments in ^{34}S. The formed S^{2-} is instead depleted in ^{34}S, and may usually be identified as negative ^{34}S-values in for example pyrites of biogenic origin. In the Forsmark area, positive in ^{34}S-values have been observed among fracture pyrites formed in the bedrock (Eva-Lena Tullborg, pers. comm.).

SO_4 concentrations in freshwater in the Forsmark region are considerably higher than in most lakes and watercourses in Sweden. As sulphate deposition this region is not deviating significantly from the rest of Sweden, the elevated SO_4 levels may be attributed to leaching from soils /Sonesten 2005/. The recent withdrawal of the sea in the Forsmark area also gives prerequisites for supply of relict marine ions as SO_4. SO_4 levels in shallow groundwater (soil tubes and private wells) in the Forsmark area are about 3–4 times elevated compared to the levels normally measured in Sweden /Tröjbom and Söderbäck 2006/.

The most compact visualisation on the origin of sulphur is shown in Figure 4-6, where the SO_4/Cl ratio is plotted versus the isotopic composition of ^{34}S and ^{32}S. Complementary plots including SO_4 concentrations are shown in Figure 4-7.

Modern sea water, marked by dashed grey lines, plots in the middle of both Figure 4-6 and Figure 4-7. Observations that plot above this horizontal line show SO_4 excess compared to the composition in sea water, and supply from non-marine sources may be considered. Observations below this line show on the contrary SO_4 deficiency, either due to removal of SO_4 or supply of non-marine Cl from e.g. shield brine. The isotopic composition, discriminating in the horizontal direction, reflects different processes and may reveal different sources of SO_4. Atmospheric composition /Kendall and McDonnel 2006/, the approximate location of biogenic pyrites /Clark and Fritz 1997/, and the SO_4 concentration in precipitation /Tröjbom and Söderbäck 2006/ concentrated three times to correct for evapotranspiration (400 mm compared to an annual precipitation or 550 mm per year) /Juston et al. 2006/, have been marked in the figure.

All observations from surface waters in Figure 4-6 plot above the marine composition line, indicating a significant contribution of non-marine SO_4 in the Forsmark area. Possible sources are atmospheric deposition and oxidation of pyrites in the Quaternary deposits. Also fertilizers may contribute, at least in the Bredviken catchment (observations PW73, S08, and S09) where the

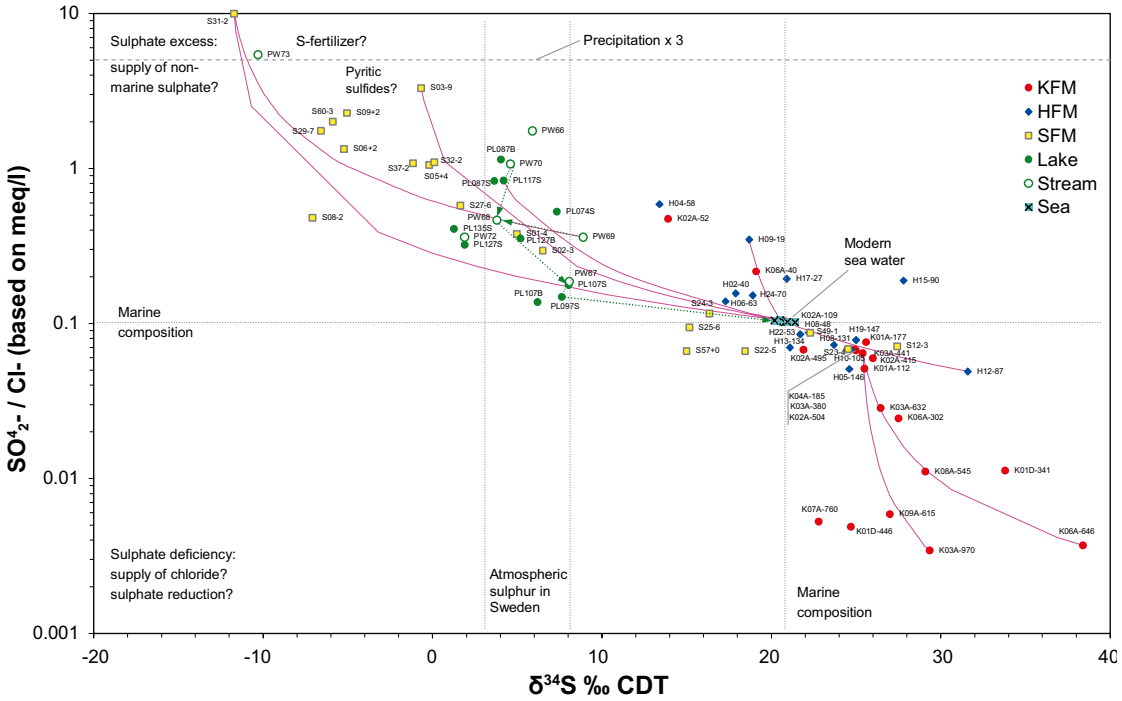

Figure 4-6. *The SO_4/Cl ratio (based on meq/L) versus the isotopic deviation of $^{34}S/^{32}S$ from the international standard (expressed as ‰ deviation from CDT). This figure is based on data selection C, cf Section 2.2.4. For explanation of labels, symbols and lines, cf Sections 2.3.12 and 2.3.13.*

proportion arable land is considerable (cf Section 7.7). The downstream evolution trend follows the hypothetical mixing line with sea water, indicating a gradually increasing importance of the marine SO_4, especially in the lakes close to the coast that are subject to sea water intrusions (cf Section 4.1.1). Due to the overlapping hypothetical mixing trends towards modern sea water, it is not possible to distinguish atmospheric from pyritic SO_4 in the surface waters in Figure 4-6.

In the lower panel of Figure 4-7, where $\delta^{34}S$ is plotted versus the SO_4 concentration, a qualitative picture of the relative importance of different sulphur sources is given. The green coloured surface, which connects three hypothetical end-members, encloses most observations from shallow groundwater and surface water and the curved shape of this surface would be a mixing triangle if plotted in a linear coordinate system. If SO_4 is regarded as a conservative constituent, the relative location within this shape corresponds to the relative proportion of each end-member in the sample. However, microbial SO_4 reduction complicates this picture by reducing the SO_4 concentration and by changing $\delta^{34}S$ towards more positive values, i.e. in a diagonal direction towards upper left. SFM0049 and most probably also SFM0015 (that are lacking $\delta^{34}S$ measurements) may have been subject to microbial SO_4 reduction, leading to the very low SO_4 concentrations observed (cf Section 7.4). If the identification of only three major end-members is not valid, i.e. there are other important end-members also contributing to the surface waters, conclusions may be more or less incorrect.

The cluster of surface water observations in Figure 4-7 gives an integrated picture of the origin of the SO_4 transported in the surface system. The relative location of this cluster indicates that atmospheric and pyritic sulphur contribute in most surface waters and that the relative contributions of marine and pyritic sulphur increase downstream (SX4). In the Eckarfjärden catchment, located in the higher inland part of the Forsmark area, the relatively low SO_4 content is probably dominated by atmospheric sulphur (i.e. these observations plot very close to the atmospheric end-member). In general, approximately one third of SO_4 in the surface water, not directly influenced by sea water intrusions, seems to originate from atmospheric deposition, whereas the remaining two thirds originate from sulphide minerals in the Quaternary deposits (cf Section 6.2.6).

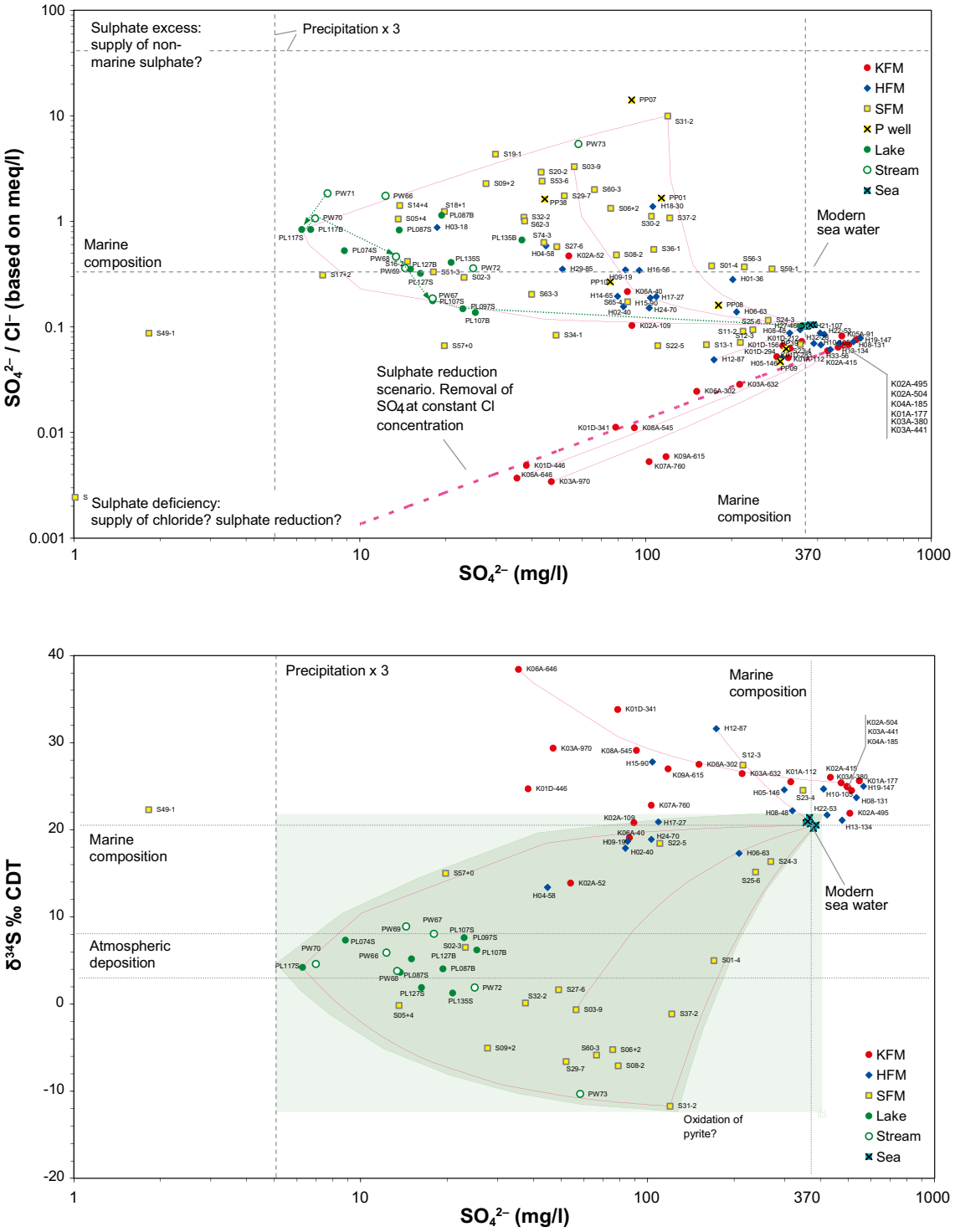

Figure 4-7. *Upper – SO_4/Cl ratio (based on meq/L) versus SO_4 concentration (mg/L). Lower – $\delta^{34}S$ (‰CDT) versus SO_4 concentration. See explanation in text for the green coloured surface in the lower panel. Based on data selection C, cf Section 2.2.4. For explanation of labels, symbols and lines, cf Sections 2.3.12 and 2.3.13.*

Many observations from shallow groundwater also plot within the surface delimited by green lines which connect the above mentioned three end-members in Figure 4-7. High SO_4 concentrations, in the order of 100 mg/L, most probably originate from mineral sulphides (pyrite) in the sediments. Among these soil tubes, two evolution trends may be distinguished: SX1 caused by mixing with marine sulphate, and SX2 probably caused by dilution with meteoric water and mixing with atmospheric SO_4.

Among the soil tubes that plot along SX1, SFM0001 differ with respect to geographical location from SFM0037, 24, and 25 which are located in close vicinity of the Baltic, or in the case of the latter two, below sea sediments in the open sea water. Pyritic SO_4 in combination with different portions of marine SO_4 are possible sulphur sources in all these soil tubes. Soil tubes plotting along the evolution trend SX2 probably represent different mixing proportions of sulphur of principally pyritic and atmospheric origin. Groundwater discharge transports this mixture into the surface water system, where both the pyritic and marine proportions seem to increase downstream along SX4.

The SO_4 concentration in the discharge from the catchment of Bredviken (cf Section 7.7) is high and shows a strong pyritic isotope signature. Agricultural activities are most probable responsible for the increased leakage of sulphur and other elements from this catchment (cf summary of catchment models in Section 6.3). Cultivation and draining aerate the soil, which leads to increased oxidation of sediments and increased leaching of SO_4. Extensive oxidation of mineral sulphides may also release large amounts of H^+, which may contribute to the weathering of calcite and other minerals /Åström and Rönnback, submitted/. Sulphur containing fertilizers may also add SO_4 with a signature close to pyritic sulphates /Clark and Fritz 1997/.

Two soil tubes, SFM0012 and SFM0023, and probably also SFM0013 and the private wells PFM0009 and PFM0039, show a deviating SO_4 signature more similar to deeper observations in the bedrock. A possible origin may be relict marine SO_4, perhaps slightly altered by microbial sulphate reduction.

When looking at deeper levels, high $\delta^{34}S$ in percussion drilled and cored boreholes may indicate a substantial influence from microbial sulphate reduction on the SO_4 of predominantly relict marine origin. The lowering of the SO_4/Cl ratio in Figure 4-7 (upper panel), compared to the composition in sea water, may also be attributed to additional supply of Cl e.g. from deep saline groundwater influenced by shield brine. According to the hypothetical mixing scenario, and the sulphate reduction scenario, it is not possible to separate SO_4 reduction from mixing with a low-sulphate shield brine component from these pictures.

In a wider context, the Quaternary deposits may have a great importance for the observed groundwater composition in the Forsmark area. For example the relict marine groundwater, prevailing both at greater depths in the bedrock and possibly also in soil tubes below lakes, may have been altered regarding sulphur when Littorina sea water percolated through the deposits into the bedrock. Due to the emerging land, the same deposits where later exposed to meteoric water and marine remnants as sulphides influence the present discharging groundwater. For example, shows the relict marine influenced groundwater elevated ^{34}S isotopic signatures (cf Figure 4-7), which theoretically may reflect a bacterially mediated precipitation of (iron-) sulphides in the sea sediments; sulphur of marine origin that passed the deposits derived enriched ^{34}S values, whereas sulphides depleted ^{34}S remained in the Quaternary deposits as solid sulphide minerals. Redox sensitive Mn shows anomalous high concentrations in the relict marine influenced groundwater, which also may be explained processes in the deposits during Littorina turnover, as discussed in /SKB 2006/ and in the conceptual model in Section 8.2.

The major conclusions regarding the origin of sulphur are summarised in the bullet list below:

- In general, approximately one third of SO_4 in the surface water, not directly influenced by sea water intrusions, seems to originate from atmospheric deposition, whereas the remaining two thirds originate from sulphide minerals in the sediments.

- The relative contributions of marine and pyritic sulphur increase downstream in the Forsmark area. In the Eckarfjärden catchment the relatively low SO_4 content is probably dominated by contributions from atmospheric sulphur deposition.
- The soil tubes SFM0049 and SFM0015 may have been subject to microbial SO_4 reduction, leading to the very low SO_4 concentrations observed.
- Two soil tubes, SFM0012 and SFM0023, and the private wells PFM0009 and PFM0039, show SO_4 isotope signatures similar to deeper observations in the bedrock. A possible origin of this isotopically altered SO_4 may be either supply of relict marine groundwater with an already altered isotope signature, or SO_4 of sea water origin locally altered by bacterial sulphate reduction.

4.1.3 On the origin of calcium

In this section is the origin of calcium explored. Rich supply of bivalent Ca^{2+} also gives prerequisites for cation exchange in the deposits, a topic outlined in Section 4.2.1.

Calcium concentrations in the Forsmark area are markedly elevated compared to the levels normally measured in Sweden. In shallow groundwater, the median value in Forsmark (110 mg/L) exceeds the 90th percentile of the distribution of national Swedish well survey /Tröjbom and Söderbäck 2006/. In surface waters, Ca concentrations are about ten times elevated compared to the median of the national surveys of streams and lakes /Sonesten 2005/. One example of the ecosystem response to the rich calcium supply is manifested in the presence of oligotrophic hardwater lakes, a unique lake type that is strongly affected by the co-precipitation of phosphorus and calcite /Brunberg and Blomquist 1999/. Flora and fauna also show typical signs of calcium influence, for example by the occurrence of rich fens /Göthberg and Wahlman 2006/ and of other types of Ca-favoured vegetation /Jonsell and Jonsell 1995/.

The explanation to the high calcium levels is found in the calcite-rich Quaternary deposits that cover the Forsmark area, and also the rest of the northern part of Uppland. These deposits originate from Gävlebukten, a wide coastal bay situated about c. 100 km north of the Forsmark site, which is covered by Cambrian and Ordovician sedimentary bedrock /Ingemar and Morborg 1976/. The calcite-rich overburden was transported from Gävlebukten and deposited in the Forsmark area during the latest glacial period /SKB 2005c/, and a calcite content of as much as 18–24% have been measured in till samples from the area /Tröjbom and Söderbäck 2006/.

In Figure 4-8, where Ca is plotted versus HCO_3, two distinct sources of Ca may be distinguished: the straight 1:1 line indicates that dissolution and precipitation of calcite plays a major role in the dynamics of Ca in surface waters and shallow groundwater. Weathering of Ca-bearing silicates is also a potential Ca source, however this process probably plays a minor role compared to the abovementioned sources in most water types in the Forsmark area.

Some soil tubes and the major part of the deeper observations in cored and percussion drilled boreholes plot above the 1:1-line. This may either be interpreted as influence from an alternative Ca source, shield brine, or alternatively withdrawal of HCO_3 by reactions. In practice, there is probably a combination of the two alternatives, but with support from a similar Cl pattern (cf Section 4.1.1) it may not be excluded that the observed Ca excess have its origin in shield brine. In such case, some shallow objects located in till below lakes and sea display possible deep water signatures (cf Section 3.2.4).

A cluster of rather shallow boreholes and a few soil tubes plot below the 1:1-line, indicating deficiency of Ca if the original Ca source is assumed to be calcite. Ion exchange may be an explanation to this pattern, which is also evident for a number of other parameters (cf cation exchange in Section 4.2.1). Moreover, supply of biogenic HCO_3 may contribute to the observed deviation, but this HCO_3-source is probably not sufficient to explain more than a fraction of the observed pattern; the lowest located observations in this cluster is hard to explain by this process which shift observations horizontally from left to right.

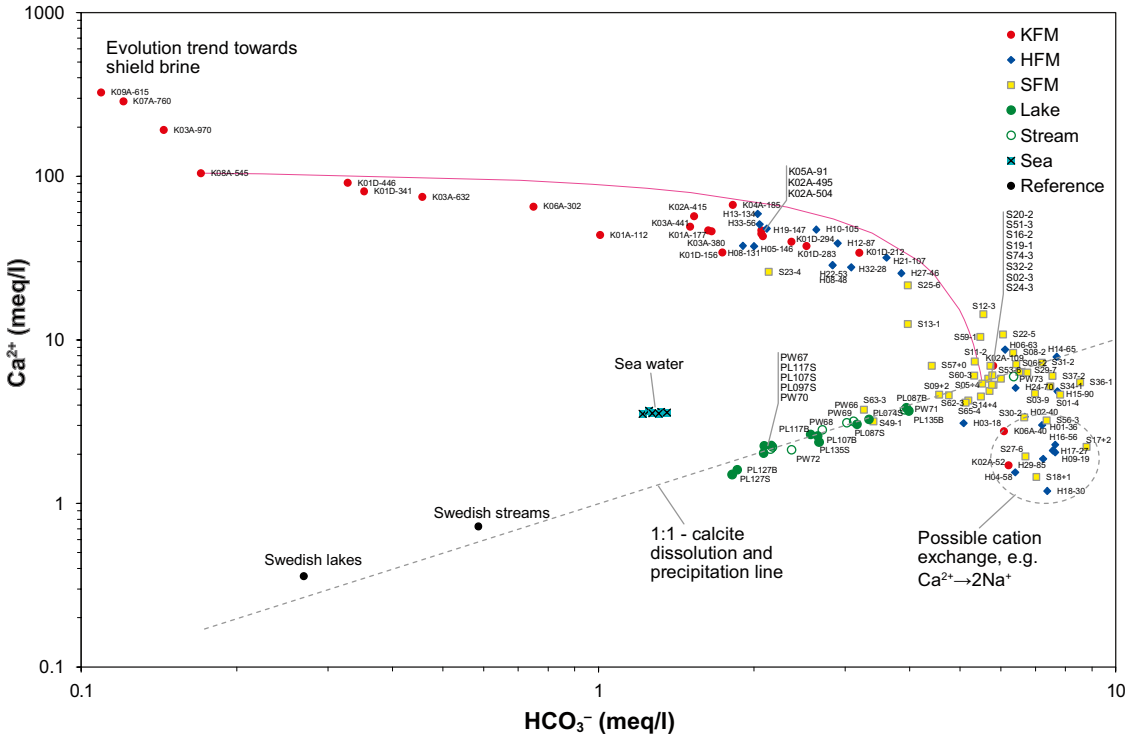

Figure 4-8. *Ca versus HCO_3 (meq/L). The grey dashed line indicates the 1:1 molar (charge) relationship between Ca and HCO_3.*

In order to understand the origin and fate of Ca, the closely related element Sr may be a supportive parameter. As different sources may have differing Ca/Sr ratios, this ratio, possibly in combination with isotopic composition of Sr, may discriminate among different Ca sources. These bivalent elements, which e.g. are able to substitute in mineral lattices, are also differently affected by specific processes which may reflect the evolution of groundwater.

In Figure 4-9, Ca is plotted versus Sr. In this log-log scaled diagram, observations that have the same Ca/Sr ratio are plotting along diagonal straight lines. From this picture the two major Ca sources, calcite and shield brine, are evident, as they show very different Ca/Sr ratios. Most soil tubes, possibly influenced by calcite, plot along a Ca/Sr ratio of 1,200, whereas shield brine shows a likely Ca/Sr ratio around 200. As a comparison, the Ca/Sr molar ratio in till samples from the Forsmark area is ranging from 600–2,600, with a median of 2,300. Thus, the till samples may be slightly more enriched in Ca compared to the water samples influenced by calcite (Figure 4-10). The median molar ratio in till of 2,300 corresponds to a Ca/Sr mass ratio of about 5,000.

A number of observations from shallow groundwater (and also some surface water samples), may, with respect to Ca and Sr, be explained by mixing between a calcite influenced water and modern sea water, according to the hypothetical mixing scenarios in Figure 4-9. There are, however, a few observations which plot outside these scenarios, reflecting possible resemblance to deeper groundwater types in the bedrock (e.g. SFM0012 and SFM0023).

Many deep observations from foremost percussion drilled boreholes, as well as some shallow groundwater objects, plot along a Ca/Sr ratio of about 300. Possible explanations to this pattern is outlined in Section 4.2.1, dealing with cation exchange.

By using Sr isotopes, further information on the origin of Ca may be revealed. The isotopic ratio $^{87}Sr/^{86}Sr$ has been measured in a subset of samples, and in Figure 4-11 is the molar Ca/Sr ratio (corresponding to the straight lines in Figure 4-9) plotted versus the $^{87}Sr/^{86}Sr$ ratio.

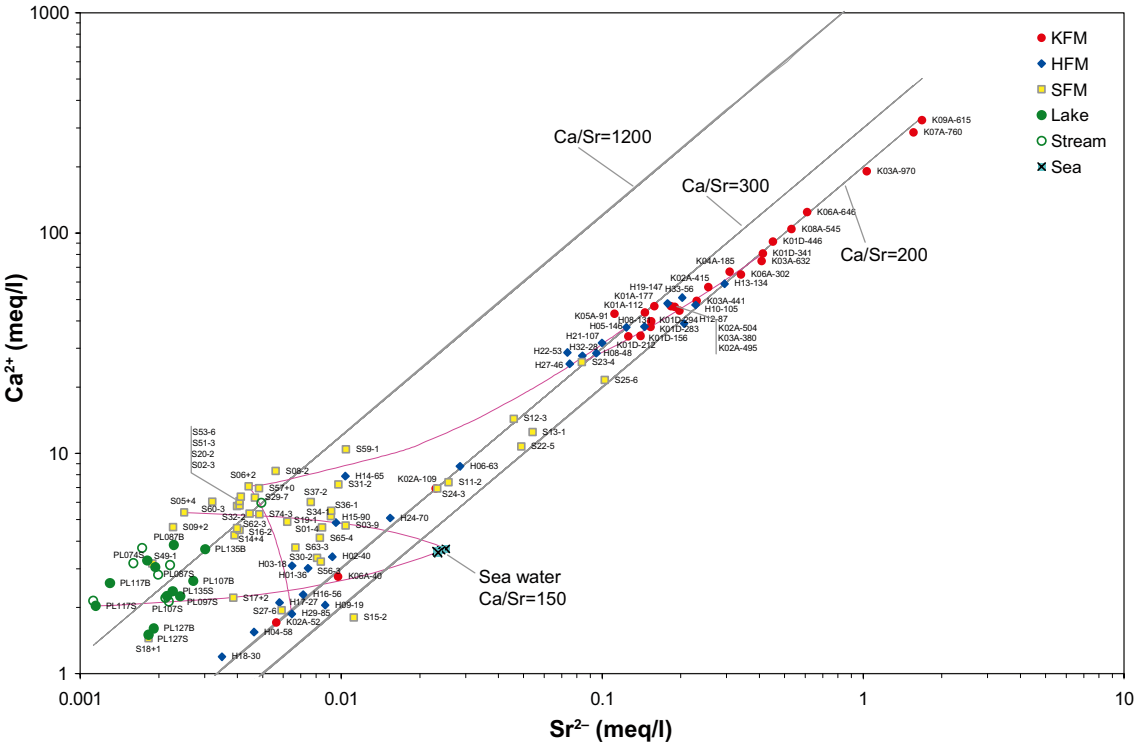

Figure 4-9. *Ca^{2+} versus Sr^{2+} (meq/L). Dashed grey lines in the log-log scaled diagram connects observations of the same Ca/Sr ratio. The figure is based on data selection C, cf Section 2.2.4. Explanation of labels, symbols and lines are given in Sections 2.3.12 and 2.3.13.*

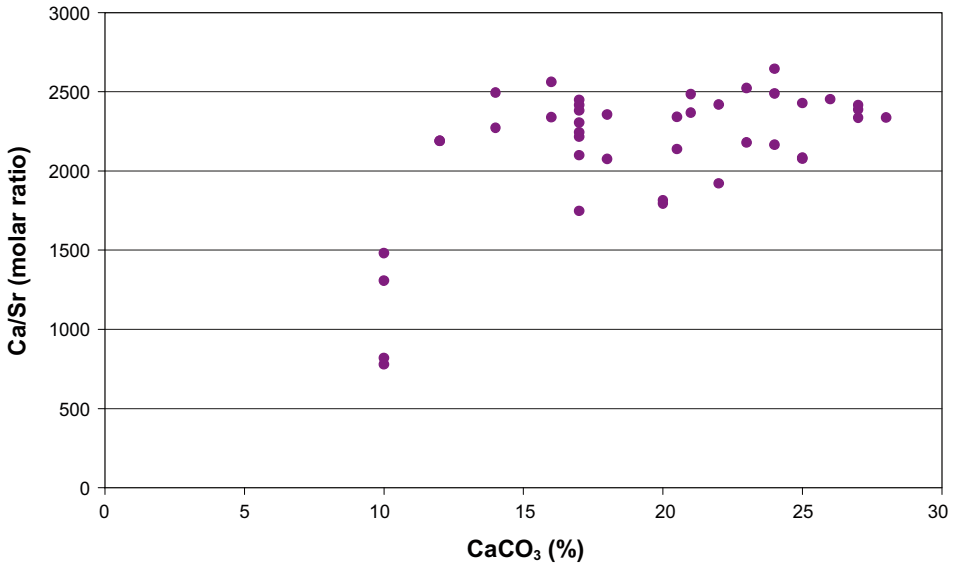

Figure 4-10. *Molar Ca/Sr ratio in till samples from Forsmark versus the measured contents of $CaCO_3$ (% of dry weight). The median molar ratio is 2,300, which corresponds to a Ca/Sr mass ratio of about 5,000.*

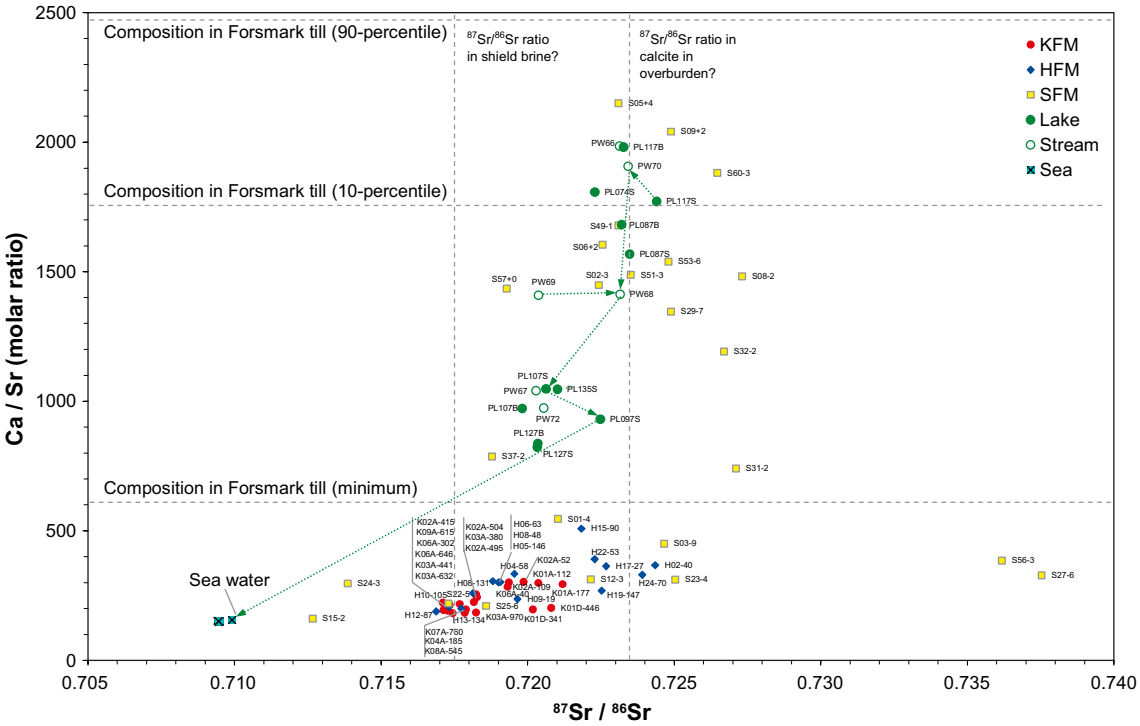

Figure 4-11. *Ca/Sr ratio versus the isotopic ratio of $^{87}Sr/^{86}Sr$. The grey lines denote the molar Ca/Sr ratio in till samples from the Forsmark area. The figure is based on data selection C, cf Section 2.2.4. Explanation of labels, symbols and lines are given in Sections 2.3.12 and 2.3.13.*

There is a clear discrimination of the Forsmark water types by these three parameters. Most soil tubes and surface waters form an extended cluster with a high Ca/Sr ratio and fairly uniform $^{87}Sr/^{86}Sr$ values. Deeper observations in percussion drilled and cored boreholes show a significantly lower ratio and overlapping $^{87}Sr/^{86}Sr$ values, but with a tendency towards depleted (lower) values when the medians are compared.

Modern sea water deviates by showing a significantly depleted $^{87}Sr/^{86}Sr$ ratio, and surface waters influenced by intrusions of modern sea water (cf Section 4.1.1) show a mixing trend towards the marine end-member, as shown by the dashed green downstream evolution line. Two soil tubes, SFM0024 and SFM0015, plot close to samples from sea water, indicating a possible marine origin of Sr.

At the other end of the horizontal scale, two soil tubes (SFM0027 and SFM0056) located in the south-eastern part of the Forsmark area are highly enriched in ^{87}Sr, perhaps reflecting a different local mineralogy.

Any interpretation of Figure 4-11 is ambiguous, since many factors may influence the isotopic composition of Sr. Besides the processes involving calcite, i.e. dissolution and precipitation, local mineralogy and ion exchange may influence the $^{87}Sr/^{86}Sr$ ratio.

With these reservations in mind, there seems to be a difference in the $^{87}Sr/^{86}Sr$ ratio between brine and calcite, probably also reflecting the different origins of Ca. Some percussion drilled boreholes and soil tubes below lake sediments show a $^{87}Sr/^{86}Sr$ ratio similar to that in shallow groundwater (0.7235), which is probably also reflecting the isotopic Sr-composition of calcite in the Quaternary deposits (there are at present date no information available about the isotopic composition of the calcite). These observations coincide approximately with the objects in Figure 4-8 that form a cluster marked as possible influence from cation exchange (cf Figure 4-2, and Section 4.2.1). Although not overall consistent, this pattern may be interpreted as if Ca and Sr, originating from calcite in the overburden, are affected in different ways by ion exchange during the infiltration through the sediments.

Another possible source of Ca is congruent dissolution of dolomite, forming equal molar amounts of Ca and Mg. In Figure 4-12 where Ca is plotted versus Mg, straight diagonal lines connect observations with the same Ca/Mg ratio. In samples from the surface and shallow waters, which are more or less strongly influenced by the calcite rich overburden, the Ca/Mg ratio scatters around 7.5, a value clearly exceeding the theoretical ratio of 1 for dolomite. This finding rejects dolomite as a major source of Ca and Mg in the Forsmark area.

In surface water at lower topographical levels, and in groundwater at greater depths, Mg is most probable supplied from a modern or relict marine source. According to the hypothetical mixing lines drawn in Figure 4-12, most observations in the surface system may be explained by mixing sea water of modern or slightly elevated salinity, e.g. Littorina, with Mg of calcite origin.

Very deep groundwater clearly influenced from Ca rich shield brine, show rapidly decreasing Mg concentrations in combination with steadily increasing Ca concentrations. The very low Ca/Mg ratio of Laxemar shield brine /Laaksoharju (ed.) in prep./ is concordant with this trend.

The major conclusions regarding the origin of calcium are summarised in the bullet list below:

- The very high calcium levels observed in surface water and shallow groundwater in the Forsmark area is a consequence of the calcite-rich Quaternary deposits that cover the Forsmark area.
- There are clear indications that dissolution and precipitation of calcite plays a major role in the dynamics of Ca in surface waters and shallow groundwater in the Forsmark area. Weathering of Ca-bearing silicates is also a potential Ca source, however this process probably plays a minor role compared to the abovementioned sources in most water types in the Forsmark area.
- Supply of Ca of deep saline origin (shield brine) is probable an significant Ca source in the groundwater of the bedrock. Also the composition of some shallower objects is difficult to explain without this deep Ca source, e.g. SFM0023 below Lake Bolundsfjärden, where the circumstances is similar for Cl (cf Section 4.1.1).

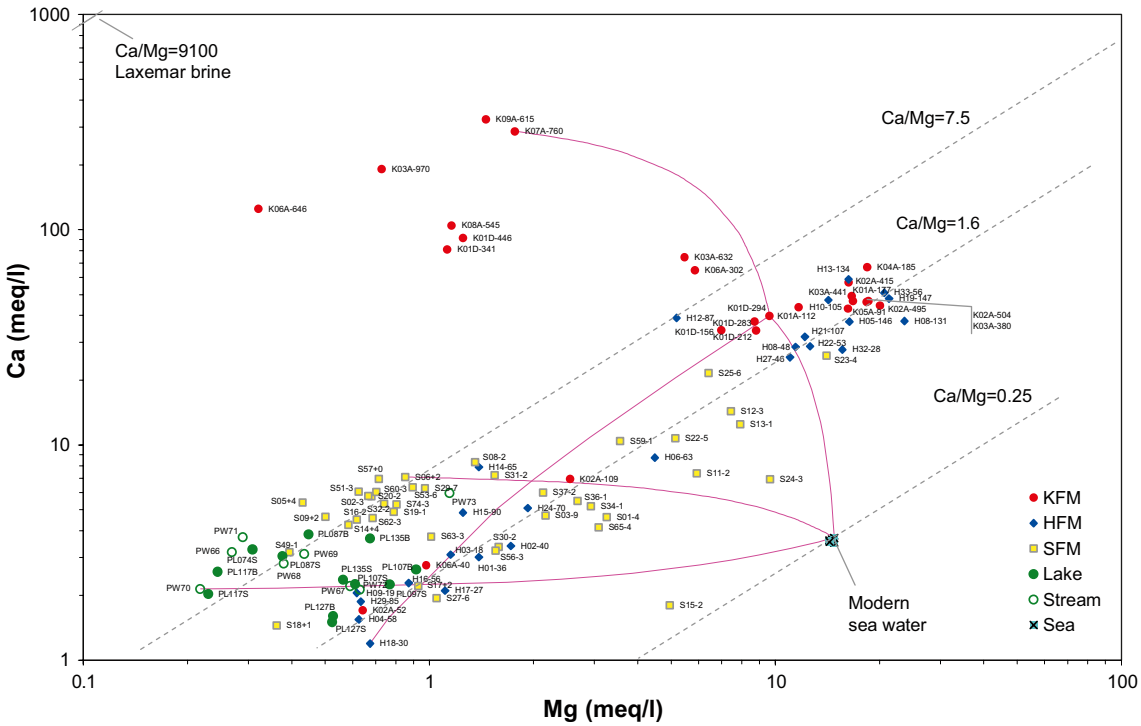

Figure 4-12. *Ca versus Mg (meq/L). Dashed grey lines in the log-log scaled diagram connects observations of the same Ca/Mg ratio. The figure is based on data selection C, cf Section 2.2.4. Explanation of labels, symbols and lines are given in Sections 2.3.12 and 2.3.13.*

- Dolomite is probably a minor source of Ca in the Forsmark area, as the Ca/Mg molar ratio in samples from the surface and shallow waters, scatters around 7.5, a value clearly exceeding the theoretical ratio of 1 for dolomite.
- Carbon isotope measurements support calcite dissolution in soil tubes, but show contradictory little evidence in surface waters (cf Section 4.1.4).

4.1.4 On the origin of carbon

Carbon in groundwater and surface water originate from the atmospheric carbon pool, from carbonates in the rock and overburden, and from microbial reactions involving fossil organic carbon relics at the site. Moreover, geogenic carbon from may also contribute at deeper levels.

Different reactions may act as sinks for carbon. Organic carbon is originally formed during photosynthesis and CO_2 assimilation from the atmosphere by plants and algae. This fixed carbon is gradually returned to the atmosphere as CO_2 during respiration by animals and bacteria. In soil, biogenic degradation of organic matter (respiration) often causes very high partial pressures of CO_2, leading to high concentrations of dissolved inorganic carbon. Precipitation of carbonates may transfer carbon to the geosphere, whereas for example biogenic processes as methanogenesis and respiration transfer carbon to the atmospheric pool.

In water, carbon occurs either as inorganic or organic compounds. Inorganic carbon involve the carbonic acid dissociation series, ranging from dissolved $CO_{2(aq)}$, to hydrated carbon dioxide (H_2CO_3 – carbonic acid), bicarbonate ions (HCO_3^-) and carbonate ions (CO_3^{2-}). The equilibrium between these species is determined by pH, and at the slightly basic conditions that prevail in the Forsmark area, most dissolved inorganic carbon, DIC, occur as HCO_3^-.

Most organic carbon enters the groundwater as dissolved organic carbon, DOC, and may be transported to deeper levels by the recharging meteoric water. In the presence of oxygen, DOC is oxidized by aerobic bacteria, forming CO_2 which contributes to DIC. When all oxygen is consumed, anaerobic bacteria take over and consume DOC using electron acceptors as NO_3^-, Fe^{3+}-oxihydroxides or SO_4^{2-}. Ultimately, methane is formed by bacteria when all other electron acceptors are depleted.

Different carbon sources often show typical carbon-isotope signatures which reflect the involved reactions. Reactions mediated by bacteria are usually accompanied by large isotope fractionations that are clearly visible in the proportions of the stable carbon isotopes ^{12}C and ^{13}C. Radiogenic ^{14}C, which is naturally formed in the upper atmosphere and present in all living matter at very low concentrations, may discriminate between modern carbon and different sources of relict carbon due to the half-life of 5,730 years (cf Section 3.5.2 dealing with age dating by ^{14}C).

The ratio between the stable isotopes $^{13}C/^{12}C$ is measured on dissolved carbon, predominantly HCO_3^-, in shallow groundwater and surface water in the Forsmark area. The relative deviation of this ratio from the international ^{13}C-standard PDB is expressed per mill, and denoted $\delta^{13}C$. Atmospheric $\delta^{13}C$ is nowadays decreasing from originally about –6.4‰, due to the extensive burning of fossil carbon depleted in ^{13}C.

Radiogenic ^{14}C is expressed in percent modern carbon, denoted pmC. The ^{14}C activities have not been constant throughout time and there is evidence that suggests a variation between 97 and 140 pmC since the last glacial maximum about 35,000 years ago. Pre-modern initial ^{14}C activities extending one half-life back in time range from 97 to 106 pmC /Clark and Fritz 1997/. In modern time, anthropogenic impact due to the atmospheric nuclear bomb tests during the fifties and sixties almost doubled radiogenic ^{14}C activities from 100 to nearly 200 pmC. At present date, ^{14}C activities in the atmosphere has decreased to about 110 pmC, not primarily due to decay, but as an effect of dilution with the large carbon pool in the oceans. Local increases are also observed in the vicinity of nuclear power stations (cf Section 3.5.3).

The distribution of dissolved carbon in different water types in the Forsmark area is outlined in Figure 4-13. Dissolved organic carbon, HCO_3 (approximately corresponding to DIC), $\delta^{13}C$ and ^{14}C isotopes are projected onto the ion source model (cf Section 3.2.3), which separate Forsmark water observations based on the contents of dissolved major ions.

- High concentrations of *dissolved organic carbon*, DOC, are predominant in surface water and shallow groundwater, and decrease towards depth where water types influenced by relict marine (Littorina) and shield brine dominate. In fresh surface water, DOC concentrations often reach 20 mg/L, whereas typical concentrations in shallow groundwater are around 10 mg/L (cf /Tröjbom and Söderbäck 2006/ and /Sonesten 2005/ for further details). In most lakes in the Forsmark area, *very high* concentrations of total organic carbon is measured according to the Swedish environmental quality criteria /Naturvårdsverket 2000/. From Figure 4-13 it can also be concluded that DOC in shallow groundwater, as well as in the upper part of the bedrock, may reach very high levels (e.g. SFM000, SFM0037, HFM19), which gives the prerequisites for drastic alterations of redox conditions in groundwater.
- *Dissolved inorganic carbon*, represented by HCO_3, which is the dominating constituent of DIC in most Forsmark water types, reach very high levels in both surface water and shallow groundwater. Compared to the national distributions, HCO_3 levels in the Forsmark area are exceeding the 90th percentile of the Swedish national surveys of both shallow groundwater in wells, as well as in lakes and streams /Tröjbom and Söderbäck 2006, Sonesten 2005/. This pattern is similar to the situation for Ca described in Section 4.1.3, where the calcite-rich overburden in the Forsmark area is described as the main factor leading to high Ca and probably also to high HCO_3 concentrations. At greater depths in the bedrock, particularly where the influence of shield brine increase, HCO_3 levels decrease to very low concentrations.

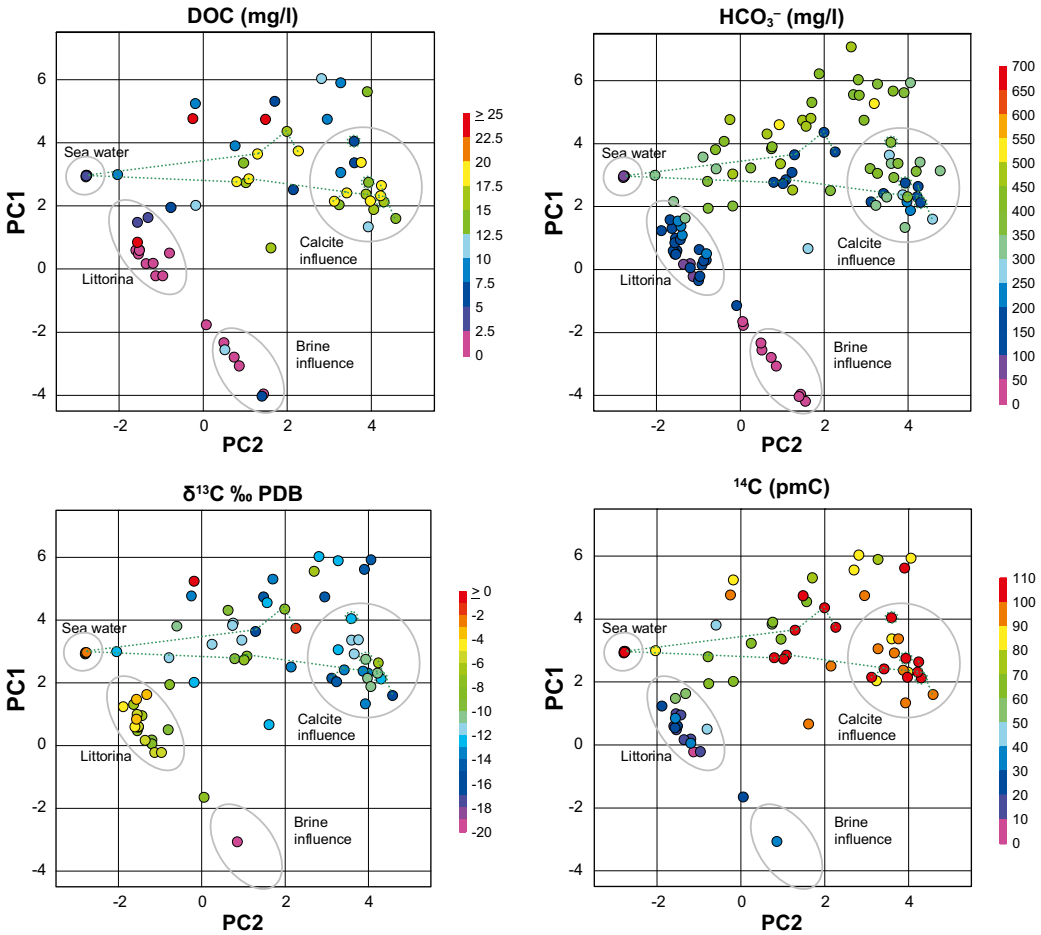

Figure 4-13. *Different carbon parameters projected onto the ion source model (cf Section 3.2.3). The figures is based on data selection C, cf Section 2.2.4. Bottom samples from lakes and sea have been excluded in this figure.*

- For $\delta^{13}C$, shown in the lower left panel of Figure 4-13, surface water and shallow groundwater in the upper half of the figure usually display negative values that range between –10 to –16, probably reflecting influence from biogenic processes (cf Figure 4-14). Modern sea water, as well as the cluster of groundwater observations in the bedrock displaying relict marine signatures (marked Littorina), show only slightly negative $\delta^{13}C$ values. The single observation from KFM06 at 646 metres depth (RHB70) that show highly negative $\delta^{13}C$ values may be an artefact due to difficulties in the determination of the isotopic composition at very low carbon concentrations (cf ^{14}C below).
- Radiogenic ^{14}C, shown in the lower right panel of Figure 4-13, reflects the proportion of modern carbon in the sample. As discussed in Section 3.5.2, this value is, beside the radioactive decay, also influenced by the initial conditions, and by the dilution of non-radiogenic carbon from dissolution of carbonates (calcite). Most surface samples in the upper half of the figure show ^{14}C activities corresponding to a fraction of more than 50% percent modern carbon, whereas objects plotting within the relict marine cluster (marked Littorina) usually contain less than 30% modern carbon. Due to the very low carbon concentrations (e.g. HCO_3) that prevail at greater depths, the determination of ^{14}C activities in these samples is ambiguous and impaired with high uncertainties.

When looking at $\delta^{13}C$ versus HCO_3 in Figure 4-14, most observations in surface water and shallow groundwater plot within a $\delta^{13}C$ span limited in the lower end by dissolved $HCO_{3(aq)}$ ($\delta^{13}C$ –15.5‰ PDB), and in the upper end by the atmospheric $\delta^{13}C$ of –7‰ PDB. At pH 7.25, a typical value in shallow groundwater in the Forsmark area /Tröjbom and Söderbäck 2006/, dissolved $HCO_{3(aq)}$ derived from biogenic $CO_{2(g)}$ ($\delta^{13}C$ –23‰ PDB) shows a theoretical $\delta^{13}C$ value of about –15.5 at 25°C, due to fractionation during hydration of $CO_{2(aq)}$ /Clark and Fritz 1997/.

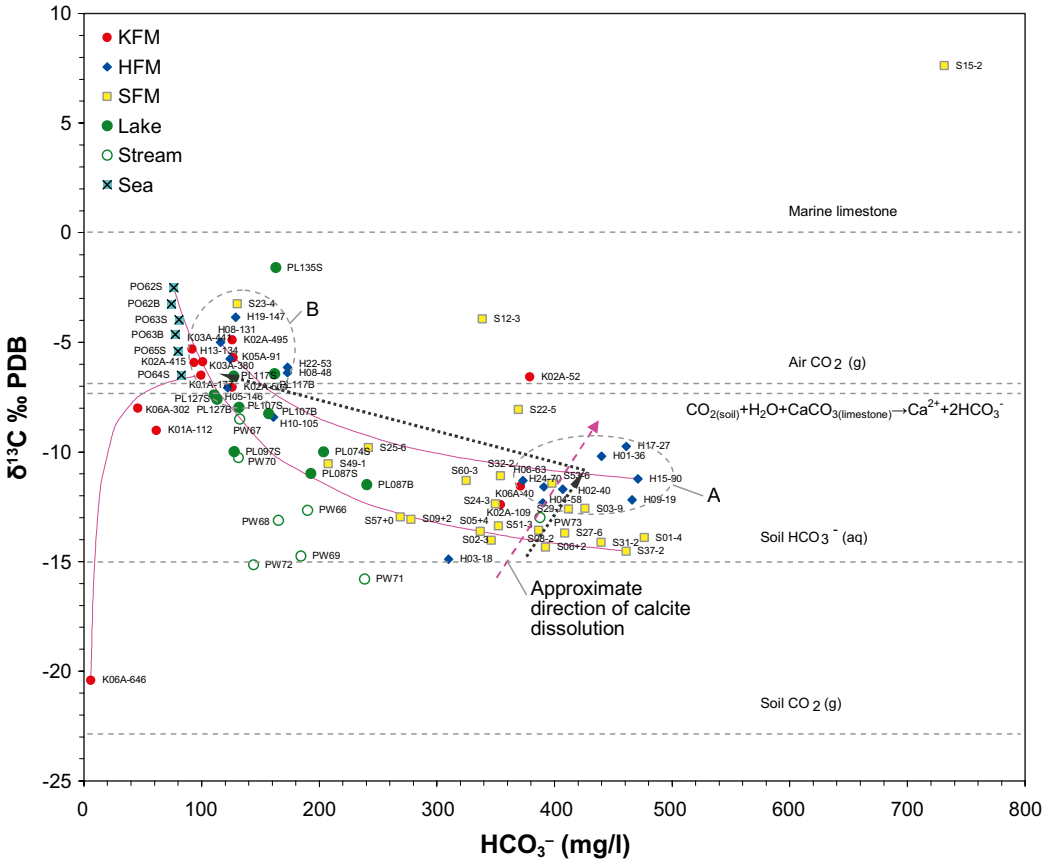

Figure 4-14. *^{13}C expressed as the ‰ deviation from the international standard PDB versus HCO_3 (mg/L). This figure is based on data selection C, cf Section 2.2.4. Explanation of labels, symbols and lines are given in Sections 2.3.12 and 2.3.13.*

Marine limestone usually has a $\delta^{13}C$ deviation from the international standard PDB (cf 2.3.3) of about 0‰. The addition of carbon enriched in ^{13}C during calcite dissolution shifts the original $\delta^{13}C$ values towards more positive values, and if all H^+ that drive the calcite dissolution are derived from dissolved biogenic CO_2, the theoretical maximum $\delta^{13}C$ value is –7.5‰ PDB (50% carbon from calcite, 50% from biogenic CO_2 according to the formula in Figure 4-14). The approximate direction of calcite dissolution is marked in Figure 4-14, a process that leads to a net supply of HCO_3 in combination with enriched $\delta^{13}C$ values. The elevated $\delta^{13}C$ values in many soil tubes in Figure 4-14, compared to the theoretical biogenic soil solution value given by /Clark and Fritz 1997/, may be interpreted as supply of HCO_3 from calcite dissolution, a conclusion concordant with the patters shown by Ca in combination with other parameters (cf Section 4.1.3). Also the location of the cluster of percussion drilled boreholes denoted "A", representing groundwater in the upper part of the bedrock, may be explained by supply of HCO_3 originating from calcite dissolution in the sediments (cf the possible role of sediments for cation exchange in Section 4.2.1). In samples from deeper groundwater, this HCO_3 supply may explain the slightly elevated HCO_3 concentrations observed in the relict marine cluster "B", compared to the levels in modern sea water.

The radiogenic isotope ^{14}C may in combination with $\delta^{13}C$ reveal further information on the origin of carbon. In Figure 4-15, $\delta^{13}C$ is plotted versus ^{14}C activity expressed as percent modern carbon. A variant of this plot is denoted "*the age model*" in Figure 3-27 (see Section 3.5.2 dealing with age dating with ^{14}C).

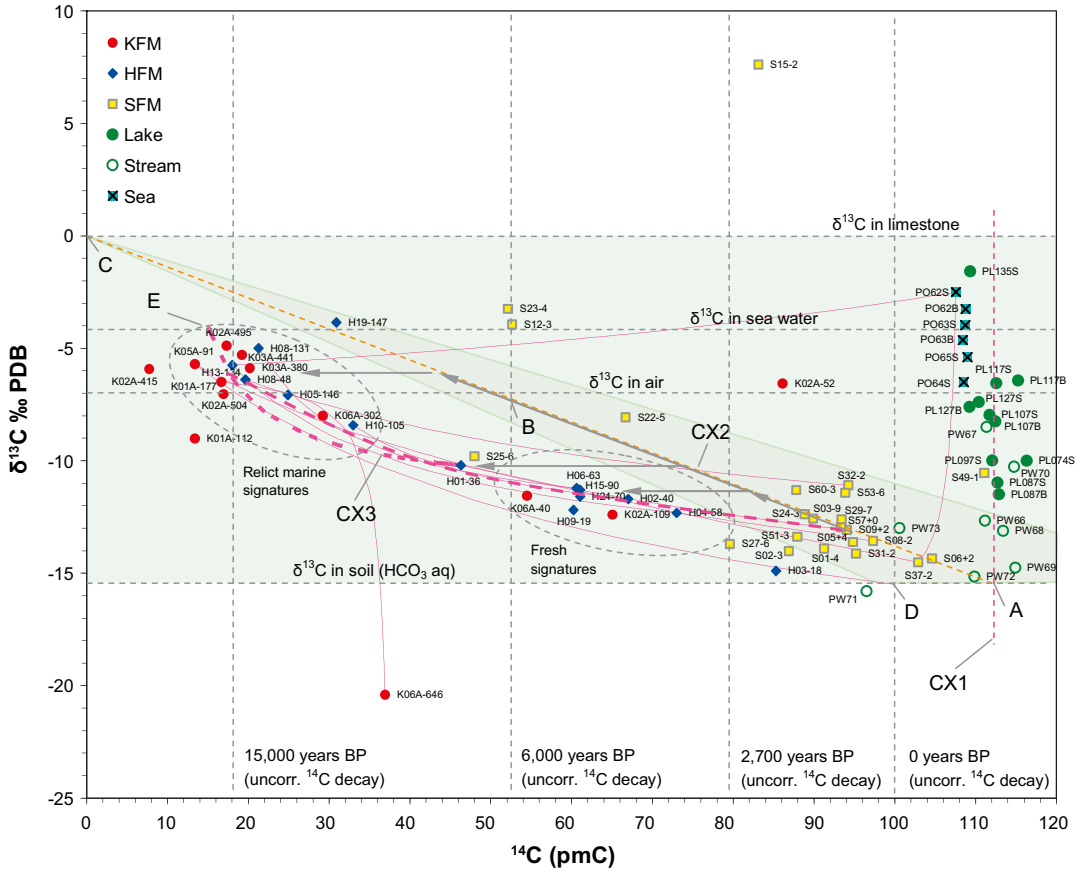

Figure 4-15. *^{13}C expressed as the deviation from the international standard PDB, versus ^{14}C activity, expressed as percent modern carbon (pmC). The yellow dashed line and the green area indicate the span of the ^{13}C-correction model used for estimating dilution due to dissolution of calcite and arrows mark hypothetical evolution paths (see text for further explanations). This figure is based on data selection C, cf Section 2.2.4. Explanation of labels, symbols and lines are given in Sections 2.3.12 and 2.3.13.*

Most observations from fresh surface waters form a vertical trend, CX1, centred at about 112 pmC, with $\delta^{13}C$ ranging from –15.5 ‰ PDB (soil $HCO_{3(aq)}$) to about –7 ‰ PDB (air $CO_{2(g)}$). Small lakes and streams show $\delta^{13}C$ values more close to the theoretical soil solution, whereas large lakes with longer retention times (e.g. Lake Eckarfjärden, PL117) show $\delta^{13}C$ values more close to the atmospheric carbon composition. This trend probably reflects the extent of equilibration with the atmospheric isotopic composition; the longer time for equilibration (i.e. longer retention time), the closer the observation will plot to a $\delta^{13}C$ value of –7 ‰ PDB. According to mass-balance calculations reported in /Nordén et al. in prep/, the small Lake Labboträsket in the Forsmark area is oversaturated with respect to CO_2, whereas Lake Eckarfjärden and Lake Bolundsfjärden are under-saturated. This is in accordance with the isotopic pattern as the rich supply of biogenic carbon in the oversaturated lakes should lower the observed $\delta^{13}C$ values.

Most soil tubes plot along the trend CX2, indicating that calcite dissolution may explain the low ^{14}C-activities observed in many of these shallow objects. This line corresponds to the ^{13}C-correction model used in Section 3.5.2 that compensate for the dilution effect of carbon supplied from calcite dissolution. Observations plotting along this line may fully be explained by calcite dissolution, given the assumption that the calcite isotopic signature corresponds to the composition of the zero point ($\delta^{13}C$ 0‰ PDB and ^{14}C activity 0 pmC), and that the dissolution process is driven by H^+ ions derived from biogenic $CO_{2(g)}$ with an isotopic signature in the soil solution ($HCO_{3(aq)}$) of $\delta^{13}C$ = –15.5‰ PDB and ^{14}C = 112 pmC. During closed conditions, calcite dissolution, driven by H^+ of biogenic CO_2 origin, shift observations in Figure 4-15 along "CX2" towards point "B", whereas more or less open conditions mask the contribution from calcite dissolution and reverse the shift towards point "A".

A few shallow groundwater observations (SFM) and most deep observations in percussion drilled (HFM) and cored boreholes (KFM) plot below the "CX2" line, indicating that radioactive decay may have significantly influenced ^{14}C in these objects. Depending on the naturally varying atmospheric ^{14}C activities during the last 35,000 years, a multitude of correction models represented by the green surface ranging from 100 to 140 pmC (at $\delta^{13}C$ –15.5‰ PDB), may be used to correct for both varying initial activities and the dilution effect from calcite dissolution. It should be noted that these corrections is applied merely to explore the limits of the age estimations based on ^{14}C, rather than finding the "true" age (cf Section 3.5.2 for age estimations based on ^{14}C).

There are several possible hypotheses explaining the carbon isotope composition in objects along CX3 in Figure 4-15. Many different combinations of calcite dissolution, ^{14}C decay and mixing of groundwater of different carbon age, may form the observed pattern. For example, the cluster which shows freshwater ion signatures according to the ion source model in Section 3.2.3, may have been formed by a combination of calcite dilution and ^{14}C decay along the evolution path marked by grey arrows. Analogous evolution paths may hypothetically explain all objects along CX3 in a similar manner according to the grey arrows. The upper cluster plotting along CX3, which shows relict marine signatures according to the ion composition, may at point "E" alternatively reflect a marine DIC component of considerable age, assuming that the initial $\delta^{13}C$ corresponds to –4‰ PDB, i.e. similar to modern sea water. The cluster showing relict marine ion signatures may in that case be a mixing product of an old marine component and a recent groundwater influenced by calcite, for example corresponding to H01–36.

Elevated $\delta^{13}C$ values may be formed in the remaining DIC as a result of bacterial methanogenesis, and a few soil tubes representing shallow groundwater in till below lake sediments, show positive deviations from CX2 (SFM0012, SFM0023, and SFM0015). This is particularly evident in SFM0015 below Lake Eckarfjärden, where a series of positive $\delta^{13}C$ values have been measured. In the list below a few shallow groundwater objects are discussed with focus on carbon:

- One possible evolution path for the DIC sampled in SFM0012 (Soil tube below Lake Gällsboträsket) and SFM0023 (soil tube below Lake Bolundsfjärden) may be calcite dissolution, and to a minor extent ^{14}C decay, during closed conditions, perhaps in combination with modern marine influences. High Ca concentrations in the range of 300–500 mg/L support the calcite dissolution path. The vertical position above CX2 may not be explained by methanogenesis due to presence of SO_4 (200–350 mg/L).

- SFM0015 shows on the contrary low Ca (36 mg/L), very low SO_4, high DOC (9 mg/L), and very high HCO_3 (740 mg/L), which in combination with extremely elevated $\delta^{13}C$ values, indicates bacterial methane production. A possible carbon source in this process may be organic carbon with an average age of a few thousands years in the sediments, a conclusion supported by the very high content of dissolved nitrogen and phosphorus (Figure 4-16). There are both hydrological /Juston et al. 2006/ and isotopic (cf Section 3.3.3 dealing with ^{2}H and ^{18}O) indications that Lake Eckarfjärden may function as a recharge area during dry periods, where lake water may reach the till below the lake sediments, perhaps after percolating the sediments.
- SFM0022 located in till below the sediments of Lake Fiskarfjärden, deviate significantly from most other soil tubes by plotting far along the CX2 line. This deviation may be explained by calcite dissolution under closed conditions, driven by H^+ of biogenic CO_2 origin. According to Figure 4-17, the composition in this soil tube may rather speculatively be explained by mixing between a groundwater altered by ion exchange and relict marine sea water.

There is a large variation in *total organic carbon* content in shallow groundwater and concentrations in the range of 10–20 mg/L are usually measured (Figure 4-16). Some soil tubes below lakes show however low organic content (e.g. SFM0012, SFM0022, SFM0023), in combination with high concentrations of nitrogen and low phosphorus content. This indicates that oxidation of organic matter may have played a role in the evolution of these groundwaters.

In conclusion, it is not possible to discriminate among different evolution paths only by examining carbon, but in combination with other parameters these hypotheses may contribute to the understanding of the role of the sediments in the Forsmark area, and ultimately, the evolution of the relict marine groundwater that seem to be present in shallow groundwater below some of the lakes.

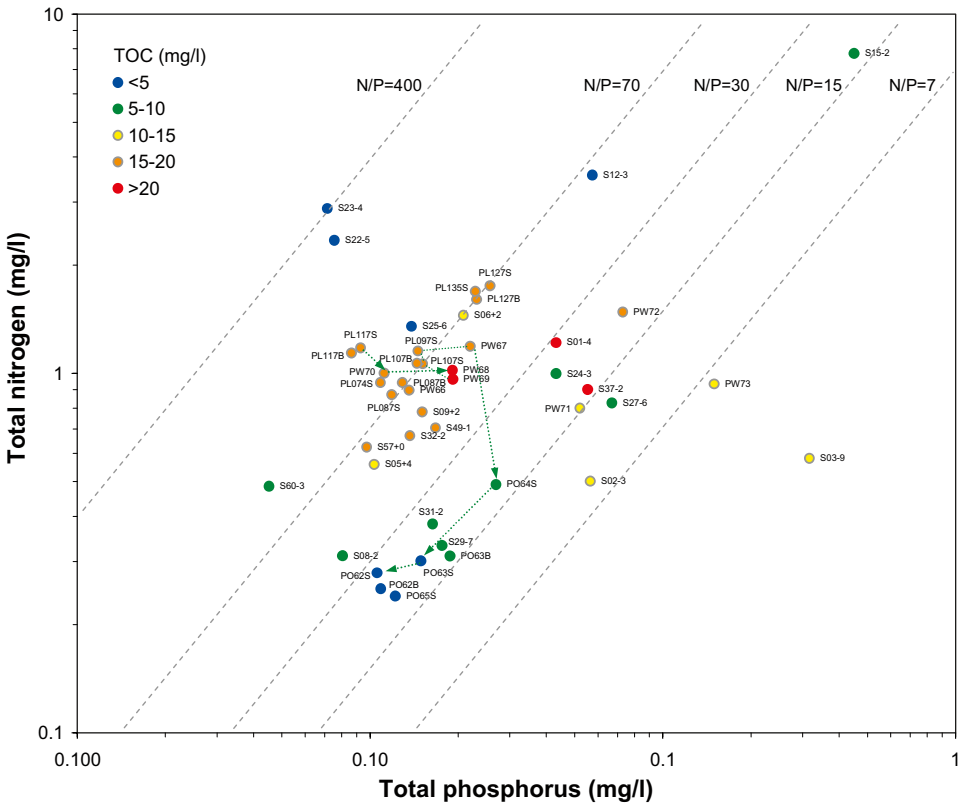

Figure 4-16. *The coupling of organic carbon to nitrogen and phorphorus in surface water and shallow groundwater in the Forsmark area. Total concentrations of nitrogen and phosphorus are plotted on the logarithmic axes, and total content of dissolved organic carbon (TOC) is shown as a colour code per object. Surface water samples are based only on data from June to September according to the SEPA /Naturvårdsverket 2000/ guidelines for interpreting the N/P ratio. Dashed grey lines connect points with the same N/P ratio (based on concentrations in mg/L). Observations in shallow groundwater represent mean values of all available samples.*

The major conclusions regarding carbon are summarised in the bullet list below:

- In the Forsmark area, very high concentrations of *total organic carbon* (TOC) are measured in the surface waters according to the Swedish environmental quality criteria. In shallow groundwater, as well as in the upper part of the bedrock, *dissolved organic carbon* (DOC) may reach very high levels which give prerequisites for drastic alterations of redox conditions in groundwater.
- *Dissolved inorganic carbon* (e.g. HCO_3 which is the dominating constituent of DIC in most Forsmark water types), reach very high levels in both surface water and shallow groundwater. Compared to the national distributions, HCO_3 levels in the Forsmark area are exceeding the 90th percentile of the Swedish national surveys of shallow groundwater in wells as well as in lakes and streams.
- According to carbon isotope measurements, calcite dissolution driven by biogenic CO_2 is the main process contributing to the very high DIC concentrations measured in both shallow groundwater and surface water in the Forsmark area.
- Carbon isotope signatures also indicate that bacterial methane production may have occurred in a few shallow groundwater objects. This is especially evident in the soil tube SFM0015, located in till below Lake Eckarfjärden, where a possible carbon source in this process may be organic carbon with an average age of a few thousands years in the sediments.

4.2 Tracing chemical reactions and processes

Besides mere mixing of different end-members, a large number of previous or ongoing chemical reactions and processes contribute to the present composition of the groundwater. This section focuses on a few important processes that alter the water composition, such as ion exchange and in redox reactions. As many reactions are facilitated by bacteria, traces of these reactions are briefly explored. Mineral weathering and calcite dissolution in particular, which are processes that are involved in transfer of solids to dissolved species (and *vice versa*), are discussed in previous sections dealing with the origin of calcium, carbon and sulphur (cf Section 4.1).

4.2.1 Cation exchange in the Quaternary deposits

When aqueous solutions come into contact with rock and soil material, dissolved elements and compounds may interact with mineral surfaces through sorption processes. During ion exchange reactions, dissolved ions switch position with ions of similar charge, adsorbed on mineral or soil surfaces. One example is cation exchange where one Ca^{2+} ion is adsorbed onto the surface and two Na^{+} ions are released to the solution.

A prerequisite for cation exchange is the movement of dissolved ions through a matrix containing exchangeable ions. In the Forsmark area, the ample supply of Ca ions derived from calcite dissolution (cf Section 4.1.3) may function as a driving force of an extensive cation exchange that seems to take place in the overburden. Weathering of minerals in the overburden, supplies the matrix with exchangeable ions as Na^{+}, which is gradually exchanged with Ca^{2+} and released to the solution. The composition of the primordial recharging groundwater may have been considerably altered when the upper parts of the bedrock are reached after percolation through the sediments. The supposed very low recharge rate of the groundwater that reaches the bedrock in the Forsmark area /Aneljung and Gustafsson 2007/ may further strengthen this pattern due to the long residence time. The ultimate driving source of this chain is supply of H^{+} derived from dissolved biogenic CO_2 (cf Section 4.1.4), and perhaps also to some extent from of oxidation of sulphides in the Quaternary deposits (cf Section 4.1.2).

There are indications of ion exchange in several plots, which are summarised in the list below:

- In Figure 4-2, many observations show Na excess compared to the Na/Cl ratio of marine sources. This is especially evident for a group of soil tubes and percussion drilled boreholes marked NX1, which contain a relatively fresh groundwater with no or very weak marine signatures. A possible source of this Na may be weathering in combination with cation exchange driven by calcite dissolution.
- The same observations also protrude in the Ca versus Na plot in Figure 4-17 as well as in the plot of the Ca/Na-ratio versus Cl in Figure 4-18. The composition of this cluster, marked by a dashed grey oval, may be explained by simple $Ca^{2+} \leftrightarrow 2Na^{+}$ exchange according to the included modelling scenario emanating from a typical groundwater composition in the upper part of the overburden.
- If Ca is derived mainly from calcite, HCO_3 should follow a 1:1 charge molar ratio to Ca. In Figure 4-8, where there is a clear 1:1 trend among observations in surface water and shallow groundwater, the above mentioned cluster is distinguished by plotting below the 1:1 line, i.e. Ca occurs in deficit compared to HCO_3 if calcite is the major Ca source. The net reaction of biogenic CO_2-driven calcite dissolution coupled to cation exchange is shown together with sub-reactions in Equation 5.
- Also in Figure 4-9, which show Ca plotted against Sr, the same observations form a deviating cluster in the lower left part of the figure. This pattern may be interpreted as if Ca and Sr, originating from calcite in the overburden, are discriminated differently by an ion exchange process during the infiltration through the sediments, resulting in an altered Ca/Sr ratio. As these observations plot below the mixing line with sea water, this pattern is not solely explained by mixing with a marine influenced groundwater component.

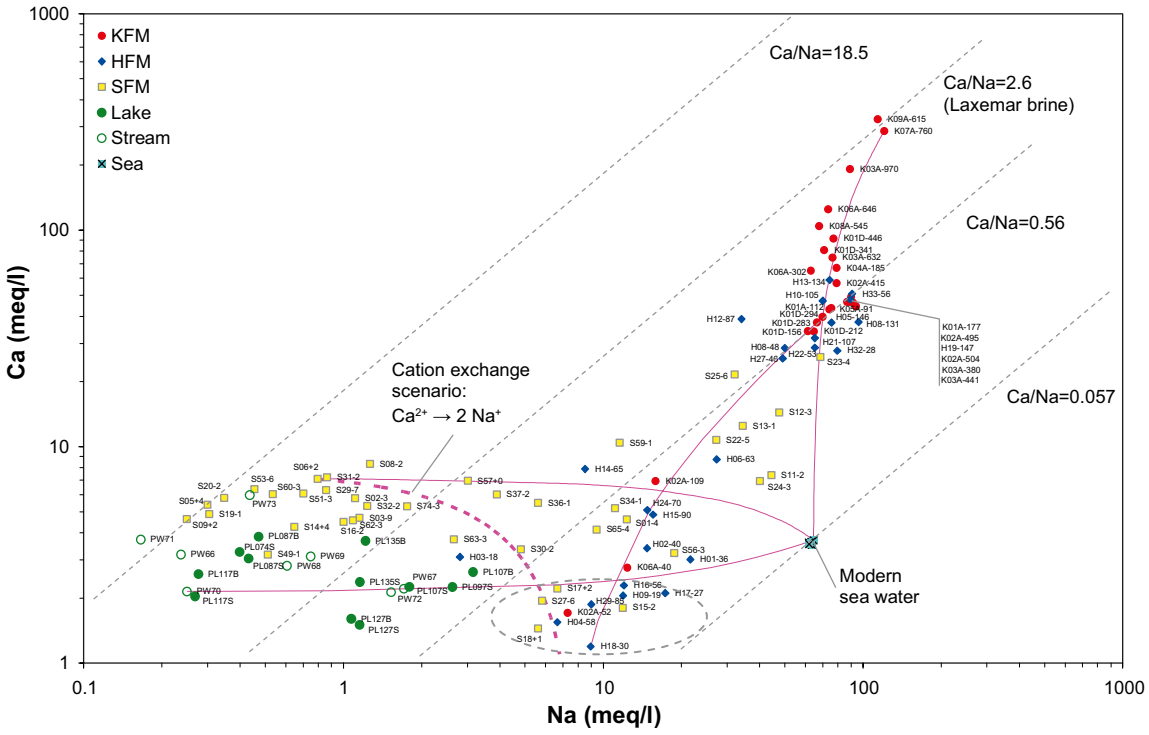

Figure 4-17. *Ca versus Na (meq/L). Dashed grey lines in the log-log scaled diagram connect observations with the same Ca/Mg ratio. This figure is based on data selection C, cf Section 2.2.4. Explanation of labels, symbols and lines are given in Sections 2.3.12 and 2.3.13.*

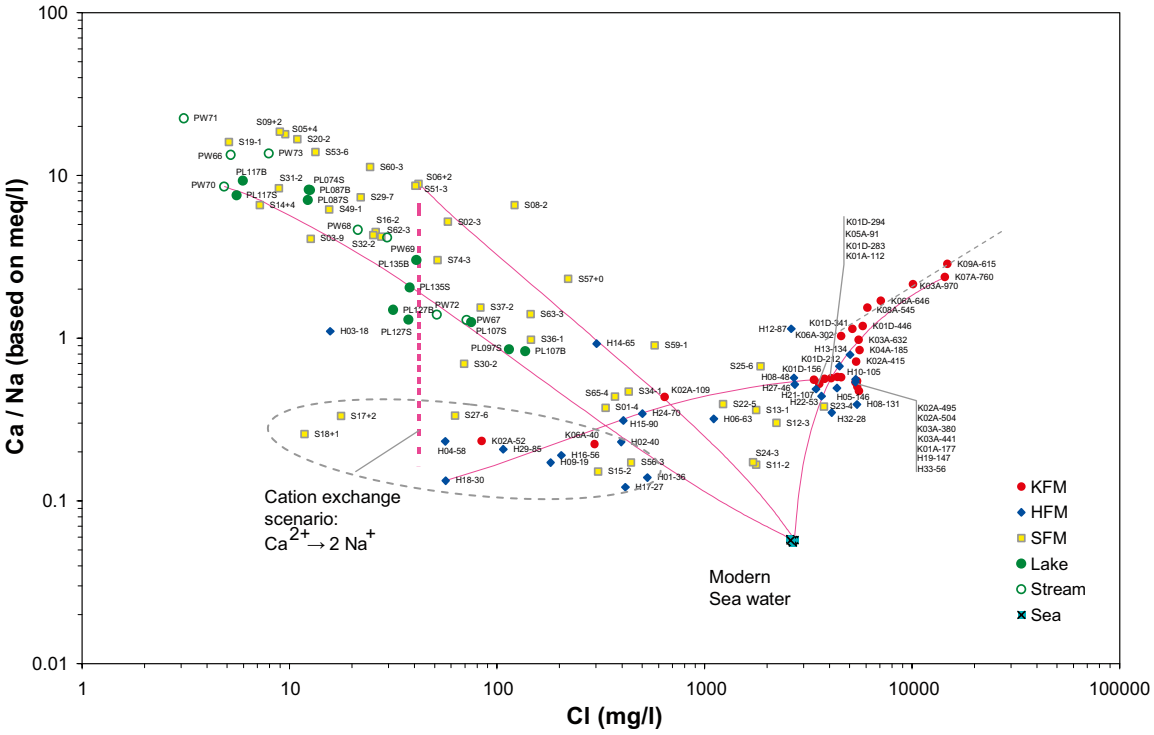

Figure 4-18. *Ca/Na (based on meq/L) versus Cl (mg/L) in water samples from the Forsmark area. Note the logarithmic scales on both axes. The figure is based on data selection C, cf Section 2.2.4. Explanation of labels, symbols and lines are given in Sections 2.3.12 and 2.3.13. Note – as this two dimensional plot is based on three parameters (three degrees of freedom), hypothetical mixing lines drawn between adjacent observations, must not necessarily follow the same path in this 2-dimensional projection.*

Equation 5. Summary of reactions that may take place in the sediments. "X" in the formulas denotes cations adsorbed onto soil or mineral surfaces. The net reaction shows how a groundwater of Na-HCO_3 type may be formed from calcite and biogenic CO_2.

$CO^2 + H_2O \rightarrow HCO^-_3 + H^+$ *(H^+ of biogenic CO_2 origin)*

$CaCO_3 + H^+ \rightarrow Ca^{2+} + HCO_3^-$ *calcite dissolution)*

$2NaX + Ca^{2+} \longleftrightarrow CaX + 2Na^+$ *(cation exchange)*

Net reaction:

$CaCO_3 + CO_2 + H_2O + 2NaX \rightarrow CaX + 2Na^+ + 2HCO_3^-$

The major conclusions regarding cat ion exchange are summarised in the bullet list below:

- In conclusion, there are several clear indications that cation exchange take place in the Quaternary deposits in the Forsmark area. These processes may have great influence on the groundwater composition in the upper part of the bedrock, as well as in some shallow groundwater samples (e.g. SFM0027 located in thick sediments).
- The rich supply of Ca ions in the Forsmark area, derived from calcite dissolution in the Quaternary deposits, is probably one important prerequisite for cation exchange that take place in the deposits during groundwater percolation to the fractured, upper parts of the bedrock. The ultimate driving source of this chain is probably supply of H^+ derived from dissolved biogenic CO_2.

4.2.2 Redox processes

Redox processes involve reactions that transfer electrons between reactants and products, i.e. reduction and oxidation reactions in common speech. Redox conditions in groundwater are controlled by the abundance of electron donors as organic carbon and NH_4, and by electron acceptors as O_2, NO_3, MnO_2, Fe_2O_3, and SO_4. As long as there are electron donors available, electron acceptors are depleted according to the sequence above, until they are consumed. If sufficient organic carbon remains in the system after all SO_4 is depleted, methanogenesis may take place reducing CO_2 to methane (CH_4).

The gradual utilization of different electron acceptors is accompanied by a gradual decrease in redox potential, measured in the field Eh, which in the case of groundwater may reflect the distance and travel time from the recharge area. Eh is however only a relative measure as the potential is controlled both by the abundance of electron donors, and by the availability of different electron acceptors in the system. All redox reactions in groundwater are also facilitated by different types of bacteria.

The redox state may be qualitatively estimated from the abundance of dissolved ions. A long as free $O_{2(aq)}$, NO_3^- and SO_4^{2-} are present, the redox potential is *oxic*. In the *suboxic* range, concentrations of dissolved Mn^{2+} and Fe^{2+} rise as NO_3^- fall to very low levels. If the supplies of reactive MnO_2 and Fe_2O_3 are consumed, SO_4^{2-} is utilized as electron acceptor by the formation of H_2S during *reducing* conditions. Concurrent with the decline in SO_4^{2-}, Fe^{2+} concentrations may decrease due to precipitation of metal sulphides. During methanogenesis methane is formed, and Fe^{2+} may increase again due to the absence of H_2S. It should be noted that this is a simplified, theoretical description of the redox reactions occurring in groundwater systems.

Very high levels of organic carbon in surface water and shallow groundwater in the Forsmark area (cf Section 4.1.4) give prerequisites for low redox potentials even at shallow depths. In Figure 4-19, a selection of parameters reflecting redox conditions are projected onto the ion source model that separate the observations into different groundwater types according to the relative composition of the major elements (cf Section 3.2.3 for further explanation of this multivariate PCA-model).

The evolution of the selected redox-parameters is consistent with the general depth trend, starting at recharging groundwater influenced by calcite, followed by shallow groundwater and groundwater in the upper part of the bedrock (represented by observations plotting along the weathering trend), further down via the relict marine groundwater cluster and finally heading towards deeper groundwater observations characterised by significant shield brine influence:

- DOC and NO_3^- are predominantly detected in the surface water and shallow groundwater whereas deeper observations in the bedrock generally show very low concentrations.
- The highest Fe^{2+} and Mn^{2+} concentrations are found in the relict marine influenced groundwater, whereas deeper levels significantly influenced by shield brine show lower concentrations of these metals.
- SO_4^{2-} decrease among deeper observations significantly influenced by shield brine, which may be explained by microbial sulphate reduction (cf Section 4.2.3). Although not consistent, increased S^{2-} concentrations are also observed at these deeper levels.

4.2.3 Microbially mediated processes

Many chemical reactions in water are mediated by different types of bacteria. In the presence of oxygen, aerobic bacteria degrade organic matter under formation of CO_2. When oxygen levels are low and NO_3 is present, facultative bacteria are able to continue degrading organic matter by using NO_3 instead of O_2 as electron acceptor. When oxygen is totally depleted, anaerobic bacteria continue the degradation of organic matter by using other electron acceptors as MnO_2,

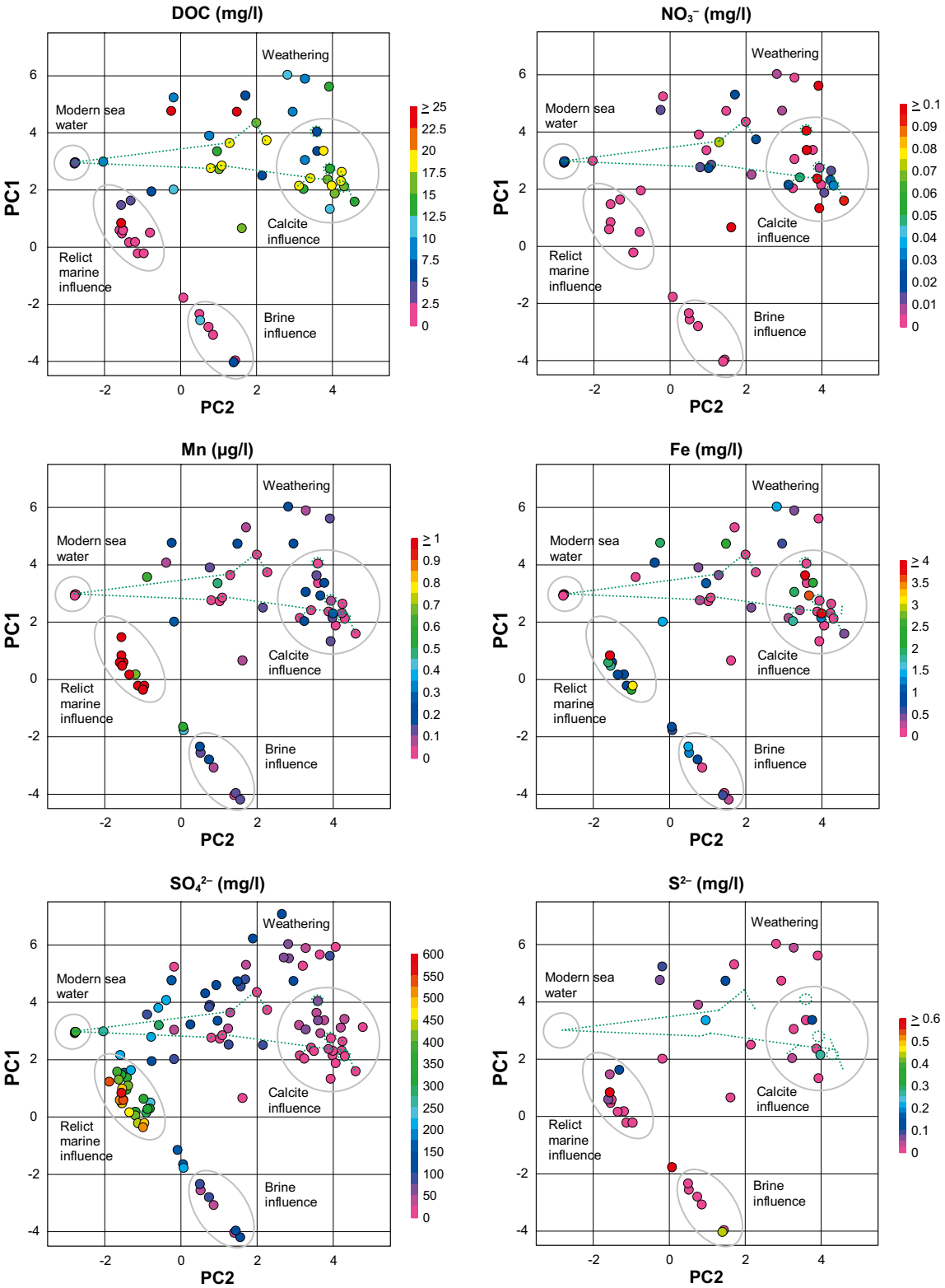

Figure 4-19. *A selection of parameters that reflect redox conditions in groundwater in the Forsmark area. Concentrations (mg/L) of dissolved organic carbon (DOC), nitrate (NO_3^-), manganese (Mn), iron (Fe), sulphate (SO_4^{2-}, and sulphide (S^{2-}) are projected onto the ion source model (cf Section 3.2.3). These figures are based on data selection C, cf Section 2.2.4. Dashed green lines mark surface waters. Bottom samples from lakes and sea have been excluded in these figures.*

Fe_2O_3 or SO_4. In absence of other electron acceptors, CO_2 is, as the last step, fermented into methane (CH_4) by methane producing bacteria. The abundance of different types of bacteria is screened in the cored boreholes in the Forsmark area, and the results and interpretations of these analyses are presented in /SKB 2005b, 2006/.

Bacterial activities make imprints in the hydrochemical parameters measured in groundwater and surface water. The very high HCO_3 concentrations observed in the Forsmark area have most probable biogenic origin according to the $\delta^{13}C$ signatures (cf Section 4.1.4). Bacterial degradation of organic matter in soil lead to very high partial pressures of $CO_{2(g)}$, a prerequisite for the high HCO_3 concentrations and the extensive calcite dissolution that take place in the sediments (cf Section 4.1.3).

In one soil tube, SFM0015 located in till below the bottom sediments of Lake Eckarfjärden, anomalous high $\delta^{13}C$ values may be an indication of methane-producing bacteria that shift $\delta^{13}C$ in the remaining DIC pool towards enriched values. The bacterial fermentation process favours the light isotope, which leads to highly negative $\delta^{13}C$ values in the gaseous methane formed. Accompanying high DOC (9 mg/L), depleted SO_4 and NO_3, in combination with very high DIC (HCO_3 740 mg/L), all support this conclusion. SFM0015 is marked by an arrow in the left panel of Figure 4-20.

Analogically, sulphate reducing bacteria favour the lighter sulphur isotope, leading to positive, enriched $\delta^{34}S$ values in the remaining SO_4 pool. The thereby formed H_2S, or precipitated sulphide minerals, are consequently depleted in ^{34}S, which leads to highly negative $\delta^{34}S$ values in these sulphur pools (cf Section 4.1.2).

The cluster influenced by relict marine sea water show slightly enriched ^{34}S values, indicating that bacterial processed may have altered the composition of this groundwater (cf Section 4.2.1). Deeper observations significantly influenced from shield brine, show low SO_4 concentrations in combination with ^{34}S enrichments in the remaining dissolved sulphur pool, which is a possible sign of ongoing bacterial sulphate reduction.

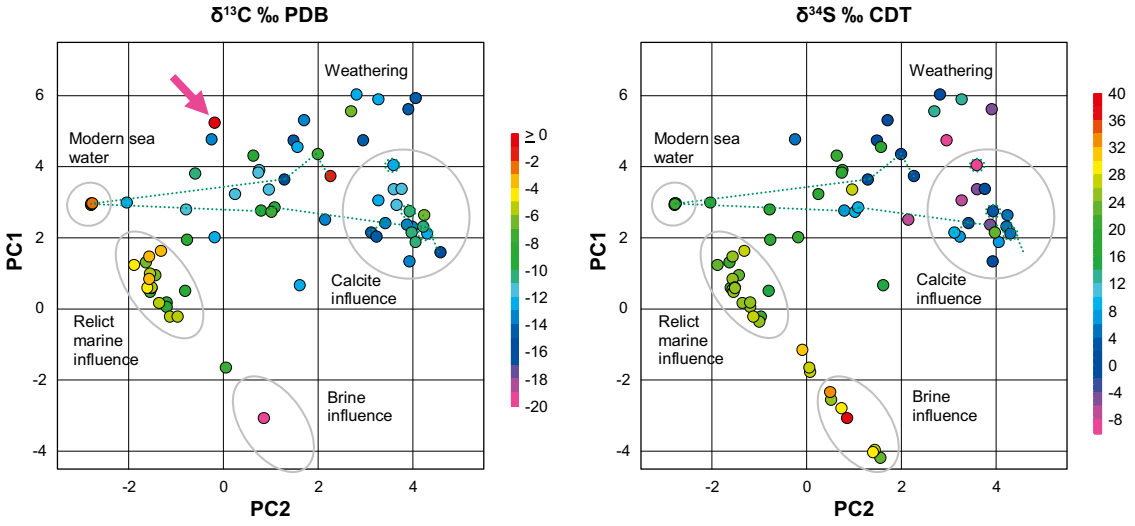

Figure 4-20. *Carbon and sulphur isotopes which are influenced by bacterial fractionation, projected onto the ion source model (cf Section 3.2.3). Isotope ratios are expressed as the ‰ deviation from international standards: $\delta^{13}C$ ‰ PDB and $\delta^{34}S$ ‰ CDT. Based on data selection C, cf Section 2.2.4. Dashed green lines mark surface waters. Bottom samples from lakes and sea have been excluded in this figure.*

4.3 Tracing deep groundwater signatures in the shallow system

In this section, possible indications of discharging deep groundwater signatures detected the shallow groundwater system are summarised. Several visualisations throughout the report are interpreted in the light of deep signatures, to find or reject the hypothesis of discharging deep groundwater components.

4.3.1 Reporting limits and dilution constraints

When discussing the possible presence of deep groundwater signatures in the surface system, an important prerequisite is the theoretical maximal dilution that is possible to detect according to the difference in concentrations and the reporting limits for the analysis technique used. In practice, the limited number of available samples also restricts the possibilities to detect very small changes on statistical grounds, as well as the uncertainties regarding factors governing the local hydrochemistry.

The dilution factors compiled in Table 4-1, give an indication of the maximal dilution of deep groundwater types that is possible to detect on theoretical grounds for different elements. There is a large variation in the dilution factors among elements, primarily due to differences in concentrations between deeper groundwater types and fresh surface water (the accuracy of the analysis method is probably selected to reflect the variation within each water type, and is accordingly a consequence of the observed concentration range).

According to Table 4-1, dilution in the magnitude of 1,000–10,000 times is possible to detect for several of the major constituents, whereas many trace elements range between a maximal dilution of 10–100 times. Consequently, concentrations and relative composition of major ions are probably best suited for detecting deep groundwater discharge, whereas most trace elements are inadequate in that respect. There are, however, a few trace elements that not follow this pattern and therefore may be theoretical candidates for detecting deep signatures: Br (ICP), Sr, Rb, Mo and Ba.

One purpose with the ion source model in Section 3.2 is to search for deep groundwater signatures among surface water samples, by looking at the relative composition of several major ions. In combination with isotope measurements reflecting the origin of water, the results from this model is used in Section 4.3.2 to summarise indications of deep signatures in the surface system.

4.3.2 Possible deep signatures in shallow objects

The first question that arises is what characterise a deep groundwater? At very deep levels, shield brine influences the groundwater composition with typical major ion signatures containing excess of Ca and Cl, and very low Mg concentrations, compared to the composition of sea water (cf ion source model in Section 3.2.3). Isotopes reflecting the origin of water, as ^{2}H and ^{18}O, also deviate in samples influenced by shield brine by showing a clear ^{2}H excess (cf Section 3.3.2).

Another water type that prevails at intermediate depths, approximately down to 400–500 metres, is the groundwater type significantly influenced by relict marine water. Observations representing this water type often form a relatively well defined cluster in many plots. According to the ion source model (cf Section 3.2.3) this cluster contains an ion mixture of marine ions, shield brine, and to a minor extent, weathering products from the local rock and overburden. A comparison with the results from the M3 mixing model (cf Section 3.2.7) reveals that about 50% of the Cl in the relict marine cluster have shield brine origin, an estimation that supports the qualitative indications of the ion source model. Regarding the origin of water, the relict marine cluster shows a strong evaporation signature supporting the sea water origin (cf Section 3.3.2).

Table 4-1. Compilation of reporting limits in fresh surface water and the maximal dilution that is possible to detect regarding two typical deep groundwater samples. HFM13-134 is a typical brackish relict marine groundwater, whereas K09A-615 represent a deep saline groundwater significantly influenced from shield brine. For comparison this factor was also calculated for typical dilute surface water in the outlet of Lake Eckarfjärden. The dilution factor shown in the three rightmost columns is calculated as the observed mean concentrations for the object at question, divided with the reporting limit for the element in fresh surface water.

	Reporting limit		Surface water PW70	Relict marine H13–134	Deep saline K09A–615
Na	0.1	mg/L	58	17,100	26,200
K	0.4	mg/L	4	63	31
Ca	0.1	mg/L	429	11,800	65,200
Mg	0.09	mg/L	29	2,200	197
HCO_3	1	mg/L	131	124	7
Cl	1	mg/L	5	5,020	14,800
SO_4	0.5	mg/L	14	952	236
Br(IC)	0.2	mg/L	0.3	119	715
Br(ICP)	0.001	mg/L	173	23,700	143,000
F	0.1	mg/L	25	13	13
Si	0.03	mg/L	3	258	155
Fe	0.4	mg/L		8	0
Mn	0.03	mg/L	0	72	4
Li	0.2	mg/L	0	0	0
Sr	0.002	mg/L	3,705	6,450	36,850
I	0.001	mg/L	867	53	525
U	0.001	µg/L	18	16,200	54
Th	0.05	µg/L	240	2	2
Al	0.2	µg/L	2	43	140
As	0.01	µg/L	2	50	240
Sc	0.05	µg/L	0	5	10
Cd	0.002	µg/L	54	13	13
Cr	0.01	µg/L	65	13	351
Cu	0.1	µg/L	1	3	11
Co	0.005	µg/L	0	5	35
Hg	0.002	µg/L	154	1	1
Ni	0.05	µg/L	40	18	67
Zn	0.2	µg/L	0	5	28
Pb	0.01	µg/L	27	15	15
V	0.005	µg/L	404	19	25
Rb	0.025	µg/L	6	2,100	1,408
Y	0.005	µg/L	49	3,680	68
Zr	0.025	µg/L	8	6	6
Mo	0.01	µg/L	3	425	9,050
In	0.05	µg/L	1	5	5
Sb	0.025	µg/L	1	2	86
Cs	0.025	µg/L	704	82	31
Ba	0.01	µg/L	8	8,910	41,300
La	0.005	µg/L	2	158	5
Eu	0.005	µg/L	4	12	5

The relict marine cluster also shows ionic and isotopic signatures indicating that interactions with sediments may have altered the original composition of this water type (cf Section 4.2.1). In conclusion, the groundwater type influenced by relict marine water displays a complex composition, not only including marine signatures but also deeper shield brine signatures and signs of alteration during formation of this groundwater.

If indications of any of the above mentioned deep groundwater types is found in shallow objects, it can not be excluded that deep groundwater reach shallow levels in the Forsmark area. It should however be noted that existence of these signatures near the ground surface not necessarily implies that they should be found at the surface. The horizontal structure in the upper part of the bedrock, the "hydrological cage", is thought to effectively drain both discharge from depth and meteoric recharge through sediments towards the sea /Follin et al. 2007a/.

There are a number of shallow objects in the Forsmark area that show possible deep groundwater signatures. These are compiled in Table 4-2, and the geographical locations are shown in the map in Figure 4-21. Two percussion drilled boreholes, HFM11 and HFM12, have also been included as they show the strongest shield brine signatures among all percussion drilled boreholes in the upper part of the bedrock. There is a large number of percussion drilled boreholes that show relict marine signatures, very similar to e.g. SFM0023 and PFM0009, but these objects are not included in this table that focus on shallow groundwater. The two subjective classifications included in Table 4-2 are based on the ion source model (cf Section 3.2.3) and the water origin model (cf Section 3.3.2).

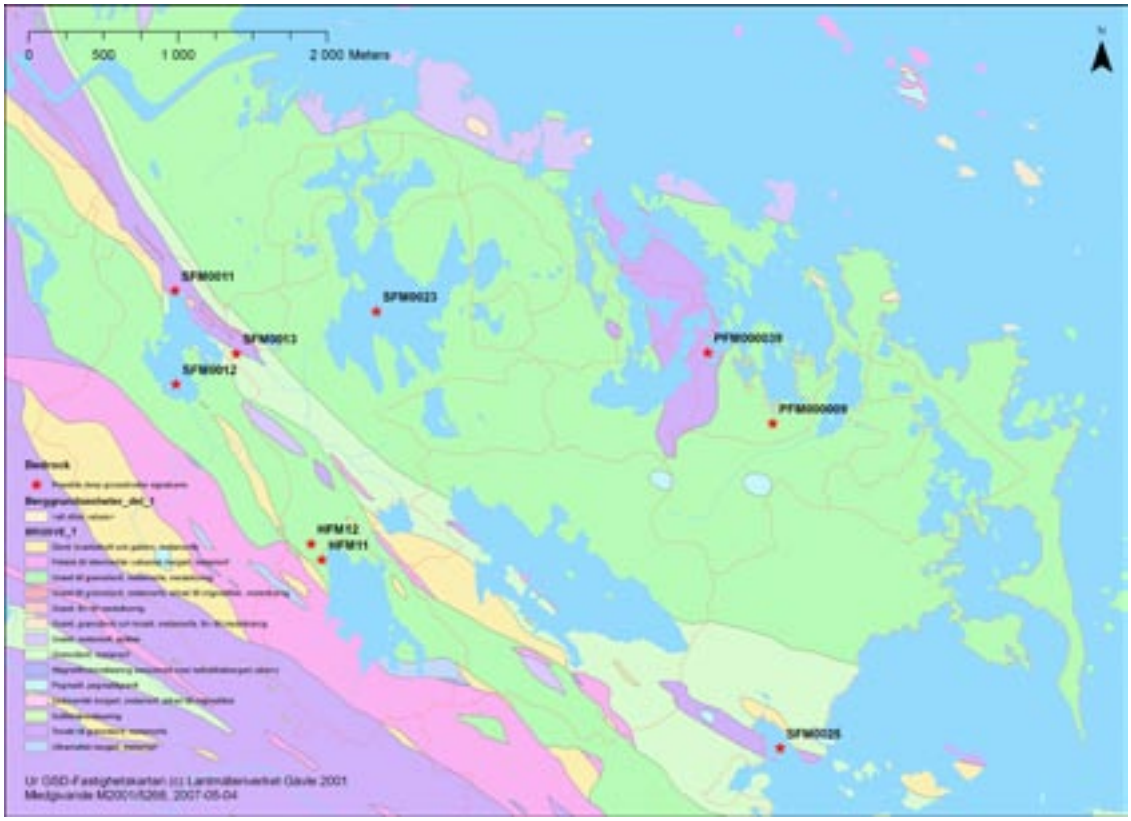

Figure 4-21. *Shallow groundwater objects (soil tubes and drilled private wells) that show possible deep groundwater signatures. See Table 4-2 for an explanation of individual objects. Two percussion drilled boreholes, HFM11 and HFM12, have also been included as they show the strongest shield brine signatures among all percussion drilled boreholes in the upper part of the bedrock.*

Table 4-2. Summary of soil tubes and private wells that show signs of deep groundwater signatures. Two percussion drilled boreholes, HFM11 and HFM12, are included as they show the strongest shield brine signatures among all percussion drilled boreholes in the upper part of the bedrock. Idcode refer to the database identification code. Label, which is based on the Idcode and contain additional depth information in RHB70, is used in all visualisations throughout the report (cf Section 2.3.12 for explanations).

Idcode	Label	Ion sources[A]	Water origin[B]	Comment
SFM0023	S23-4	MA+(WP)+(SB)	E	Soil tube located in till below bottom sediments of Lake Bolundsfjärden
SFM0011	S11-2	MA+WP+(SB)	E+(M)	Soil tube located in till close to Lake Gällsboträsket
SFM0012	S12-3	MA+WP+(SB)	E+(M)	Soil tube located in till below bottom sediments of Lake Gällsboträsket
SFM0013	S13-1	MA+WP+(SB)	–	Soil tube located in till near outlet of Lake Gällsboträsket
SFM0025	S25-6	(MA)+WP+SB	M+(G)	Soil tube located in till below bottom sea sediments of Kallriga bay (below sea water)
PFM0009	PP09	MA+SB	M+(G)	Private well drilled to 70 m
PFM0039	PP39	MA+SB	E+M	Private well drilled to 60 m
HFM11	H11–25	(MA)+(WP)+SB	M+(G)	Percussion drilled borehole in Eckarfjärden deformation zone
HFM12	H12–87	(MA)+SB	M+G	Percussion drilled borehole in Eckarfjärden deformation zone

A: Ion sources: MA = marine ions, WP = weathering products, SB = ions of shield brine origin.

B: Water origin: E = influence from evaporation, M = meteoric, G = glacial influence.

From observations of major elements and environmental isotopes in some shallow groundwater objects, it can be concluded that deep groundwater signatures are present at relatively shallow levels in the Quaternary deposits. There are, however, no indications that these signatures actually reach the surface (cf possible explanations in the conceptual model in Section 8.2)

According to /Rönnback and Åström, in press[a]/, differ deeper groundwater types significantly from shallow groundwater with respect to concentrations and fractionation patterns among REE (Rare Earth Elements), and there are accordingly no indications regarding these elements of surface discharge of deep groundwater. This conclusion is however contradicted by the dilution constraints discussed in Section 4.3.1 (cf La and Eu).

5 Integrated evaluation of hydrochemical and hydrological data in the surface system

In this section, the couplings between hydrochemistry and hydrological data in shallow groundwater and surface systems are explored. A hydrological field classification of soil tubes, according to recharge and discharge characteristics, is compared to the hydrochemical measurements in shallow groundwater in order to explore possible correlations. Discharge measurements in streams are further compared to the hydrochemical composition of streaming water, and possible correlations are explored between water flow and measured concentrations. Finally, discharge measurements are used in combination with hydrochemical data in order to estimate transport of elements in Forsmark watercourses. These transport estimations are the basis for the catchment modelling described in Section 6.

5.1 Evaluation of observed hydrochemistry in relation to hydrological recharge/discharge characteristics

Here, the observed hydrochemistry in shallow groundwater is evaluated in relation to a qualitative, hydrological field classification of soil tubes in the Forsmark area. The purpose of this evaluation is to explore whether chemical parameters can support field estimations of recharge and discharge characteristics. A matrix where the hydrological characteristics of soil tubes are compiled can be found in Appendix B, and further explanations and hydrological evaluations are found in /Werner et al. 2007/.

The correlation structure among a selection of hydrochemical parameters, representing either the variability or mean values, was studied in relation to the semi-quantitative recharge/discharge parameter. Parameters included in the analysis are listed in Section 2.2.1 along with an explanation of the recharge-discharge parameter (RDPO). This parameter is further evaluated in relation to other hydrological and physical parameters in Appendix C. The complete chemical data matrix is found in Appendix B.

In the last section a few hydrochemical classifications are compared with the hydrological field classification in order to explore similarities and dissimilarities among different approaches to the recharge-discharge question.

5.1.1 Correlation analysis by Principal Component Analysis

A standard principal component analysis (PCA – cf Section 2.3.10 for explanation), based on a Pearson correlation matrix, is used to visualise the correlation structure among the selected hydrochemical parameters and the recharge-discharge parameter RDPO (Figure 5-1). A few additional parameters, e.g. temperature and ground water level, are included to facilitate comparisons. The strongest correlations identified in the PCA are visualised in scatter plots in Figure 5-2, to give a conception of the strength (or weakness) of the relationships.

When the selected hydrochemical parameters are analysed in combination with RDPO and a few additional parameters, the patterns in Figure 5-1 describe 45% of the total variation in data from these soil tubes. In the score plot in the lower panel, the first principal component discriminate the observations in three distinct groups with respect to the hydrological classification. Soil tubes hydrologically classified as recharge are ringed with red, discharge soil tubes located below lakes or sea are ringed with green, whereas discharge soil tubes located on land have no additional marking.

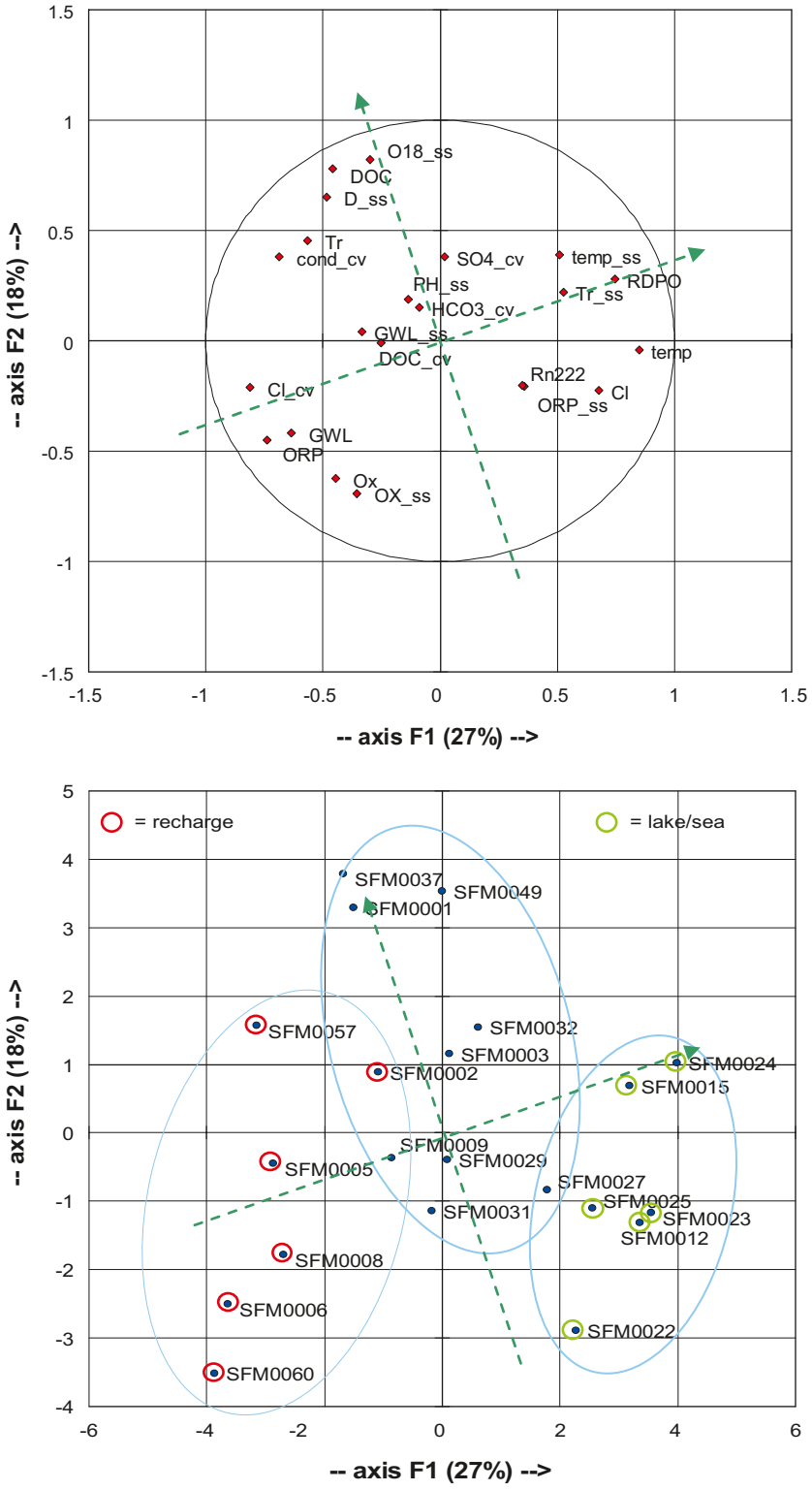

Figure 5-1. *Principal Component Analysis (PCA) on all data from soil tubes with more than 2 observations. Loading plot of parameters (upper) and score plot of observations (lower), cf Section 2.3.10 for an explanation of multivariate plots. Parameters in the upper panel that plot along the dashed green arrow pointing to the right are correlated to the RDPO parameter, whereas parameters associated with the perpendicular arrow show little correlation to RDPO. See text for an explanation of the marking of observations.*

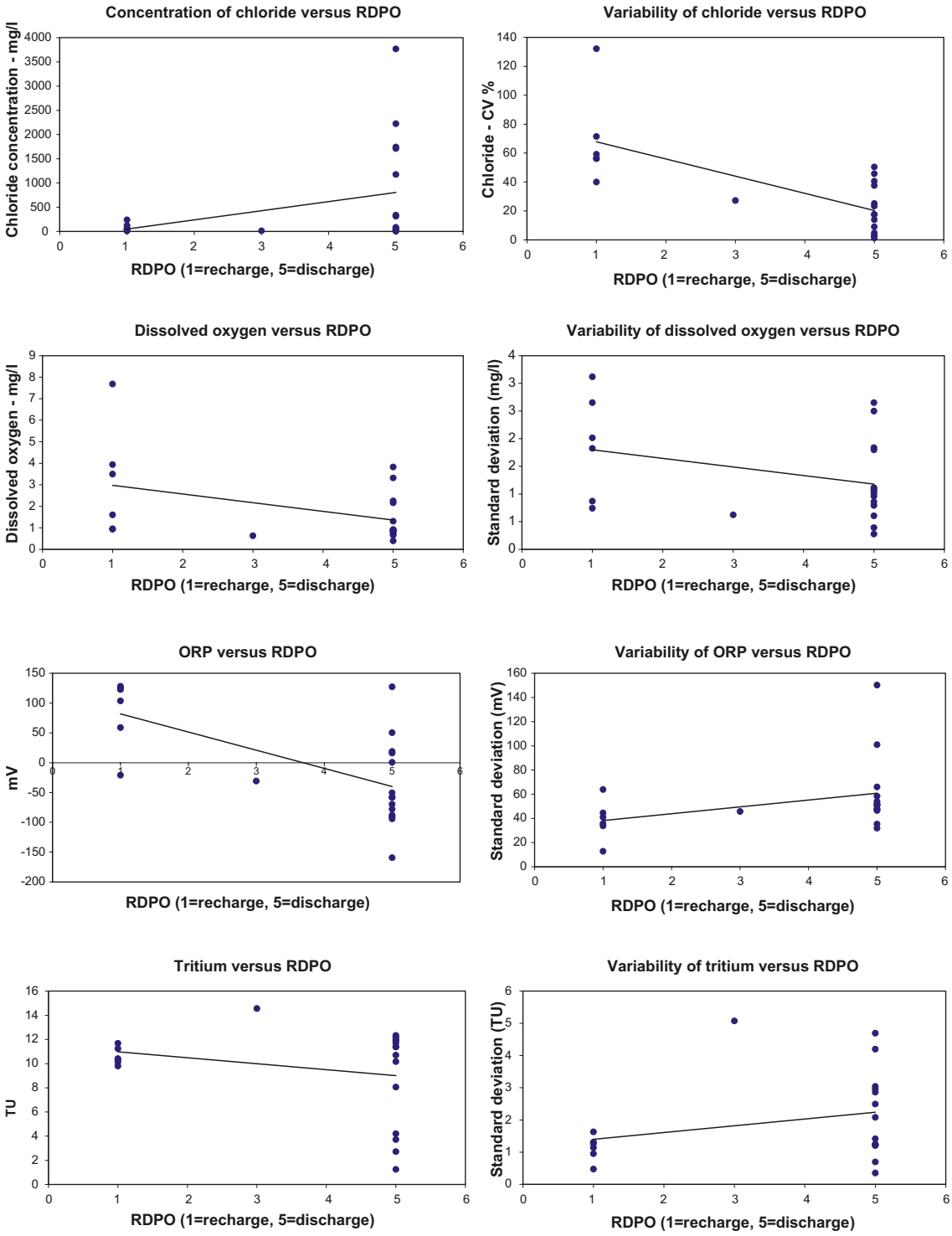

Figure 5-2. *Scatterplot showing the strongest relationships that were identified in the principal component analysis in Figure 5-1. Data from all soil tubes with more than 2 observations are included in the plots. The trendlines in the figures are adapted by least squares regression.*

On the right side of the score plot, all soil tubes located in lakes and at sea form a cluster. All soil tubes on the left side are classified as recharge, and the middle section is dominated by soil tubes on land classified as discharge. Soil tubes in the encircled groups are consequently both discriminated both with respect to the selected chemical parameters and to the recharge/discharge parameter RDPO. This indicates a correlation between the hydrological classification and the observed hydrochemical patterns.

The recharge/discharge parameter RDPO, located to the right in Figure 5-1, shows positive correlation to the parameters describing the variability of temperature and ^{3}H, as well as to the mean values of Cl and temperature. The strongest negative correlations are found for the variability parameters of Cl, dissolved O_2 and conductivity, as well as the mean values of field measured redox potential Eh (ORP), ground water level (GWL) and dissolved O_2 (Ox).

Soil tubes with *hydrological recharge characteristics* (left side) therefore show:

- High relative variability of Cl and low absolute Cl concentrations.
- Higher redox potential (Eh) and greater mean depth to the groundwater table.
- Low mean temperature and low variability of temperature.
- Low variability of ^{3}H.

The opposite pattern applies to soil tubes with *hydrological discharge characteristics,* located at the right side of the plot. Pair-wise scatter-plots in Figure 5-2 show the strongest, but still rather weak, correlations identified in the PCA. As most of the soil tubes are classified either as recharge or discharge on the discrete RDPO-scale in Figure 5-2, many points cluster around 1 and 5 making the scatter plots harder to interpret.

Some parameters, such as the variability of the ^{18}O-isotope and the concentration of dissolved organic carbon (DOC), show little correlation to the almost horizontal recharge/discharge gradient, which is most associated to the first principal component in the PCA. There are examples among soil tubes, classified either as recharge or discharge that show high concentrations of DOC and high variability of ^{2}H and ^{18}O, which is reflected in the overlapping, vertical extensions of the encircled clusters in Figure 5-1 The same conclusion may be drawn from Figure 5-3, where no correlation is evident between any of these parameters and RDPO.

When the hydrological/physical parameters temp, temp_ss, GWL, GWL_ss are excluded from the PCA, the general pattern and the conclusions are unchanged. The same is true when soil tubes located in lakes or at sea are excluded from the analysis; the main pattern among the remaining parameters and observations is maintained.

The main variation described by the two first principal components of the PCA may alternatively be visualised in a scatter plot. In Figure 5-4, the variability of oxygen-18 is plotted versus the variability of chloride. The relative locations of the soil tubes in the plot are very similar to the PCA score plot, though slightly rotated and mirrored to the vertical axis, due to the random sign of the latent variable in the PCA plot. The horizontal variation in the plot corresponds to the

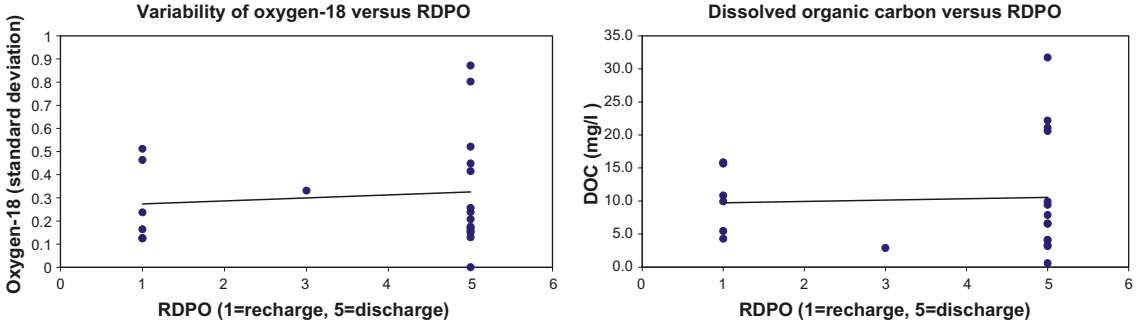

Figure 5-3. *Variability of ^{18}O and DOC versus the hydrological recharge/discharge classification RDPO.*

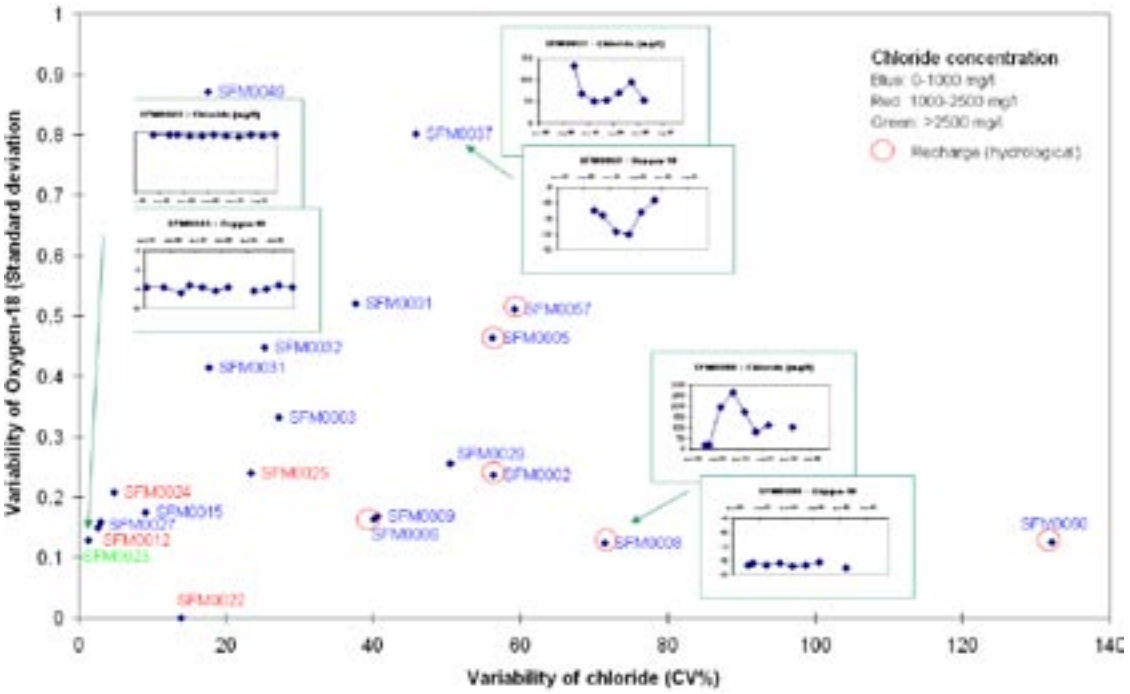

Figure 5-4. *Variability of ^{18}O versus variability of Cl in soil tubes from the Forsmark area, sampled at least three times. Cut-in figures show underlying time series for three soil tubes located at different extremes in the plot: SFM0023, SFM0037 and SFM0008.*

main variation of the first principal component, which is most correlated to RDPO. The vertical variation show less correlation to RDPO, possibly indicating a common physical/hydrological factor influencing soil tubes classified as both recharge and discharge.

Two of the parameters that are independent of RDPO, the variability of oxygen-18 and dissolved organic carbon (DOC), show a close correlation to each other according to Figure 5-5. The concomitant variation shown by these parameters is orthogonal (independent) of the recharge/discharge gradient, and probably reflects a hydrological property common to both recharge and discharge soil tubes. The length of the flow path or the water retention time is two possible candidates.

The co-variation of these parameters with tritium, where high ^{3}H values are accompanied by high DOC and high variability of ^{18}O, support this explanation. Another supportive fact is that DOC is negatively correlated to the mean screen depth relative ground, according to Figure 5-6.

5.1.2 Evaluation of relationships between the groundwater temperature and hydrological parameters

Both mean temperature and the seasonal variability of temperature show higher values in soil tubes with hydrological discharge characteristics according to Figure 5-7. Soil tubes located in lakes or at sea form a deviating group (encircled in the figure). Two extremes within this group are shown by the sea-located soil tubes SFM0024 and SFM0025. The former soil tube has an estimated depth from sediment surface to the intake screen of 2 m, whereas the screen of SFM0025 is located at greater depth (4.7 m). According to the green labels in Figure 5-7, the rest of the soil tubes located in lakes fit well into this hypothetical trend related to screen depth.

A possible explanation to the elevated mean temperature below lakes and sea water may be the influence from the bottom water, probably not falling below 4°C during winter. The elevated temperature variability among some of these soil tubes, predominantly located below thinner sediment layers, may possibly be explained by a higher degree of seasonal temperature fluctuations due to heat transfer through the sediments. Land based soil tubes show similar tendencies, with lower variation below thicker soil layers.

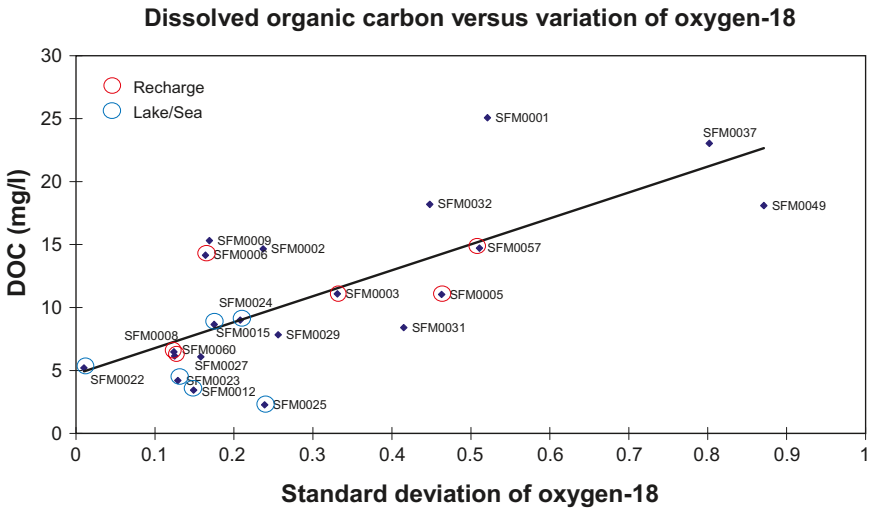

Figure 5-5. *Concentration of dissolved organic carbon versus standard deviation of ^{18}O in Forsmark soil tubes. Red circles denote recharge soil tubes, blue discharge soil tubes below lake or sea, whereas observations with no mark denote discharge soil tubes located on land.*

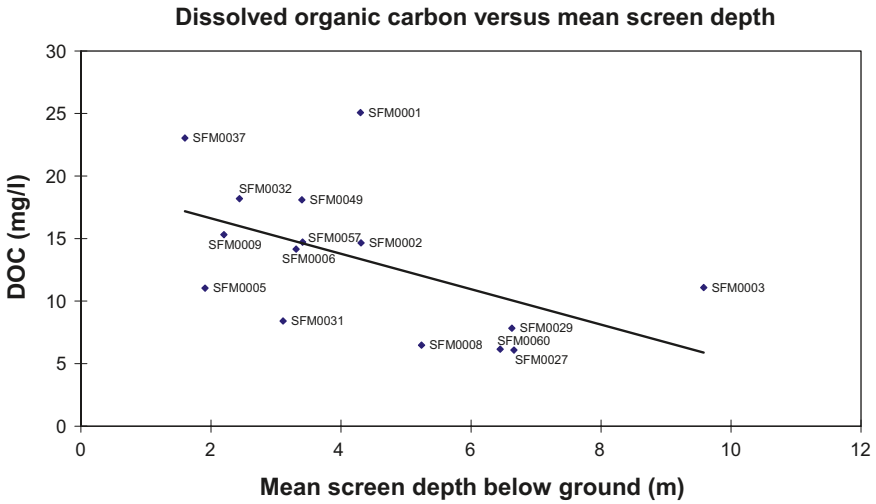

Figure 5-6. *Dissolved organic carbon (DOC) versus mean intake screen depth relative ground (MSD). Only soil tubes located on land are included in this plot.*

A separate correlation analysis of the land-based soil tubes (both recharge and discharge classified) reveals the correlation structure among the temperature parameters, ground water level, mean screen depth and the recharge/discharge parameter RDPO (Figure 5-8). RDPO is positive correlated to both of the temperature parameters (i.e. the highest mean temperatures and highest variability is found in discharge soil tubes), and negatively correlated to the mean ground water level (i.e. ground water is closer to ground in discharge soil tubes).

The parameter describing mean screen depth shows little correlation to RDPO, indicating that there is no bias regarding the screen depth in the selected soil tubes. Furthermore, this parameter is positively correlated to the mean temperature, and negatively correlated to the temperature variation (i.e. higher mean temperature and less variation at greater screen depth).

The variation observed among the temperature parameters is complex and probably an effect of several superimposed factors. The following conclusions may be drawn from Figure 5-7 and the correlation analysis in Figure 5-8:

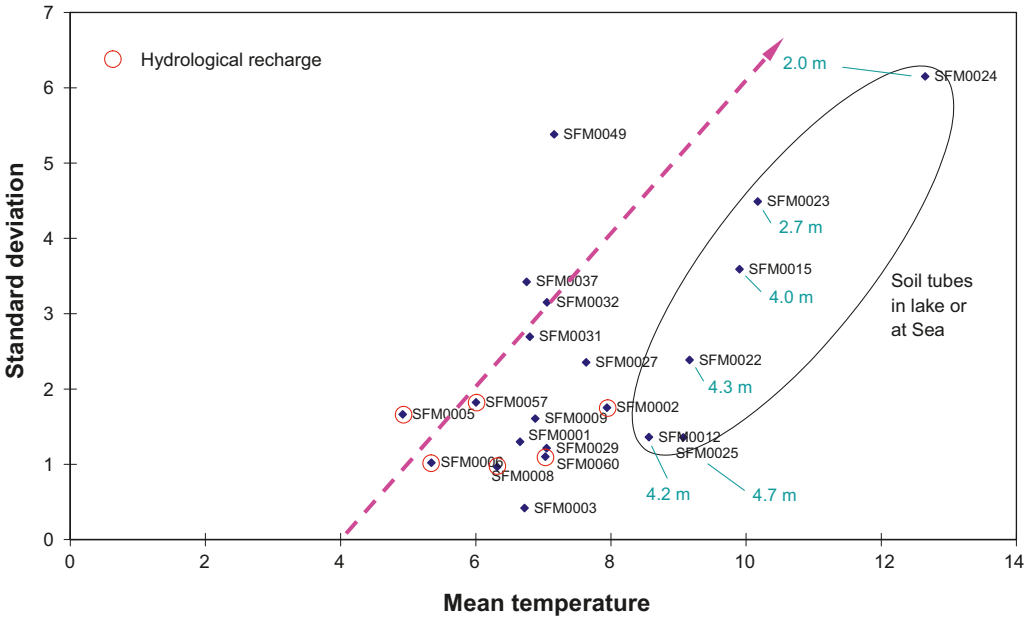

Figure 5-7. *Standard deviation of temperature versus mean temperature in Forsmark soil tubes (°C). Green labels denote the relative depth from sediment surface to intake screen of the soil tube. Red marks indicate soil tubes classified as hydrological recharge.*

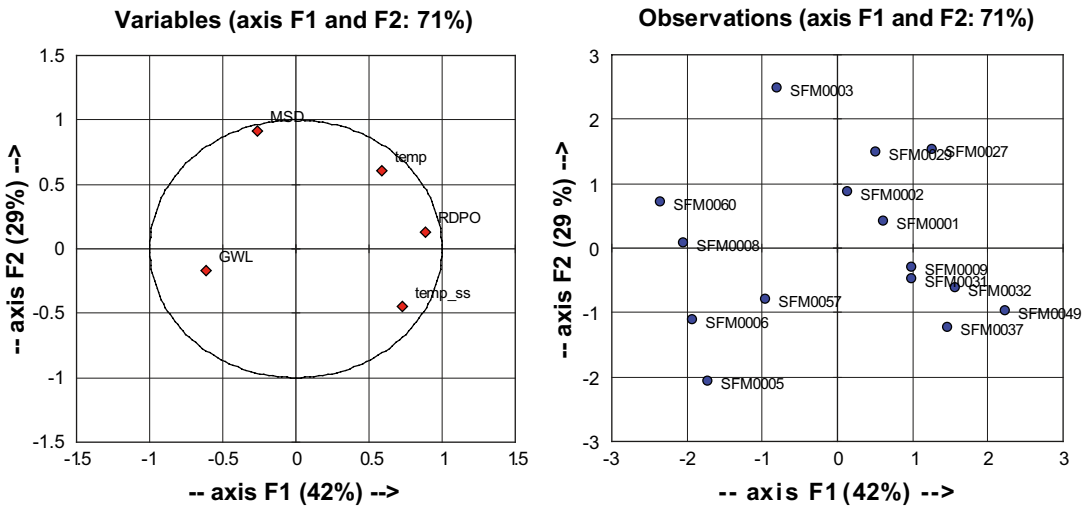

Figure 5-8. *Correlation analysis by PCA (cf Section 2.3.10 for explanation) of temperature parameters, ground water level, mean screen depth and the recharge/discharge parameter on a selection of soil tubes located on land. SFM0012, SFM0015, SFM0022, SFM0023, SFM0024, SFM0025 were excluded compared to the selection in Figure 5-7. Loading plot to the left and score plot to the right.*

- Soil tubes in till below lake and sea sediments generally show higher mean temperature compared to both recharge and discharge soil tubes on land. A possible explanation is the influence from bottom water not falling below 4°C during winter.
- The lake/sea soil tubes also show high temperature variability, with a tendency of less variation at thicker sediment layers.
- Soil tubes located on land show higher mean temperature and lower variation below thicker soil layers (greater mean screen depths, MSD).
- Soil tubes on land hydrologically classified as discharge, show both higher mean temperature and more seasonal induced variation, as compared to the soil tubes classified as recharge.

5.1.3 Comparisons of recharge/discharge classifications

In this section comparisons are made among three classifications of soil tubes with the purpose of discriminating between recharge/discharge characteristics. All three classifications are based on independent parameters reflecting different aspects that may be coupled to the question of recharge/discharge in shallow groundwater. In combination with other supportive parameters and auxiliary classifications reflecting redox potential (cf /Tröjbom and Söderbäck 2006/ and groundwater residence time (based on minimum ^3H activities per soil tube and the classification scheme in Table 3-1), these recharge-discharge classifications are compiled in a condensed matrix in Table 5-3. The use of classifications instead of original parameter values facilitates comparisons and interpretations in the table.

The subjective hydrological field classification probably best reflects the recharge-discharge properties of the soil tubes, and is therefore used as reference when other classifications are evaluated. A thorough description of the prerequisites of this field classification is given in /Werner et al. 2007/. It should however be held in mind that the field classification is solely based on surface characteristics, but measurements in soil tubes may reflect conditions at several metres depth where the intake screen is located. In a relatively flat terrain as the Forsmark area, probably dominated by small-scale groundwater circulation patterns /Werner et al. 2007/, discrepancies between surface estimations and actual conditions at deeper levels can not be excluded.

The hydrochemical recharge-discharge classification is based on the relative composition of major constituents of groundwater. The traditional water type classification plot in Figure 5-9 was used to classify the soil tubes in recharge-discharge characteristics, assuming that waters of Ca-HCO_3 type correspond to recharging groundwater (encircled in the figure), whereas groundwaters of Na-HCO_3 to Na-Cl types correspond to discharging groundwater. See Sections 2.3.5 and 3.1.2 for further explanations of the so-called Piper plot. It should be noted that this classification is mainly included to emphasise the difference between the simplified chemical generalisation and the hydrological field assessment. As the evaluations later in this section indicate, this classification is probably not valid in the small scale groundwater circulation patterns that seem to prevail in the surface system in the Forsmark area.

As a result of the explorative analysis in Section 5.1.1, an alternative chemical recharge-discharge classification based on the relative variability of Cl was tested. The rather close correlation between the recharge-discharge parameter, RDPO, and the relative variability of Cl may in recharging groundwater reflect fluctuations due to seasonal variations in the water balance, whereas more constant conditions is manifested as low variability of Cl in discharging groundwater. This is a pure statistical classification based on 20/40/60/80-percentiles of the range measured in soil tubes of the Forsmark area (Table 5-1).

It should be noted that the alternative classifications presented in this section are a part of the explorative analysis, and they should be regarded as a formalised approach to get a condensed compilation in Table 5-3 of possible important aspects on the question of recharge-discharge characteristics in shallow groundwater.

Table 5-1. Statistical Cl variability classification of recharge/discharge characteristics based on the coefficient of variation for Cl (%). Class limits correspond to 20/40/60/80-percentiles of the range measured in Forsmark soil tubes.

Class limits Coefficient of variation for Cl (%)	Cl variability class Recharge (1) – discharge (5)
< 10	5
10–23	4
23–40	3
40–56	2
> 56	1

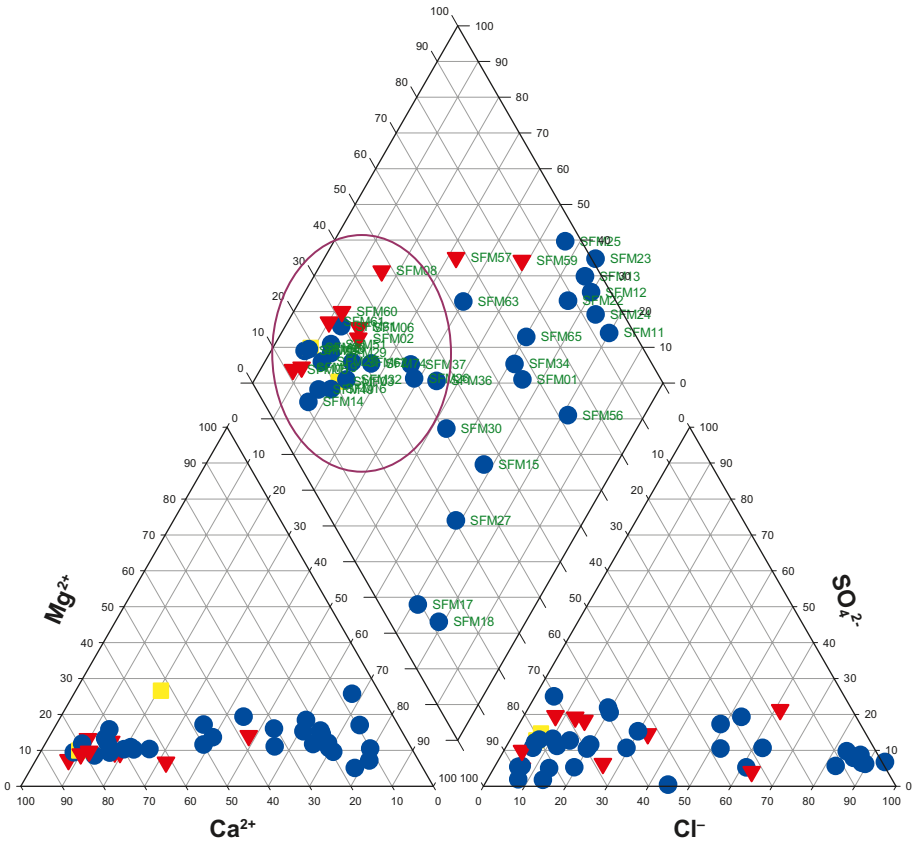

Figure 5-9. *Traditional water type classification Piper plot (cf Section 2.3.5) based on mean values, used for the hydrochemical recharge-discharge classification of shallow groundwater in the Forsmark area. Encircled points are assumed to represent recharging groundwater. Red triangles correspond to hydrological recharge characteristics, yellow varying and blue dots discharge characteristics according to the hydrological field characterisation.*

When examining the three classifications in Table 5-3 the most pronounced deviations from the hydrological classification are shown by the hydrochemical ”Piper-classification”. These classifications are compared in Table 5-2, and the main difference is shown by a group of soil tubes that were hydrologically classified as discharge but showing recharge characteristics according to the chemical Piper-classification (This “H5-C1” group is located within the circle corresponding to Ca-HCO_3 groundwater in the Piper plot, and is marked red in Table 5-2).

The geographical distribution of the six available combinations in Table 5-2 are visualised in Figure 5-10. As supposed, most soil tubes classified as hydrological recharge are located on topographical heights. All soil tubes classified both as hydrological and chemical discharge are located within or in close vicinity of streams, lakes or the coast.

Table 5-2. Comparison of the hydrological field classification and the Piper based chemical classification of recharge/discharge characteristics. As classes C2-C4 have not been used they are omitted in the table.

Hydrological field classification	Chemical Piper classification	
	C1 (recharge)	C5 (discharge)
H1 (recharge)	7	2
H2 (prob. recharge)	–	–
H3 (varying)	3	–
H4 (prob. discharge)	1	–
H5 (discharge)	13	16

Table 5-3. Compilation of recharge-discharge classifications of soil tubes in the Forsmark area, based on different independent parameters, complemented by a few auxiliary parameters and classifications. The hydrological field classification in labelled "Hydro field", the chemical classification based on major constituents is labelled "Chemical Piper", an additional chemical classification summarising the relative variability is labelled "Cl variability". Supportive classifications summarise redox potential and estimations of groundwater residence time based on ^{3}H measurements. Figures marked with red colour deviate from the hydrological classification with more than one class.

ID code	Supportive parameters			Supportive classifications		Recharge (1) – discharge (5) classifications		
	Cl mg/L	Mean groundwater depth (m)	Mean screen depth (m)	Redox potential	^{3}H age	Hydro field (H)	Chemical Piper (C)	Cl variability (V)
Hydrological recharge								
SFM0002	64	0.38	4.31	Low	Modern	1	1	1
SFM0005	10	1.17	1.91	Moderate	Modern	1	1	1
SFM0006	42	1.23	3.31	Moderate	Modern	1	1	3
SFM0008	122	2.91	5.24	Low	Modern	1	1	1
SFM0019	5	0.50	3.90	–	Modern	1	1	–
SFM0057	241	0.72	3.41	Low	Modern	1	5	1
SFM0059	576	3.94	4.98	–	Modern	1	5	–
SFM0060	24	4.26	6.45	High	Modern	1	1	1
SFM0061	12	4.33	5.46	–	Modern	1	1	–
Hydrological varying								
SFM0003	13	0.19	9.58	Low	Modern	3	1	3
SFM0010		0.64	1.20	–	Submodern	3	1	–
SFM0020	11	0.28	2.92	–	Modern	3	1	–
Hydrological discharge								
SFM0021		0.43	1.96	–	Modern	4	1	–
SFM0001	335	0.44	4.30	Low	Modern	5	5	3
SFM0009	9	0.37	2.20	High	Modern	5	1	2
SFM0011	1,778	0.08	3.35	–	Mix	5	5	–
SFM0012	2,223	–0.01	4.75	Low	Submodern	5	5	5
SFM0013	1,777	0.02	4.28	–	Modern	5	5	–
SFM0014	7	0.25	1.48	–	Modern	5	1	–
SFM0015	314	–0.01	6.35	Very low	Submodern	5	5	4
SFM0016	26	0.01	7.03	–	Modern	5	1	–
SFM0017	18	0.11	3.46	–	Modern	5	5	–
SFM0018	12	0.50	4.10	–	Modern	5	5	–
SFM0022	1,177	0.02	4.63	Moderate	Submodern	5	5	4
SFM0023	3,767	0.03	3.73	Low	Mix	5	5	5
SFM0024	1,712	0.03	2.45	–	Modern	5	5	5
SFM0025	1,743	0.08	5.66	Low	Modern	5	5	3
SFM0026	97	–0.15	15.51	–	Anthropog. inf.	5	1	–
SFM0027	62		6.66	Moderate	Modern	5	5	5
SFM0028	13	0.00	6.65	–	Anthropog. inf.	5	1	–
SFM0029	23	0.00	6.63	Low	Modern	5	1	2
SFM0030	69	0.58	3.38	–	Modern	5	5	–
SFM0031	9	0.65	3.11	Low	Modern	5	1	4
SFM0032	25	0.08	2.44	Low	Modern	5	1	3
SFM0034	432	0.19	1.59	–	Modern	5	5	–
SFM0036	146	0.30	1.60	–	Modern	5	1	–
SFM0037	84	0.28	1.60	Low	Modern	5	1	2
SFM0049	16	0.62	3.40	Very low	Modern	5	1	4
SFM0062	28	–0.08	2.65	Low	Modern	5	1	–
SFM0063	145		2.57	Moderate	Modern	5	5	–
SFM0065	370	0.08	3.81	Moderate	–	5	5	–
SFM0074	49		7.05	Low	Modern	5	1	–

Figure 5-10. *Map showing the geographical distribution of soil tubes according to the six available combinations in Table 5-2. "H" denotes hydrological class and "C" chemical class.*

The deviating "H5-C1"-group (marked red in Table 5-2), which is hydrologically classified as discharge but showing recharge characteristics according to the hydrochemical classification, is predominantly located in the vicinity of lakes, a fact that support the hydrological view. One possible explanation may be local recharge-discharge patterns close to wetlands and lakes, characterised by short residence times and little alteration of the recharging groundwater. In the calcite-rich soils of the Forsmark area (cf Section 4.1.3), recharging groundwater may be saturated with respect to calcite at relatively shallow depths, which implies that this type of discharging groundwater may be interpreted as recharging groundwater hydrochemically (see /Werner et al. 2007/ for further discussions on this topic). The chemical "recharge" characteristics of the hydrological discharge "H5-C1" group may be an indication of more local flow regimes in this selection of soil tubes, leading to a less altered water composition comparable to the composition of the recharging water. It can also be concluded that an uncritical use of a chemical characterisation tool, such as the Piper classification plot, may lead to erroneous conclusions when applied at conditions prevailing in the Forsmark area.

Soil tubes in the "H1-C5" group are located close to water divides, hence indicating recharge, but show discharge characteristics according to the hydrochemistry. SFM0057, which is located close to the border of the Lake Gällsboträsket depression, show relict marine signatures similar to the soil tubes below this lake. SFM0059, located close to the Baltic coast, is correlated to the Sea water level according to groundwater level studies /Juston et al. 2006/.

The alternative chemical classification based on the variability of Cl is difficult to evaluate due to the limited number of objects with more than two observations over time.

5.1.4 Conclusions – recharge/discharge characteristics

- There are few clear, straightforward relationships between the hydrological field classification (the recharge/discharge parameter) and the selected chemical parameters according to the correlation study, which also are manifested as a relatively low explanatory power of the two first principal components in the PCA.
- The recharge/discharge parameter is strongest correlated to the redox potential (ORP), to dissolved O_2 (ox), and to the variability of chloride. This means that both lower redox potential and lower concentration of dissolved O_2 are observed in discharging compared to recharging groundwater. The increased variability observed for chloride in recharging groundwater may be explained as a effect of fluctuations induced by seasonal variations in the water balance, and, consequently, this variation is generally smaller in discharging groundwater.
- Parameters as the variability of ^{2}H and ^{18}O, as well as the presence of DOC, on the contrary, show no correlation to the recharge/discharge parameter RDPO. These co-variant parameters probably reflect a hydrological property common to both recharge and discharge soil tubes, such as the length of the flow path or the groundwater retention time.
- Both mean and variability of groundwater temperature are correlated to the recharge/discharge parameter RDPO. These relationships are however complex and probably an effect of several superimposed factors or different mechanisms.
- The overall conclusion is that the surface system in the Forsmark area is difficult to understand from a recharge/discharge point of view. The observed patterns are probably the result of several superimposed processes working on different scales and are ultimately an effect of the specific hydrological conditions in the Forsmark area: the relatively flat and small-scale topography, the increasing hydraulic conductivity by depth in the Quaternary deposits and the horizontally fractured upper parts of the bedrock. All these factors contribute to the supposed shallow (local) flow regimes that prevail in the Forsmark area.

5.2 Evaluation of concentrations and water flow

Concentrations measured in streams and lakes show variations depending on many different factors, and in this section, influence of water flow on the concentrations of a large number of parameters is explored. Depending on the nature of the underlying processes and pathways that bring different elements to the streams, different responses to variations in water flow may be expected.

The most obvious response to a supply of e.g. meteoric water that contain small amounts of dissolved ions or compounds, is dilution and lowered concentrations as a consequence. However, episodes of high flow rates may also mediate release and transport of elements to the surface waters through erosion and floods, e.g. particulate matter and ions adsorbed to particles, with increasing concentrations as a consequence. High flow episodes may also lead to a greater fraction of overland discharge, possibly contributing to higher concentrations of e.g. organic compounds and elements associated with organic matter. During episodes of lower flow rates, usually a greater fraction of the surface water originate from discharging groundwater, which influence the concentrations in different directions depending on element. Variations in recharge may also influence the chemical environment in soil and sediments, which often results in changed pH or altered redox conditions, which in turn either may lead to release or retention of specific elements.

This simplified, but still complex picture should be held in mind when observed concentrations are correlated to measured discharge in watercourses. In order to facilitate comparisons that involve about two orders of magnitude, concentrations and discharge measurements are displayed in log-log plots. Relationships following power laws (e.g. $y = ax^b$), for example dilution of a point source, form straight lines in this type of plots. However, it should however be noted that observations that seem to plot along straight lines in these plots, not necessarily have to be an effect of mechanisms that follow power-laws, as straightness is a necessary, but not a sufficient condition for data following a power-law relation.

In Table 5-4, correlation coefficients have been calculated for two years of measured discharge (cf Section 5.3.1) and monthly concentrations of selected elements. Only data from three streams (PFM000066, PFM000068 and PFM000069) and one very small lake (PFM000074) are included in the analyses as data from larger lakes (as well as outlets of large lakes, e.g. PFM000070) are thought to integrate and disguise possible relationships.

From Table 5-4 could be concluded that about half of the studied parameters show significant correlations with water flow in streams at the $p < 0.05$ significance level. Among these significant relationships, most parameters are negatively correlated to water flow, which implies that dilution is a mechanism that influences many parameters at elevated flow rates. It should be held in mind when the significance of a large number of correlations is calculated, that about 5% of the relationships are erroneously regarded as significant at the chosen significance level, i.e. about 4 of 74 in Table 5-4.

Parameter groups representing different major sources also show different responses to changes in discharge according to Table 5-4. Three major groups have been colour coded in the table: marine ions, ions originating from calcite dissolution and compounds originating from organic matter. Among the marine ions, Na, Mg and Cl show strong negative correlations to discharge especially in the lower located stations (PFM000068, PFM000069). Ions of calcite origin also show negative correlations, but contrary to the marine ions, there are only minor differences among different catchments, probably reflecting the rather uniform distribution of calcite dissolution over the Forsmark area.

Elements and compounds associated to organic matter show, with a few exceptions, little correlation to water flow in streams. This fact reflects that fundamentally different processes mediate release and transport of these compounds, compared to ions released by inorganic weathering processes.

Simple dilution may however only to some extent explain these descending patterns according to scenario 1 in Figure 5-11, where water flow is plotted versus Cl concentration. The straight line of scenario 1 represents dilution of a point source assuming an initial Cl concentration of 39 mg/L at a discharge of 2 L/s. This chloride concentration may represent the concentration of the base flow in the catchments of PFM0068 (inlet to Lake Bolundsfjärden) and PFM0069 (outlet of Gällsboträsket), as there is tendency of constant concentrations when discharge fall below about 2–3 L/s. An interpretation of scenario 1, descending with a steeper slope compared to the observed patterns, is that additional Cl is supplied through discharging groundwater and overland flow, which counteracts the dilution effect. One possible source is addition of Cl by deposition, which is accounted for in scenario 2. If a Cl concentration corresponding to the observed concentration in precipitation is corrected for the concentrating effects of evapotranspiration by a factor 3 (according to the approximate relation between evapotranspiration and precipitation in the Forsmark area /Juston et al. 2006/), and the approximate additional supply through dry deposition estimated as the same magnitude as the wet deposition (P.O. Johansson, pers. comm.), a concentration in discharge of about 4 mg/L should be the result according to scenario 2. From Figure 5-11 it is evident that deposition may not explain the observed additional supply of Cl, and one probable additional source is supply of Cl originating from marine relics in the sediments (cf Section 4.1.1). This source is however not able to maintain constant concentrations and the observed descending pattern is formed as a result of increased dilution of groundwater discharge containing marine ions.

There are apparent differences in the response to water flow among the catchments in Figure 5-11. PFM000068 and PFM000069, located at lower topographical levels in the catchments, show a clear decrease in Cl concentration with increasing discharge, whereas PFM000066, draining higher areas in the north-western part of the area, shows almost constant concentrations at a level about twice the concentrations measured in precipitation. These differences probably reflect varying soil conditions within the catchments (see Section 6 for interpretations of the importance of varying soil conditions on the observed water quality).

Table 5-4. Spearman rank correlation coefficients calculated for the correlation between discharge (Q, L/s) and concentrations of selected elements. Figures marked in bold are significant at the p < 0.05 level. Colour coding indicate the major sources of these ions: marine ions (blue), calcite dissolution (brown) and organic matter (green). The analysis is based on a two year period from 2004-06-01 to 2006-05-31, with a monthly sampling interval at all stations. PFM000074, Lake Labboträsket, is sampled in a small lake downstream the stream sampling point PFM000066. PFM000069 is located downstream the small Lake Gällsboträsket and PFM000068 is located further downstream near the inlet to Lake Bolundsfjärden.

	All stations	PFM000066	PFM000068	PFM000069	PFM000074
Na	**–0.36**	–0.41	**–0.98**	**–0.86**	**–0.53**
K	**0.42**	0.24	**0.41**	**0.55**	**0.61**
Ca	–0.15	0.07	**–0.42**	–0.02	0.05
Mg	**–0.33**	–0.15	**–0.85**	**–0.61**	**–0.45**
HCO_3	**–0.30**	0.00	**–0.59**	–0.25	–0.19
Cl	**–0.24**	0.09	**–0.97**	**–0.86**	**–0.45**
SO_4	**0.36**	0.38	0.10	**0.51**	**0.65**
SO_4_S	**0.33**	0.39	0.10	**0.48**	**0.48**
Br	–0.15	0.11	**–0.85**	**–0.51**	0.18
F	**–0.32**	**–0.49**	**–0.52**	**–0.45**	–0.28
I	–0.12	–0.19	–0.22	–0.14	–0.03
Si	–0.05	0.17	–0.17	0.14	–0.22
SiO_2-Si	–0.11	0.14	–0.33	0.05	–0.28
Fe	–0.18	**–0.68**	**–0.71**	**–0.61**	0.00
Mn	–0.14	–0.27	**–0.46**	**–0.41**	0.13
Li	–0.09	0.13	–0.11	–0.09	–0.26
Sr	**–0.40**	–0.24	**–0.87**	**–0.44**	**–0.51**
pH	**–0.60**	**–0.42**	**–0.70**	**–0.65**	**–0.60**
E. conductivity	**–0.30**	0.02	**–0.75**	–0.29	–0.04
Tot-N	**–0.28**	**–0.60**	–0.01	**–0.52**	**–0.62**
NO_3-N	**0.38**	0.10	0.29	0.21	**0.63**
NH_4-N	0.02	–0.22	–0.11	**–0.45**	0.10
PON	–0.13	–0.37	0.06	0.12	**–0.44**
Tot-P	–0.20	–0.40	–0.29	–0.38	–0.15
PO_4-P	**–0.22**	–0.30	–0.42	–0.40	–0.07
POP	–0.06	–0.37	0.00	0.30	–0.22
DIC	–0.09	0.14	–0.37	–0.09	0.16
TOC	–0.12	**–0.42**	0.08	–0.30	–0.31
DOC	–0.06	–0.32	0.24	–0.23	–0.34
POC	–0.13	–0.35	0.00	0.10	**–0.47**
Absorbance 436 nm	–0.12	1	–0.31	**–0.65**	–0.08
Field measured parameters					
Temperature	**–0.52**	–0.40	**–0.54**	**–0.51**	**–0.59**
pH	**–0.54**	**–0.46**	**–0.66**	**–0.58**	**–0.57**
Conductivity	**–0.29**	–0.01	**–0.86**	–0.25	0.05
Salinity	**–0.31**	–0.06	**–0.88**	–0.26	0.04
Dissolved O_2	0.14	0.22	0.21	–0.40	**–0.49**

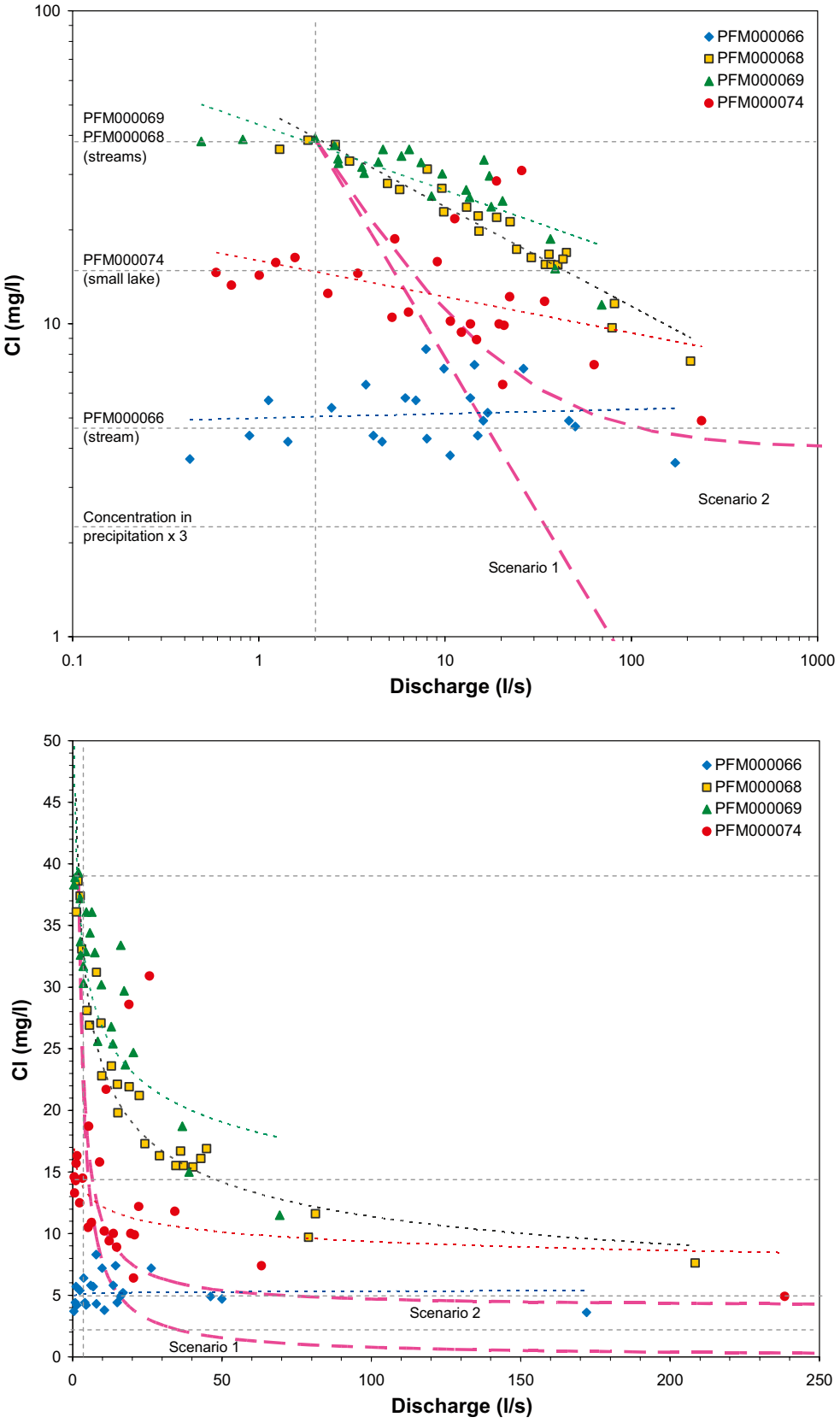

Figure 5-11. *Upper panel – Log-log plot showing discharge (L/s) plotted versus Cl (mg/L). Straight lines in the figures are power functions (e.g. $y = ax^n$) fitted to the observations. Lower panel – exactly the same information as above, but with linear axes for comparison. Two dilution scenarios are shown by dashed pink lines (see text for explanation).*

Twelve plots, analogous to the Cl-figure, are shown for selected elements in Figure 5-12 and Figure 5-13. Patterns identified in these plots give information on how concentrations of selected parameters and parameter groups of Table 5-4 respond in relation to variations in concomitant discharge measurements in streams. Conclusions and comments are summarised per parameter in the list below followed by a general conclusion in Section 5.2.1.

- Cl show a general negative correlation to discharge in all catchments except for PFM000066, where the relatively low Cl concentrations are almost constant despite great variations in water flow similar to the other catchments (cf Section 5.3.1). The observed pattern is probably explained by a combination of dilution and supply of marine ions in the lower parts of the Forsmark area.
- Na shows a pattern very similar to Cl, probably due to the major common source of marine ions.
- K shows a pattern completely different from e.g. Na, indicating that other sources and mechanisms may mediate the distribution of this element. The Spearman correlation analysis in Table 5-4 indicate significant positive relationships with discharge, i.e. concentrations of K increase slightly when water flow in streams increase.
- Mg is negatively correlated to discharge similar to Na and Cl, but display a significantly lower spatial variation range within the Forsmark area compared to these ions, notified by a more compressed distribution in the vertical range. A possible explanation to this pattern may be an additional Mg source that partly disguises the supply of marine ions at lower levels in the area. A possible source may be calcite dissolution (cf Section 4.1.3).
- Ca and HCO_3 show very similar relationships with discharge, as both ions show significant negative correlations and analogue spatial distributions with rather constant concentrations in all catchments. Most probably are the distributions of these ions controlled by the same processes and sources, e.g. dissolution and precipitation of calcite (cf Section 4.1.3), and is only to a minor extent diluted when water flow increase in streams.
- SO_4 show similar to K tendencies for a positive correlation between concentrations and discharge, i.e. concentrations in streams tend to increase with increasing discharge. Similar to other marine ions as Na and Cl, there is a clear discrepancy between different catchments within the Forsmark area indicating an uneven spatial distribution of the SO_4-source (cf Section 4.1.2 dealing with the origin of sulphur). The major process behind this pattern during high flow episodes is probably flushing of SO_4 formed by oxidising sulphide minerals during the preceding dryer period.
- Total contents of elements and compounds associated with organic matter as carbon (TOC), nitrogen (tot-N) and phosphorus (tot-P), show small variations when discharge in streams varies several orders of magnitude, compared to for example Cl. The spatial distribution is also rather uniform regarding TOC and tot-N, which implies that the sources of these major constituents of organic matter are rather uniformly distributed throughout the area. Tot-P on the other hand shows a clear spatial variation with generally lower concentrations in PFM000066 and PFM000074 compared to for example the inlet to Lake Bolundsfjärden (PFM000068), a pattern with similarities to the distribution of several marine ions. This may be caused by an additional phosphorus source associated to the soils containing marine relics.
- Among the compounds associated to organic matter, NO_3-N, shows a highly deviating pattern. The concentrations vary within four orders of magnitude, compared to one or two for the rest of the parameters, and in all catchments NO_3-N is positively correlated to discharge according to the correlation analysis in Table 5-4. This is especially evident in the small lake Labboträsket, PFM000074, where very low NO_3-N concentrations are measured during low discharge episodes. This pattern may be the result of two superimposed mechanisms: during the vegetation period, NO_3-N is consumed by primary production, especially when the water turnover is low, whereas low NO_3-N concentrations during winter may be the result of noxic conditions when NH_4-N is formed.

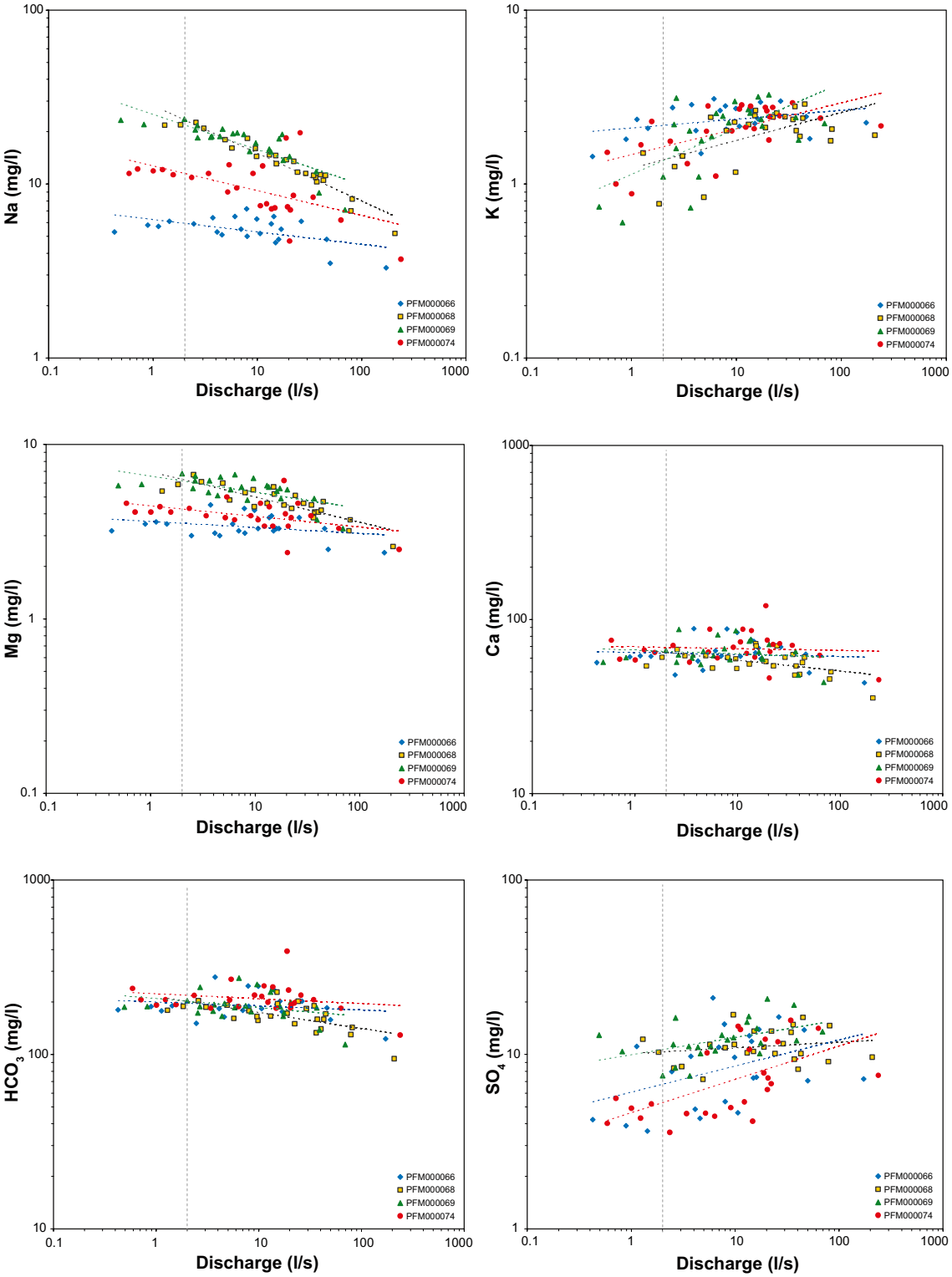

Figure 5-12. *Log-log plots showing discharge (L/s) plotted versus selected parameters (Na, K, Mg, Ca, HCO_3, and SO_4). Straight lines in the figures are power functions (e.g. $y = ax^n$) fitted to the observations (cf explanation in previous figure).*

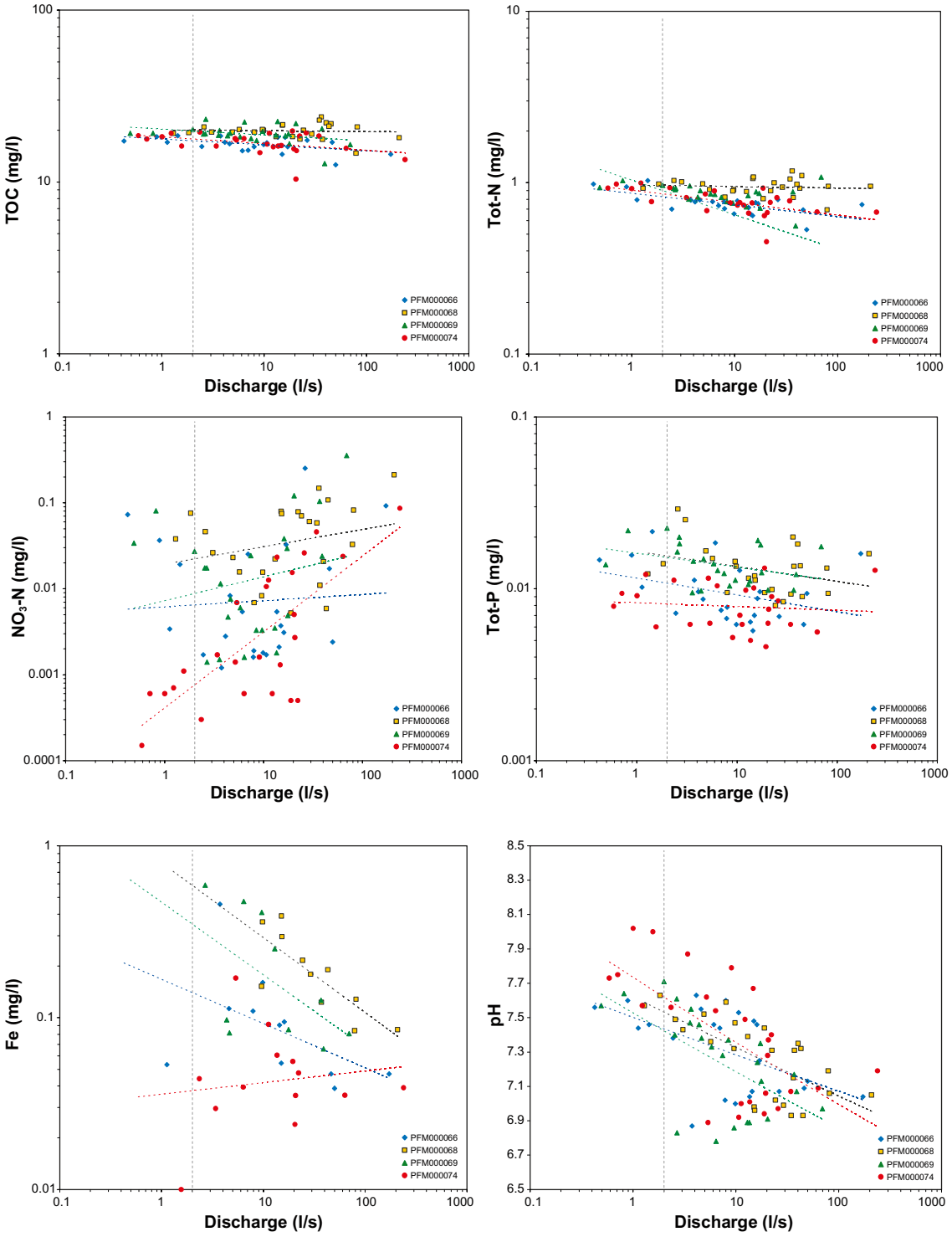

Figure 5-13. *Log-log plots showing discharge (L/s) plotted versus selected parameters (TOC, tot-N, NO_3-N, tot-P, Fe, and pH). Straight lines in the figures are power functions (e.g. $y = ax^n$) fitted to the observations (cf explanation in previous figure).*

- Fe concentrations show negative correlations to discharge in all catchments according to the correlation analysis in Table 5-4, which is especially evident in the catchments where the relict marine influence is significant.
- The pattern shown by pH is contradictory and further evaluation of the included observations is needed to find an explanation. Normally, pH decrease when flow increase due to the supply of organic acids in combinations with generally lower buffer capacity in water discharging via the shallow flow paths that prevail during high flow episodes.

The results from Figure 5-12 and Figure 5-13 are summarised in Table 5-5, where the exponents of the fitted power relationships of PFM000068 and PFM000066 may be compared. Negative exponents indicate negative correlations (and *vice versa*), and similar exponent values may be an indication that these parameters are influenced from the same major factors with respect to the relationship to discharge, e.g. Na and Cl,. Parameters with exponents close to zero show little correlation to discharge, and nothing can be said about the correlation structure among these parameters from this analysis.

5.2.1 Conclusions – concentrations and water flow

The exploration of measured discharge versus concentrations of a large number of elements in streams in the Forsmark area shows that the concentrations of most elements either decrease or stay rather constant when discharge increase:

- Marine ions as Cl, Na, and Mg show a clear negative correlation to discharge in lower located catchments, where marine relics are the probable source. The rapidly decreasing concentrations evident at flow rates exceeding 2–3 L/s, may be explained by dilution as an effect of the more shallow flow regimes that predominate at high flow episodes.
- Ions that originate from calcite dissolution, as Ca, HCO_3 and Sr, show a more uniform distribution over the Forsmark area, with no marked differences in spatial distribution. These ions are negatively correlated to the discharge according to the correlation analysis in Table 5-4, but the measured concentrations show a very small absolute decrease when discharge varies several orders of magnitude, which implies that the sources of Ca and HCO_3 are distributed along the major pathways of water.

Table 5-5. Compilation of exponents from the fitted power relationships marked by straight lines in Figure 5-12 and Figure 5-13 (the exponent b in the fitted power relationship $y = ax^b$). The higher located PFM000066 is compared to PFM000068, located in the inlet to Lake Bolundsfjärden. Negative correlations between the parameters and discharge are indicated by negative exponents, values close to zero indicate no correlation and positive exponents a positive correlation.

Element	PFM000068	PFM000066
Fe	–0.44	–0.26
Cl	–0.32	0.01
Na	–0.27	–0.07
Mg	–0.14	–0.03
HCO_3	–0.09	–0.02
Tot-P	–0.09	–0.10
Ca	–0.06	–0.01
pH	–0.02	–0.01
TOC	–0.01	–0.03
Tot-N	–0.01	–0.07
SO_4	0.03	0.15
K	0.16	0.05
NO_3-N	0.20	0.07

- A similar conclusion may also be applied on the total concentrations of carbon, nitrogen and phosphorus, which all are closely associated to decomposition and forming of organic matter. These elements show relatively constant concentrations analogous to Ca, both spatially and compared to water flow, even if measured discharge varies several orders of magnitude. Total phosphorus deviate slightly from this pattern by showing a spatial variation similar to some of the marine ions, implicating that an additional phosphorus source is associated to these soils.

5.3 Estimation of mass transports in Forsmark watercourses

Estimations of mass transports are based on concomitant measurements of concentrations and discharge in streams. Daily transports are calculated by multiplying total daily discharge with a concentration representative for the same time-period, and these daily estimations are further summarised to monthly and yearly transports. In the Forsmark area, daily discharge measurements are available from four gauge stations, and monthly concentration measurements are available from eight stream locations and from seven sampling sites in lakes (station identities are shown in Figure 5-14 and summarised in Table 5-8). Due to a mismatch among the discharge and chemistry stations with respect to time periods, sampling interval and spatial coverage of the stations, there is, however, a need for extrapolations in both time and space in order to make any transport estimations possible. These prerequisites are described in the following sections, and the results are compiled in Section 5.3.4.

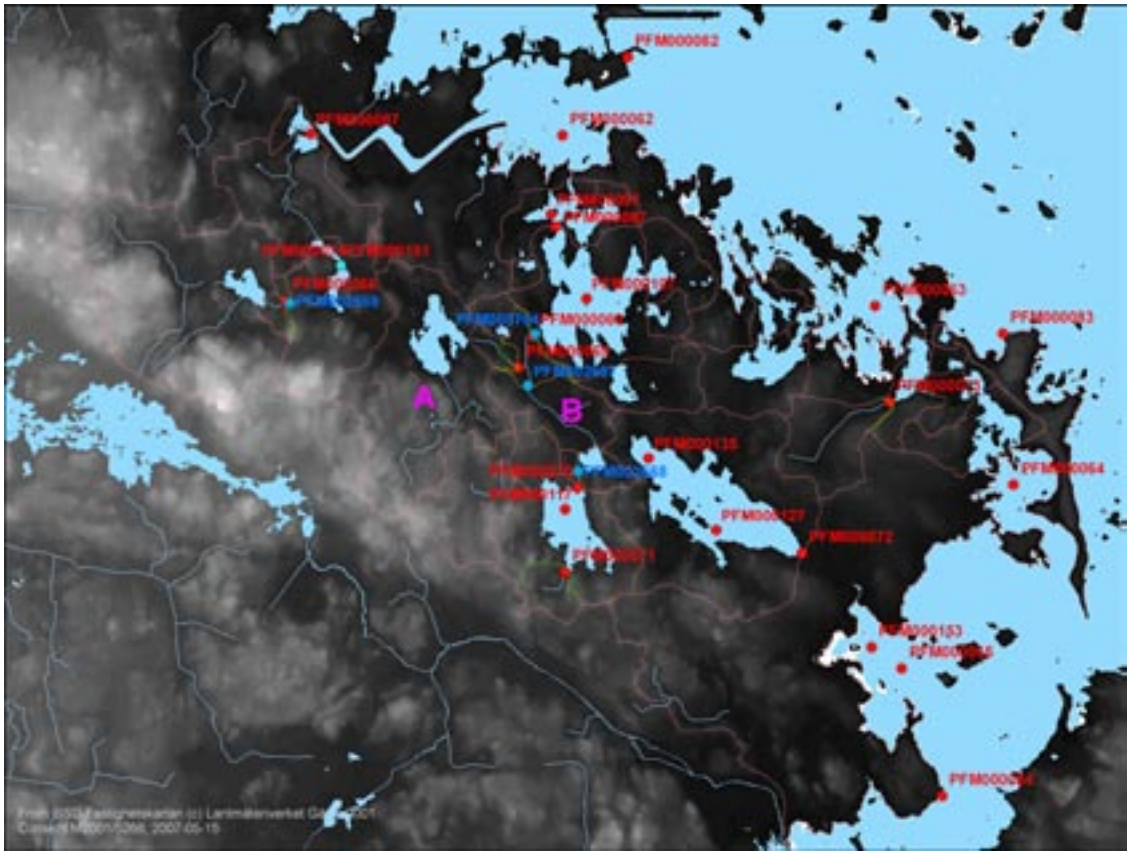

Figure 5-14. *Locations of hydrochemical stations (red) and hydrological discharge stations (blue) in the Forsmark area. The "official" catchments in the Forsmark area /Brunberg et al. 2004/ are marked in red and further divisions based on the locations of hydrochemical stations are coloured in green and discharge stations orange. Sub-catchments denoted "A" and "B" are discussed in the text.*

5.3.1 Evaluation of discharge measurements used for transport estimations

All four automatic discharge gauge stations in the Forsmark area show very good agreement, which is especially evident when the normalised time series are plotted in the lower panel in Figure 5-15. Despite the localisation in independent catchments, as PFM002669 and PFM005764, these stations show a very high degree of correlation according to Figure 5-16. This fact may be interpreted as if flow in probably all parts of the Forsmark area are controlled by the same underlying factors, and also that the area is rather homogenous with respect to hydrological driving variables as precipitation and evapotranspiration. Spatial extrapolation of discharge time-series, described in Section 5.3.2 is therefore straightforward due to the negligible spatial variation within the Forsmark area /cf Johansson and Juston 2007/.

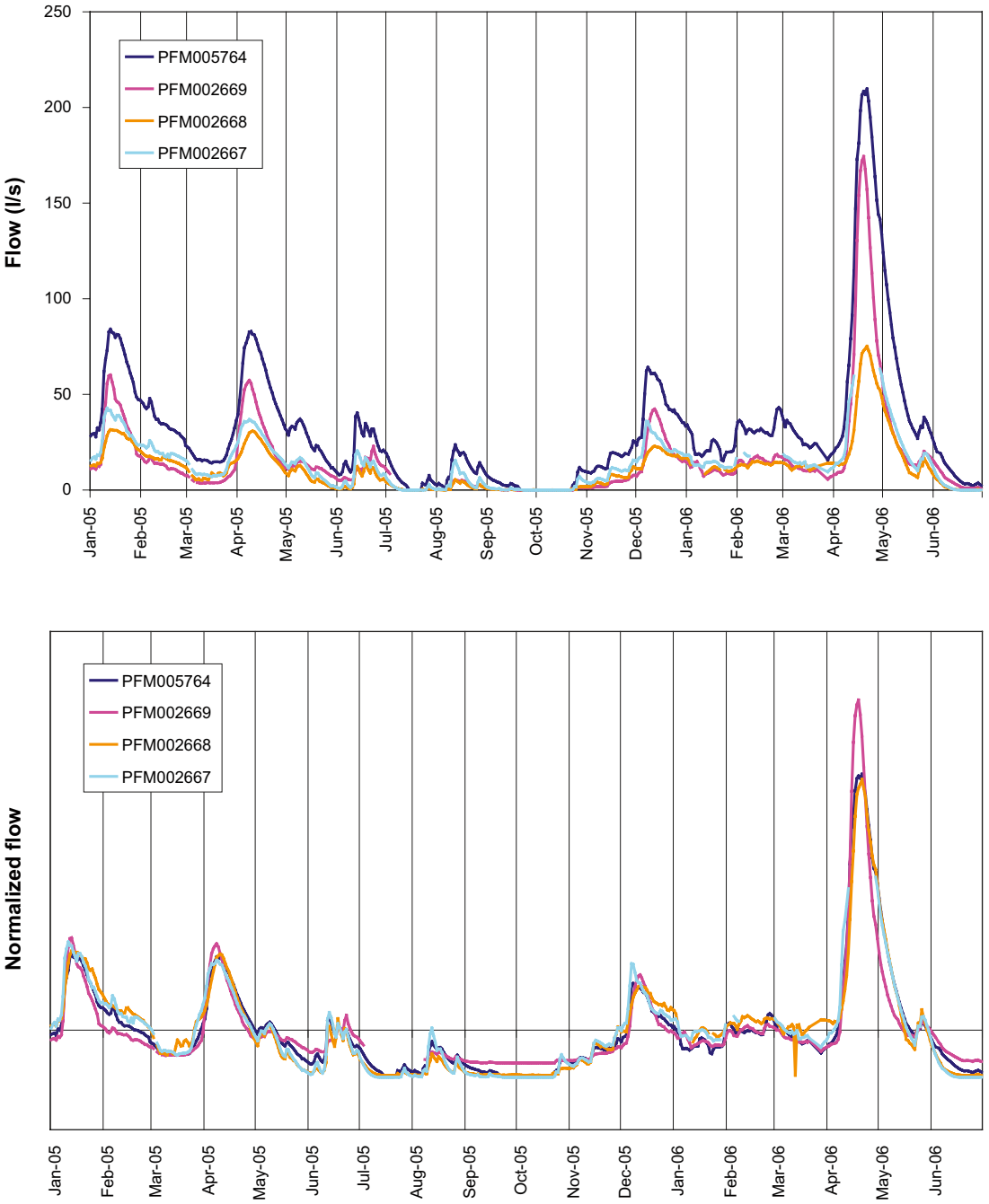

Figure 5-15. *Discharge time series registered automatically at four discharge stations in the Forsmark area. Original time series in L/s (upper), and a time series normalised to unit mean and variance (lower).*

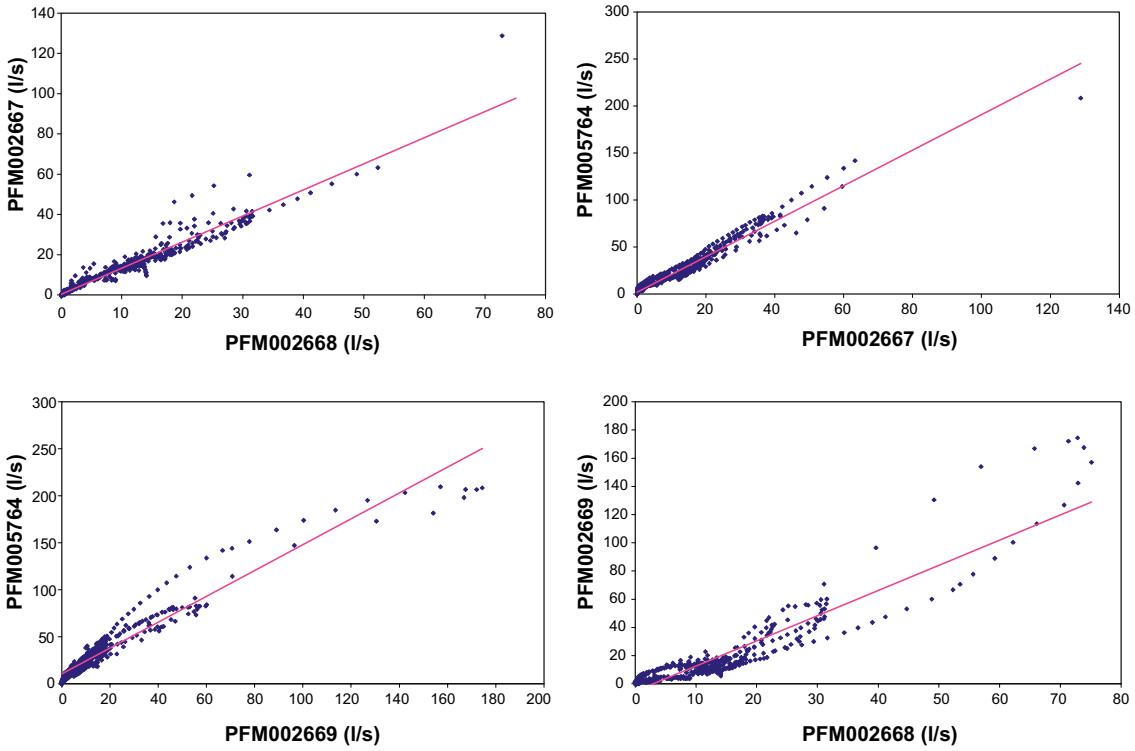

Figure 5-16. *Pair-wise comparisons of discharge time series at the four automatic discharge gauge stations. The plots are based on the time period from 2005-01-01 to 2006-06-30.*

A principal component analysis of the time-series shown in the cross-plots in Figure 5-16 and the time-series in Figure 5-15, further strengthens the conclusion of very high degree of correlation between discharge stations and adjacent catchments. The first component comprises as much as 96% of the total variation among these four discharge stations, i.e. the differences between the time series is only 4%. The second principal component comprises further 3% of the total variation, leaving only 1% not to be described in Figure 5-17.

From this analysis may be concluded that the variation patterns are most similar in PFM005764 and PFM002667, which is expected as these stations are located close to each other in the lower part of the same catchment. The largest discrepancy among the discharge stations is shown by PFM002668 and PFM002669, which are located in separate catchments. One possible explanation to this discrepancy is the differing lake proportions of the total catchment area: PFM002668 is located in the outlet of Lake Eckarfjärden with a relatively small drainage area, whereas PFM002669 drain a larger catchment containing only a very small and shallow lake.

From the score plot in the lower panel of Figure 5-17, where the number of the sampling month is shown, can be concluded that the minor difference comprised by the second principal component is mostly manifested by PFM002668, which show slightly higher discharge during January to March (blue ellipse), and during the spring flood in 2006 (green ellipse). PFM002669 shows an opposing pattern, whereas PFM005764 and PFM002667, placed in between (red ellipse), show little connection to this probably lake-induced pattern.

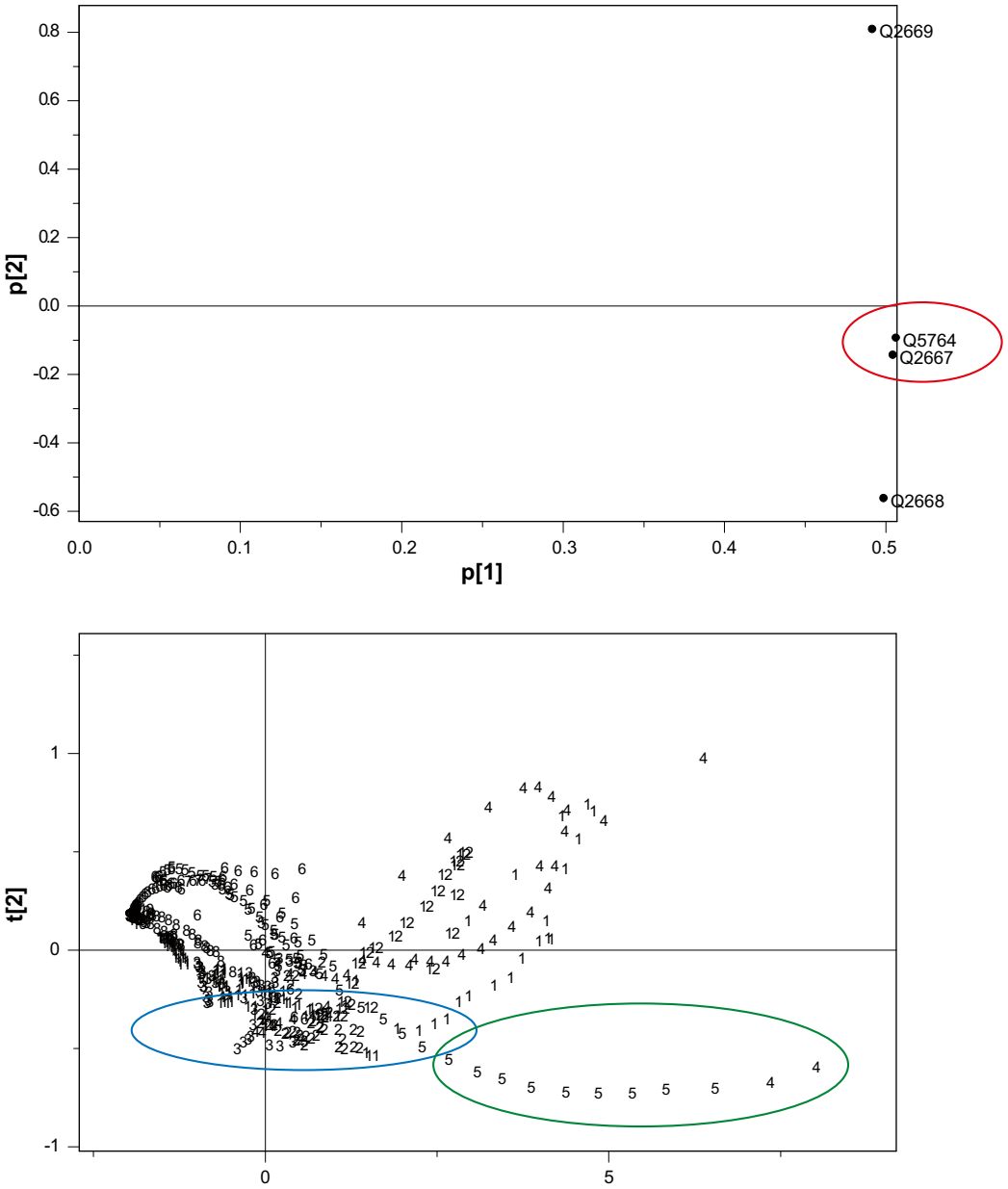

Figure 5-17. *Principal component analysis of discharge data from 2005-01-01 to 2006-06-30. The upper panel is a loading plot showing how the stations are related (cf Section 2.3.10 for an explanation of PCA), and in the score plot in the lower panel is shown how individual samples are related (numbers correspond to the number of the month). Only complete observations (i.e. with contemporary measurements from all four stations) were included in the analysis. This resulted for example in the exclusion of a part in the spring flood of 2006. The first, horizontal, component comprises 96% of the total variation and the second component further 3%, giving a total of 99%.*

When the specific discharge (i.e. discharge per unit area expressed in L/s,km^2) in Table 5-6 is compared among discharge stations, together with calculated values for two intermediate areas, the specific discharge is rather uniform all over the Forsmark area, further strengthening the conclusions based on previous PCA analysis. Specific discharge for the two intermediate areas of Lake Gällsboträsket and Lake Stocksjön, marked “A” and “B” respectively in Figure 5-14, represent the difference between two adjacent discharge stations, and these values are therefore extra susceptible for errors in either discharge measurements or in the determination of catchments areas.

Table 5-6. Specific discharge (L/s,km²) estimated for catchments upstream discharge gauging stations and difference areas around Lake Gällsboträsket (PFM005764–PFM002667) and Lake Stocksjön (PFM002667–PFM002668), denoted A and B respectively in Figure 5-14. The figures represent monthly mean values from the time period 2005-01-01 to 2006-06-30. In case of missing data PFM005764 was used to fill in series in order to achieve maximum comparability over months (cf Section 5.3.2).

Month	5764	2669	2668	2667	$Q_{gäll}$ (A)	Q_{stock} (B)
1	7.3	7.5	7.2	7.2	7.3	7.3
2	6.2	5.0	6.5	5.6	6.8	2.9
3	4.0	2.9	4.5	4.0	3.9	2.6
4	16.3	20.0	14.0	13.6	19.4	12.4
5	7.1	6.0	5.6	5.7	8.7	5.9
6	2.8	2.7	1.7	1.9	3.9	2.5
7	0.9	0.9	0.3	0.3	1.5	0.4
8	2.1	1.0	0.9	1.6	2.6	4.0
9	0.4	0.1	0.1	0.1	0.8	0.2
10	0.4	0.1	0.2	0.4	0.4	1.1
11	2.8	1.3	2.6	2.8	2.8	3.7
12	8.1	8.4	7.9	7.8	8.5	7.2
Mean	**4.9**	**4.7**	**4.3**	**4.3**	**5.6**	**4.2**

In conclusion, both variation patterns and specific discharge seem to be rather constant throughout the Forsmark area, a fact that justifies the simple proportional extrapolation in both time and space of the discharge series as explained in Section 5.3.2 below.

5.3.2 Extrapolation of discharge time series

Complete discharge time series extending over two full years are available only from PFM005764 at the inlet to Lake Bolundsfjärden, where measurements are available from April 2004, about half a year before the other three stations. In order to extrapolate these time series half a year back in time, discharge was calculated by proportionalisation with a constant determined from the parallel measurements during December 2004 to June 2006. Constants used are compiled in Table 5-7 and a graphical visualisation of the results is shown in Figure 5-18.

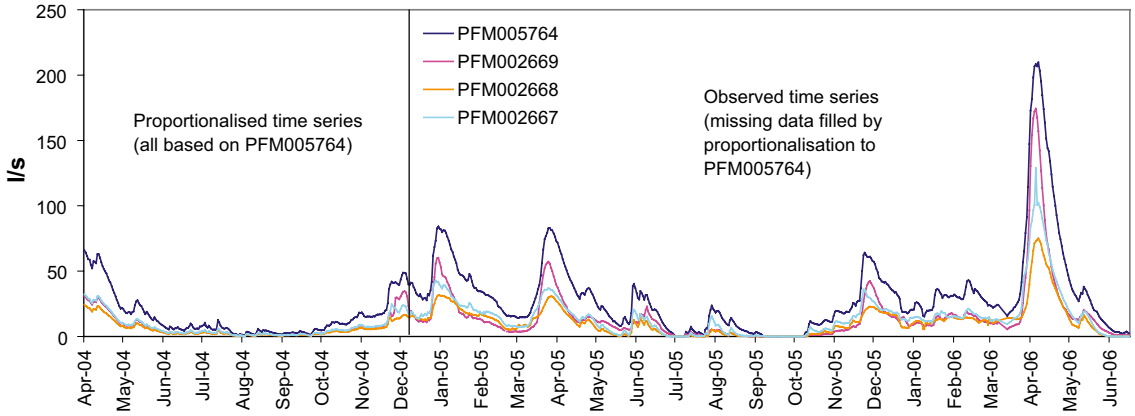

Figure 5-18. *Proportionalised and observed discharge time series from the automatic discharge gauge stations in the Forsmark area.*

Table 5-7. Constants used for extrapolation of discharge series back in time based on the automatic gauge discharge station PFM005764. These constants are based on parallel measurements of discharge during the period December 2004 to June 2006.

Discharge station	PFM005764	PFM002669	PFM002668	PFM002667
Ratio to PFM005764	1	0.467	0.366	0.488

Based on the good agreement among all discharge stations as described in Section 5.3.1, the extrapolation of the discharge time series back in time is regarded as sufficient in the light of the chemical sampling taking place only once a month (cf Section 5.3.3). This extrapolation only affects the estimated mass transports one of the two complete years that are accounted for in the compilations in Section 5.3.4.

As shown in Figure 5-14, the location of the hydrochemical sampling points usually not coincide with the automatic discharge stations, making a spatial extrapolation of the discharge necessary in order to estimate transports in all chemical sampling points. More or less sophisticated extrapolation methods may be used for this purpose, from simple calculations based on area proportions to complicated discharge models including snow models and varying soil conditions. The evaluation of discharge time series in previous section indicates that an uncomplicated proportionalisation model probably is sufficient in this case.

The uniform discharge conditions that seems to prevail in the whole Forsmark area, as stated in Section 5.3.1, implies that a simple model based on area proportionalisation may be sufficient for the spatial extrapolation used in this section. In Table 5-8 are available hydrochemical sampling points listed, together with information of which discharge stations are used for the extrapolation (in one case, PFM000069, is the difference between two discharge stations used). About half of the hydrochemical sampling points in this table are disqualified due to changes in the chemical sampling programme and terminated measurement series (cf Section 5.3.3). Constants used for spatial extrapolation are based on the catchments boundaries described in /Brunberg et al. 2004/ (compiled in Table 5-9). The resulting proportionalised time series are visualised in Figure 5-19.

Specific discharge during the period 2004-06-01 and 2006-05-31 are 4.7 L/s,km^2 for PFM005764 and 4.8L/s,km^2 for PFM002669 (cf Table 5-6). The average of 4.75 L/s,km^2 (150 mm/year) is supposed to represent average conditions in the Forsmark area.

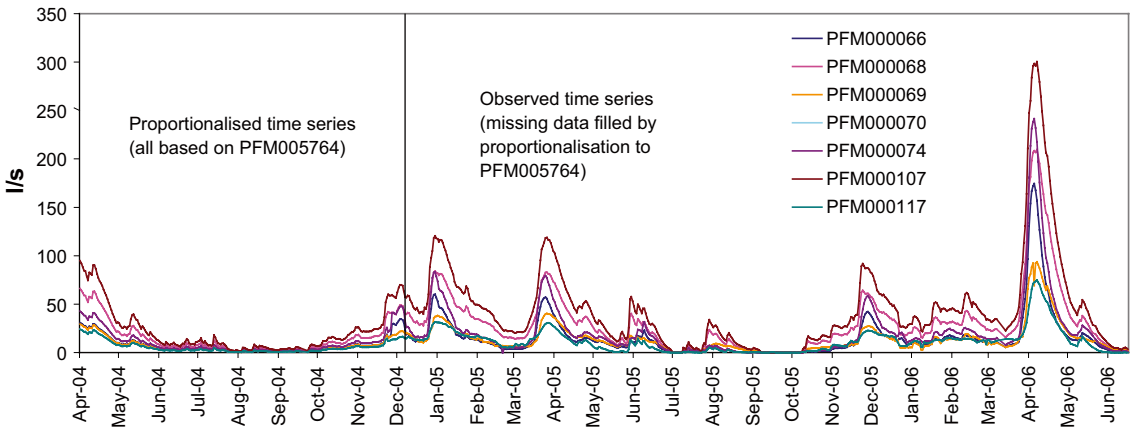

Figure 5-19. *Discharge time series for hydrochemical sampling points based on area proportionalisation of results from the automatic discharge gauging stations.*

Table 5-8. Compilation of available hydrochemical stations and hydrological discharge stations in the Forsmark area. Transport estimations were possible to conduct for hydrochemical stations marked in blue.

Hydrochemical sampling point	Water type	Geographical description	Possible discharge station	
			Overlapping	In vicinity
PFM000066	Stream	East Gunnarsboträsket	PFM002669	
PFM000074	Lake	Labboträsket		PFM002669
PFM000087	Lake	Gunnarsbo-Lillfjärden		PFM002669
PFM000071	Stream	South Eckarfjärdenn (inlet)		PFM002668
PFM000117	Lake	Eckarfjärden		PFM002668
PFM000070	Stream	North Eckarfjärden (outlet)	PFM002668	
PFM000069	Stream	Bolundskogen		PFM002667 and PFM2668
PFM000068	Stream	Kungsträsket	PFM005764	
PFM000107	Lake	Bolundsfjärden		PFM005764
PFM000067	Stream	Lillputtsundet		PFM005764
PFM000097	Lake	Norra Bassängen		*PFM005764*
PFM000127	Lake	Fiskarfjärden		*PFM005764*
PFM000135	Lake	Fiskarfjärden		*PFM005764*
PFM000072	Stream	Flottbron		*PFM005764*
PFM000073	Stream	South Bredviken (inlet)		*PFM005764*

Table 5-9. Coefficients used for the spatial extrapolation of discharge time series for hydrochemical sampling points. These coefficients are based on the catchment boundaries described in /Brunberg et al. 2004/.

Hydrochemical sampling point	PFM000066	PFM000068	PFM000069	PFM000070	PFM000074	PFM000107	PFM000117
Based on discharge station	PFM002669	PFM005764	PFM005764–PFM002667	PFM002668	PFM002669	PFM005764	PFM002668
Coefficient	1.00	1.00	0.871	0.996	1.39	1.43	0.996

5.3.3 Description of hydrochemical data used for transport estimations

A considerable source of error behind the calculations of mass transports in the Forsmark area is the estimation of representative concentrations. The spatial error regarding concentrations is negligible, since all mass transports are calculated for the specific hydrochemical sampling points, but the temporal resolution is more limited due to the monthly sampling interval.

As mass transports are estimated by multiplication of daily discharge and the concentration representative for this time interval (one day), daily concentrations have to be interpolated from the monthly measurements according to the calculation technique commonly used. This rough generalisation may of course lead to a great impact on the estimated mass transport if concentrations fluctuate between the sampling occasions. Concentrations show however usually much less variation compared to variations in discharge, which also was concluded in Section 5.2 where discharge contra concentrations was explored in Forsmark watercourses. Depending on element, this error varies. For total contents of major nutrients and carbon, concentrations showed a weak correlation to water flow, implicating that mass calculations for these elements are less affected by variations in water flow. Cl as well as other marine ions, show on the other hand a clear negative correlation with discharge in the downstream parts of the catchment, which may lead to overestimated transport of these ions during episodes of high discharge (see Table 5-4 and Table 5-5) for details on each parameter).

Parameters and hydrochemical sampling points with enough data for the transport calculation are summarised in Table 5-10, where complete time-series of monthly measurements are marked in blue. About half of the hydrochemical sampling points in this table are disqualified due to changes in the chemical sampling programme and terminated measurement series /Nilsson and Borgiel 2005b/.

5.3.4 Compilation of transports, areal specific transports and flow weighted concentrations

Daily mass transports were estimated by multiplying daily discharge (cf Section 5.3.2) with the interpolated daily concentrations (cf Section 5.3.3). These transports were further summarised to monthly and yearly transports.

Table 5-10. Compilation of available hydrochemical data used for transport estimations. The figures represent the available number of observations per sampling point during 2004-05-01 to 2006-06-30. Transport estimations were possible to calculate only for sampling points with complete monthly time series, marked in blue in the table.

ID code	Na	K	Ca	Mg	HCO_3	Cl	SO_4	SO_4_S	Br	F	Si	Sr
PFM000066	23	23	23	23	23	23	23	23	23	23	23	23
PFM000067	4	4	4	4	4	4	4	4	4	4	4	4
PFM000068	26	26	26	26	26	26	26	26	26	26	26	26
PFM000069	25	25	25	25	25	25	25	25	25	25	25	25
PFM000070	26	26	26	26	26	26	26	26	26	26	26	25
PFM000071	4	4	4	4	4	4	4	4	4	4	4	4
PFM000072	4	4	4	4	4	4	4	4	4	4	4	4
PFM000073	3	3	3	3	3	3	3	3	3	3	3	2
PFM000074	27	27	27	27	27	27	27	27	27	27	27	27
PFM000087	4	4	4	4	4	4	4	4	4	4	4	4
PFM000097	4	4	4	4	4	4	4	4	4	4	4	4
PFM000107	26	26	26	26	26	26	26	26	26	26	26	26
PFM000117	26	26	26	26	26	26	26	26	26	26	26	26
PFM000135	7	7	7	7	6	7	7	7	7	7	7	7

ID code	NH_4-N	NO_3-N	N-TOT	P-TOT	PO_4-P	POP	PON	SiO_2-Si	POC	TOC	DOC	DIC
PFM000066	25	25	25	25	25	24	24	25	24	25	25	25
PFM000067	4	4	4	4	4	4	4	4	4	4	4	4
PFM000068	27	27	27	27	27	27	27	27	27	27	27	27
PFM000069	26	26	26	26	26	26	26	26	26	26	26	26
PFM000070	28	28	28	28	28	27	28	28	28	28	28	28
PFM000071	4	4	4	4	4	4	4	4	4	4	4	4
PFM000072	4	4	4	4	4	4	4	4	4	4	4	4
PFM000073	3	3	3	3	3	3	3	3	3	3	3	3
PFM000074	29	29	29	29	29	29	29	29	29	29	29	29
PFM000082	3	3	3	3	3	3	3	3	3	3	3	3
PFM000087	4	4	4	4	4	4	4	4	4	4	4	4
PFM000097	4	4	4	4	4	4	4	4	4	4	4	4
PFM000107	29	29	29	29	29	29	28	29	28	29	29	29
PFM000117	28	28	28	28	28	28	28	28	28	28	28	28
PFM000135	9	9	9	9	9	9	9	9	9	9	9	9

In order to fully utilise available hydrochemical data and available time series of discharge measurements, transports are not compiled for calendar years, but for two consecutive hydrological years extending over the period 2004-06-01 to 2006-05-31. To give a conception of the variation between years, transports are summarised both per year and over the whole two year period (cf Section 5.3.3 for further discussions on uncertainties in transport estimations).

Estimated mass transports at stream sampling points may also be presented as area specific transports (mass transport per unit area and year) or flow weighted concentrations (total transport divided by total discharge volume). In Appendix E are mass transports, area-specific transports and flow weighted concentrations compiled per year (not calendar years), and as averages for the two year period. Monthly values representing averages of the two year period are also compiled in this appendix.

The relative differences in estimated transports are compiled in Table 5-11. Year 2 show generally about 30% higher transports compared to year 1, a figure that agree with the general difference in discharge of about 30% between the years. It can therefore be concluded that variations in discharge is the major factor causing the observed variations in mass transports. Phosphorus species and F deviate from this pattern by showing greater differences in the range of 50–100%, a fact that may indicate a coupling to variations in water flow, although this is not indicated by the correlation analysis in Section 5.2.

5.3.5 Visualisation of area-specific transports

In this section are area-specific transports shown in bar graphs. These visualisations emphasize differences in underlying sources of the selected parameters by the normalisation with the whole catchment area upstream each sampling point. If the supply of ions and substances are evenly distributed throughout the Forsmark area, the bars will be equal in height.

Table 5-11. Relative difference (%) between estimated transports in year 1 and year 2, calculated as 100×(year 2-year 1)/year 1, i.e. the figures show how transport changed from year 1 to year 2. Deviations exceeding ±20% have been colour marked in the table: yellow +20 to +39%, brown > +40%, blue < –20%.

	q (L/s)	Na	K	Ca	Mg	HCO_3	DIC	Cl	SO_4	SO_4S	Br	F	Sr
PFM000066	34	39	43	38	39	34	32	43	9	13	–37	110	30
PFM000074	34	22	48	34	34	27	22	33	28	30	30	64	25
PFM000117	24	18	19	39	27	30	35	18	10	17	–39	92	25
PFM000070	24	31	24	20	26	21	14	32	4	9	170	87	19
PFM000069	28	36	49	33	34	29	23	35	19	24	160	60	28
PFM000068	30	38	47	36	39	32	29	39	24	27	141	77	30
PFM000107	30	3	19	34	15	34	30	1	4	11	–33	91	16

	q (L/s)	TotN	NH_4N	NO_3N	PON	TotP	PO_4P	POP	TOC	DOC	POC	Si	SiO_2Si
PFM000066	34	51	93	700	98	85	105	84	40	43	87	46	44
PFM000074	34	28	–54	427	14	51	125	36	28	27	–4	42	18
PFM000117	24	16	–1	70	7	65	93	16	31	30	–1	104	72
PFM000070	24	25	59	23	38	48	65	47	15	14	33	16	11
PFM000069	28	40	26	418	62	53	54	84	33	34	45	37	27
PFM000068	30	38	69	120	33	40	125	34	30	31	26	41	32
PFM000107	30	31	29	92	35	51	97	12	31	30	34	62	46

The bars in the diagrams represent area-specific transports calculated for the individual years, where year 1 corresponds to the period 2004-06-01 to 2005-05-31, and year 2 2005-06-01 to 2006-05-31 (see Table 5-2 for explanation and Figure 5-14 for localisation of sampling points). PFM000066, PFM000070, PFM000069 and PFM000068 represent stream sampling points, whereas PFM000074, PFM000117 and PFM0000107 represent lake sampling points (Lake Labboträsket, Lake Eckarfjärden and Lake Bolundsfjärden, respectively). Lake Bolundsfjärden is influenced from sea water intrusions, which is the main explanation to the elevated transports of marine ions, e.g. Ca, Na, and Mg (cf Section 4.1.1).

Area-specific transports for Cl are shown in Figure 5-20, and in Figure 5-21 are the other major constituents (Ca, Mg, Na, HCO_3, SO_4) visualised together with Br and F. Organic substances and nutrients are shown in Figure 5-22, together with total contents of Si. Conclusions based on these figures are summarised in the list below:

- For ions of predominantly marine origin (Na, Cl, Br, and to some extent Mg and SO_4), the hydrochemical sampling points PFM000069 and PFM000107 show elevated supply per unit area compared to the rest of the points. The explanation to the elevated levels in PFM000107 (Lake Bolundsfjärden), as previously mentioned, most probably are the recurring salt water intrusions (cf Section 4.1.1). PFM000069 located at the outlet of Lake Gällsboträsket is on the other hand located well above sea level and modern salt water intrusion can not be an explanation to the observed elevated area-specific discharge from this catchment. A possible explanation may in this case (as well as to some extent in PFM000074) be old marine remnants in the Quaternary deposits (cf Section 6 for further analysis of the coupling between specific transports and distribution of sediments in the Forsmark area).
- Ca, HCO_3 and to some extent K, show very similar patterns with only minor fluctuations throughout the Forsmark area. The sampling points within and in the outlet of Lake Eckarfjärden deviate by showing slightly lower area-specific transports, probably due to influences from the lake.

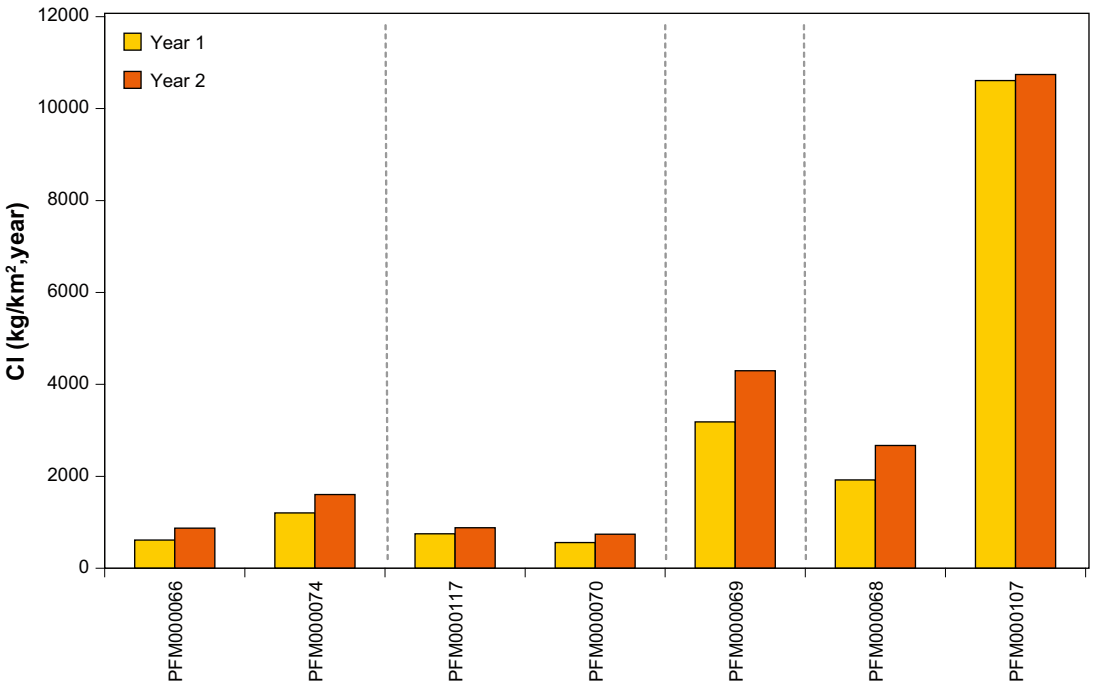

Figure 5-20. *Area-specific Cl transport in the Forsmark area (kg/km²,year). The bars in the diagram represent specific transports calculated for the individual years, where year 1 corresponds to the period 2004-06-01 to 2005-05-31, and year 2 2005-06-01 to 2006-05-31. See Table 5-8 for explanation and Figure 5-14 for localisation of sampling points.*

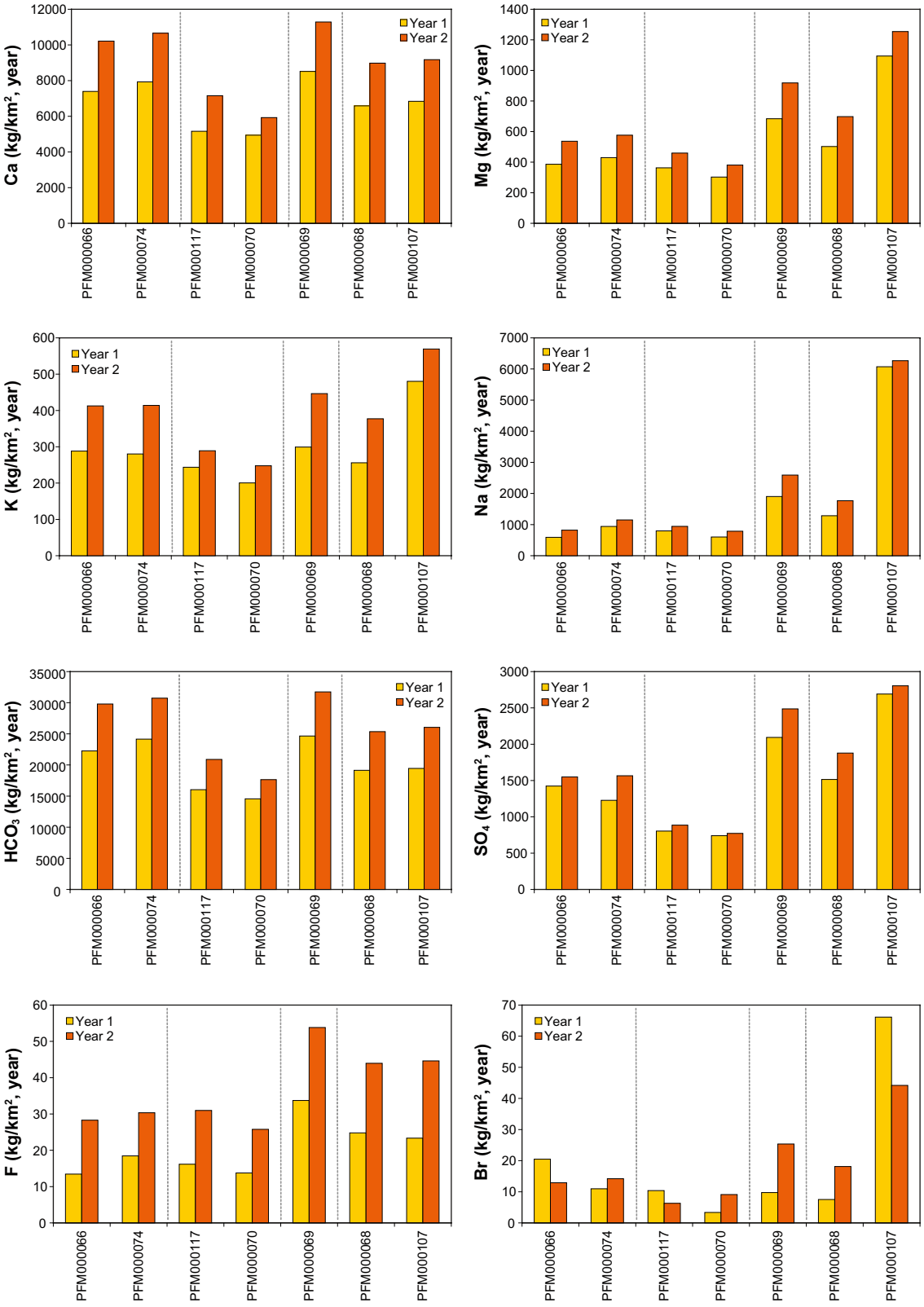

Figure 5-21. *Area-specific transports of Ca, Mg, K, Na, HCO_3, SO_4, F, and Br in the Forsmark area (kg/km²,year). See Figure 5-20 for an explanation to the diagrams, and Figure 5-14 for localisation of sampling points.*

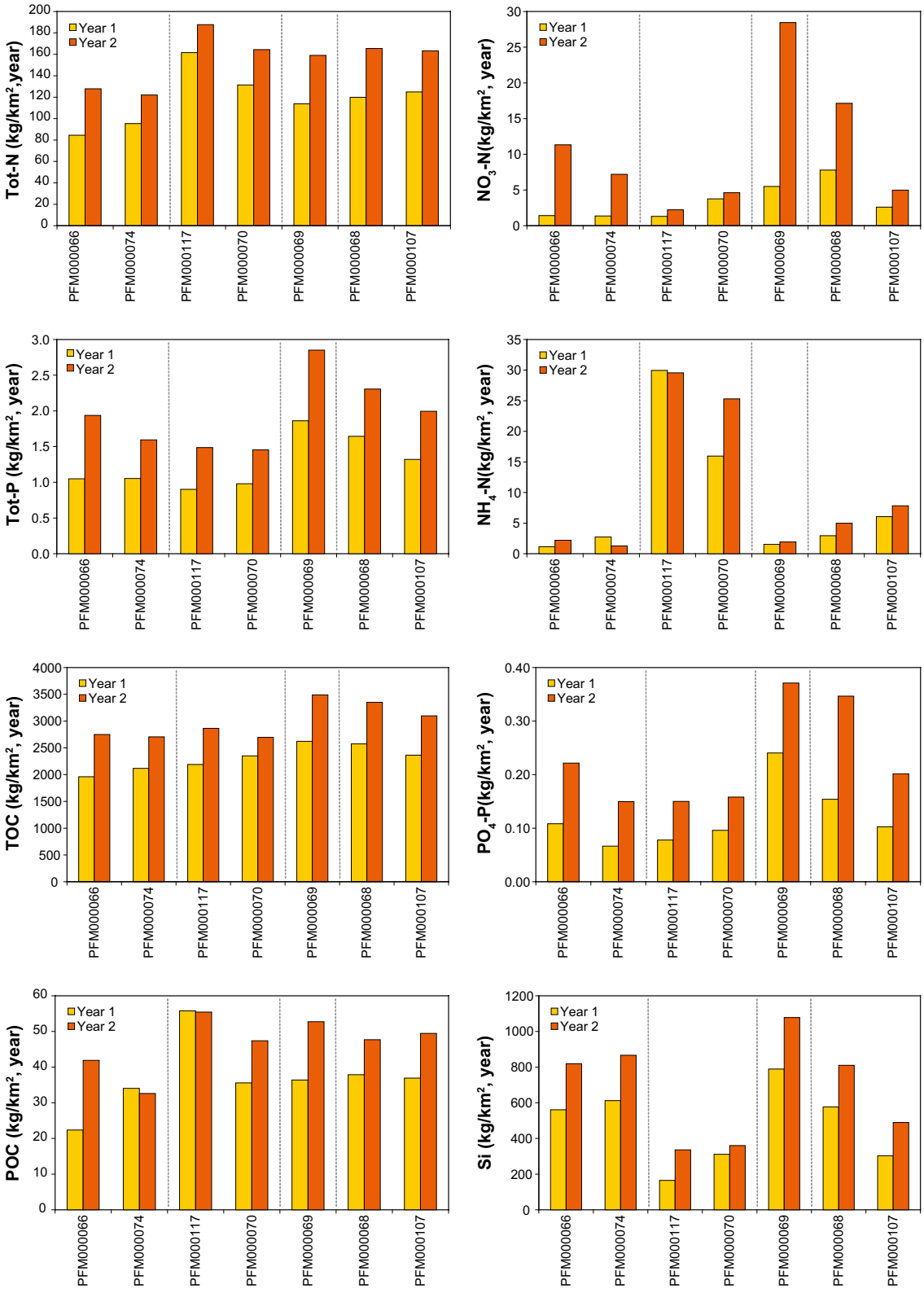

Figure 5-22. *Area-specific transports of Tot-N, NO_3-N, Tot-P, NH_4-N, TOC, PO_4-P, POC, and Si in the Forsmark area (kg/km²,year). See Figure 5-20 for an explanation to the diagrams, and Figure 5-14 for localisation of sampling points.*

- Fluoride shows pronounced difference between the two studied years, as area-specific transports are almost doubled year 2 compared to year 1. A similar, but weaker pattern, is also seen among other ions, e.g. Ca and K. According to the correlation analysis in Section 5.2, where water flow is correlated to a large number of parameters, the relationship between F and discharge is negative, indicating that another factor than water flow may be the explanation, e.g. differences in weathering rates between the two years.
- The spatial distribution of the organic substances and related ions in Figure 5-22, differ from the "inorganic" ion species by showing a relatively uniform area-specific transport in the included sampling points. Tot-P and PO_4-P deviate to some extent from tot-N and TOC by showing slightly elevated specific transports in the outlet of Lake Gällsboträsket, in concordance with e.g. marine ions, which may indicate the presence of an additional phosphorus source in this area, e.g. a specific regolith category.
- Nitrogen compounds, as NO_3-N and NH_4-N, as well as total silicon, show deviating characteristics within lake surface water and in the outlet of Lake Eckarfjärden (PFM000117 and PFM000070, respectively). These patterns probably reflect the influence from processes in the lake ecosystem as bacterial degradation of organic matter and uptake of Si in diatoms. The sampling point in Lake Bolundsfjärden (PFM000107), show a similar pattern regarding these compounds with the exception of NH_4-N.

It should be noted that there are probably greater variations among the organic species and related substances within the Forsmark area than reflected by this selection of sampling points. For example PFM000073 in the outlet of Bredviken, a catchment significantly influenced from farming activities, show high concentrations of tot-P (0.08 mgP/L compared to Forsmark average of 0.024 mgP/L) and tot-N (2.8 mgN/L compared to Forsmark average of 1.2 mgN/L) in combination with low TOC, probably an effect of leakage of nutrients from arable land /Sonesten 2005/ (cf Section 7.7).

5.3.6 Estimated transports of trace elements

Based on the estimated transport of major constituents in Section 5.3.4 and a correlation analysis of concentrations of a large number of trace elements versus these major constituents, mass transports and area-specific transports were estimated for almost 40 trace elements. The results in the form of mass transports per year and area-specific transports per year are compiled in Table 5-13 and Table 5-14.

The basis for the selection of which major constituent should be used as a representative for each trace element is a standard Pearson correlation analysis conducted on 56 samples from fresh surface water in the Forsmark area with complete characterisation of trace elements, which is summarised in Table 5-12. The scale factor in the rightmost column represents the ratio between the average concentration of the trace element and the average of the selected major constituent that show the largest significant ($p < 0.05$) correlation coefficient (it should be noted, however, that the use of Pearson correlation coefficients may violate the condition of normally distributed variables). This coefficient is multiplied with the previously estimated transport of the current major constituent, thus giving a coarse estimation of the transport of the trace element at interest. This estimation, which accordingly is based on several assumptions, may foremost be regarded as estimation of the order of magnitude of transports of trace elements in Forsmark watercourses.

Four selected trace elements are visualised in Figure 5-23, analogous to previous visualisations of area-specific transports (cf Figure 5-20).

It should be noted that errors in transport estimations due to the statistical approach are expected, especially when the correlation coefficients are low or erroneously regarded as significant. When the significance of a large number of correlations are investigated, about 5% of the relationships should erroneously be regarded as significant due to the assumptions of the underlying statistical testing, i.e. 8 out of 153 significant relationships in Table 5-12.

Table 5-12. Pearson correlation coefficients for concentrations in fresh surface water of trace elements and selected major elements for which transports are estimated. The largest significant ($p < 0.05$) correlation coefficient per trace element used for the transport estimation is marked red in the table (other significant coefficients are shaded blue). The scale factor in the rightmost column is the ratio between the average concentration of the trace element and the average of the selected major constituent in freshwaters in the Forsmark area.

Element	TOC	POC	Na	K	Ca	Mg	HCO_3	Cl	SO_4	Si	Scale factor
Ba	–0.05	–0.11	0.10	**0.47**	**0.83**	**0.48**	**0.75**	0.10	**0.60**	**0.57**	4.2E–04
Cd	–0.14	0.13	**0.50**	**0.32**	0.06	**0.43**	0.06	**0.48**	0.14	–0.17	2.1E–07
Ce	**0.54**	–0.11	0.25	0.05	0.06	0.08	–0.08	**0.32**	0.20	**0.29**	1.3E–06
Co	0.14	**0.52**	0.22	**0.43**	**0.36**	**0.47**	**0.46**	0.18	**0.50**	0.08	1.9E–04
Cr	**0.58**	–0.14	0.21	0.05	0.11	0.03	–0.02	**0.27**	0.18	**0.35**	2.5E–05
Cs	0.00	0.00	0.00	0.00	0.00	0.00	0.00	0.00	0.00	0.00	–
Cu	–0.14	**–0.27**	–0.15	**0.29**	**0.40**	0.14	**0.38**	–0.10	**0.37**	0.17	1.4E–05
Dy	**0.57**	**–0.32**	0.06	0.00	0.22	–0.07	0.05	0.15	0.16	**0.51**	1.1E–06
Er	**0.57**	**–0.33**	0.06	–0.03	0.24	–0.07	0.07	0.14	0.15	**0.53**	8.5E–07
Eu	0.21	–0.17	**0.34**	–0.01	0.00	0.16	–0.08	**0.36**	–0.01	0.02	7.6E–08
Fe	**0.56**	0.23	**0.27**	0.11	0.21	0.18	0.11	**0.31**	**0.27**	**0.35**	7.4E–03
Gd	0.56	**–0.30**	0.09	–0.03	0.18	–0.05	0.02	0.17	0.14	**0.46**	1.1E–06
HF	**0.44**	**–0.30**	–0.18	0.01	**0.29**	–0.15	0.17	–0.08	0.19	**0.49**	3.7E–06
Hg	**0.44**	0.09	0.16	–0.01	0.10	0.04	0.04	0.21	0.01	**0.35**	1.1E–07
Ho	**0.42**	–0.23	**0.30**	0.12	0.13	0.15	0.01	**0.34**	0.20	**0.31**	2.8E–07
I	**0.35**	**0.34**	**0.26**	0.17	–0.21	0.12	–0.16	0.21	0.03	–0.02	4.0E–04
La	**0.54**	–0.24	0.15	0.01	0.09	0.00	–0.06	0.23	0.15	**0.35**	5.0E–06
Li	**–0.38**	**0.31**	0.24	**0.79**	**0.54**	**0.78**	**0.63**	0.21	**0.78**	–0.05	1.0E–03
Lu	–0.06	–0.06	**0.47**	0.16	–0.09	**0.28**	–0.11	**0.44**	0.06	–0.16	1.9E–07
Mn	**0.33**	**0.31**	–0.12	–0.02	**0.29**	–0.02	**0.28**	–0.13	0.14	**0.32**	2.2E–03
Mo	**–0.53**	0.10	0.23	**0.58**	0.21	**0.58**	**0.32**	0.21	**0.49**	**–0.31**	1.8E–04
Nd	**0.57**	**–0.26**	0.07	–0.01	0.14	–0.06	–0.01	0.15	0.15	**0.43**	1.1E–06
Ni	–0.08	–0.05	0.14	**0.62**	**0.69**	**0.56**	**0.67**	0.17	**0.74**	**0.30**	2.7E–05
Pb	0.07	**0.31**	**0.76**	**0.28**	**–0.34**	**0.49**	**–0.33**	**0.74**	0.13	**–0.46**	4.5E–06
Pr	**0.54**	**–0.26**	0.15	–0.01	0.10	–0.02	–0.05	0.23	0.14	**0.38**	5.2E–06
Rb	0.20	0.11	**0.51**	**0.57**	–0.14	**0.38**	–0.22	**0.51**	**0.52**	–0.13	8.7E–04
Sb	–0.14	**0.36**	**0.40**	**0.48**	–0.22	**0.43**	–0.13	**0.41**	**0.34**	**–0.60**	2.7E–05
Sc	0.18	–0.13	–0.07	–0.02	–0.01	–0.07	–0.02	–0.05	0.01	0.15	–
Sm	**0.55**	**–0.29**	0.13	0.00	0.15	–0.03	–0.01	0.21	0.15	**0.42**	2.3E–07
Sr	**–0.34**	0.06	**0.39**	**0.74**	**0.72**	**0.87**	**0.73**	**0.39**	**0.76**	0.14	1.5E–02
Tb	0.09	–0.04	**0.29**	0.22	–0.03	0.18	–0.11	**0.27**	0.13	0.16	4.3E–07
Th	0.51	**–0.27**	–0.02	0.04	0.11	–0.09	–0.01	0.07	0.15	**0.40**	1.1E–06
Tl	–0.02	0.03	0.16	0.14	0.01	0.15	0.01	0.16	0.17	–0.21	6.3E–06
Tm	0.08	–0.10	**0.50**	0.21	0.00	**0.32**	–0.05	**0.49**	0.15	–0.05	1.2E–07
U	**–0.50**	–0.09	–0.09	**0.60**	**0.76**	**0.57**	**0.81**	–0.09	**0.69**	0.16	1.7E–05
V	–0.12	**0.48**	**0.41**	0.25	**–0.28**	**0.35**	–0.23	**0.38**	0.20	–0.51	7.1E–04
Y	**0.58**	**–0.32**	–0.06	–0.02	0.25	–0.14	0.08	0.04	0.16	**0.54**	9.5E–06
Yb	**0.57**	**–0.33**	0.04	0.01	**0.29**	–0.06	0.12	0.12	0.19	**0.57**	9.1E–07
Zn	**0.28**	–0.05	0.12	0.15	0.06	0.05	–0.02	0.14	**0.27**	0.26	1.1E–04
Zr	**0.31**	**–0.28**	–0.14	0.12	**0.31**	–0.06	0.19	–0.06	**0.30**	**0.43**	9.1E–05

Table 5-13. Estimated mass transports of trace elements in the Forsmark area (g or kg per year). The calculation, which is based on several uncertain assumptions, may foremost be regarded as an estimation of the order of magnitude of transports of trace elements in Forsmark watercourses.

Element	Unit	PFM000066	PFM000074	PFM000117	PFM000070	PFM000069	PFM000068	PFM000107
Ba	g	10,495	15,347	5,875	5,185	9,335	18,283	26,942
Cd	g	0.4	0.9	0.4	0.3	1.1	1.8	10.6
Ce	g	42	60	36	36	43	104	138
Co	g	17	25	24	18	19	45	65
Cr	g	169	239	145	145	173	418	552
Cs	g	Not calculated due to no significant relationship with major constituents						
Cu	g	344	503	193	170	306	600	884
Dy	g	8	11	6	6	8	19	25
Er	g	6	8	5	5	6	14	19
Eu	g	0.2	0.4	0.1	0.1	0.6	1.0	6.5
Fe	kg	50	70	43	43	51	123	162
Gd	g	7	11	6	6	8	18	24
HF	g	7	11	2	3	8	14	12
Hg	g	0.7	1.0	0.6	0.6	0.7	1.8	2.3
Ho	g	2	3	2	2	2	5	6
I	kg	3	4	2	2	3	7	9
La	g	34	48	29	29	35	83	110
Li	kg	1.0	1.4	0.6	0.5	0.9	1.8	4.3
Lu	g	0.4	0.8	0.4	0.3	1.0	1.7	9.6
Mn	kg	15	21	13	13	15	36	48
Mo	g	176	242	107	90	148	314	744
Nd	g	35	50	30	30	36	87	115
Ni	g	115	150	52	47	140	259	601
Pb	g	9	19	9	7	23	39	224
Pr	g	9	12	8	7	9	22	29
Rb	g	864	1,186	526	443	727	1,539	3,654
Sb	g	27	37	16	14	23	48	114
Sc	g	Not calculated due to no significant relationship with major constituents						
Sm	g	7	11	6	6	8	18	24
Sr	kg	20	30	14	12	27	51	143
Tb	g	0.9	1.8	0.9	0.7	2.2	3.7	21.4
Th	g	7	10	6	6	7	18	23
Tl	g	Not calculated due to no significant relationship with major constituents						
Tm	g	0.2	0.5	0.2	0.2	0.6	1.0	6.1
U	g	1,234	1,802	701	612	1,058	2,080	3,045
V	g	65	94	90	67	71	171	247
Y	g	63	90	54	54	65	156	207
Yb	g	6	9	5	5	6	15	20
Zn	g	731	1,037	628	627	750	1,812	2,392
Zr	g	178	264	52	69	190	352	288

Table 5-14. Estimated area-specific transports of trace elements in the Forsmark area (g or kg per year). The calculation, which is based on several uncertain assumptions, may foremost be regarded as an estimation of the order of magnitude of specific transports of trace elements in Forsmark watercourses.

Element	Unit	PFM000066	PFM000074	PFM000117	PFM000070	PFM000069	PFM000068	PFM000107
Ba	g/km²	3,702	3,908	2,588	2,284	4,163	3,272	3,366
Cd	g/km²	0.2	0.2	0.2	0.1	0.5	0.3	1.3
Ce	g/km²	15	15	16	16	19	19	17
Co	g/km²	6	6	10	8	8	8	8
Cr	g/km²	60	61	64	64	77	75	69
Cs[A]	g/km²	Not calculated as all observations in surface water fall below reporting limit						
Cu	g/km²	121	128	85	75	137	107	110
Dy	g/km²	3	3	3	3	3	3	3
Er	g/km²	2	2	2	2	3	3	2
Eu	g/km²	0.1	0.1	0.1	0.0	0.3	0.2	0.8
Fe	kg/km²	18	18	19	19	23	22	20
Gd	g/km²	3	3	3	3	3	3	3
HF	g/km²	3	3	1	1	3	3	1
Hg	g/km²	0.25	0.26	0.27	0.27	0.32	0.31	0.29
Ho	g/km²	0.7	0.7	0.7	0.7	0.9	0.8	0.8
I	kg/km²	0.9	1.0	1.0	1.0	1.2	1.2	1.1
La	g/km²	12	12	13	13	15	15	14
Li	kg/km²	0.4	0.4	0.3	0.2	0.4	0.3	0.5
Lu	g/km²	0.1	0.2	0.2	0.1	0.4	0.3	1.2
Mn	kg/km²	5	5	6	6	7	7	6
Mo	g/km²	62	62	47	40	66	56	93
Nd	g/km²	12	13	13	13	16	16	14
Ni	g/km²	41	38	23	21	63	46	75
Pb	g/km²	3	5	4	3	10	7	28
Pr	g/km²	3	3	3	3	4	4	4
Rb	g/km²	305	302	232	195	324	275	457
Sb	g/km²	10	9	7	6	10	9	14
Sc	g/km²	Not calculated due to no significant relationship with major constituents						
Sm	g/km²	3	3	3	3	3	3	3
Sr	kg/km²	7	8	6	5	12	9	18
Tb	g/km²	0.3	0.5	0.4	0.3	1.0	0.7	2.7
Th	g/km²	3	3	3	3	3	3	3
Tl	g/km²	Not calculated due to no significant relationship with major constituents						
Tm	g/km²	0.1	0.1	0.1	0.1	0.3	0.2	0.8
U	g/km²	435	459	309	269	472	372	381
V	g/km²	23	24	40	30	32	31	31
Y	g/km²	22	23	24	24	29	28	26
Yb	g/km²	2	2	2	2	3	3	2
Zn	g/km²	258	264	277	276	335	324	299
Zr	g/km²	63	67	23	31	85	63	36

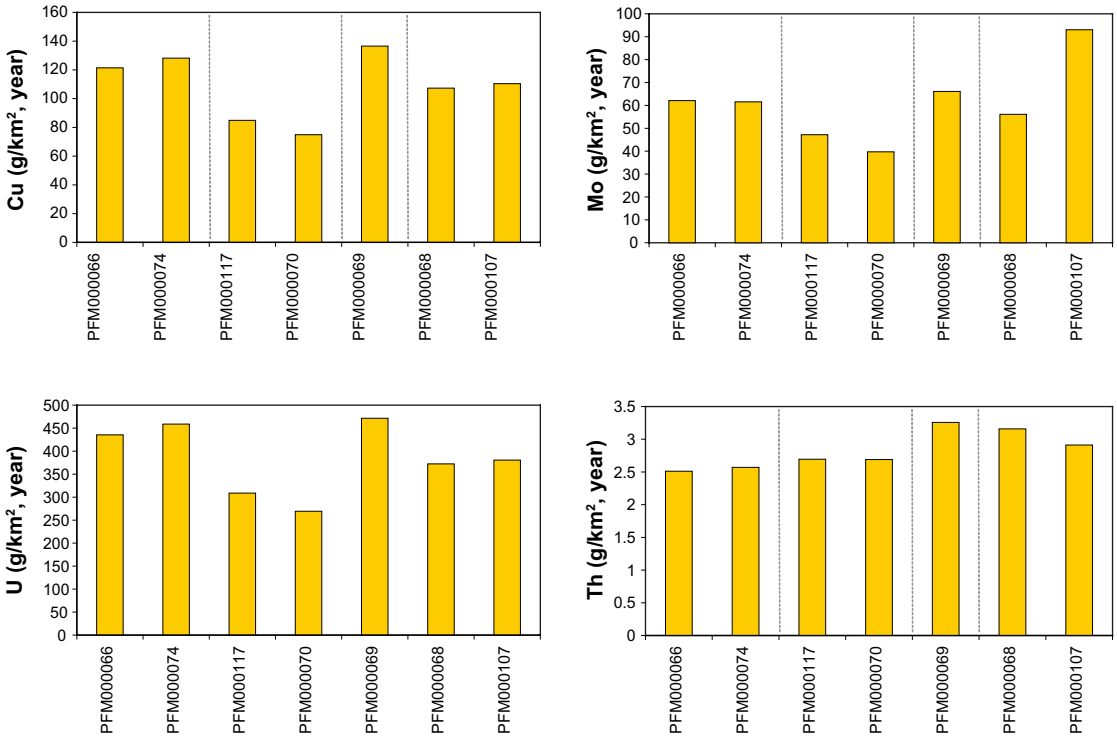

Figure 5-23. *Estimated area-specific transports of Cu, Mo, U and Th (g/km²,year).*

6 Evaluation of hydrochemistry on catchment scale

In this section a catchment model is used to evaluate Forsmark hydrochemistry at a catchment level. The objective with these scenarios is to explore if the observed hydrochemistry may be explained by spatially distributed factors as regolith characteristics and land-use, and in the prolongation to explain the causes to the observed variation within the Forsmark area. The calibrated catchment model is also a tool which may be used to extrapolate the results into areas where no measurements are conducted.

6.1 Catchment model VBX-VI

The catchment model VBX-VI (WaterBox version VI), couples hydrochemistry in surface water with hydrology and spatial environmental factors as land-use, regolith category, elevation distribution, and vegetation. Retention in lakes and emission from point sources are also handled in the model. Previous model versions are reported in /Naturvårdsverket 2003/ and /Tröjbom and Lindeström 2004/. A similar approach was also used in e.g. /Kvarnäs 1997/. VBX-VI is a static model, thus describing the average conditions over a fixed time-period, as in the Forsmark case, two hydrological years from 2004-06-01 to 2006-05-31 (cf Section 5.3.2).

VBX-VI is applied on all elements for which mass transports were estimated in Section 5.3.4 (except for F and Br where the reporting limit is reached in many surface water samples). The outcome of the model should be regarded as one possible solution on the mass balance for a specific element, and it should be noted that there may be other alternative scenarios working as well. In most cases however, the model converge towards only one stable solution regarding the selected factors (cf Section 6.1.4). As the model is calibrated against the observed transports in the outlets of the catchments, the model consequently describes the net balance per sub-catchment, i.e. if looking at organic carbon, only the net fixation or loss is included in the model and nothing is said about the total exchange with the atmosphere.

When the catchment model satisfactorily describes the variation within the studied area, the major underlying factors are probably understood. Deviations in the model may also contribute to the overall understanding of the site, by indicating where unknown sources are influencing specific areas. Output from the model is the yearly mass transports or flow weighted concentrations in the outflow of each sub-catchment. If the element at issue is subject for retention in lakes, the model gives estimations of this loss (or reversely, the gain if this is the case). The results may also be summarised per source giving source apportionments at sub-catchment or catchment scales.

6.1.1 Hydrological network and water balance

The sub-catchment is the smallest spatial unit in the catchment model, and all information is aggregated and related to this unit. Sub-catchments used in VBX-VI are based on the water divides described in /Brunberg et al. 2004/ and in a few cases further divided in order to form sub-catchments that intersect the hydrochemical sampling points (these catchments have an additional letter at the end of the idcode in Figure 6-1).

Sub-catchments are related to each other according to the hydrological network formed by streams and lakes in the area. A schematic representation of this network is shown in Figure 6-1 by arrows that connect catchment labels. There are two larger catchments in the Forsmark area containing of a number of sub-catchments, the Gunnarsbo-Lillfjärden catchment (outlet via AFM001099) and Norra Bassängen catchment (outlet via AFM001101), and a large number of smaller catchments that are more ore less directly connected to the Baltic Sea.

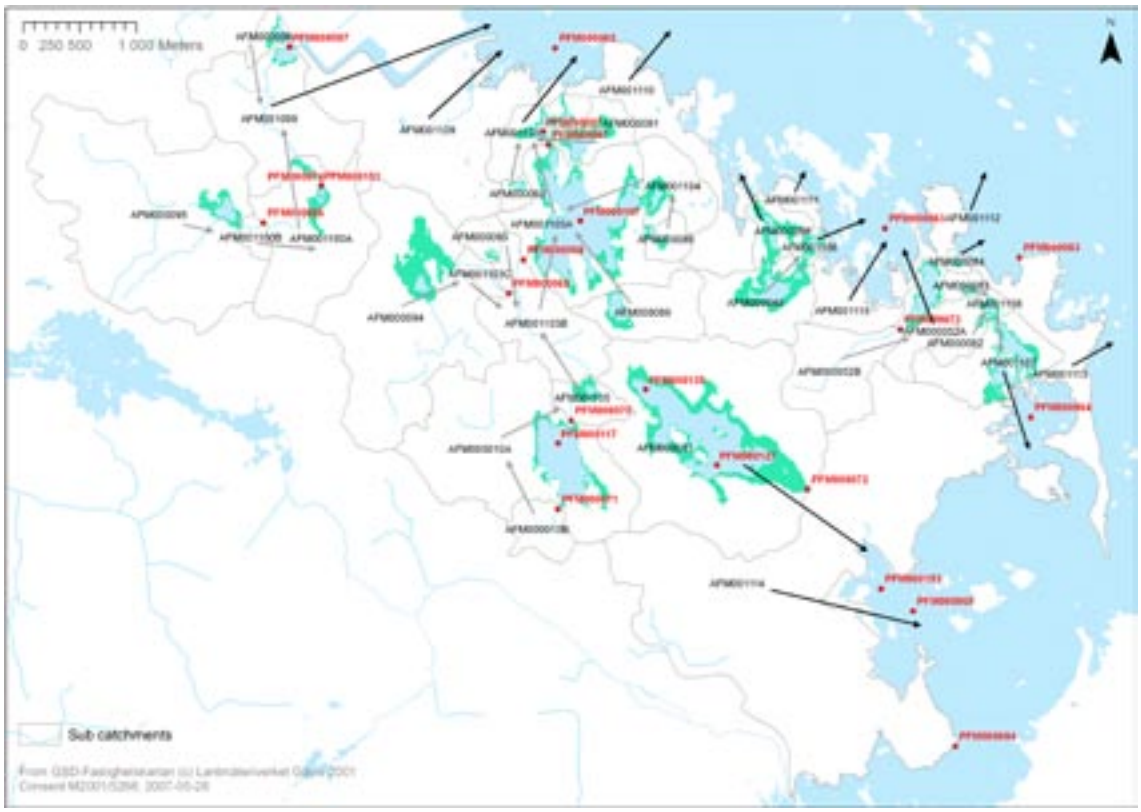

Figure 6-1. *Hydrological network of the Forsmark area. Grey arrows show schematically how sub-catchments (black labels) are interconnected and black arrow discharge to Baltic Sea. Red labels show locations of the hydrochemical sampling points. Blue-green borders around lakes mark the difference between two map layers, mainly reflecting wetland areas covered by vegetation as reed. Catchments AFM001100, AFM001103, AFM000010 and AFM000052 are further divided in order to form sub-catchments that intersect the hydrochemical sampling points (sub-catchments are denoted by an additional letter at the end of the idcode, e.g. AFM001103A).*

This hydrological network is implemented in VBX-VI in a spreadsheet according to the mathematical model structure described in Section 6.1.2. Additional information as land-use and other prerequisites are also included in this spreadsheet (see Section 6.1.3), where diffuse sources and point sources are summarised downstream along the flow paths. The spreadsheet also includes calibration procedures (cf Section 6.1.4) and visualisation of the results (cf Section 6.2).

Annual discharge from a specific catchment is estimated by a multiplying the specific discharge for a catchment with the catchment area. The specific discharge, which is assumed to be constant for the entire Forsmark area as supported by the analysis in Section 5.3.1, have been estimated to 150 mm/year during the modelled time period 2004-06-01 to 2006-05-31 (see Section 5.3.2).

Modelled and observed discharge in the outlet of the sub-catchments can be compared in Figure 6-2. Modelled discharge is based on a specific discharge of 150 mm/year multiplied with the catchment area, whereas the observed discharge is based on actual proportionalised discharge measurements (cf Table 5-8 and Table 5-9). The good agreement among all six stations indicates that the assumption of constant discharge in the Forsmark area probably is valid, and that these estimations are probably enough accurate in the light of other uncertainties associated with the catchment model.

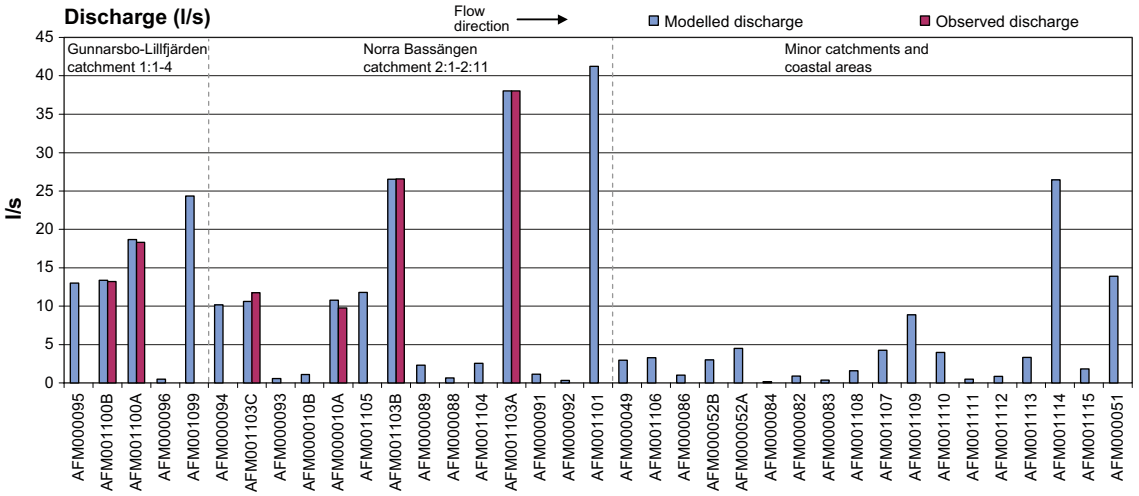

Figure 6-2. *Modelled and observed discharge (L/s) in outlet of sub-catchments in the Forsmark area.*

6.1.2 Mathematical description of the VBX-VI model

In the catchment model VBX-VI, the average mass balance per sub-catchment is calculated as the sum of all inputs from upstream sub-catchments, as well as the sum of diffuse and point sources, minus retention and output through the outlet of the sub-catchment. Depending on the character of the source, these may be implemented in the catchment model by three different methods, as shown in Equation 6 and in the example in Table 6-1:

- Distributed diffuse sources as weathering are modelled by a *typical concentration* per category (mg/L), multiplied with the discharge from this category (class) within each sub-catchment (cf Section 6.1.3 for a listing of categories and included classes). When discharge increases, concentrations are assumed constant and transports increase proportionally.
- Distributed diffuse sources as deposition may also be modelled by a *typical area-specific loss* per category (kg/km^2,yr), multiplied with the area of this category (class) in each sub-catchment (cf Section 6.1.3). In this case, concentrations in watercourses decrease when discharge increase, whereas transports stay constant.
- Point sources are modelled as *constant supply* of elements (kg/yr). In this case concentrations decrease due to dilution effects, when discharge increase, whereas transports stay constant.

The average flow weighed concentration in the outlet of the catchment is derived by dividing the yearly mass transport in the outlet with the yearly discharge, as shown in the generalised mathematical description for an arbitrary catchment in Equation 6. This quantity is compared to the measured concentrations at the calibration of the catchment model (cf Section 6.1.4). Parameter abbreviations and units are explained in Table 6-1, where the calculation sequence is exemplified for a hypothetical two-catchment model.

Equation 6. Mathematical formulation of the relationship used for calculating the flow weighted concentration, c_a, in the outlet of catchment "a". The lower equation is the statistical relationship used for retention apportionment describing the proportion that is lost due to retention. Parameters and units are explained in Table 6-1. In the generalised equation below is e.g. the typical concentration $c_{typ,i}$ for different diffuse sources denoted $c_{typ,1}$, $c_{typ,2}$,…$c_{typ,n}$.

$$c_a = \left[\sum_{i=1} c_{typ,i} A_{a,typ,i} Q + \sum_{j=1} M_{a,spec,j} A_{a,spec,j} + \sum_{k=1} m_{pmt,k} + \sum_{l=1} T_{a,in,l} \right] \cdot \left[1 - f(\lambda, V_{a,lake}, q_a)\right] / q_a$$

$$q_a = A_a Q$$

$$f(\lambda, V_{a,lake}, q_a) = 1 - \frac{1}{1 + \lambda \frac{V_{a,lake}}{q_a}}$$

Table 6-1. Generalised scheme showing the calculation order of different sources for the hypothetical catchments a and b, where catchment a is located upstream catchment b. Red arrows emphasize the direction of summation, blue arrows subtraction due to retention processes and green arrows denote transfer to catchments downstream. Conversion constants k_1 and k_2 are added to correct for the different units used in the calculations. $V_{a,lake}$ denotes the total lake volume of catchment a.

Catchment	Area	Specific discharge	Discharge	Typical concentration	Typical areal loss	Point source	Estimated transport	Comment
	A	Q	q	c_{typ}	M_{spec}	m_{pnt}	T	Abbreviation
	km^2	mm/yr	m^3/yr	mg/L	kg/km^2,yr	kg/yr	kg/yr	Unit
a	$A_{a,typ1}$	Q	$q_{a,typ1}=k_1\times A_{a,typ1}\times Q$	c_{typ1}			$T_{a,1}=k_2\times c_{typ1}\times q_{a,typ1}$	Diffuse source 1
a	$A_{a,typ2}$	Q	$q_{a,typ2}=k_1\times A_{a,typ2}\times Q$	c_{typ2}			$T_{a,2}=k_2\times c_{typ2}\times q_{a,typ2}$	Diffuse source 2
a	$A_{a,spec1}$	Q			M_{spec1}		$T_{a,3}=M_{spec1}\times A_{a,spec1}$	Diffuse source 3
a						m_{point1}	$T_{a,4}=m_{pnt1}$	Point source 1
a							$T_{a,tot}=T_{a,1}+T_{a,2}+T_{a,3}+T_{a,4}$	Total input, Gross
a	$A_{a,lake}$		$q_a= k_1\times A_a\times Q$				$T_{a,ret}=f(\lambda, V_{a,lake}, q_a)\times T_{a,tot}$	Retention in lakes
a	A_a	Q	$q_a= k_1\times A_a\times Q$				$T_{a,out}=T_{a,tot}-T_{a,ret}$	Total output, Net
b							$T_{b,in}=T_{a,out}$	Upstream input
b	$A_{b,typ1}$	Q	$q_{typ1,b}= k_1\times A_{typ1,b}\times Q$	c_{typ1}			$T_{b,1}=k_2\times c_{typ1}\times q_{b,typ1}$	Diffuse source 1
b	$A_{b,typ2}$	Q	$q_{a,typ2}= k_1\times A_{a,typ2}\times Q$	c_{typ2}			$T_{b,2}=k_2\times c_{typ2}\times q_{b,typ2}$	Diffuse source 2
b	$A_{b,spec1}$	Q			M_{spec1}		$T_{b,3}=M_{spec1}\times A_{b,spec1}$	Diffuse source 3
b						m_{point2}	$T_{b,4}=m_{pnt2}$	Point source 2
b							$T_{b,tot}=T_{b,in}+T_{b,1}+T_{b,2}+T_{b,3}+T_{b,4}$	Total input, Gross
b	$A_{b,lake}$						$T_{b,ret}=f(\lambda, V_{b,lake}, q_b)\times T_{b,tot}$	Retention in lakes
b	A_b	Q	$q_b= k_1\times A_b\times Q$				$T_{b,out}=T_{b,tot}-T_{b,ret}$	Total output, Net

Unit conversion factors: k_1 = 1,000, k_2 = 0.001.

The total retention in the studied area is distributed among the sub-catchments by a statistical model where the total retention time in the lakes and a general retention constant (λ) are parameters. This model reflects how the proportion of retention of the specific element increase when residence time increase, i.e. there is a larger loss in the lake when the retention time is long. At the interval where most sub-catchments in the Forsmark area end up, this model is approximately linear (Lake Bolundsfjärden 77 days and Lake Eckarfjärden 328 days /Brunberg et al. 2004/), according to the relationships in Figure 6-3. A similar statistical relationship was used by /Grimwall and Stålnacke 1996/ in the MESAW model. If the retention parameter arrive at negative values during calibration (cf Section 6.1.4), a net gain is modelled in the lakes instead of a loss.

6.1.3 Distributed land characteristics and prerequisites for retention

Modelling of emission from diffuse sources in the catchment model is based on statistical information of the areas of different distributed characteristics within each sub-catchment (cf Section 6.1.2 for a description of the methodology). A compilation and description of original and aggregated classifications used in the VBX–VI model can be found in Appendix D, together the areas listed per class and catchment. Four major categories, each describing different distributed characteristics, are compiled per sub-catchment and may be implemented in the model:

- **Regolith**: The area of each of six regolith classes within each sub-catchment, based on aggregated classes from the soil survey /Sohlenius et al. 2004/: jWater, jSand, jPeat, jRock, jClay, and jTill.

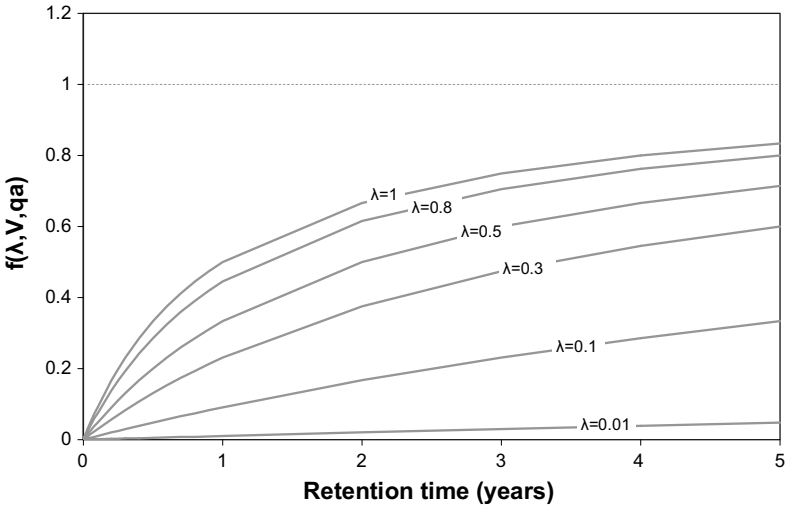

Figure 6-3. *Visualisation of the relationship f(λ,V,q), which describes the proportion of an element that is lost by retention, as a function of retention time (years) for different values of λ (year^{-1}). See Equation 6 for a mathematical description of this function.*

- **Land-use**: The area of each of six land-use categories within each sub-catchment, based on the topographical map: mWater, mForest, mClear, mArable, mOpen, and mHard.
- **Vegetation cover**: The areas of eight different vegetation classes from the vegetation map in each sub-catchment /Boresjö Bronge and Wester 2003/: vWater, vWet, vRock, vForest, vClear, vArable, vOpen, and vHard.
- **Elevation distribution**: The topographical elevation distribution per sub-catchment of seven classes was calculated from the digital elevation model /Brydsten and Strömgren 2004/: 0–2 m, 2–4 m, 4–6 m, 6–8 m, 8–10 m, 10–15 m, and > 15 m.

As the sources of different elements are coupled to different environmental factors, the categories and classes included in the models differ between specific elements as well as between element groups. The same geographical spot may also, as indicated in the mathematical description in Section 6.1.2, be subject for several sources from different environmental categories. Besides the spatial information listed above is the total lake volume per sub-catchment used as parameter for the retention model (data derived from /Brunberg et al. 2004/).

6.1.4 Model setup, calibration and validation

Model setup and calibration is an iterative process with the aim of finding an as simple model as possible that satisfactorily describes the spatial variation within the Forsmark area. There is necessarily a subjective stage in this process, when the governing parameters are selected based on the PLS explorative analysis described below, and on expert knowledge of the behaviour of different elements.

Prior to model setup, a partial least squares regression (see Section 2.3.11 for an explanation of PLS) was conducted on the relative areas of the distributed characteristics (cf Section 6.1.3) upstream the hydrochemical sampling points, in relation to the observed concentrations. This analysis gives a rough indication of which factors that are most correlated to the observed concentrations of the element at interest, and therefore are candidates in the initial model setup.

During calibration of the catchment model, general parameters valid for the whole area, as typical concentrations, typical area loss and the retention constant are varied in order to achieve maximal agreement between modelled and observed concentrations. The automatic calibration procedure uses the relationship in Equation 7 to find local minima which represent maximal agreement between modelled and observed concentrations. In most cases, the solver converges towards a stable single solution when a decent initial guess is applied.

Equation 7. Relationship used by the automatic calibration procedure to calculate the total deviation, dev, between modelled and observed concentrations in the catchment model.

$$dev = \sum ABS(c_{\mathrm{mod}} - c_{obs}) / c_{obs}$$

Calibration was carried out on three sets of data with different levels of confidence:

- Primary (high confidence): Flow weighed concentrations estimated for 6 streams and lake outlets, as described in Section 5.3.4, representing average conditions during the period 2004-06-01 and 2006-05-31 (PFM000066, 68, 69, 70, 74, 107).
- Secondary A (moderate confidence): A limited number of samples from two lakes (PFM000087, PFM000072 and PFM000097) from the beginning of the two-year model period. As these samples only represent a few months from the summer season, these average concentrations may be biased for parameters that show large seasonal variability (cf Table 5-10 and Section 5.3.3 for a description of these data).
- Secondary B (low confidence): Similar to the lakes described above there are also a few samples available from streams from the beginning of the two year model period (PFM000071 and PFM000073). These average concentrations show however low confidence as they represent very small streams with presumably high seasonal variability and no smoothing lakes upstream.

Generally, both the primary and secondary data sets were used for calibration. It should, however, be held in mind when evaluating the calbration results, that the secondary data sets show lower confidence compared to the primary data set, and that the greatest uncertainities within the secondary dataset are shown by elements with large seasonal variability, due to the limited seasonal representativeness. In the element-wise presentations in Section 6.2, the dataset with the highest confidence is denoted “primary” and the latter two are denoted “secondary”. The specific use of these datasets is declared in connection to the presentations below.

In some cases it is convenient to add a hypothetical point source to the model scenario in order to neutralize anomalies, for example sea water intrusions in Lake Bolundsfjärden. These point sources are quantified in the summary tables, and marked in the mass-balance figures as a dashed blue bar. In case of retention in the lakes, this loss is also quantified in the summary tables and larger sinks are marked in the mass-balance figures as green bars.

As a final validation step, calibrated typical concentrations from different land-use classes, regolith or vegetation types are compared to local observations in shallow groundwater (cf /Tröjbom and Söderbäck 2006/) and, when applicable, to distributions of nation-wide surveys of streams and lakes, to give a conception if these values are plausible.

6.2 Mass balance scenarios

In this section, mass balance scenarios are shown for a large number of elements. It should be noted that this is just scenarios and that there may be other plausible solutions on the mass balances of the Forsmark area. In most cases however, the models converge towards only one stable solution from the selected prerequisites, and in case of equivalent solutions, these are mentioned in text or shown in alternative presentations.

The results of the mass balance models are presented for each element as bar graphs showing the flow weighted concentrations and transports in the outlets of the catchments. Modelled values are shown together with observed values from the primary and secondary calibration/ validation sets of data, described in Section 6.1.4. Model parameters are listed in a table in each section, as well as in the summary in Table 6-16.

As supportive information is the calibrated typical concentrations plotted into the concentration distributions from the Swedish survey of lakes and stream /IMA 2007/. A partial least square regression model (PLS) is also included, showing the correlation structure between observed concentrations and the relative area proportion of the different distributed characteristics (cf Section 2.3.11 for a description of PLS).

6.2.1 Mass balance for chloride (Cl)

Among the distributed characteristics, only the elevation category was able to satisfactorily model the variation pattern for chloride within the Forsmark area, shown in the scenario 1 in Figure 6-4. The correlation analysis in Figure 6-5 also indicates that lower topographical elevations as well as parameters coupled to these lower levels, e.g. the occurrence of water and wetlands, are most correlated to the Cl concentration. Model details are listed below:

- The deficiency of Cl indicated by the model in Lake Bolundsfjärden (AFM001103A) may be explained by sea water intrusions from the Baltic Sea (cf Section 4.1.1). This anomaly was implemented as a point source in the model and estimated by calibration to 57,000 kg/year as indicated by the blue striped bar in the lower panel.
- The agreement between modelled and observed concentrations was further improved when the regolith class jClay (clay and gyttja classes, cf Appendix D for an explanation of the regolith category) was taken into account, which was especially evident in the outlet of Lake Gällsboträsket (AFM001103C).
- Both the primary and secondary datasets were used for calibration of the Cl model. Parameter values for Cl and a source apportionment for the Forsmark area (i.e. the modelled catchments) are compiled in Table 6-2. In Appendix E are model details compiled.

By adjusting the typical concentrations of three parameters (‘jClay’, ‘0–2 m’ and ‘4–6 m’), the variation in Cl concentration is satisfactorily modelled by scenario 1 within the Forsmark area. The largest deviations are shown by the small streams in the secondary calibration dataset B

Table 6-2. Compilation of parameters from the Cl mass balance model. Categories not used have been omitted from the table. The two rightmost columns show the total contribution from each category to the entire modelled area in Forsmark.

Diffuse sources		**mg/L**	**kg/km^2,yr**	**kg/year**	**%**
Cathegory	**Class**				
Regolith	jClay	72	–	25,628	14
Land-use	–	–	–	–	
Vegetation	–	–	–	–	
Topography	0–2 m	47	–	48,883	27
	2–4 m	='0–2 m'	–	48,282	27
	4–6 m	0.8'	–	591	0.3
	6–8 m	='4–6 m'	–	408	0.2
	8–10 m	='4–6 m'	–	273	0.2
	10–15 m	='4–6 m'	–	324	0.2
	> 15 m	='4–6 m'	–	170	0.1
Point sources					
Sea water intrusions in Lake Bolundsfjärden				57,000	31
Total					
Gross				181,560	100
Retention (λ), yr^{-1}				0	0
Net				181,560	100

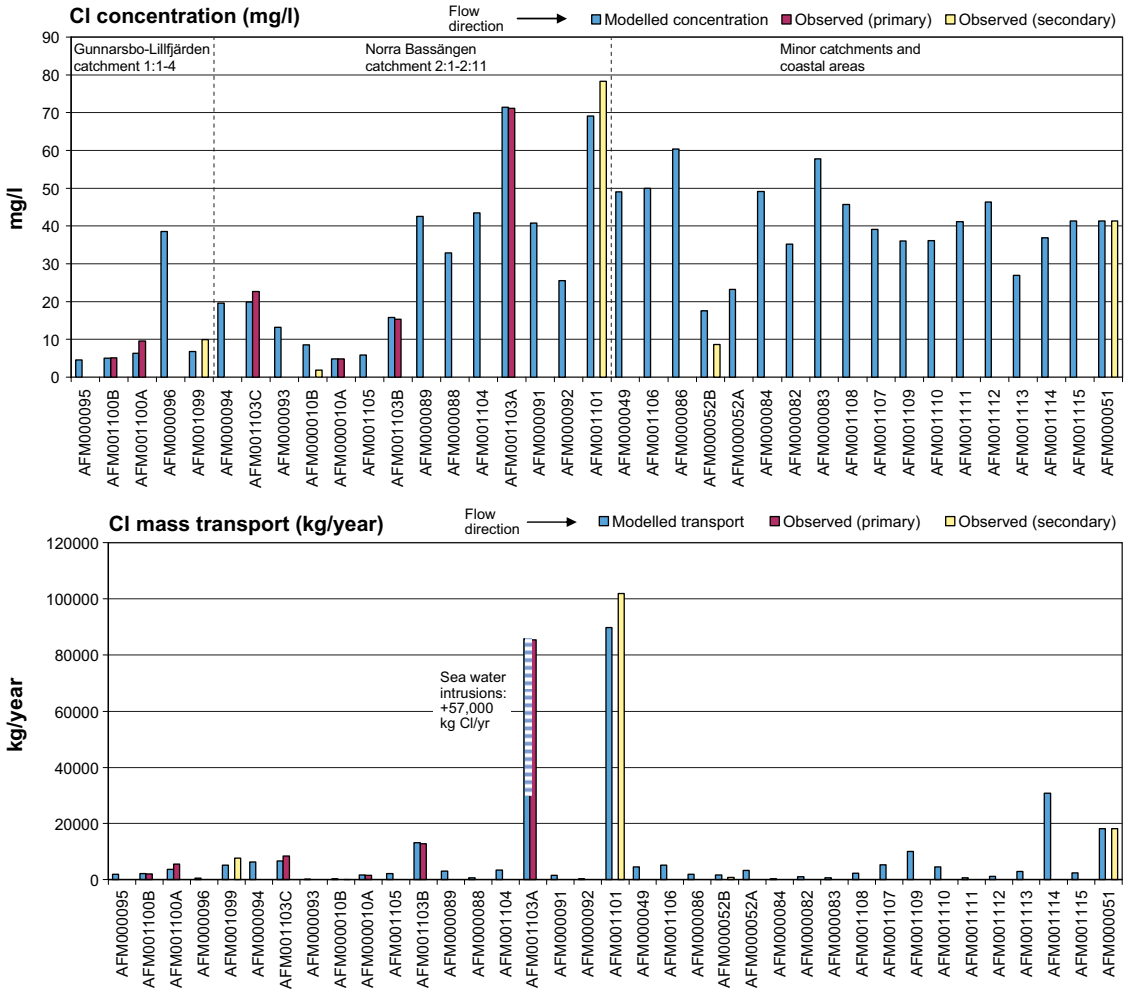

Figure 6-4. *Mass balance scenario 1 for Cl in the Forsmark area. Flow weighted concentrations (mg/L) above, and transports (kg/year) below, describing the conditions in the outlet of each catchment.*

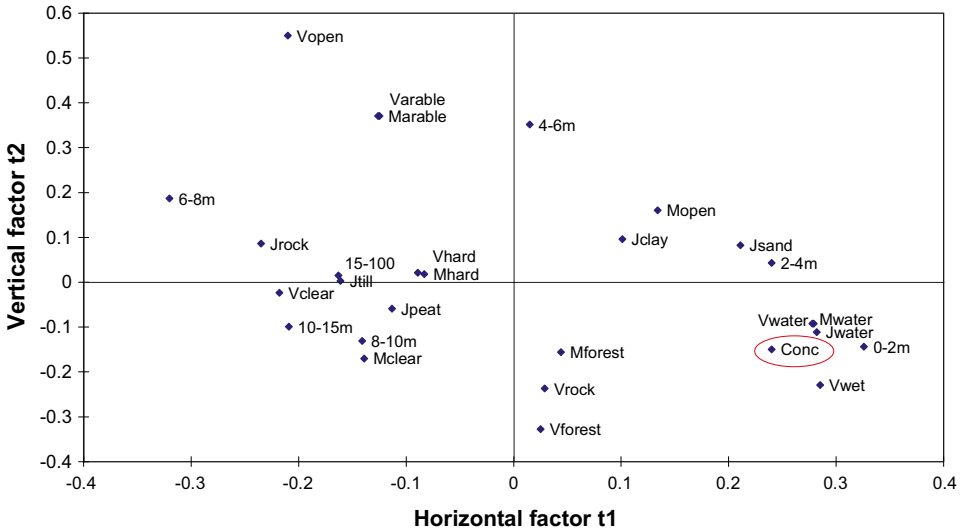

Figure 6-5. *Partial least square regression model, PLS, (cf Section 2.3.11 for an explanation of PLS) showing the correlation structure among distributed catchment characteristics, and the observed Cl concentration (encircled in red). The parameters represent the relative distribution of each regolith, land-use, vegetation and elevation class upstream the hydrochemical sampling point in the outlet of the catchments. Factor t1 describes 37% of the variation among the explanatory variables and t2 27%. 51% of the variance in 'Conc' is described by t1 and 12% by t2.*

(AFM000010B and AFM000052B), which probably are the least representative among the calibration sample points (cf Section 6.1.4). The average deviation between modelled and observed concentrations is 8% in the primary calibration dataset (104% in secondary, most depending on two observations in small streams, AFM000010B and AFM000052B).

The alternative scenario 2 in Table 6-3, based only on the topographical parameters, show similar results, but with a larger average deviation between modelled and observed values. The conclusions below and all visualisations in this section are based on Scenario 1.

From the mass balance scenario 1, the following conclusions may be drawn about sources of Cl:

- Diffuse sources of Cl are most probable connected to the topographical elevation distribution rather than factors as regolith or land-use within the catchments. The catchment model indicates that areas located below 4 metres altitude, show increased Cl supply (47 mg/L compared to the background of 0.8 mg/L prevailing at higher topographical elevations).
- The background level in discharge from higher elevations was calibrated to 0.8 mg/L, which is in level with the concentration in precipitation of about 0.7 mg/L /Tröjbom and Söderbäck 2006/. These levels correspond to the 20th percentile in the distribution from the Swedish national survey of lakes and streams according to Figure 6-7.
- At episodes of high water levels in the Baltic, sea water intrusions add significant amounts of Cl into Lake Bolundsfjärden, corresponding to an amount of 57,000 kg/year or 66% of the total input to the lake.
- The results indicate that soils that contain clay or gyttja are coupled to leakage of additional amounts of Cl, e.g. in the area around Lake Gällsboträsket (AFM000094) where the total Cl concentration in discharge from these soils possibly reach about 120 mg/L (72 + 47 = 119 mg/L). Concentrations in this order of magnitude are also observed in shallow groundwater in soil tubes located at low altitude in the vicinity of lakes /Tröjbom and Söderbäck 2006/. The distribution of the 'jClay' regolith class is shown in Figure 6-6 (cf Appendix D for an explanation of regolith classes).
- There are, as presumed, no indications of retention for Cl.

Table 6-3. Comparison of the major Scenario 1, which is shown in all presentations, and the alternative Scenario 2, based on topographical parameters only.

Diffuse sources		**Scenario 1**	**Scenario 2**
Cathegory	**Class**	**mg/L**	**mg/L**
Regolith	jClay	72	–
Land–use	–	–	–
Vegetation	–	–	–
Topography	0–2 m	47	69
	2–4 m	='0–2 m'	53
	4–6 m	0.8	5
	6–8 m	='4–6 m'	='4–6 m'
	8–10 m	='4–6 m'	='4–6 m'
	10–15 m	='4–6 m'	='4–6 m'
	> 15 m	='4–6 m'	='4–6 m'
Point sources			
Bolundsfjärden	kg/yr	57,000	53,000
Average deviation			
Primary dataset		8%	17%
Secondary dataset		104%	73%

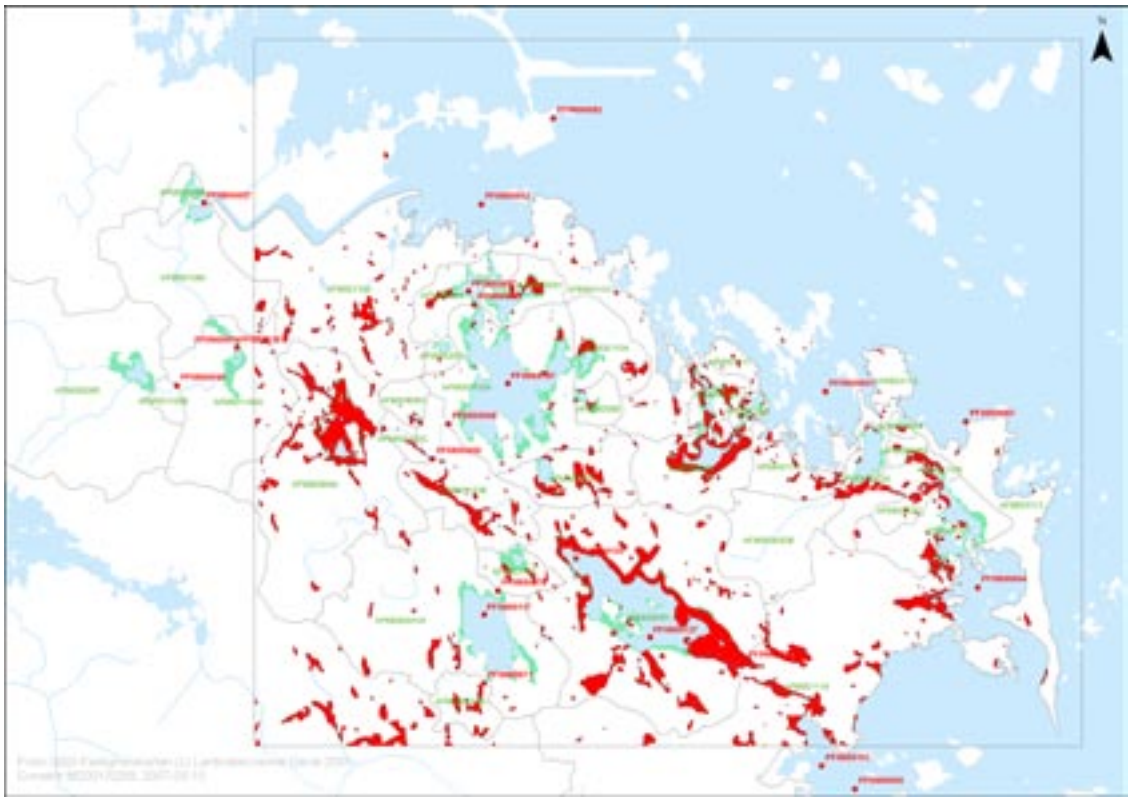

Figure 6-6. *The distribution of the jClay soil class in within the Forsmark area (cf Appendix D for explanation of regolith categories). A detailed soil survey has been conducted within the marked rectangle, whereas regional data have been used outside.*

Compared to Swedish lakes and streams, the calibrated typical concentration of scenario 1 representing higher topographical levels, correspond to the 20th percentile of the national distribution shown in Figure 6-7. When the median concentration of precipitation of 0.7 mg/L is corrected for evapotranspiration (about 400 mm/year of a total precipitation of c 550 mm/year /Juston et al. 2006/), a background concentration of about 2.1 mg/L should be measured if these values are representative also for higher topographical locations in the Forsmark area.

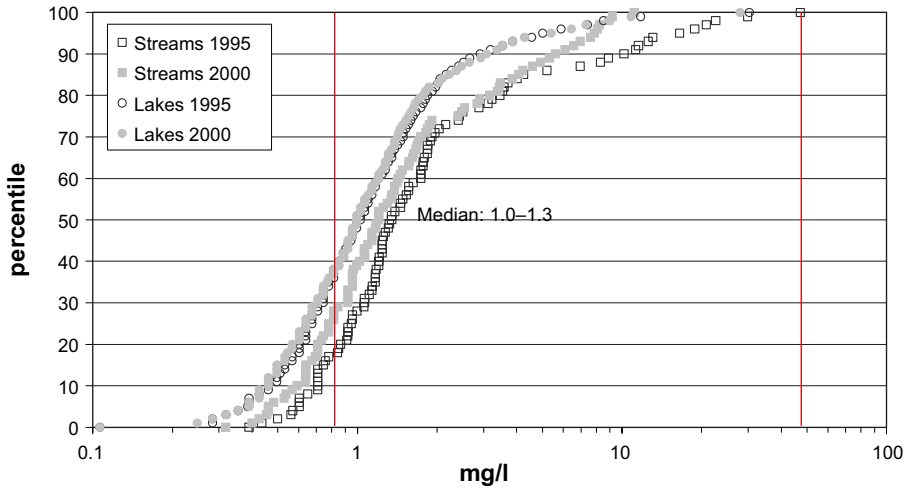

Figure 6-7. *Distribution of Cl concentrations in the Swedish surveys of lakes and streams 1995 and 2000 /IMA 2007/. Typical concentrations in the Forsmark area calibrated within the VBX-VI model, are marked as red lines.*

The discrepancy between 0.8 mg/L and 2.1 mg/L is accounted for by supply from the regolith category 'jClay' in Scenario 1, which is included within the topographical class in Scenario 2 by the calibrated value of 5 mg/L for all areas above 4 metres. It is not possible to determine which model is most correct regarding the background level, but these results may be an indication that the origin of the background supply of Cl is uncertain. The difference between 5 mg/L (above 4 metres in Scenario 2) and 2.1 mg/L (contribution from precipitation corrected for evapotranspiration) may be attributed to dry deposition, which is supposed to add 50 to 100% to the wet deposition value in these areas (P.O. Johansson 2007, pers. comm.).

The estimated Cl supply to Lake Bolundsfjärden through sea water intrusions in Scenario 1 is further used for estimating the sea water supply of other marine ions, e.g. sodium, magnesium and potassium. These estimations, which are listed in Table 6-4, are included as initial assumptions in the models for the different elements in the following sections.

6.2.2 Mass balance for sodium (Na)

The mass balance for Na is very similar to the Cl balance in Scenario 2 (Section 6.2.1), and the Na supply is therefore supposed to be controlled primarily by the topographical elevation rather than factors as regolith or land-use. The dependence of the topographical elevation is also evident in the correlation analysis in Figure 6-9. Model details are listed below:

- An addition of Na to Lake Bolundsfjärden of 31,000 kg/year due to sea water intrusions was assumed as an initial condition in the model (cf Table 6-4).
- Both the primary and the secondary datasets were used for calibration of the Na model shown in Figure 6-8. Parameter values and a source apportionment for the entire Forsmark area are compiled in Table 6-5. In Appendix F are model details compiled.

By adjusting the typical concentrations of three topographical parameters ('0–2 m', '2–4 m' and '4–6 m'), the variation in Na concentration within the Forsmark area is satisfactorily modelled. There are no major deviations between modelled and observed concentrations, and the average deviation between modelled and observed concentrations is 10% in the primary calibration dataset (14% in secondary). The least confident observations from the secondary dataset B also shows good agreement with modelled concentrations (AFM000010A, and AFM000052B), probably due to small seasonal fluctuations for Na.

Table 6-4. Estimated yearly supply of marine ions into Lake Bolundsfjärden due to sea water intrusions. The amounts are based on the calibrated value of chloride, multiplied with the relative fractions of sea water according to Figure 4-1.

Element	Abbreviation	Inflow (kg/yr)
Chloride	Cl	57,000 kg
Sodium	Na	31,000 kg
Sulphate	SO_4	8,100 kg
Magnesium	Mg	3,800 kg
Calcium	Ca	1,600 kg
Potassium	K	1,200 kg
Strontium	Sr	21 kg

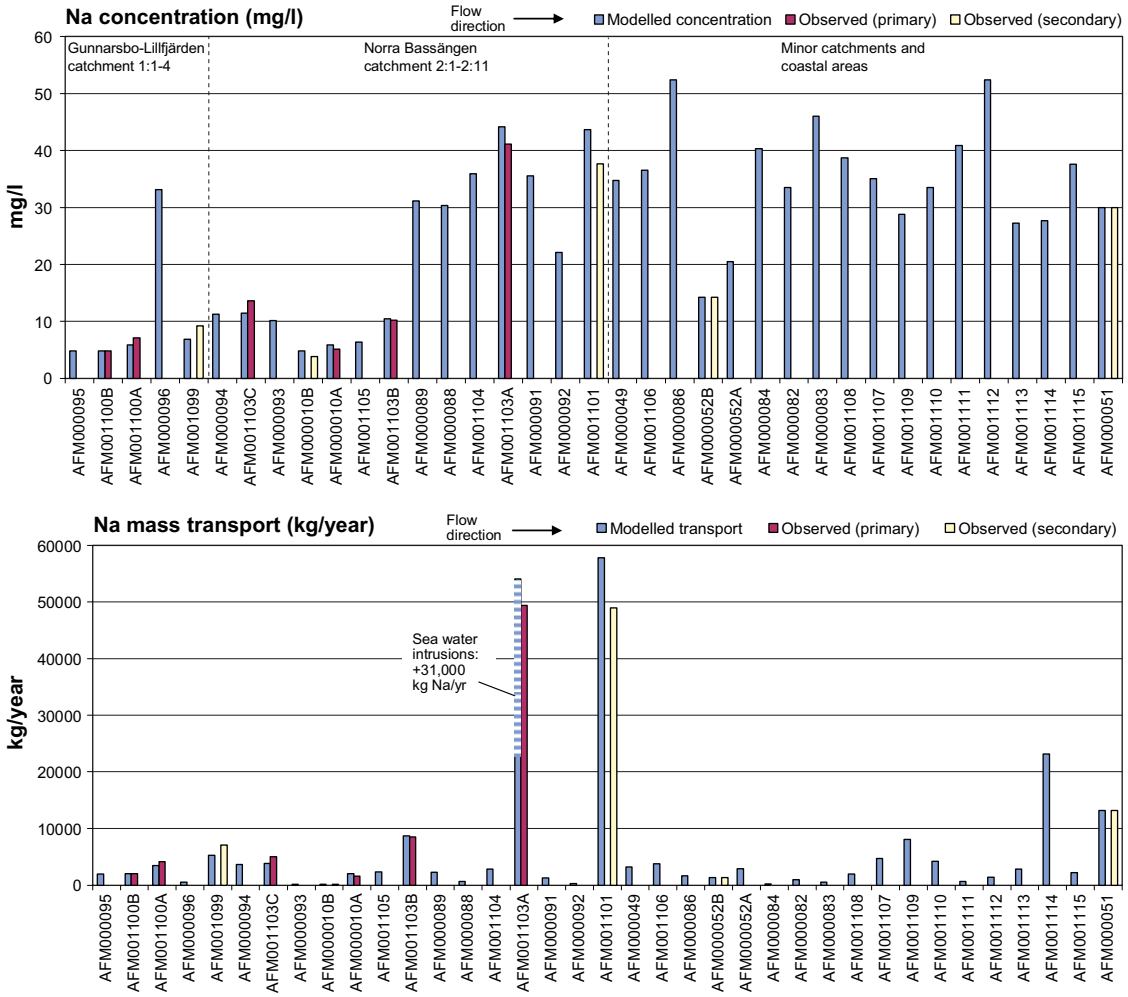

Figure 6-8. *Mass balance for Na in the Forsmark area. Flow weighted concentrations (mg/L) above, and transports (kg/year) below, describing the conditions in the outlet of each catchment.*

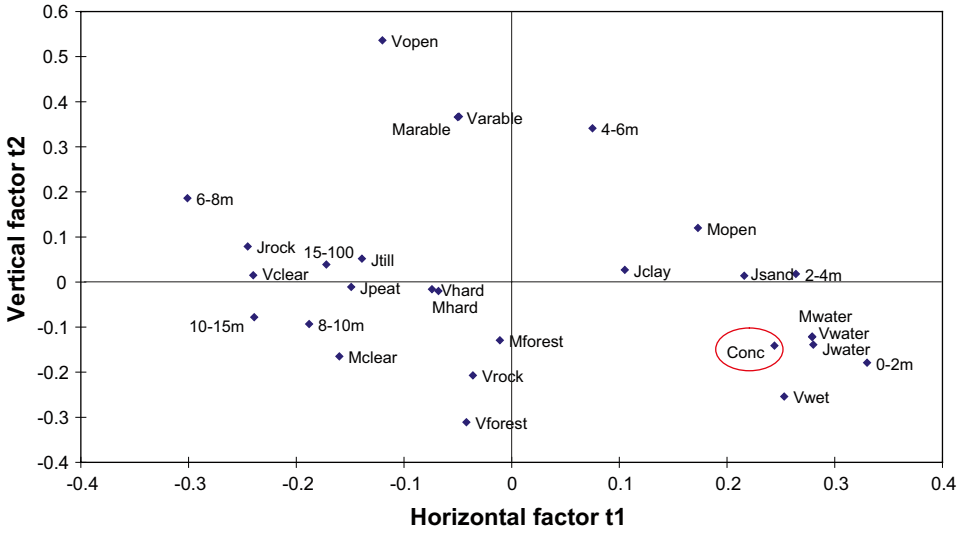

Figure 6-9. *Partial least square regression model, PLS, (cf Section 2.3.11 for an explanation of PLS) showing the correlation structure among distributed catchment characteristics, and the observed Na concentration (encircled in red). The parameters represent the relative distribution of each regolith, land-use, vegetation and elevation class upstream the hydrochemical sampling point in the outlet of the catchments. Factor t1 describe 40% of the variation among the explanatory variables and t2 24%. 61% of the variance in 'Conc' is described by t1 and 10% by t2.*

Table 6-5. Compilation of parameters from the Na mass balance model. Categories not used have been omitted from the table. The two rightmost columns show the total contribution from each category to the entire modelled area in Forsmark.

Diffuse sources		mg/L	kg/km^2,yr	kg/year	%
Cathegory	**Class**				
Regolith	–	–	–	–	–
Land–use	–	–	–	–	
Vegetation	–	–	–	–	
Topography	0–2 m	56	–	58,666	44
	2–4 m	30	–	31,340	24
	4–6 m	5	–	3,675	3
	6–8 m	='4–6 m'	–	2,532	2
	8–10 m	='4–6 m'	–	1,697	1
	10–15 m	='4–6 m'	–	2,014	2
	> 15 m	='4–6 m'	–	1,054	1
Point sources					
Sea water intrusions in Lake Bolundsfjärden				31,000	23
Total					
Gross				131,978	100
Retention (λ), yr^{-1}				0	0
Net				131,978	100

From the mass balance scenario, the following conclusions can be drawn about sources of Na:

- Diffuse sources of Na are most probable coupled to the topographical elevation rather than to factors as regolith category or land-use within the catchments. The catchment model indicates that areas located below 4 metres altitude, show increased Na supply (30–56 mg/L compared to the background of 5 mg/L prevailing at higher topographical elevations).
- The background level in discharge from higher elevations was calibrated to 5 mg/L, which is 10 times higher than the median concentration in precipitation of 0.5 mg/L /Tröjbom and Söderbäck 2006/. These levels correspond to the 90th percentile in the distribution from the Swedish national survey of lakes and streams according to Figure 6-10. When the concentration of precipitation is corrected for evapotranspiration (about 400 mm/yr of a total precipitation of 550 mm/yr /Juston et al. 2006/), a background concentration of about 1.5 mg/L should be measured if these values are representative also for higher topographical locations in the Forsmark area. The difference between 5 mg/L (typical concentration in discharge from higher locations) and 1.5 mg/L (evapotranspiration corrected concentration of precipitation) of 3.5 mg/L, may be explained by supply from relict remnants, mineral weathering or dry deposition not included in the measurements of precipitation (cf Section 6.2.1). If this figure is compared to the average concentration from the whole Forsmark area of 30 mg/L (see compilation in Appendix E), about 10% or less of the total Na leakage originate from weathering reactions.
- At episodes of high water levels in the Baltic, sea water intrusions add significant amounts of Na into Lake Bolundsfjärden, corresponding to an amount of 31,000 kg/year or 57% of the total input to the lake.
- There are, as presumed, no indications of retention for Na.

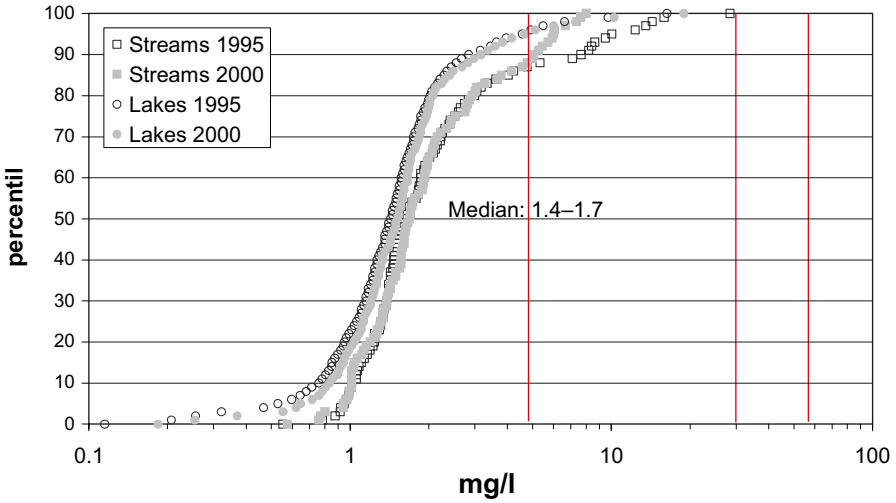

Figure 6-10. *Distribution of Na concentrations in the Swedish surveys of lakes and streams 1995 and 2000 /IMA 2007/. Typical concentrations in the Forsmark area calibrated within the VBX-VI model, are marked as red lines.*

6.2.3 Mass balance for potassium (K)

The distribution of K differs from Na and Cl by showing lower spatial variability within the Forsmark area. The correlation analysis shown in Figure 6-12 gives a scattered picture where e.g. arable land shows positive correlation to observed K concentrations. Due to the low K variability among the hydrochemical sampling points, the perquisite for elucidating the factors behind the presence of K in Forsmark surface water is limited, and only a very simple model is applied. Model details are listed below:

- An addition of K to Lake Bolundsfjärden of 1,200 kg/year due to sea water intrusions was assumed as an initial condition in the model (cf Table 6-4).
- Both the primary and the secondary datasets were used for calibration of the K model shown in Figure 6-11. Parameter values and a source apportionment for the entire Forsmark area are compiled in Table 6-6. In Appendix F are model details compiled.

By using only one calibrated typical concentration, representing the discharge from all regolith categories, together with the estimated deposition on lakes, the K model describes the variation reasonably well with an average deviation of 9% in the primary calibration dataset (28% in secondary). The typical concentration in deposition was estimated as three times the observed mean concentration in precipitation as a correction for evapotranspiration (400 mm/year of a total precipitation of approximately 550 mm/year /Juston et al. 2006/).

The largest deviations in the K model are encircled in red in Figure 6-11. Both AFM000052B and AFM000051 belong to the secondary dataset B that show higher uncertainty due to biased data (cf Section 6.1.4), which may be a partial explanation to the deviation. AFM000052B, the catchment upstream Lake Bredviken contains a high proportion arable land, which probably is the explanation to the elevated K transport from this area /Åström and Rönnback, submitted/.

From the mass balance scenario, the following conclusions about sources of K can be drawn:

- Diffuse sources of K are more uniformly distributed over the Forsmark area compared to e.g. marine ions as Cl and Na. A simple mass balance model based on only one typical concentration in the discharge from all regolith classes in combination with estimated deposition on lakes, can explain the variability within the area reasonably well, indicating that no distributed factors as topographical elevation, regolith type, land-use or vegetation cover seem to have any important influence.

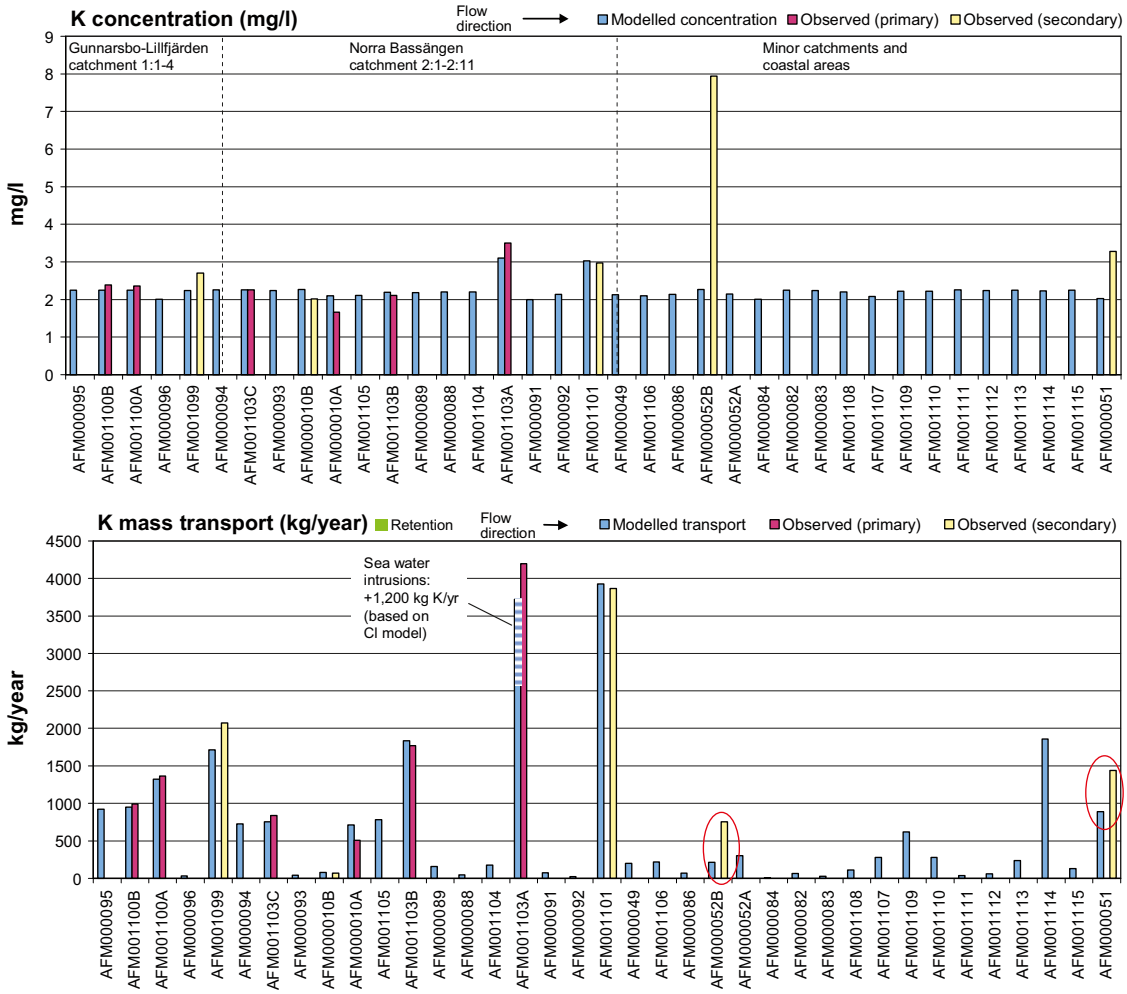

Figure 6-11. *Mass balance for K in the Forsmark area. Flow weighted concentrations (mg/L) above, and transports (kg/year) below, describing the conditions in the outlet of each catchment.*

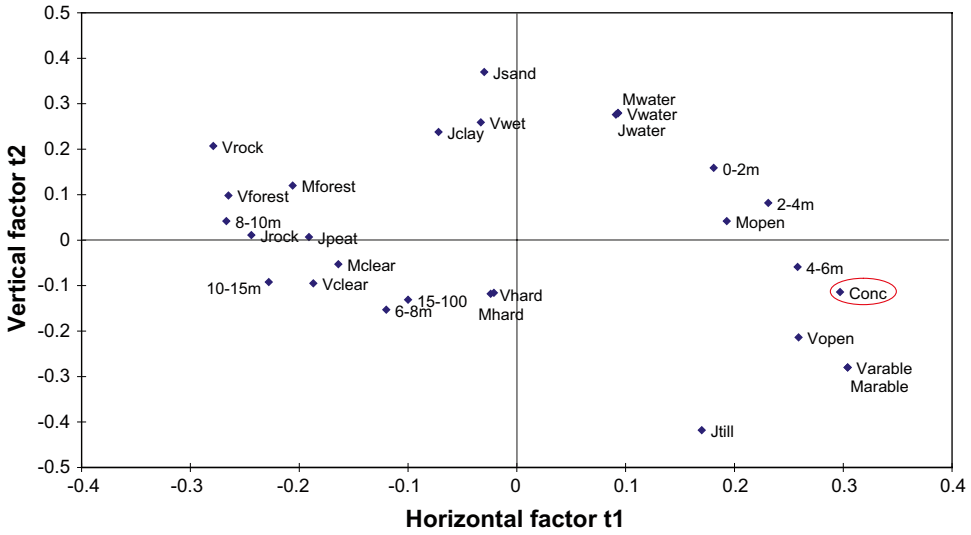

Figure 6-12. *Partial least square regression model, PLS, (cf Section 2.3.11 for an explanation of PLS) showing the correlation structure among distributed catchment characteristics, and the observed K concentration (encircled in red). The parameters represent the relative distribution of each regolith, land-use, vegetation and elevation class upstream the hydrochemical sampling point in the outlet of the catchments. Factor t1 describe 40% of the variation among the explanatory variables and t2 26%. 89% of the variance in 'Conc' is described by t1 and 9% by t2.*

Table 6-6. Compilation of parameters from the K mass balance model. Categories not used have been omitted from the table. The two rightmost columns show the total contribution from each category to the entire modelled area in Forsmark.

Diffuse sources		mg/L	kg/km²,yr	kg/year	%
Cathegory	**Class**				
Regolith	jWater	0.45	–	117	1
	jSand	2.3	–	306	3
	jPeat	='jSand'	–	413	4
	jRock	='jSand'	–	641	6
	jClay	='jSand'	–	807	8
	jTill	='jSand'	–	7,145	67
Land-use	–	–	–	–	
Vegetation	–	–	–	–	
Topography	–	–	–	–	–
Point sources					
Sea water intrusions in Lake Bolundsfjärden				1,200	11
Total					
Gross				10,630	100
Retention (λ), yr^{-1}				0	0
Net				10,630	100

- The calibrated background level of about 2 mg/L in discharge from all soil categories in the Forsmark area is about 15 times higher than the median concentration in precipitation of 0.15 mg/L /Tröjbom and Söderbäck 2006/. If this value is corrected for evapotranspiration (cf Section 6.2.1), the discrepancy is 4 times corresponding to a concentration of 0.5 mg/L. When compared to the average concentration in the discharge from the entire Forsmark area of 2 mg/L (cf model compilation in Appendix E), a significant fraction (50–75%) probably originates from either weathering reactions or relict remnants in the Quaternary deposits, depending on the contribution from dry deposition not included in the measurements of precipitation. Both these concentrations exceed the 70th percentile of the Swedish distributions shown in Figure 6-13.

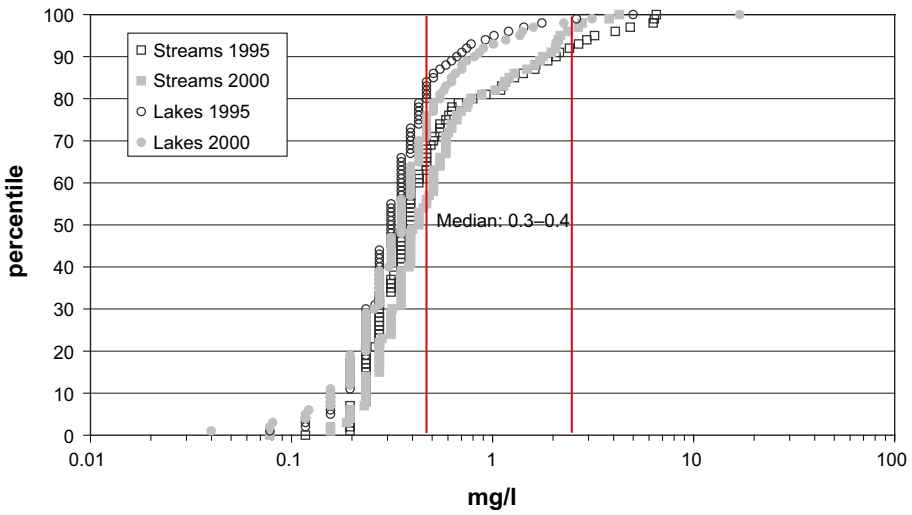

Figure 6-13. *Distribution of K concentrations in the Swedish surveys of lakes and streams 1995 and 2000 /IMA 2007/. Typical concentrations calibrated within the VBX-VI model are marked as red lines.*

- At episodes of high water levels in the Baltic, sea water intrusions add significant amounts of K into Lake Bolundsfjärden corresponding to an amount of 1,200 kg/year or 30% of the total input to the lake.
- There are no indications of significant retention of K in the lakes.

6.2.4 Mass balance for calcium (Ca)

The spatial variability of Ca show a clear pattern of influence from retention processes as precipitation in lakes (i.e. concentrations in the outlet of lakes are significantly lower than expected from the typical concentrations in the discharge from land). In the correlation analysis in Figure 6-15, the regolith class 'jTill' and land-use classes 'arable' and 'open' correlate to the calcium concentrations, indicating two possible sources (or processes) which release calcium to the surface waters. Model details are listed below:

- Due to almost similar Ca levels in Lake Bolundsfjärden and the Baltic Sea, the net effect of sea water intrusions is assumed to be negligible (a net input in the order of 500 kg/year is expected when mean concentrations in lake and sea are concerned cf Table 6-4).
- Both the primary and the secondary datasets were used for calibration of the Ca model shown in Figure 6-14. Parameter values and a source apportionment for the entire Forsmark area are compiled in Table 6-7. In Appendix F are model details compiled.

By only one calibrated typical concentration, representing discharge from all regolith classes, and a general retention parameter, λ, the Ca model describes the concentration variation within the Forsmark area well, with an average deviation of 5% in the primary calibration dataset (22% in secondary).

The largest deviations in the Ca model are encircled in red in Figure 6-14. The discrepancy in Lake Bolundsfjärden (AFM001103A), in combination with an opposite deviation in Lake Norra Bassängen (AFM001101) close downstream, indicates increased uncertainties in the Ca model in these lakes. The catchment upstream Lake Bredviken (AFM000052B) shows almost doubled concentrations of Ca, compared to what is expected in the model. This catchment contains a high proportion arable land, and, in accordance with the situation for K, this may be an explanatory factor to the elevated Ca transport from this area /Åström and Rönnback, submitted/.

From the mass balance scenario, the following conclusions about sources of Ca can be drawn:

- Diffuse Ca sources are rather uniformly distributed over the Forsmark area and no distributed factors, as topographical elevation, regolith type, land-use or vegetation cover seem to have any clear influence. The typical concentration in discharge from all soil categories is estimated to 62 mg/L, which corresponds to the 95th percentile of the national distribution (cf Figure 6-16). This high value reflects influence from the calcite-rich till that covers the area and gives prerequisites for deviant chemistry in shallow groundwater and also affects the structure of freshwater ecosystems /Brunberg and Blomquist 2000/ (cf Section 4.1.3).
- The Ca retention in lakes in the Forsmark area is substantial. The calibrated retention parameter implies a total retention of 12% in the whole area. This portion is substantially higher in some catchments that contain lakes, and reach about 30% in AFM000010A (Lake Eckarfjärden), AFM000084 (Lake Simpviken), and AFM000091 (Lake Puttan). Calcite-bearing gyttja-clays have also been observed in the lake sediments in the Forsmark area /Hedenström 2004/. See Appendix F for a compilation of retention details.
- Sea water intrusions at episodes of high water levels in the Baltic have little influence on the Ca input to Lake Bolundsfjärden and other lakes located close to sea level. Differences between modelled and observed values for Lake Bolundsfjärden and Lake Norra Bassängen may however indicate that Ca sources and sinks are less understood in these lakes with strong marine influences.

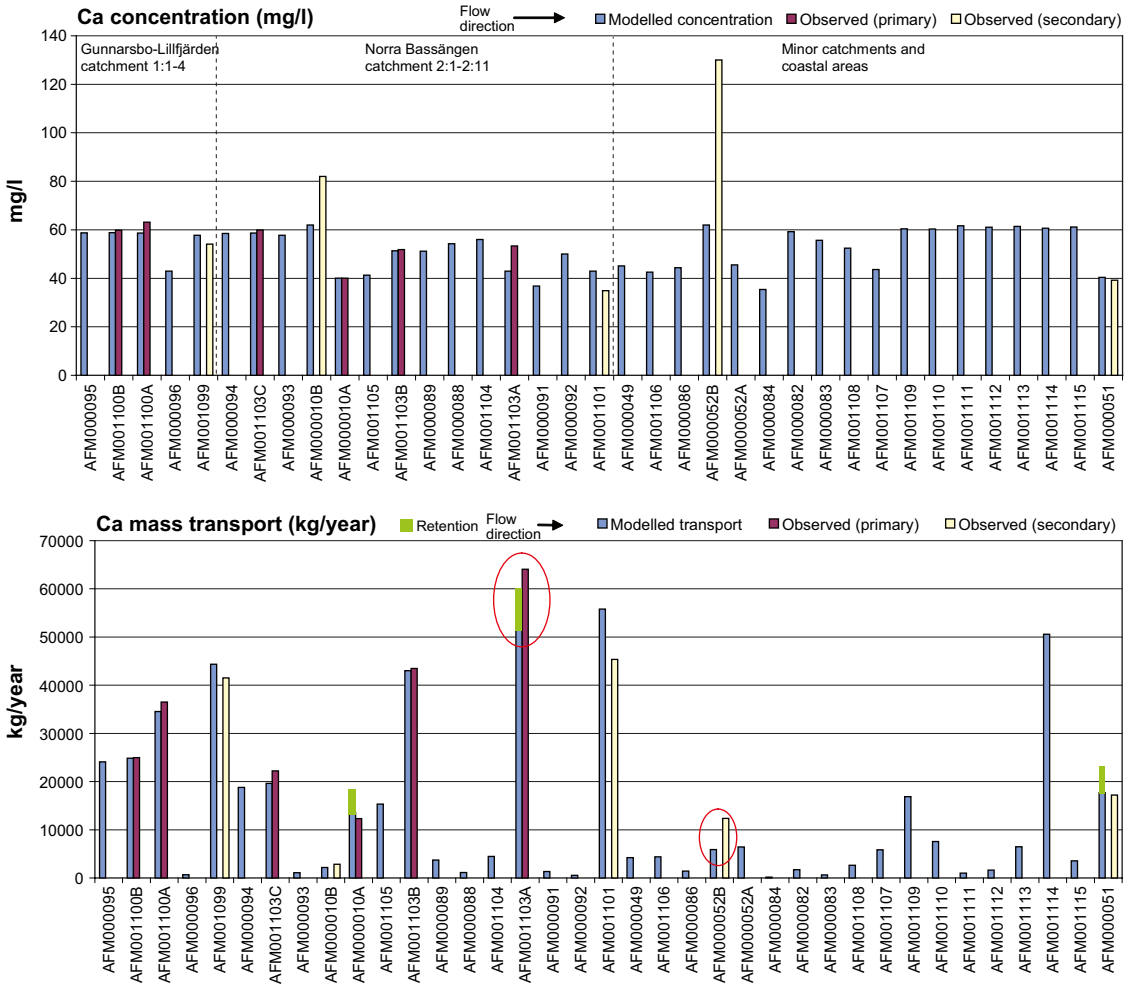

Figure 6-14. *Mass balance for Ca in the Forsmark area. Flow weighted concentrations (mg/L) above, and transports (kg/year) below, describing the conditions in the outlet of each catchment. Green bars mark the retention loss in lakes.*

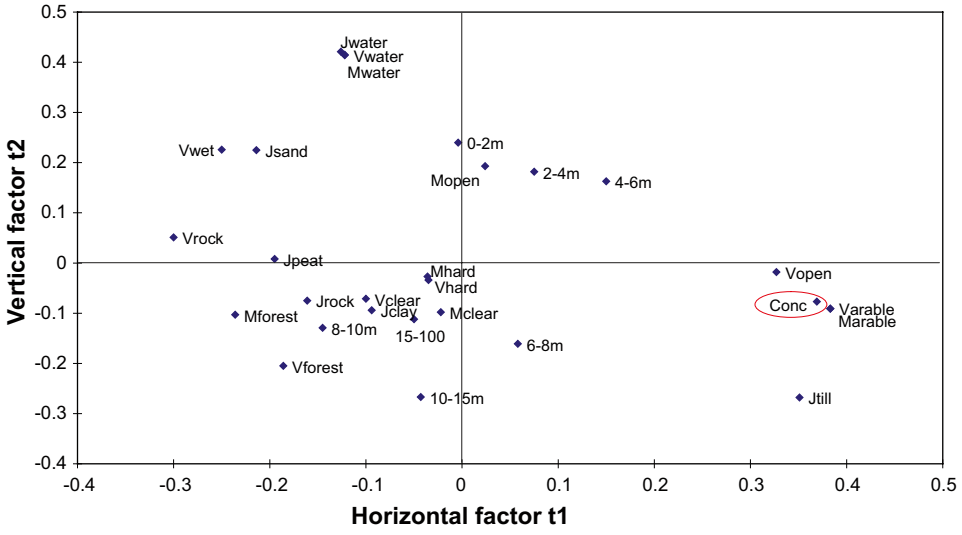

Figure 6-15. *Partial least square regression model, PLS, (cf Section 2.3.11 for an explanation of PLS) showing the correlation structure among distributed catchment characteristics, and the observed Ca concentration (encircled in red). The parameters represent the relative distribution of each regolith, land-use, vegetation and elevation class upstream the hydrochemical sampling point in the outlet of the catchments. Factor t1 describe 26% of the variation among the explanatory variables and t2 38%. 89% of the variance in 'Conc' is described by t1 and 5% by t2.*

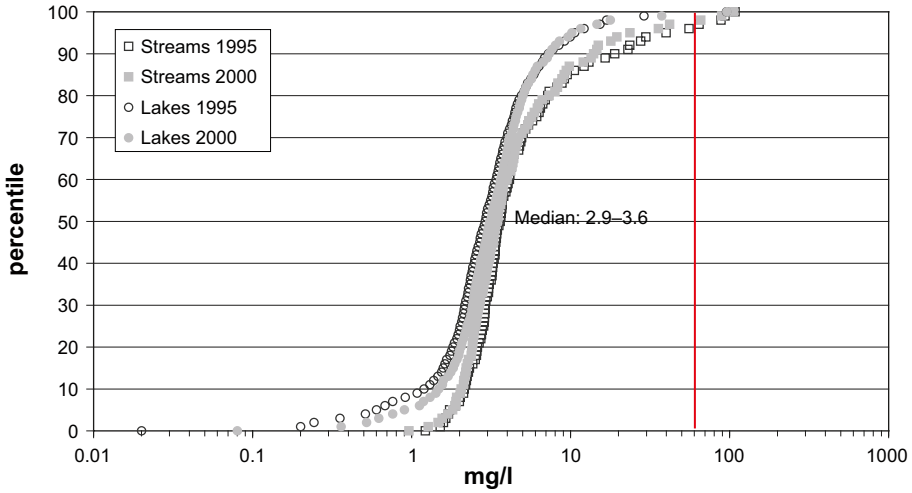

Figure 6-16. Distribution of Ca concentrations in the Swedish surveys of lakes and streams 1995 and 2000 /IMA 2007/. Typical concentrations calibrated within the VBX-VI model is marked as a red line.

Table 6-7. Compilation of parameters from the Ca mass balance model. Categories not used have been omitted from the table. The two rightmost columns show the total contribution from each category to the entire modelled area in Forsmark.

Diffuse sources		mg/L	kg/km²,yr	kg/year	%
Cathegory	**Class**				
Regolith	jWater	–	–	–	–
	jSand	62	–	8,377	3
	jPeat	='jSand'	–	11,298	4
	jRock	='jSand'	–	17,553	7
	jClay	='jSand'	–	22,081	9
	jTill	='jSand'	–	195,423	77
Land–use	–	–	–	–	
Vegetation	–	–	–	–	
Topography	–	–	–	–	–
Point sources					
Sea water intrusions in Lake Bolundsfjärden				–	–
Total					
Gross				254,732	100
Retention (λ = 0.53 yr^{-1})				30,860	12
Net				223,872	88

6.2.5 Mass balance for magnesium (Mg)

Mg shows a distribution pattern intermediate to e.g. Na and Ca, reflecting at least two major sources of this element. According to the correlation analysis in Figure 6-18, the topographical elevation and the regolith class 'jTill', as well as the land-use classes 'arable' and 'open', are positively correlated to the Mg concentration. Possible sources are sea water intrusions, relict marine remnants and dissolution of Mg-bearing calcite. Model details are listed below:

- An addition of Mg to Lake Bolundsfjärden of 3,800 kg/year due to sea water intrusions was assumed as an initial condition in the model (cf Table 6-4).
- Both the primary and the secondary datasets were used for calibration of the Mg model shown in Figure 6-17. Parameter values and a source apportionment for the entire Forsmark area are compiled in Table 6-8. In Appendix F are model details compiled.

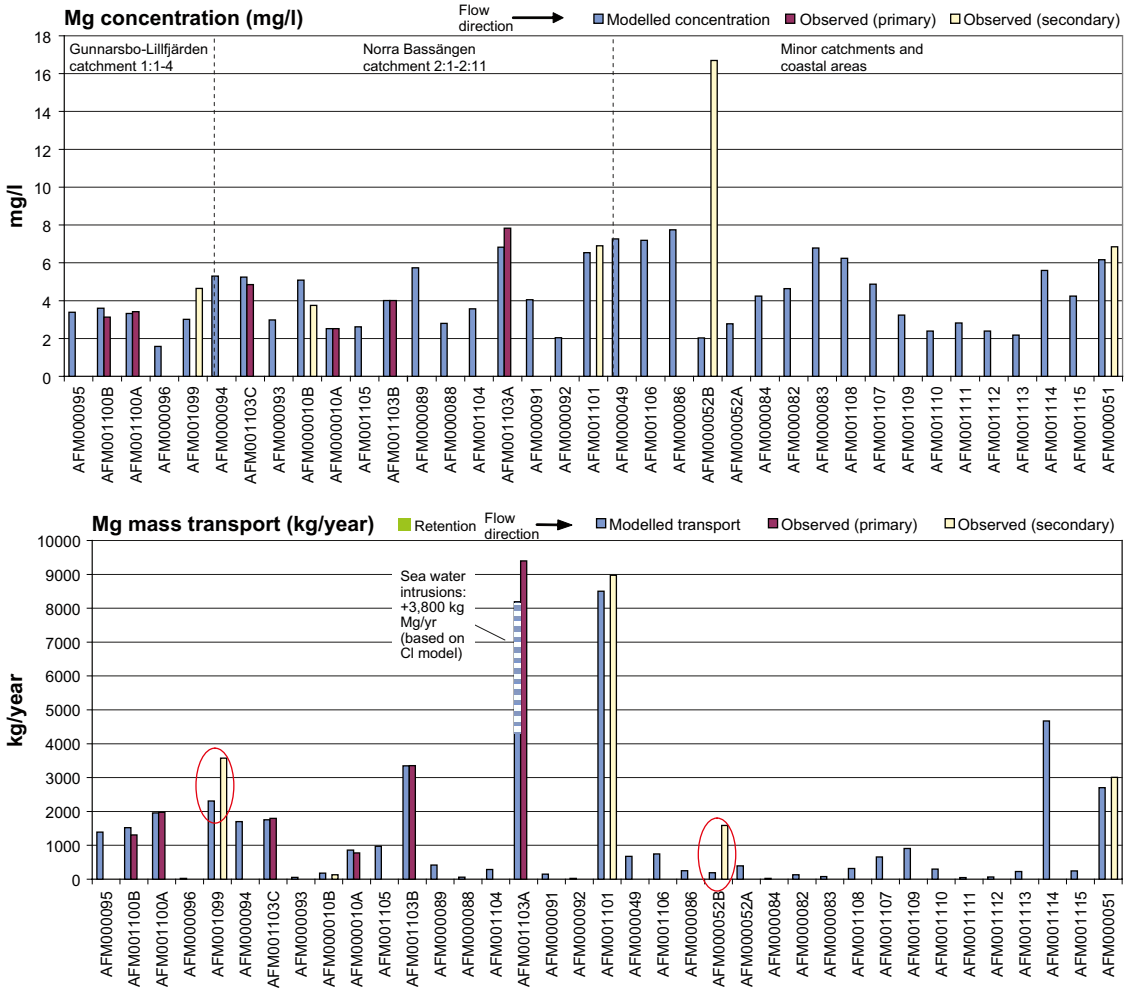

Figure 6-17. *Mass balance for Mg in the Forsmark area. Flow weighted concentrations (mg/L) above, and transports (kg/year) below, describing the conditions in the outlet of each catchment.*

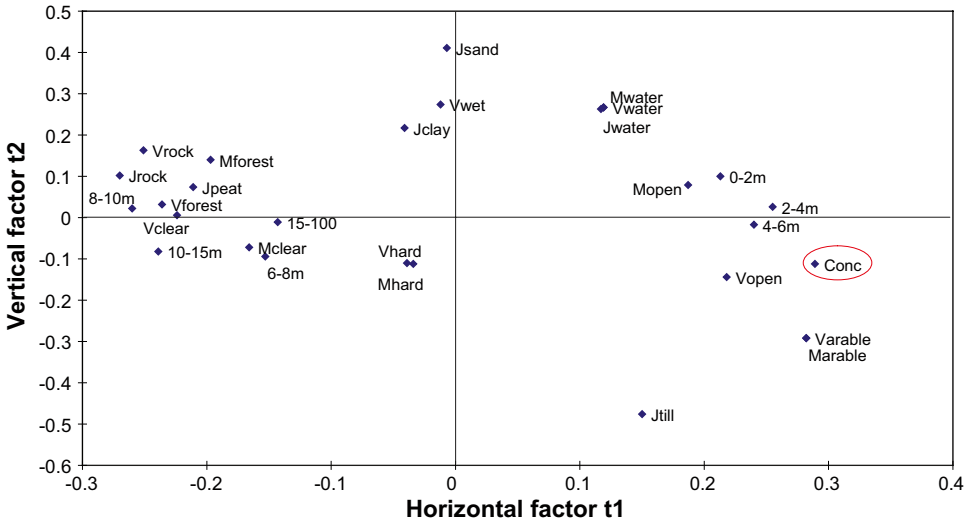

Figure 6-18. *Partial least square regression model, PLS, (cf Section 2.3.11 for an explanation of PLS) showing the correlation structure among distributed catchment characteristics, and the observed Mg concentration (encircled in red). The parameters represent the relative distribution of each regolith, land-use, vegetation and elevation class upstream the hydrochemical sampling point in the outlet of the catchments. Factor t1 describe 41% of the variation among the explanatory variables and t2 24%. 88% of the variance in 'Conc' is described by t1 and 7% by t2.*

Table 6-8. Compilation of parameters used in the Mg mass balance model. Categories not used have been omitted from the table. The two rightmost columns show the total contribution from each category to the entire modelled area in Forsmark.

Diffuse sources		mg/L	kg/km^2,yr	kg/year	%
Cathegory	Class				
Regolith	jWater	–	–	–	–
	jSand	2	–	250	1
	jPeat	='jSand'	–	336	2
	jRock	='jSand'	–	522	2
	jClay	32	–	11,321	51
	jTill	='jSand'	–	5,815	26
Land-use	–	–	–	–	
Vegetation	–	–	–	–	
Topography	–	–	–	–	
Point sources					
Sea water intrusions in Lake Bolundsfjärden				3,800	18
Total					
Gross				22,044	100
Retention (λ), yr^{-1}				0	0
Net				22,044	100

By adjusting two parameters, which represent typical concentrations in water from different regolith classes, the Mg concentration within the Forsmark area is satisfactorily modelled with an average model deviation of 6% between modelled and observed concentrations in the primary calibration dataset (35% in secondary).

Two catchments encircled in red deviate in the Mg scenario. Both belong to the secondary calibration dataset, thus showing higher uncertainty due to limited data (cf Section 6.1.4), which may be, at least partly, the explanation to the deviation of AFM001099. The inlet to Bredviken, AFM000052B, shows similar to other ions, e.g. K and SO_4, elevated concentrations of Mg compared to the modelled results, which may be explained by the large portion of arable land in this catchment /Åström and Rönnback, submitted/.

From the mass balance scenario, the following conclusions about sources of Mg can be drawn:

- The calibrated background level of about 2 mg/L in discharge from all soil categories except for 'jClay' is about 25 times higher than the median concentration in precipitation of 0.08 mg/L /Tröjbom and Söderbäck 2006/. If these values are corrected for evapotranspiration, the discrepancy is 8 times corresponding to a concentration of 0.24 mg/L, which means that deposition is a minor source contributing with only 10% of the background level. This fraction is probably slightly higher if there is a fraction of dry deposition not included in the measurements of precipitation, but probably not exceeding 20% as dry deposition in these areas add approximately 50–100% to the wet deposition value (P.O. Johansson, pers. comm.). The major source of the background level of 2 mg/L is probably attributed to weathering reactions as dissolution of Mg-bearing calcite (cf Section 4.1.3 that deals with the origin of calcium). Compared to the national distribution, this background level corresponds to the 80–90th percentile, which supports that calcite, rather than a more widespread mineral, is the major Mg source (cf Figure 6-19).
- Discharge from the regolith class 'jClay', contains according to the Mg model, more than ten times Mg compared to the background level. The spatial distribution of this regolith category is shown in Figure 6-6, and the original source of this Mg is most probable marine Mg trapped in the sediments. As tested in an alternative, but not reported, model scenario, topographical parameters did not reproduce the spatial variability as good as the 'jClay' regolith parameter.

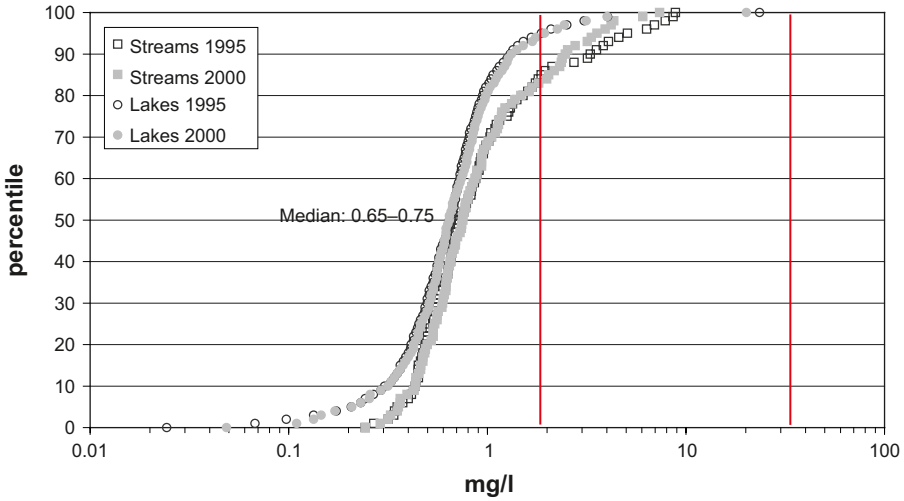

Figure 6-19. *Distribution of Mg concentrations in the Swedish surveys of lakes and streams 1995 and 2000 /IMA 2007/. Typical concentrations calibrated within the VBX-VI model are marked as red lines.*

- When the background level of about 2 mg/L is compared to the average concentration in discharge from the entire Forsmark area (5 mg/L), approximately 30–40% of the Mg that reaches the sea probably originates from weathering reactions, whereas the rest originates from sea water intrusions or relict marine remnants in sediments. The estimated sea water intrusions into Lake Bolundsfjärden, contributing with 3,800 kg/year, account for a relative portion of 18%, leaving 40–50% to diffuse leaching from sediments.
- There are no indications of significant retention of Mg in the lakes.

6.2.6 Mass balance for sulphate (SO_4)

SO_4 in surface water originates from three major sources according to the qualitative analysis in Section 4.1.2, where the origin of sulphur is explored. These are atmospheric deposition, marine remnants either in form of sulphide minerals or sulphate, and ongoing sea water intrusions in lakes located close to the sea level. According to the correlation analysis in Figure 6-21, the topographical elevation and the regolith category 'jTill', as well as the land-use categories 'arable' and 'open', are positively correlated to the SO_4 concentration, similar to the pattern for Mg. In a correlation analysis of the element contents in till samples from the Forsmark area in /Tröjbom and Söderbäck 2006/, Ca and SO_4 were positively correlated, indicating a similar spatial distribution pattern of the source of these elements. A possible candidate is the Quaternary deposits which contain large amounts of calcite, and probably also sulphide minerals of marine origin from the Littorina period when the Forsmark area was submerged by Sea water (cf conceptual model in Section 8.2). Model details are listed below:

- A point source addition of Mg to Lake Bolundsfjärden of 8,100 kg/year due to sea water intrusions was assumed as an initial condition in the model (cf Table 6-4).
- Both the primary and the secondary datasets were used for calibration of the SO_4 model shown in Figure 6-20. Parameter values and a source apportionment for the entire Forsmark area are compiled in Table 6-9. In Appendix F are model details compiled.

By adjusting two parameters, which represent typical concentrations in water from different regolith categories, the SO_4 concentration within the Forsmark area is satisfactorily modelled, with an average model deviation of 13% between modelled and observed concentrations in the primary calibration dataset (69% in secondary).

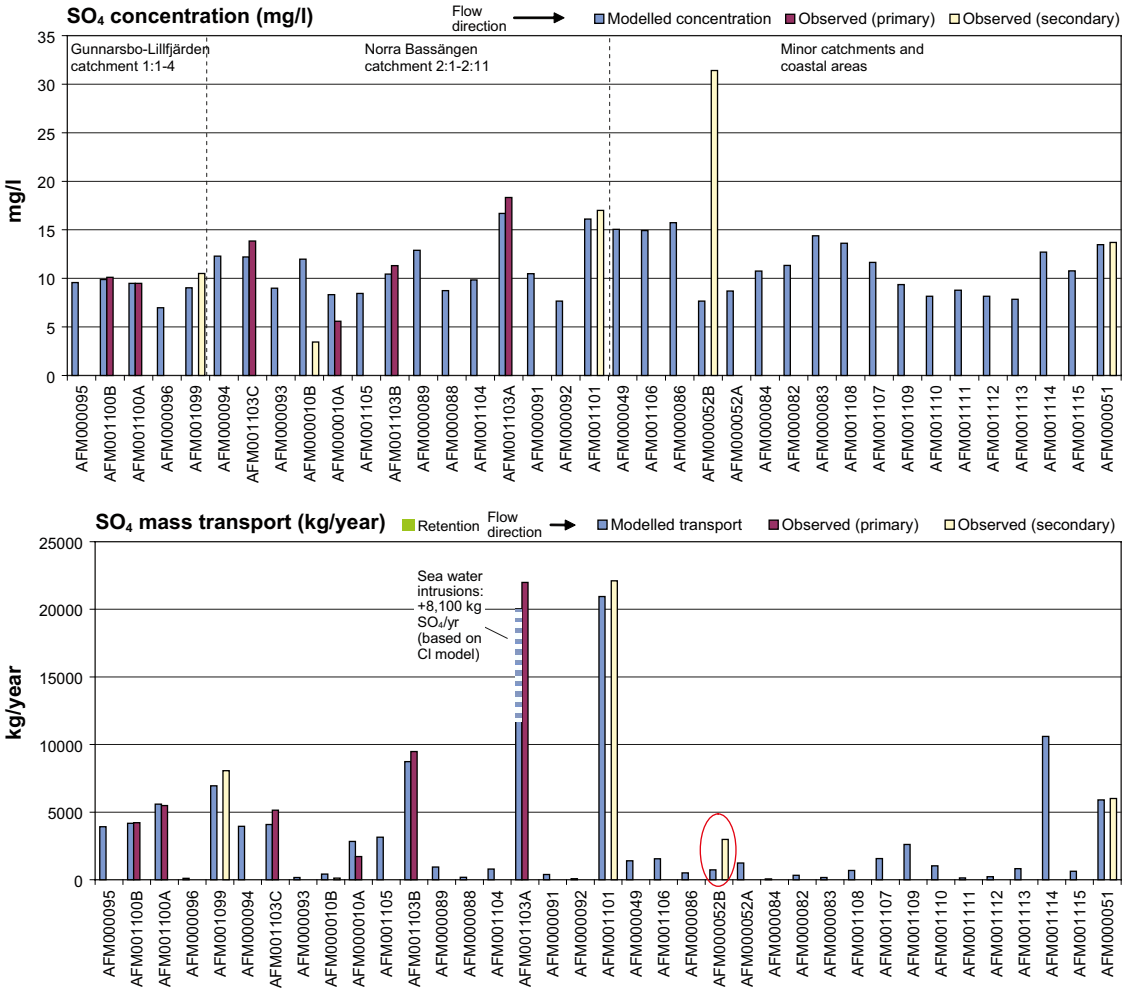

Figure 6-20. *Mass balance for SO_4 in the Forsmark area. Flow weighted concentrations (mg/L) above, and transports (kg/year) below, describing the conditions in the outlet of each catchment.*

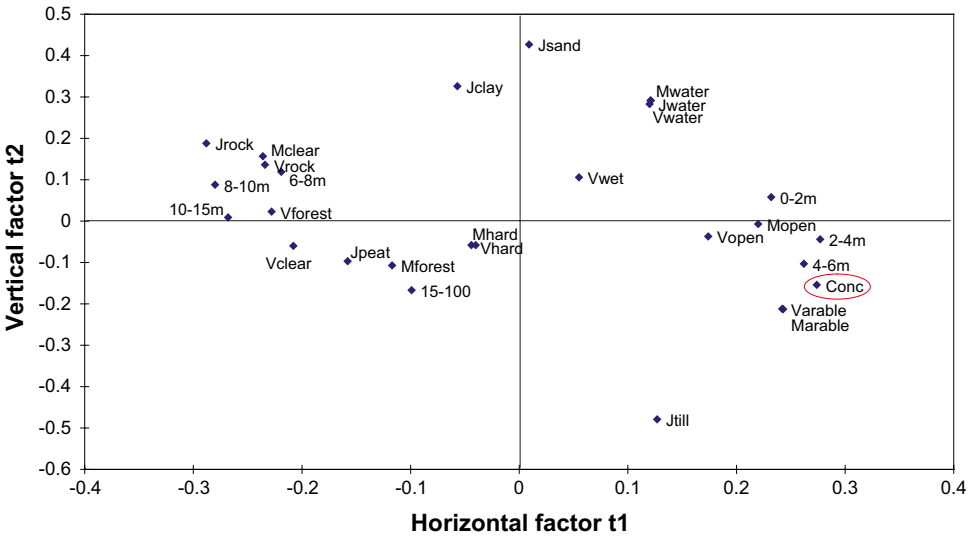

Figure 6-21. *Partial least square regression model, PLS, (cf Section 6.5.3 for an explanation of PLS) showing the correlation structure among distributed catchment characteristics, and the observed SO_4 concentration (encircled in red). The parameters represent the relative distribution of each regolith, land-use, vegetation and elevation class upstream the hydrochemical sampling point in the outlet of the catchments. Factor t1 describe 42% of the variation among the explanatory variables and t2 20%. 81% of the variance in 'Conc' is described by t1 and 10% by t2.*

Table 6-9. Compilation of parameters used in the SO_4 mass balance model. Categories not used have been omitted from the table. The two rightmost columns show the total contribution from each category to the entire modelled area in Forsmark.

Diffuse sources		mg/L	kg/km²,yr	kg/year	%
Cathegory	**Class**				
Regolith	jWater	4.5[A]	–	1,174	2
	jSand	7.4	–	999	2
	jPeat	='jSand'	–	1,347	2
	jRock	='jSand'	–	2,092	4
	jClay	50	–	17,737	32
	jTill	='jSand'	–	23,300	43
Land-use	–	–	–	–	
Vegetation	–	–	–	–	
Topography	–	–	–	–	
Point sources					
Sea water intrusions in Lake Bolundsfjärden				8,100	15
Total					
Gross				54,750	100
Retention (λ), yr^{-1}				0	0
Net				54,750	100

A: average concentration in precipitation x 3 to correct for evapotranspiration.

The major deviation in the SO_4-model is, similarly to the situation for K and Mg, shown by the catchment that discharges into Lake Bredviken (AFM000052B). A possible explanation to the elevated SO_4 concentrations may be the large portion of arable land in this catchment, where either farming activities as cultivating or draining enhance the oxidation and release of sulphur from sulphide minerals /Åström and Rönnback, submitted/. Also sulphur bearing fertilizers may be a partial explanation to the elevated SO_4 transport, corresponding to an additional area-specific loss of 35 kg/ha,yr from this catchment.

From the mass balance scenario, the following conclusions about sources of SO_4 can be drawn:

- The calibrated background level of 7.4 mg SO_4/L in discharge from all soil categories except for 'jClay' is about 6 times higher than the median SO_4 concentration in precipitation of 1.5 mg/L /Tröjbom and Söderbäck 2006/. If these values are corrected for evapotranspiration (cf Section 6.2.1), the discrepancy to the background level is less than 2 times corresponding to a concentration of 4.5 mg/L. An interpretation of this result is that deposition may be a major source contributing to the background level in the Forsmark area. If the estimated concentration in precipitation is compared to the average concentration in discharge from the entire Forsmark area (13 mg/L), approximately one third of the SO_4 that reaches the sea originates from deposition. Of this airborne fraction, only 0.1 mg/L out of 4.5 mg/L, or 2%, originate from sea spray, if the marine part is estimated from local Cl measurements in precipitation, and the rest originate from regional sulphur deposition. Compared to the national distribution, this background level corresponds to the 80–90th percentile in lakes and streams (Figure 6-22). The measurements of SO_4 in precipitation, which is sampled in a container located in an open field, may to some extent discriminate the additional supply from dry deposition. According to measurements in the region this part may contribute with further 50–100% compared to observed wet deposition (P.O. Johansson, pers. comm.), which means that the total background level of 7.4 mg SO_4/L could be explained by deposition.

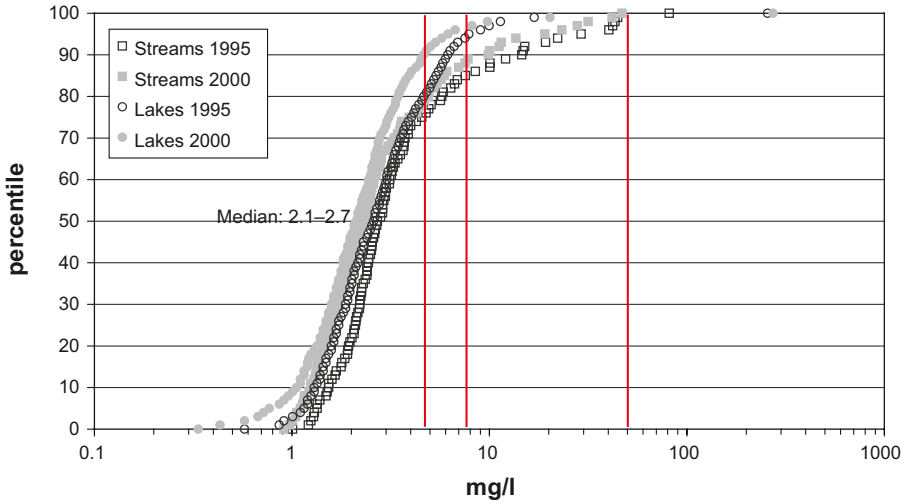

Figure 6-22. *Distribution of SO_4 concentrations in the Swedish surveys of lakes and streams 1995 and 2000 /IMA 2007/. Typical concentrations calibrated within the VBX-VI model are marked as red lines.*

- Discharge from the regolith class 'jClay', contains according to the SO_4 model, more than six times SO_4 compared to the background level. The spatial distribution of this regolith class is shown in Figure 6-6 and the original source of this SO_4 is most probable marine sulphur in the sediments (sulphide minerals). Approximately one third of all SO_4 that leaves the area originate from this regolith class according to the mass balance model.
- The remaining third part (the other two where deposition and discharge from 'jClay') originates from sea water intrusions or relict marine remnants in regolith classes other than 'jClay'. The estimated intrusions into Lake Bolundsfjärden of 8,100 kg/year account for 50% of this last third, whereas diffuse leakage makes the rest. Depending on the unknown contribution from dry deposition, described under the first bullet in the list, this diffuse post may be explained by dry deposition.
- There are no indications of significant retention of SO_4 in the lakes.

6.2.7 Mass balance for bicarbonate (HCO_3)

The spatial variability of HCO_3 is in most details similar to the situation for Ca, described in Section 6.2.4, despite independent models which are calibrated separately. HCO_3 also show a clear pattern of influence from retention processes as precipitation in lakes (i.e. concentrations in the outlet of lakes are significantly lower than expected from the typical concentrations in the discharge from land). The regolith class 'jTill' and land-use classes 'arable' and 'open' are positively correlated to 'Conc' in the correlation analysis in Figure 6-24. Model details are listed below:

- Contrary to most other ions, sea water intrusions in the lower located lakes theoretically lead to a minor net outflow of HCO_3 due to about halved concentrations in the Baltic compared to most surface waters in the Forsmark area.
- Both the primary and the secondary datasets were used for calibration of the HCO_3 model shown in Figure 6-23. Parameter values and a source apportionment for the entire Forsmark area are compiled in Table 6-10. In Appendix F are model details compiled.

By one calibrated typical concentration representing discharge from all regolith categories and a general retention parameter, λ, the HCO_3 model describes the concentration variation within the Forsmark area well, with an average deviation of 5% in the primary calibration dataset (34% in secondary).

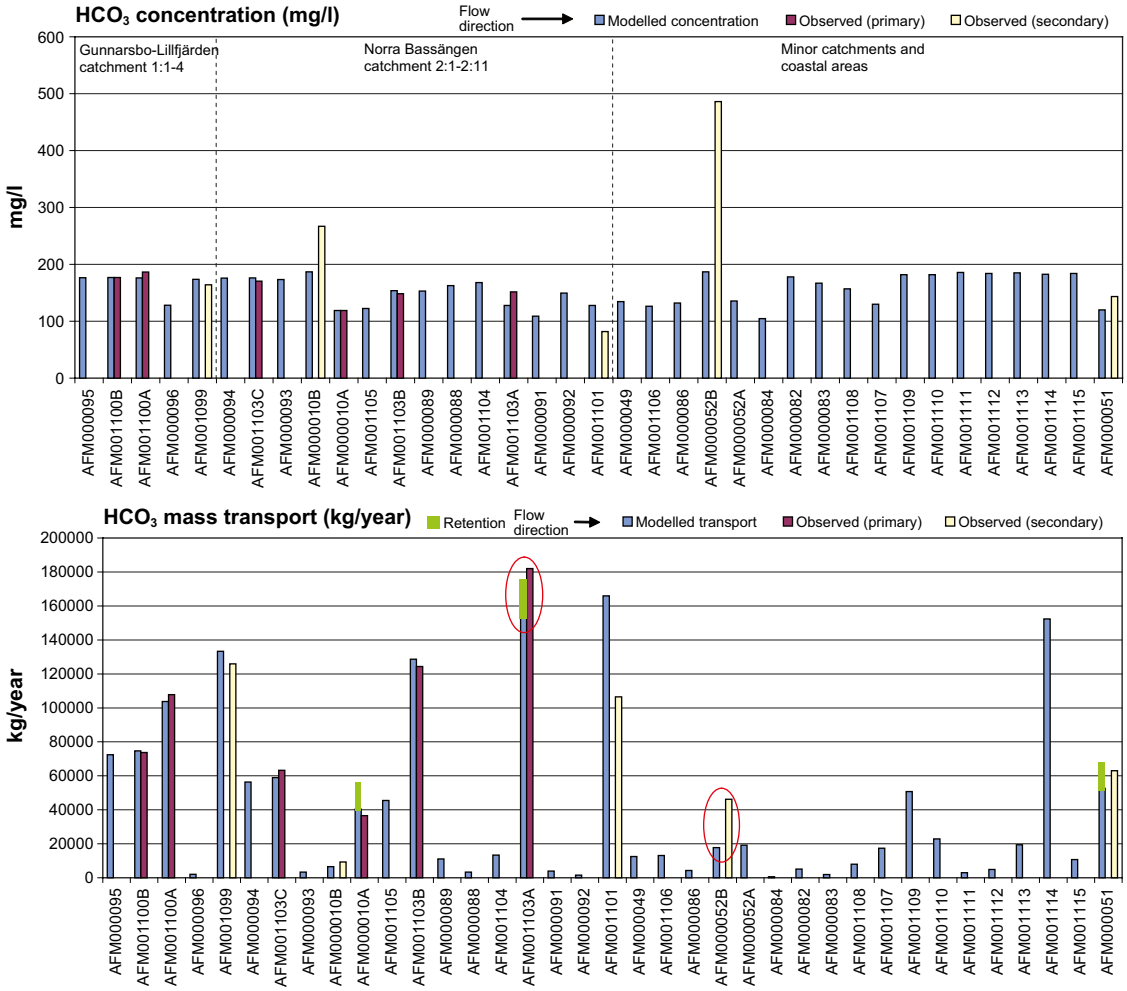

Figure 6-23. *Mass balance for HCO_3 in the Forsmark area. Flow weighted concentrations (mg/L) above, and transports (kg/year) below, describing the conditions in the outlet of each catchment. Green bars mark the retention loss in lakes.*

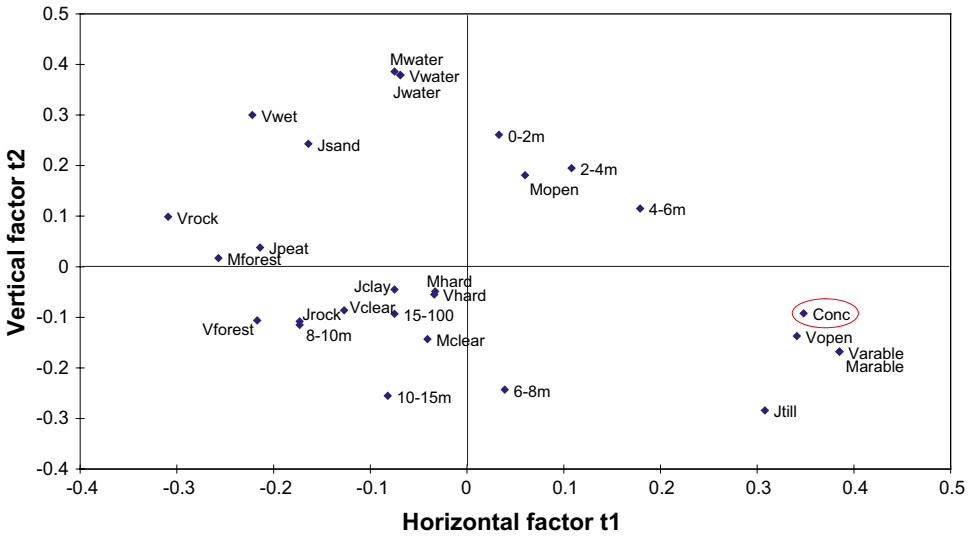

Figure 6-24. *Partial least square regression model, PLS, (cf Section 6.5.3 for an explanation of PLS) showing the correlation structure among distributed catchment characteristics, and the observed HCO_3 concentration (encircled in red). The parameters represent the relative distribution of each regolith, land-use, vegetation and elevation class upstream the hydrochemical sampling point in the outlet of the catchments. Factor t1 describe 29% of the variation among the explanatory variables and t2 36%. 86% of the variance in 'Conc' is described by t1 and 7% by t2.*

Table 6-10. Compilation of parameters used in the HCO_3 mass balance model. Categories not used have been omitted from the table. The two rightmost columns show the total contribution from each category to the entire modelled area in Forsmark.

Diffuse sources		mg/L	kg/km²,yr	kg/year	%
Cathegory	**Class**				
Regolith	jWater	–	–	–	–
	jSand	187	–	25,230	3
	jPeat	='jSand'	–	34,026	4
	jRock	='jSand'	–	52,867	7
	jClay	='jSand'	–	66,503	9
	jTill	='jSand'	–	588,575	77
Land-use	–	–	–	–	
Vegetation	–	–	–	–	
Topography	–	–	–	–	
Point sources					
Sea water intrusions in Lake Bolundsfjärden				–	–
Total					
Gross				767,202	100
Retention (λ=0.56 yr^{-1})				–96,947	13
Net				670,254	87

The largest deviations in the HCO_3 model are encircled in red in Figure 6-23. The discrepancy in Lake Bolundsfjärden (AFM001103A), in combination with an opposite, even larger deviation compared to the Ca-model in Lake Norra Bassängen (AFM001101) close downstream, indicates that the uncertainties regarding HCO_3 are substantial in these lakes influenced by sea water intrusions.

The catchment upstream Lake Bredviken (AFM000052B) deviates with respect to HCO_3 in a similar manner as many ions (e.g. Ca, Mg, K, SO_4), showing more than doubled HCO_3 concentrations compared to the model. This catchment contains a high proportion arable land, which at least partly may explain the elevated HCO_3 transport from this area (cf Section 7.7 and /Åström and Rönnback, submitted/).

From the mass balance scenario, the following conclusions about sources of HCO_3 may be drawn:

- Diffuse HCO_3 sources are rather uniformly distributed over the Forsmark area, and no distributed factors as topographical elevation, regolith type, land-use or vegetation cover seems to have any clear influence. The typical concentration in discharge from all soil categories is estimated to 187 mg/L, which corresponds to the 95th percentile of the national distribution (cf Figure 6-25). This high value reflects the influence from the calcite rich till that covers the area (cf Section 4.1.3).
- There is a substantial HCO_3 retention in the lakes in the Forsmark area indicated by the model. The calibrated retention parameter implies a total retention of 13% in the entire area. This portion is substantially higher in some catchments that contain lakes, and reaches about 30% in AFM000010A (Lake Eckarfjärden), AFM000084 (Lake Simpviken), and AFM000091 (Lake Puttan). See Appendix E for a compilation of retention details.

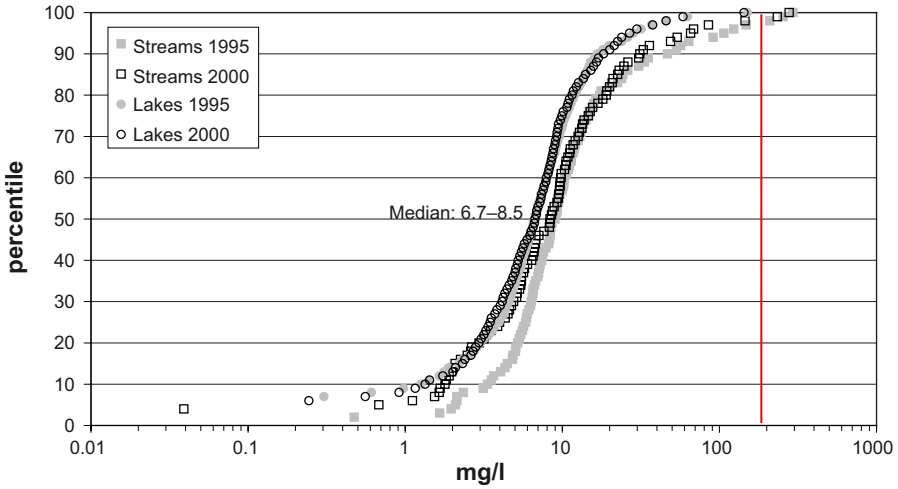

Figure 6-25. *Distribution of HCO_3 concentrations in the Swedish surveys of lakes and streams 1995 and 2000 /IMA 2007/. Typical concentrations calibrated within the VBX-VI model are marked as red lines.*

- When the amount HCO_3 that is lost in the lakes by retention is compared to the corresponding Ca loss, the mass ratio of the total amounts estimated by the independent models fits very closely to the theoretical ratio between these ions when calcite is precipitated according to the reaction in Equation 8. The mass ratio of modelled retention loss from the models is 3.14 (HCO_3/Ca), compared to the theoretical mass ratio according to Equation 8 of 3.05 (2×61/40). This finding probably gives a rough indication of the uncertainties of the catchment models, or at least, the Ca and HCO_3-models.
- Sea water intrusions at episodes of high water levels in the Baltic have contrary to most ions, theoretically a negative net effect on the HCO_3 concentrations to Lake Bolundsfjärden and other lakes located close to sea level. Large positive deviations between the model and observed values for Lake Bolundsfjärden and Lake Norra Bassängen may, however, indicate that HCO_3 sources and sinks are poorly understood in these lakes influenced by sea water intrusions.

Equation 8. Calcite precipitation. This net reaction is the reverse of the two upper formulas in Equation 5.

$$Ca^{2+} + 2HCO_3^- \rightarrow CaCO_3 + CO_2 + H_2O$$

6.2.8 Mass balance for total organic carbon (TOC)

According to the correlation analysis in Figure 6-27, several land-use and vegetation parameters are either positively or negatively correlated to TOC concentrations, indicating that factors coupled to e.g. vegetation have large impact on the release of TOC. There are no known point sources of TOC in the Forsmark area, and sea water intrusions in the lower located lakes dilute the freshwater with respect to TOC, leading to a minor net loss of TOC. Model details are listed below:

- Both the primary and the secondary datasets were used for calibration of the TOC model shown in Figure 6-26. Parameter values and a source apportionment for the entire Forsmark area are compiled in Table 6-11. In Appendix F are model details compiled.

By adjusting three parameters, which represent typical concentrations in water from different types of vegetation and land-use, the TOC concentration within the Forsmark area is satisfactorily modelled, with an average model deviation of 8% between modelled and observed concentrations in the primary calibration dataset (5% in secondary).

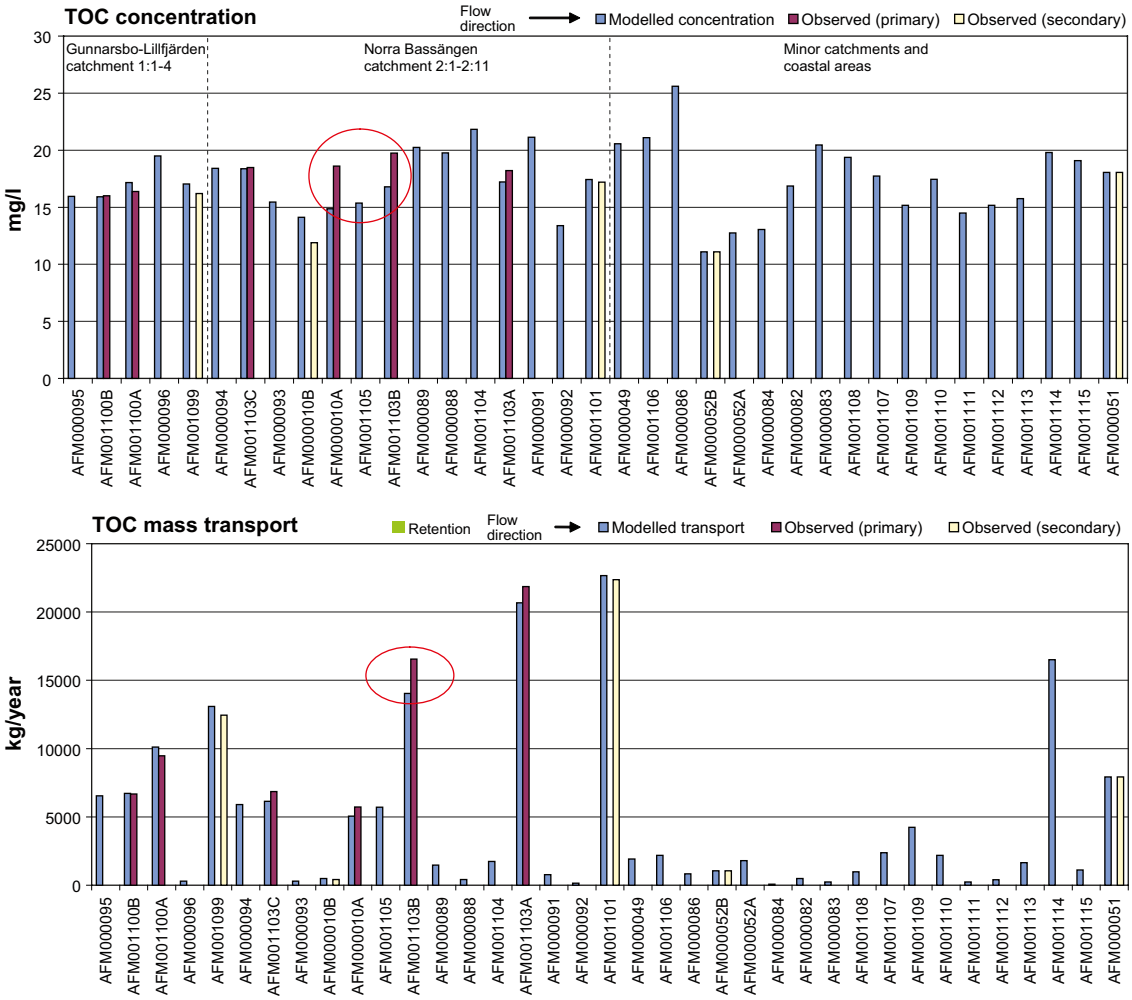

Figure 6-26. *Mass balance for TOC in the Forsmark area. Flow weighted concentrations (mg/L) above, and transports (kg/year) below, describing the conditions in the outlet of each catchment.*

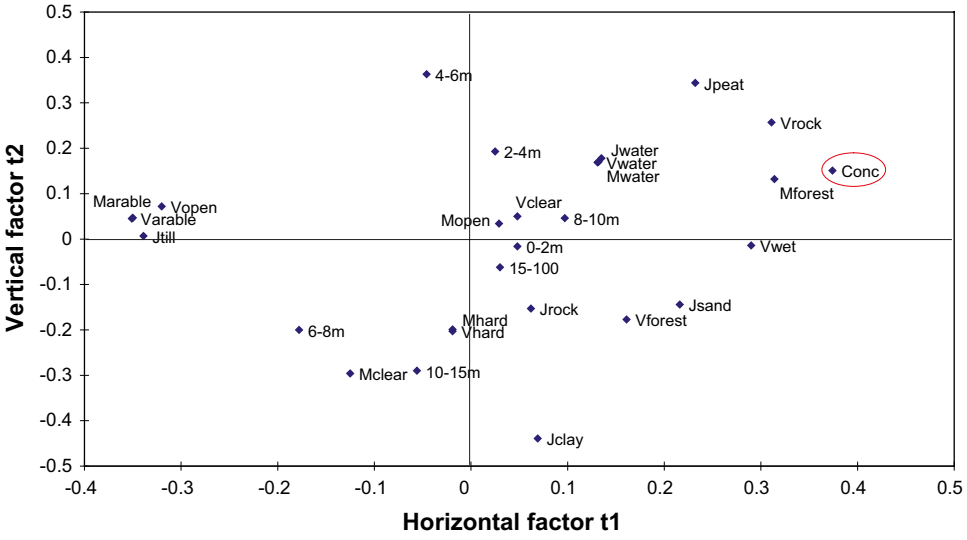

Figure 6-27. *Partial least square regression model, PLS, (cf Section 6.5.3 for an explanation of PLS) showing the correlation structure among distributed catchment characteristics, and the observed TOC concentration (encircled in red). The parameters represent the relative distribution of each regolith, land-use, vegetation and elevation class upstream the hydrochemical sampling point in the outlet of the catchments. Factor t1 describe 37% of the variation among the explanatory variables and t2 15%. 83% of the variance in 'Conc' is described by t1 and 7% by t2.*

Table 6-11. Compilation of parameters from the TOC mass balance model. Categories not used have been omitted from the table. The two rightmost columns show the total contribution from each category to the entire modelled area in Forsmark.

Diffuse sources		mg/L	kg/km^2,yr	kg/year	%
Cathegory	**Class**				
Regolith	–	–	–	–	–
Land–use	–	–	–	–	–
Vegetation	vWater	–	–	0	0
	vWet	51	–	28,477	37
	vRock	15	–	1,634	2
	vForest	='vRock'	–	42,313	55
	vClear	='vRock'	–	2,751	4
	vArable	9	–	1,149	1
	vOpen	='vArable'	–	965	1
	vHard	–	–	0	0
Topography	–	–	–	–	–
Point sources					
–				–	–
Total					
Gross				77,288	100
Retention (λ, yr^{-1})				–	0
Net				77,288	100

The major deviation in the model is shown by the catchment AFM001103B, located downstream Lake Stocksjön and upstream Lake Bolundsfjärden, corresponding to an area-specific loss of 2,500 kg/km^2,year or an addition of 2 mg/L in discharge from this area. There is no clear explanation to this discrepancy, but deviating concentrations in the upstream catchment AFM000010A may be an indication that this discrepancy actually applies to the whole catchment. Clear-cuts and other changes in land-use may be responsible for deviations of this order of magnitude, and one candidate is the burning of debris after a clear-cut in sub-catchment AFM001103B.

From the mass balance scenario, the following conclusions about sources of TOC can be drawn:

- Typical concentrations of TOC from wetlands are more than three times elevated compared to concentrations in discharge from forest land. According to the TOC model, wetlands covering about 14 % of the land area answer for 37% of the total output of TOC to the Baltic.
- Forest land, which covers 70% of the land area, contributes with slightly more than 50% of the total output. The typical TOC concentration of 15 mg/L corresponds to the 70–95th percentiles of the national distributions in Figure 6-28, which may be an indication that area-specific TOC loss is rather high in the Forsmark area, both regarding forest and wetland.
- Arable land and open land release less amounts of TOC per unit area according to the mass balance model. A typical concentration for these vegetation categories was calibrated to a value almost half the discharge from forest land.
- There are no indications of any significant retention loss of TOC in the lakes. This finding is in accordance with other mass balance models from the Forsmark area, where these lakes were found to be slightly autotrophic (i.e. the outflow of carbon is larger than the inflow) /Andersson and Sobek 2006/. The accumulation of carbon in the bottom sediments are therefore a least balanced by the net fixation of carbon from the atmosphere.

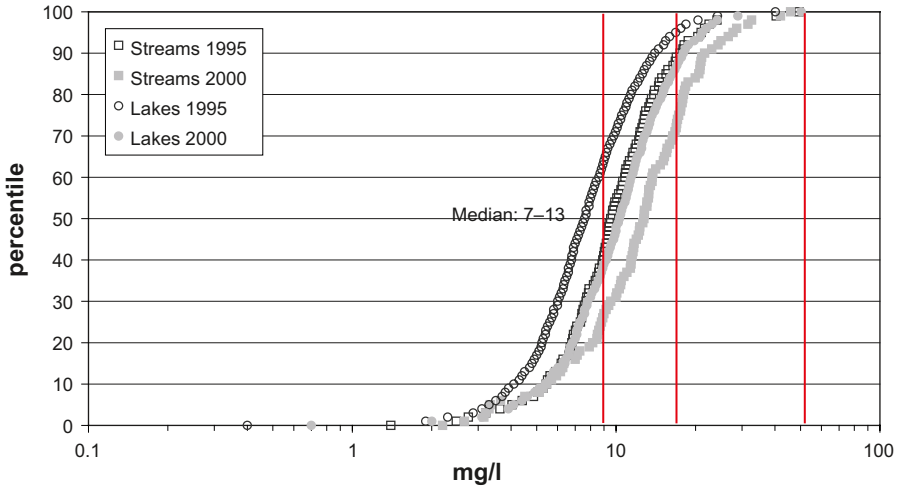

Figure 6-28. *Distribution of TOC concentrations in the Swedish surveys of lakes and streams 1995 and 2000 /IMA 2007/. Typical concentrations calibrated within the VBX-VI model are marked as red lines.*

6.2.9 Mass balance for total nitrogen (Tot-N)

The mass balance model for total nitrogen, tot-N, differs from previous models with respect to the background information of governing factors. Tot-N is thoroughly investigated in many catchment models, and consequently, there is much detailed information available about deposition and typical concentrations for this element.

The correlation analysis in Figure 6-30 indicates that high tot-N concentrations in surface water are correlated to a high proportion of water in the catchment. Also the regolith class ‘jPeat’ shows a positive correlation to tot-N according to the vertical factor in the PLS plot, whereas ‘jTill’ shows a negative correlation. Model details are listed below:

- In /TRK 2007/ and originally /Löfgren 1990/, typical concentrations from different land-use categories (Clear-cut:Wetland:Forest:Open land were estimated for northern Sweden to 3:2:1:1) These values were used in the VBX-VI model for tot-N.
- Both the the primary and the secondary datasets were used for calibration of the tot-N model shown in Figure 6-29. Parameter values and a source apportionment for the entire Forsmark area are compiled in Table 6-12. In Appendix F are model details compiled.

By adjusting three parameters, which either represent typical concentrations of different vegetation types or area-specific loss per year, the tot-N concentrations within the Forsmark area are satisfactorily modelled. The average model deviation is 5% between modelled and observed concentrations in the primary dataset and the secondary dataset shows a mean deviation of 9%.

The clearest deviation in the model is shown by AFM001103C (probably also valid for the catchment upstream, AFM000094), where the model slightly underestimate the transports.

From the mass balance scenario, the following conclusions about sources of tot-N can be drawn:

- The calibrated parameter ‘vForest’, which also controls the typical concentrations of the parameters ‘vClear’, ‘vWet’ and ‘vOpen‘ according to the relationship adopted from /TRK 2007/, was estimated to 0.47 mg/L. This value agree well with the typical concentrations from forest land according to /TRK 2007/, which are 0.33 mg/L for northern Sweden and 0.62 mg/L for the parts of southern Sweden that discharge into the Baltic, as the Forsmark area is located on the border between these administrative regions. This concentration corresponds to the 50–70th percentile of the national distribution shown in Figure 6-31. About one third of the tot-N leakage is attributed to forest land.

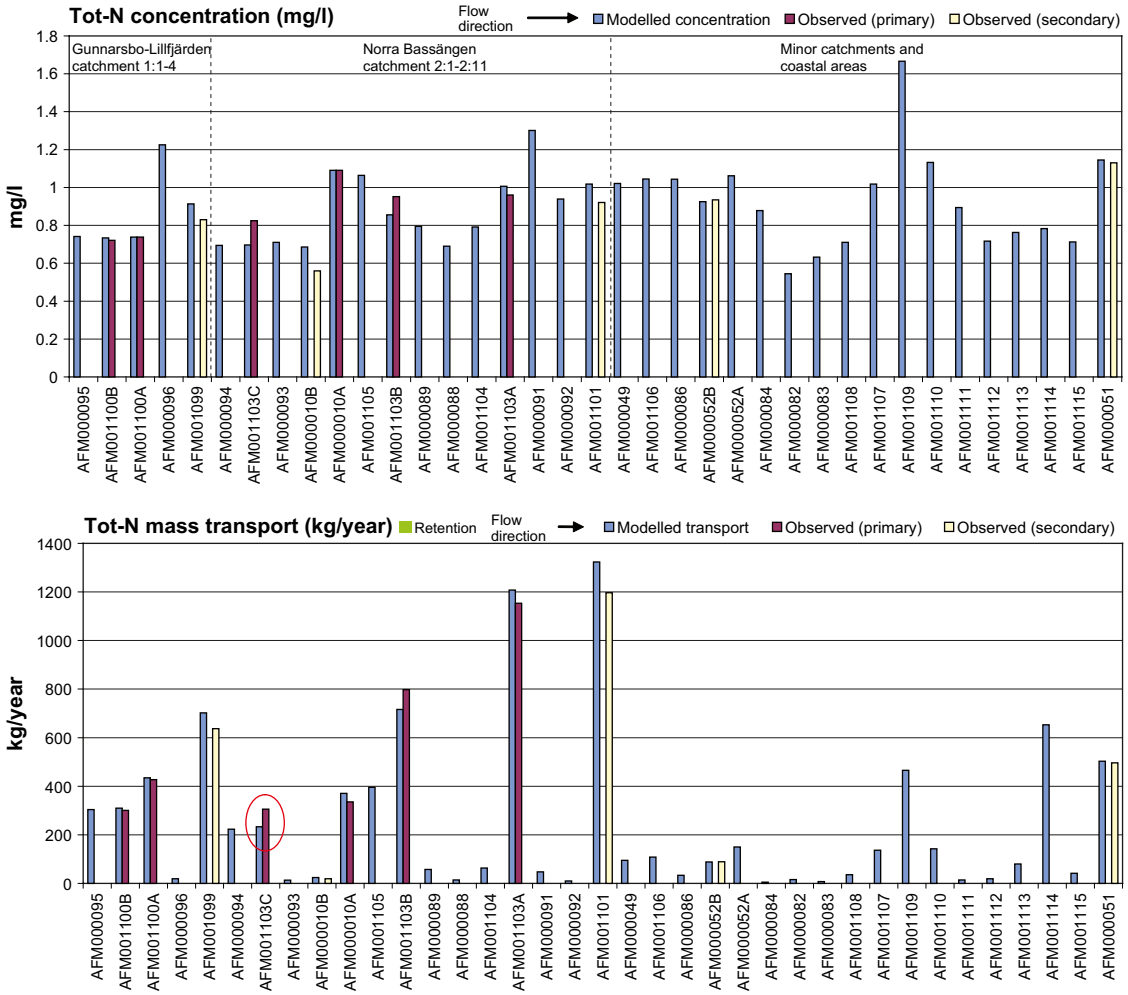

Figure 6-29. *Mass balance for Tot-N in the Forsmark area. Flow weighted concentrations (mg/L) above, and transports (kg/year) below, describing the conditions in the outlet of each catchment.*

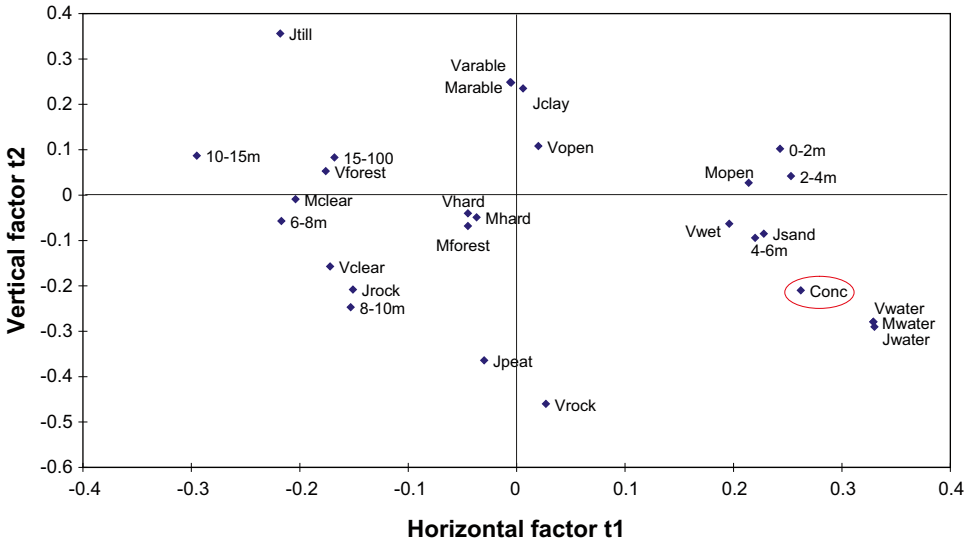

Figure 6-30. *Partial least square regression model, PLS, (cf Section 6.5.3 for an explanation of PLS) showing the correlation structure among distributed catchment characteristics, and the observed tot-N concentration (encircled in red). The parameters represent the relative distribution of each regolith, land-use, vegetation and elevation class upstream the hydrochemical sampling point in the outlet of the catchments. Factor t1 describe 41% of the variation among the explanatory variables and t2 19%. 70% of the variance in 'Conc' is described by t1 and 17% by t2.*

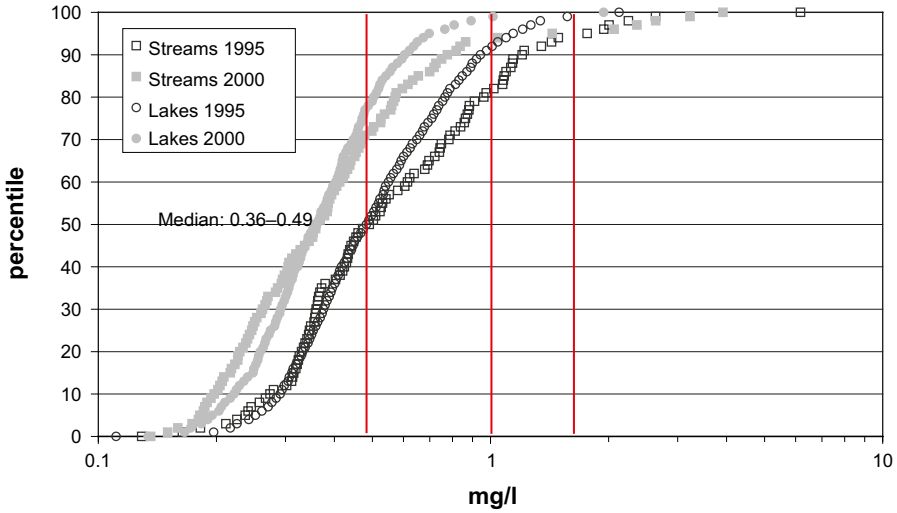

Figure 6-31. *Distribution of Tot-N concentrations in the Swedish surveys of lakes and streams 1995 and 2000 /IMA 2007/. Typical concentrations calibrated within the VBX-VI model are marked as red lines.*

Table 6-12. Compilation of parameters from the Tot-N mass balance model. Categories not used have been omitted from the table. The two rightmost columns show the total contribution from each category to the entire modelled area in Forsmark.

Diffuse sources		**mg/L**	**kg/km²,yr**	**kg/year**	**%**
Cathegory	**Class**				
Regolith	–	–	–	–	–
Land-use	–	–	–	–	–
Vegetation	vWater	–	619[A]	1,142	26
	vWet	0.94[C]	–	529	12
	vRock	–	619[A]	459	10
	vForest	0.47[B]	–	1,368	31
	vClear	1.41[D]	–	267	6
	vArable	–	225[F]	200	5
	vOpen	0.47[E]	–	53	1
	vHard	–	619[A]	358	8
Topography	–	–	–	–	–
Point sources					
–				–	–
Total					
Gross				4,377	100
Retention (λ, yr^{-1})				–	0
Net				4,377	100

A: calibrated supply per km^2 representing deposition per year.
B: calibrated typical concentration representing discharge from forest land.
C: 2 x vForest according to /TRK 2007/, representing discharge from wetland.
D: 3 x vForest according to /TRK 2007/, representing discharge from clear-cuts.
E: 1 x vForest according to /TRK 2007/, representing discharge from open land (not arable).
F: Calibrated specific area loss representing arable land.

- Wetlands contribute with 12% of the tot-N output to the sea, whereas the corresponding figure for TOC is as much as 37%. This discrepancy probably reflects the important input from deposition, which is substantial for tot-N, but negligible for TOC
- According to the tot-N model, the area-specific loss from the 'vArable' class was calibrated to 225 kg/km^2,year, which is a rather low value compared to estimations in adjacent areas and almost corresponds to the background levels. In /TRK 2007/, the area loss for the coastal area 53058 (TRK catchment number) including the Forsmark area was estimated to 1,100 kg/km^2,year, with an average background loss of 120 kg/km^2,year. The corresponding figures for the adjacent catchment of Forsmarksån (55-003) was estimated to 1,200 kg/ m^2,year and 200 kg/km^2,year respectively. An area loss of 225 kg/km^2,year is therefore not unrealistic depending on the intensity of the farming activities prevailing in the Forsmark area. The low portion of arable land in the studied area (3 % of total area) may also contribute to increased uncertainties regarding conclusions about this land-use category.
- Tot-N deposition on lakes, rock and other hard surfaces was calibrated to 619 kg/km^2,year. Compared to values estimated for coastal area 53,058 (cf previous bullet) and for the catchment of Forsmarksån (55-003) of 430 kg/km^2,year and 850 kg/km^2,year, respectively, the calibrated value of 619 kg/km^2,year seems reasonable. These categories contribute with almost half of the tot-N that reaches the sea.
- If the calibrated value of deposition on lakes and hard surfaces is adapted to the entire Forsmark area, a total of about 18,000 kg/year is supplied through deposition. Of this amount, only about 4,500 kgN/year reach the Baltic Sea via discharge and about 13,500 kg/year or 75% is lost to the atmosphere or stored as e.g. organic sediments.
- N-retention seems, however, to be marginal in the lakes in the Forsmark area according to the tot-N model. In /TRK 2007/, the total retention in the lakes in the catchment of Forsmarksån was estimated to 19% of the total input. The calibration sample sites are not optimally located in order to detect retention in lakes within the Forsmark area, which may partially explain the discrepancy. A possible explanation to the indicated low N-retention may be the low phosphorus concentrations that characterise lakes in the area, which leads to oligotrophic hardwater lakes with N-excess.
- The discrepancy between modelled and observed concentrations was less than 10% for both the primary and secondary datasets, indicating a fairly good agreement for all sites with measurements (including the secondary B dataset with limited seasonal coverage, cf Section 6.1.4).

6.2.10 Mass balance for total phosphorus (Tot-P)

The tot-P model is, similar to the total nitrogen model in Section 6.2.9, based on literature information on the relative contribution from different land-use categories. The correlation analysis in Figure 6-33 indicates that high tot-P concentrations are correlated to land-use categories as forest land and arable land. There is also an indication that the topographical location may have importance for the supply of tot-P. Model details are listed below:

- Adopted from /TRK 2007/, the relative proportion of the typical tot-P concentrations from the land-use categories Clear-cut:Wetland:Forest:Open land was assumed 2:2:1:1 in the Forsmark area.
- Deposition was assumed to be negligible for tot-P.
- Both the primary and secondary datasets were used for calibration of the tot-P model shown in Figure 6-32. Parameter values and a source apportionment for the entire Forsmark area are compiled in Table 6-13. In Appendix F are model details compiled.

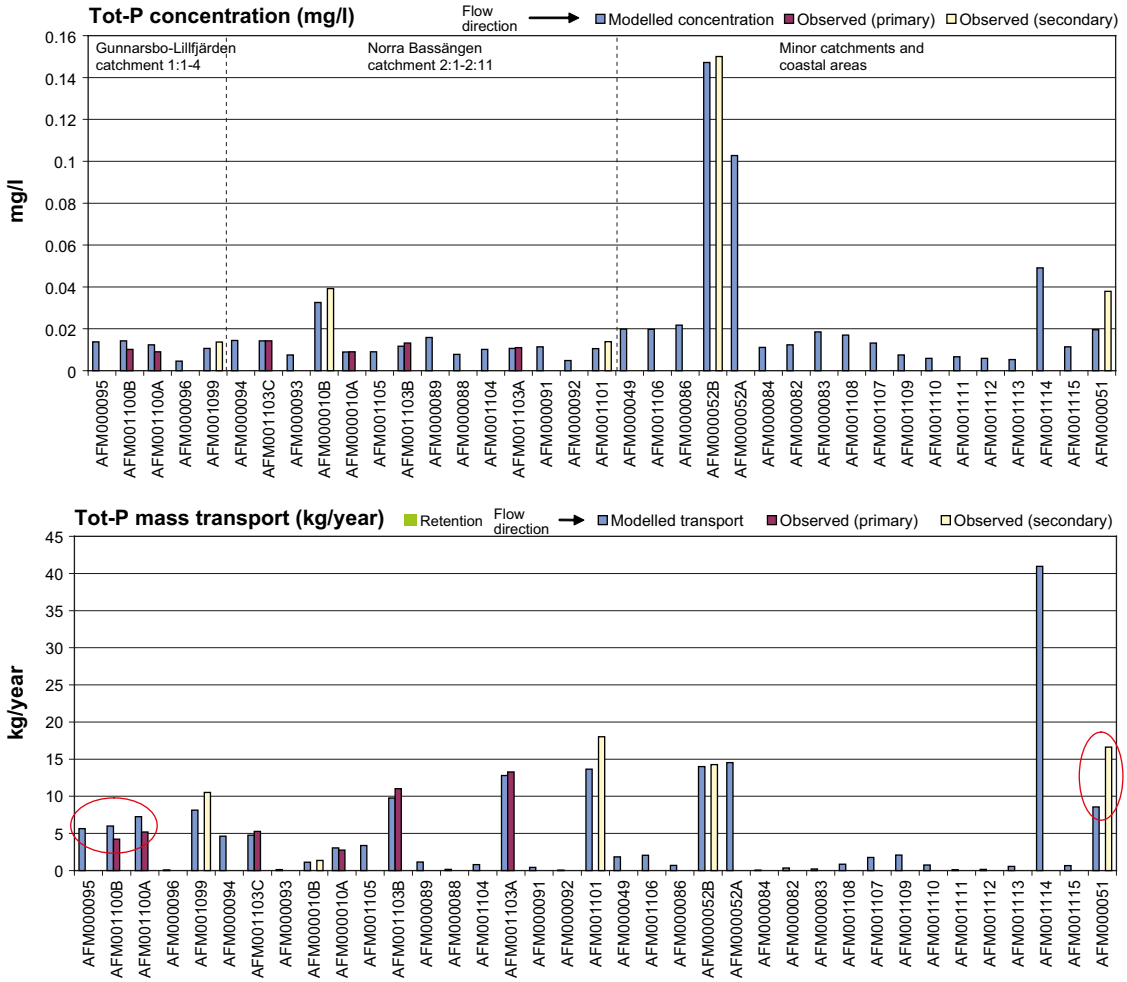

Figure 6-32. *Mass balance for Tot-P in the Forsmark area. Flow weighted concentrations (mg/L) above, and transports (kg/year) below, describing the conditions in the outlet of each catchment.*

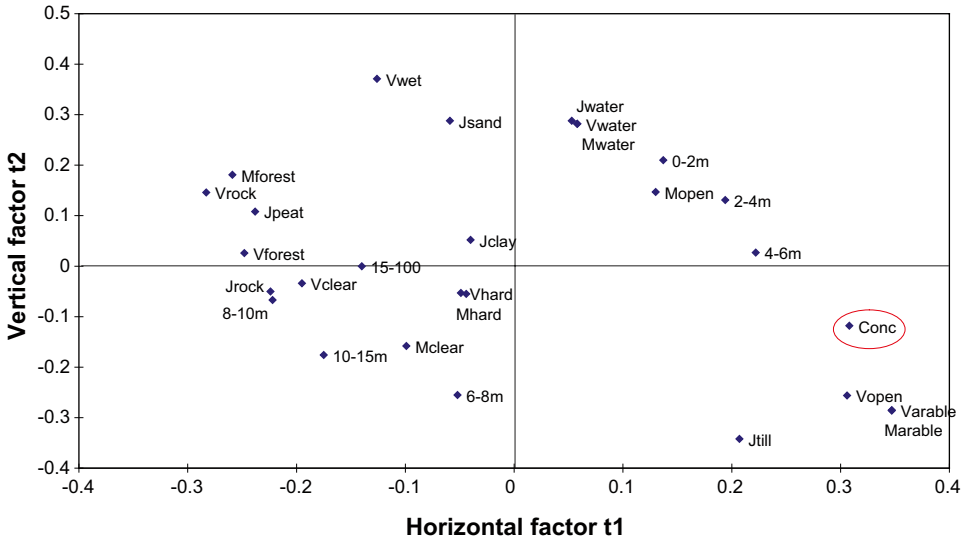

Figure 6-33. *Partial least square regression model, PLS (cf Section 6.5.3 for an explanation of PLS) showing the correlation structure among distributed catchment characteristics, and the observed tot-P concentration (encircled in red). The parameters represent the relative distribution of each regolith, land-use, vegetation and elevation class upstream the hydrochemical sampling point in the outlet of the catchments. Factor t1 describe 37% of the variation among the explanatory variables and t2 28%. 87% of the variance in 'Conc' is described by t1 and 10% by t2.*

Table 6-13. Compilation of parameters from the Tot-P mass balance model. Categories not used have been omitted from the table. The two rightmost columns show the total contribution from each category to the entire modelled area in Forsmark.

Diffuse sources		mg/L	kg/km²,yr	kg/year	%
Cathegory	**Class**				
Regolith	jClay	0.080	–	29	30
Land–use	–	–	–	–	–
Vegetation	vWater	–	–	0	0
	vWet	0.009[A]	–	5	5
	vRock	–	–	0	0
	vForest	0.005[B]	–	13	14
	vClear	0.009[C]	–	2	2
	vArable	0.340[D]	–	46	48
	vOpen	0.005[E]	–	1	1
	vHard	–	–	0	0
Topography	–	–	–	–	–
Point sources					
–				–	–
Total					
Gross				95	100
Retention (λ, yr^{-1})				–	0
Net				95	100

A: 2 x vForest according to /TRK 2007/, representing discharge from wetland.
B: calibrated typical concentration representing discharge from forest land.
C: 2 x vForest according to /TRK 2007/, representing discharge from clear-cuts.
D: Calibrated value.
E: 1 x vForest according to /TRK 2007/, representing discharge from open land (not arable).

By adjusting three parameters (‘vForest’, ‘vArable’ and ‘jClay’) the tot-P concentrations within the Forsmark area are satisfactorily modelled. The average deviation between modelled and observed concentrations is 15% for the primary dataset, and the secondary validation shows a mean deviation of 23%.

The most obvious deviations in the model are shown by the Gunnarsbo-Lillfjärden catchment (AFM000095, AFM001100B and AFM001100A), and the outlet of Lake Fiskarfjärden (AFM000051). The systematic overestimation in the Gunnarsbo-Lillfjärden sub-catchments may be attributed to either erroneous assumptions regarding the typical concentrations from different land-use categories, or be an effect of the lower resolution of the soil survey in this area. The deviation in the outlet of Lake Fiskarfjärden, may in addition to the previous explanation, also be attributed to the low representativeness of the secondary dataset (cf Section 6.1.4), which probably affects a biogenic element to a higher degree than e.g. Cl.

From the mass balance scenario, the following conclusions about sources of tot-P can be drawn:

- The typical concentration in water from forest land was calibrated to 0.005 mg/L, about half the estimation in /TRK 2007/ of 0.0012 mg/L. According to this reference, an area-specific loss of 1.8 kg/km²,year should be expected, which corresponds to a concentration of 0.012 mg/L at a specific discharge of 150 mm/yr. About 15% of the total output to the sea may be attributed to forest land (‘vForest’ and ‘vClear’ classes).

- The addition of the regolith class ‘jClay’ to the tot-P model improved the model, especially in the area of Lake Gällsboträsket, where this regolith class is common (cf Figure 6-6). Approximately 30% of the output to the sea from the Forsmark area may be attributed to this regolith class according to this scenario.
- Arable land constitutes 3% of the land area in Forsmark, but contributes with as much as 50% of the tot-P output to the sea due to the high typical concentration in the discharge from this land-use category. According to the tot-P model, a typical concentration of 0.34 mg/L may be expected in the discharge from arable land (corresponding to 50 kg/km^2,year at a specific discharge of 150 mm/yr). This value is in level with area-specific tot-P loss estimated within the TRK project /TRK 2007/ for adjacent areas. The coastal area 53058 (TRK catchment number) show a specific loss of 41 kg/km^2,year, whereas the inland catchment of Forsmarksån (55-003) show a area-specific loss of tot-P from arable land of 60 kg/km^2,year. It can be concluded that the calibrated value for the Forsmark area of 50 kg/km^2,year fits well in-between these two adjacent estimations.
- According to the tot-P model, retention in lakes is negligible. This finding may seem contradictory as phosphorus retention usually is significant in lakes and co-precipitation with Ca have been proposed as an explanation to the usually low phosphorus concentrations that prevail in surface waters in the Forsmark area (cf national distribution in Figure 6-34 and /Tröjbom and Söderbäck 2006/). One possible explanation, which may be supported by the low typical concentration calibrated for e.g. forest land, may be that a substantial local phosphorus retention take place before the water reaches the lakes (e.g. in wetlands and small streams). If this is the case, a rough estimation based on the generic concentration in discharge from forest land of 0.0012 mg/L (cf first bullet in list) and the calibrated concentration in the Forsmark area of 0.005 mg/L, approximately 18 kg or 18% of the total amount of phosphorus is precipitated locally.

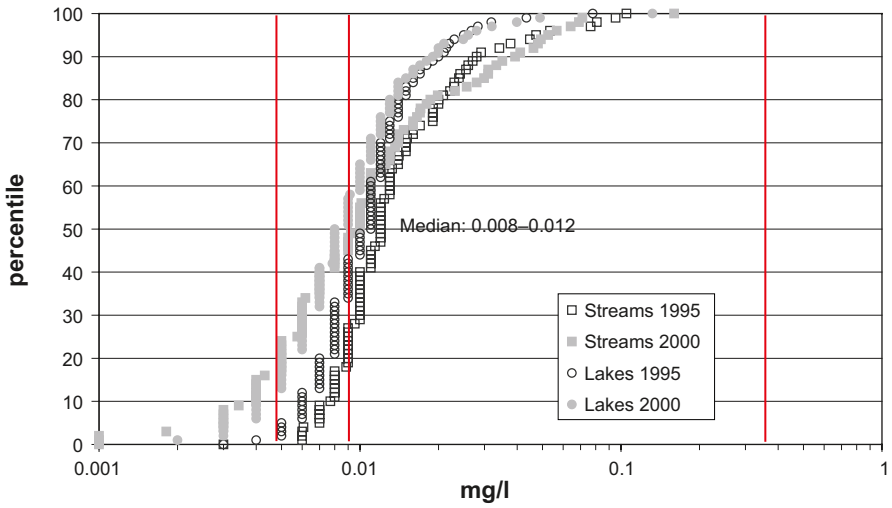

Figure 6-34. *Distribution of Tot-P concentrations in the Swedish surveys of lakes and streams 1995 and 2000 /IMA 2007/. Typical concentrations calibrated within the VBX-VI model are marked as red lines.*

6.2.11 Mass balance for total silicon (Si)

The spatial variability of Si in the Forsmark area is, similarly to Ca, clearly influenced from retention processes, such as precipitation in lakes (i.e. concentrations in the outlet of lakes are significantly lower than expected from the typical concentrations in the discharge from land). The correlation structure in Figure 6-36 differs however significantly from all other studied elements: the regolith class 'jTill', the land-use class 'Forest', and the topographical parameters representing higher elevations are positively correlated to the Si concentration, whereas the water parameters are negatively correlated. Model details are listed below:

- Due to about 10 times higher Si levels in Lake Bolundsfjärden compared to the Baltic Sea, the net effect of sea water intrusions is assumed to be negligible.
- Only the primary dataset was used for calibration of the Si model due to probably low representativeness for this element of the secondary dataset. Model results are shown in Figure 6-35, and parameter values and a source apportionment for the entire Forsmark area are compiled in Table 6-14. In Appendix F are model details compiled.

By adjusting two parameters and the retention constant, the Si concentrations within the Forsmark area are satisfactorily modelled when the primary calibration dataset is concerned. The average model deviation between modelled and observed concentrations is 7% in the primary calibration dataset, whereas the secondary dataset shows a very large mean deviation (1985%), mostly due to seasonal effects in AFM001101. The very large average deviation shown by the secondary dataset most probably reflects the non-representativeness of these data (particularly secondary B dataset), which is an effect of the biased selection only representing a few summer months (cf Section 6.1.4). Si shows large seasonal variations in surface waters due to the utilisation of this element by diatom algae species.

Table 6-14. Compilation of parameters from the Si mass balance model. Categories not used have been omitted from the table. The two rightmost columns show the total contribution from each category to the entire modelled area in Forsmark.

Diffuse sources		**mg/L**	**kg/km²,yr**	**kg/year**	**%**
Cathegory	**Class**				
Regolith	jWater	–	–	–	–
	jSand	0	–	0	0
	jPeat	='jSand'	–	0	0
	jRock	='jSand'	–	0	0
	jClay	='jSand'	–	0	0
	jTill	7.5	–	23,732	100
Land–use	–	–	–	–	
Vegetation	–	–	–	–	
Topography	–	–	–	–	
Point sources					
–				–	–
Total					
Gross				23,732	100
Retention (λ=1.4 yr^{-1})				5,677	24
Net				18,056	76

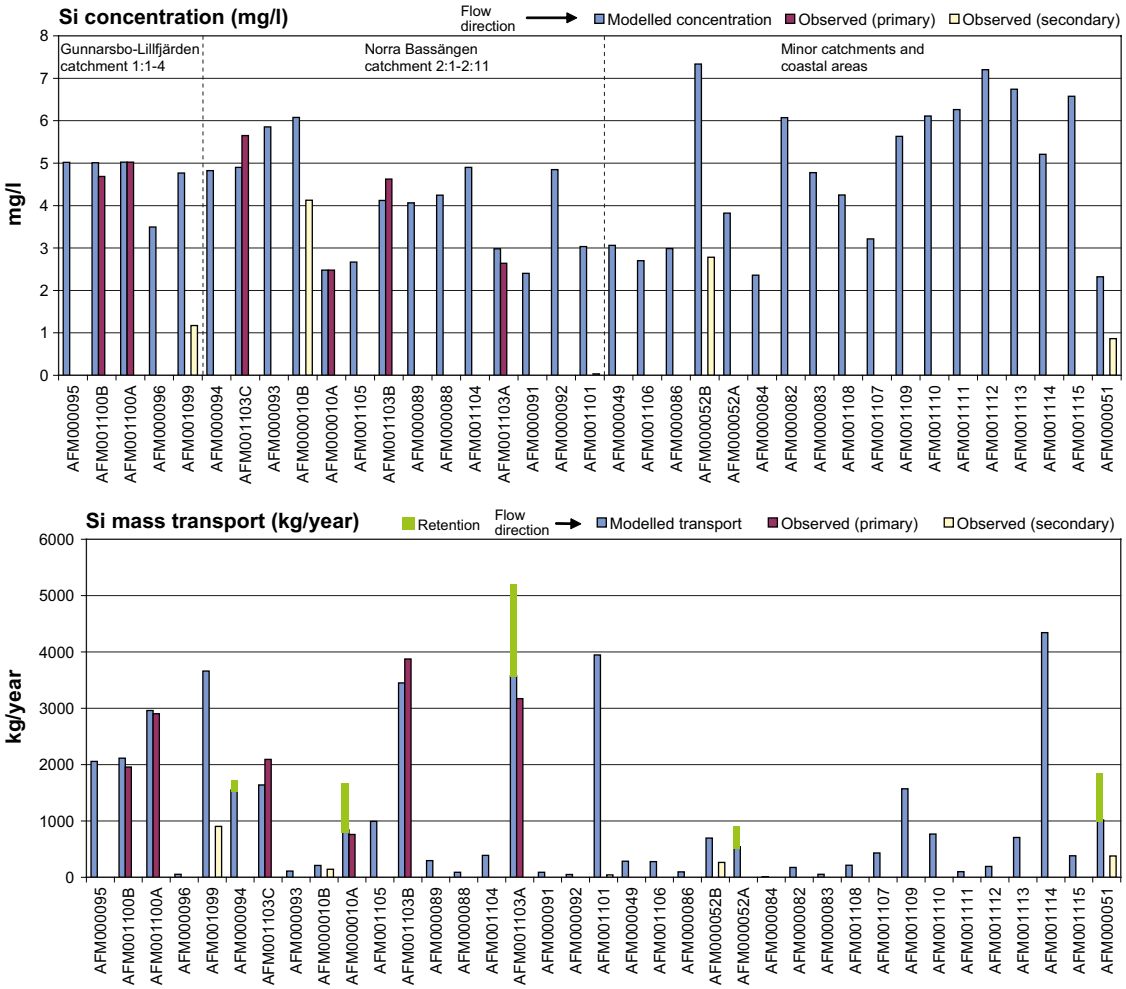

Figure 6-35. *Mass balance for Si in the Forsmark area. Flow weighted concentrations (mg/L) above, and transports (kg/year) below, describing the conditions in the outlet of each catchment. Green bars mark the retention loss in lakes.*

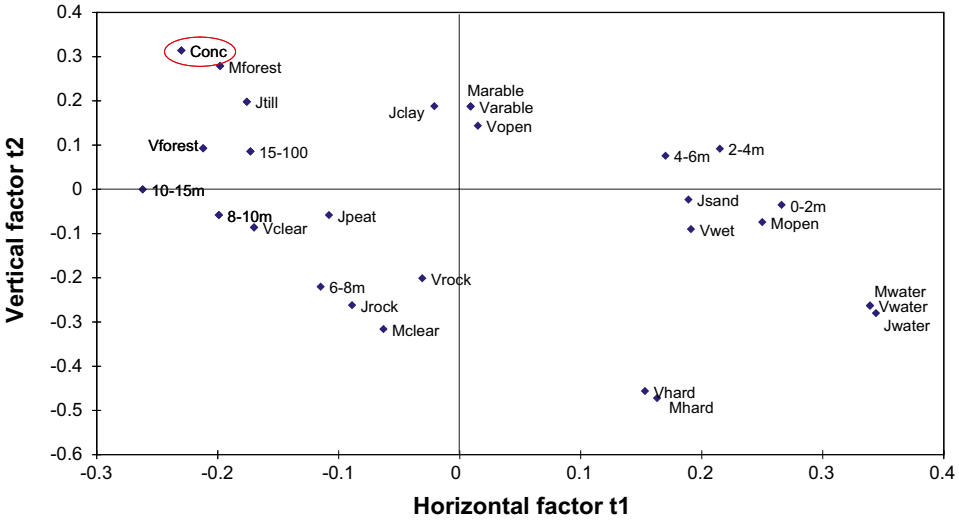

Figure 6-36. *Partial least square regression model, PLS (cf Section 6.5.3 for an explanation of PLS) showing the correlation structure among distributed catchment characteristics, and the observed total-Si concentration (encircled in red). The parameters represent the relative distribution of each regolith, land-use, vegetation and elevation class upstream the hydrochemical sampling point in the outlet of the catchments. Factor t1 describe 37% of the variation among the explanatory variables and t2 28%. 87% of the variance in 'Conc' is described by t1 and 10% by t2.*

From the mass balance scenario, the following conclusions about sources of Si can be drawn:

- The regolith class ‘jTill’ is the completely dominating source of Si according to the Si model, as all other soil categories converged towards zero during calibration. This fact, most probably reflects the evenly distributed source of Si in the Forsmark area. The typical concentration in the discharge from the regolith class ‘jTill’ is calibrated to 7.5 mg/L, which is slightly higher than the median of shallow groundwater in the Forsmark area of 6.3 mg/L /Tröjbom and Söderbäck 2006/.
- There is a substantial retention of Si in lakes, corresponding to 24% of the total output to the sea. In some catchments containing lakes, 50–60% of the supplied Si is precipitated, e.g. Lake Eckarfjärden (AFM000010A), Lake Simpviken (AFM000084) and Lake Puttan (AFM000091). Sedimentation of diatoms is probably the process responsible for this Si-sink in the lakes. Analyses of biogenic Si in the sediments of Lake Eckarfjärden revealed that the biogenic Si fraction varies between 2–12% depending on the sampling depth in the sediment profile /Baxter et al. 2007/.

6.2.12 Mass balance for strontium (Sr)

The prevalence of strontium is often closely coupled to the prevalence of calcium. According to Figure 4-9, many observations from different water types within the Forsmark area plot along specific Ca/Sr ratios, reflecting the signatures of different sources. The correlation analysis in Figure 6-38 differs, however, from the corresponding analysis for Ca (cf Figure 6-15), by indicating a possible marine Sr source besides Sr originating from calcite in the overburden, which is indicated by the correlation to the lower topographical parameters (similar to Cl in Section 6.2.1). Model details are listed below:

- An addition of Sr to Lake Bolundsfjärden of 21 kg/year due to sea water intrusions was assumed as an initial condition in the model (cf Table 6-4).
- Both the primary and the secondary datasets were used for calibration of the Sr model shown in Figure 6-37. Parameter values and a source apportionment for the entire Forsmark area are compiled in Table 6-15. In Appendix F are model details compiled.

Table 6-15 Compilation of parameters from the Sr mass balance model. Categories not used have been omitted from the table. The two rightmost columns show the total contribution from each category to the entire modelled area in Forsmark.

Diffuse sources Cathegory	Class	mg/L	kg/km^2,yr	kg/year	%
Regolith	jTill	0.08	–	249	44
Land–use	–	–	–		
Vegetation	–	–	–		
Topography	0–2 m	0.10	–	109	19
	2–4 m	=’0–2 m’		108	19
	4–6 m	=’0–2 m’		80	14
Point sources					
Sea water intrusions in Lake Bolundsfjärden				21	4
Total					
Gross				567	100
Retention (λ=0.72 yr^{-1})				–81	14
Net				486	86

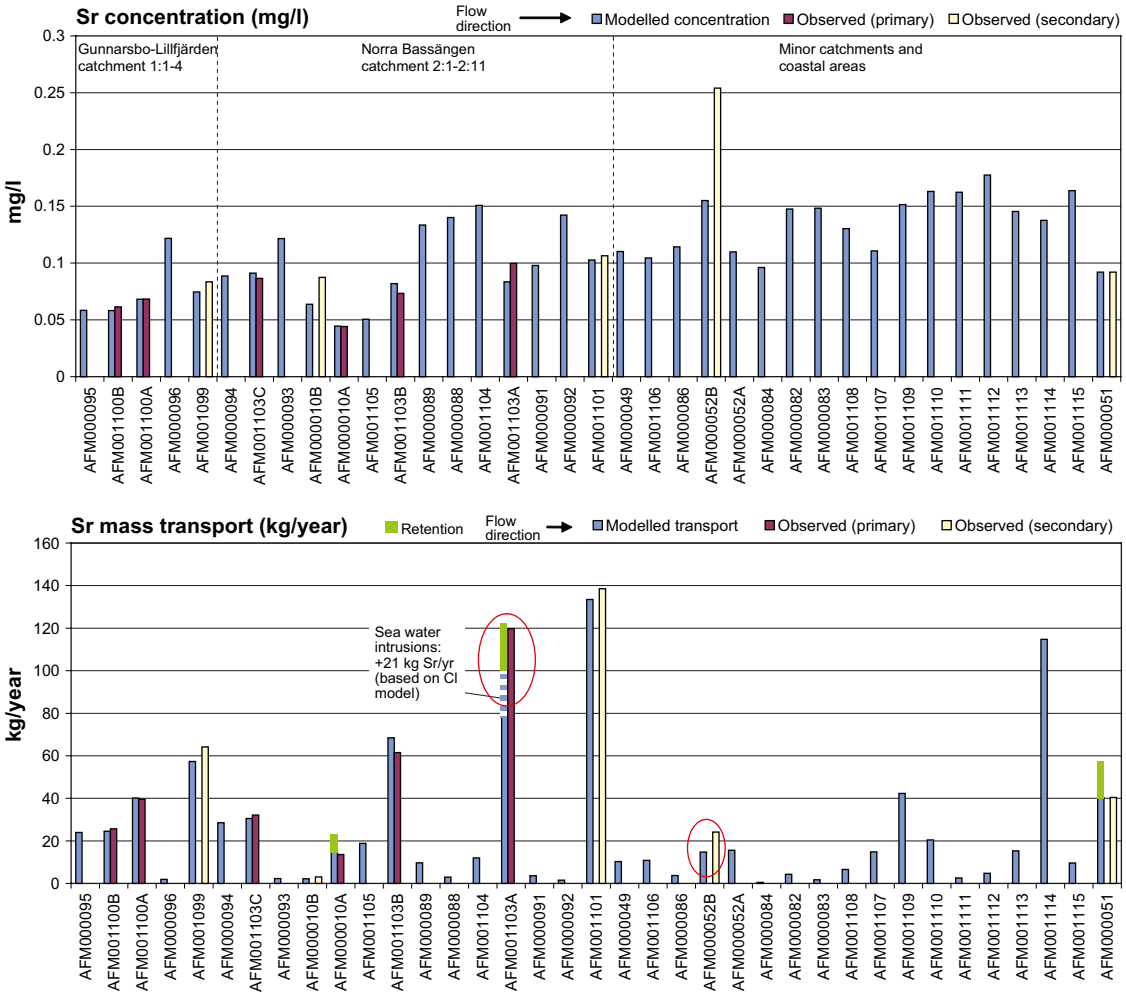

Figure 6-37. *Mass balance for Sr in the Forsmark area. Flow weighted concentrations (mg/L) above, and transports (kg/year) below, describing the conditions in the outlet of each catchment. Green bars mark the retention loss in lakes.*

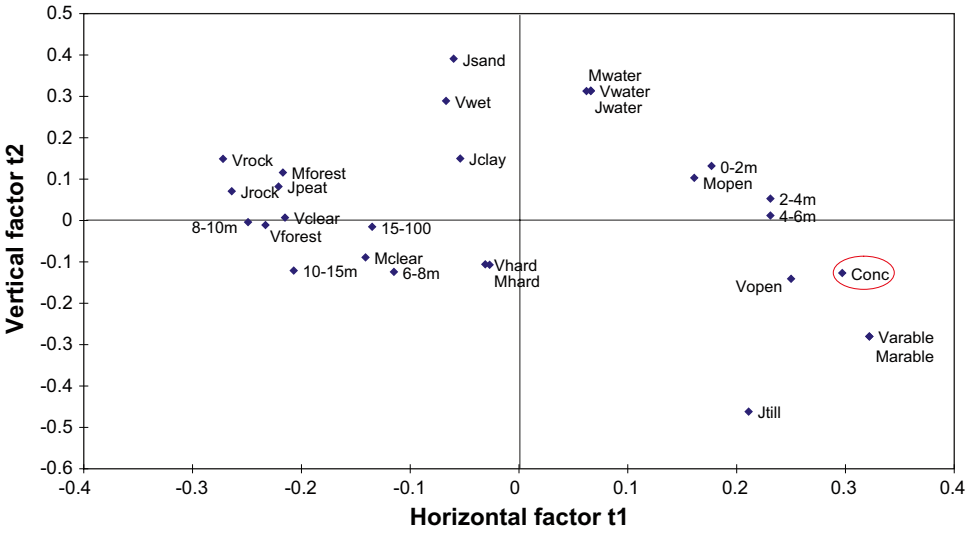

Figure 6-38. *Partial least square regression model, PLS (cf Section 6.5.3 for an explanation of PLS) showing the correlation structure among distributed catchment characteristics, and the observed Sr concentration (encircled in red). The parameters represent the relative distribution of each regolith, land-use, vegetation and elevation class upstream the hydrochemical sampling point in the outlet of the catchments. Factor t1 describe 39% of the variation among the explanatory variables and t2 26%. 86% of the variance in 'Conc' is described by t1 and 11% by t2.*

By adjusting two parameters and the general retention constant, the Sr concentrations within the Forsmark area are satisfactorily modelled. The average model deviation between modelled and observed concentrations in the primary dataset is 7%, and the secondary dataset shows a mean deviation of 16%.

The largest deviations in the Sr model are encircled in red in Figure 6-37. The discrepancy in Lake Bolundsfjärden (AFM001103A) indicates possible uncertainties regarding Sr in these lakes influenced by sea water intrusions (cf Ca model in Section 6.2.4).

The catchment upstream Lake Bredviken (AFM000052B) deviates with respect to Sr in a similar manner as many ions (e.g. Ca, Mg, K, SO_4), showing more than doubled Sr concentrations compared with those expected in the model. This catchment contains a high proportion arable land, which may be one explanatory factor to the elevated Sr transport from this area (cf Section 7.7 and /Åström and Rönnback, submitted/).

From the mass balance scenario, the following conclusions about sources of Sr can be drawn:

- Sr shows a spatial distribution pattern in the Forsmark area similar to Ca, but with addition of a marine source at lower altitudes.
- The regolith class ‘jTill’ is an important source of Sr according to the Sr model, contributing with 44% of the total input to the surface waters in the area. The typical concentration in discharge from ‘jTill’ is calibrated to 0.08 mg/L, which is significantly lower than the median for shallow groundwater of 0.25 mg/L /Tröjbom and Söderbäck 2006/. Calcite in the overburden is most probably the major source of this Sr.
- Areas situated at lower altitudes, which also may be covered by the regolith class ‘jTill’, contribute with significant amounts of Sr, corresponding to 52% of the total input to the surface waters. In the presence of till, the total typical concentration from lower located areas (0–4 m) may reach 0.18 mg/L (0.08 + 0.10). This concentration is in level with the median value of groundwater, cf above.
- Similar to Ca, there is a substantial retention of Sr in lakes, corresponding to 14% of the total input to the surface waters. In some catchments up to 40% of the supplied Sr is precipitated, e.g. Lake Eckarfjärden (AFM000010A), Lake Simpviken (AFM000084) and Lake Puttan (AFM000091).

6.3 Summary and conclusions of catchment modelling

The catchment model is a formalised method, which couples distributed spatial information about the catchment with the water balance and observed concentrations in watercourses and lakes into an integrated model that results in a scenario describing the over all mass balance of an element. It should, however, be noted that the presented models are just scenarios representing one probable solution of the mass balance of respective element, and that there are other possible solutions as well. The establishment and calibration of each model have followed identical schemes, with the over-all objective to find an as simple model as possible that satisfactorily describes the observed variation within the Forsmark area. In most cases the calibration of the model converge towards only one stable, probable solution for the selected set of parameters, but the subjective element regarding the selection of the governing parameters can not be circumvented. The use of an initial PLS correlation analysis gives, however, an objective picture of the correlation structure among the parameters, and may give an indication on which parameters may be fruitful to include into the model.

When catchment models for different elements are compared, a few general patterns may be distinguished. Environmental factors, such as the strong marine influence due to the recent withdrawal of the Baltic Sea, in combination with calcite-rich deposits in the Forsmark area make clear imprints in the models depending on the sources of each element.

The occurrence of marine ions as Cl and Na in surface waters is mainly coupled to low altitude areas rather than a specific land-use or regolith category. Sources of ions as Ca and HCO_3 are on the other hand more evenly distributed over the entire area. There are also examples of ions which seem to be coupled to a specific regolith category, e.g. SO_4 and Si, whereas ions as Mg and Sr show a mixed pattern probably indicating the dual origin of these elements (both marine and calcite origin).

Carbon, nitrogen and phosphorus, which all are part of organic matter and cycled in the biosphere, show radically different patterns coupled to land-use and vegetation rather than to regolith and elevation.

In all models, retention has been tested as an initial scenario, but only a few elements show clear indications of retention loss in lakes. There is always a possibility that retention takes place at a local level, in riparian zones, in wetlands or in small streams which are not separated in the model; in this case the catchment model to some extent describe net transports and net concentrations in surface waters rather than representing a typical concentration from a specific regolith type or land-use category. According to Table 6-16, where all model parameters are compiled, only Sr, Ca, HCO_3 and Si show significant retention in lakes. The prerequisites for detecting retention are however not optimal in the Forsmark area due to the limited time series available for some of the hydrochemical sampling stations located downstream lakes, and it can not be excluded that these results to some extent is a consequence of the limited precision in the model.

Table 6-16. Overview of model parameters and calibration results. Typical concentrations (mg/L) per category (see Section 6.1.3 and Appendix D for descriptions of categories) are marked in black, whereas red figures correspond to area loss expressed in kg/km^2,year. The retention parameter λ and total retention in the Forsmark area (Ret %) are shown when applicable. The calibration result, expressed as the mean deviation between modelled and observed concentrations, is shown in the Dev % columns (calculated for the primary and secondary datasets respectively, cf Section 6.1.4).

Categories	jClay	jTill	0–2 m	2–4 m	4–6 m	6–8 m	8–10 m	10–15 m	> 15 m	λ yr^{-1}	Ret %	Dev % prim	Dev % sec
Cl	72	–	47	47	0.8	0.8	0.8	0.8	0.8	–	–	8	104
Na	–	–	56	30	4.8	4.8	4.8	4.8	4.8	–	–	10	14
Sr	–	0.08	0.10	0.10	0.10	–	–	–	–	0.72	14	7	16
Categories	**jWater**	**jSand**	**jPeat**	**jRock**	**jClay**	**jTill**							
K	0.45	2.3	2.3	2.3	2.3	2.3				–	–	9	28
Ca	–	62	62	62	62	62				0.53	12	5	22
Mg	–	2	2	2	32	2				–	–	6	35
HCO_3	–	187	187	187	187	187				0.56	13	5	34
SO_4	4.5	7.4	7.4	7.4	50	7.4				–	–	13	69
Si	0	0	0	0	0	7.6				1.4	24	7	1,985
Categories	**vWater**	**vWet**	**vRock**	**vForest**	**vClear**	**vArable**	**vOpen**	**vHard**					
TOC	–	51	15	15	15	9	9	–		–	–	8	5
Tot-N	620	0.95	620	0.47	1.4	225	0.47	620		–	–	5	9
Tot-P	–	0.009	–	0.005	0.009	0.340	0.005	–		–	–	15	23

In Table 6-16 below, model parameters and calibration results are compiled in order to facilitate comparisons among elements. The middle section of this table lists calibrated typical concentrations in discharge from each topographical, regolith, land-use and vegetation category (cf Section 6.1.3 and Appendix D for explanations of these categories). In the case of retention in lakes, the calibrated parameter is listed together with an estimation of the total retention in the entire Forsmark area. The calibration result, expressed as the average deviation between modelled and observed concentrations, is calculated for two sets of data: the primary and the secondary datasets, which differ strongly in reliability depending on element (cf Section 6.1.4).

In the bullet list below are the main conclusions per element summarised:

- Diffuse sources of **chloride** (Cl) are most probable connected to the topographical elevation distribution rather than to factors as regolith type or land-use within the catchments. At episodes of high water levels in the Baltic, sea water intrusions add significant amounts of Cl into Lake Bolundsfjärden. The results indicates that areas containing clay or gyttja leak additional amounts of Cl, e.g. in the area around Lake Gällsboträsket (AFM000094) where the total Cl concentration in discharging groundwater possibly reach about 120 mg/L. There are, as presumed, no indications of retention for Cl.
- Diffuse sources of **sodium** (Na) are, similar to Cl, most probable coupled to the topographical elevation rather than to factors as regolith or land-use within the catchments. The catchment model indicates that areas located below 4 metres of altitude, show increased Na supply compared to higher topographical elevations. At episodes of high water levels in the Baltic, sea water intrusions add significant amounts of Na into the lower located lakes. Less than 10% of the total Na leakage is estimated to originate from weathering reactions.
- Diffuse sources of **potassium** (K) are more uniformly distributed over the Forsmark area than those of marine ions as Cl and Na, and no distributed factors as topographical elevation, regolith, land-use or vegetation cover seem to have any particular influence on K. At episodes of high water levels in the Baltic, sea water intrusions add significant amounts of K into Lake Bolundsfjärden, corresponding to c. 30% of the total input into this lake. About 75% of the K was estimated to originate from either weathering reactions or relict remnants in the sediments. There are no indications of significant retention of K in the lakes.
- Diffuse **calcium** (Ca) sources are also rather uniformly distributed over the Forsmark area and no distributed factors as topographical elevation, regolith, land-use or vegetation cover, seem to have any clear influence. The typical concentration in discharge from all regolith classes, which was estimated to 62 mg/L, reflects the influence from the calcite rich till that covers the area. The high level gives rich prerequisites for deviant chemistry in shallow groundwater and also affects the structure of freshwater ecosystems. There is a substantial retention of Ca in the lakes and a total retention of 12% was estimated for the Forsmark area. In some catchments this portion reach about 30%, e.g. AFM000010A (Lake Eckarfjärden), AFM000085 (Lake Simpviken), and AFM000091 (Lake Puttan).
- **Magnesium** (Mg) shows a dual origin, with both marine relics and calcite dissolution as sources. Discharge from the regolith class ‘jClay’, contains according to the Mg model, more than ten times Mg compared to the background level, probably reflecting the marine remnants attributed to this regolith category. Approximately 30–40% of the Mg that reaches the sea probably originates from weathering reactions (e.g. calcite), whereas the rest originates from sea water intrusions or relict marine remnants in sediments. The estimated sea water intrusion into Lake Bolundsfjärden answer to a relative portion of 18%, leaving 40–50% to diffuse leaching from marine remnants in sediments. There are no indications of significant retention of Mg in the lakes.
- For **sulphate** (SO_4), deposition is probably a major source contributing to the background level in the Forsmark area, and approximately one third of the SO_4 that reaches the sea originates from deposition. Of this airborne fraction, only 2%, originate from sea spray if the marine part is estimated from local Cl measurements in precipitation, and the rest originate from regional sulphur deposition. Discharge from the regolith class ‘jClay’, contain according to the SO_4 model, more than six times SO_4 compared to the background

level from other regolith categories, and about one third of all SO_4 that leaves the Forsmark area originate from this regolith class where sulphide minerals probably is an important source. The remaining third part originates from sea water intrusions or leaching from relict marine remnants from regolith classes other than 'jClay'. The estimated intrusions into Lake Bolundsfjärden answer to 50% of this third, whereas diffuse leaching makes the rest. According to the argumentation in Section 6.2.6 this rest could be explained by dry deposition, and in that case deposition probably contributes with more than a third of the total sulphur supply. There are no indications of significant retention of SO_4 in the lakes.

- The distribution of **bicarbonate** (HCO_3) is in all details similar to calcium, implicating a concomitant origin and fate of these elements. Typical concentrations in discharge from all regolith classes was estimated to 187 mg/L, which corresponds to the 95th percentile of the national distribution and reflects the anomalous conditions with respect to HCO_3 in the Forsmark area. There is a substantial retention of HCO_3 and almost similar to Ca is 13% of the total input lost the lakes. This portion is substantially higher in some catchments and reach about 30% in AFM000010A (Lake Eckarfjärden), AFM000085 (Lake Simpviken), and AFM000091 (Lake Puttan). When the amount HCO_3 that is lost in the lakes by retention is compared to the corresponding Ca loss, the mass ratio of the total amounts estimated by the independent models fits closely to the theoretical ratio between these ions when calcite is precipitated.
- Typical concentrations of **total organic carbon** (TOC) from wetlands are elevated more than three times compared to concentrations in discharge from forest land, and answer for 37% of the total output of TOC to the Baltic. Forest land, which covers 70% of the land area, contributes with slightly more than 50% of the total output. The typical concentration of forest land corresponds to the 70–95th percentiles of the national distribution, which may be an indication that area-specific TOC loss is relatively high in the Forsmark area. There are no indications of any significant retention of TOC in the lakes.
- Deposition is a major source of **total nitrogen** (tot-N) in the Forsmark area. Almost half of the tot-N that reaches the sea originates from deposition on land-use categories comprising lakes, rocks and hard surfaces, which together cover only about 17 % of the modelled area. Wetlands contribute with 12% of the tot-N output to the sea, whereas forest land that covers almost 70% of the land area contributes with the remaining 37%. The area-specific loss from arable land is low compared to adjacent areas and almost corresponds to the background levels. If the calibrated value of deposition on lakes and hard surfaces is adapted to the entire Forsmark area, a total of about 18,000 kg/year is supplied through deposition. Of this amount, only about 4,500 kgN/year reach the Baltic Sea via discharge and about 13,500 kg/year or 75% is lost to the atmosphere or stored as e.g. organic sediments. N-retention seems, however, to be marginal in the lakes in the Forsmark area, and a possible explanation to the indicated low N-retention could be the low phosphorus concentrations that characterise the area, which leads to oligotrophic hard water lakes with N-excess.
- Contrary to total nitrogen, deposition is a negligible source for **total phosphorus** (tot-P). Arable land, which constitutes about 3% of the total land area, contributes with as much as 50% of the total phosphorus output into the Baltic, whereas forest land with clear-cuts included contribute with 15% of the total output from an area corresponding to 70% of the land surface. The model scenario also indicates that there is an additional tot-P source from the soil category 'jClay', contributing with approximately 30% of the total output. According to the tot-P model, retention in lakes is negligible. This finding may seem contradictory as phosphorus retention usually is significant in lakes and co-precipitation with Ca have been proposed as an explanation to the usually low phosphorus concentrations that prevail in surface waters in the Forsmark area. One possible explanation, which is supported by the low typical concentration calibrated for e.g. forest land, may be that substantial local phosphorus retention takes place in wetlands and even in soil before the water reaches the lakes. As a rough estimation based on generic concentrations in discharge from forest land, about 20% of the total amount of phosphorus release to surface waters is precipitated locally.

- The regolith class that contains various classes of till ('jTill') is the major source of dissolved **silicon** (Si) according to the Si model. This fact, most probably reflects the evenly distributed source of Si in the Forsmark area. There is a substantial retention of Si in lakes, corresponding to 24% of the total output to the sea. In some catchments containing lakes, 50–60% of the supplied Si is precipitated, e.g. Lake Eckarfjärden (AFM000010A), Lake Simpviken (AFM000084) and Lake Puttan (AFM000091). Analyses of biogenic Si in the sediments of Lake Eckarfjärden revealed that the biogenic Si fraction varies between 2–12% depending on the sampling depth in the sediment profile /Baxter et al. 2007/.
- **Strontium** (Sr) shows a spatial distribution in the Forsmark area similar to Ca, but with additional marine influences at lower locations. Calcite in the overburden is most probably one of the major sources of Sr, contributing with 44% of the total input to the surface waters in the area. Lower located areas contribute with significant amounts of Sr, corresponding to 52% of the total input to the surface waters. Similar to Ca, there is a substantial retention of Sr in lakes, corresponding to 14% of the total input to the surface waters. In some catchments up to 40% of the supplied Sr is precipitated.

The overall uncertainties of the models are difficult to estimate, but the subjective impression is that most models converge towards rather stable solutions despite the large number of uncertainties regarding water balance, representativeness of hydrochemical sampling, and the classification and aggregation of different regolith, land-use and vegetation types. The models also describe the average situation of two specific years (2004-06-01 to 2006-05-31), and as indicated in Table 5-11, there is probably a large variation between years due to climatic factors.

The ratio of the amounts of Ca and HCO_3 which are lost in the lakes by retention closely fits the theoretical ratio between these ions when calcite is precipitated. This may, if not a coincidence, be an indication that these independent models show a rather good agreement. Moreover, comparisons of typical concentrations and area losses calibrated within the VBX-VI model with estimations from adjacent areas and generic data show generally good agreement.

Due to the limited number of hydrochemical sampling points available, a true validation of the models is in most cases not possible to perform. A further problem is that the secondary dataset, which for a few elements may be used for validation, is characterised by a significantly higher degree of uncertainty compared to the primary calibration dataset, leading to limited value of these validations. A further improvement of the VBX-VI model probably demands better spatial representativity of the hydrochemical sampling points and preferably also additional points only used for validation purposes.

7 Integrated hydrochemical evaluation of selected objects and subareas

With focus on specific objects and subareas of particular interest, the integrated evaluation in this section attempts to explain the observed hydrochemical patterns by compiling information from previous chapters. As a complement, additional visualisations based on the model of regolith layers /Nyman et al. in prep./, interpolated ground water levels /Werner et al. 2007/ and topography, are shown in order to visualise hydrochemical conditions and physical/hydrological prerequisites in the presented subareas (cf Section 2.3.7).

7.1 Identification of subareas of special interest

A number of sampling points in shallow groundwater and surface water show deviating characteristics in many visualisations throughout this report. These objects, of which many are soil tubes located in till below lakes, were the basis when the subareas shown in Figure 7-1 were selected.

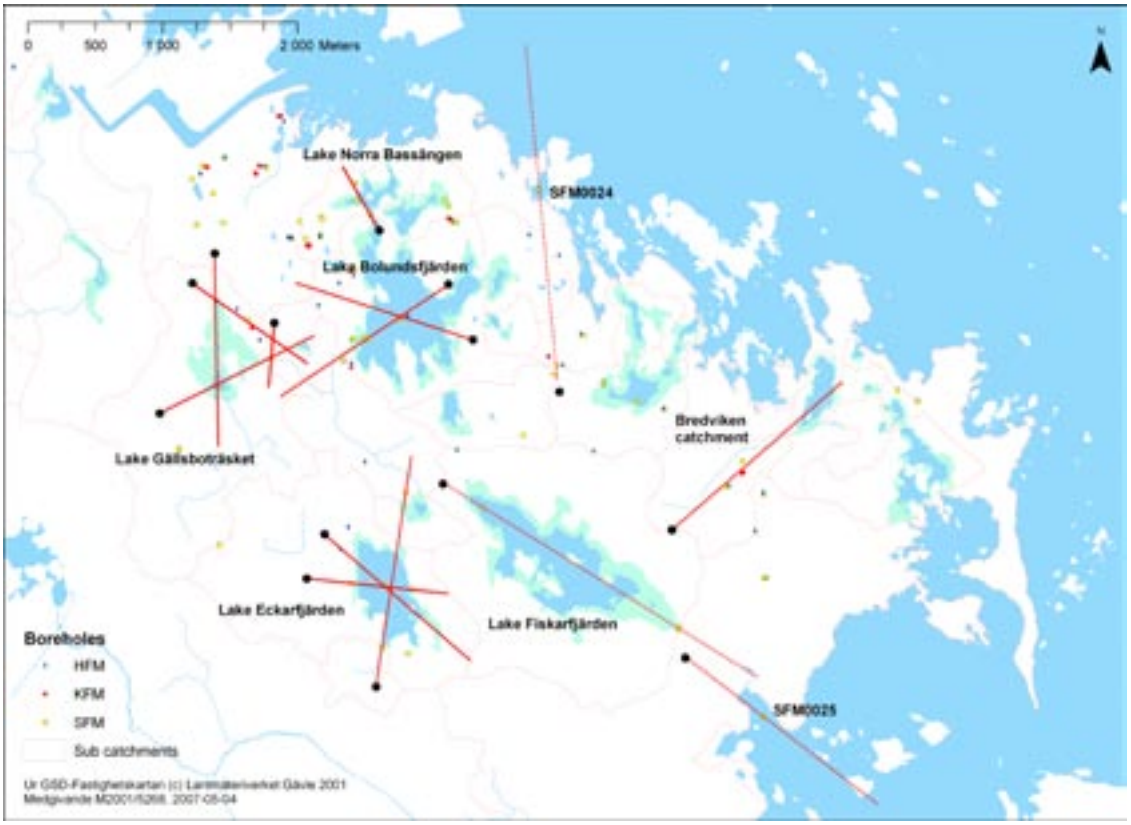

Figure 7-1. *Selected objects and subareas evaluated in this section. Straight red lines denote the location of profiles including cross sections of soil layers, groundwater levels and boreholes in the vicinity of these transects (profiles start at the end marked with a black dot). Thin red lines denote surface water divides, and point objects are labelled according to the legend: percussion drilled boreholes (HFM), cored boreholes (KFM) and soil tubes (SFM).*

Each subarea is briefly characterised in the bullet list below, and in the following sections are hydrochemical conditions and possibly important prerequisites compiled per subarea.

- In the subarea of **Lake Bolundsfjärden,** SFM0023 is a soil tube located in till below the lake sediments, which shows highly deviating hydrochemical characteristics with possible influences from a deep ion signature. An adjacent percussion drilled borehole on the small island in the middle of Bolundsfjärden, HFM32, shows similar signatures towards depth.
- Discharging water from the subarea of **Lake Gällsboträsket** (PFM000069) shows significantly increased area-specific transports of several ions, which in combination with possible deep signatures in a few soil tubes located below or in the vicinity of the lake (SFM11, 12, 13) are anomalous features of this catchment.
- The catchment of **Lake Eckarfjärden** is characterised by relatively high topographical elevations compared to the low elevations that usually prevail in the Forsmark regional model area (cf Figure 2-2). Among the studied lakes in the area, Lake Eckarfjärden was the first to be separated from the Baltic Sea, and one soil tube located in till below the rather thick sediments of this lake (SFM0015) shows deviating hydrochemistry.
- A large portion of arable land characterise the **catchment of Lake Bredviken**, which shows deviating hydrochemical characteristics both in discharging stream water (PFM000073) and shallow groundwater (SFM0006 and SFM00008).
- **Lake Fiskarfjärden** is located in a low elevated area characterised by thick sediments, which may influence shallow groundwater in the soil tubes in this subarea.
- The small lake **Norra Bassängen**, located almost at sea level near the outlet to the Baltic Sea, is influenced both from discharge from a relatively large catchment, and sea water intrusions from the Baltic at high water episodes.
- Two soil tubes, **SFM0024** and **SFM0025**, are located in till below sea water sediments. Despite similar settings, the hydrochemical composition of shallow groundwater in these soil tubes are quite different, and in the latter tube are possible deep water signatures revealed.

7.2 Bolundsfjärden subarea

The Bolundsfjärden subarea is characterised by a flat topography and is located very close to the present sea level, according to the cross-sections in Figure 7-3. During episodes of high sea level, sea water intrusions may reach Lake Bolundsfjärden, which leads to increased marine signatures in the lake water (cf Section 4.1.1). In the catchment model scenario in Section 6.2.1, the total Cl input to Lake Bolundsfjärden through these sea water intrusions was estimated to 66% of the total input per year.

Shallow groundwater in this area is also characterised by marine influences. Most soil tubes located within or in the vicinity of the lake show moderate marine influences, with a composition corresponding to dilute modern sea water according to the ion signatures (cf Section 4.1.1) and to a varying degree mixing with meteoric water. According to the conceptual model in Section 8.3, the composition may be explained by a varying degree of flushing of marine remnants by meteoric recharge from local recharge.

One soil tube located in till below lake sediments in the middle of the lake (SFM0023), as well as a percussion drilled borehole located on the small island nearby (HFM32, cf Figures 7-2 and 7-4), shows, contrary to the other soil tubes, strong marine signatures, probably influenced by relict marine groundwater and possibly also influence from deep saline signatures (cf ion source model in Sections 3.2 and 4.3.2). Similar to the relict marine groundwater in the bedrock, there is also high concentrations of Mn^{2+} in this soil tube (cf Section 4.2.2). According to hydrological head measurements in HFM32, there is at present date no indication on deep discharge in this area (P.O. Johansson, pers. comm.). This observation contradicts ongoing discharge of deeper signatures, but may be explained by an altered flow regime since this part of the Forsmark area was covered by the Baltic less than hundred years ago (cf conceptual model in Section 8.2).

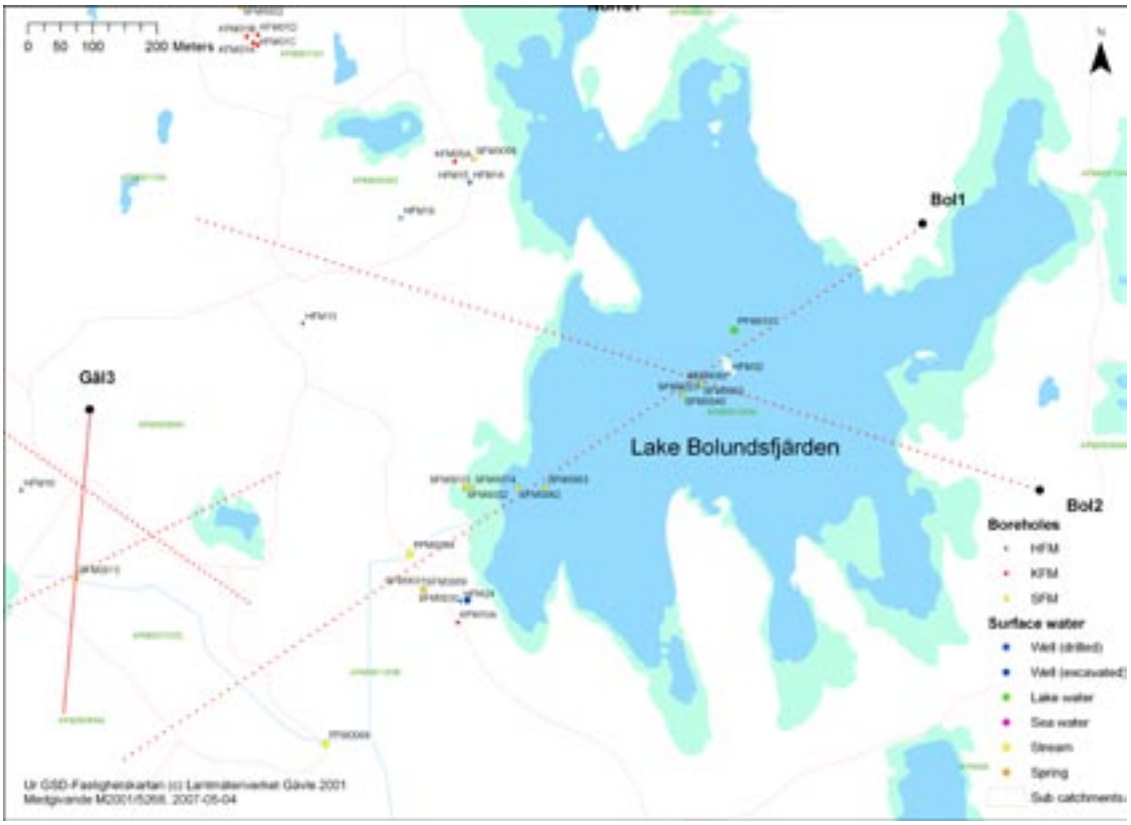

Figure 7-2. *Detail of the subarea of Bolundsfjärden. Red dotted lines denote the location of vertical profiles showing cross sections including soil layers, groundwater levels and boreholes in the vicinity of these transects (profiles start at the end marked with a black dot).*

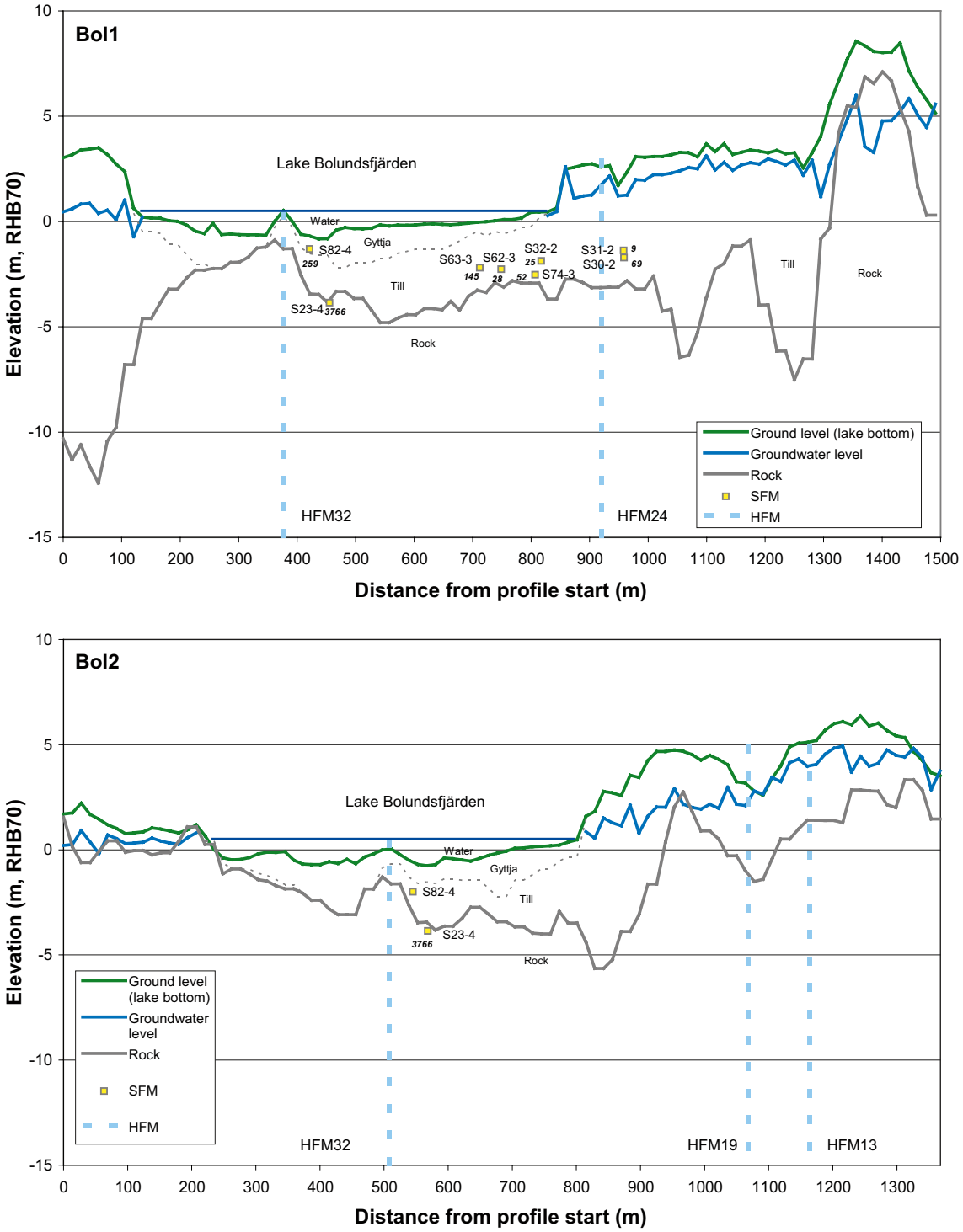

Figure 7-3. *Profiles showing ground level, soil layers and the upper part of the rock, together with borehole samples in the vicinity of the transect and average groundwater level. See Figure 7-2 for a description of profiles. Below lakes, boundaries between different regolith layers are marked by a thin dashed line and the actual regolith categories are labelled. Outside lakes, the soils is in most cases entirely dominated by till, and therefore no division of the soil is shown there. Average chloride concentrations in shallow groundwater are shown in italics.*

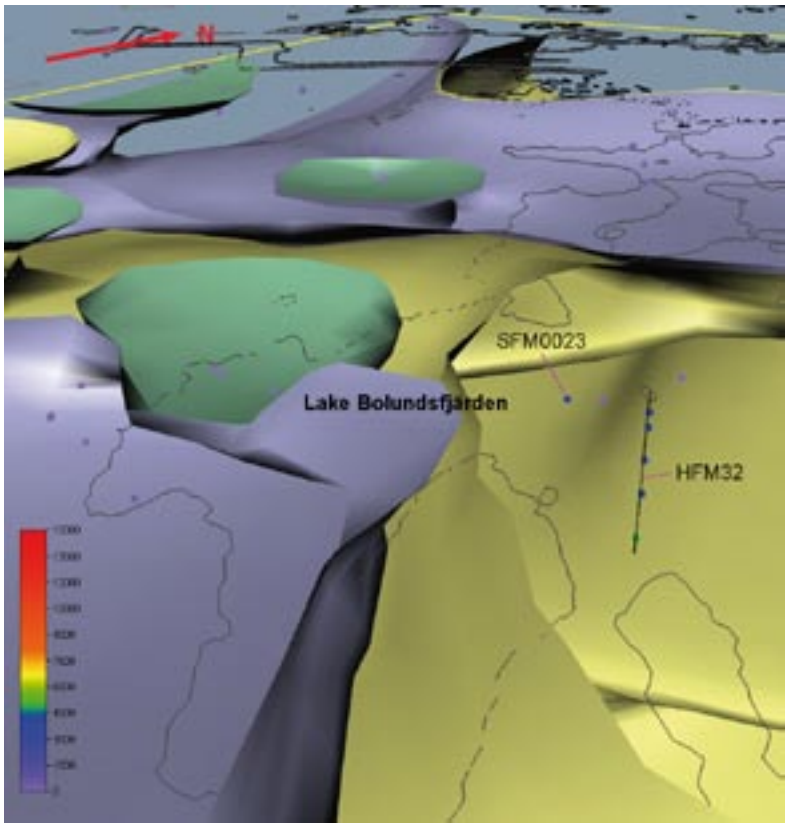

Figure 7-4. *3D model showing the vicinity of SFM0023 and a part of Lake Bolundsfjärden (the shoreline is approximately indicated by the grey elevation curve). Coloured volumes enclose observations in shallow groundwater in the Quaternary deposits and groundwater in the bedrock, representing the same water type according to the multivariate classification in Section 3.2.5. Green and lilac denote fresh groundwater types, whereas yellow denote brackish marine groundwater. The colour scale represents the Cl concentration of each sampling point.*

7.3 Gällsboträsket subarea

Lake Gällsboträsket is a shallow lake located in a local depression about 2 metres above sea level, as shown in the overview in Figure 7-5 and in the cross-sections in Figures 7-6 and 7-7. South-west of this lake, topography rises and the catchment boundary coincides with the regional water-divide towards Forsmarksån and the Forsmark reservoir (cf overview of the Norra Bassängen catchment in Figure 7-14). The Gällsboträsket subarea is located outside the tectonic lens as well as the candidate area for the repository /Olofsson et al. 2007/.

Discharging water from the subarea of Lake Gällsboträsket (PFM000069) shows significantly increased area-specific transport of particularly Cl, but also of several other marine ions (cf Figures 5-20 and 5-21). According to the catchment mass-balance scenarios in Section 6.2, the clay layer which covers a significant part of the depression (cf Figure 6-6) may in combination with the relatively low elevation above sea level, be one important factor explaining this deviation (see comparisons with the conceptual model in Section 8.3 for further details). The attraction of PFM000069 towards the relict marine "pole" in the ion source model in Section 3.2.3, compared to the position of PFM000068 located downstream, may be an additional indication that the ion source in the Lake Gällsboträsket sub-catchment to some extent contains ions of relict marine origin (and possibly also a minor influence from a deep saline component).

Shallow groundwater in the area also shows marine signatures in the Quaternary deposits below and in the vicinity of Lake Gällsboträsket. According to the ion source model in Section 3.2, dilute shallow groundwater in several soil tubes shows a relict marine signature with possible influence from deep saline groundwater (shield brine). Adjacent deep boreholes in the bedrock (KFM04A and HFM10, see Figures 7-5 and 7-8), show similar relict marine groundwater signatures, but with an even more pronounced deep saline signature. HFM10 shows one of the strongest deep saline (shield brine) signatures among all percussion drilled boreholes in the Forsmark area, according to the ion source model in Section 3.2.3.

When the Gällsboträsket area is compared to the whole catchment of Norra Bassängen (of which Gällsboträsket is a part), there are indications that high Cl concentrations in the shallow groundwater occur at higher absolute elevation in this area compared to other areas within this catchment (upper panels in Figures 7-16 and 7-17). A similar, and even more pronounced pattern is also evident for the Mg/Br ratio in the lower panels of Figures 7-16 and 7-17 (cf Figure 4-4 and Section 4.1.1 for an explanation of this ratio). This is the two-element combination that shows the strongest discrimination between modern sea water and shield brine (deep saline groundwater), according to the ion source model in Section 3.2.3. These patterns, which could be interpreted as if deep ion signatures occur at shallower depths in the area of Gällsboträsket compared to e.g. the areas of Lake Eckarfjärden and Lake Stocksjön, may have two explanations:

- Marine remnants has not yet been flushed out from the Quaternary deposits in the area of Gällsboträsket, and these remnants may contain relict deep ion signatures from the time when this area was submerged under the Baltic Sea according to the conceptual model in Section 8.2. The rich occurrence of clay in the Gällsboträsket depression may be an important factor explaining the stagnant conditions which generate deviant hydrochemical conditions in this sub-catchment.
- Hypothetically, this pattern may be an indication of a current (regional) discharge of deeper groundwater components in this area (if this pattern reflects a steady-state). The topographical gradient raising south-west of Lake Gällsboträsket, which is evident in Figure 7-16, may perhaps constitute a potential hydrological driving force for this type of flow pattern. There are, however, no indications of such a flow regime as the major water divide between Forsmarksån and the Forsmark reservoir is located on top of this ridge.

According to the overall hydrological flow pattern in the Forsmark area based on measured groundwater pressure gradients /Follin et al. 2007a/, and also according the conceptual model in Section 8.2, the former alternative is most probable. As there are no measurements of differential groundwater heads in the bedrock in the area of Gällsboträsket, there is, however, no possibility to definitively discard the latter alternative of discharge of deep groundwater.

In one soil tube located in the vicinity of Lake Gällsboträsket (SFM0057), which is classified as recharge according to the hydrological field classification (cf Section 5.1.3), traces of a possible influence from a deep signature is detected according to the ion source model in Section 3.2.3. The location SFM0057 within the Quaternary deposits is shown in the profile “Gäl2” in the lower panel of Figure 7-6. The shallow groundwater in this soil tube is rather dilute and shows a Cl concentration of about 200 mg/L, compared to about 20 mg/L in the discharge from the Gällsboträsket area. The groundwater composition also shows typical indications of calcite dissolution, indicating supply of a relatively immature and shallow groundwater component (cf Sections 4.1.3 and 4.1.4).

Similar to the area of Gällsboträsket, the area of Bredviken (cf Section 7.7) is also characterised by elevated discharge of several major ions, which is mostly explained by enhanced weathering and leakage due to agricultural activities according to the catchment models in Section 6. There is, however, a difference in area-specific discharge of Cl between these catchments, where the Gällsboträsket area show considerably higher discharge of Cl compared to the Bredviken catchment. This difference is probably attributed to supply of Cl of marine remnants in the catchment of Gällsboträsket.

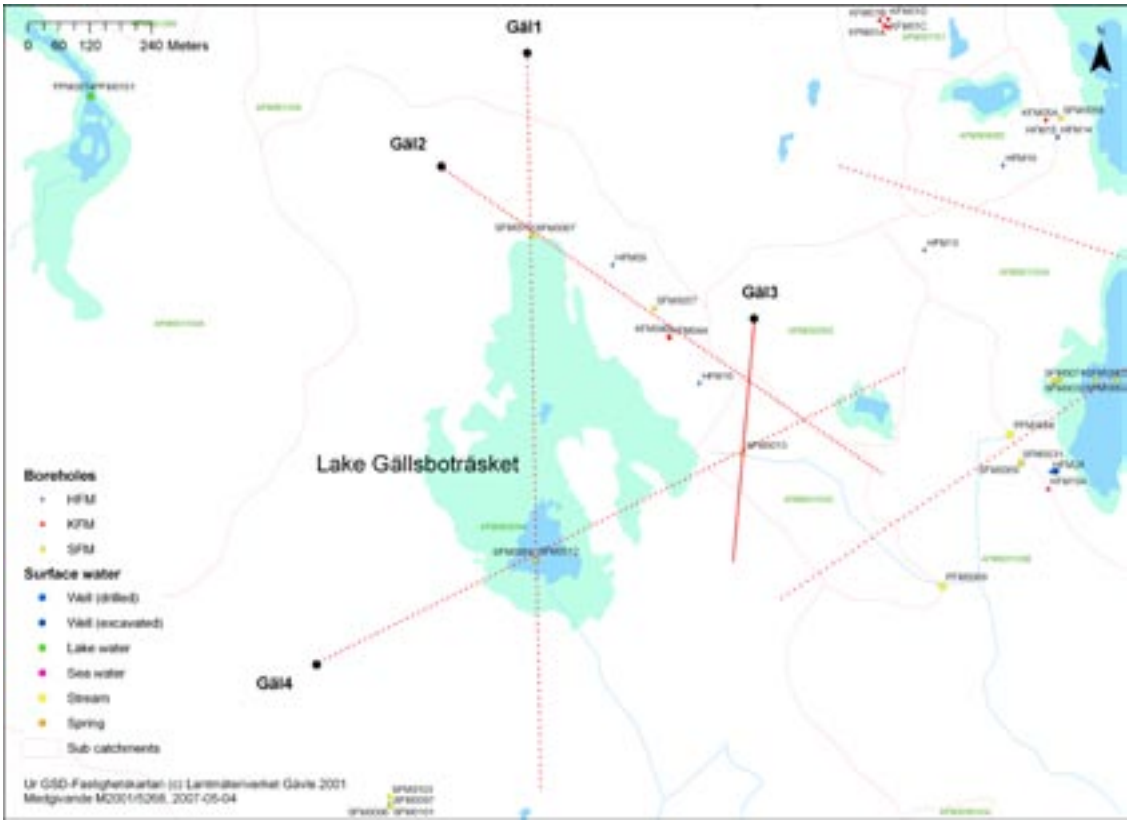

Figure 7-5. *Detail of the subarea of Lake Gällsboträsket. Red dotted lines denote the location of vertical profiles showing cross sections including soil layers, groundwater levels and boreholes in the vicinity of these transects (profiles start at the end marked with a black dot).*

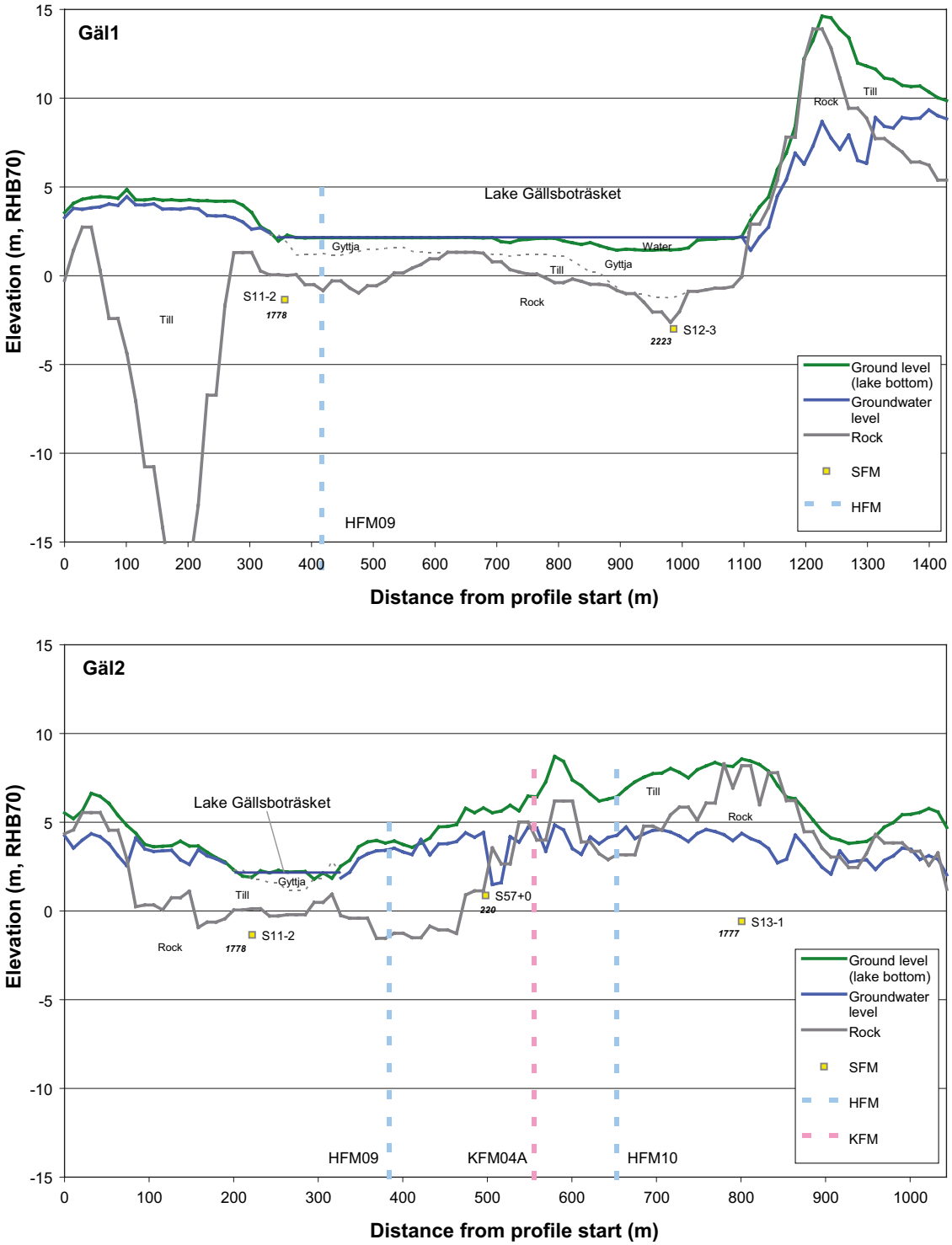

Figure 7-6. *Profiles showing ground level, soil layers and the upper part of the rock, together with borehole samples in the vicinity of the transect and average groundwater level. See Figure 7-5 for a description of profiles. Below lakes, boundaries between different regolith layers are marked by a thin dashed line and the actual regolith categories are labelled. Outside lakes, the soils is in most cases entirely dominated by till, and therefore no division of the soil is shown there. Average chloride concentrations in shallow groundwater are shown in italics.*

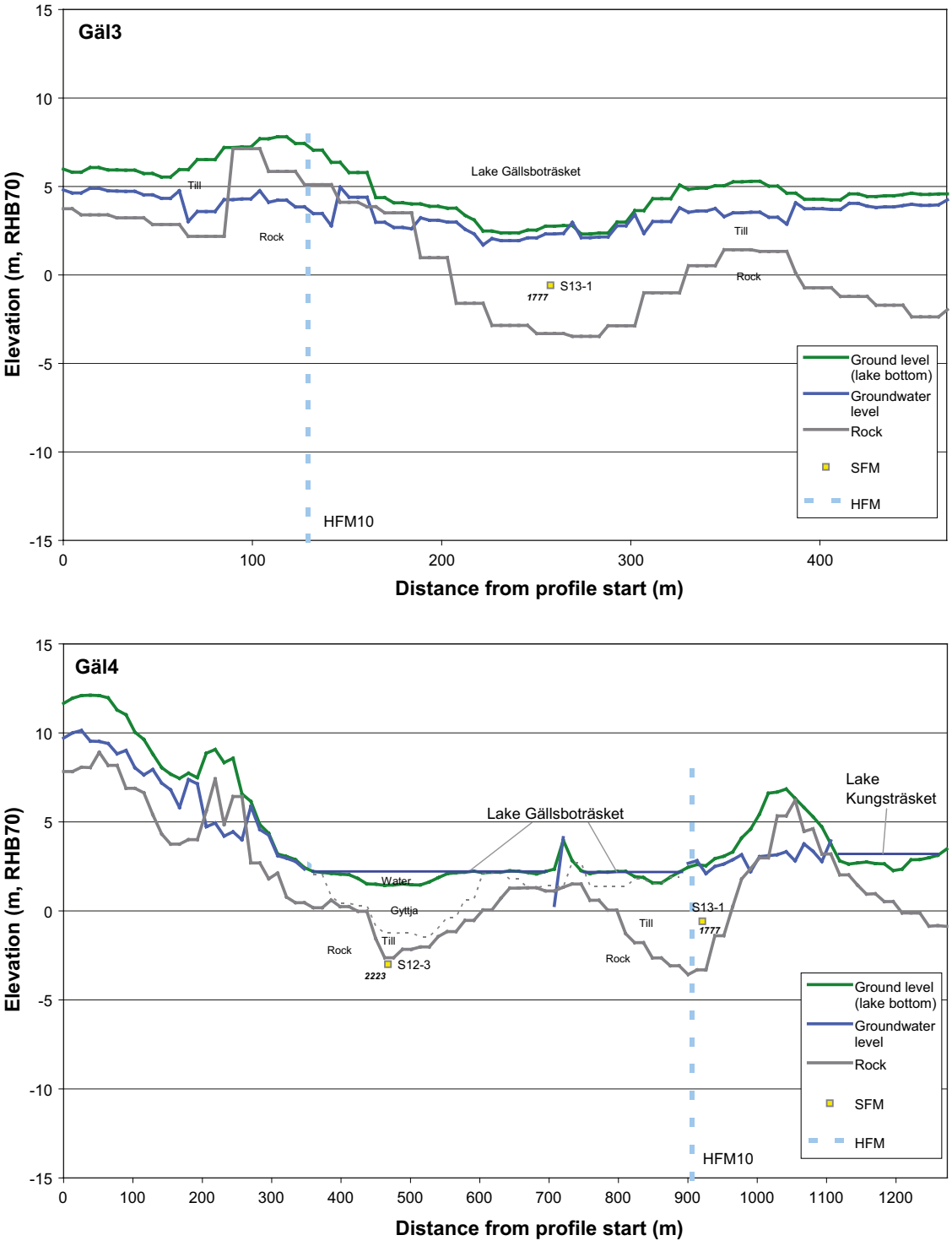

Figure 7-7. *Profiles showing ground level, soil layers and the upper part of the rock, together with borehole samples in the vicinity of the transect and average groundwater level. See Figure 7-5 for a description of profiles. Below lakes, boundaries between different regolith layers are marked by a thin dashed line and the actual regolith categories are labelled. Outside lakes, the soils is in most cases entirely dominated by till, and therefore no division of the soil is shown there. Average chloride concentrations in shallow groundwater are shown in italics.*

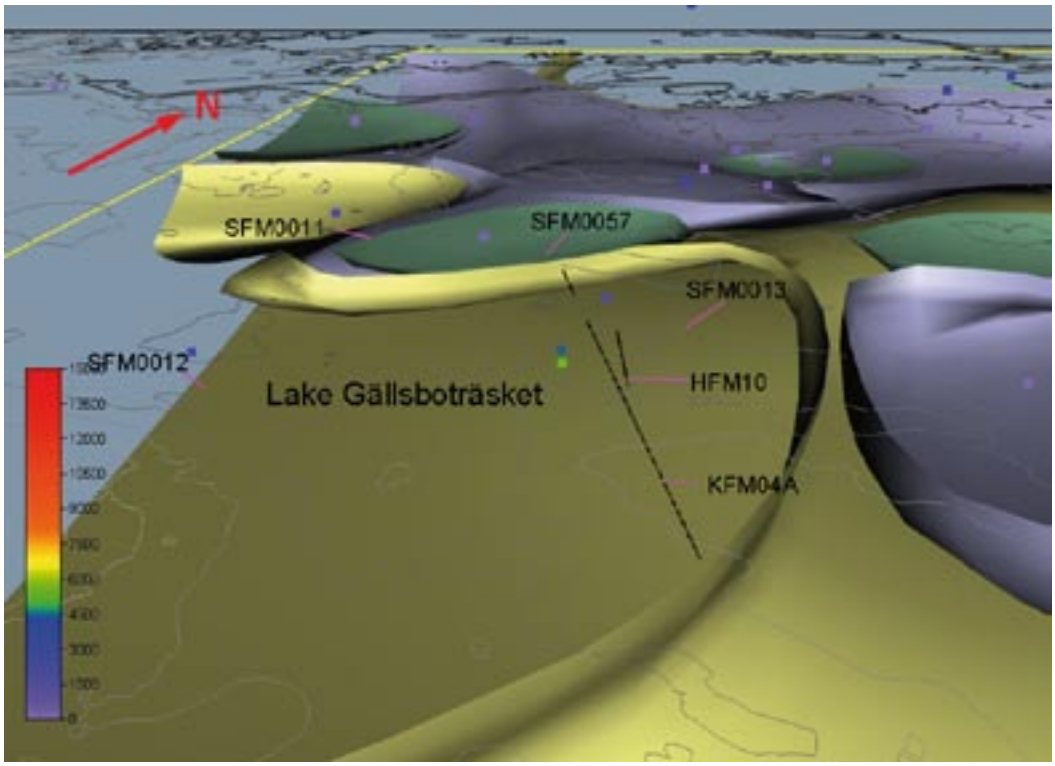

Figure 7-8. *3D model showing borehole sampling points in the vicinity of Lake Gällsboträsket (the shoreline is approximately indicated by the grey elevation curve). Coloured volumes enclose observations in shallow groundwater in the Quaternary deposits and groundwater in the bedrock, representing the same water type according to the multivariate classification in Section 3.2.5. Green and lilac denote fresh groundwater types, whereas yellow denote brackish marine groundwater. The colour scale represents the Cl concentration of each sampling point.*

7.4 Eckarfjärden subarea

The catchment of Lake Eckarfjärden is located at relatively high topographical elevations, compared to the major part of the Forsmark model area. Among the studied lakes in the area, Lake Eckarfjärden was the first to be separated from the Baltic Sea. A few observations and conclusions on this area are summarised in the bullet list below (cf overview in Figure 7-9 and cross-sections in Figures 7-10 and 7-11):

- Discharge from the Eckarfjärden area show low area-specific transport of e.g. Na, Cl, Ca, HCO_3, and Si, compared to the lower located parts of the Forsmark area, according to the comparisons in Section 5.3.5.
- Concerning the marine constituents as Na and Cl, the low area-specific discharge of these ions may be explained by almost completed flushing of marine remnants at these topographical elevations (cf the evaluation of the conceptual model in Section 8.3).
- The slightly lowered area-specific transport of Ca, HCO_3 and Si observed in the outlet of Lake Eckarfjärden compared to average conditions in the Forsmark area, may be explained by the retention that seem to take place in the lake, according to the catchment scale mass-balance models in Section 6.2.
- In case of organic carbon and nutrients, this area shows no discrepancy regarding the area-specific transports.

SFM0015, a soil tube located in the Quaternary deposits below Lake Eckarfjärden (cf Figure 7-10), deviates hydrochemically from soil tubes at similar settings in other lakes in the Forsmark area. In the bullet list below, conditions concerning this soil tube are summarised:

- Water isotope measurements in SFM0015 show a clear evaporation signature corresponding to the mean isotopic signature of the lake water (cf water isotope evaluation in Section 3.3.3). Hydrological pressure measurements below the sediments of Lake Eckarfjärden probably also indicate that this lake serves as a recharge area during the dry season /Juston et al. 2006/. These observations indicate that the groundwater in the Quaternary deposits below the lake originates from the lake water rather than from meteoric recharge from the surrounding topographical heights.
- The residence time in SFM0015 is however probably rather long, which is indicated by sub-modern ^{3}H-activies (cf Section 3.5.1). ^{14}C-activity measurements of DIC, corresponding to a non-corrected carbon age of 1,500 years, suggests that the carbon source in this shallow groundwater is rather old, and one possible origin of DIC could be organic matter in sediments.
- According to ^{13}C measurements and other supporting observations in SFM0015 (cf Section 4.1.4), there are typical evidence of anoxic bacterial processes as sulphate reduction and methanogenesis in this groundwater (cf Section 4.2.3).
- Dilute marine signatures according to the ions source model in Section 3.2.3 and Cl concentrations of 300 mg/L probably indicates that the flushing of sea water remnants have gone relatively far in the case of SFM0015.
- To summarise: the shallow groundwater in SFM0015 may represent a brackish marine groundwater successively diluted by lake water during relatively closed and stagnant conditions.

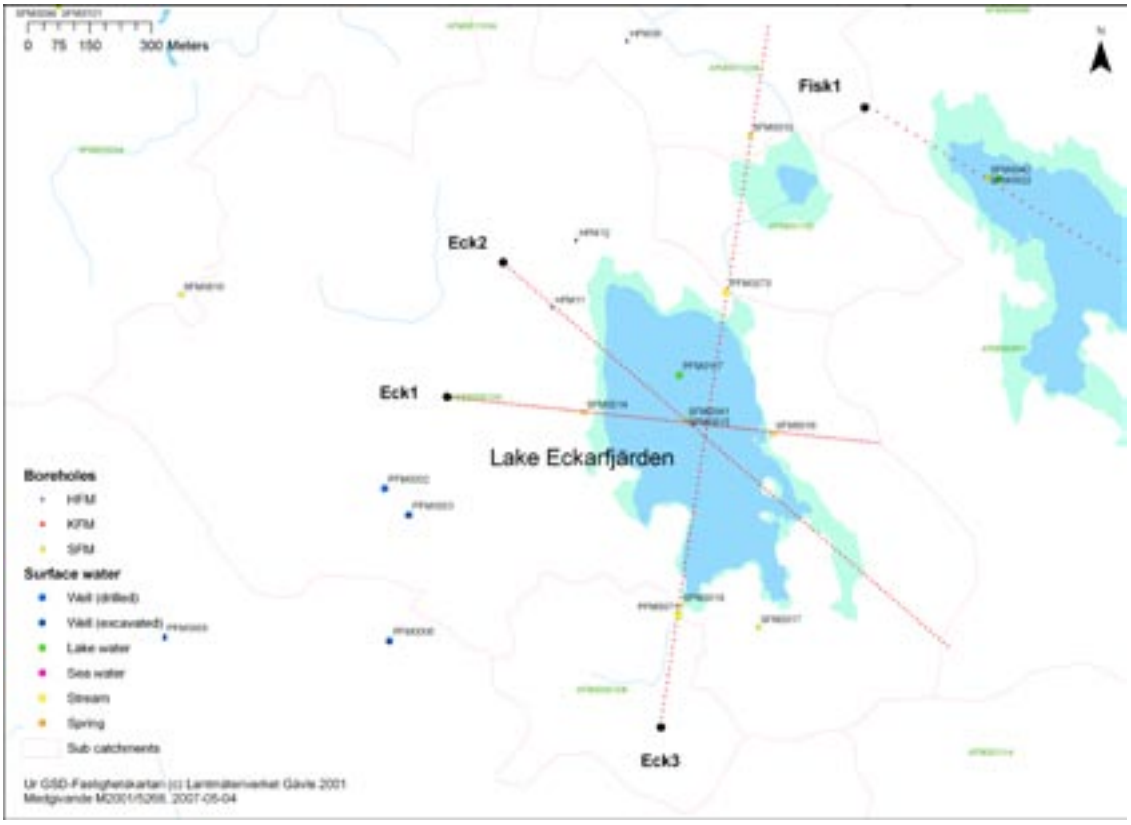

Figure 7-9. *Detail of the subarea of Lake Eckarfjärden. Red dotted lines denote the location of vertical profiles showing cross sections including soil layers, groundwater levels and boreholes in the vicinity of these transects (profiles start at the end marked with a black dot).*

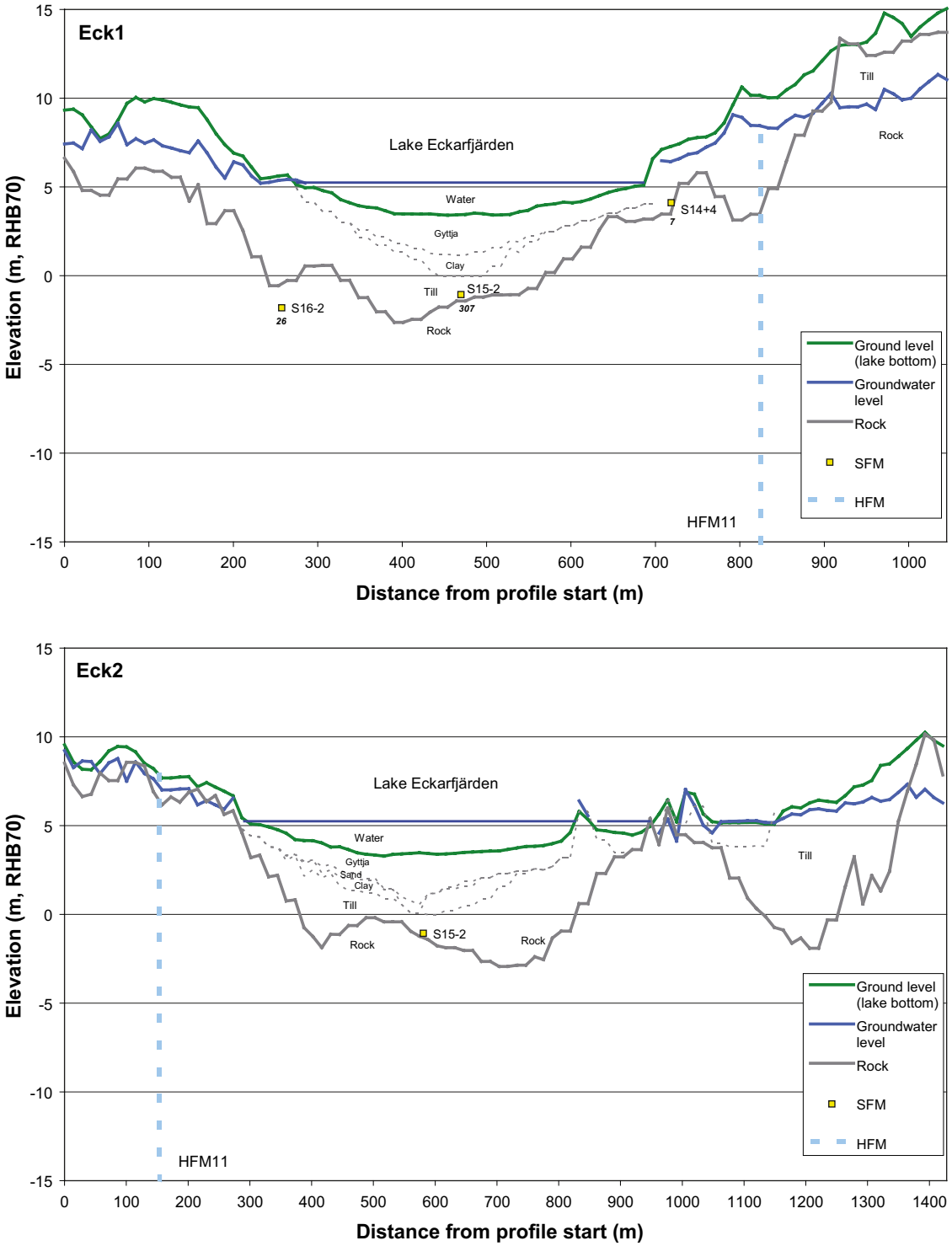

Figure 7-10. *Profiles showing ground level, soil layers and the upper part of the rock, together with borehole samples in the vicinity of the transect and average groundwater level. See Figure 7-9 for a description of profiles. Below lakes, boundaries between different regolith categories are marked by a thin dashed line and the actual regolith layers are labelled. Outside lakes, the soils is in most cases entirely dominated by till, and therefore no division of the soil is shown there. Average chloride concentrations in shallow groundwater are shown in italics.*

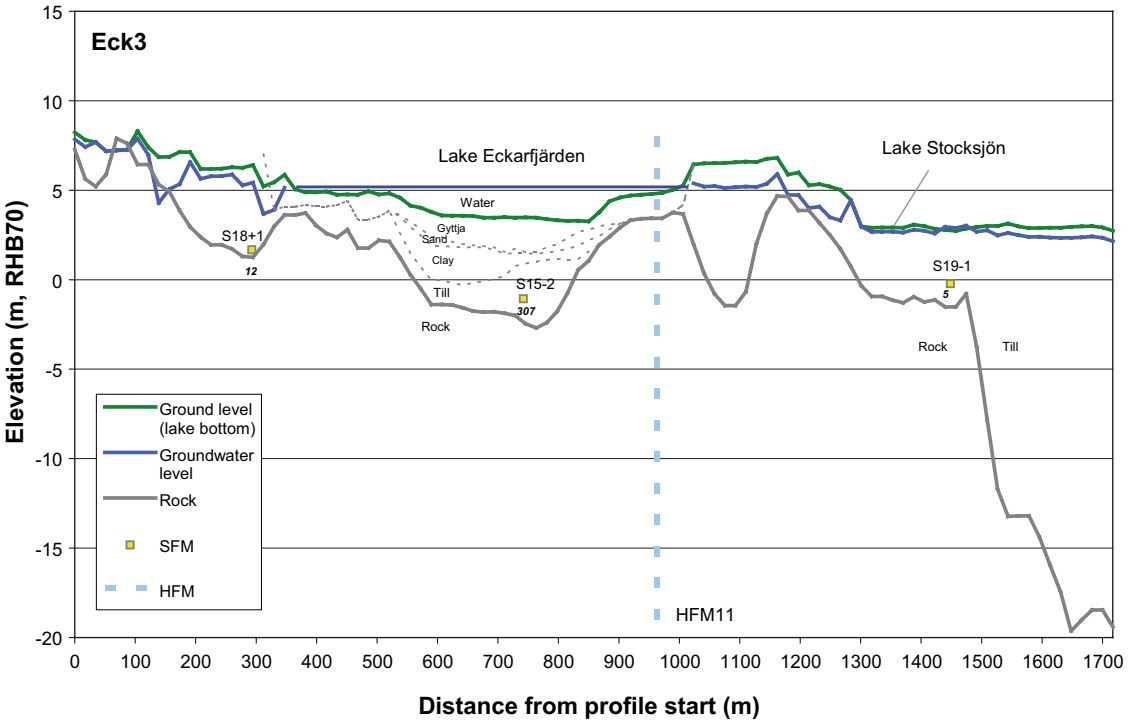

Figure 7-11. *Profile showing ground level, soil layers and the upper part of the rock, together with borehole samples in the vicinity of the transect and average groundwater level. See Figure 7-9 for a description of profiles. Below lakes, boundaries between different regolith layers are marked by a thin dashed line and the actual regolith categories are labelled. Outside lakes, the soils is in most cases entirely dominated by till, and therefore no division of the soil is shown there. Average chloride concentrations in shallow groundwater are shown in italics.*

There are no indications of a connection between the groundwater types sampled in the Eckarfjärden deformation zone (HFM11 and HFM12) and the composition of the shallow groundwater sampled in this subarea. This deformation zone extends across the lake according to Figure 7-20. The percussion drilled boreholes HFM11 and HFM12, show according to the ion source model significant influence from deep saline groundwater (cf Section 3.2.4), and also possible influence from glacial (cold) water isotope signatures according to the water origin model in Section 3.3.2.

The Eckarfjärden subarea, which is part of the Norra Bassängen catchment, is further discussed in Section 7.6, and in the evaluation of the conceptual model in Section 8.3.

7.5 Fiskarfjärden subarea

The Fiskarfjärden subarea is characterised by relatively thick Quaternary deposits and the relatively large and shallow Lake Fiskarfjärden. An overview of the area is shown in Figure 7-12, and a profile showing a cross-section along the lake is shown in Figure 7-13. A few observations and conclusions from this subarea are summarised in the bullet list below:

- The catchment scale mass-balance models in Section 6 indicates that discharge from the Fiskarfjärden subarea is influenced from clays and gyttja that cover parts of the subarea, similar to the situation in the Gällsboträsket subarea (cf Figure 6-6). Agricultural activities coupled the land-use categories arable and open land are also supposed to influence the hydrochemistry in the subarea, e.g. by slightly elevated phosphorus concentrations.

- The significant portion of the land-use category “water” in the Fiskarfjärden catchment compared to the land area gives rich prerequisites for retention in the lake. The mass-balance models in Section 6.2 indicate that there is a substantial retention in Lake Fiskarfjärden for elements as Ca, Sr, HCO_3 and Si. Depending on element, as much as 25–50% of the total supply is trapped in the sediments of the lake.
- Shallow groundwater below Lake Fiskarfjärden, which is sampled in the soil tube SFM0022, shows elevated salinity (c 1,000 mgCl/L) similar to other soil tubes located in the Quaternary deposits below lakes. The Cl concentration is lower than what is observed below Lake Gällsboträsket and higher than shallow groundwater below Lake Eckarfjärden, giving Lake Fiskarfjärden an intermediate position among these lakes. The isotopic signature of the water shows influence from a meteoric recharge groundwater component, which implies that meteoric recharge may have diluted the originally brackish groundwater below this lake (cf Section 3.3.3 where four lakes in the area are compared with respect to the water origin).
- Thick Quaternary deposits and sediments characterise the Fiskarfjärden subarea according to the cross-section in Figure 7-13. The soil tubes SFM0026 and SFM0027, which both are located in the Quaternary deposits at fifteen and six metres depth respectively, show according to the ion source model in Section 3.2.3 and the visualisations in Section 4.2.1 a hydrochemical composition affected by cation exchange. The possible long residence time in these deposits probably enhance the effects of cation exchange. Supporting parameters are however ambiguous in these sampling points, such as there is a high ^{222}Rn activity observed in SFM0027 possibly indicating a long residence time for groundwater at these depths in the deposits (there are no measurements of ^{222}Rn in SFM0026), in combination with ^{3}H-activities indicating a substantial supply of modern recharge (or contamination during drilling).

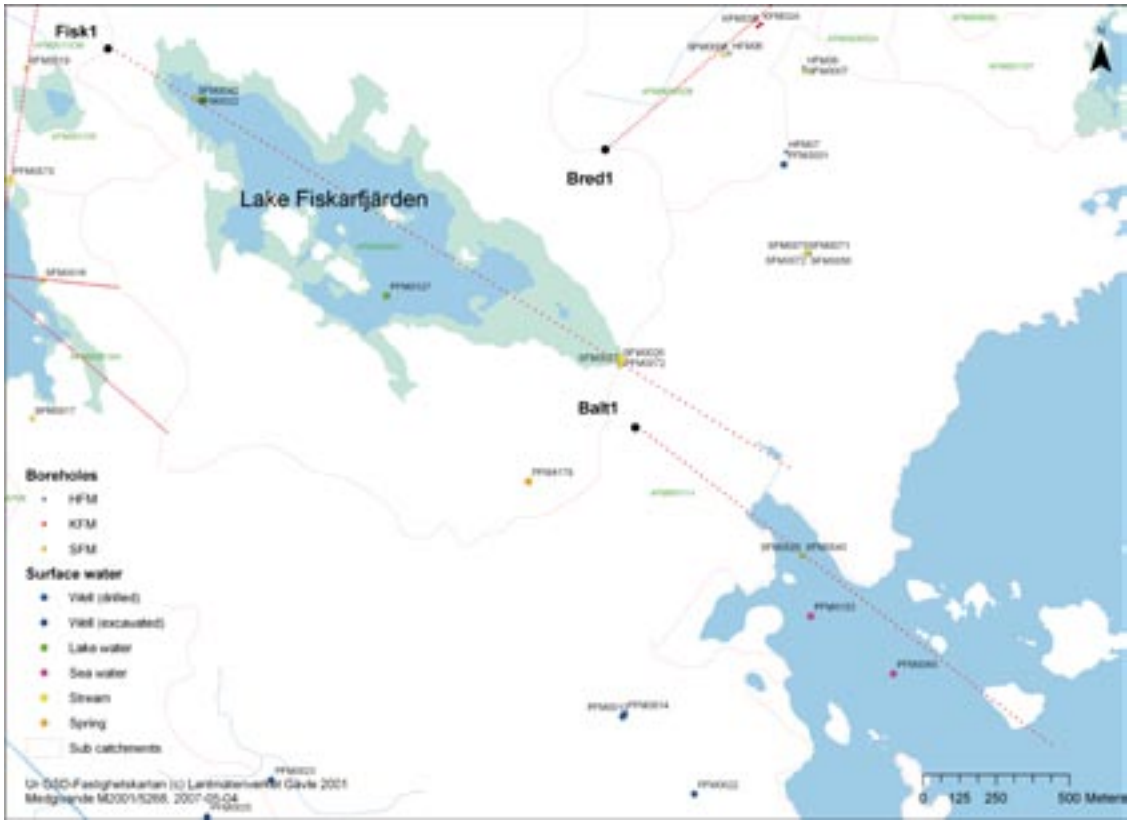

Figure 7-12. *Detail of the subarea of Lake Fiskarfjärden. Red dotted lines denote the location of vertical profiles showing cross sections including soil layers, groundwater levels and boreholes in the vicinity of these transects (profiles start at the end marked with a black dot).*

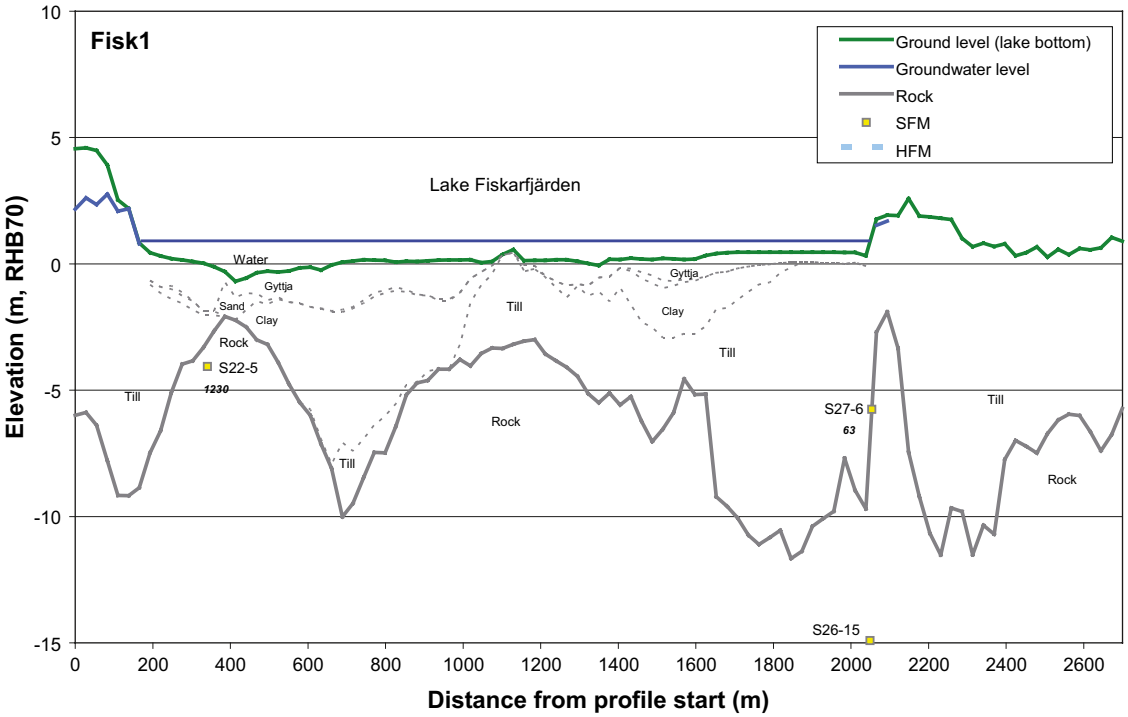

Figure 7-13. *Profile showing ground level, soil layers and the upper part of the rock, together with borehole samples in the vicinity of the transect and average groundwater level. See Figure 7-12 for a description of profiles. Below lakes, boundaries between different regolith layers are marked by a thin dashed line and the actual regolith categories are labelled. Outside lakes, the soils is in most cases entirely dominated by till, and therefore no division of the soil is shown there. Average chloride concentrations in shallow groundwater are shown in italics.*

7.6 Subarea Norra Bassängen

The Norra Bassängen subarea is the largest catchment in the Forsmark area, and includes the previously described subareas of Bolundsfjärden, Gällsboträsket and Eckarfjärden as well as the catchment of Norra Bassängen close to the Baltic coast. In this section, two longer profiles extending from the Baltic Sea towards the Gällsboträsket subarea and the Eckarfjärden subarea respectively are explored. Both these transects follow the major topographical SW-NE gradient. An overview of the whole Norra Bassängen catchment is shown in Figure 7-14, and profiles showing cross-sections are shown in Figure 7-15 to Figure 7-16.

In shallow groundwater in the Norra Bassängen catchment, close to the Baltic coast, the hydrochemical composition in several soil tubes may be explained by simple mixing between different proportions of modern sea water and meteoric recharge (Figure 7-15). The composition in these soil tubes therefore probably reflects varying degrees of flushing of sea water remnants by meteoric recharge; Cl and Na concentrations in SFM0037, 36, 34 may according to the scenario in Figure 4-2 (lower panel) be explained by simple mixing as these points plot along a binary mixing line. A similar pattern applies to the series SFM0031, 32, 63 and 74 in the Bolundsfjärden catchment (cf Figure 7-3, upper panel). Different starting points of these mixing scenarios probably reflect different local conditions with respect to theses parameters, e.g. regarding weathering and groundwater residence time.

If the perspective is extended to the entire Norra Bassängen catchment along the transects "Norra2" and "Norra3", Cl gradients are evident at larger scale as shown in Figures 7-16 and 7-17:

- Along the "Norra3" which is extending from Lake Eckarfjärden towards the Baltic Sea, the shift to higher Cl concentrations occur at relatively constant absolute depth, in spite of a varying topography.
- Along the profile "Norra2" in Figure 7-16, higher Cl concentrations are observed at lower absolute depth in the Gällsboträsket subarea compared to e.g. Eckarfjärden subarea shown in the "Norra3" transect. It should be noted that this is an uncertain conclusion due to the limited spatial coverage of the sampling points.
- This pattern is further strengthened if the Mg/Br ratio is plotted onto the profiles (see explanation of this ratio in Sections 7.3 and 4.1.1), which could be interpreted as influence from relict marine groundwater in the Gällsboträsket subarea. This pattern may either be explained by regional discharge of relict marine groundwater, or most probably, reflect relict marine remnants trapped in the Quaternary deposits (cf Section 7.3). The Gällsboträsket subarea forms a depression covered by clayey sediments, which may have preserved the relict marine signatures in the shallow groundwater in this area.

These overall patterns may be explained in the light of the paleo-hydrological history of the Forsmark area, as is described in the conceptual model in Section 8.2, where the ongoing land-uplift in combination with earlier hydrological flow regimes are important factors forming the present hydrochemistry.

Figure 7-14. *The catchment of Norra Bassängen. Red dotted lines denote the location of vertical profiles showing cross sections including soil layers, groundwater levels and boreholes in the vicinity of these transects (profiles start at the end marked with a black dot). Boreholes within a specified distance from the transects are included in the profile plots (Norra 1: 100 m, Norra 2: 700 m, Norra 3: 500 m respectively).*

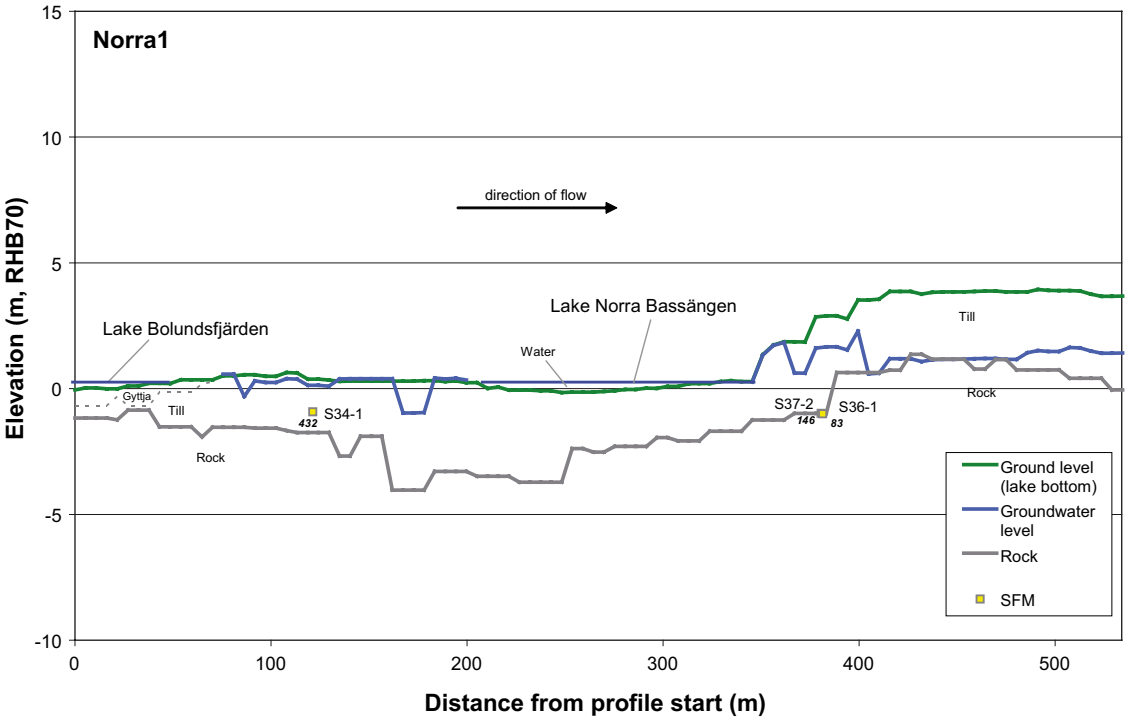

Figure 7-15. *Profile showing ground level, soil layers and the upper part of the rock, together with borehole samples in the vicinity of the transect and average groundwater level. See Figure 7-14 for a description of profiles. Below lakes in the soil model, boundaries between different regolith layers are marked by a thin dashed line, and the actual regolith categories are labelled. Outside lakes no additional soil divisions are shown and the range between ground level and upper part of the rock is dominated by till. Average chloride concentrations in shallow groundwater are shown in italics.*

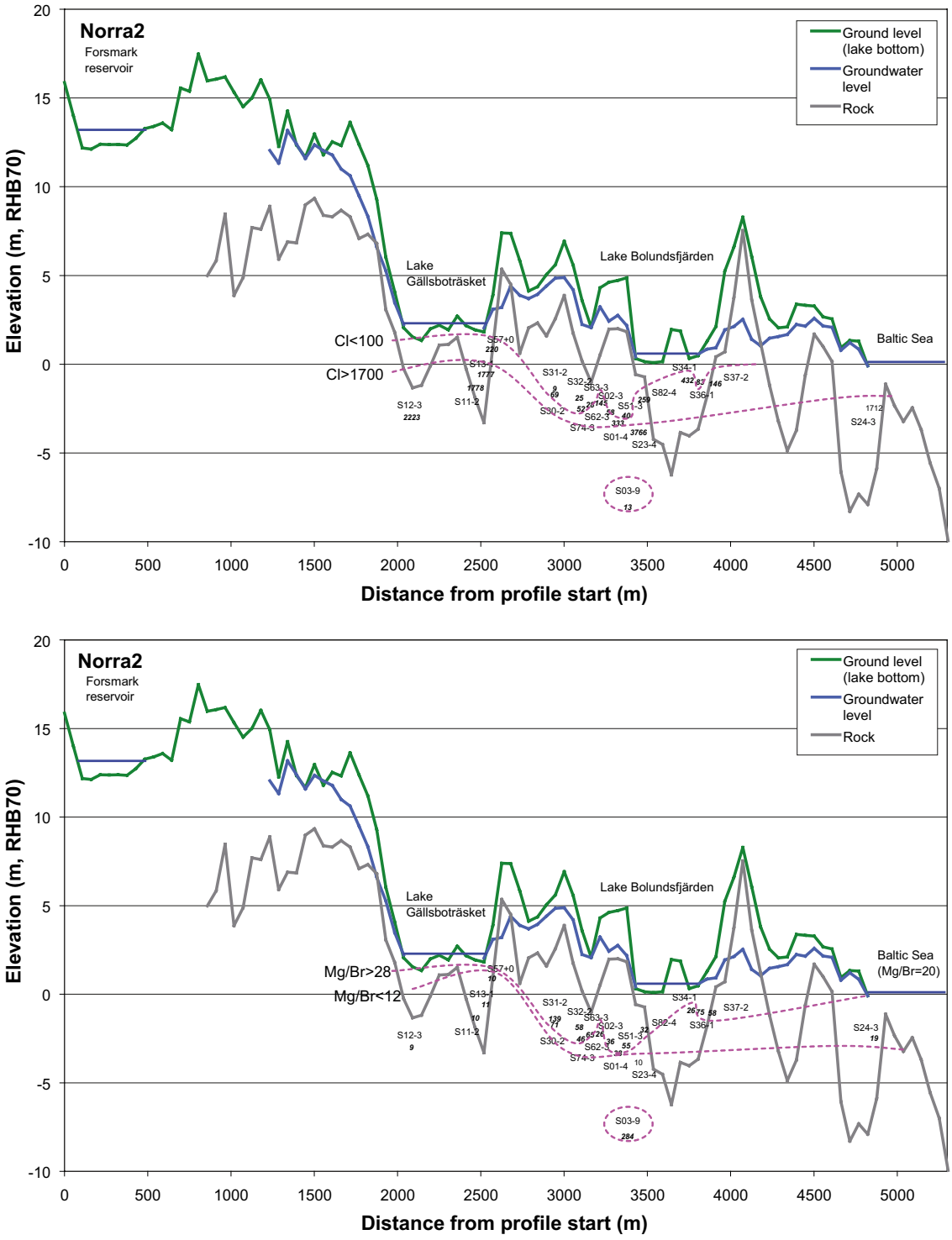

Figure 7-16. *Profiles showing ground level, soil layers and the upper part of the rock, together with borehole samples in the vicinity of the transect and average groundwater level. See Figure 7-14 for a description of profiles. Below lakes in the soil model, boundaries between different regolith layers are marked by a thin dashed line, and the actual regolith categories are labelled. Outside lakes no additional soil divisions are shown and the range between ground level and upper part of the rock is dominated by till. Average chloride concentrations in shallow groundwater (mg/L) are shown in italics in the upper panel, and the Mg/Br ratio (mass ratio)in the lower. Demarcations between groups of similar values are emphasized by dashed pink lines.*

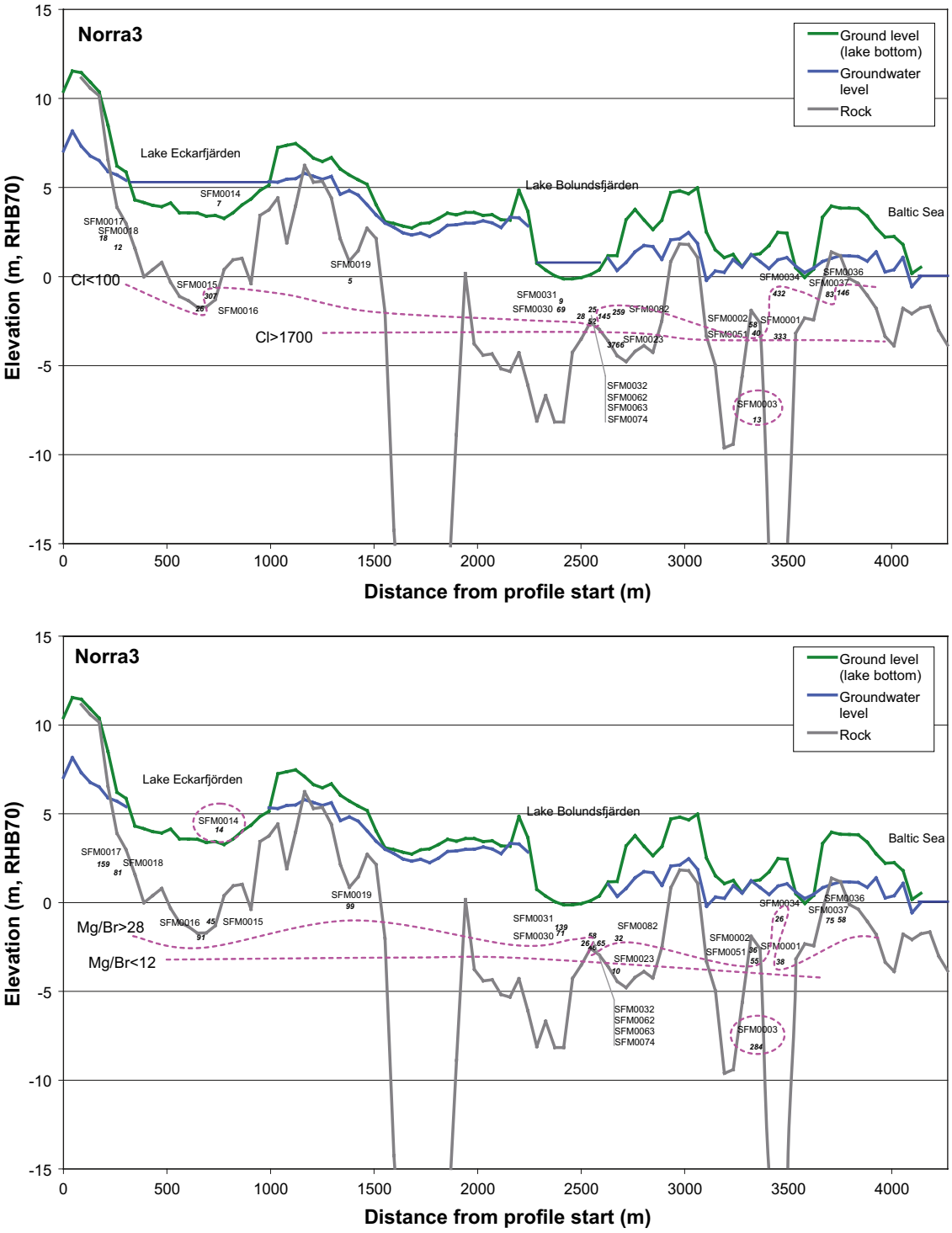

Figure 7-17. *Profiles showing ground level, soil layers and the upper part of the rock, together with borehole samples in the vicinity of the transect and average groundwater level. See Figure 7-14 for a description of profiles. Below lakes in the soil model, boundaries between different regolith layers are marked by a thin dashed line, and the actual regolith categories are labelled. Outside lakes no additional soil divisions are shown and the range between ground level and upper part of the rock is dominated by till. Average chloride concentrations in shallow groundwater (mg/L) are shown in italics in the upper panel, and the Mg/Br ratio (mass ratio) in the lower. Demarcations between groups of similar values are emphasized by dashed pink lines.*

7.7 Subarea Bredviken

The subarea of Bredviken shows a deviating hydrochemistry in both surface water and shallow groundwater with respect to many parameters. According to the catchment scale mass-balance models in Section 6.2, the main explanation for is anomaly is most probably accounted for by the large portion of arable land in this catchment (Figure 7-18). Marine influences are also evident in this catchment due to the vicinity to the Baltic Sea (cf Section 4.1.1).

Agricultural activities as cultivation and draining soils are supposed to lead to enhanced weathering rates and increased leakage of several ions and nutrients as phosphorus and dissolved nitrogen species:

- According to the mass-balance for phosphorus in Section 6.2.10, the area-specific transport of phosphorus is about 50 times higher than from forest land, whereas leakage of total nitrogen in Section 6.2.9 is only elevated three times according to the calibrated parameters. Area-specific transports of total carbon are lower from arable land compared to forest land and wetlands.
- In surface water discharge in the inlet to Lake Bredviken concentrations of K, Ca, Mg, SO_4 and HCO_3 are significantly elevated compared to most other catchments in the Forsmark area /Sonesten 2005/. Concentrations of Na and Cl are contrary relatively normal in discharge from this area, compared to adjacent catchments.

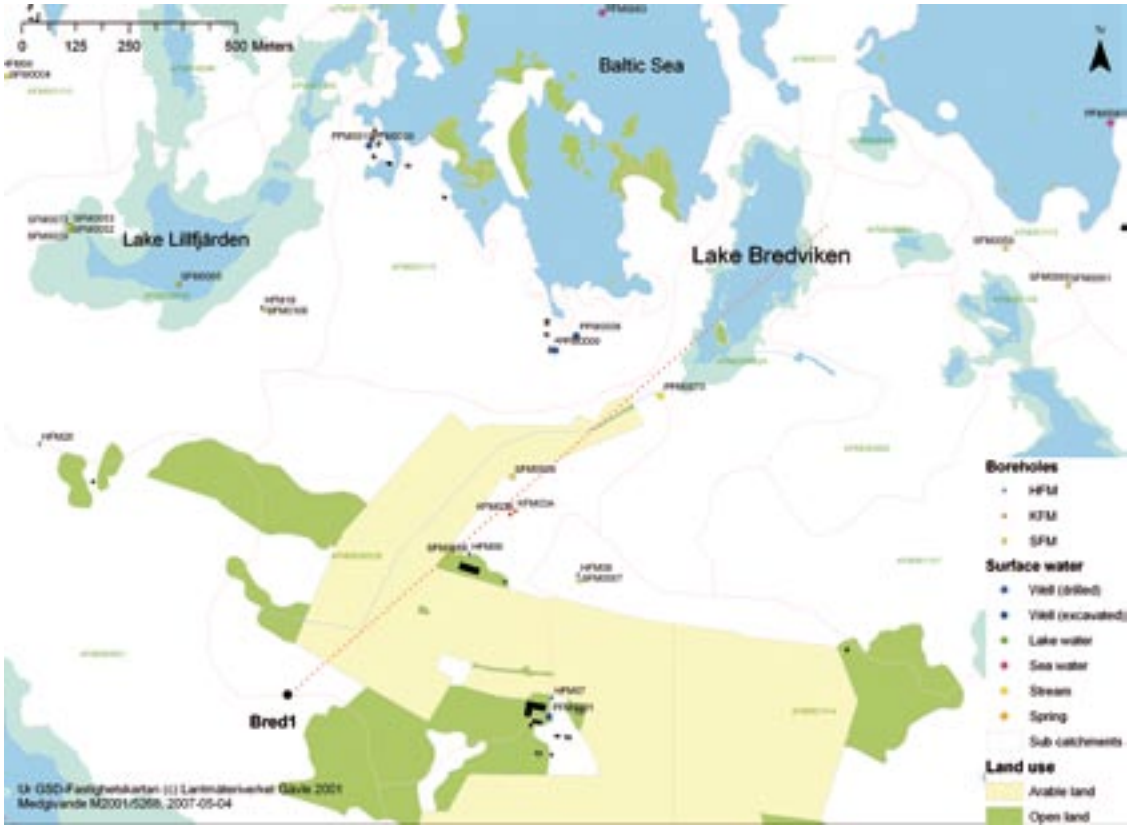

Figure 7-18. *The subarea of Lake Bredviken. Red dotted lines denote the location of vertical profiles showing cross sections including soil layers, groundwater levels and boreholes in the vicinity (100 m) of these transects (profiles start at the end marked with a black dot).*

The anomalous conditions observed in the Bredviken catchment is most probably caused by increased rates of weathering of calcite and other minerals, according to the prevailing ion signatures in the discharging surface water. As proposed by /Åström and Rönnback, submitted/, this process, which is mainly driven by H^+ of biogenic origin, may be further enhanced by H^+ derived from oxidation of biogenic sulphides in postglacial clays. In combination with relatively low concentrations of Na and Cl, the negative ^{34}S isotope signature also indicates significant contributions of SO_4 from sulphide minerals rather than a marine source (cf Section 4.1.2).

Shallow groundwater in the Bredviken subarea, sampled in the two soil tubes SFM0006 and SFM0008 (see profile in Figure 7-19), show hydrochemical characteristics similar to the observations in the discharging surface water. Very high concentrations of Ca, not fully matched by HCO_3 according to the molar ratio in calcite, are in these sampling points accompanied with negative ^{34}S isotope signatures, which may indicate that enhanced weathering of calcite due to oxidation of sulphide minerals is a probable process influencing the shallow groundwater in the Bredviken subarea.

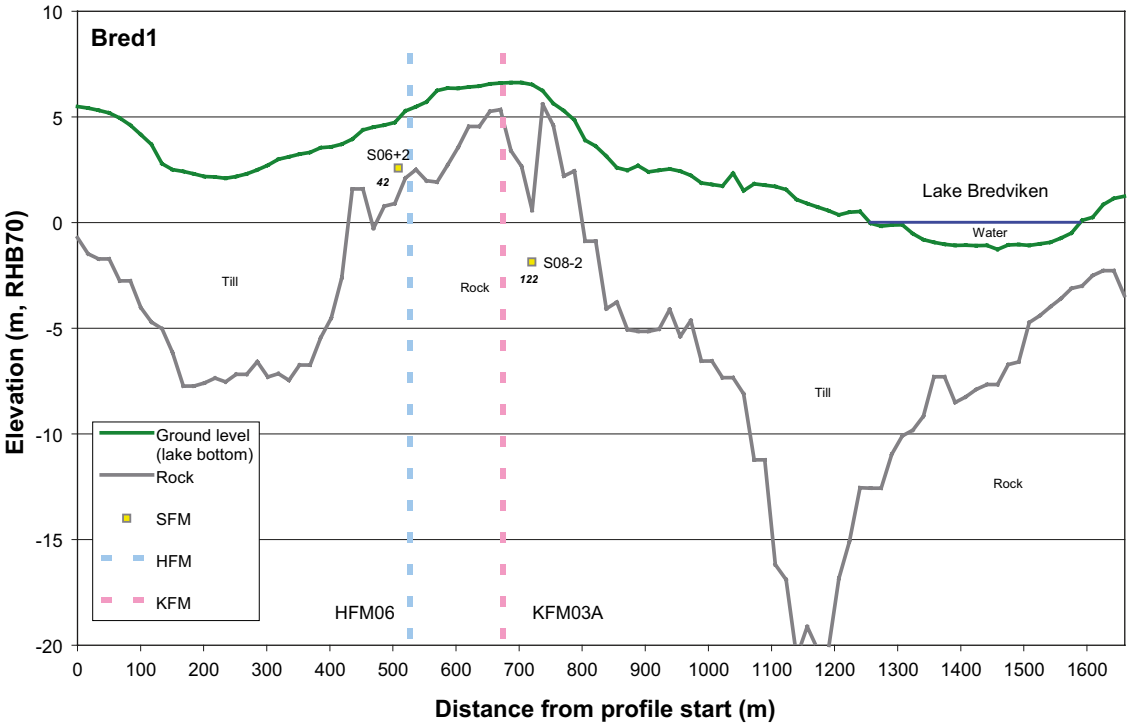

Figure 7-19. *Profile showing ground level, soil layers and the upper part of the rock, together with borehole samples in the vicinity of the transect and average groundwater level. See Figure 7-14 for a description of profiles. Below lakes in the soil model, boundaries between different regolith layers are marked by a thin dashed line, and the actual regolith categories are labelled. Outside lakes no additional soil divisions are shown and the range between ground level and upper part of the rock is dominated by till. Average chloride concentrations in shallow groundwater are shown in italics.*

7.8 Soil tubes located below sea water

Two soil tubes are located in till below sea sediments of the Baltic Sea (SFM0024 and SFM0025). The locations of these sampling points are shown in Figure 7-20, and in two cross-sections extending from land towards sea in Figure 7-21. These shallow groundwater sampling points, which hypothetically may represent discharge areas, show both similarities and dissimilarities with respect to the observed hydrochemistry:

- Sea water signatures dominate in SFM0024 according to the ion source model in Section 3.2.3, as well as the water origin model in Section 3.3.2. This soil tube is also located closer to the sea bottom, which is e.g. manifested in a greater temperature variability compared to SFM0025 (cf Section 5.1.2).
- SFM0025 is characterised by relict marine ion signatures (cf Section 3.2.3), in combination with a meteoric recharge component according to the water origin model (cf Section 3.3.2). The groundwater residence time in this soil tube may be several thousands years according to the interpretation of the ^{14}C-activity in Section 3.5.2. Compared to SFM0024 this soil tube is located closer to the bedrock below thick Quaternary deposits (cf 5.1.2).

The discrepancy between SFM0024 and SFM0025 probably reflects two different hydrological flow regimes in the hypothetical discharge zone in the vicinity of the coast. SFM00024 probably represents relatively modern sea water slightly diluted by meteoric recharge, whereas SFM0025, which have a potentially long residence time, probably contain a mixture of a relict marine groundwater component and meteoric recharge.

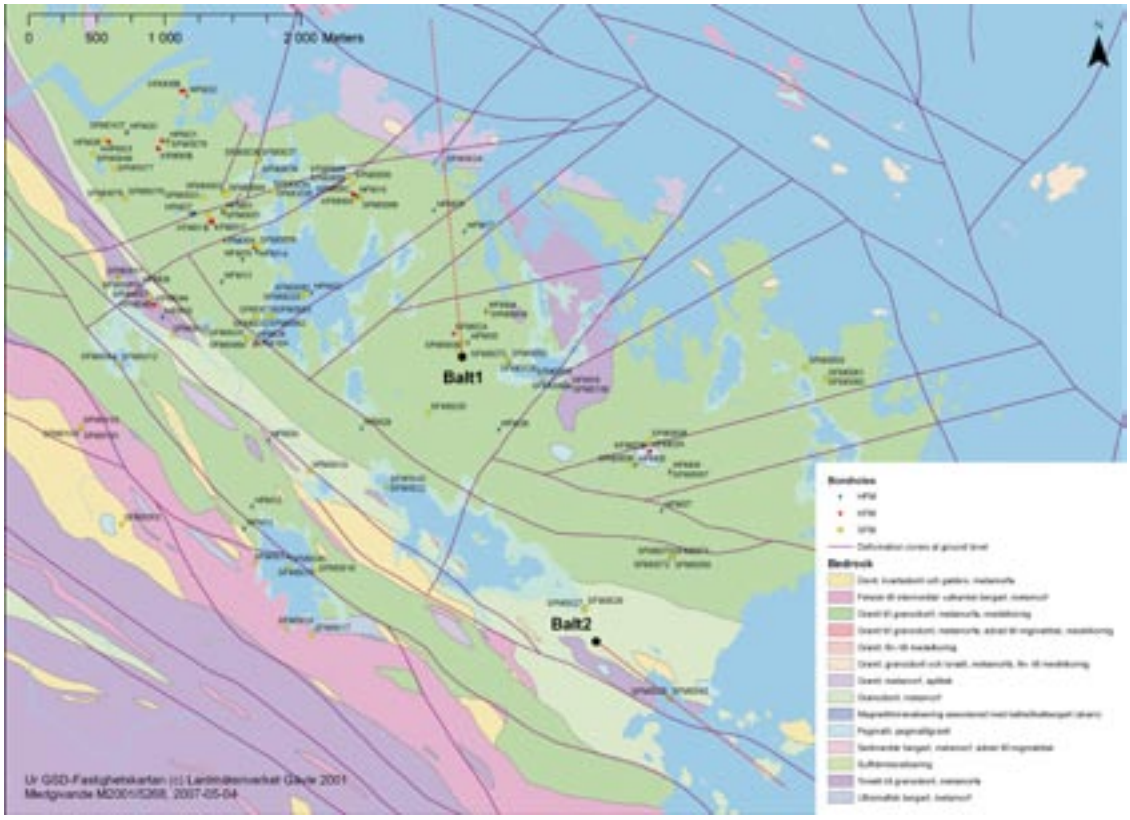

Figure 7-20. *The location of the two transects that extend into the Baltic Sea, 'Balt1' and 'Balt2'. Red dotted lines denote the location of vertical profiles showing cross sections including soil layers, groundwater levels and boreholes in the vicinity (100 m) of these transects (profiles start at the end marked with a black dot).*

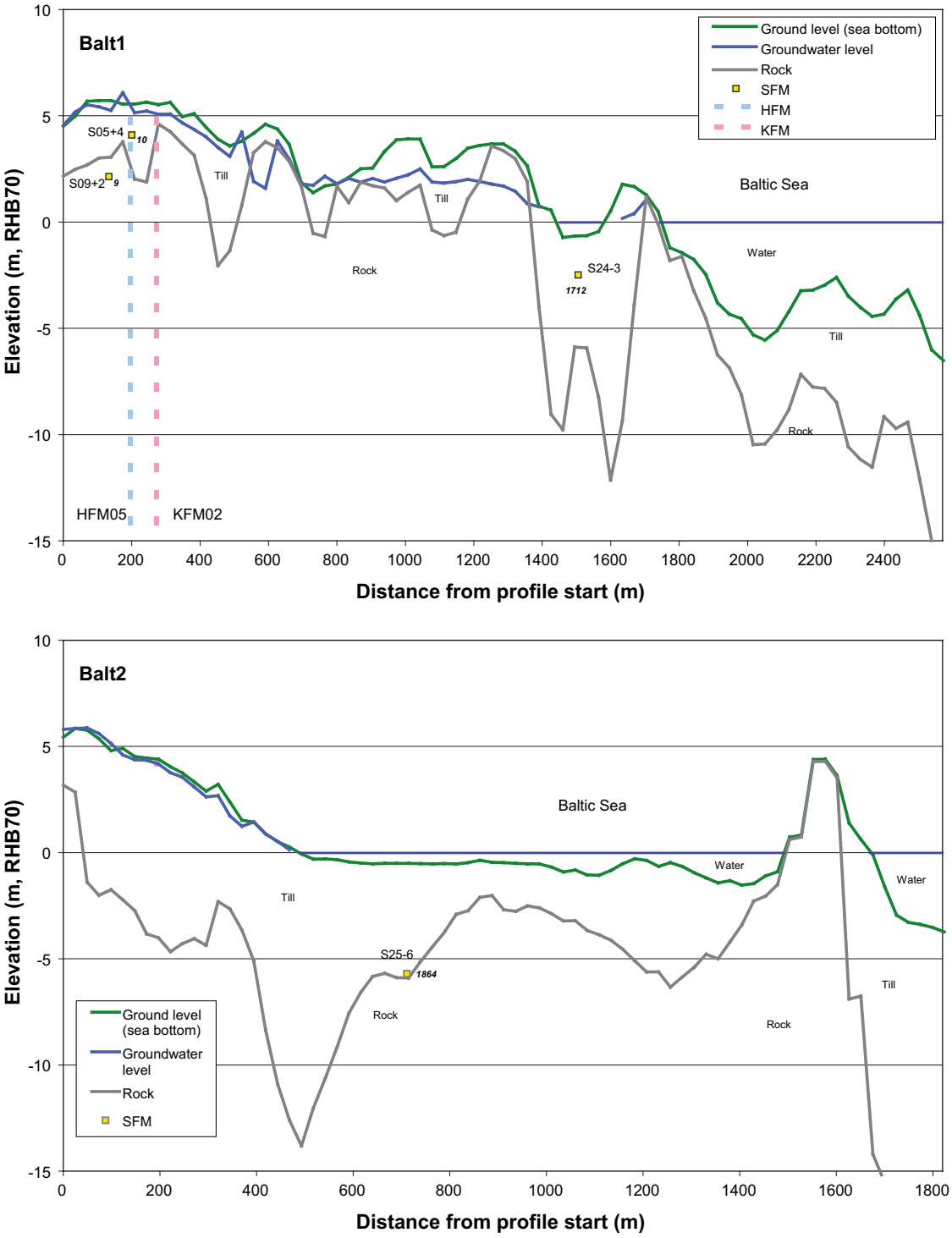

Figure 7-21. *Profiles showing ground level, soil layers and the upper part of the rock, together with borehole samples in the vicinity of the transect and average groundwater level. See Figure 7-14 for a description of profiles. Below lakes in the soil model, boundaries between different regolith layers are marked by a thin dashed line, and the actual regolith categories are labelled. Outside lakes no additional soil divisions are shown and the range between ground level and upper part of the rock is dominated by till. Average chloride concentrations in shallow groundwater (mg/L) are shown in italics.*

8 A conceptual model for the hydrochemistry in surface systems in the Forsmark area

In this report a large number of visualisations and models of different complexity reflect the hydrochemistry in the Forsmark area, with the intention to give an understanding of important processes and factors that affect the hydrochemistry in the surface systems. In order to widen the perspective, all data including observations from different levels of the bedrock as well as hydrological measurements and characterisations of the Quaternary deposits (QD), have been included in the analyses. The purpose of this report is to give a general understanding of the site and to explain observed overall patterns as well as anomalies, and, ultimately, to present a conceptual model that explains the present hydrochemistry in the light of the past. Together with the conceptual model presented in this section, supportive references are included that point back into the report, and in the final section, specific observations from the Forsmark area are related to the conceptual model.

8.1 Important prerequisites forming the hydrochemistry in the surface systems

The flat topography and the recent withdrawal of the Baltic Sea due to the isostatic land-uplift are two important factors determining the hydrochemistry in the Forsmark area /Lindborg et al. 2005/. Marine remnants in the Quaternary deposits, as well as modern sea water intrusions, are therefore strongly influencing the hydrochemistry, especially in areas at low altitude close to the coast (cf Section 4.1.1).

The Forsmark area is dominated by glacial remnants, mostly in the form of a till layer, which was deposited during the Weichselian glaciation and de-glaciation /Fredén 2002/. When the ice cover retreated about 11,000 years ago these deposits was exposed the sea floor. This till layer is characterized by a rich content of calcite, originating from the sedimentary bedrock of Gävlebukten about 100 km north of Forsmark /Fredén 2002/, and it has a central role in the forming of today's hydrochemistry in surface systems, and probably also on the composition of the dilute groundwater in the upper parts of the bedrock. The rich supply of calcium and high alkalinity affects the structure of the whole ecosystem, for example by forming the oligotrophic hardwater lakes which are characteristic for the area /Brunberg and Blomquist 1999/.

In samples from the upper parts of the bedrock extending down to depths of several hundred metres, as well as in some shallow groundwater sampling points, a brackish groundwater type with a clear relict marine signature prevail. Major ions in these groundwaters seem to originate mainly from a marine source but, at least to some extent, also from a deeper saline source (cf Section 3.2). The isotope signatures of the water (i.e. ^{2}H, ^{18}O) also show a clear evaporation signature, which reflects the marine (Littorina) origin of the solvent (cf Section 3.3). However, the relict marine groundwater differs in isotopic water composition from the present-day sea water in the Baltic, which may be interpreted as influence of meteoric recharge during a period of cold climate.

8.2 Conceptual model with paleo-hydrologic perspective

In the following sections, the development of the hydrochemistry in the Forsmark area since the latest deglaciation 11,000 years ago is outlined in a series of figures. Each figure describes a generalised hydrological picture (cf /Follin et al. 2007a/), in combination with some reactions involving a few elements important for the interpretation of past and present hydrological patterns in the surface system and in groundwater in the upper parts of the bedrock.

8.2.1 The period from deglaciation until onset of the Littorina stage

Shortly after the deglaciation (c 9,000 BC), the groundwater in the fractured bedrock consisted of a mixture of glacial water, old meteoric water and deep saline groundwater (abbreviated GOD in the figures below), originating from the previous glacial period and earlier interglacials /Follin et al. 2007a/. After the withdrawal of the ice cover, Glacial (Quaternary) deposits were exposed at the bottom of the freshwater lake, which was formed by the melting glaciers. These deposits were probably saturated with glacial melt water. In the Forsmark area, these deposits also contained large amounts of limestone originating from Gävlebukten about 100 km north of the area, represented by the mineral $CaCO_3$ in Figure 8-1. Perhaps Mn and Fe oxides were precipitated onto the sea floor during this freshwater stage, as indicated by the grey arrows in the figure (cf Section 8.2.2).

During this period, when the Forsmark area was covered by non-saline water (c 9,000–7,500 BC, during the Ancylus stage), there was probably little exchange of water and elements through the Quaternary deposits due to the lack of hydrological driving forces (the density of the saline/brackish groundwater in the bedrock was higher than in the freshwater). There were probably also layers of glacial clay deposited on top, which further reduced the permeability of the Quaternary deposits (Gustav Sohlenius, SGU, pers. comm.).

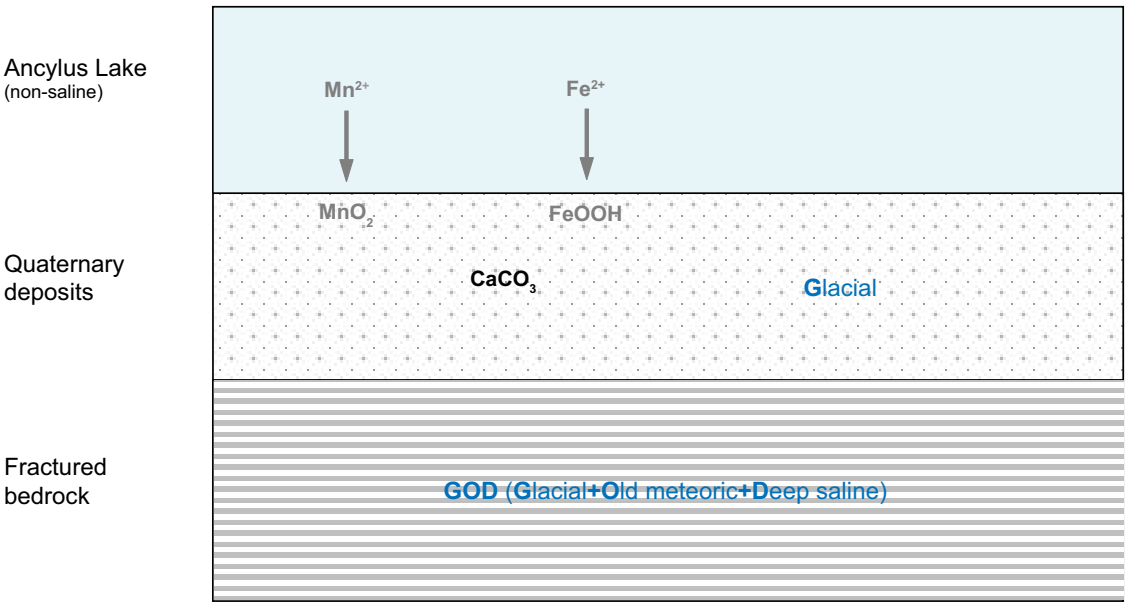

Figure 8-1. *Important characteristics of the hydrochemistry in different parts of the surface system when the Forsmark area was covered by non-saline water, e.g. during the Ancylus Lake (c 9,000–7,500 BC). Typical for the period is the lack of strong hydrological driving forces leading to little water exchange through the Quaternary deposits. Constituents, important for the understanding of the development of the hydrochemistry in the surface system, are denoted by chemical abbreviations in the figure. Grey colour on text and arrows denote more uncertain assumptions.*

8.2.2 The Forsmark area covered by Littorina Sea water

When the Forsmark area was covered by the brackish Littorina Sea with increasing salinity (c 7,500–3,000 BC), the difference in density between Littorina Sea water and the GOD mixture in the bedrock gave prerequisites for a density turnover, which may have infiltrated sea water through the bottom sediments and the minerogenic Quaternary deposits. There is at present date no information available how fast this shift took place, and to what extent the Littorina Sea water actually passed the Quaternary deposits, or if the inflow penetrated uncovered fractures directly (Sven Follin, pers. comm.). A similar scenario may also have occurred during earlier brackish periods, e.g. the Yoldia Sea stage, but since the Forsmark area was ice-covered during this period /cf SKB 2005c/, it was probably unaffected by density turnover.

If there was suitable conditions, organic sediments may have accumulated onto the sea floor during the Littorina period, and perhaps also during the previous non-brackish stage. According to a dynamic sedimentation model (Lars Brydsten, pers. comm.), sediments were accumulating during the Littorina stage in the deeper areas between Forsmark and Gräsö, but only to a minor extent in the present Forsmark area. According to the general situation in the Baltic Sea (Gustav Sohlenius, pers. comm.), there were, however, small prerequisites for accumulation of organic sediments in the Forsmark region during the Littorina Sea stage. The discrepancy between the general situation and the site specific Forsmark model may perhaps be explained by the local-specific conditions, e.g. the sheltering effects of Gräsö.

If present, organic sediments on top of the minerogenic Quaternary deposits gave prerequisites for altered redox conditions within the deposits due to oxygen consumption by microbial decomposition of organic matter. The lowered redox conditions also gave prerequisites for anoxic reactions to take place within the sediments/deposits:

- Manganese and iron present on the sea floor as oxides, was mobilised as Mn^{2+} and Fe^{2+} ions due to the lowered redox state. These oxides may have precipitated already during the freshwater stage, previous to the brackish Littorina stage, as indicated in Figure 6-1.
- SO_4 originating from sea water was reduced to hydrogen sulphide by sulphate-reducing bacteria. This process altered the isotope composition of the marine SO_4, in that the lighter ^{32}S-isotope was trapped in the QD as e.g. pyrite when S^{2-} was precipitated by Fe^{2+} (characterised by negative $\delta^{34}S$ values), whereas the SO_4 that reached the bedrock consequently became enriched in the heavier ^{34}S-isotope (positive $\delta^{34}S$ values, cf Section 4.1.2).

If there was a density-driven flow pattern from Littorina Sea through the Quaternary deposits, mobilised Mn^{2+}, as well as SO_4 with an altered ^{34}S-isotopic signature, may have been transferred with the relict marine groundwater into the upper parts of the bedrock.

According to the scenario proposed in /SKB 2006/, the high Mn^{2+} concentrations that prevail in the present relict marine groundwater in the bedrock may originate from the marine environment during the Littorina stage. The rich occurrence of manganese-reducing bacteria (MRB) in this groundwater (Lotta Hallbäck, pers. comm.), could, however, be an indication that some Mn^{2+} also originate from local bedrock minerals.

The resulting mixing of Littorina Sea water and the GOD mixture gave the groundwater in the fractured bedrock a distinct marine signature regarding ions as Na, Cl and Mg, as well as a typical marine evaporation signature of the water (the solvent) (cf Sections 3.2 and 3.3). Additionally, a possible infiltration through the sediments may have altered the isotopic composition of the marine SO_4 (cf Section 4.1.2) and may have also added large amounts of Mn^{2+} to the groundwater in the fractured bedrock (cf Section 4.2.2), according to the scenario outlined in Figure 8-2.

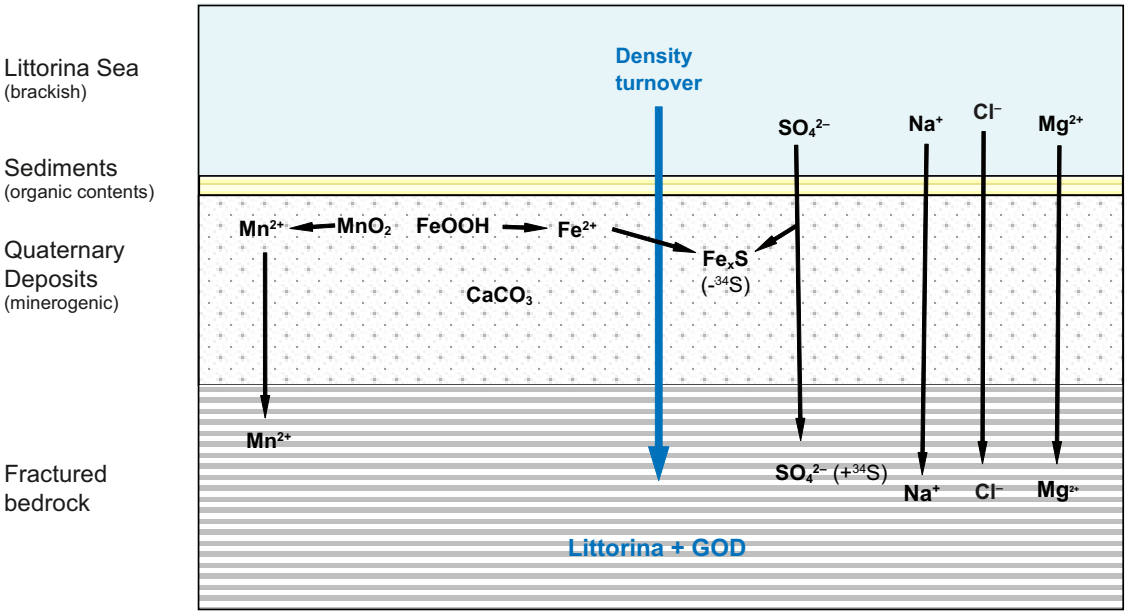

Figure 8-2. *Important characteristics of the hydrochemistry in different parts of the surface system in Forsmark during the first part of the Littorina stage (7,500–3,000 BC). A strong density-driven hydrological driving force, directed from the saline sea water towards the bedrock, is indicated by the blue arrow. Constituents, important for the understanding of the development of the hydrochemistry in the surface system and shallow groundwater, are denoted by chemical abbreviations, whereas the direction of major processes and reactions are schematically marked by black arrows in the figure.*

8.2.3 The Forsmark area covered by Baltic Sea water

When the Forsmark area was still covered by Baltic Sea water after the Littorina salinity maximum (c 3,000–0 BC), there was no driving force transporting ions and water from the less saline sea water to the heavier, more saline groundwater in the bedrock. On the contrary, there was a possible discharge of groundwater from the fractured bedrock upwards through the QD, driven by the topographical gradient near the coast (Per-Olof Johansson, pers. comm.). This flow regime may have transported the Littorina dominated groundwater from the fractured bedrock, as well as any residual signature of the GOD mixture, into the QD, according to the scenario outlined in Figure 8-3. Glacial clay layers deposited on top of the till after the withdrawal of the ice, was probably eroded in the vicinity of the coast due to wave induced erosion (Lars Brydsten, pers. comm.), which resulted in a higher permeability of the upper parts of the QD.

8.2.4 The Forsmark area emerging from the sea

From around 0 BC until present date, when parts of the Forsmark area have emerged from the sea due to the isostatic uplift, the conditions in the Quaternary deposits (QD) are significantly altered. Recharge of meteoric water leads to a completely new flow pattern in the QD, compared to the conditions prevailing when the area was submerged under sea water. This new situation results in local discharge in streams and lakes, as well as recharge through the QD down to the upper parts of the fractured bedrock. The widespread and horizontally extended fracture systems, which are characteristic for the upper parts of the bedrock in the Forsmark area, effectively channel the recharging groundwater to discharge points, e.g. near or below the Baltic Sea. Any potential regional discharge of deeper groundwater is probably also channelled to these exit points through the horizontal fracture system /Follin et al. 2007a/. Hydrological measurements indicate that there are no deeper flow patterns that reach the surface, not even in the lower located lakes as Lake Bolundsfjärden. However, during dry summer conditions there are observations of groundwater levels in QD dropping below groundwater levels in the bedrock at some locations due to the influence of evapotranspiration. If a continuous upward gradient

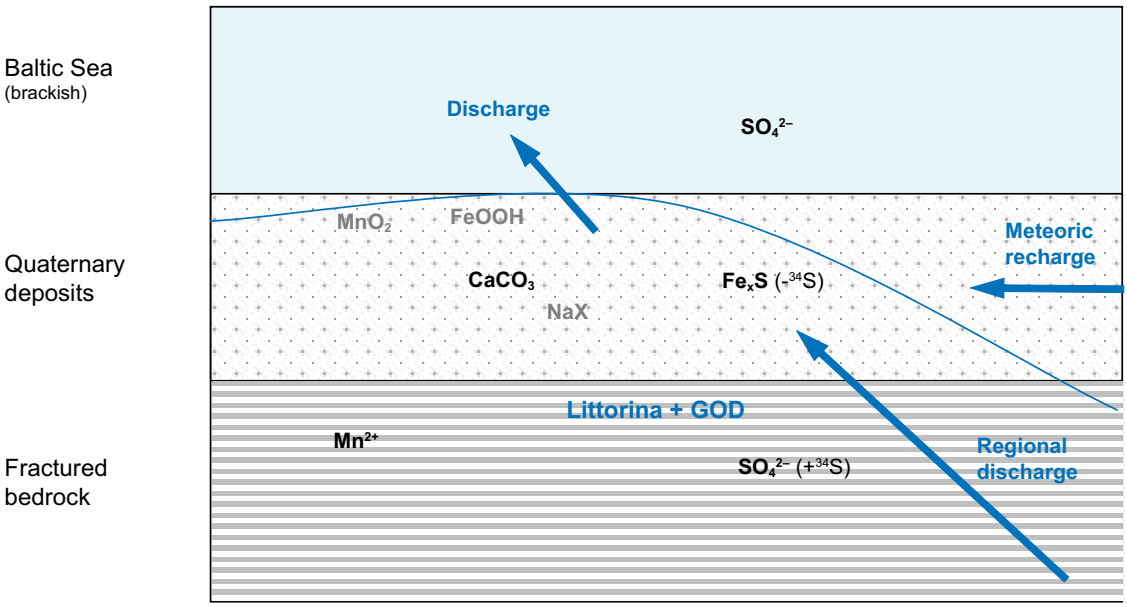

Figure 8-3. *Important characteristics of the hydrochemistry in different parts of the surface system in Forsmark during the period after the salinity maximum of the Littorina stage, until the first islands emerged from the sea (3,000–0 BC). Due to reduced salinity of the sea water, there was no longer any density-driven transport of sea water downwards. Instead, the dotted blue arrow indicates a potential regional discharge gradient, which may transport Littorina and GOD water types into the Quaternary deposits. Blue arrows mark the major groundwater flow regime in the Quaternary deposits in case of meteoric recharge from land. Constituents important for the understanding of the development of the hydrochemistry in the surface system and shallow groundwater are denoted by chemical abbreviations in the figure. Grey colour on text and arrows denote more uncertain assumptions.*

prevails in the bedrock at these occasions prerequisites exist, at least theoretically, for an upward flow of water from depth all the way up to the QD. The role of this phenomenon is currently being investigated and will be further addressed in the final hydrogeological description of modelling stage 2.3 /Werner et al. 2007, Follin et al. 2007b/.

The effective recharge into the lower parts of the QD and further down into the upper parts of the bedrock is probably low /Aneljung and Gustafsson 2007/, due to the low permeability of the till (the permeability is relatively high in the upper parts of the profile, and decrease gradually with depth to a very low permeability deeper down in the till profile). This may lead to a possibly slow washout of marine remnants from the time submerged under the Baltic Sea, and in areas with supposed low turnover, e.g. areas covered by low permeable clay layers, relict marine signatures should be more pronounced in the shallow groundwater, e.g. the area around Lake Gällsboträsket (cf Section 7.3).

When looking at the sulphur system in Figure 8-4, the aeration of the deposits by recharging meteoric water leads to oxidation of the sulphide minerals. This process is reflected in the surface system by the presence of SO_4 depleted in ^{34}S in the surface water and shallow groundwater (cf Section 4.1.2). As a rough estimation, at least one third of the sulphur that discharges from the Forsmark area originates from sulphide minerals (cf Section 6.2.6). According to the scenario outlined in Section 8.2.2 these biogenic pyrites may either have been formed in the Littorina Sea sediments, or at a later stage in post-glacial sediments when smaller basins were isolated from the Baltic Sea. Clayey sediments are a significant sulphur source according to the mass-balance in Section 6.2.6. There are also some indications that there is a distributed sulphur source in the Forsmark area, not fully explained by atmospheric sulphur deposition, which may be explained by the presence of pyrites in the QD from the Littorina stage.

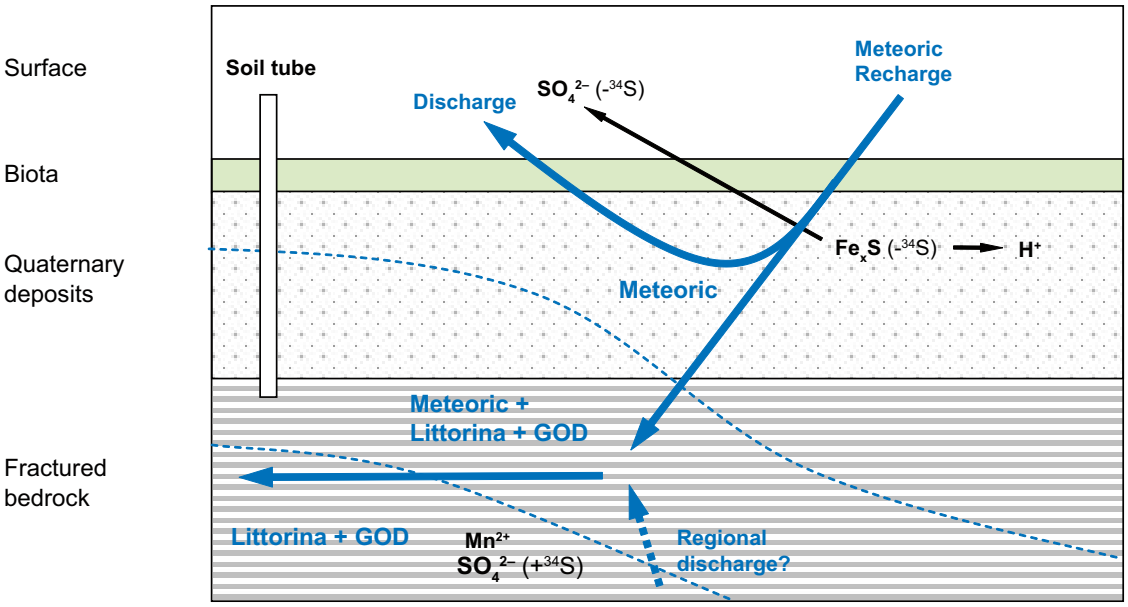

Figure 8-4. *The present situation in the Forsmark area regarding the sulphur system. Blue arrows mark the major groundwater flow regime in the Quaternary deposits and the fractured bedrock. Generalised water types are shown in blue text, together with dashed blue lines that mark the gradients between these water types. Constituents important for the understanding of the development of the hydrochemistry in the surface system and shallow groundwater are denoted by chemical abbreviations, whereas the direction of major processes and reactions are schematically marked by black arrows in the figure.*

In some shallow groundwater objects (e.g. the schematic soil tube in Figure 8-4), characterised by relict marine signatures regarding other major constituents, SO_4 enriched in ^{34}S is observed. Elevated Mn^{2+} concentrations are also observed in these objects, similar to what is observed in the relict marine groundwater (cf Sections 7.2 and 7.3). This pattern could be explained by influence from stagnant marine remnants (Littorina water and possibly also an older GOD mixture), as indicated in Figure 8-4. The occurrence of shallow groundwater objects with a clear relict marine signature (cf Section 3.2), found in areas characterised by clay layers with low permeability, may be interpreted as a "memory" of the past. These conditions have probably been created under a previous hydrological regime and are preserved because of the stagnant conditions in these areas.

The development of a biologically active layer and the accompanying supply of organic carbon to the QD also give prerequisites for drastic alterations in the hydrochemical conditions in the shallow groundwater. Concentrations of total organic carbon, TOC, in surface water and shallow groundwater in the Forsmark are high in a national perspective /Tröjbom and Söderbäck 2006/. Increased supply of H^+ ions, mostly derived from decomposition of biogenic carbon or oxidation of sulphide minerals (see Figure 8-4), is the ultimate driving force for weathering reactions that take place in the QD or bedrock.

The QD in the Forsmark area are also characterised by especially high contents of calcite ($CaCO_3$) /Tröjbom and Söderbäck 2006/, which in combination with rich supply of H^+ from organic carbon (cf Section 4.1.4) leads to an extensive dissolution of calcite in the till (cf Section 4.1.3) as outlined in the scenario in Figure 8-5. Calcite dissolution releases large amounts of Ca^{2+} ions into the shallow groundwater system.

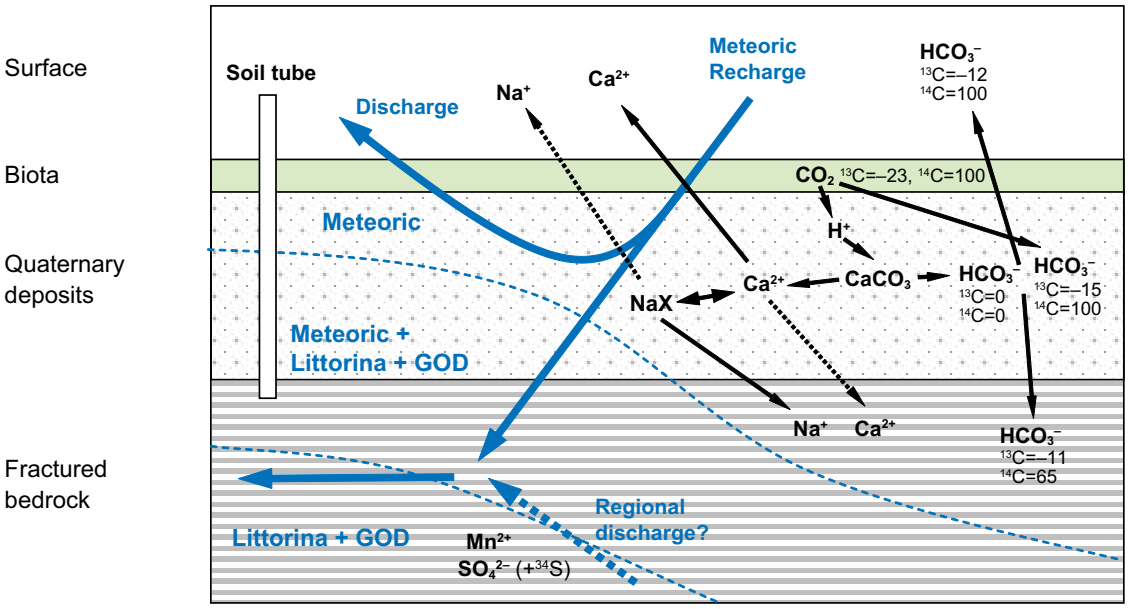

Figure 8-5. *The present situation in the Forsmark area regarding biogenic CO_2, calcite dissolution and ion exchange reactions in the Quaternary deposits. Blue arrows mark the major groundwater flow regime in the Quaternary deposits and the fractured bedrock. Generalised water types are shown in blue text, together with dashed blue lines that mark the gradients between these water types. Constituents important for the understanding of the development of the hydrochemistry in the surface system and shallow groundwater are denoted by chemical abbreviations, whereas the direction of major processes and reactions are schematically marked by black and dotted (minor importance) arrows in the figure.*

Some Ca^{2+} are discharged into streams and lakes through the local hydrological recharge/discharge patterns, and contribute to the forming of the Ca-rich oligotrophic hardwater lakes which are characteristic for the Forsmark area /Brunberg and Blomquist 1999/. The rich supply of Ca^{2+} ions is also an important prerequisite and driving force for an extensive cation exchange that seem to take place in the Quaternary deposits (cf Section 4.2.1). Na^{+} and other cations, released by e.g. weathering of rock minerals, exchange with Ca^{2+} and get into the solution. Groundwater with long residence time, e.g. groundwater that reaches down to the upper parts of the bedrock, may be considerably depleted in Ca^{2+} but enriched in e.g. Na^{+}, and shows therefore a more "mature" signature than groundwater found at more shallow depths. The supposed very low rate of recharge to the upper parts of the bedrock in the Forsmark area /Aneljung and Gustafsson 2007/, a consequence of the low permeable QD as described above, leads to a long groundwater residence time and consequently long time for processes as weathering and cation exchange to operate within the QD.

There are indications that Sr^{2+}, which is released during calcite dissolution, shows a fractionation pattern different from Ca^{2+}, due to the slightly different chemical properties of this ion. Cation exchange in the QD therefore discriminate between these ions, and a larger fraction of Sr^{2+} reaches the fractured bedrock, which is reflected by an altered Ca/Sr ratio evident in many non-brackish groundwater samples in the upper parts of the bedrock and also in some shallow groundwater objects in the deeper parts of the QD (cf Section 4.1.3). The interpretation of Sr is however complicated by the fact that this element is also derived from other sources than calcite, as other Sr-bearing minerals and sea water (cf Section 6.2.12).

HCO_3^-, mostly derived from hydration of biogenic CO_2 and dissolution of calcite in the QD, contributes significantly to the very high alkalinity observed in surface water and shallow groundwater in the Forsmark area (cf Section 4.1.4). The isotopic fractionation patterns of carbon in the surface water and shallow groundwater show important influence from biogenic CO_2, as well as clear contributions of carbon of calcite origin, according to the generalised picture outlined in Figure 8-5.

8.3 Conclusions concerning observations in the Forsmark area in relation to the conceptual model

The ongoing uplift after the latest glaciation, in combination with marine remnants from the past, are factors that have great impact on the present surface hydrochemistry observed in the Forsmark area.

Large-scale marine gradients in the surface system are consistent with the conceptual model described in previous section and the paleo-hydrological history; areas recently emerged from the Baltic Sea show stronger marine influences compared to areas located at higher altitude. Discharge from Lake Eckarfjärden, located at c 5 m absolute elevation (RT90) contain low concentrations marine ions, whereas Lake Gällsboträsket, which was more recently separated from the Baltic and now is located at c 2 m elevation, still show significantly elevated concentrations e.g. Na and Cl in discharge. At a smaller scale, for example in the area of Lake Bolundsfjärden and Lake Norra Bassängen, there are marine gradients among shallow groundwater sampling points, most probably reflecting different stages of washout of marine remnants by meteoric recharge.

In shallow groundwater in the Quaternary deposits below the lakes, more or less stagnant conditions have preserved relict marine signatures, even at relatively shallow depths. These signatures, which are generally found in the groundwater of the bedrock down to several hundred metres depth, reflects a trapped relict marine groundwater which may have entered the deposits from below when the area was covered by the Baltic Sea, according to the conceptual model. The possible presence of deep saline influences (shield brine) at these locations are difficult to explain without a vertical discharge gradient at any time during the paleo-hydrological history, especially as there are no hydrological indications of any deep discharge at present date (cf reservation in Section 8.2.4).

The marine signature in the soil tubes located in the Quaternary deposits below the lakes shows, similar to the marine influence in the discharge from the lakes, a topographical gradient which probably reflects the time for influence from meteoric recharge. Among these soil tubes, only a weak marine influence is observed in the soil tube SFM0015 below Lake Eckarfjärden, whereas SFM0023 below Lake Bolundsfjärden shows a typical relict marine signature and a salinity exceeding the present-day salinity of the Baltic Sea. In SFM0011, 12, and 13, located in the deposits below Lake Gällsboträsket, relict marine signatures are evident, but e.g. Cl concentrations are intermediate compared to soil tubes below Lake Eckarfjärden and Lake Bolundsfjärden. There are, however, exceptions from this general trend, which reflects the importance of the local recharge/discharge patterns; SFM0065, located in deposits below Lake Lillfjärden, at a similar setting as SFM0023, but adjacent to the present-day coastline, shows significantly lower concentrations of marine ions in combination with a meteoric recharge isotope signature. The presence of low permeable deposits as clay, such is the case for Lake Gällsboträsket, may be an important prerequisite governing the local recharge/discharge patterns.

SFM0025, located in Quaternary deposits below the present Baltic Sea, contain brackish groundwater diluted with meteoric recharge (cf water origin model in Section 3.3), but show, according to the ion source model in Section 3.2, possible influence from a deep saline (shield brine) signature. Perhaps the situation outlined in the conceptual model when the Forsmark area was covered by the Baltic Sea (cf Section 8.2.3) is applicable on this soil tube; meteoric recharge from the land nearby, mix with relict marine groundwater, which in turn show possible influence from a deep saline signature representing a deep discharge component.

The deep groundwater signature evident in shallow groundwater at some locations are most probably explained by relict remnants, not yet flushed out from the Quaternary deposits, according to the conceptual model and the present hydrological flow patterns. There is no clear evidence of deep groundwater discharge into the fresh surface system according to hydrochemical measurements in streams and lakes (however, due to dilution effects, a small potential discharge may not be detected, cf Section 4.3.1). Discharge from the catchment of Lake Gällsboträsket (PFM0069), show higher concentrations of most marine ions, which could be explained by the ongoing washout of marine remnants in the sediments according to the conceptual model (cf Section 8.2.4). In the ion source model (cf Section 3.2) there is, however, a weak indication of a slightly more deep signature in this stream, compared to the downstream sampling site PFM0068, which could be explained by washout of relict marine groundwater and deep saline remnants (the latter was included in the GOD mixture, cf Section 8.2.1 for an explanation of this abbreviation).

The only remaining potential source for supply of present deep saline groundwater components into the fresh surface system is man-induced artificial “discharge” in brackish groundwater wells. Two private wells drilled in the bedrock in the Forsmark area, as well as many of the percussion drilled boreholes in the SKB site investigation, show very clear relict marine and possibly also deep saline signatures according to the ion source model (PFM0009 and PFM0039, cf Section 4.3.2 and Figure 2-5).

9 References

Aitchison J, Greenacre M, 2002. Biplots for compositional data. Applied Statistics 51 (4), 375–392.

Andersson E, Sobek S, 2006. Comparison of a mass balance and an ecosystem model approach when evaluating the carbon cycling in a lake ecosystem. Ambio 35:8 p. 476–483.

Aneljung M, Gustafsson L-G, 2007. Sensitivity analysis and development of calibration methodology for near-surface hydrogeology model of Forsmark. SKB R-07-27. SvenskKärnbränslehantering AB.

Baxter D, Hannu S, Karlsson S, 2007. Analyses of biogenic silicon in sediment from Lake Eckarfjärden. SKB P-07-40. Svensk Kärnbränslehantering AB.

Boresjö Bronge L, Wester K, 2003. Vegetation mapping with satellite data of the Forsmark, Tierp and Oskarshamn regions. SKB R-03-83. Svensk Kärnbränslehantering AB.

Brunberg A-K, Blomquist P, 1999. Characteristics and ontogeny of oligotrophic hardwater lakes in the Forsmark area, central Sweden. SKB R-99-68. Svensk Kärnbränslehantering AB.

Brunberg A-K, Blomquist P, 2000. Post-glacial, land rise-induced formation and development of lakes in the Forsmark area, central Sweden. SKB TR-00-02. Svensk Kärnbränslehantering AB.

Brunberg A-K, Carlsson T, Blomquist P, Brydsten L, Strömgren M, 2004. Forsmark area – Identification of catchments, lake related drainage parameters and lake habitats. SKB P-04-25. Svensk Kärnbränslehantering AB.

Brydsten L, Strömgren M, 2004. Digital elevation models for site investigation programme in Forsmark. Site description version 1.2. SKB R-04-70. Svensk Kärnbränslehantering AB.

Clark I, Fritz P, 1997. Environmental Isotopes in Hydrogeology. Boca Raton, FL:CRC Press.

Fredén C (ed), 2002. Berg och jord. Sveriges nationalatlas. Tredje utgåvan. 208 pp.

Follin S, Johansson P-O, Levén J, Hartley L, Holton D, McCharty R, Roberts D, 2007a. Updated strategy and test of new concepts for groundwater flow modelling in Forsmark in preparation of site descriptive modelling stage 2.2. SKB R-07-20. Svensk Kärnbränslehantering AB.

Follin S, Levén J, Hartley L, Jackson P, Joyce S, Roberts D, Swift B, 2007b. Hydrogeological characterisation and modelling of deformation zones and fracture domains in Forsmark, stage 2.2. SKB R-07-48. Svensk Kärnbränslehantering AB.

Gómez J B, Laaksoharju M, Skårman E, Gurban I, 2006. M3 version 3.0: Concepts, methods, and mathematical formulation. SKB TR-06-27. Svensk Kärnbränslehantering AB.

Grimwall U, Stålnacke P, 1996. Statistical methods for source apportionment of riverine loads of pollutants. Environmentrics 7:201–213.

Göthberg A, Wahlman H, 2006. Inventory of vascular plants and classification of calcareous wetlands in the Forsmark area. Forsmark site investigation. SKB P-06-115. Svensk Kärnbränslehantering AB.

Hedenström A, 2004. Forsmark site investigation. Investigation of marine and lacustrine sediment in lakes – Stratigraphical and analytical data. SKB P-04-86. Svensk Kärnbränslehantering AB.

Hedenström A, Sohlenius G, in prep. Properties of the regolith at Forsmark. Site descriptive modelling, SDM-Site Forsmark. SKB R-08-XX. Svensk Kärnbränslehantering AB.

Ingemar T, Moreborg K, 1976. The leaching and original content of calcium carbonate in till in Northern Uppland, Sweden. Geol. Fören. Stockh. Förh. 98:120–132. (The Geological Society, Stockholm, Sweden).

Johansson P-O, Werner K, Bosson E, Berglund S, Juston J, 2005. Description of climate, surface hydrology, and near-surface hydrogeology. Forsmark 1.2. SKB R-05-06. Svensk Kärnbränslehantering AB.

Johansson P-O, Juston J, 2007. Forsmark site investigation. Monitoring of brook levels, water electrical conductivities, temperatures and discharges from April 2004 until March 2007. SKB P-07-135. Svensk Kärnbränslehantering AB.

Jonsell B, Jonsell L, 1995. Floran i Hållnäs socken. (Vasculan plants in the parish of Hållnäs, N Uppland, Sweden). Svensk Botanisk Tidskrift 89: 257–312.

Juston J, Johansson P-O, 2005. Analysis of meteorological data, surface water level data, and groundwater level data. Forsmark site investigation. SKB P-05-152. Svensk Kärnbränslehantering AB.

Juston J, Johansson P-O, Levén J, Tröjbom M, Follin S, 2006. Forsmark 2.1 Analysis of meteorological, hydrological and hydrogeological monitoring data. SKB R-06-49. Svensk Kärnbränslehantering AB.

Kendall C, McDonnell J, 2006. Isotope tracers in catchment hydrology. Amsterdam, Elsevier**.**

Kvarnäs H, 1997. Modellering av näringsämnen i Vätterns tillrinningsområde – Källfördelning och retention. Vätternvårdsförbundet, Rapport nr 46.

Laaksoharju M, Skårman C, Skårman E, 1999. Multivariate Mixing and Mass-balance (M3) calculations, a new tool for decoding hydrogeochemical information. Applied Geochemistry Vol. 14, #7, 1999, Elsevier Science Ltd. pp861–871.

Laaksoharju (ed.) in prep. Hydrochemistry Forsmark. Site descriptive modelling, SDM-Site. SKB R-08-XX. Svensk Kärnbränslehantering AB.

Lindborg T (ed.), 2005. Description of the surface systems, Forsmark area – version 1.2. SKB R-05-03. Svensk Kärnbränslehantering AB.

Löfgren A, Lindborg T, 2003. A descriptive ecosystem model – a strategy for model development during site investigations. SKB R-03-06. Svensk Kärnbränslehantering AB.

Löfgren S, 1990. Tillförsel av kväve och fosfor till vattendrag i Sveriges inland: underlagsrapport till Hav -90. Naturvårdsverket report 3692. (in Swedish)

Ludvigson J-E, 2002. Brunnsinventering i Forsmark. SKB R-02-17. Svensk Kärnbränslehantering AB. (in Swedish)

Naturvårdsverket, 2000. Environmental Quality Criteria – Lakes and water courses. Swedish Environmental Protection Agency Report 5050.

Naturvårdsverket, 2003. Åtgärder och kostnader för minskade fosforutsläpp från enskilda avlopp, industrier m.m. till sjön Glan : underlagsrapport (2) till Miljökvalitetsnormer för fosfor i sjöar redovisning av ett regeringsuppdrag. Swedish Environmental Protection Agency Report 5050.

Nilsson A-C, 2003a. Forsmark site investigation – Sampling and analyses of groundwater in percussion drilled boreholes and shallow monitoring wells at drillsite DS1 Results from the percussion boreholes HFM01, HFM02, HFM03, KFM01A (borehole section 0–100 m) and the monitoring wells SFM0001, SFM0002 and SFM0003. SKB P-03-47. Svensk Kärnbränslehantering AB.

Nilsson A-C, 2003b. Forsmark site investigation Sampling and analyses of groundwater in percussion drilled boreholes and shallow monitoring wells at drillsite DS2 Results from the percussion boreholes HFM04, HFM05, KFM02A (borehole section 0–100 m) and the monitoring wells SFM0004 and SFM0005. SKB P-03-48. Svensk Kärnbränslehantering AB.

Nilsson A-C, 2003c. Sampling and analyses of groundwater in percussion drilled boreholes at drillsite DS3. Results from the percussion boreholes HFM06 and HFM08. Forsmark site investigation. SKB P-03-49. Svensk Kärnbränslehantering AB.

Nilsson A-C, Borgiel M, 2005a. Sampling and analyses of near surface groundwaters. Results from sampling of shallow monitoring wells in soil, BAT pipes, a natural spring and private wells, May 2003–April 2005. SKB P-05-171. Svensk Kärnbränslehantering AB.

Nilsson A-C, Borgiel M, 2005b. Sampling and analyses of surface waters. Results from sampling in the Forsmark area, March 2004–June 2005. Forsmark site investigation. SKB P-05-274. Svensk Kärnbränslehantering AB.

Nilsson A-C, Karlsson S, Borgiel M, 2003. Forsmark site investigations – Sampling and analyses of surface waters – Results from sampling in the Forsmark area, March 2002 to March 2003. SKB P-03-27. Svensk Kärnbränslehantering AB.

Nordén S, Andersson E, Söderbäck B, in prep. The limnic ecosystems at Forsmark and Laxemar. Site descriptive modelling, SDM-Site. SKB R-08-XX. Svensk Kärnbränslehantering AB.

Nyman H, Hedenström A, Strömgren M, in prep. Depth and stratigraphy of regolith at Forsmark. Site descriptive modelling, SDM-Site Forsmark. SKB R-08-XX. Svensk Kärnbränslehantering AB.

Olofsson I, Simeonov, A, Stephens M, Follin S, Nilsson A-C, Röshoff K, Lindberg U, Lanaro F, Fredriksson A, Persson L, 2007. Site descriptive modelling Forsmark, stage 2.2. A fracture domain concept as a basis for the statistical modelling of fractures and minor deformation zones, and interdisciplinary coordination. SKB R-07-15. Svensk Kärnbränslehantering AB.

Rozanski K, Araguás-Araguás L, Gonfiantini R, 1993. Isotopic patterns in modern global precipitation. In: Continental Isotope Indicators of climate, American Geophysical Union Monograph.

Rönnback P, Åström M, in press[a]. Concentrations and fractionation patterns of rare earth elements in surface waters and ground waters in a granite and till environment. Accepted for publication in Applied Geochemistry.

Rönnback P, Åström M, in press[b]. Hydrochemical patterns of a small lake and a stream in an uplifting area proposed as a repository site for spent nuclear fuel, Forsmark, Sweden. Accepted for publication in Journal of Hydrology.

SKB, 2001. Site investigations. Investigation methods and general execution programme. SKB TR-01-29. Svensk Kärnbränslehantering AB.

SKB, 2005a. Forsmark site investigation. Programme for further investigations of geosphere and biosphere. SKB R-05-14. Svensk Kärnbränslehantering AB.

SKB, 2005b. Hydrogeochemical evaluation for Forsmark model version 1.2. Preliminary site description of the Forsmark area. SKB R-05-17. Svensk Kärnbränslehantering AB.

SKB, 2005c. Preliminary site description Forsmark area – version 1.2. SKB R-05-18. Svensk Kärnbränslehantering AB.

SKB, 2006. Hydrogeochemical evaluation of the Forsmark site, modelling stage 2.1 – issue report. SKB R-06-69. Svensk Kärnbränslehantering AB.

Sohlenius G, Hedenström A, Rudmark L, 2004. Mapping of unconsolidated Quaternary deposits 2002–2003. Map description. SKB R-04-39. Svensk Kärnbränslehantering AB.

Sonesten L, 2005. Chemical characteristics of surface waters in the Forsmark area. Evaluation of data from lakes, streams, and coastal sites. SKB R-05-41. Svensk Kärnbränslehantering AB.

Tröjbom M, Lindeström L, 2004. Ämnestransporter i Dalälven 1990–2003. Länsstyrelsen i Dalarna rapport 2004:22.

Tröjbom M, Söderbäck B, 2006. Chemical characteristics of surface systems in the Forsmark area. Visualisation and statistical evaluation of data from shallow groundwater, precipitation, and regolith. SKB R-06-19. Svensk Kärnbränslehantering AB.

Werner K, Johansson P-O, Brydsten L, Bosson E, Berglund S, Tröjbom M, Nyman H, 2007. Recharge and discharge of near-surface groundwater in Forsmark. Comparison of classification methods. SKB R-07-08. Svensk Kärnbränslehantering AB.

Åström M, Rönnback P, Submitted. Evidence of sulphide-oxidation products in a circumneutral stream in a boreal area recently risen above the sea level, Forsmark, Sweden. Submitted to Boreal Environment Research.

Web based references

EZ Profiler, 2007. EZ profiler 9.0 for ArcMap 9.x at http://arcscripts.esri.com

IMA, 2007. IMA, 2007. The national survey of Lakes and Streams at http://info1.ma.slu.se/db.html (accessed 2007-05-30).

TRK, 2007. Nitrogen and phosphorus load to the sea. Joint project of SMHI, SLU, and Swedish EPA. http://www-nrciws.slu.se/TRK/ (accessed 2007-05-30).

Voxler, 2006. Voxler Software version 1.0. at http://www.goldensoftware.com.

Database references

SKB GIS database, 2007. SDEADM.POS_FM_HOJ_4529. N-STH-SDEAPP. ArcSDE ver. 9.1, ESRI. Oracle9i Release 9.2.

Appendix A

Additional visualisation of the ion source model

The ion source model presented in Section **3.2**, including all observations from the cored boreholes based on data from data set A, and corrected flushing water content.

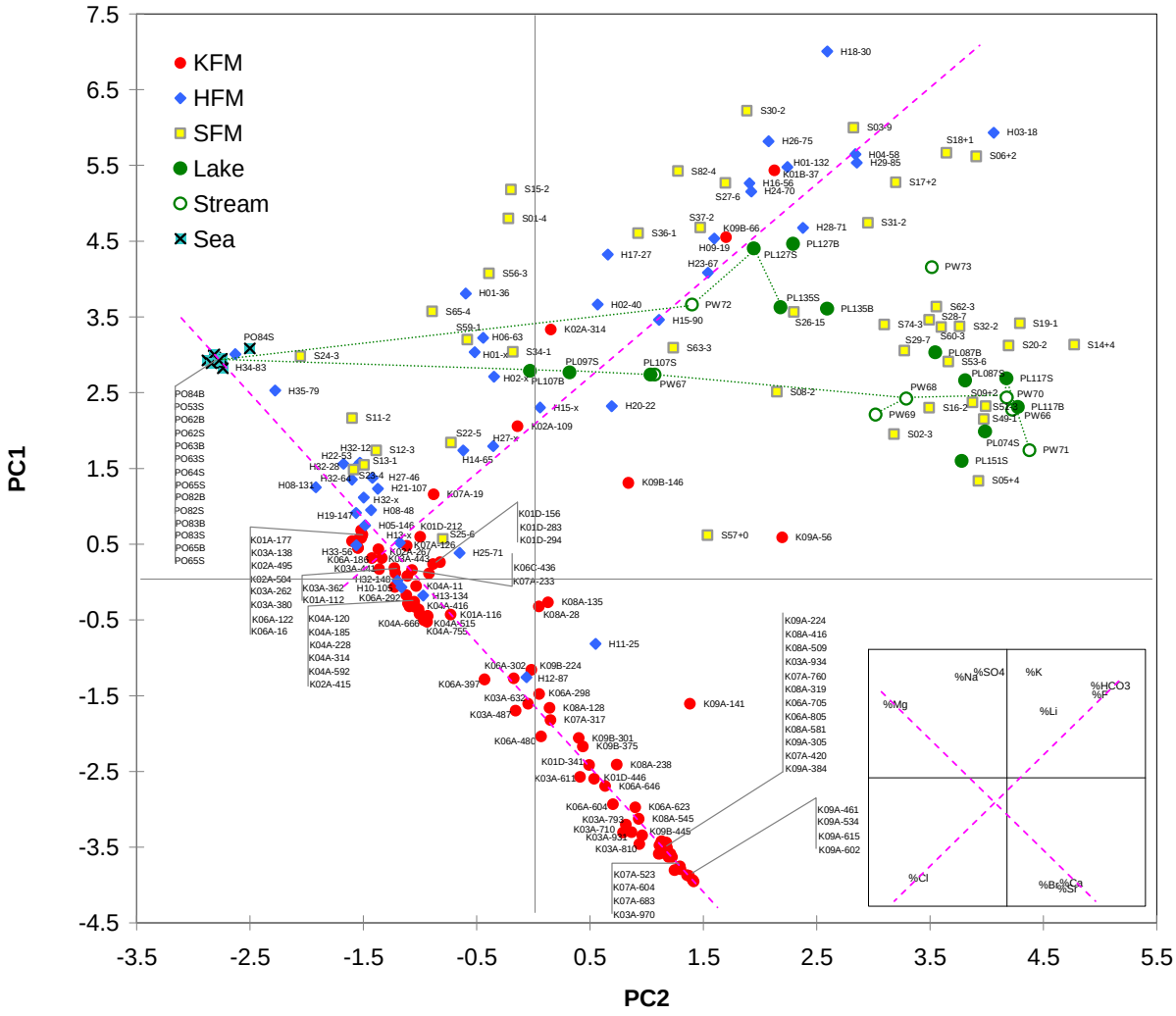

Appendix B

Compilations of hydrological data

Hydrological tables

Table B1. Statistics for the parameters used in the evaluation of hydrological properties in relation to hydrochemistry.

IDCODE	count	RDPO	Cl	Cl_cv	cond_cv	D_ss	DOC	DOC_cv	GWL	GWL_ss	HCO3_cv	O18_ss	ORP	ORP_ss	Ox	OX_ss	PH_ss	Rn222	SO4_cv	temp	temp_ss	Tr	Tr_ss
SFM0001	15	5	335,3	37,6	38,3	5,3	25,1	23,3	0,8	0,3	20,6	0,5	-58,2	47,2	0,9	1,1	0,2	27,8	23,7	6,7	1,3	11,4	2,9
SFM0002	12	1	63,7	56,3	18,4	4,1	14,7	8,9	0,9	0,2	5,5	0,2	-20,8	40,9	1,0	0,9	0,2	52,3	36,3	7,9	1,8	11,7	1,3
SFM0003	12	3	13,3	27,2	5,5	3,7	11,1	9,0	0,8	0,2	2,9	0,3	-30,8	45,7	0,6	0,6	0,1	18,3	18,1	6,7	0,4	14,6	5,1
SFM0005	7	1	9,5	56,2	12,2	3,9	11,0	15,4	2,0	0,3	15,7	0,5	103,7	63,9	3,5	1,8	0,5	74,9	29,2	4,9	1,7	11,3	0,5
SFM0006	6	1	41,9	40,0	17,6	2,7	14,2	9,5	2,1	1,2	10,9	0,2	122,7	33,8	7,7	3,1	0,1	7,7	27,8	5,3	1,0	10,1	1,6
SFM0008	9	1	121,5	71,5	18,6	3,1	6,5	20,8	3,2	0,6	10,0	0,1	58,9	35,6	1,6	2,0	0,1	30,1	16,9	6,3	1,0	10,4	1,1
SFM0009	9	5	8,8	40,6	15,4	2,5	15,3	10,5	0,9	0,2	9,9	0,2	127,3	66,0	2,2	1,8	0,1	40,0	62,6	6,9	1,6	11,7	0,7
SFM0012	10	5	2223,2	2,5	2,5	2,4	3,4	7,3	1,0	0,1	6,6	0,1	-57,8	51,7	0,9	1,1	0,1	64,6	5,4	8,6	1,4	2,7	4,2
SFM0015	11	5	314,2	9,1	2,1	2,0	8,7	5,6	0,5	0,1	3,2	0,2	-91,0	31,9	0,7	0,4	0,1	74,7	127,4	9,9	3,6	4,2	2,1
SFM0022	4	5	1176,8	14,0	2,5	3,5	5,2	10,2	1,0	0,1	7,9	0,0	0,8	150,3	3,3	2,5	0,0		16,6	9,2	2,4	1,3	0,4
SFM0023	12	5	3767,3	1,3	2,6	2,7	4,2	39,3	0,8	0,2	31,7	0,1	-159	51,3	2,3	2,6	0,3		4,6	10,2	4,5	3,7	3,0
SFM0024	3	5	1711,9	4,9	4,5	2,3	9,0	1,6	0,9	0,8	0,6	0,2	-88,0		0,4	0,3	0,2		5,8	12,7	6,2	10,2	4,7
SFM0025	9	5	1743,3	23,4	2,8	1,5	2,3	7,9	1,0	0,2	6,6	0,2	-50,5	53,9	0,9	1,1	0,1		13,4	9,1	1,4	8,1	3,0
SFM0027	9	5	62,4	2,9	1,6	2,5	6,1	13,7	1,0	0,4	22,2	0,2	16,2	101,0	1,3	0,6	0,1	163,0	3,6	7,6	2,4	10,7	1,2
SFM0029	8	5	22,8	50,4	5,9	2,0	7,8	8,1	0,9	0,2	4,1	0,3	18,8	48,2	0,9	0,9	0,1	12,1	6,5	7,1	1,2	11,9	1,2
SFM0031	8	5	8,9	17,7	4,2	2,3	8,4	15,9	1,7	0,5	4,1	0,4	50,5	58,4	3,8	1,8	0,1	88,8	3,9	6,8	2,7	12,0	1,2
SFM0032	13	5	25,4	25,2	4,3	3,0	18,2	11,3	1,2	0,3	3,3	0,4	-94,1	35,3	0,8	1,0	0,1	33,5	13,2	7,1	3,2	11,4	2,5
SFM0037	11	5	83,8	45,8	20,7	6,0	23,0	19,4	1,5	0,9	21,1	0,8	-69,7	50,8	0,7	0,8	0,1	31,0	25,0	6,8	3,4	12,2	1,4
SFM0049	9	5	15,7	17,6	6,9	4,9	18,1	5,5	1,8	0,2	9,4	0,9	-78,1	46,5	0,8	1,0	0,1	18,7	95,3	7,2	5,4	12,3	1,2
SFM0057	7	1	240,6	59,2	38,3	4,9	14,7	27,4	1,4	0,3	15,9	0,5	128,2	44,5	0,9	0,7	0,2	29,1	33,4	6,0	1,8	10,3	1,3
SFM0060	5	1	23,9	132,2	11,6	3,0	6,2	16,6	4,9	0,2	4,3	0,1	125,4	12,8	3,9	2,7	0,1	36,3	3,6	7,0	1,1	9,8	1,0

Table B2. Hydrological data for soil tubes in the Forsmark area. The original table also includes parameters describing the local topography at two different scales and a land-use classification (excluded here, c.f. /Werner et al. 2007/). Soil tubes marked by green are located in till below in lakes or sea.

IDCODE	Ground elevation or mean surface water level (RHB70)	Mean sceen elevation (RHB70)	Mean screen depth (m below ground or mean water level)	Mean groundwater elevation (RHB70)	Mean groundwater depth below ground (m)	Min groundwater elevation	Max groundwater depth below ground (m)	Max groundwater elevation	Min groundwater depth below ground (m)	Groundwater level amplitude (m)	Soil depth	Soil at screen depth	Site hydrology	Recharge/ Discharge area
SFM0001	0.95	-3.35	4.30	0.51	0.44	-0.48	1.44	0.87	0.08	1.35	4.80	Clayey sandy silty till	M	D
SFM0002	1.61	-2.69	4.31	1.23	0.38	0.16	1.45	1.57	0.05	1.41	4.80	Sandy till	F	R
SFM0003	1.46	-8.04	9.58	1.27	0.19	0.22	1.24	1.56	-0.10	1.34	10.20	Sand	FM	I
SFM0004	3.52	-1.38	4.92	2.93	0.59	2.17	1.36	3.47	0.05	1.31	5.10	Till	F	R
SFM0005	5.99	4.09	1.91	4.82	1.17	4.28	1.71	5.41	0.58	1.13	2.10	Sandy till	F	R
SFM0006	5.75	2.58	3.31	4.52	1.23	2.78	2.97	5.32	0.44	2.53	3.40	Till	F	R
SFM0007	6.60	1.95	4.65	<1,10			>5,50	<1,10			5.50	Till	F	R
SFM0008	3.36	-1.87	5.24	0.45	2.91	-0.25	3.61	1.45	1.91	1.70	5.50	Clayey sandy till	F	R
SFM0009	4.34	2.13	2.20	3.97	0.37	3.21	1.13	4.40	-0.06	1.19	2.50	Clayey till	FM	D
SFM0010	13.24	12.04	1.20	12.59	0.64	11.44	1.80	13.19	0.05	1.75	1.60	Clayey sandy silty till	M	I
SFM0011	2.00	-1.35	3.35	1.93	0.07	1.46	0.54	2.18	-0.18	0.72	3.90	Sandy till	M	D
SFM0012	1.81	-2.94	4.75	1.82	-0.01	1.62	0.18	2.06	-0.25	0.44	5.33	Till	Open water	D

SFM0013	3.68	-0.60	4.28	3.66	0.02	3.20	0.48	3.96	-0.28	0.76	4.60	Till	M, W	D
SFM0014	5.59	1.31	1.48	5.34	0.25	4.86	0.73	5.56	0.03	0.70	2.00	Till	M	D
SFM0015	5.27	-1.08	6.35	5.28	-0.01	5.06	0.21	5.43	-0.16	0.37		Till	Open water	D
SFM0016	5.22	-1.82	7.03	5.20	0.01	4.94	0.28	5.39	-0.18	0.46	7.20	Clayey sandy till	M	D
SFM0017	5.65	2.19	3.46	5.53	0.11	5.15	0.50	5.73	-0.08	0.58	4.00	Clayey sandy silty till	W	D
SFM0018	5.77	1.67	4.10	5.27	0.50	4.91	0.86	5.46	0.31	0.55	4.50	Clayey gravelly till	W	D
SFM0019	3.67	-0.23	3.90	3.17	0.50	2.08	1.59	3.59	0.08	1.51	4.80	Sandy till	F	R
SFM0020	1.67	-1.25	2.92	1.38	0.28	0.76	0.91	1.80	-0.13	1.04	3.20	Clayey sandy till	FM	I
SFM0021	1.43	-0.53	1.96	1.00	0.43	-0.33	1.76	1.45	-0.02	1.78	2.10	Clayey sandy till	FM	(D)
SFM0022	0.57	-4.06	4.63	0.55	0.02	0.40	0.17	0.68	-0.11	0.28		Sandy till	Open water	D
SFM0023	0.38	-3.35	3.73	0.35	0.03	-0.10	0.48	0.57	-0.19	0.67	4.40	Till	Open water	D
SFM0024	-0.04	-2.49	2.45	-0.07	0.03	-0.31	0.27	0.25	-0.29	0.56	2.40	Till	Open water	D
SFM0025	-0.04	-5.70	5.66	-0.12	0.08	-0.52	0.48	0.69	-0.73	1.21		Till	Open water	D
SFM0026	0.70	-14.82	15.51	0.85	-0.15	-0.34	1.04	1.79	-1.09	2.13	16.10	Till	W	D
SFM0027	1.05	-5.75	6.66								7.00	Silty till	M	D
SFM0028	0.22	-6.43	6.65	0.21	0.00	-0.61	0.83	0.88	-0.66	1.49	7.10	Clayey sandy till	W	D
SFM0029	0.21	-6.42	6.63	0.21	0.00	-0.61	0.82	0.88	-0.67	1.49	7.10	Clayey sandy till	W	D
SFM0030	1.67	-1.71	3.38	1.09	0.58	-0.94	2.61	1.78	-0.11	2.72	3.60	Clayey sandy till	M	D
SFM0031	1.74	-1.37	3.11	1.09	0.65	-0.94	2.68	1.78	-0.04	2.72	3.60	Clayey sandy till	M	D

SFM0032	0.57	-1.87	2.44	0.49	0.08	-0.63	1.20	0.81	-0.24	1.44	2.90	Till	W	D
SFM0033	0.53	-1.81	2.34	0.49	0.05	-0.63	1.17	0.81	-0.28	1.44	2.60	Till	W	D
SFM0034	0.67	-0.93	1.59	0.48	0.19	-0.06	0.73	0.86	-0.20	0.92	2.00	Sandy till	M, W	D
SFM0035	0.66	-1.01	1.67	0.48	0.18	-0.06	0.72	0.86	-0.20	0.92	2.30	Sandy till	M, W	D
SFM0036	0.62	-0.99	1.60	0.32	0.30	-0.80	1.42	0.84	-0.23	1.64	1.80	Sandy till	W	D
SFM0037	0.60	-1.00	1.60	0.32	0.28	-0.80	1.40	0.84	-0.24	1.64	2.00	Sandy till	W	D
SFM0049	2.93	-0.47	3.40	2.31	0.62	1.79	1.14	2.65	0.28	0.86	3.90	Grusig Till	FM, M	D
SFM0057	4.27	0.86	3.41	3.55	0.72	2.74	1.53	4.34	-0.07	1.60	3.80	Till	FM	R
SFM0058	3.20	0.25	2.95	1.27	1.93	0.56	2.64	2.46	0.74	1.90	3.50	Till	F	R
SFM0059	4.03	-0.85	4.98	0.09	3.94	-0.13	4.16	0.67	3.36	0.80	5.30	Sand, gravel	F	R
SFM0060	4.26	-2.19	6.45	0.00	4.26	-0.19	4.45	0.54	3.72	0.73	7.00	Gravel, stone	D	R
SFM0061	4.33	-1.13	5.46	0.00	4.33	-0.19	4.52	0.54	3.79	0.73	6.50	Gravel, stone	D	R
SFM0062	0.38	-2.27	2.65	0.46	-0.08	0.20	0.18	0.71	-0.33	0.51		Sandy till	Open water	D
SFM0063	0.38	-2.19	2.57									Sandy till	Open water	D
SFM0065	0.13	-3.68	3.81	0.05	0.08	-0.45	0.58	0.47	-0.34	0.92		Clayey sandy till	Open water	D
SFM0067	2.11	1.04	1.07				2.11		2.11			Till	M	D
SFM0068	1.61	0.77	0.84				1.61		1.61			Till	FM	(D)
SFM0069	1.87	1.00	0.87				1.87		1.87			Sandy gravel	M	D
SFM0070	3.26	1.54	1.72				3.26		3.26			Clayey sandy silty till	F	R
SFM0071	3.29	-1.90	5.19				3.29		3.29			Clayey till	F	R

SFM0072	3.27	-5.31	8.58				3.27		3.27			Clayey sandy silty till	F	R
SFM0073	0.23	-3.37	3.60				0.23		0.23			Till	W	D
SFM0074	0.52	-6.53	7.05				0.52		0.52			Silty till	W	D
SFM0075	3.27	-4.38	7.65				3.27		3.27			Silty till	F	R
SFM0076	3.37	1.82	1.55	1.62	1.75	1.31	2.06	1.79	1.58	0.48	2.37	Till	F	R

Site hydrology: D=dry, F=fresh, FM=fresh/moist, M=moist, W=wet

Recharge/discharge classification: D=discharge, (D)=probable discharge, I=varying, (R)=probable recharge, R=recharge

Appendix C

Evaluation of correlations among hydrological parameters

Text in Swedish. This appendix describes the correlation structure among the hydrological parameters presented in Appendix B, Table B2.

Fysikaliska underlagsdata

Per-Olof Johansson har sammanställt en matris som sammanfattar en mängd olika fysikaliska egenskaper för jordrören i Forsmark (RechargeDischargeField060314MT.xls). I matrisen ingår hydrologiska parametrar som speglar grundvattenhydrologin och omgivningsfaktorer som speglar närområdet, t ex markanvändning, lokal topografi, jordart vid intagssil etc.

Flera parametrar som utgörs av diskreta klasser har gjorts om till numeriska variabler för att de skall kunna ingå i analysen tillsammans med övriga numeriska variabler. Detta gäller till exempel markfuktighet som klassats på en skala från fuktig till torr, eller 'local topography', som baserat på DEM:en, klassar den lokala topografin från topp till sänka. Även den av P.O Johansson subjektiva bedömningen som klassar 'recharge/discharge' på en femgradig skala (recharge, probable recharge, varying, probable discharge, discharge) ingår i utvärderingen som en numerisk parameter.

Sammanlagt ingår data från 56 jordrör i Forsmark. De olika parametrarna sammanfattas i tabell 1.

Tabell 1. Sammanställning av de förkortningar som används för de fysikaliska parametrarna.

AQT	1-3 (confined)	Aquifer type (numerical)
B%100	%	Built up area (%) (100 x 100 m)
B%20	%	Built up area (%) (20 x 20 m)
F%100	%	Forest % (100 x 100 m)
F%20	%	Forest % (20 x 20 m)
GEL	m	Ground elevation or mean surface water level (RHB70)
GLA	m	Groundwater level amplitude (m)
LT100	1 (peak) – 10	Local topography (100 x 100 m) (numerical)
LT20	1 (peak) – 10	Local topography (20 x 20 m) (numerical)
MaGD	m	Max groundwater depth below ground (m)
MaGE	m (absolut RHB70)	Max groundwater elevation
MGD	m	Mean groundwater depth below ground (m)
MGE	m (absolut RHB70)	Mean groundwater elevation (RHB70)
MiGD	m	Min groundwater depth below ground (m)
MiGE	m (absolut RHB70)	Min groundwater elevation
MSD	m	Mean screen depth (m below ground or mean water level)
MSE	m (absolut RHB70)	Mean screen elevation (RHB70)
O%100	%	Open land (100 x 100 m) %
O%20	%	Open land (20 x 20 m) %
RDPO	1(rech.) – 5 (disch.)	Recharge/Discharge area (numerical)
SCD	1(grov) -5 (fin)	Soil at screen depth (numerical)
Shyd	1 (dry) – 6 (wet)	Site hydrology (numerical)
SOD	m	Soil depth
SWD	m	If influence by surface water distance m
W%20	%	Water (%) (20 x 20 m)
W&100	%	Water (%) (100 x 100 m)

Korrelationer bland de fysikaliska parametrarna

Med en principalkomponentanalys undersöktes hur de fysikaliska parametrarna samvarierar och hur de förhåller sig till klassningen av jordrören i ”recharge-discharge” egenskaper. Samtliga parametrar var centrerade och skalade till samma varians vilket innebär att de ges samma vikt vid analysen.

I figurerna 1-2 nedan redovisas de fyra första principalkomponenterna som tillsammans förklarar 70% av den totala variationen hos de fysikaliska parametrarna. De två första komponenterna fångar tillsammans upp cirka 50% av variationen i materialet medan principalkomponenterna 3 och 4 fångar upp sammanlagt ytterligare cirka 20% av variationen.

Principalkomponenterna som beskrivs nedan är underliggande faktorer som var och en är olika starkt kopplade till de olika parametrarna. Idealt har principalkomponenterna en verklig innebörd genom att de speglar någon grundläggande egenskap som påverkar ett antal variabler i en viss riktning. Genom att studera hur de olika parametrarna förhåller sig till principalkomponenterna får man en uppfattning om korrelationsmönstren mellan de olika variablerna (’loading plot’). Genom att studera hur observationerna (jordrören) förhåller sig till principalkomponenterna får man också en uppfattning om hur dessa relaterar till varandra (’score plot’). Jämförs ’loading’-figuren med motsvarande ’score’-figur får man en uppfattning om vilka observationer som har stor inverkan på respektive principalkomponent och man kan dra slutsatser hur de olika observationerna inverkar på variablerna.

Den *första principalkomponenten,* som fångar upp 31% av variationen i materialet, är starkast positivt korrelerad med parametrarna som beskriver lokal topografi (LT20 och LT100), markfuktighet (’site hydrology’), akviferens slutenhet (AQT) samt klassningen i recharge/discharge (RDPO). Negativt korrelerad till denna parameter är grundvattenytans djup relativt mark (MGD, MaGD, MiGD) enligt figur 1.

Jordrören som är lokaliserade i sjöarna uppvisar höga värden för dessa variabler, dvs lokal topografi, markfuktighet mm, samtidigt som grundvattenytan ligger nära markytan (låga värden på MGD mfl). Motsatsen till ”sjörören”, m a p principalkomponent 1, är de jordrör som är belägna på Börstilsåsen, samt några jordrör som ligger på lokala maxima (SFM0005 och SFM0006). Den subjektiva klassningen i recharge-discharge (RDPO) är också starkast korrelerad till principalkomponent 1.

Principalkomponent 2 speglar främst en regional topografisk gradient från lågt till högt (höga värden på MGE, MiGE och MaGE). Omvänt korrelerade till dessa parametrar är bland annat ’Soil depth’ (SOD) och intagssilens djup relativt jordytan (MSD). Komponenten speglar således att jordlagren är mäktigare i de lägre liggande delarna av området. Kopplingen mellan denna komponent och klassningen i recharge/discharge är svag.

Principalkomponent 3 som speglar motsättningen mellan öppen mark och skog, visar svag koppling till klassningen i recharge/discharge enligt figur 2.

Grundvattenytans amplitud (GLA) är korrelerad till *principalkomponent 4.* Störst är amplituden i SFM0026 och SFM0011 och lägst i SFM0062, 63, 65, 12. Andelen vatten i närområdet är negativt korrelerad till GLA, vilket innebär att amplituden är låg i ett antal jordrör som ligger i nära anslutning till vatten (höga värden på W%100 och W%20). Klassningen i recharge/discharge (RDPO) visar svag koppling till denna komponent.

Sammanfattande slutsatser

- Klassningen i recharge/discharge (RDPO) är tydligt korrelerad till lokal topografi och markfuktighet. Samtidigt är endast cirka 30% av den totala variationen hos de undersökta variablerna kopplade till denna parameter.

- Kopplingen mellan de absoluta höjdparameterarna (MGE, MiGE, MaGE och MSE) och klassningen i recharge/discharge är svag, vilket troligen är en effekt av att de lokala strömningsmönstren dominerar i området.

- Den subjektiva fältklassningen ’site hydrology’ (Shyd) är starkt korrelerad till den objektiva klassningen ’local topography’ (LT20 och LT100).

- Grundvattenytans amplitud är tenderar att vara negativt kopplad till andelen vatten i närområdet

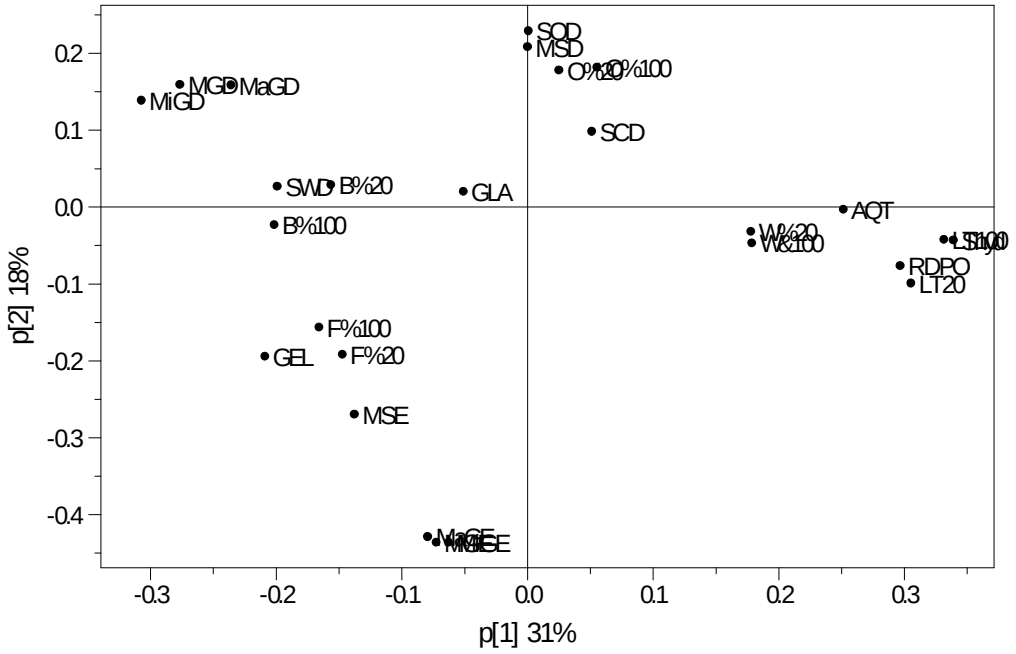

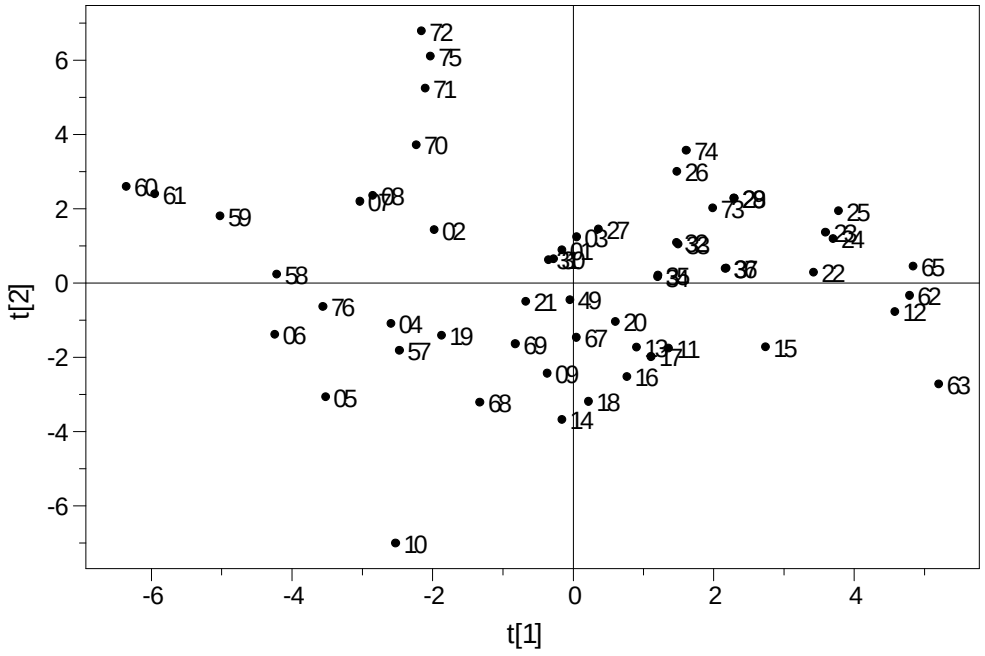

Figur 1. Första och andra principalkomponenterna som tillsammans beskriver cirka 50% av variationen i materialet. Överst 'loading plot' som beskriver hur de olika parametrarna förhåller sig til varandra med avseende på de två första principalkomponenterna. Nederst 'score plot' som visar jordrörens koppling till dessa komponenter. Endast de två sista siffrorna i idkoderna SFM00XX visas i figuren. Observationerna i det nedre diagrammet uppvisar höga värden för de parametrar som ligger i motsvarande position i det övre diagrammet. Parametrar och objekt som ligger på motstående sidor om origo är omvänt korrelerade med avseende på dessa komponenter.

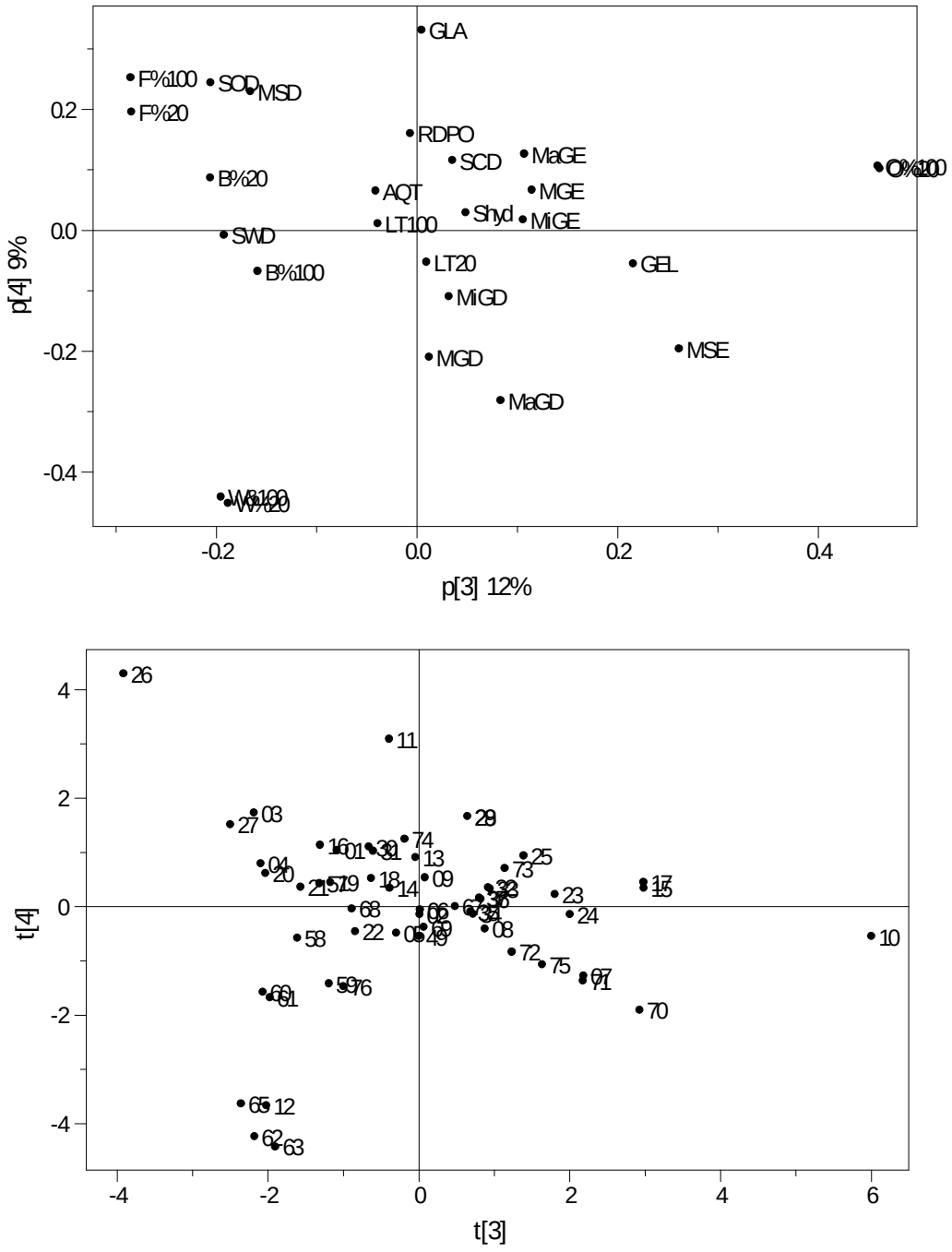

Figur 2. Tredje och fjärde principalkomponenterna som tillsammans beskriver cirka 50% av variationen i materialet. Överst 'loading plot' som beskriver hur de olika parametrarna förhåller sig till varandra med avseende på de två första principalkomponenterna. Nederst 'score plot' som visar jordrörens koppling till dessa komponenter. Endast de två sista siffrorna i idkoderna SFM00XX visas i figuren. Observationerna i det nedre diagrammet uppvisar höga värden för de parametrar som ligger i motsvarande position i det övre diagrammet. Parametrar och objekt som ligger på motstående sidor om origo är omvänt korrelerade med avseende på dessa komponenter

PLS-modell för recharge/discharge-klassning

För att undersöka hur stor del av variationen i RDPO-parametern som kan förklaras av några av de starkast korrelerade fysikaliska parametrarna gjordes en PLS-modell (se förklaring under avsnittet som beskriver kopplingen mellan fysikaliska och kemiska variabler). Enligt PCA-analysen är dessa Shyd (’site hydrology’), LT100 (’local topography’ 100x100m), MGD (’mean groundwater depth’).

Med en enkel PLS-modell baserad på en signifikant komponent går det att beskriva 70% av variationen i parametern RDPO med hjälp av parametrarna Shyd, LT100 och MGD enligt figur 3. Jordrören SFM0002, 19 och 57, som är inringade med blått, är svaga outliers i modellen.

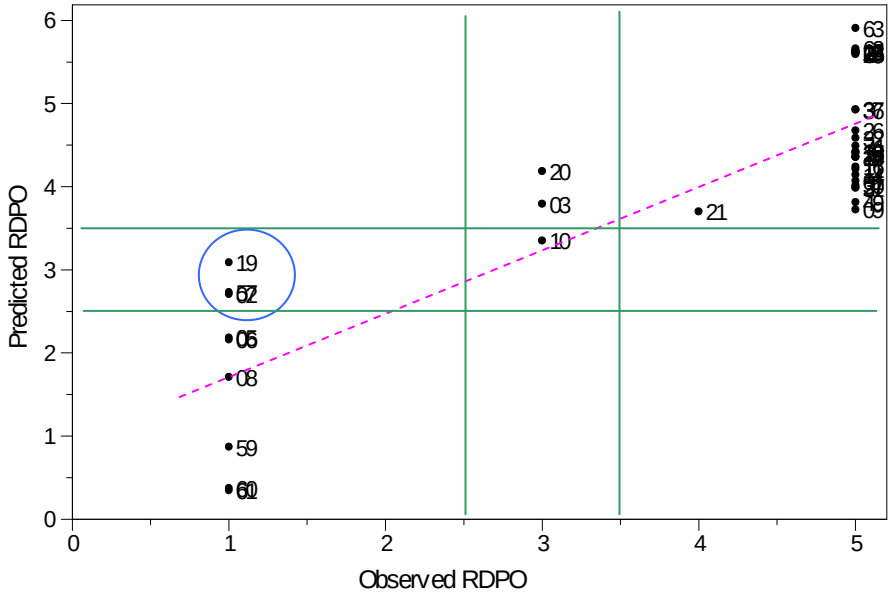

Figur 3. RDPO uppskattat med PLS-modellen utifrån parametrarna Shyd, LT100 och MGD avsatt mot observerad RDPO. PLS-modellen beskrivs av följande samband: RDPO=0.372*Shyd+0.213*LT100-0.395*MGD+1.26.

Eftersom RDPO är en diskret parameter radar de modellerade värdena upp sig vid heltalsvärdena. De gröna linjerna avgränsar den intermediära klassen ’varying’, dvs varierande recharge/discharge egenskaper.

Av de jordrör som klassats som ’recharge’ (1) klassar modellen merparten i klass 1 eller klass 2 , dvs ’recharge’ eller ’probable recharge’. Undantaget är SFM0002, 19 och 57 som hamnar i klassen ’varying’ (3).

Samtliga jordrör som klassats som ’probable discharge’ (4) eller ’dicharge’ (5) klassas av modellen i samma klasser.

Sammanfattningsvis kan man konstatera att PLS-modellen verkar modellera RDPO-parametern relativt väl utifrån parametrarna ’site hydrology’ (Shyd), ’local topography’ (LT100) och ’mean groundwater depth’ (MGD). Att sambandet är så starkt beror främst på att dessa parametrar utgjort underlag vid den subjektiva klassningen i recharge-discharge (RDPO). PLS-modellen kan därmed ses som ett empiriskt samband som sammanfattar denna subjektiva process.

Appendix D

Spatial distribution of regolith, land-use and vegetation classifications

Table D1. Compilation of original and aggregated classes of regolith, land-use and vegetation classifications.

Regolith classification

VBX-VI class	Original code	Description
jClay	J6	Gyttja
jClay	J16	Lergyttja--gyttjelera
jClay	J17	Postglacial lera, ospecificerad
jClay	J40	Glacial lera, ospecificerad
jClay	J416	Lergyttja--gyttjelera med tunt ytlager av torv
jClay	J440	Glacial lera, ospecificerad med tunt ytlager av torv
jClay	J9401	Glacial lera, ospecificerad med tunt ytlager av svallsediment, sand
jClay	J9402	Glacial lera, ospecificerad med tunt ytlager av svallsediment, grus
jClay	J9405	Glacial lera, ospecificerad med tunt ytlager av postglacialt sediment, lergyttja--gyttjelera
jClay	J9406	Postglacial lera, ospecificerad med tunt ytlager av postglacialt sediment, lergyttja--
jPeat	J1	Torv; mosse
jPeat	J5	Torv; kärr
jRock	J890	Urberg
jRock	J4111	Urberg; med tunt ytlager av morän, sandig
jRock	J4112	Urberg; med tunt ytlager av torv
jRock	J4113	Urberg; med tunt ytlager av svallsediment, sand
jSand	J29	Postglacial mellansand--grovsand
jSand	J30	Svallsediment, sand
jSand	J32	Postglacialt grus
jSand	J33	Svallsediment, grus
jSand	J34	Svallsediment, sten--block (klapper)
jSand	J92	Sten--block (glacial och postglacial)
jSand	J290	Fyllning pä okänt underlag
jSand	J429	Postglacial mellansand--grovsand med tunt ytlager av torv
jSand	J430	Svallsediment, sand med tunt ytlager av torv
jSand	J432	Postglacialt grus med tunt ytlager av torv
jSand	J433	Svallsediment, grus med tunt ytlager av torv
jSand	J9403	Svallsediment, sand med tunt ytlager av postglacialt sediment, lergyttja--gyttjelera
jTill	J50	Isälvssediment, grovsilt--block
jTill	J59	Morän pä isälvssediment, grovsilt--block
jTill	J94	Morän, lerig sandig
jTill	J95	Morän, sandig
jTill	J96	Morän, lerig sandig-siltig
jTill	J495	Morän, sandig; med tunt ytlager av torv
jTill	J496	Morän, lerig sandig-siltig; med tunt ytlager av torv
jTill	J9487	Morän, lerig sandig-siltig; med tunt ytlager av svallsediment, sand
jTill	J9489	Morän, sandig; med tunt ytlager av svallsediment, sand
jTill	J9490	Morän, sandig; med tunt ytlager av postglacialt sediment, lergyttja--gyttjelera
jTill	J9491	Morän, sandig; med tunt ytlager av glacial lera, ospecificerad
jWater	J91	Vatten

Land-use classification

VBX-VI class	Original code	Description
mArable	Ma4	Åker
mClear	Ma6	Hygge
mForest	Ma2	Skog, barr- och blandskog
mForest	Ma19	Lövskog
mHard	Ma14	Låghusbebyggelse
mHard	Ma15	Industriområde
mOpen	Ma5	Annan öppen mark
mOpen	Ma17	Annan öppen mark utan skogskontur

mWater	Ma1	Vattenyta

Vegetation classification

VBX-VI class	Original code	Description
x	Veg0	Information saknas
x	Veg1	Oklassificerad
vClear	Veg45	Äldre hyggen, sly/ängsartat frodigt
vClear	Veg46	Äldre hyggen, ringa återväxt/block, stenar
vClear	Veg50	Nya hyggen ej hygge -89
vForest	Veg11	Äldre gran, frisk-fuktig
vForest	Veg12	Yngre gran, frisk-fuktig
vForest	Veg13	Äldre tall, frisk-fuktig
vForest	Veg14	Yngre tall, frisk-fuktig
vForest	Veg21	Björkdominerad skog
vForest	Veg26	Askdominerad skog
vForest	Veg30	Blandskog barr-löv
vForest	Veg41	Granungskog
vForest	Veg42	Tallungskog
vForest	Veg43	Ospecificerad barrungskog
vForest	Veg44	Sly på hygge huvudsakl. björk
vHard	Veg92	Industri
vHard	Veg93	Låghus
vHard	Veg96	Övriga hårda ytor/grus etc
vOpen	Veg81	Odlad mark enligt topokarta
vOpen	Veg82	Övrig öppen mark
vRock	Veg15	Hällmarkstallskog
vRock	Veg83	Kustklippor
vWater	Veg100	Vatten
vWet	Veg61	Grandominerad sankmark
vWet	Veg62	Talldominerad sankmark
vWet	Veg63	Björkdominerad sankmark
vWet	Veg64	Hygge på myr
vWet	Veg72	Frodig blöt myr
vWet	Veg74	Frodig fastmattemyr
vWet	Veg75	Frodig fastmattemyr med viden
vWet	Veg76	Frodig fastmattemyr med björk
vWet	Veg77	Vassdominerad torrare myr
vWet	Veg78	Vass/frodigare, ev. buskar
vWet	Veg79	Vassdominerad blötare myr

Table D2. Area per catchment of regolith classes described in Table D1.

Catchment	Regolith class					
	jWater km^2	jSand km^2	jPeat km^2	jRock km^2	jClay km^2	jTill km^2
AFM000095	0.029	0.048	0.249	0.230	0.142	2.036
AFM001100B	0.000	0.002	0.002	0.000	0.025	0.051
AFM001100A	0.017	0.010	0.161	0.046	0.030	0.849
AFM000096	0.015	0.000	0.007	0.004	0.000	0.079
AFM001099	0.028	0.001	0.173	0.172	0.007	0.708
AFM000094	0.015	0.055	0.160	0.099	0.248	1.565
AFM001103C	0.000	0.001	0.001	0.003	0.007	0.081
AFM000093	0.002	0.002	0.001	0.003	0.005	0.113
AFM000010B	0.000	0.001	0.002	0.017	0.025	0.187
AFM000010A	0.214	0.038	0.226	0.159	0.039	1.358
AFM001105	0.006	0.001	0.024	0.007	0.013	0.159
AFM001103B	0.000	0.009	0.004	0.029	0.080	0.625
AFM000089	0.023	0.017	0.003	0.008	0.064	0.368
AFM000088	0.005	0.025	0.000	0.004	0.005	0.100
AFM001104	0.015	0.038	0.000	0.008	0.027	0.304
AFM001103A	0.447	0.022	0.002	0.011	0.017	0.907
AFM000091	0.036	0.013	0.001	0.005	0.020	0.168
AFM000092	0.005	0.001	0.000	0.000	0.001	0.064
AFM001101	0.039	0.002	0.000	0.001	0.012	0.296
AFM000049	0.048	0.006	0.000	0.018	0.115	0.433
AFM001106	0.016	0.001	0.000	0.001	0.012	0.039
AFM000086	0.016	0.002	0.000	0.002	0.043	0.153
AFM000052B	0.000	0.001	0.000	0.012	0.004	0.618
AFM000052A	0.064	0.004	0.000	0.005	0.029	0.208
AFM000084	0.005	0.000	0.000	0.001	0.003	0.026
AFM000082	0.002	0.001	0.000	0.001	0.018	0.170
AFM000083	0.002	0.001	0.000	0.001	0.013	0.061
AFM001108	0.009	0.005	0.000	0.000	0.019	0.035
AFM001107	0.081	0.022	0.000	0.002	0.046	0.406
AFM001109	0.049	0.011	0.045	0.275	0.090	1.392
AFM001110	0.023	0.034	0.000	0.084	0.017	0.679
AFM001111	0.001	0.001	0.000	0.012	0.004	0.089
AFM001112	0.003	0.001	0.000	0.001	0.003	0.170
AFM001113	0.007	0.053	0.000	0.005	0.008	0.627
AFM001114	0.123	0.235	0.128	0.524	0.705	3.846
AFM001115	0.005	0.006	0.000	0.006	0.031	0.340
AFM000051	0.390	0.232	0.026	0.130	0.446	1.701

Table D3. Area per catchment of land-use classes described in Table D1.

Cachment	Landuse class					
	mWater km^2	mForest km^2	mClear km^2	mArable km^2	mOpen km^2	mHard km^2
AFM000095	0.025	2.124	0.273	0.037	0.275	0.000
AFM001100B	0.000	0.078	0.000	0.000	0.002	0.000
AFM001100A	0.015	0.760	0.177	0.000	0.160	0.000
AFM000096	0.010	0.084	0.000	0.000	0.010	0.000
AFM001099	0.023	0.678	0.088	0.000	0.296	0.005
AFM000094	0.016	1.895	0.002	0.000	0.228	0.000
AFM001103C	0.000	0.083	0.000	0.000	0.007	0.000
AFM000093	0.004	0.087	0.031	0.000	0.004	0.000
AFM000010B	0.000	0.135	0.076	0.013	0.009	0.000
AFM000010A	0.222	1.306	0.321	0.000	0.186	0.000
AFM001105	0.007	0.163	0.000	0.000	0.041	0.000
AFM001103B	0.000	0.568	0.144	0.000	0.033	0.000
AFM000089	0.026	0.340	0.048	0.000	0.070	0.000
AFM000088	0.005	0.112	0.000	0.000	0.022	0.000
AFM001104	0.022	0.279	0.000	0.000	0.091	0.000
AFM001103A	0.447	0.633	0.117	0.000	0.212	0.000
AFM000091	0.042	0.142	0.000	0.000	0.060	0.000
AFM000092	0.006	0.032	0.033	0.000	0.000	0.000
AFM001101	0.044	0.211	0.033	0.000	0.062	0.000
AFM000049	0.076	0.410	0.000	0.000	0.135	0.000
AFM001106	0.012	0.031	0.000	0.000	0.026	0.000
AFM000086	0.024	0.124	0.000	0.000	0.067	0.000
AFM000052B	0.000	0.262	0.000	0.266	0.107	0.000
AFM000052A	0.068	0.203	0.000	0.000	0.039	0.000
AFM000084	0.004	0.031	0.000	0.000	0.000	0.000
AFM000082	0.002	0.178	0.000	0.000	0.012	0.000
AFM000083	0.002	0.062	0.000	0.000	0.013	0.000
AFM001108	0.011	0.032	0.000	0.000	0.025	0.000
AFM001107	0.101	0.368	0.000	0.000	0.089	0.000
AFM001109	0.060	1.166	0.059	0.000	0.436	0.142
AFM001110	0.033	0.706	0.000	0.000	0.098	0.000
AFM001111	0.002	0.105	0.000	0.000	0.000	0.000
AFM001112	0.008	0.164	0.000	0.000	0.006	0.000
AFM001113	0.030	0.636	0.000	0.000	0.035	0.000
AFM001114	0.061	3.908	0.039	0.553	1.000	0.000
AFM001115	0.007	0.343	0.000	0.000	0.039	0.000
AFM000051	0.421	1.989	0.008	0.023	0.485	0.000

Table D4. Area per catchment of vegetation classes described in Table D1.

Catchment	Vegetation class							
	vWater km^2	vWet km^2	vRock km^2	vForest km^2	vClear km^2	vArable km^2	vOpen km^2	vHard km^2
AFM000095	0.025	0.192	0.040	1.707	0.455	0.035	0.137	0.000
AFM001100B	0.000	0.001	0.000	0.078	0.000	0.000	0.000	0.000
AFM001100A	0.015	0.182	0.021	0.834	0.051	0.000	0.000	0.011
AFM000096	0.010	0.019	0.006	0.066	0.000	0.000	0.000	0.003
AFM001099	0.023	0.135	0.057	0.580	0.109	0.000	0.000	0.185
AFM000094	0.016	0.228	0.052	1.711	0.122	0.000	0.013	0.000
AFM001103C	0.000	0.007	0.006	0.078	0.000	0.000	0.000	0.000
AFM000093	0.004	0.004	0.004	0.114	0.000	0.000	0.000	0.000
AFM000010B	0.000	0.000	0.005	0.187	0.018	0.013	0.009	0.000
AFM000010A	0.221	0.120	0.066	1.280	0.253	0.000	0.093	0.000
AFM001105	0.007	0.038	0.006	0.157	0.000	0.000	0.003	0.000
AFM001103B	0.000	0.047	0.025	0.644	0.029	0.000	0.000	0.000
AFM000089	0.026	0.084	0.003	0.360	0.011	0.000	0.000	0.000
AFM000088	0.005	0.022	0.000	0.112	0.000	0.000	0.000	0.000
AFM001104	0.022	0.094	0.001	0.266	0.009	0.000	0.000	0.000
AFM001103A	0.448	0.239	0.008	0.686	0.026	0.000	0.000	0.000
AFM000091	0.042	0.060	0.006	0.136	0.000	0.000	0.000	0.000
AFM000092	0.006	0.000	0.003	0.062	0.000	0.000	0.000	0.000
AFM001101	0.044	0.073	0.006	0.226	0.000	0.000	0.000	0.000
AFM000049	0.076	0.132	0.000	0.408	0.000	0.000	0.006	0.000
AFM001106	0.012	0.026	0.000	0.031	0.000	0.000	0.000	0.000
AFM000086	0.024	0.074	0.000	0.117	0.000	0.000	0.000	0.000
AFM000052B	0.000	0.000	0.000	0.247	0.013	0.266	0.107	0.000
AFM000052A	0.068	0.040	0.000	0.201	0.001	0.000	0.000	0.000
AFM000084	0.004	0.000	0.000	0.031	0.000	0.000	0.000	0.000
AFM000082	0.002	0.012	0.000	0.178	0.000	0.000	0.000	0.000
AFM000083	0.002	0.013	0.000	0.062	0.000	0.000	0.000	0.000
AFM001108	0.012	0.024	0.000	0.032	0.000	0.000	0.000	0.000
AFM001107	0.102	0.075	0.000	0.364	0.000	0.000	0.017	0.000
AFM001109	0.057	0.202	0.141	1.069	0.013	0.000	0.000	0.381
AFM001110	0.033	0.077	0.103	0.608	0.016	0.000	0.000	0.000
AFM001111	0.002	0.000	0.011	0.095	0.000	0.000	0.000	0.000
AFM001112	0.008	0.006	0.003	0.161	0.000	0.000	0.000	0.000
AFM001113	0.034	0.034	0.017	0.616	0.000	0.000	0.000	0.000
AFM001114	0.068	0.944	0.100	3.556	0.093	0.553	0.247	0.000
AFM001115	0.008	0.050	0.011	0.319	0.001	0.000	0.000	0.000
AFM000051	0.422	0.464	0.042	1.832	0.027	0.023	0.115	0.000

Table D5. Area per catchment of topographical elevation classes described in Table D1.

Catchment	Topographical elevation class						
	0-2m km^2	2-4m km^2	4-6m km^2	6-8m km^2	8-10m km^2	10-15m km^2	>15m km^2
AFM000095	0.000	0.000	0.082	0.533	0.399	0.703	1.017
AFM001100B	0.000	0.000	0.000	0.041	0.025	0.013	0.002
AFM001100A	0.000	0.163	0.238	0.242	0.223	0.109	0.137
AFM000096	0.029	0.056	0.015	0.003	0.000	0.000	0.000
AFM001099	0.037	0.059	0.422	0.306	0.225	0.039	0.000
AFM000094	0.051	0.434	0.278	0.180	0.195	0.798	0.206
AFM001103C	0.003	0.036	0.030	0.018	0.004	0.000	0.000
AFM000093	0.000	0.026	0.046	0.048	0.005	0.000	0.000
AFM000010B	0.000	0.000	0.000	0.057	0.075	0.101	0.000
AFM000010A	0.000	0.097	0.229	0.368	0.422	0.815	0.103
AFM001105	0.000	0.054	0.077	0.053	0.020	0.006	0.000
AFM001103B	0.000	0.461	0.139	0.066	0.035	0.044	0.000
AFM000089	0.157	0.180	0.130	0.015	0.000	0.000	0.000
AFM000088	0.048	0.041	0.047	0.003	0.000	0.000	0.000
AFM001104	0.152	0.199	0.040	0.000	0.000	0.000	0.000
AFM001103A	0.878	0.370	0.137	0.024	0.001	0.000	0.000
AFM000091	0.112	0.069	0.056	0.007	0.001	0.000	0.000
AFM000092	0.011	0.026	0.031	0.004	0.000	0.000	0.000
AFM001101	0.185	0.128	0.034	0.003	0.000	0.000	0.000
AFM000049	0.251	0.219	0.094	0.044	0.012	0.001	0.000
AFM001106	0.062	0.004	0.001	0.000	0.000	0.000	0.000
AFM000086	0.188	0.023	0.004	0.001	0.000	0.000	0.000
AFM000052B	0.007	0.217	0.248	0.143	0.018	0.000	0.000
AFM000052A	0.162	0.019	0.076	0.052	0.001	0.000	0.000
AFM000084	0.016	0.015	0.003	0.000	0.000	0.000	0.000
AFM000082	0.099	0.016	0.041	0.035	0.000	0.000	0.000
AFM000083	0.048	0.027	0.002	0.000	0.000	0.000	0.000
AFM001108	0.047	0.012	0.008	0.001	0.000	0.000	0.000
AFM001107	0.265	0.078	0.147	0.060	0.002	0.000	0.000
AFM001109	0.457	0.822	0.363	0.139	0.067	0.006	0.000
AFM001110	0.318	0.297	0.176	0.032	0.004	0.000	0.000
AFM001111	0.062	0.026	0.011	0.006	0.001	0.000	0.000
AFM001112	0.159	0.011	0.003	0.000	0.000	0.000	0.000
AFM001113	0.229	0.155	0.116	0.150	0.034	0.000	0.000
AFM001114	1.708	1.537	1.160	0.611	0.428	0.092	0.000
AFM001115	0.203	0.089	0.060	0.026	0.002	0.000	0.000
AFM000051	0.990	0.883	0.570	0.249	0.159	0.074	0.000

Appendix E

Compilation of mass-transports

Table E1: Estimated mass transports per year
Table E2: Area-specific transports
Table E3: Flow weighted concentrations
Table E4: Monthly transports

Table E1. Estimated mass transports in the Forsmark area (kg/year). Year 1 corresponds to the period 2004-06-01 to 2005-05-31, and year 2 2005-06-01 to 2006-05-31. PFM000074, FM000117 and PFM00107 are lakes. See *Fel! Hittar inte referenskälla.* ***for localisation of sampling points.***

Year 1	q (L/s)	Na	K	Ca	Mg	HCO_3	Cl	SO_4	SO_4S	Br	F	Sr	TotN	NH_4N	NO_3N	PON	TotP	PO_4P	POP	TOC	DOC	POC	DIC	Si	SiO_2Si
PFM000066	11	1676	817	20967	1094	63099	1735	4037	1503	58	38	22	240	3.2	4.0	9	3.0	0.31	1.3	5559	5492	63	11937	1590	1441
PFM000074	16	3690	1101	31152	1688	94825	4733	4820	1830	43	73	35	375	10.8	5.4	18	4.1	0.26	1.9	8313	8249	134	18959	2405	2567
PFM000117	9	1812	553	11710	824	36388	1700	1826	731	24	37	14	367	68.0	3.0	16	2.0	0.18	1.1	4969	4991	127	6204	374	396
PFM000070	9	1365	455	11214	687	33050	1269	1681	677	8	31	12	298	36.2	8.5	10	2.2	0.22	1.0	5336	5305	81	6316	707	658
PFM000069	10	4268	671	19097	1534	55286	7144	4695	1737	22	76	28	255	3.4	12.3	11	4.2	0.54	1.5	5881	5776	82	11182	1770	1710
PFM000068	23	7175	1430	36811	2807	107004	10728	8464	3207	42	139	53	670	16.4	43.5	27	9.2	0.86	4.0	14381	14121	212	20555	3222	3052
PFM000107	33	48594	3845	54749	8758	155676	84900	21539	7739	529	187	111	1000	48.5	20.8	42	10.6	0.82	4.9	18917	18743	296	27874	2425	2429
Year 2																									
PFM000066	15	2326	1170	28961	1522	84468	2477	4395	1692	37	80	29	362	6.2	32.1	18	5.5	0.63	2.4	7793	7837	119	15722	2321	2081
PFM000074	21	4513	1626	41862	2265	120684	6293	6149	2388	56	119	44	479	5.0	28.3	20	6.3	0.59	2.6	10625	10498	128	23108	3404	3030
PFM000117	11	2138	656	16240	1043	47432	2003	2011	857	14	70	18	426	67.1	5.0	17	3.4	0.34	1.2	6503	6470	126	8389	763	680
PFM000070	11	1789	563	13453	865	40070	1681	1753	735	21	59	15	373	57.4	10.5	14	3.3	0.36	1.5	6119	6066	108	7219	817	729
PFM000069	13	5813	1001	25313	2059	71167	9639	5577	2150	57	121	36	357	4.3	63.8	18	6.4	0.83	2.7	7824	7713	118	13761	2419	2164
PFM000068	30	9873	2108	50171	3901	141693	14919	10496	4082	101	246	70	925	27.8	95.8	36	12.9	1.94	5.3	18726	18479	266	26481	4527	4030
PFM000107	43	50147	4557	73424	10039	208454	85965	22451	8614	354	357	129	1307	62.6	39.8	56	16.0	1.61	5.4	24794	24458	396	36113	3917	3536
Average year 1&2																									
PFM000066	13	2001	993	24964	1308	73784	2106	4216	1597	47	59	26	301	4.7	18.1	13	4.2	0.47	1.8	6676	6665	91	13829	1956	1761
PFM000074	18	4102	1363	36507	1977	107754	5513	5485	2109	49	96	40	427	7.9	16.8	19	5.2	0.42	2.3	9469	9374	131	21033	2904	2798
PFM000117	10	1975	605	13975	934	41910	1852	1918	794	19	54	16	397	67.6	4.0	16	2.7	0.26	1.1	5736	5731	126	7296	568	538
PFM000070	10	1577	509	12333	776	36560	1475	1717	706	14	45	14	336	46.8	9.5	12	2.8	0.29	1.3	5727	5686	94	6767	762	693
PFM000069	12	5041	836	22205	1797	63227	8391	5136	1944	39	98	32	306	3.9	38.1	14	5.3	0.69	2.1	6852	6744	100	12472	2094	1937
PFM000068	27	8524	1769	43491	3354	124349	12824	9480	3644	72	192	61	797	22.1	69.7	31	11.0	1.40	4.7	16553	16300	239	23518	3875	3541
PFM000107	38	49371	4201	64086	9398	182065	85432	21995	8177	441	272	120	1153	55.6	30.3	49	13.3	1.22	5.2	21855	21601	346	31993	3171	2982

Table E2. Estimated area-specific transports in the Forsmark area (kg/km^2,year). Year 1 corresponds to the period 2004-06-01 to 2005-05-31, and year 2 2005-06-01 to 2006-05-31. PFM000074, FM000117 and PFM00107 are lakes. See *Fel! Hittar inte referenskälla.* ***for localisation of sampling points.***

Year 1	Q (L/s,km^2)	Na	K	Ca	Mg	HCO_3	Cl	SO_4	SO_4S	Br	F	Sr	TotN	NH4N	NO3_N	PON	TotP	PO_4P	POP	TOC	DOC	POC	DIC	Si	SiO_2Si
PFM000066	4.0	591	288	7396	386	22257	611.9	1424	530	20	13	8	85	1.1	1.4	3.2	1.0	0.11	0.46	1961	1937	22	4210	561	508
PFM000074	4.0	940	280	7932	429.8	24144	1205	1227	466	11	18	9	95	2.7	1.4	4.6	1.1	0.07	0.49	2117	2100	34	4827	612	654
PFM000117	3.8	798	244	5159	363	16030	748.7	804.5	322	10	16	6	162	30.0	1.3	6.9	0.9	0.08	0.46	2189	2199	56	2733	165	175
PFM000070	3.8	601	201	4940	302.8	14560	559.2	740.5	298	3	14	5	131	16.0	3.8	4.5	1.0	0.10	0.45	2350	2337	36	2782	311	290
PFM000069	4.6	1903	299	8516	684.1	24654	3186	2094	775	10	34	13	114	1.5	5.5	4.9	1.9	0.24	0.66	2623	2576	36	4987	789	763
PFM000068	4.1	1284	256	6588	502.3	19149	1920	1515	574	8	25	10	120	2.9	7.8	4.8	1.6	0.15	0.71	2574	2527	38	3678	577	546
PFM000107	4.1	6072	480	6841	1094	19452	10608	2691	967	66	23	14	125	6.1	2.6	5.2	1.3	0.10	0.61	2364	2342	37	3483	303	304
Year 2																									
PFM000066	5.3	820	413	10216	536.8	29795	873.8	1550	597	13	28	10	128	2.2	11.3	6.3	1.9	0.22	0.84	2749	2764	42	5546	819	734
PFM000074	5.3	1149	414	10659	576.8	30729	1602	1566	608	14	30	11	122	1.3	7.2	5.2	1.6	0.15	0.66	2705	2673	33	5884	867	771
PFM000117	4.8	942	289	7154	459.6	20895	882.6	885.7	377	6	31	8	188	29.6	2.2	7.4	1.5	0.15	0.54	2865	2850	55	3695	336	300
PFM000070	4.8	788	248	5926	380.9	17652	740.5	772.4	324	9	26	6	164	25.3	4.6	6.1	1.5	0.16	0.66	2696	2672	47	3180	360	321
PFM000069	5.9	2592	446	11288	918.3	31736	4299	2487	959	25	54	16	159	1.9	28.5	7.9	2.9	0.37	1.21	3489	3439	53	6136	1078	965
PFM000068	5.4	1767	377	8978	698.1	25357	2670	1878	730	18	44	12	165	5.0	17.2	6.4	2.3	0.35	0.95	3351	3307	48	4739	810	721
PFM000107	5.4	6266	569	9174	1254	26047	10741	2805	1076	44	45	16	163	7.8	5.0	7.0	2.0	0.20	0.68	3098	3056	49	4512	489	442
Average year 1&2																									
PFM000066	4.7	706	350	8806	461.4	26026	742.9	1487	563	17	21	9	106	1.7	6.4	4.7	1.5	0.16	0.65	2355	2351	32	4878	690	621
PFM000074	4.7	1044	347	9295	503.3	27436	1404	1396	537	13	24	10	109	2.0	4.3	4.9	1.3	0.11	0.57	2411	2387	33	5355	740	713
PFM000117	4.3	870	266	6156	411.3	18463	815.6	845.1	350	8	24	7	175	29.8	1.8	7.2	1.2	0.11	0.50	2527	2525	56	3214	250	237
PFM000070	4.3	695	224	5433	341.8	16106	649.8	756.5	311	6	20	6	148	20.6	4.2	5.3	1.2	0.13	0.55	2523	2505	41	2981	336	305
PFM000069	5.2	2248	373	9902	801.2	28195	3742	2290	867	18	44	14	136	1.7	17.0	6.4	2.4	0.31	0.93	3056	3008	45	5562	934	864
PFM000068	4.8	1525	317	7783	600.2	22253	2295	1696	652	13	34	11	143	4.0	12.5	5.6	2.0	0.25	0.83	2962	2917	43	4209	693	634
PFM000107	4.8	6169	525	8008	1174	22749	10675	2748	1022	55	34	15	144	6.9	3.8	6.1	1.7	0.15	0.64	2731	2699	43	3998	396	373

Table E3. Flow weighted concentrations (mg/L). Year 1 corresponds to the period 2004-06-01 to 2005-05-31, and year 2 2005-06-01 to 2006-05-31. PFM000074, FM000117 and PFM00107 are lakes. See *Fel! Hittar inte referenskälla.* ***for localisation of sampling points.***

Year 1	Na	K	Ca	Mg	HCO_3	Cl	SO_4	SO_4S	Br	F	Sr	TotN	NH_4N	NO_3N	PON	TotP	PO_4P	POP	TOC	DOC	POC	DIC	Si	SiO_2Si
PFM000066	4.7	2.3	59	3.1	177	4.9	11.3	4.2	0.16	0.11	0.06	0.67	0.01	0.01	0.025	0.008	0.0009	0.0036	16	15	0.18	33	4.5	4.0
PFM000074	7.5	2.2	63	3.4	192	9.6	9.8	3.7	0.09	0.15	0.07	0.76	0.02	0.01	0.036	0.008	0.0005	0.0039	17	17	0.27	38	4.9	5.2
PFM000117	6.6	2.0	43	3.0	133	6.2	6.6	2.7	0.09	0.13	0.05	1.34	0.25	0.01	0.057	0.007	0.0006	0.0038	18	18	0.46	23	1.4	1.4
PFM000070	5.0	1.7	41	2.5	120	4.6	6.1	2.5	0.03	0.11	0.05	1.09	0.13	0.03	0.037	0.008	0.0008	0.0037	19	19	0.29	23	2.6	2.4
PFM000069	13	2.1	59	4.7	170	21.9	14.4	5.3	0.07	0.23	0.09	0.78	0.01	0.04	0.034	0.013	0.0017	0.0045	18	18	0.25	34	5.4	5.2
PFM000068	9.8	2.0	50	3.8	147	14.7	11.6	4.4	0.06	0.19	0.07	0.92	0.02	0.06	0.037	0.013	0.0012	0.0055	20	19	0.29	28	4.4	4.2
PFM000107	46	3.7	52	8.4	149	81.2	20.6	7.4	0.51	0.18	0.11	0.96	0.05	0.02	0.040	0.010	0.0008	0.0047	18	18	0.28	27	2.3	2.3
År2																								
PFM000066	4.9	2.4	61	3.2	177	5.2	9.2	3.5	0.08	0.17	0.06	0.76	0.01	0.07	0.037	0.011	0.0013	0.0050	16	16	0.25	33	4.9	4.4
PFM000074	6.8	2.5	63	3.4	182	9.5	9.3	3.6	0.08	0.18	0.07	0.72	0.01	0.04	0.031	0.009	0.0009	0.0039	16	16	0.19	35	5.1	4.6
PFM000117	6.3	1.9	48	3.1	139	5.9	5.9	2.5	0.04	0.21	0.05	1.25	0.20	0.01	0.049	0.010	0.0010	0.0036	19	19	0.37	25	2.2	2.0
PFM000070	5.2	1.7	39	2.5	118	4.9	5.1	2.2	0.06	0.17	0.04	1.09	0.17	0.03	0.041	0.010	0.0011	0.0044	18	18	0.32	21	2.4	2.1
PFM000069	14	2.4	61	5.0	171	23.2	13.4	5.2	0.14	0.29	0.09	0.86	0.01	0.15	0.043	0.015	0.0020	0.0065	19	19	0.28	33	5.8	5.2
PFM000068	10.	2.2	53	4.1	150	15.8	11.1	4.3	0.11	0.26	0.07	0.98	0.03	0.10	0.038	0.014	0.0020	0.0056	20	20	0.28	28	4.8	4.3
PFM000107	37	3.4	54	7.4	154	63.4	16.6	6.4	0.26	0.26	0.09	0.96	0.05	0.03	0.041	0.012	0.0012	0.0040	18	18	0.29	27	2.9	2.6
Medel År1&2																								
PFM000066	4.8	2.4	60	3.1	177	5.0	10.1	3.8	0.11	0.14	0.06	0.72	0.01	0.04	0.032	0.010	0.0011	0.0044	16	16	0.22	33	4.7	4.2
PFM000074	7.1	2.4	63	3.4	186	9.5	9.5	3.6	0.09	0.17	0.07	0.74	0.01	0.03	0.033	0.009	0.0007	0.0039	16	16	0.23	36	5.0	4.8
PFM000117	6.4	2.0	45	3.0	136	6.0	6.2	2.6	0.06	0.17	0.05	1.29	0.22	0.01	0.053	0.009	0.0008	0.0037	19	19	0.41	24	1.8	1.7
PFM000070	5.1	1.7	40	2.5	119	4.8	5.6	2.3	0.05	0.15	0.04	1.09	0.15	0.03	0.039	0.009	0.0009	0.0041	19	18	0.31	22	2.5	2.3
PFM000069	14	2.3	60	4.8	171	22.6	13.9	5.2	0.11	0.26	0.09	0.82	0.01	0.10	0.039	0.014	0.0018	0.0057	18	18	0.27	34	5.6	5.2
PFM000068	10	2.1	52	4.0	148	15.3	11.3	4.3	0.09	0.23	0.07	0.95	0.03	0.08	0.037	0.013	0.0017	0.0055	20	19	0.29	28	4.6	4.2
PFM000107	41	3.5	53	7.8	152	71.2	18.3	6.8	0.37	0.23	0.10	0.96	0.05	0.03	0.041	0.011	0.0010	0.0043	18	18	0.29	27	2.6	2.5

Table E4. Monthly transports (kg/month) compiled for PFM000066, PFM000068 and PFM000069 (c.f. *Fel! Hittar inte referenskälla.* ***and*** *Fel! Hittar inte referenskälla.****). Based on mean values for two years. Year 1 corresponds to the period 2004-06-01 to 2005-05-31, and year 2 2005-06-01 to 2006-05-31.***

Idcode	Month	q	Na	K	Ca	Mg	HCO_3	Cl	SO_4	SO_4S	Br	F	Sr	TotN	NH_4N	NO_3N	PON	TotP	PO_4P	POP	TOC	DOC	POC	DIC	Si	SiO_2Si
PFM000066	1	21	608	291	7724	399	22410	647	1622	604	4	15	7.9	82	1.4	3.4	2.1	0.7	0.09	0.3	1993	2005	15	4318	662	580
PFM000066	2	14	387	171	4780	246	14348	437	830	310	8	11	4.8	47	0.5	0.3	1.1	0.4	0.04	0.1	1190	1167	8	2884	399	384
PFM000066	3	8	231	104	3010	153	9029	268	414	160	7	8	3.0	27	0.4	0.2	0.9	0.3	0.03	0.1	676	663	5	1769	238	223
PFM000066	4	57	1069	636	14453	763	42805	1219	2156	841	56	34	14.2	201	2.6	16.1	13.0	3.8	0.39	1.8	4233	4191	81	8279	1233	1110
PFM000066	5	17	421	209	5747	287	17035	415	640	259	6	16	5.7	68	1.6	1.5	2.8	0.9	0.12	0.3	1513	1504	21	3119	372	332
PFM000066	6	8	218	85	2466	134	7531	165	189	84	2	5	2.8	33	0.9	0.2	1.9	0.5	0.06	0.3	696	686	15	1197	120	107
PFM000066	7	3	87	29	874	50	2741	67	69	30	1	3	1.1	14	0.6	0.2	0.8	0.2	0.03	0.1	273	272	6	451	39	36
PFM000066	8	2	62	20	624	36	1963	48	52	23	1	3	0.8	10	0.3	0.4	0.3	0.1	0.03	0.1	194	193	2	348	39	36
PFM000066	9	1	22	9	199	12	628	20	27	10	0	1	0.2	3	0.0	0.0	0.1	0.0	0.00	0.0	65	65	1	113	11	11
PFM000066	10	2	54	25	492	29	1478	50	109	40	1	1	0.6	7	0.0	0.0	0.3	0.1	0.01	0.0	143	142	2	266	31	31
PFM000066	11	5	163	77	1735	92	4977	154	454	163	1	4	1.9	21	0.2	0.5	0.9	0.3	0.03	0.1	422	416	8	855	126	115
PFM000066	12	22	681	331	7825	416	22621	723	1871	671	6	20	8.3	89	0.9	13.3	2.7	0.9	0.11	0.4	1955	2027	18	4061	643	558
PFM000068	1	41	2086	488	11972	890	33971	3040	3094	1177	9	34	16.6	220	6.5	18.3	5.4	2.2	0.25	0.8	4663	4529	41	6502	1139	1011
PFM000068	2	34	1628	370	9284	688	26960	2326	2064	786	10	34	12.7	166	7.6	10.4	4.7	1.5	0.14	0.6	3489	3483	35	5829	842	817
PFM000068	3	22	1132	262	6805	494	19623	1630	1245	490	9	29	9.2	109	6.8	7.3	3.5	1.1	0.12	0.4	2248	2245	27	3899	588	547
PFM000068	4	91	3166	919	20104	1462	55812	4602	4513	1722	40	109	26.3	414	7.7	60.8	22.3	6.8	0.66	3.3	8275	8187	161	10278	1844	1671
PFM000068	5	39	2166	463	11137	848	31577	3279	2052	819	20	56	15.1	192	3.7	8.5	8.5	3.1	0.40	1.3	4184	4160	66	5814	923	826
PFM000068	6	16	1174	155	4474	386	13153	1772	765	310	11	22	7.2	78	2.1	1.4	3.6	1.4	0.25	0.6	1739	1715	29	2344	357	326
PFM000068	7	6	581	45	1839	169	5606	927	338	134	5	9	3.2	31	1.5	0.9	1.4	0.6	0.16	0.2	658	641	13	997	135	131
PFM000068	8	7	804	44	2455	241	7585	1308	339	149	6	13	4.4	39	1.4	1.5	1.3	0.8	0.27	0.3	788	707	11	1356	188	174
PFM000068	9	3	276	15	829	81	2591	461	125	52	2	4	1.5	13	0.2	0.6	0.5	0.2	0.05	0.1	272	247	4	463	72	67
PFM000068	10	4	379	54	1308	118	3898	631	287	108	4	6	2.1	21	0.2	0.4	0.9	0.4	0.04	0.1	466	463	7	702	122	118
PFM000068	11	15	1115	180	4371	364	12547	1792	1018	380	9	20	6.7	74	1.2	4.6	2.7	1.0	0.12	0.4	1534	1512	22	2258	405	377
PFM000068	12	41	2540	544	12404	966	35374	3879	3119	1162	19	50	18.1	236	5.2	24.7	7.7	2.8	0.33	1.2	4790	4712	62	6595	1136	1016
PFM000069	1	16	1164	224	6057	458	17099	1913	1612	615	4	21	8.5	73	1.1	6.6	2.3	1.0	0.12	0.3	1852	1805	16	3408	603	541
PFM000069	2	14	943	172	4745	361	13820	1575	1104	418	6	18	6.6	55	0.4	0.7	2.2	0.8	0.07	0.3	1421	1402	14	3078	463	462
PFM000069	3	9	634	116	3226	244	9422	1083	632	237	5	13	4.4	34	0.4	0.8	1.6	0.5	0.05	0.2	853	843	11	1910	303	290
PFM000069	4	40	1883	447	10164	785	27988	3123	2683	994	19	50	13.6	185	1.4	43.3	11.4	3.2	0.27	1.6	3313	3296	77	5788	960	863
PFM000069	5	20	1393	234	5671	476	15912	2275	1242	473	12	30	8.2	96	1.1	14.8	4.6	1.6	0.21	0.7	1875	1865	33	3031	522	467
PFM000069	6	8	775	88	2463	226	7047	1228	422	172	7	11	4.0	35	0.6	0.8	1.4	0.7	0.13	0.2	767	760	10	1223	202	179
PFM000069	7	3	374	24	1067	104	3227	614	179	72	3	5	1.8	16	0.4	0.3	0.5	0.3	0.09	0.1	342	335	4	570	79	73
PFM000069	8	4	412	17	1211	122	3749	678	163	71	3	7	2.1	18	0.3	0.4	0.5	0.3	0.10	0.1	382	364	4	655	91	81
PFM000069	9	2	165	7	489	49	1517	278	72	30	1	3	0.9	8	0.1	0.3	0.2	0.1	0.03	0.0	156	153	2	264	42	38
PFM000069	10	2	212	20	628	60	1895	377	113	44	2	3	1.0	10	0.2	0.2	0.4	0.2	0.02	0.1	197	194	3	335	62	61
PFM000069	11	6	639	69	2158	191	6305	1108	401	154	5	9	3.4	29	0.6	0.8	1.1	0.5	0.08	0.2	620	608	8	1149	216	208
PFM000069	12	18	1487	254	6530	518	18472	2531	1650	607	11	26	9.7	52	1.3	7.1	2.5	1.3	0.22	0.4	1926	1863	17	3532	645	611

Appendix F

Detailed results from mass-balance calculations

Detailed compilations of results from mass balance calculations catchment model VBX-VI.

Catchments are denoted by the Sicada IDCODE, starting with “AFM”. When applicable, catchments are sorted in the tables from upstream to downstream parts.

Results for the following elements are presented in the tables below:

Chloride
Sodium
Potassium
Calcium
Magnesium
Sulphate
Bicarbonate
Total organic carbon
Total nitrogen
Total phosphorus
Silicon
Strontium

Element: Chloride (Cl), scenario 1			Water balance			Sources per catchment (Gross)			Total including upstream catchments					Calibration data[noteA]			
Idcode	Name	Area	Q_{catch}	Q_{out}	q	Diffuse	Point	Total	Total IN	Retention		Total OUT	Conc.	Reference	Concentration	q	Deviation
		km^2	m^3/yr	m^3/yr	L/s	kg/yr	kg/yr	kg/yr	kg/yr	kg/yr	%	kg/yr	mg/L		mg/L	L/s	%
AFM000095	Gunnarsboträsket	2.73	410100	410100	13.0	1851	0	1851	1851	0	0	1851	5				
AFM001100B	Sub-area: Labboträsket	0.08	12000	422100	13.4	279	0	279	2130	0	0	2130	5	**PFM000066**	**5**	**13.2**	**0**
AFM001100A	Sub-area: Labboträsket	1.11	166950	589050	18.7	1582	0	1582	3712	0	0	3712	6	**PFM000074**	**10**	**18.3**	**34**
AFM000096	Gunnarsbo - Lillfjärden (north)	0.10	15600	15600	0.5	601	0	601	601	0	0	601	39				
AFM001099	Gunnarsbo - Lillfjärden (south)	1.09	163350	768000	24.4	871	0	871	5185	0	0	5185	7	PFM000087	10		32
AFM000094	Gällsboträsket	2.14	321150	321150	10.2	6289	0	6289	6289	0	0	6289	20				
AFM001103C	Sub-area: Bolundsfjärden	0.09	13650	334800	10.6	352	0	352	6641	0	0	6641	20	**PFM000069**	**23**	**11.8**	**12**
AFM000093	Kungsträsket	0.13	18900	18900	0.6	250	0	250	250	0	0	250	13				
AFM000010B	Eckarfjärden	0.23	34800	34800	1.1	298	0	298	298	0	0	298	9	PFM000071	2		375
AFM000010A	Eckarfjärden	2.04	305250	340050	10.8	1332	0	1332	1630	0	0	1630	5	**PFM000070**	**5**	**9.8**	**0**
AFM001105	Sub-area: Stocksjön	0.21	31500	371550	11.8	539	0	539	2169	0	0	2169	6				
AFM001103B	Sub-area: Bolundsfjärden	0.75	111750	837000	26.5	4147	0	4147	13206	0	0	13206	16	**PFM000068**	**15**	**26.6**	**3**
AFM000089	Vambörsfjärden	0.48	72600	72600	2.3	3092	0	3092	3092	0	0	3092	43				
AFM000088	Fräkengropen	0.14	20850	20850	0.7	686	0	686	686	0	0	686	33				
AFM001104	Sub-area: Graven	0.39	58800	79650	2.5	2772	0	2772	3459	0	0	3459	43				
AFM001103A	Sub-area: Bolundsfjärden	1.41	211200	1200450	38.1	8996	57000	65996	85752	0	0	85752	71	**PFM000107**	**71**	**38.1**	**0**
AFM000091	Puttan	0.24	36600	36600	1.2	1494	0	1494	1494	0	0	1494	41				
AFM000092	No name	0.07	10650	10650	0.3	271	0	271	271	0	0	271	25				
AFM001101	Sub-area: Norra bassängen	0.35	52500	1300200	41.2	2342	0	2342	89859	0	0	89859	69	PFM000097	78		12
AFM000049	Lillfjärden	0.62	93150	93150	3.0	4575	0	4575	4575	0	0	4575	49				
AFM001106	Sub-area: AFM000085	0.07	10350	103500	3.3	597	0	597	5171	0	0	5171	50				
AFM000086	Tallsundet	0.22	32250	32250	1.0	1948	0	1948	1948	0	0	1948	60				
AFM000052B	Bredviken	0.63	95100	95100	3.0	1673	0	1673	1673	0	0	1673	18	PFM000073	9		105
AFM000052A	Bredviken	0.31	46500	141600	4.5	1608	0	1608	3282	0	0	3282	23				
AFM000084	Simpviken	0.04	5250	5250	0.2	258	0	258	258	0	0	258	49				
AFM000082	No name	0.19	28800	28800	0.9	1013	0	1013	1013	0	0	1013	35				
AFM000083	No name	0.08	11550	11550	0.4	667	0	667	667	0	0	667	58				
AFM001108	Sub-area: Märrbadet	0.07	10200	50550	1.6	629	0	629	2309	0	0	2309	46				
AFM001107	Sub-area: AFM000080	0.56	83700	134250	4.3	2941	0	2941	5250	0	0	5250	39				
AFM001109	Coastal area	1.86	279300	279300	8.9	10052	0	10052	10052	0	0	10052	36				
AFM001110	Coastal area	0.84	125550	125550	4.0	4541	0	4541	4541	0	0	4541	36				
AFM001111	Coastal area	0.11	16050	16050	0.5	660	0	660	660	0	0	660	41				
AFM001112	Coastal area	0.18	26700	26700	0.8	1238	0	1238	1238	0	0	1238	46				
AFM001113	Coastal area	0.70	105150	105150	3.3	2830	0	2830	2830	0	0	2830	27				
AFM001114	Coastal area	5.56	834150	834150	26.5	30745	0	30745	30745	0	0	30745	37				
AFM001115	Coastal area	0.39	58350	58350	1.9	2411	0	2411	2411	0	0	2411	41				
AFM000051	Fiskarfjärden	2.93	438900	438900	13.9	18130	0	18130	18130	0	0	18130	41	PFM000072	41		0
	Lillfjärden catchment	0.69	103500	103500	3.3	5171	0	5171		0	0	5171	50				
	Bredviken Catchment	0.94	141600	141600	4.5	3282	0	3282		0	0	3282	23				
	Fiskarfjärden	2.93	438900	438900	13.9	18130	0	18130		0	0	18130	41				
	Gunnarsbo-Lillfjärden	5.12	768000	768000	24.4	5185	0	5185		0	0	5185	7				
	Norra Bassängen	8.67	1300200	1300200	41.2	32859	57000	89859		0	0	89859	69				
	Forsmark area (all catchments)	29.13	4369200	4369200	138.5	124560	57000	181560		0	0	181560	42				

Note A: Primary calibration dataset is marked in bold.

Element: Sodium (Na), scenario 2			Water balance			Sources per catchment (Gross)			Total including upstream catchments					Calibration data[noteA]			
Idcode	Name	Area	Q_{catch}	Q_{out}	q	Diffuse	Point	Total	Total IN	Retention		Total OUT	Conc.	Reference	Concentration	q	Deviation
		km^2	m^3/yr	m^3/yr	L/s	kg/yr	kg/yr	kg/yr	kg/yr	kg/yr	%	kg/yr	mg/L		mg/L	L/s	%
AFM000095	Gunnarsboträsket	2.73	410100	410100	13.0	1964	0	1964	1964	0	0	1964	5				
AFM001100B	Sub-area: Labboträsket	0.08	12000	422100	13.4	58	0	58	2022	0	0	2022	5	**PFM000066**	**5**	**13.2**	**0**
AFM001100A	Sub-area: Labboträsket	1.11	166950	589050	18.7	1429	0	1429	3451	0	0	3451	6	**PFM000074**	**7**	**18.3**	**17**
AFM000096	Gunnarsbo - Lillfjärden (north)	0.10	15600	15600	0.5	517	0	517	517	0	0	517	33				
AFM001099	Gunnarsbo - Lillfjärden (south)	1.09	163350	768000	24.4	1294	0	1294	5262	0	0	5262	7	PFM000087	9		26
AFM000094	Gällsboträsket	2.14	321150	321150	10.2	3616	0	3616	3616	0	0	3616	11				
AFM001103C	Sub-area: Bolundsfjärden	0.09	13650	334800	10.6	227	0	227	3843	0	0	3843	11	**PFM000069**	**14**	**11.8**	**16**
AFM000093	Kungsträsket	0.13	18900	18900	0.6	192	0	192	192	0	0	192	10				
AFM000010B	Eckarfjärden	0.23	34800	34800	1.1	167	0	167	167	0	0	167	5	PFM000071	4		26
AFM000010A	Eckarfjärden	2.04	305250	340050	10.8	1836	0	1836	2003	0	0	2003	6	**PFM000070**	**5**	**9.8**	**15**
AFM001105	Sub-area: Stocksjön	0.21	31500	371550	11.8	361	0	361	2364	0	0	2364	6				
AFM001103B	Sub-area: Bolundsfjärden	0.75	111750	837000	26.5	2320	0	2320	8718	0	0	8718	10	**PFM000068**	**10**	**26.6**	**2**
AFM000089	Vambörsfjärden	0.48	72600	72600	2.3	2261	0	2261	2261	0	0	2261	31				
AFM000088	Fräkengropen	0.14	20850	20850	0.7	633	0	633	633	0	0	633	30				
AFM001104	Sub-area: Graven	0.39	58800	79650	2.5	2228	0	2228	2861	0	0	2861	36				
AFM001103A	Sub-area: Bolundsfjärden	1.41	211200	1200450	38.1	9227	30000	39227	53067	0	0	53067	44	**PFM000107**	**41**	**38.1**	**7**
AFM000091	Puttan	0.24	36600	36600	1.2	1302	0	1302	1302	0	0	1302	36				
AFM000092	No name	0.07	10650	10650	0.3	235	0	235	235	0	0	235	22				
AFM001101	Sub-area: Norra bassängen	0.35	52500	1300200	41.2	2176	0	2176	56780	0	0	56780	44	PFM000097	38		16
AFM000049	Lillfjärden	0.62	93150	93150	3.0	3234	0	3234	3234	0	0	3234	35				
AFM001106	Sub-area: AFM000085	0.07	10350	103500	3.3	548	0	548	3783	0	0	3783	37				
AFM000086	Tallsundet	0.22	32250	32250	1.0	1691	0	1691	1691	0	0	1691	52				
AFM000052B	Bredviken	0.63	95100	95100	3.0	1353	0	1353	1353	0	0	1353	14	PFM000073	14		0
AFM000052A	Bredviken	0.31	46500	141600	4.5	1548	0	1548	2901	0	0	2901	20				
AFM000084	Simpviken	0.04	5250	5250	0.2	212	0	212	212	0	0	212	40				
AFM000082	No name	0.19	28800	28800	0.9	964	0	964	964	0	0	964	33				
AFM000083	No name	0.08	11550	11550	0.4	531	0	531	531	0	0	531	46				
AFM001108	Sub-area: Märrbadet	0.07	10200	50550	1.6	461	0	461	1957	0	0	1957	39				
AFM001107	Sub-area: AFM000080	0.56	83700	134250	4.3	2750	0	2750	4706	0	0	4706	35				
AFM001109	Coastal area	1.86	279300	279300	8.9	8048	0	8048	8048	0	0	8048	29				
AFM001110	Coastal area	0.84	125550	125550	4.0	4200	0	4200	4200	0	0	4200	33				
AFM001111	Coastal area	0.11	16050	16050	0.5	656	0	656	656	0	0	656	41				
AFM001112	Coastal area	0.18	26700	26700	0.8	1398	0	1398	1398	0	0	1398	52				
AFM001113	Coastal area	0.70	105150	105150	3.3	2863	0	2863	2863	0	0	2863	27				
AFM001114	Coastal area	5.56	834150	834150	26.5	23121	0	23121	23121	0	0	23121	28				
AFM001115	Coastal area	0.39	58350	58350	1.9	2191	0	2191	2191	0	0	2191	38				
AFM000051	Fiskarfjärden	2.93	438900	438900	13.9	13167	0	13167	13167	0	0	13167	30	PFM000072	30		0
	Lillfjärden catchment	0.69	103500	103500	3.3	3783	0	3783		0	0	3783	37				
	Bredviken Catchment	0.94	141600	141600	4.5	2901	0	2901		0	0	2901	20				
	Fiskarfjärden	2.93	438900	438900	13.9	13167	0	13167		0	0	13167	30				
	Gunnarsbo-Lillfjärden	5.12	768000	768000	24.4	5262	0	5262		0	0	5262	7				
	Norra Bassängen	8.67	1300200	1300200	41.2	26780	30000	56780		0	0	56780	44				
	Forsmark area (all catchments)	29.13	4369200	4369200	138.5	100979	30000	130979		0	0	130979	30				

Note A: Primary calibration dataset is marked in bold.

Element: Potassium (K), scenario 1			Water balance			Sources per catchment (Gross)			Total including upstream catchments					Calibration data[noteA]			
Idcode	Name	Area	Q_{catch}	Q_{out}	q	Diffuse	Point	Total	Total IN	Retention		Total OUT	Conc.	Reference	Concentration	q	Deviation
		km^2	m^3/yr	m^3/yr	L/s	kg/yr	kg/yr	kg/yr	kg/yr	kg/yr	%	kg/yr	mg/L		mg/L	L/s	%
AFM000095	Gunnarsboträsket	2.73	410100	410100	13.0	922	0	922	922	0	0	922	2				
AFM001100B	Sub-area: Labboträsket	0.08	12000	422100	13.4	27	0	27	949	0	0	949	2	**PFM000066**	**2.4**	**13.2**	**6**
AFM001100A	Sub-area: Labboträsket	1.11	166950	589050	18.7	374	0	374	1323	0	0	1323	2	**PFM000074**	**2.4**	**18.3**	**5**
AFM000096	Gunnarsbo - Lillfjärden (north)	0.10	15600	15600	0.5	31	0	31	31	0	0	31	2				
AFM001099	Gunnarsbo - Lillfjärden (south)	1.09	163350	768000	24.4	363	0	363	1717	0	0	1717	2	PFM000087	2.7		17
AFM000094	Gällsboträsket	2.14	321150	321150	10.2	724	0	724	724	0	0	724	2				
AFM001103C	Sub-area: Bolundsfjärden	0.09	13650	334800	10.6	31	0	31	755	0	0	755	2	**PFM000069**	**2.3**	**11.8**	**0**
AFM000093	Kungsträsket	0.13	18900	18900	0.6	42	0	42	42	0	0	42	2				
AFM000010B	Eckarfjärden	0.23	34800	34800	1.1	79	0	79	79	0	0	79	2	PFM000071	2.0		13
AFM000010A	Eckarfjärden	2.04	305250	340050	10.8	634	0	634	712	0	0	712	2	**PFM000070**	**1.7**	**9.8**	**27**
AFM001105	Sub-area: Stocksjön	0.21	31500	371550	11.8	70	0	70	782	0	0	782	2				
AFM001103B	Sub-area: Bolundsfjärden	0.75	111750	837000	26.5	254	0	254	1833	0	0	1833	2	**PFM000068**	**2.1**	**26.6**	**4**
AFM000089	Vambörsfjärden	0.48	72600	72600	2.3	158	0	158	158	0	0	158	2				
AFM000088	Fräkengropen	0.14	20850	20850	0.7	46	0	46	46	0	0	46	2				
AFM001104	Sub-area: Graven	0.39	58800	79650	2.5	129	0	129	175	0	0	175	2				
AFM001103A	Sub-area: Bolundsfjärden	1.41	211200	1200450	38.1	356	1200	1556	3723	0	0	3723	3	**PFM000107**	**3.5**	**38.1**	**11**
AFM000091	Puttan	0.24	36600	36600	1.2	73	0	73	73	0	0	73	2				
AFM000092	No name	0.07	10650	10650	0.3	23	0	23	23	0	0	23	2				
AFM001101	Sub-area: Norra bassängen	0.35	52500	1300200	41.2	108	0	108	3927	0	0	3927	3	PFM000097	3.0		2
AFM000049	Lillfjärden	0.62	93150	93150	3.0	198	0	198	198	0	0	198	2				
AFM001106	Sub-area: AFM000085	0.07	10350	103500	3.3	19	0	19	217	0	0	217	2				
AFM000086	Tallsundet	0.22	32250	32250	1.0	69	0	69	69	0	0	69	2				
AFM000052B	Bredviken	0.63	95100	95100	3.0	216	0	216	216	0	0	216	2	PFM000073	7.9		71
AFM000052A	Bredviken	0.31	46500	141600	4.5	88	0	88	303	0	0	303	2				
AFM000084	Simpviken	0.04	5250	5250	0.2	11	0	11	11	0	0	11	2				
AFM000082	No name	0.19	28800	28800	0.9	65	0	65	65	0	0	65	2				
AFM000083	No name	0.08	11550	11550	0.4	26	0	26	26	0	0	26	2				
AFM001108	Sub-area: Märrbadet	0.07	10200	50550	1.6	21	0	21	111	0	0	111	2				
AFM001107	Sub-area: AFM000080	0.56	83700	134250	4.3	168	0	168	279	0	0	279	2				
AFM001109	Coastal area	1.86	279300	279300	8.9	620	0	620	620	0	0	620	2				
AFM001110	Coastal area	0.84	125550	125550	4.0	278	0	278	278	0	0	278	2				
AFM001111	Coastal area	0.11	16050	16050	0.5	36	0	36	36	0	0	36	2				
AFM001112	Coastal area	0.18	26700	26700	0.8	60	0	60	60	0	0	60	2				
AFM001113	Coastal area	0.70	105150	105150	3.3	236	0	236	236	0	0	236	2				
AFM001114	Coastal area	5.56	834150	834150	26.5	1858	0	1858	1858	0	0	1858	2				
AFM001115	Coastal area	0.39	58350	58350	1.9	131	0	131	131	0	0	131	2				
AFM000051	Fiskarfjärden	2.93	438900	438900	13.9	888	0	888	888	0	0	888	2	PFM000072	3.3		38
	Lillfjärden catchment	0.69	103500	103500	3.3	217	0	217		0	0	217	2				
	Bredviken Catchment	0.94	141600	141600	4.5	303	0	303		0	0	303	2				
	Fiskarfjärden	2.93	438900	438900	13.9	888	0	888		0	0	888	2				
	Gunnarsbo-Lillfjärden	5.12	768000	768000	24.4	1717	0	1717		0	0	1717	2				
	Norra Bassängen	8.67	1300200	1300200	41.2	2727	1200	3927		0	0	3927	3				
	Forsmark area (all catchments)	29.13	4369200	4369200	138.5	9430	1200	10630		0	0	10630	2				

Note A: Primary calibration dataset is marked in bold.

Element: Calcium (Ca), scenario 1			Water balance			Sources per catchment (Gross)			Total including upstream catchments					Calibration data[noteA]			
Idcode	Name	Area	Q_{catch}	Q_{out}	q	Diffuse	Point	Total	Total IN	Retention		Total OUT	Conc.	Reference	Concentration	q	Deviation
		km^2	m^3/yr	m^3/yr	L/s	kg/yr	kg/yr	kg/yr	kg/yr	kg/yr	%	kg/yr	mg/L		mg/L	L/s	%
AFM000095	Gunnarsboträsket	2.73	410100	410100	13.0	25160	0	25160	25160	1060	4	24100	59				
AFM001100B	Sub-area: Labboträsket	0.08	12000	422100	13.4	742	0	742	24841	0	0	24841	59	**PFM000066**	**60**	**13.2**	**2**
AFM001100A	Sub-area: Labboträsket	1.11	166950	589050	18.7	10197	0	10197	35039	498	1	34541	59	**PFM000074**	**63**	**18.3**	**7**
AFM000096	Gunnarsbo - Lillfjärden (north)	0.10	15600	15600	0.5	829	0	829	829	159	19	670	43				
AFM001099	Gunnarsbo - Lillfjärden (south)	1.09	163350	768000	24.4	9867	0	9867	45077	705	2	44372	58	PFM000087	54		7
AFM000094	Gällsboträsket	2.14	321150	321150	10.2	19773	0	19773	19773	993	5	18780	58				
AFM001103C	Sub-area: Bolundsfjärden	0.09	13650	334800	10.6	853	0	853	19633	0	0	19633	59	**PFM000069**	**60**	**11.8**	**2**
AFM000093	Kungsträsket	0.13	18900	18900	0.6	1152	0	1152	1152	61	5	1091	58				
AFM000010B	Eckarfjärden	0.23	34800	34800	1.1	2158	0	2158	2158	0	0	2158	62	PFM000071	82		24
AFM000010A	Eckarfjärden	2.04	305250	340050	10.8	16933	0	16933	19091	5464	29	13627	40	**PFM000070**	**40**	**9.8**	**0**
AFM001105	Sub-area: Stocksjön	0.21	31500	371550	11.8	1894	0	1894	15521	175	1	15346	41				
AFM001103B	Sub-area: Bolundsfjärden	0.75	111750	837000	26.5	6942	0	6942	43012	0	0	43012	51	**PFM000068**	**52**	**26.6**	**1**
AFM000089	Vambörsfjärden	0.48	72600	72600	2.3	4289	0	4289	4289	571	13	3718	51				
AFM000088	Fräkengropen	0.14	20850	20850	0.7	1246	0	1246	1246	115	9	1130	54				
AFM001104	Sub-area: Graven	0.39	58800	79650	2.5	3507	0	3507	4638	178	4	4459	56				
AFM001103A	Sub-area: Bolundsfjärden	1.41	211200	1200450	38.1	8921	0	8921	60110	8527	14	51583	43	**PFM000107**	**53**	**38.1**	**20**
AFM000091	Puttan	0.24	36600	36600	1.2	1932	0	1932	1932	586	30	1346	37				
AFM000092	No name	0.07	10650	10650	0.3	612	0	612	612	80	13	533	50				
AFM001101	Sub-area: Norra bassängen	0.35	52500	1300200	41.2	2893	0	2893	56356	547	1	55809	43	PFM000097	35		23
AFM000049	Lillfjärden	0.62	93150	93150	3.0	5330	0	5330	5330	1126	21	4205	45				
AFM001106	Sub-area: AFM000085	0.07	10350	103500	3.3	489	0	489	4694	293	6	4401	43				
AFM000086	Tallsundet	0.22	32250	32250	1.0	1854	0	1854	1854	424	23	1431	44				
AFM000052B	Bredviken	0.63	95100	95100	3.0	5898	0	5898	5898	0	0	5898	62	PFM000073	130		52
AFM000052A	Bredviken	0.31	46500	141600	4.5	2285	0	2285	8182	1739	21	6444	46				
AFM000084	Simpviken	0.04	5250	5250	0.2	279	0	279	279	94	34	186	35				
AFM000082	No name	0.19	28800	28800	0.9	1768	0	1768	1768	63	4	1705	59				
AFM000083	No name	0.08	11550	11550	0.4	702	0	702	702	59	8	643	56				
AFM001108	Sub-area: Märrbadet	0.07	10200	50550	1.6	552	0	552	2900	250	9	2650	52				
AFM001107	Sub-area: AFM000080	0.56	83700	134250	4.3	4433	0	4433	7083	1227	17	5856	44				
AFM001109	Coastal area	1.86	279300	279300	8.9	16862	0	16862	16862	0	0	16862	60				
AFM001110	Coastal area	0.84	125550	125550	4.0	7575	0	7575	7575	0	0	7575	60				
AFM001111	Coastal area	0.11	16050	16050	0.5	989	0	989	989	0	0	989	62				
AFM001112	Coastal area	0.18	26700	26700	0.8	1631	0	1631	1631	0	0	1631	61				
AFM001113	Coastal area	0.70	105150	105150	3.3	6455	0	6455	6455	0	0	6455	61				
AFM001114	Coastal area	5.56	834150	834150	26.5	50581	0	50581	50581	0	0	50581	61				
AFM001115	Coastal area	0.39	58350	58350	1.9	3568	0	3568	3568	0	0	3568	61				
AFM000051	Fiskarfjärden	2.93	438900	438900	13.9	23579	0	23579	23579	5867	25	17712	40	PFM000072	39		3
	Lillfjärden catchment	0.69	103500	103500	3.3	5820	0	5820		1419	24	4401	43				
	Bredviken Catchment	0.94	141600	141600	4.5	8182	0	8182		1739	21	6444	46				
	Fiskarfjärden	2.93	438900	438900	13.9	23579	0	23579		5867	25	17712	40				
	Gunnarsbo-Lillfjärden	5.12	768000	768000	24.4	46795	0	46795		2423	5	44372	58				
	Norra Bassängen	8.67	1300200	1300200	41.2	73106	0	73106		17297	24	55809	43				
	Forsmark area (all catchments)	29.13	4369200	4369200	138.5	254732	0	254732		30860	12	223872	51				

Note A: Primary calibration dataset is marked in bold.

Element: Magnesium (Mg), scenario 1			Water balance			Sources per catchment (Gross)			Total including upstream catchments					Calibration data[noteA]			
Idcode	Name	Area	Q_{catch}	Q_{out}	q	Diffuse	Point	Total	Total IN	Retention		Total OUT	Conc.	Reference	Concentration	q	Deviation
		km^2	m^3/yr	m^3/yr	L/s	kg/yr	kg/yr	kg/yr	kg/yr	kg/yr	%	kg/yr	mg/L		mg/L	L/s	%
AFM000095	Gunnarsboträsket	2.73	410100	410100	13.0	1387	0	1387	1387	0	0	1387	3.4				
AFM001100B	Sub-area: Labboträsket	0.08	12000	422100	13.4	134	0	134	1522	0	0	1522	3.6	**PFM000066**	**3.1**	**13.22989**	**15**
AFM001100A	Sub-area: Labboträsket	1.11	166950	589050	18.7	438	0	438	1960	0	0	1960	3.3	**PFM000074**	**3.4**	**18.32779**	**3**
AFM000096	Gunnarsbo - Lillfjärden (north)	0.10	15600	15600	0.5	25	0	25	25	0	0	25	1.6				
AFM001099	Gunnarsbo - Lillfjärden (south)	1.09	163350	768000	24.4	327	0	327	2311	0	0	2311	3.0	PFM000087	4.7		35
AFM000094	Gällsboträsket	2.14	321150	321150	10.2	1701	0	1701	1701	0	0	1701	5.3				
AFM001103C	Sub-area: Bolundsfjärden	0.09	13650	334800	10.6	55	0	55	1756	0	0	1756	5.2	**PFM000069**	**4.8**	**11.75793**	**8**
AFM000093	Kungsträsket	0.13	18900	18900	0.6	56	0	56	56	0	0	56	3.0				
AFM000010B	Eckarfjärden	0.23	34800	34800	1.1	177	0	177	177	0	0	177	5.1	PFM000071	3.8		36
AFM000010A	Eckarfjärden	2.04	305250	340050	10.8	680	0	680	857	0	0	857	2.5	**PFM000070**	**2.5**	**9.759476**	**0**
AFM001105	Sub-area: Stocksjön	0.21	31500	371550	11.8	114	0	114	971	0	0	971	2.6				
AFM001103B	Sub-area: Bolundsfjärden	0.75	111750	837000	26.5	566	0	566	3349	0	0	3349	4.0	**PFM000068**	**4.0**	**26.58018**	**0**
AFM000089	Vambörsfjärden	0.48	72600	72600	2.3	417	0	417	417	0	0	417	5.7				
AFM000088	Fräkengropen	0.14	20850	20850	0.7	58	0	58	58	0	0	58	2.8				
AFM001104	Sub-area: Graven	0.39	58800	79650	2.5	226	0	226	285	0	0	285	3.6				
AFM001103A	Sub-area: Bolundsfjärden	1.41	211200	1200450	38.1	343	3800	4143	8193	0	0	8193	6.8	**PFM000107**	**7.8**	**38.06818**	**13**
AFM000091	Puttan	0.24	36600	36600	1.2	148	0	148	148	0	0	148	4.1				
AFM000092	No name	0.07	10650	10650	0.3	22	0	22	22	0	0	22	2.0				
AFM001101	Sub-area: Norra bassängen	0.35	52500	1300200	41.2	140	0	140	8504	0	0	8504	6.5	PFM000097	6.9		5
AFM000049	Lillfjärden	0.62	93150	93150	3.0	676	0	676	676	0	0	676	7.3				
AFM001106	Sub-area: AFM000085	0.07	10350	103500	3.3	67	0	67	744	0	0	744	7.2				
AFM000086	Tallsundet	0.22	32250	32250	1.0	250	0	250	250	0	0	250	7.7				
AFM000052B	Bredviken	0.63	95100	95100	3.0	193	0	193	193	0	0	193	2.0	PFM000073	16.7		88
AFM000052A	Bredviken	0.31	46500	141600	4.5	200	0	200	393	0	0	393	2.8				
AFM000084	Simpviken	0.04	5250	5250	0.2	22	0	22	22	0	0	22	4.2				
AFM000082	No name	0.19	28800	28800	0.9	133	0	133	133	0	0	133	4.6				
AFM000083	No name	0.08	11550	11550	0.4	78	0	78	78	0	0	78	6.8				
AFM001108	Sub-area: Märrbadet	0.07	10200	50550	1.6	104	0	104	315	0	0	315	6.2				
AFM001107	Sub-area: AFM000080	0.56	83700	134250	4.3	339	0	339	654	0	0	654	4.9				
AFM001109	Coastal area	1.86	279300	279300	8.9	904	0	904	904	0	0	904	3.2				
AFM001110	Coastal area	0.84	125550	125550	4.0	301	0	301	301	0	0	301	2.4				
AFM001111	Coastal area	0.11	16050	16050	0.5	45	0	45	45	0	0	45	2.8				
AFM001112	Coastal area	0.18	26700	26700	0.8	64	0	64	64	0	0	64	2.4				
AFM001113	Coastal area	0.70	105150	105150	3.3	229	0	229	229	0	0	229	2.2				
AFM001114	Coastal area	5.56	834150	834150	26.5	4673	0	4673	4673	0	0	4673	5.6				
AFM001115	Coastal area	0.39	58350	58350	1.9	247	0	247	247	0	0	247	4.2				
AFM000051	Fiskarfjärden	2.93	438900	438900	13.9	2704	0	2704	2704	0	0	2704	6.2	PFM000072	6.9		10
	Lillfjärden catchment	0.69	103500	103500	3.3	744	0	744		0	0	744	7.2				
	Bredviken Catchment	0.94	141600	141600	4.5	393	0	393		0	0	393	2.8				
	Fiskarfjärden	2.93	438900	438900	13.9	2704	0	2704		0	0	2704	6.2				
	Gunnarsbo-Lillfjärden	5.12	768000	768000	24.4	2311	0	2311		0	0	2311	3.0				
	Norra Bassängen	8.67	1300200	1300200	41.2	4704	3800	8504		0	0	8504	6.5				
	Forsmark area (all catchments)	29.13	4369200	4369200	138.5	18244	3800	22044		0	0	22044	5.0				

Note A: Primary calibration dataset is marked in bold.

Element: Sulphate (SO_4), scenario 1			Water balance			Sources per catchment (Gross)			Total including upstream catchments					Calibration data[noteA]			
Idcode	Name	Area	Q_{catch}	Q_{out}	q	Diffuse	Point	Total	Total IN	Retention		Total OUT	Conc.	Reference	Concentration	q	Deviation
		km^2	m^3/yr	m^3/yr	L/s	kg/yr	kg/yr	kg/yr	kg/yr	kg/yr	%	kg/yr	mg/L		mg/L	L/s	%
AFM000095	Gunnarsboträsket	2.73	410100	410100	13.0	3924	0	3924	3924	0	0	3924	10				
AFM001100B	Sub-area: Labboträsket	0.08	12000	422100	13.4	247	0	247	4171	0	0	4171	10	**PFM000066**	**10**	**13.2**	**2**
AFM001100A	Sub-area: Labboträsket	1.11	166950	589050	18.7	1418	0	1418	5590	0	0	5590	9	**PFM000074**	**9**	**18.3**	**0**
AFM000096	Gunnarsbo - Lillfjärden (north)	0.10	15600	15600	0.5	109	0	109	109	0	0	109	7				
AFM001099	Gunnarsbo - Lillfjärden (south)	1.09	163350	768000	24.4	1243	0	1243	6941	0	0	6941	9	PFM000087	11		14
AFM000094	Gällsboträsket	2.14	321150	321150	10.2	3943	0	3943	3943	0	0	3943	12				
AFM001103C	Sub-area: Bolundsfjärden	0.09	13650	334800	10.6	143	0	143	4087	0	0	4087	12	**PFM000069**	**14**	**11.8**	**12**
AFM000093	Kungsträsket	0.13	18900	18900	0.6	170	0	170	170	0	0	170	9				
AFM000010B	Eckarfjärden	0.23	34800	34800	1.1	417	0	417	417	0	0	417	12	PFM000071	3		247
AFM000010A	Eckarfjärden	2.04	305250	340050	10.8	2414	0	2414	2830	0	0	2830	8	**PFM000070**	**6**	**9.8**	**49**
AFM001105	Sub-area: Stocksjön	0.21	31500	371550	11.8	312	0	312	3143	0	0	3143	8				
AFM001103B	Sub-area: Bolundsfjärden	0.75	111750	837000	26.5	1336	0	1336	8735	0	0	8735	10	**PFM000068**	**11**	**26.6**	**8**
AFM000089	Vambörsfjärden	0.48	72600	72600	2.3	936	0	936	936	0	0	936	13				
AFM000088	Fräkengropen	0.14	20850	20850	0.7	182	0	182	182	0	0	182	9				
AFM001104	Sub-area: Graven	0.39	58800	79650	2.5	601	0	601	783	0	0	783	10				
AFM001103A	Sub-area: Bolundsfjärden	1.41	211200	1200450	38.1	1475	8100	9575	20029	0	0	20029	17	**PFM000107**	**18**	**38.1**	**9**
AFM000091	Puttan	0.24	36600	36600	1.2	383	0	383	383	0	0	383	10				
AFM000092	No name	0.07	10650	10650	0.3	82	0	82	82	0	0	82	8				
AFM001101	Sub-area: Norra bassängen	0.35	52500	1300200	41.2	448	0	448	20943	0	0	20943	16	PFM000097	17		5
AFM000049	Lillfjärden	0.62	93150	93150	3.0	1401	0	1401	1401	0	0	1401	15				
AFM001106	Sub-area: AFM000085	0.07	10350	103500	3.3	144	0	144	1545	0	0	1545	15				
AFM000086	Tallsundet	0.22	32250	32250	1.0	507	0	507	507	0	0	507	16				
AFM000052B	Bredviken	0.63	95100	95100	3.0	728	0	728	728	0	0	728	8	PFM000073	31		76
AFM000052A	Bredviken	0.31	46500	141600	4.5	503	0	503	1231	0	0	1231	9				
AFM000084	Simpviken	0.04	5250	5250	0.2	56	0	56	56	0	0	56	11				
AFM000082	No name	0.19	28800	28800	0.9	327	0	327	327	0	0	327	11				
AFM000083	No name	0.08	11550	11550	0.4	166	0	166	166	0	0	166	14				
AFM001108	Sub-area: Märrbadet	0.07	10200	50550	1.6	195	0	195	688	0	0	688	14				
AFM001107	Sub-area: AFM000080	0.56	83700	134250	4.3	877	0	877	1565	0	0	1565	12				
AFM001109	Coastal area	1.86	279300	279300	8.9	2613	0	2613	2613	0	0	2613	9				
AFM001110	Coastal area	0.84	125550	125550	4.0	1025	0	1025	1025	0	0	1025	8				
AFM001111	Coastal area	0.11	16050	16050	0.5	141	0	141	141	0	0	141	9				
AFM001112	Coastal area	0.18	26700	26700	0.8	218	0	218	218	0	0	218	8				
AFM001113	Coastal area	0.70	105150	105150	3.3	826	0	826	826	0	0	826	8				
AFM001114	Coastal area	5.56	834150	834150	26.5	10600	0	10600	10600	0	0	10600	13				
AFM001115	Coastal area	0.39	58350	58350	1.9	629	0	629	629	0	0	629	11				
AFM000051	Fiskarfjärden	2.93	438900	438900	13.9	5910	0	5910	5910	0	0	5910	13	PFM000072	14		2
	Lillfjärden catchment	0.69	103500	103500	3.3	1545	0	1545		0	0	1545	15				
	Bredviken Catchment	0.94	141600	141600	4.5	1231	0	1231		0	0	1231	9				
	Fiskarfjärden	2.93	438900	438900	13.9	5910	0	5910		0	0	5910	13				
	Gunnarsbo-Lillfjärden	5.12	768000	768000	24.4	6941	0	6941		0	0	6941	9				
	Norra Bassängen	8.67	1300200	1300200	41.2	12843	8100	20943		0	0	20943	16				
	Forsmark area (all catchments)	29.13	4369200	4369200	138.5	46650	8100	54750		0	0	54750	13				

Note A: Primary calibration dataset is marked in bold.

Element: Bicarbonate (HCO_3), scenario 1			Water balance			Sources per catchment (Gross)			Total including upstream catchments					Calibration data[noteA]			
Idcode	Name	Area	Q_{catch}	Q_{out}	q	Diffuse	Point	Total	Total IN	Retention		Total OUT	Conc.	Reference	Concentration	q	Deviation
		km^2	m^3/yr	m^3/yr	L/s	kg/yr	kg/yr	kg/yr	kg/yr	kg/yr	%	kg/yr	mg/L		mg/L	L/s	%
AFM000095	Gunnarsboträsket	2.73	410100	410100	13.0	75777	0	75777	75777	3364	4	72413	177				
AFM001100B	Sub-area: Labboträsket	0.08	12000	422100	13.4	2233	0	2233	74647	0	0	74647	177	**PFM000066**	**177**	**13.2**	**0**
AFM001100A	Sub-area: Labboträsket	1.11	166950	589050	18.7	30712	0	30712	105359	1579	1	103780	176	**PFM000074**	**186**	**18.3**	**5**
AFM000096	Gunnarsbo - Lillfjärden (north)	0.10	15600	15600	0.5	2498	0	2498	2498	502	20	1996	128				
AFM001099	Gunnarsbo - Lillfjärden (south)	1.09	163350	768000	24.4	29717	0	29717	135492	2236	2	133256	174	PFM000087	164		6
AFM000094	Gällsboträsket	2.14	321150	321150	10.2	59551	0	59551	59551	3149	5	56402	176				
AFM001103C	Sub-area: Bolundsfjärden	0.09	13650	334800	10.6	2569	0	2569	58971	0	0	58971	176	**PFM000069**	**171**	**11.8**	**3**
AFM000093	Kungsträsket	0.13	18900	18900	0.6	3470	0	3470	3470	194	6	3276	173				
AFM000010B	Eckarfjärden	0.23	34800	34800	1.1	6500	0	6500	6500	0	0	6500	187	PFM000071	267		30
AFM000010A	Eckarfjärden	2.04	305250	340050	10.8	50999	0	50999	57499	17105	30	40394	119	**PFM000070**	**119**	**9.8**	**0**
AFM001105	Sub-area: Stocksjön	0.21	31500	371550	11.8	5706	0	5706	46100	550	1	45550	123				
AFM001103B	Sub-area: Bolundsfjärden	0.75	111750	837000	26.5	20909	0	20909	128706	0	0	128706	154	**PFM000068**	**148**	**26.6**	**4**
AFM000089	Vambörsfjärden	0.48	72600	72600	2.3	12917	0	12917	12917	1801	14	11116	153				
AFM000088	Fräkengropen	0.14	20850	20850	0.7	3751	0	3751	3751	364	10	3387	162				
AFM001104	Sub-area: Graven	0.39	58800	79650	2.5	10563	0	10563	13950	565	4	13385	168				
AFM001103A	Sub-area: Bolundsfjärden	1.41	211200	1200450	38.1	26869	0	26869	180075	26762	15	153314	128	**PFM000107**	**152**	**38.1**	**16**
AFM000091	Puttan	0.24	36600	36600	1.2	5819	0	5819	5819	1831	31	3988	109				
AFM000092	No name	0.07	10650	10650	0.3	1844	0	1844	1844	251	14	1593	150				
AFM001101	Sub-area: Norra bassängen	0.35	52500	1300200	41.2	8714	0	8714	167608	1716	1	165893	128	PFM000097	82		56
AFM000049	Lillfjärden	0.62	93150	93150	3.0	16053	0	16053	16053	3538	22	12515	134				
AFM001106	Sub-area: AFM000085	0.07	10350	103500	3.3	1474	0	1474	13989	920	7	13069	126				
AFM000086	Tallsundet	0.22	32250	32250	1.0	5585	0	5585	5585	1330	24	4255	132				
AFM000052B	Bredviken	0.63	95100	95100	3.0	17762	0	17762	17762	0	0	17762	187	PFM000073	486		62
AFM000052A	Bredviken	0.31	46500	141600	4.5	6882	0	6882	24644	5464	22	19180	135				
AFM000084	Simpviken	0.04	5250	5250	0.2	842	0	842	842	293	35	549	105				
AFM000082	No name	0.19	28800	28800	0.9	5326	0	5326	5326	199	4	5126	178				
AFM000083	No name	0.08	11550	11550	0.4	2115	0	2115	2115	187	9	1928	167				
AFM001108	Sub-area: Märrbadet	0.07	10200	50550	1.6	1661	0	1661	8715	790	9	7925	157				
AFM001107	Sub-area: AFM000080	0.56	83700	134250	4.3	13351	0	13351	21275	3854	18	17422	130				
AFM001109	Coastal area	1.86	279300	279300	8.9	50784	0	50784	50784	0	0	50784	182				
AFM001110	Coastal area	0.84	125550	125550	4.0	22814	0	22814	22814	0	0	22814	182				
AFM001111	Coastal area	0.11	16050	16050	0.5	2979	0	2979	2979	0	0	2979	186				
AFM001112	Coastal area	0.18	26700	26700	0.8	4914	0	4914	4914	0	0	4914	184				
AFM001113	Coastal area	0.70	105150	105150	3.3	19441	0	19441	19441	0	0	19441	185				
AFM001114	Coastal area	5.56	834150	834150	26.5	152340	0	152340	152340	0	0	152340	183				
AFM001115	Coastal area	0.39	58350	58350	1.9	10746	0	10746	10746	0	0	10746	184				
AFM000051	Fiskarfjärden	2.93	438900	438900	13.9	71016	0	71016	71016	18403	26	52613	120	PFM000072	144		16
	Lillfjärden catchment	0.69	103500	103500	3.3	17527	0	17527		4458	25	13069	126				
	Bredviken Catchment	0.94	141600	141600	4.5	24644	0	24644		5464	22	19180	135				
	Fiskarfjärden	2.93	438900	438900	13.9	71016	0	71016		18403	26	52613	120				
	Gunnarsbo-Lillfjärden	5.12	768000	768000	24.4	140937	0	140937		7681	5	133256	174				
	Norra Bassängen	8.67	1300200	1300200	41.2	220180	0	220180		54288	25	165893	128				
	Forsmark area (all catchments)	29.13	4369200	4369200	138.5	767202	0	767202		96947	13	670254	153				

Note A: Primary calibration dataset is marked in bold.

Element: Total organic carbon (TOC), scenario 1			Water balance			Sources per catchment (Gross)			Total including upstream catchments					Calibration data[noteA]			
Idcode	Name	Area	Q_{catch}	Q_{out}	q	Diffuse	Point	Total	Total IN	Retention		Total OUT	Conc.	Reference	Concentration	q	Deviation
		km^2	m^3/yr	m^3/yr	L/s	kg/yr	kg/yr	kg/yr	kg/yr	kg/yr	%	kg/yr	mg/L		mg/L	L/s	%
AFM000095	Gunnarsboträsket	2.73	410100	410100	13.0	6539	0	6539	6539	0	0	6539	16				
AFM001100B	Sub-area: Labboträsket	0.08	12000	422100	13.4	183	0	183	6721	0	0	6721	16	**PFM000066**	**16**	**13.2**	**0**
AFM001100A	Sub-area: Labboträsket	1.11	166950	589050	18.7	3388	0	3388	10109	0	0	10109	17	**PFM000074**	**16**	**18.3**	**5**
AFM000096	Gunnarsbo - Lillfjärden (north)	0.10	15600	15600	0.5	304	0	304	304	0	0	304	19				
AFM001099	Gunnarsbo - Lillfjärden (south)	1.09	163350	768000	24.4	2675	0	2675	13088	0	0	13088	17	PFM000087	16		5
AFM000094	Gällsboträsket	2.14	321150	321150	10.2	5910	0	5910	5910	0	0	5910	18				
AFM001103C	Sub-area: Bolundsfjärden	0.09	13650	334800	10.6	239	0	239	6149	0	0	6149	18	**PFM000069**	**18**	**11.8**	**1**
AFM000093	Kungsträsket	0.13	18900	18900	0.6	292	0	292	292	0	0	292	15				
AFM000010B	Eckarfjärden	0.23	34800	34800	1.1	491	0	491	491	0	0	491	14	PFM000071	12		19
AFM000010A	Eckarfjärden	2.04	305250	340050	10.8	4566	0	4566	5057	0	0	5057	15	**PFM000070**	**19**	**9.8**	**20**
AFM001105	Sub-area: Stocksjön	0.21	31500	371550	11.8	650	0	650	5707	0	0	5707	15				
AFM001103B	Sub-area: Bolundsfjärden	0.75	111750	837000	26.5	1897	0	1897	14046	0	0	14046	17	**PFM000068**	**20**	**26.6**	**15**
AFM000089	Vambörsfjärden	0.48	72600	72600	2.3	1470	0	1470	1470	0	0	1470	20				
AFM000088	Fräkengropen	0.14	20850	20850	0.7	412	0	412	412	0	0	412	20				
AFM001104	Sub-area: Graven	0.39	58800	79650	2.5	1327	0	1327	1739	0	0	1739	22				
AFM001103A	Sub-area: Bolundsfjärden	1.41	211200	1200450	38.1	3422	0	3422	20676	0	0	20676	17	**PFM000107**	**18**	**38.1**	**5**
AFM000091	Puttan	0.24	36600	36600	1.2	774	0	774	774	0	0	774	21				
AFM000092	No name	0.07	10650	10650	0.3	143	0	143	143	0	0	143	13				
AFM001101	Sub-area: Norra bassängen	0.35	52500	1300200	41.2	1072	0	1072	22664	0	0	22664	17	PFM000097	17		1
AFM000049	Lillfjärden	0.62	93150	93150	3.0	1915	0	1915	1915	0	0	1915	21				
AFM001106	Sub-area: AFM000085	0.07	10350	103500	3.3	269	0	269	2184	0	0	2184	21				
AFM000086	Tallsundet	0.22	32250	32250	1.0	826	0	826	826	0	0	826	26				
AFM000052B	Bredviken	0.63	95100	95100	3.0	1056	0	1056	1056	0	0	1056	11	PFM000073	11		0
AFM000052A	Bredviken	0.31	46500	141600	4.5	749	0	749	1805	0	0	1805	13				
AFM000084	Simpviken	0.04	5250	5250	0.2	69	0	69	69	0	0	69	13				
AFM000082	No name	0.19	28800	28800	0.9	486	0	486	486	0	0	486	17				
AFM000083	No name	0.08	11550	11550	0.4	236	0	236	236	0	0	236	20				
AFM001108	Sub-area: Märrbadet	0.07	10200	50550	1.6	258	0	258	980	0	0	980	19				
AFM001107	Sub-area: AFM000080	0.56	83700	134250	4.3	1400	0	1400	2380	0	0	2380	18				
AFM001109	Coastal area	1.86	279300	279300	8.9	4238	0	4238	4238	0	0	4238	15				
AFM001110	Coastal area	0.84	125550	125550	4.0	2191	0	2191	2191	0	0	2191	17				
AFM001111	Coastal area	0.11	16050	16050	0.5	233	0	233	233	0	0	233	14				
AFM001112	Coastal area	0.18	26700	26700	0.8	405	0	405	405	0	0	405	15				
AFM001113	Coastal area	0.70	105150	105150	3.3	1656	0	1656	1656	0	0	1656	16				
AFM001114	Coastal area	5.56	834150	834150	26.5	16515	0	16515	16515	0	0	16515	20				
AFM001115	Coastal area	0.39	58350	58350	1.9	1114	0	1114	1114	0	0	1114	19				
AFM000051	Fiskarfjärden	2.93	438900	438900	13.9	7922	0	7922	7922	0	0	7922	18	PFM000072	18		0
	Lillfjärden catchment	0.69	103500	103500	3.3	2184	0	2184		0	0	2184	21				
	Bredviken Catchment	0.94	141600	141600	4.5	1805	0	1805		0	0	1805	13				
	Fiskarfjärden	2.93	438900	438900	13.9	7922	0	7922		0	0	7922	18				
	Gunnarsbo-Lillfjärden	5.12	768000	768000	24.4	13088	0	13088		0	0	13088	17				
	Norra Bassängen	8.67	1300200	1300200	41.2	22664	0	22664		0	0	22664	17				
	Forsmark area (all catchments)	29.13	4369200	4369200	138.5	77288	0	77288		0	0	77288	18				

Note A: Primary calibration dataset is marked in bold.

Element: Total nitrogen (Tot-N), scenario 1			Water balance			Sources per catchment (Gross)			Total including upstream catchments					Calibration data[noteA]			
Idcode	Name	Area	Q_{catch}	Q_{out}	q	Diffuse	Point	Total	Total IN	Retention		Total OUT	Conc.	Reference	Concentration	q	Deviation
		km^2	m^3/yr	m^3/yr	L/s	kg/yr	kg/yr	kg/yr	kg/yr	kg/yr	%	kg/yr	mg/L		mg/L	L/s	%
AFM000095	Gunnarsboträsket	2.73	410100	410100	13.0	304	0	304	304	0	0	304	1				
AFM001100B	Sub-area: Labboträsket	0.08	12000	422100	13.4	6	0	6	310	0	0	310	1	**PFM000066**	**0.72**	**13.2**	**2**
AFM001100A	Sub-area: Labboträsket	1.11	166950	589050	18.7	125	0	125	435	0	0	435	1	**PFM000074**	**0.74**	**18.3**	**0**
AFM000096	Gunnarsbo - Lillfjärden (north)	0.10	15600	15600	0.5	19	0	19	19	0	0	19	1				
AFM001099	Gunnarsbo - Lillfjärden (south)	1.09	163350	768000	24.4	247	0	247	702	0	0	702	1	PFM000087	0.83		10
AFM000094	Gällsboträsket	2.14	321150	321150	10.2	223	0	223	223	0	0	223	1				
AFM001103C	Sub-area: Bolundsfjärden	0.09	13650	334800	10.6	10	0	10	233	0	0	233	1	**PFM000069**	**0.82**	**11.8**	**16**
AFM000093	Kungsträsket	0.13	18900	18900	0.6	13	0	13	13	0	0	13	1				
AFM000010B	Eckarfjärden	0.23	34800	34800	1.1	24	0	24	24	0	0	24	1	PFM000071	0.56		23
AFM000010A	Eckarfjärden	2.04	305250	340050	10.8	347	0	347	371	0	0	371	1	**PFM000070**	**1.09**	**9.8**	**0**
AFM001105	Sub-area: Stocksjön	0.21	31500	371550	11.8	24	0	24	395	0	0	395	1				
AFM001103B	Sub-area: Bolundsfjärden	0.75	111750	837000	26.5	74	0	74	716	0	0	716	1	**PFM000068**	**0.95**	**26.6**	**10**
AFM000089	Vambörsfjärden	0.48	72600	72600	2.3	58	0	58	58	0	0	58	1				
AFM000088	Fräkengropen	0.14	20850	20850	0.7	14	0	14	14	0	0	14	1				
AFM001104	Sub-area: Graven	0.39	58800	79650	2.5	49	0	49	63	0	0	63	1				
AFM001103A	Sub-area: Bolundsfjärden	1.41	211200	1200450	38.1	371	0	371	1208	0	0	1208	1	**PFM000107**	**0.96**	**38.1**	**5**
AFM000091	Puttan	0.24	36600	36600	1.2	48	0	48	48	0	0	48	1				
AFM000092	No name	0.07	10650	10650	0.3	10	0	10	10	0	0	10	1				
AFM001101	Sub-area: Norra bassängen	0.35	52500	1300200	41.2	58	0	58	1323	0	0	1323	1	PFM000097	0.92		11
AFM000049	Lillfjärden	0.62	93150	93150	3.0	95	0	95	95	0	0	95	1				
AFM001106	Sub-area: AFM000085	0.07	10350	103500	3.3	13	0	13	108	0	0	108	1				
AFM000086	Tallsundet	0.22	32250	32250	1.0	34	0	34	34	0	0	34	1				
AFM000052B	Bredviken	0.63	95100	95100	3.0	88	0	88	88	0	0	88	1	PFM000073	0.94		1
AFM000052A	Bredviken	0.31	46500	141600	4.5	62	0	62	150	0	0	150	1				
AFM000084	Simpviken	0.04	5250	5250	0.2	5	0	5	5	0	0	5	1				
AFM000082	No name	0.19	28800	28800	0.9	16	0	16	16	0	0	16	1				
AFM000083	No name	0.08	11550	11550	0.4	7	0	7	7	0	0	7	1				
AFM001108	Sub-area: Märrbadet	0.07	10200	50550	1.6	13	0	13	36	0	0	36	1				
AFM001107	Sub-area: AFM000080	0.56	83700	134250	4.3	101	0	101	137	0	0	137	1				
AFM001109	Coastal area	1.86	279300	279300	8.9	465	0	465	465	0	0	465	2				
AFM001110	Coastal area	0.84	125550	125550	4.0	142	0	142	142	0	0	142	1				
AFM001111	Coastal area	0.11	16050	16050	0.5	14	0	14	14	0	0	14	1				
AFM001112	Coastal area	0.18	26700	26700	0.8	19	0	19	19	0	0	19	1				
AFM001113	Coastal area	0.70	105150	105150	3.3	80	0	80	80	0	0	80	1				
AFM001114	Coastal area	5.56	834150	834150	26.5	653	0	653	653	0	0	653	1				
AFM001115	Coastal area	0.39	58350	58350	1.9	42	0	42	42	0	0	42	1				
AFM000051	Fiskarfjärden	2.93	438900	438900	13.9	503	0	503	503	0	0	503	1	PFM000072	1.13		1
	Lillfjärden catchment	0.69	103500	103500	3.3	108	0	108		0	0	108	1				
	Bredviken Catchment	0.94	141600	141600	4.5	150	0	150		0	0	150	1				
	Fiskarfjärden	2.93	438900	438900	13.9	503	0	503		0	0	503	1				
	Gunnarsbo-Lillfjärden	5.12	768000	768000	24.4	702	0	702		0	0	702	1				
	Norra Bassängen	8.67	1300200	1300200	41.2	1323	0	1323		0	0	1323	1				
	Forsmark area (all catchments)	29.13	4369200	4369200	138.5	4377	0	4377		0	0	4377	1				

Note A: Primary calibration dataset is marked in bold.

Element: Total phosphorus (Tot-P), scenario 1			Water balance			Sources per catchment (Gross)			Total including upstream catchments					Calibration data[noteA]			
Idcode	Name	Area	Q_{catch}	Q_{out}	q	Diffuse	Point	Total	Total IN	Retention		Total OUT	Conc.	Reference	Concentration	q	Deviation
		km^2	m^3/yr	m^3/yr	L/s	kg/yr	kg/yr	kg/yr	kg/yr	kg/yr	%	kg/yr	mg/L		mg/L	L/s	%
AFM000095	Gunnarsboträsket	2.73	410100	410100	13.0	5.6	0.0	5.6	5.6	0	0	5.6	0.014				
AFM001100B	Sub-area: Labboträsket	0.08	12000	422100	13.4	0.4	0.0	0.4	6.0	0	0	6.0	0.014	**PFM000066**	**0.010**	**13.2**	**40**
AFM001100A	Sub-area: Labboträsket	1.11	166950	589050	18.7	1.2	0.0	1.2	7.2	0	0	7.2	0.012	**PFM000074**	**0.009**	**18.3**	**37**
AFM000096	Gunnarsbo - Lillfjärden (north)	0.10	15600	15600	0.5	0.1	0.0	0.1	0.1	0	0	0.1	0.005				
AFM001099	Gunnarsbo - Lillfjärden (south)	1.09	163350	768000	24.4	0.8	0.0	0.8	8.1	0	0	8.1	0.011	PFM000087	0.014		23
AFM000094	Gällsboträsket	2.14	321150	321150	10.2	4.6	0.0	4.6	4.6	0	0	4.6	0.014				
AFM001103C	Sub-area: Bolundsfjärden	0.09	13650	334800	10.6	0.1	0.0	0.1	4.8	0	0	4.8	0.014	**PFM000069**	**0.014**	**11.8**	**0**
AFM000093	Kungsträsket	0.13	18900	18900	0.6	0.1	0.0	0.1	0.1	0	0	0.1	0.008				
AFM000010B	Eckarfjärden	0.23	34800	34800	1.1	1.1	0.0	1.1	1.1	0	0	1.1	0.033	PFM000071	0.039		17
AFM000010A	Eckarfjärden	2.04	305250	340050	10.8	1.9	0.0	1.9	3.0	0	0	3.0	0.009	**PFM000070**	**0.009**	**9.8**	**0**
AFM001105	Sub-area: Stocksjön	0.21	31500	371550	11.8	0.3	0.0	0.3	3.4	0	0	3.4	0.009				
AFM001103B	Sub-area: Bolundsfjärden	0.75	111750	837000	26.5	1.5	0.0	1.5	9.8	0	0	9.8	0.012	**PFM000068**	**0.013**	**26.6**	**11**
AFM000089	Vambörsfjärden	0.48	72600	72600	2.3	1.2	0.0	1.2	1.2	0	0	1.2	0.016				
AFM000088	Fräkengropen	0.14	20850	20850	0.7	0.2	0.0	0.2	0.2	0	0	0.2	0.008				
AFM001104	Sub-area: Graven	0.39	58800	79650	2.5	0.6	0.0	0.6	0.8	0	0	0.8	0.010				
AFM001103A	Sub-area: Bolundsfjärden	1.41	211200	1200450	38.1	1.0	0.0	1.0	12.8	0	0	12.8	0.011	**PFM000107**	**0.011**	**38.1**	**4**
AFM000091	Puttan	0.24	36600	36600	1.2	0.4	0.0	0.4	0.4	0	0	0.4	0.011				
AFM000092	No name	0.07	10650	10650	0.3	0.1	0.0	0.1	0.1	0	0	0.1	0.005				
AFM001101	Sub-area: Norra bassängen	0.35	52500	1300200	41.2	0.4	0.0	0.4	13.7	0	0	13.7	0.011	PFM000097	0.014		24
AFM000049	Lillfjärden	0.62	93150	93150	3.0	1.8	0.0	1.8	1.8	0	0	1.8	0.020				
AFM001106	Sub-area: AFM000085	0.07	10350	103500	3.3	0.2	0.0	0.2	2.0	0	0	2.0	0.020				
AFM000086	Tallsundet	0.22	32250	32250	1.0	0.7	0.0	0.7	0.7	0	0	0.7	0.022				
AFM000052B	Bredviken	0.63	95100	95100	3.0	14.0	0.0	14.0	14.0	0	0	14.0	0.147	PFM000073	0.150		2
AFM000052A	Bredviken	0.31	46500	141600	4.5	0.5	0.0	0.5	14.5	0	0	14.5	0.103				
AFM000084	Simpviken	0.04	5250	5250	0.2	0.1	0.0	0.1	0.1	0	0	0.1	0.011				
AFM000082	No name	0.19	28800	28800	0.9	0.4	0.0	0.4	0.4	0	0	0.4	0.012				
AFM000083	No name	0.08	11550	11550	0.4	0.2	0.0	0.2	0.2	0	0	0.2	0.019				
AFM001108	Sub-area: Märrbadet	0.07	10200	50550	1.6	0.3	0.0	0.3	0.9	0	0	0.9	0.017				
AFM001107	Sub-area: AFM000080	0.56	83700	134250	4.3	0.9	0.0	0.9	1.8	0	0	1.8	0.013				
AFM001109	Coastal area	1.86	279300	279300	8.9	2.1	0.0	2.1	2.1	0	0	2.1	0.008				
AFM001110	Coastal area	0.84	125550	125550	4.0	0.7	0.0	0.7	0.7	0	0	0.7	0.006				
AFM001111	Coastal area	0.11	16050	16050	0.5	0.1	0.0	0.1	0.1	0	0	0.1	0.007				
AFM001112	Coastal area	0.18	26700	26700	0.8	0.2	0.0	0.2	0.2	0	0	0.2	0.006				
AFM001113	Coastal area	0.70	105150	105150	3.3	0.6	0.0	0.6	0.6	0	0	0.6	0.005				
AFM001114	Coastal area	5.56	834150	834150	26.5	40.9	0.0	40.9	40.9	0	0	40.9	0.049				
AFM001115	Coastal area	0.39	58350	58350	1.9	0.7	0.0	0.7	0.7	0	0	0.7	0.011				
AFM000051	Fiskarfjärden	2.93	438900	438900	13.9	8.6	0.0	8.6	8.6	0	0	8.6	0.020	PFM000072	0.038		48
	Lillfjärden catchment	0.69	103500	103500	3.3	2.0	0.0	2.0		0	0	2.0	0.020				
	Bredviken Catchment	0.94	141600	141600	4.5	14.5	0.0	14.5		0	0	14.5	0.103				
	Fiskarfjärden	2.93	438900	438900	13.9	8.6	0.0	8.6		0	0	8.6	0.020				
	Gunnarsbo-Lillfjärden	5.12	768000	768000	24.4	8.1	0.0	8.1		0	0	8.1	0.011				
	Norra Bassängen	8.67	1300200	1300200	41.2	13.7	0.0	13.7		0	0	13.7	0.011				
	Forsmark area (all catchments)	29.13	4369200	4369200	138.5	94.8	0.0	94.8		0	0	94.8	0.022				

Note A: Primary calibration dataset is marked in bold.

Element: Total silicon (Si), scenario 1			Water balance			Sources per catchment (Gross)			Total including upstream catchments					Calibration data[noteA]			
Idcode	Name	Area	Q_{catch}	Q_{out}	q	Diffuse	Point	Total	Total IN	Retention		Total OUT	Conc.	Reference	Concentration	q	Deviation
		km^2	m^3/yr	m^3/yr	L/s	kg/yr	kg/yr	kg/yr	kg/yr	kg/yr	%	kg/yr	mg/L		mg/L	L/s	%
AFM000095	Gunnarsboträsket	2.73	410100	410100	13.0	2300	0	2300	2300	242	11	2058	5.0				
AFM001100B	Sub-area: Labboträsket	0.08	12000	422100	13.4	57	0	57	2115	0	0	2115	5.0	**PFM000066**	**4.7**	**13.2**	**7**
AFM001100A	Sub-area: Labboträsket	1.11	166950	589050	18.7	959	0	959	3074	114	4	2960	5.0	**PFM000074**	**5.0**	**18.3**	**0**
AFM000096	Gunnarsbo - Lillfjärden (north)	0.10	15600	15600	0.5	89	0	89	89	35	39	55	3.5				
AFM001099	Gunnarsbo - Lillfjärden (south)	1.09	163350	768000	24.4	800	0	800	3815	155	4	3659	4.8	PFM000087	1.2		305
AFM000094	Gällsboträsket	2.14	321150	321150	10.2	1767	0	1767	1767	219	12	1548	4.8				
AFM001103C	Sub-area: Bolundsfjärden	0.09	13650	334800	10.6	92	0	92	1640	0	0	1640	4.9	**PFM000069**	**5.6**	**11.8**	**13**
AFM000093	Kungsträsket	0.13	18900	18900	0.6	127	0	127	127	17	13	111	5.9				
AFM000010B	Eckarfjärden	0.23	34800	34800	1.1	211	0	211	211	0	0	211	6.1	PFM000071	4.1		47
AFM000010A	Eckarfjärden	2.04	305250	340050	10.8	1533	0	1533	1745	903	52	842	2.5	**PFM000070**	**2.5**	**9.8**	**0**
AFM001105	Sub-area: Stocksjön	0.21	31500	371550	11.8	179	0	179	1021	30	3	991	2.7				
AFM001103B	Sub-area: Bolundsfjärden	0.75	111750	837000	26.5	706	0	706	3448	0	0	3448	4.1	**PFM000068**	**4.6**	**26.6**	**11**
AFM000089	Vambörsfjärden	0.48	72600	72600	2.3	416	0	416	416	121	29	295	4.1				
AFM000088	Fräkengropen	0.14	20850	20850	0.7	113	0	113	113	24	21	89	4.2				
AFM001104	Sub-area: Graven	0.39	58800	79650	2.5	344	0	344	432	42	10	390	4.9				
AFM001103A	Sub-area: Bolundsfjärden	1.41	211200	1200450	38.1	1025	0	1025	5158	1581	31	3577	3.0	**PFM000107**	**2.6**	**38.1**	**13**
AFM000091	Puttan	0.24	36600	36600	1.2	190	0	190	190	102	54	88	2.4				
AFM000092	No name	0.07	10650	10650	0.3	72	0	72	72	21	29	52	4.8				
AFM001101	Sub-area: Norra bassängen	0.35	52500	1300200	41.2	334	0	334	4051	103	3	3947	3.0	PFM000097	0.0		9242
AFM000049	Lillfjärden	0.62	93150	93150	3.0	490	0	490	490	204	42	285	3.1				
AFM001106	Sub-area: AFM000085	0.07	10350	103500	3.3	44	0	44	330	50	15	280	2.7				
AFM000086	Tallsundet	0.22	32250	32250	1.0	173	0	173	173	76	44	96	3.0				
AFM000052B	Bredviken	0.63	95100	95100	3.0	698	0	698	698	0	0	698	7.3	PFM000073	2.8		164
AFM000052A	Bredviken	0.31	46500	141600	4.5	234	0	234	932	391	42	541	3.8				
AFM000084	Simpviken	0.04	5250	5250	0.2	29	0	29	29	17	57	12	2.4				
AFM000082	No name	0.19	28800	28800	0.9	192	0	192	192	17	9	175	6.1				
AFM000083	No name	0.08	11550	11550	0.4	69	0	69	69	14	20	55	4.8				
AFM001108	Sub-area: Märrbadet	0.07	10200	50550	1.6	39	0	39	269	54	20	215	4.2				
AFM001107	Sub-area: AFM000080	0.56	83700	134250	4.3	459	0	459	674	242	36	432	3.2				
AFM001109	Coastal area	1.86	279300	279300	8.9	1573	0	1573	1573	0	0	1573	5.6				
AFM001110	Coastal area	0.84	125550	125550	4.0	767	0	767	767	0	0	767	6.1				
AFM001111	Coastal area	0.11	16050	16050	0.5	101	0	101	101	0	0	101	6.3				
AFM001112	Coastal area	0.18	26700	26700	0.8	192	0	192	192	0	0	192	7.2				
AFM001113	Coastal area	0.70	105150	105150	3.3	709	0	709	709	0	0	709	6.7				
AFM001114	Coastal area	5.56	834150	834150	26.5	4344	0	4344	4344	0	0	4344	5.2				
AFM001115	Coastal area	0.39	58350	58350	1.9	384	0	384	384	0	0	384	6.6				
AFM000051	Fiskarfjärden	2.93	438900	438900	13.9	1922	0	1922	1922	903	47	1019	2.3	PFM000072	0.9		168
	Lillfjärden catchment	0.69	103500	103500	3.3	534	0	534		254	48	280	2.7				
	Bredviken Catchment	0.94	141600	141600	4.5	932	0	932		391	42	541	3.8				
	Fiskarfjärden	2.93	438900	438900	13.9	1922	0	1922		903	47	1019	2.3				
	Gunnarsbo-Lillfjärden	5.12	768000	768000	24.4	4205	0	4205		546	13	3659	4.8				
	Norra Bassängen	8.67	1300200	1300200	41.2	7111	0	7111		3163	44	3947	3.0				
	Forsmark area (all catchments)	29.13	4369200	4369200	138.5	23733	0	23733		5677	24	18056	4.1				

Note A: Primary calibration dataset is marked in bold.

Element: Strontium (Sr), scenario 1			Water balance			Sources per catchment (Gross)			Total including upstream catchments					Calibration data[noteA]			
Idcode	Name	Area	Q_{catch}	Q_{out}	q	Diffuse	Point	Total	Total IN	Retention		Total OUT	Conc.	Reference	Concentration	q	Deviation
		km^2	m^3/yr	m^3/yr	L/s	kg/yr	kg/yr	kg/yr	kg/yr	kg/yr	%	kg/yr	mg/L		mg/L	L/s	%
AFM000095	Gunnarsboträsket	2.73	410100	410100	13.0	25	0	25	25	1	6	24	0.06				
AFM001100B	Sub-area: Labboträsket	0.08	12000	422100	13.4	1	0	1	25	0	0	25	0.06	**PFM000066**	**0.06**	**13.2**	**5**
AFM001100A	Sub-area: Labboträsket	1.11	166950	589050	18.7	16	0	16	41	1	2	40	0.07	**PFM000074**	**0.07**	**18.3**	**0**
AFM000096	Gunnarsbo - Lillfjärden (north)	0.10	15600	15600	0.5	3	0	3	3	1	24	2	0.12				
AFM001099	Gunnarsbo - Lillfjärden (south)	1.09	163350	768000	24.4	17	0	17	59	1	2	57	0.07	PFM000087	0.08		11
AFM000094	Gällsboträsket	2.14	321150	321150	10.2	31	0	31	31	2	7	28	0.09				
AFM001103C	Sub-area: Bolundsfjärden	0.09	13650	334800	10.6	2	0	2	31	0	0	31	0.09	**PFM000069**	**0.09**	**11.8**	**5**
AFM000093	Kungsträsket	0.13	18900	18900	0.6	2	0	2	2	0	7	2	0.12				
AFM000010B	Eckarfjärden	0.23	34800	34800	1.1	2	0	2	2	0	0	2	0.06	PFM000071	0.09		27
AFM000010A	Eckarfjärden	2.04	305250	340050	10.8	21	0	21	23	8	35	15	0.04	**PFM000070**	**0.04**	**9.8**	**1**
AFM001105	Sub-area: Stocksjön	0.21	31500	371550	11.8	4	0	4	19	0	2	19	0.05				
AFM001103B	Sub-area: Bolundsfjärden	0.75	111750	837000	26.5	17	0	17	68	0	0	68	0.08	**PFM000068**	**0.07**	**26.6**	**12**
AFM000089	Vambörsfjärden	0.48	72600	72600	2.3	12	0	12	12	2	17	10	0.13				
AFM000088	Fräkengropen	0.14	20850	20850	0.7	3	0	3	3	0	12	3	0.14				
AFM001104	Sub-area: Graven	0.39	58800	79650	2.5	10	0	10	13	1	5	12	0.15				
AFM001103A	Sub-area: Bolundsfjärden	1.41	211200	1200450	38.1	33	0	33	123	23	18	100	0.08	**PFM000107**	**0.10**	**38.1**	**16**
AFM000091	Puttan	0.24	36600	36600	1.2	6	0	6	6	2	37	4	0.10				
AFM000092	No name	0.07	10650	10650	0.3	2	0	2	2	0	17	2	0.14				
AFM001101	Sub-area: Norra bassängen	0.35	52500	1300200	41.2	9	21	30	135	2	1	133	0.10	PFM000097	0.11		4
AFM000049	Lillfjärden	0.62	93150	93150	3.0	14	0	14	14	4	27	10	0.11				
AFM001106	Sub-area: AFM000085	0.07	10350	103500	3.3	2	0	2	12	1	8	11	0.10				
AFM000086	Tallsundet	0.22	32250	32250	1.0	5	0	5	5	1	29	4	0.11				
AFM000052B	Bredviken	0.63	95100	95100	3.0	15	0	15	15	0	0	15	0.16	PFM000073	0.25		39
AFM000052A	Bredviken	0.31	46500	141600	4.5	6	0	6	21	6	27	16	0.11				
AFM000084	Simpviken	0.04	5250	5250	0.2	1	0	1	1	0	41	1	0.10				
AFM000082	No name	0.19	28800	28800	0.9	4	0	4	4	0	5	4	0.15				
AFM000083	No name	0.08	11550	11550	0.4	2	0	2	2	0	11	2	0.15				
AFM001108	Sub-area: Märrbadet	0.07	10200	50550	1.6	1	0	1	7	1	11	7	0.13				
AFM001107	Sub-area: AFM000080	0.56	83700	134250	4.3	13	0	13	19	4	22	15	0.11				
AFM001109	Coastal area	1.86	279300	279300	8.9	42	0	42	42	0	0	42	0.15				
AFM001110	Coastal area	0.84	125550	125550	4.0	20	0	20	20	0	0	20	0.16				
AFM001111	Coastal area	0.11	16050	16050	0.5	3	0	3	3	0	0	3	0.16				
AFM001112	Coastal area	0.18	26700	26700	0.8	5	0	5	5	0	0	5	0.18				
AFM001113	Coastal area	0.70	105150	105150	3.3	15	0	15	15	0	0	15	0.15				
AFM001114	Coastal area	5.56	834150	834150	26.5	115	0	115	115	0	0	115	0.14				
AFM001115	Coastal area	0.39	58350	58350	1.9	10	0	10	10	0	0	10	0.16				
AFM000051	Fiskarfjärden	2.93	438900	438900	13.9	59	0	59	59	18	31	40	0.09	PFM000072	0.09		0
	Lillfjärden catchment	0.69	103500	103500	3.3	16	0	16		5	30	11	0.10				
	Bredviken Catchment	0.94	141600	141600	4.5	21	0	21		6	27	16	0.11				
	Fiskarfjärden	2.93	438900	438900	13.9	59	0	59		18	31	40	0.09				
	Gunnarsbo-Lillfjärden	5.12	768000	768000	24.4	61	0	61		4	7	57	0.07				
	Norra Bassängen	8.67	1300200	1300200	41.2	153	21	174		41	23	133	0.10				
	Forsmark area (all catchments)	29.13	4369200	4369200	138.5	546	21	567		81	14	486	0.11				

Note A: Primary calibration dataset is marked in bold.

Appendix G

Compilation of number of hydrochemical observations

Table G1. Compilation of the total number of observations of representative parameters (c.f. *Fel! Hittar inte referenskälla.****) in surface water and shallow groundwater in the Forsmark area. Surface and bottom samples in lakes and sea are denoted with 'S' and 'B' respectively, at the end of the label code. This compilation includes all available samples including the few non-representative samples excluded in presentations and models due to large errors in charge balance. Label codes used in all visualisations are shown in the third column, and elevation in the fourth column denotes the vertical elevation to the sampling point (RHB70, masl).***

IDCODE	Water type	Label	Elevation	pH	Cl	Sr	Si	Fe	S^2	N_{tot}	DOC	^2H	^{13}C	^{14}C	^{34}S	^{87}Sr	Cu	La	U	^{222}Rn
PFM000001	Private well	PP01	-39	5	5	3	3	2	0	2	3	3	0	0	0	0	2	0	0	0
PFM000002	Private well	PP02	-30	1	1	0	0	1	0	0	0	0	0	0	0	0	1	0	0	0
PFM000003	Private well	PP03	9	1	1	0	0	1	0	0	0	0	0	0	0	0	1	0	0	0
PFM000004	Private well	PP04	8	1	1	0	0	1	0	0	0	0	0	0	0	0	1	0	0	0
PFM000005	Private well	PP05	8	1	1	0	0	1	0	0	0	0	0	0	0	0	1	0	0	0
PFM000006	Private well	PP06	8	1	1	0	0	1	0	0	0	0	0	0	0	0	1	0	0	0
PFM000007	Private well	PP07	-1	4	5	3	3	2	0	2	3	3	0	0	0	0	2	0	0	0
PFM000008	Private well	PP08	-1	4	5	3	3	2	0	2	3	3	0	0	0	0	2	0	0	0
PFM000009	Private well	PP09	-69	4	5	3	3	2	0	2	3	3	0	0	0	0	2	0	0	0
PFM000010	Private well	PP10	-3	2	3	2	2	2	0	1	1	1	0	0	0	0	1	0	0	0
PFM000011	Private well	PP11	-61	1	1	0	0	1	0	0	0	0	0	0	0	0	1	0	0	0
PFM000012	Private well	PP12	-2	1	1	0	0	1	0	0	0	0	0	0	0	0	1	0	0	0
PFM000013	Private well	PP13	1	1	1	0	0	1	0	0	0	0	0	0	0	0	1	0	0	0
PFM000014	Private well	PP14	-55	1	1	0	0	1	0	0	0	0	0	0	0	0	1	0	0	0
PFM000015	Private well	PP15	-55	1	1	0	0	1	0	0	0	0	0	0	0	0	1	0	0	0
PFM000016	Private well	PP16	-32	1	1	0	0	1	0	0	0	0	0	0	0	0	1	0	0	0
PFM000017	Private well	PP17	-27	1	1	0	0	1	0	0	0	0	0	0	0	0	1	0	0	0
PFM000018	Private well	PP18	-2	1	1	0	0	1	0	0	0	0	0	0	0	0	1	0	0	0
PFM000019	Private well	PP19	-3	1	1	0	0	1	0	0	0	0	0	0	0	0	1	0	0	0
PFM000020	Private well	PP20	-47	1	1	0	0	1	0	0	0	0	0	0	0	0	1	0	0	0
PFM000021	Private well	PP21	-1	1	1	0	0	1	0	0	0	0	0	0	0	0	1	0	0	0
PFM000022	Private well	PP22	-52	1	1	0	0	1	0	0	0	0	0	0	0	0	1	0	0	0
PFM000023	Private well	PP23	-19	1	1	0	0	1	0	0	0	0	0	0	0	0	1	0	0	0
PFM000024	Private well	PP24	-42	1	1	0	0	1	0	0	0	0	0	0	0	0	1	0	0	0
PFM000025	Private well	PP25	2	1	1	0	0	1	0	0	0	0	0	0	0	0	1	0	0	0
PFM000038	Private well	PP38	-38	1	1	1	1	0	0	0	0	1	0	0	0	0	0	0	0	0
PFM000039	Private well	PP39	-57	3	5	4	4	1	0	3	4	4	0	0	0	0	1	0	0	0
PFM000062	Sea Water	PO62B	-3	14	16	16	16	5	1	15	15	3	2	2	1	1	3	2	2	1
PFM000062	Sea Water	PO62S	-1	55	56	56	56	21	0	55	56	15	5	5	6	5	15	8	10	3
PFM000063	Sea Water	PO63B	-5	18	21	21	21	6	0	20	21	4	3	3	1	1	4	3	3	0
PFM000063	Sea Water	PO63S	-1	39	41	41	41	11	0	40	40	10	5	5	6	5	10	6	9	3
PFM000064	Sea Water	PO64S	-1	51	56	56	56	15	0	54	56	12	6	6	5	4	12	9	10	2
PFM000065	Sea Water	PO65S	-1	34	36	36	36	9	0	35	36	10	4	4	5	4	9	6	8	2
PFM000066	Streaming Water	PW66	7	58	58	58	58	22	1	58	57	16	3	3	3	2	7	6	7	0
PFM000067	Streaming Water	PW67	0	41	42	44	44	12	0	43	44	11	4	4	4	3	7	4	5	0
PFM000068	Streaming Water	PW68	1	66	67	67	67	23	1	66	65	18	4	4	4	3	8	5	6	0
PFM000069	Streaming Water	PW69	3	65	66	66	66	23	0	65	66	14	4	4	1	1	3	1	1	0
PFM000070	Streaming Water	PW70	6	60	58	59	59	20	0	60	60	17	3	3	2	2	7	5	6	0
PFM000071	Streaming Water	PW71	5	33	33	33	33	9	0	33	33	4	3	3	0	0	1	0	0	0
PFM000072	Streaming Water	PW72	0	40	39	40	40	12	2	40	39	10	4	4	4	3	6	4	5	0
PFM000073	Streaming Water	PW73	1	23	23	23	23	5	0	23	23	4	1	1	2	1	3	2	3	0
PFM000074	Lake Water	PL074S	3	60	62	62	62	26	1	61	62	18	6	6	6	6	15	7	9	3
PFM000087	Lake Water	PL087B	0	23	25	25	25	10	1	24	25	7	5	5	3	3	3	2	3	1
PFM000087	Lake Water	PL087S	1	36	38	38	38	12	1	37	38	9	5	5	4	4	7	5	7	1
PFM000097	Lake Water	PL097S	0	35	37	37	37	9	1	36	37	9	4	4	3	2	5	4	6	1
PFM000107	Lake Water	PL107B	-1	28	30	30	30	13	1	29	30	7	4	4	1	1	4	2	3	1
PFM000107	Lake Water	PL107S	0	62	63	64	64	25	1	62	63	16	7	7	6	5	12	7	9	3
PFM000117	Lake Water	PL117B	3	27	30	30	30	12	0	28	28	6	4	4	0	1	5	2	3	1
PFM000117	Lake Water	PL117S	4	59	62	62	62	23	0	61	61	15	6	6	4	4	13	7	9	3
PFM000127	Lake Water	PL127B	-1	7	9	9	9	3	0	8	9	3	2	2	1	1	2	1	1	0
PFM000127	Lake Water	PL127S	0	11	14	14	14	3	0	13	14	3	2	2	1	1	1	0	0	0
PFM000135	Lake Water	PL135B	-1	1	1	1	1	0	0	1	1	0	0	0	0	0	0	0	0	0
PFM000135	Lake Water	PL135S	0	18	19	19	19	5	0	19	19	5	2	2	3	3	5	3	4	2
PFM002457	Precipitation	PN2457	2	6	6	0	0	0	0	0	6	6	0	0	0	0	0	0	0	0
PFM002564	Precipitation	PN2564	11	8	19	0	0	0	0	1	8	19	0	0	0	0	0	0	0	0
SFM0001	Ground Water	S01-4	-4	16	16	16	16	14	11	14	15	16	10	8	10	9	12	10	10	4
SFM0002	Ground Water	S02-3	-3	12	12	12	12	9	4	11	12	12	9	7	10	9	7	7	7	4
SFM0003	Ground Water	S03-9	-9	12	12	12	12	9	8	11	12	12	9	7	10	9	8	7	7	4
SFM0005	Ground Water	S05+4	4	7	7	7	7	6	5	6	6	7	5	3	6	5	5	4	4	1
SFM0006	Ground Water	S06+2	2	6	6	6	6	5	5	6	6	6	5	3	6	4	4	3	4	1
SFM0008	Ground Water	S08-2	-2	9	9	9	9	7	5	8	9	9	6	4	9	8	6	6	6	3

IDCODE	Water type	Label	Elevation	pH	Cl	Sr	Si	Fe	S^{2}	N_{tot}	DOC	^{2}H	^{13}C	^{14}C	^{34}S	^{87}Sr	Cu	La	U	^{222}Rn
SFM0009	Ground Water	S09+2	2	9	9	9	9	6	5	7	8	9	5	4	8	8	6	6	6	2
SFM0010	Ground Water	S10+12	12	1	0	1	1	0	0	0	0	1	0	0	0	0	0	0	0	0
SFM0011	Ground Water	S11-2	-2	1	1	1	1	0	0	0	0	1	0	0	0	0	0	0	0	0
SFM0012	Ground Water	S12-3	-3	10	10	10	10	0	1	8	9	10	8	6	9	8	1	1	1	1
SFM0013	Ground Water	S13-1	-1	1	1	1	1	0	0	0	0	1	0	0	0	0	0	0	0	0
SFM0014	Ground Water	S14+4	4	1	1	1	1	0	0	0	0	1	0	0	0	0	0	0	0	0
SFM0015	Ground Water	S15-2	-2	9	9	9	9	0	1	7	8	9	8	6	0	7	1	1	1	1
SFM0016	Ground Water	S16-2	-2	1	1	1	1	0	0	0	0	1	0	0	0	0	0	0	0	0
SFM0017	Ground Water	S17+2	2	1	1	1	1	0	0	0	0	1	0	0	0	0	0	0	0	0
SFM0018	Ground Water	S18+1	1	1	1	1	1	0	0	0	0	1	0	0	0	0	0	0	0	0
SFM0019	Ground Water	S19-1	-1	1	1	1	1	0	0	0	0	1	0	0	0	0	0	0	0	0
SFM0020	Ground Water	S20-2	-2	1	1	1	1	0	0	0	0	1	0	0	0	0	0	0	0	0
SFM0021	Ground Water	S21-1	-1	1	0	1	1	0	0	0	0	1	0	0	0	0	0	0	0	0
SFM0022	Ground Water	S22-5	-5	4	4	4	4	1	0	3	3	3	3	2	3	3	0	0	0	0
SFM0023	Ground Water	S23-4	-4	12	12	12	12	0	1	9	10	12	6	3	8	8	2	2	2	0
SFM0024	Ground Water	S24-3	-3	3	3	3	3	0	0	1	2	3	2	2	2	2	0	0	0	0
SFM0025	Ground Water	S25-6	-6	9	9	9	9	0	0	7	8	9	6	4	8	8	1	1	1	0
SFM0026	Ground Water	S26-15	-15	1	1	1	1	0	0	0	0	1	0	0	0	0	0	0	0	0
SFM0027	Ground Water	S27-6	-6	9	9	9	9	6	4	7	8	9	6	4	8	8	6	6	6	2
SFM0028	Ground Water	S28-7	-7	1	1	1	1	0	0	0	0	1	0	0	0	0	0	0	0	0
SFM0029	Ground Water	S29-7	-7	8	8	8	8	6	5	6	7	8	5	3	8	8	6	6	6	2
SFM0030	Ground Water	S30-2	-2	1	1	1	1	0	0	0	0	1	0	0	0	0	0	0	0	0
SFM0031	Ground Water	S31-2	-2	8	8	8	8	6	4	7	8	8	6	4	8	8	6	6	6	2
SFM0032	Ground Water	S32-2	-2	14	14	14	14	9	9	10	11	14	8	5	8	8	9	9	9	2
SFM0034	Ground Water	S34-1	-1	1	1	1	1	0	0	0	0	1	0	0	0	0	0	0	0	0
SFM0035	Ground Water	S35-2	-2	0	0	0	0	0	0	0	0	0	0	0	0	0	0	0	0	0
SFM0036	Ground Water	S36-1	-1	1	1	1	1	0	0	0	0	1	0	0	0	0	0	0	0	0
SFM0037	Ground Water	S37-2	-2	12	12	12	12	9	7	10	11	12	6	4	8	8	8	8	8	2
SFM0049	Ground Water	S49-1	-1	10	10	10	10	8	6	7	7	10	4	3	1	4	7	7	7	1
SFM0051	Ground Water	S51-3	-3	25	25	25	25	19	0	0	0	25	16	12	0	16	21	21	21	0
SFM0053	Ground Water	S53-6	-6	16	16	16	16	10	0	0	0	16	16	12	0	16	12	12	12	0
SFM0056	Ground Water	S56-3	-3	16	16	16	16	10	0	0	0	16	0	0	0	2	12	12	12	0
SFM0057	Ground Water	S57+0	0	7	7	7	7	6	5	6	7	7	6	4	7	7	6	6	6	2
SFM0059	Ground Water	S59-1	-1	1	1	1	1	0	0	0	0	1	0	0	0	0	0	0	0	0
SFM0060	Ground Water	S60-3	-3	5	5	5	5	4	2	5	5	5	5	3	5	5	4	4	4	1
SFM0062	Ground Water	S62-3	-3	3	3	3	3	3	0	0	0	3	0	0	0	0	0	0	0	0
SFM0063	Ground Water	S63-3	-3	2	2	2	2	0	0	0	0	2	0	0	0	0	0	0	0	0
SFM0065	Ground Water	S65-4	-4	1	1	1	1	1	0	0	0	1	0	0	0	0	0	0	0	0
SFM0074	Ground Water	S74-3	-3	11	11	11	11	0	0	0	0	11	0	0	0	0	0	0	0	0
SFM0082	Ground Water	S82-4	-1.3	1	1	1	1	1	0	0	0	1	0	0	0	0	0	0	0	0

Table G2. Compilation of the total number of observations of representative (c.f. *Fel! Hittar inte referenskälla.****) parameters in the groundwater of the bedrock in the Forsmark area. This compilation includes all available samples with acceptable charge balance and measurements of flushing water content in KFM-samples. Label codes used in all visualisations are shown in the second column, and elevation in the third column marked 'Elev' denotes the vertical elevation to the midpoint of the sampled section in the RHB70 reference system (masl). For HFM-samples marked with an asterisk, this elevation reflects the elevation of the main supply level rather than the mid point of the section /Forsmark 2.1 data compilation, Laaksoharju et al., in prep./. ChemNet representative samples (dataset C c.f. Section*** *Fel! Hittar inte referenskälla.****) are selected from levels marked in bold.***

IDCODE	Label	Elev	pH	Cl	Sr	Si	Fe	S^2	N_{tot}	DOC	^2H	^{13}C	^{14}C	^{34}S	^{87}Sr	Cu	La	U	^{222}Rn
HFM01	**H01-36**	**-36***	**1**	**1**	**1**	**1**	**0**	**0**	**0**	**0**	**1**	**1**	**1**	**0**	**0**	**0**	**0**	**0**	**0**
HFM01	H01-x	-36*	8	8	8	8	2	0	0	0	7	4	4	3	3	0	0	0	0
HFM01	H01-132	-132	1	1	1	1	0	0	0	0	0	0	0	0	0	0	0	0	0
HFM02	**H02-40**	**-40***	**3**	**3**	**3**	**3**	**2**	**1**	**0**	**1**	**3**	**1**	**1**	**1**	**1**	**1**	**1**	**1**	**1**
HFM02	H02-x	-40*	2	2	2	2	0	0	0	0	0	0	0	0	0	0	0	0	0
HFM03	**H03-18**	**-18***	**1**	**1**	**1**	**1**	**0**	**0**	**0**	**0**	**1**	**1**	**1**	**0**	**0**	**0**	**0**	**0**	**0**
HFM04	**H04-58**	**-58***	**6**	**6**	**6**	**6**	**2**	**1**	**0**	**1**	**6**	**3**	**3**	**4**	**4**	**1**	**1**	**1**	**1**
HFM05	**H05-146**	**-146***	**9**	**9**	**9**	**9**	**4**	**0**	**0**	**0**	**9**	**7**	**7**	**8**	**9**	**1**	**1**	**1**	**0**
HFM06	**H06-63**	**-63***	**4**	**4**	**4**	**4**	**0**	**0**	**0**	**0**	**4**	**4**	**4**	**4**	**4**	**0**	**0**	**0**	**0**
HFM08	**H08-48**	**-48**	**1**	**1**	**1**	**1**	**0**	**0**	**0**	**0**	**1**	**1**	**1**	**1**	**1**	**0**	**0**	**0**	**0**
HFM08	**H08-131**	**-131***	**2**	**2**	**2**	**2**	**0**	**0**	**0**	**0**	**2**	**2**	**2**	**2**	**2**	**0**	**0**	**0**	**0**
HFM09	**H09-19**	**-19***	**4**	**4**	**4**	**4**	**0**	**0**	**0**	**0**	**2**	**2**	**2**	**2**	**2**	**0**	**0**	**0**	**0**
HFM10	**H10-105**	**-105***	**4**	**4**	**4**	**4**	**0**	**0**	**0**	**0**	**4**	**4**	**4**	**4**	**4**	**0**	**0**	**0**	**0**
HFM11	H11-25	-25*	3	3	3	3	0	0	0	0	3	1	1	2	2	0	0	0	0
HFM12	**H12-87**	**-87***	**3**	**3**	**3**	**3**	**0**	**0**	**0**	**0**	**3**	**1**	**1**	**3**	**3**	**0**	**0**	**0**	**0**
HFM13	H13-x	-77	4	4	4	4	0	0	0	0	4	2	2	4	4	0	0	0	0
HFM13	**H13-134**	**-134***	**3**	**3**	**3**	**3**	**2**	**1**	**0**	**1**	**3**	**1**	**1**	**1**	**1**	**1**	**1**	**1**	**1**
HFM14	**H14-65**	**-65**	**9**	**9**	**9**	**9**	**0**	**0**	**0**	**0**	**4**	**1**	**1**	**3**	**3**	**0**	**0**	**0**	**0**
HFM15	**H15-90**	**-90**	**3**	**3**	**3**	**3**	**2**	**1**	**0**	**1**	**3**	**1**	**1**	**1**	**1**	**1**	**1**	**1**	**1**
HFM15	H15-x	-100	3	3	3	3	1	0	0	0	3	1	1	3	3	0	0	0	0
HFM16	**H16-56**	**-56***	**4**	**4**	**4**	**4**	**0**	**0**	**0**	**0**	**2**	**1**	**1**	**1**	**1**	**0**	**0**	**0**	**0**
HFM17	**H17-27**	**-27***	**3**	**3**	**3**	**3**	**0**	**0**	**0**	**0**	**1**	**1**	**0**	**1**	**1**	**0**	**0**	**0**	**0**
HFM18	H18-30	-30*	3	3	3	3	0	0	0	0	1	1	0	1	1	0	0	0	0
HFM19	**H19-147**	**-147***	**3**	**3**	**3**	**3**	**2**	**1**	**0**	**1**	**3**	**1**	**1**	**1**	**1**	**1**	**1**	**1**	**1**
HFM20	H20-22	-22*	3	3	3	3	0	0	0	0	1	1	1	1	1	0	0	0	0
HFM21	H21-107	-107	6	6	6	6	2	0	0	1	4	4	4	3	4	0	0	0	0
HFM22	**H22-53**	**-53***	**8**	**8**	**8**	**8**	**2**	**0**	**0**	**0**	**8**	**8**	**6**	**8**	**8**	**0**	**0**	**2**	**0**
HFM23	H23-67	-67	3	3	3	3	0	0	0	0	1	0	0	0	0	0	0	0	0
HFM24	**H24-70**	**-70**	**5**	**5**	**5**	**5**	**1**	**0**	**0**	**0**	**2**	**1**	**1**	**1**	**1**	**0**	**0**	**1**	**0**
HFM25	H25-71	-71	1	1	1	1	0	0	0	0	1	0	0	0	0	0	0	0	0
HFM26	H26-75	-75	3	3	3	3	0	0	0	0	1	0	0	0	0	0	0	0	0
HFM27	**H27-46**	**-46**	**1**	**1**	**1**	**1**	**0**	**0**	**0**	**0**	**1**	**0**	**0**	**0**	**0**	**0**	**0**	**0**	**0**
HFM27	H27-x	-57	3	3	3	3	0	0	0	0	1	0	0	0	0	0	0	0	0
HFM28	H28-71	-71	3	3	3	3	0	0	0	0	1	0	0	0	0	0	0	0	0
HFM29	**H29-85**	**-85**	**2**	**2**	**2**	**2**	**0**	**0**	**0**	**0**	**1**	**0**	**0**	**0**	**0**	**0**	**0**	**0**	**0**
HFM32	H32-12	-12	1	1	1	1	0	0	0	0	1	0	0	0	0	0	0	0	0
HFM32	**H32-28**	**-28**	**2**	**2**	**2**	**2**	**0**	**0**	**0**	**0**	**2**	**0**	**0**	**0**	**0**	**0**	**0**	**0**	**0**
HFM32	H32-64	-64	1	1	1	1	0	0	0	0	1	0	0	0	0	0	0	0	0
HFM32	H32-x	-100	4	4	4	4	0	0	0	0	2	0	0	0	0	0	0	0	0
HFM32	H32-148	-148	1	1	1	1	0	0	0	0	1	0	0	0	0	0	0	0	0
HFM33	**H33-56**	**-56**	**3**	**3**	**3**	**3**	**0**	**0**	**0**	**0**	**1**	**0**	**0**	**0**	**0**	**0**	**0**	**0**	**0**
HFM34	H34-83	-83	3	3	3	3	0	0	0	0	1	0	0	0	0	0	0	0	0
HFM35	H35-79	-79	2	2	2	2	0	0	0	0	0	0	0	0	0	0	0	0	0
KFM01A	**K01A-112**	**-112**	**1**	**8**	**7**	**7**	**7**	**1**	**0**	**1**	**6**	**1**	**1**	**3**	**3**	**0**	**1**	**1**	**1**
KFM01A	K01A-116	-116	1	1	1	1	1	0	0	0	1	0	0	0	0	0	0	0	0
KFM01A	**K01A-177**	**-177**	**3**	**9**	**9**	**9**	**9**	**3**	**0**	**3**	**9**	**4**	**4**	**4**	**4**	**0**	**5**	**5**	**1**
KFM01B	K01B-37	-37	1	1	1	1	1	0	0	0	1	1	1	1	1	0	0	0	0
KFM01D	**K01D-156**	**-156**	**1**	**1**	**1**	**1**	**0**	**0**	**0**	**0**	**1**	**0**	**0**	**0**	**0**	**0**	**0**	**0**	**0**
KFM01D	**K01D-212**	**-212**	**1**	**1**	**1**	**1**	**0**	**0**	**0**	**0**	**1**	**0**	**0**	**0**	**0**	**0**	**0**	**0**	**0**
KFM01D	**K01D-283**	**-283**	**1**	**1**	**1**	**1**	**0**	**0**	**0**	**0**	**1**	**0**	**0**	**0**	**0**	**0**	**0**	**0**	**0**
KFM01D	**K01D-294**	**-294**	**1**	**1**	**1**	**1**	**0**	**0**	**0**	**0**	**1**	**0**	**0**	**0**	**0**	**0**	**0**	**0**	**0**
KFM01D	**K01D-341**	**-341**	**3**	**6**	**6**	**6**	**6**	**3**	**0**	**3**	**6**	**0**	**0**	**3**	**3**	**3**	**3**	**3**	**0**
KFM01D	**K01D-446**	**-446**	**4**	**4**	**4**	**4**	**4**	**4**	**0**	**4**	**4**	**0**	**0**	**4**	**4**	**4**	**4**	**4**	**0**
KFM02A	**K02A-109**	**-109**	**1**	**3**	**3**	**3**	**3**	**1**	**0**	**1**	**3**	**1**	**1**	**1**	**1**	**0**	**1**	**1**	**1**
KFM02A	K02A-267	-267	1	1	1	1	0	0	0	0	0	0	0	0	0	0	0	0	0
KFM02A	**K02A-415**	**-415**	**4**	**4**	**4**	**4**	**3**	**3**	**0**	**3**	**4**	**2**	**2**	**2**	**2**	**1**	**1**	**2**	**2**
KFM02A	**K02A-495**	**-495**	**2**	**2**	**2**	**2**	**2**	**2**	**0**	**2**	**2**	**2**	**1**	**2**	**2**	**2**	**2**	**2**	**1**
KFM02A	**K02A-504**	**-504**	**3**	**10**	**10**	**10**	**10**	**3**	**0**	**3**	**2**	**1**	**1**	**2**	**2**	**0**	**5**	**5**	**2**
KFM03A	K03A-138	-138	1	1	1	1	0	0	0	0	1	1	1	1	1	0	0	0	0
KFM03A	K03A-262	-262	1	1	1	1	0	0	0	0	1	1	1	0	1	0	0	0	0
KFM03A	K03A-362	-362	1	1	1	1	0	0	0	0	1	1	1	0	1	0	0	0	0
KFM03A	**K03A-380**	**-380**	**1**	**4**	**4**	**4**	**4**	**0**	**0**	**1**	**4**	**1**	**1**	**1**	**1**	**0**	**1**	**1**	**1**
KFM03A	**K03A-441**	**-441**	**1**	**2**	**2**	**2**	**2**	**1**	**0**	**1**	**2**	**1**	**1**	**1**	**1**	**0**	**1**	**1**	**1**
KFM03A	K03A-443	-443	1	2	2	2	2	1	0	0	2	1	0	2	2	0	0	0	1
KFM03A	K03A-487	-487	1	1	1	1	0	0	0	0	0	0	0	0	0	0	0	0	0
KFM03A	K03A-611	-611	1	1	1	1	0	0	0	0	0	0	0	0	0	0	0	0	0
KFM03A	**K03A-632**	**-632**	**6**	**9**	**10**	**10**	**9**	**4**	**0**	**5**	**9**	**0**	**0**	**6**	**6**	**3**	**4**	**6**	**4**
KFM03A	K03A-710	-710	1	1	1	1	0	0	0	0	0	0	0	0	0	0	0	0	0
KFM03A	K03A-793	-793	1	1	1	1	1	0	0	1	1	1	0	1	1	0	0	0	0
KFM03A	K03A-810	-810	1	1	1	1	0	0	0	0	0	0	0	0	0	0	0	0	0
KFM03A	K03A-934	-934	1	1	1	1	0	0	0	0	1	0	0	1	1	0	0	0	0
KFM03A	**K03A-970**	**-970**	**4**	**11**	**11**	**11**	**10**	**2**	**0**	**2**	**11**	**0**	**0**	**4**	**4**	**1**	**4**	**4**	**1**
KFM04A	K04A-11	-11	1	1	1	1	0	0	0	0	1	0	0	0	0	0	0	0	0

KFM04A	K04A-120	-120	1	1	1	1	0	0	0	0	1	1	1	1	1	0	0	0	0
KFM04A	**K04A-185**	**-185**	**2**	**6**	**6**	**6**	**6**	**2**	**0**	**2**	**6**	**0**	**0**	**2**	**2**	**0**	**2**	**2**	**0**
IDCODE	**Label**	**Elev**	**pH**	**Cl**	**Sr**	**Si**	**Fe**	**S^2**	**N_{tot}**	**DOC**	**^2H**	**^{13}C**	**^{14}C**	**^{34}S**	**^{87}Sr**	**Cu**	**La**	**U**	**^{222}Rn**
KFM04A	K04A-228	-228	1	1	1	1	0	0	0	0	1	1	1	0	0	0	0	0	0
KFM04A	K04A-314	-314	1	1	1	1	0	0	0	0	0	0	0	0	0	0	0	0	0
KFM04A	K04A-416	-416	1	1	1	1	0	0	0	0	0	0	0	0	0	0	0	0	0
KFM04A	K04A-515	-515	1	1	1	1	0	0	0	0	0	0	0	0	0	0	0	0	0
KFM04A	K04A-592	-592	1	1	1	1	1	0	0	0	0	0	0	0	0	0	0	0	0
KFM04A	K04A-666	-666	1	1	1	1	0	0	0	0	0	0	0	0	0	0	0	0	0
KFM04A	K04A-755	-755	1	1	1	1	0	0	0	0	0	0	0	0	0	0	0	0	0
KFM05A	**K05A-91**	**-91**	**1**	**1**	**1**	**1**	**0**	**0**	**0**	**0**	**1**	**1**	**1**	**0**	**0**	**0**	**0**	**0**	**0**
KFM06A	K06A-16	-16	1	1	1	1	1	0	0	0	1	0	0	0	0	0	0	0	0
KFM06A	K06A-122	-122	1	1	1	1	1	0	0	0	1	1	1	1	1	0	0	0	0
KFM06A	K06A-186	-186	1	1	1	1	1	0	0	0	1	1	1	0	1	0	0	0	0
KFM06A	K06A-292	-292	1	1	1	1	1	0	0	0	0	0	0	0	0	0	0	0	0
KFM06A	K06A-298	-298	1	1	1	1	0	0	0	0	1	0	0	0	0	0	0	0	0
KFM06A	**K06A-302**	**-302**	**1**	**8**	**8**	**8**	**8**	**0**	**0**	**0**	**7**	**1**	**1**	**4**	**4**	**0**	**4**	**4**	**1**
KFM06A	K06A-397	-397	1	1	1	1	1	0	0	0	0	0	0	0	0	0	0	0	0
KFM06A	K06A-480	-480	1	1	1	1	1	0	0	0	0	0	0	0	0	0	0	0	0
KFM06A	K06A-604	-604	1	1	1	1	1	0	0	0	0	0	0	0	0	0	0	0	0
KFM06A	K06A-623	-623	1	1	1	1	0	0	0	0	1	0	0	0	0	0	0	0	0
KFM06A	**K06A-646**	**-646**	**1**	**9**	**9**	**9**	**9**	**1**	**0**	**1**	**9**	**1**	**1**	**5**	**5**	**0**	**0**	**0**	**0**
KFM06A	K06A-705	-705	1	1	1	1	1	0	0	0	0	0	0	0	0	0	0	0	0
KFM06A	K06A-805	-805	1	1	1	1	1	0	0	0	0	0	0	0	0	0	0	0	0
KFM06C	K06C-436	-436	1	1	1	1	1	0	0	0	0	0	0	0	0	0	0	0	0
KFM07A	K07A-19	-19	1	1	1	1	1	0	0	0	0	0	0	0	0	0	0	0	0
KFM07A	K07A-126	-126	1	1	1	1	1	0	0	0	0	0	0	0	0	0	0	0	0
KFM07A	K07A-233	-233	1	1	1	1	1	0	0	0	0	0	0	0	0	0	0	0	0
KFM07A	K07A-317	-317	1	1	1	1	1	0	0	0	1	1	1	0	1	0	0	0	0
KFM07A	K07A-420	-420	1	1	1	1	1	0	0	0	1	0	0	1	1	0	0	0	0
KFM07A	K07A-523	-523	1	1	1	1	1	0	0	0	1	0	0	0	1	0	0	0	0
KFM07A	K07A-604	-604	1	1	1	1	1	0	0	0	1	0	0	0	1	0	0	0	0
KFM07A	K07A-683	-683	1	1	1	1	1	0	0	0	1	0	0	0	1	0	0	0	0
KFM07A	**K07A-760**	**-760**	**1**	**10**	**10**	**10**	**10**	**1**	**0**	**1**	**10**	**0**	**0**	**5**	**5**	**1**	**5**	**5**	**1**
KFM08A	K08A-28	-28	1	1	1	1	1	0	0	0	1	1	1	0	1	0	0	0	0
KFM08A	K08A-128	-128	1	1	1	1	1	0	0	0	1	0	0	1	1	0	0	0	0
KFM08A	K08A-135	-135	1	1	1	1	1	0	0	0	1	1	1	1	1	0	0	0	0
KFM08A	K08A-238	-238	1	1	1	1	1	0	0	0	1	1	1	0	1	0	0	0	0
KFM08A	K08A-319	-319	1	1	1	1	1	0	0	0	0	0	0	0	0	0	0	0	0
KFM08A	K08A-416	-416	1	1	1	1	1	0	0	0	0	0	0	0	0	0	0	0	0
KFM08A	K08A-509	-509	1	1	1	1	1	0	0	0	0	0	0	0	0	0	0	0	0
KFM08A	**K08A-545**	**-547**	**8**	**13**	**13**	**13**	**13**	**7**	**0**	**8**	**13**	**0**	**0**	**7**	**7**	**7**	**7**	**7**	**1**
KFM08A	K08A-581	-581	1	1	1	1	1	0	0	0	0	0	0	0	0	0	0	0	0
KFM09A	K09A-56	-56	1	1	1	1	1	0	0	0	0	0	0	0	0	0	0	0	0
KFM09A	K09A-141	-141	1	1	1	1	1	0	0	0	0	0	0	0	0	0	0	0	0
KFM09A	K09A-224	-224	1	1	1	1	1	0	0	0	0	0	0	0	0	0	0	0	0
KFM09A	K09A-305	-305	1	1	1	1	1	0	0	0	0	0	0	0	0	0	0	0	0
KFM09A	K09A-384	-384	1	1	1	1	1	0	0	0	0	0	0	0	0	0	0	0	0
KFM09A	K09A-461	-461	1	1	1	1	1	0	0	0	1	0	0	0	0	0	0	1	0
KFM09A	K09A-534	-534	1	1	1	1	1	0	0	0	1	0	0	0	0	0	0	1	0
KFM09A	K09A-602	-602	1	1	1	1	1	0	0	0	1	0	0	0	0	0	0	1	0
KFM09A	**K09A-615**	**-615**	**3**	**4**	**4**	**4**	**4**	**3**	**0**	**3**	**4**	**0**	**0**	**2**	**2**	**2**	**2**	**2**	**0**
KFM09B	K09B-66	-66	1	1	1	1	0	0	0	0	0	0	0	0	0	0	0	0	0
KFM09B	K09B-146	-146	1	1	1	1	0	0	0	0	0	0	0	0	0	0	0	0	0
KFM09B	K09B-224	-224	1	1	1	1	0	0	0	0	0	0	0	0	0	0	0	0	0
KFM09B	K09B-301	-301	1	1	1	1	0	0	0	0	0	0	0	0	0	0	0	0	0
KFM09B	K09B-375	-375	1	1	1	1	0	0	0	0	0	0	0	0	0	0	0	0	0
KFM09B	K09B-445	-445	1	1	1	1	0	0	0	0	0	0	0	0	0	0	0	0	0

Appendix H

Title: Compilation of hydrochemical data

Compilation of hydrochemical data from percussion drilled boreholes (HFM), cored boreholes (KFM), lakes, streams, sea water, precipitation, private wells, springs (PFM) and soil tubes (SFM). The table shows mean values of available samples per section or depth level, based on ChemNet representative data selection (c.f. Section 2.2.4).

Data from percussion boreholes should be used with caution as they may represent mixed ground water of different origin.

The number at the end of the label code represents the vertical elevation of the mid point (RHB70) of the sampled section when the borehole is sectioned by packers, or the midpoint of the borehole if there is only one section. If there is information about the main supply level in percussion drilled boreholes, this elevation replace the mid section value /Forsmark 2.1 data compilation, Laaksoharju et al., in prep./.

IDCODE	Label	First	Last	Na	K	Ca	Mg	HCO3	Cl	SO_4	Br	Li	Sr	Fe	Mn	pH	U	Th	La	D	Tr	^{18}O	^{14}C	^{13}C	^{34}S	^{87}Sr	Ntot	Ptot	TOC
HFM01	H01-36	2002-05-16	2002-05-16	498	14	60	17	440	530	202	1.62	0.015	0.3			8.4				-64	3.7	-9.5	46	-10.2					10
HFM02	H02-40	2005-11-09	2005-11-09	339	14	68	21	407	396	84	1.91	0.014	0.4	0.42	0.13	7.8	11.2	0.01	0.04	-82	9.6	-11.5	67	-11.7	17.9	0.724			10
HFM03	H03-18	2002-05-29	2002-05-29	65	10	62	14	310	16	19	0.10	0.011	0.3			7.6				-80	12.0	-11.8	85	-14.9					
HFM04	H04-58	2005-11-07	2005-11-07	153	6	31	8	390	56	45	0.23	0.006	0.2	0.35	0.08	7.7	3.2	0.03	0.12	-84	10.6	-11.7	73	-12.3	13.4	0.720			8
HFM05	H05-146	2002-12-19	2002-12-19	1740	41	749	199	122	4340	299	21.98	0.043	5.4			7.4				-75	<0.8	-10.3	25	-7.1	24.6	0.719			3
HFM06	H06-63	2003-01-21	2003-01-21	629	28	175	55	373	1108	208	3.71	0.017	1.3			7.6				-80	5.7	-10.6	61	-11.3	17.3	0.719			5
HFM08	H08-48	2003-03-20	2003-03-20	1150	33	572	139	173	2694	319	10.98	0.033	4.2			7.3				-73	1.2	-9.4	20	-6.4	22.2	0.719			
HFM08	H08-131	2003-03-18	2003-03-18	2210	68	754	287	116	5422	534	24.12	0.052	6.4			7.3				-66	<0.8	-8.4	21	-5.0	23.7	0.718			
HFM09	H09-19	2004-02-18	2004-02-18	274	6	41	8	466	181	85	0.57	0.014	0.4			7.9				-81	12.1	-11.1	60	-12.2	18.7	0.720			9
HFM10	H10-105	2003-08-21	2003-08-21	1610	22	945	173	161	4466	410	16.70	0.043	10.0			7.2				-73	1.9	-9.5	33	-8.4	24.7	0.717			3
HFM12	H12-87	2003-09-26	2003-09-26	783	6	779	63	177	2617	174	12.10	0.036	9.0			7.4				-94	<0.8	-12.6			31.6	0.717			5
HFM13	H13-134	2005-11-09	2005-11-09	1710	25	1180	198	124	5020	476	23.70	0.052	12.9	3.11	2.15	7.3	16.2	0.10	0.79	-72	<0.8	-9.5	18	-5.8	21.1	0.718			2
HFM14	H14-65	2006-04-04	2006-04-04	196	9	158	17	469	302	80	1.04	0.010	0.5			6.9				-82	8.1	-11.5							15
HFM15	H15-90	2005-11-09	2005-11-09	358	9	97	15	471	406	104	2.02	0.013	0.4	1.02	0.47	7.4	18.1	0.04	0.18	-81	6.0	-9.4	61	-11.2	27.8	0.722			13
HFM16	H16-56			276	7	46	11	466	204	95	0.78	0.011	0.3			7.7				-81	6.7	-11.1							
HFM17	H17-27	2004-01-27	2004-01-27	399	13	42	14	461	415	109	1.07	0.011	0.3			7.9				-80	7.8	-10.9		-9.8	20.9	0.723			14
HFM18	H18-30	2004-02-10	2004-02-10	206	9	24	8	450	57	106	0.14	0.011	0.2			7.9													6
HFM19	H19-147	2005-11-09	2005-11-09	2050	57	960	259	129	5330	565	23.60	0.058	7.8	5.40	1.93	7.2	5.0	0.10	0.10	-65	1.0	-8.5	31	-3.9	25.0	0.723			40
HFM21	H21-107	2004-08-10	2004-08-10	1500	32	637	148	220	3440	408	12.20	0.052	4.4			7.4													4
HFM22	H22-53	2004-09-24	2004-09-24	1500	40	575	153	173	3660	422	12.50	0.053	3.2			7.4				-68	1.6	-8.9		-6.1	21.7	0.722			3
HFM24	H24-70	2006-04-06	2006-04-06	340	14	102	23	391	501	103	1.63	0.017	0.7			7.7	16.6	0.01		-80	7.5	-10.9	61	-11.6	18.9	0.724			11
HFM27	H27-46	2006-05-30	2006-05-30	1130	34	512	134	235	2720	347	9.20	0.040	3.3			7.4				-74	1.7	-9.6							
HFM29	H29-85	2006-05-15	2006-05-15	207	8	38	8	442	107	51	0.30	0.015	0.3			8.1				-85	6.5	-11.5							10
HFM32	H32-28	2006-06-01	2006-06-01	1830	61	556	190	188	4100	388	14.70	0.063	3.7			7.1				-70	<0.8	-9.0							
HFM33	H33-56	2006-05-09	2006-05-09	2090	33	1020	251	125	5350	443	18.80	0.062	8.9			7.3				-68	1.2	-8.7							1
KFM01A	K01A-112	2003-02-24	2003-02-24	1740	26	874	142	62	4563	316	18.35	0.046	6.4	0.79	0.69	7.5	1.5	0.10	0.03	-88	<0.8	-11.6	13	-9.0	25.5	0.720			
KFM01A	K01A-177	2003-03-31	2003-03-31	2000	29	934	204	100	5330	547	20.09	0.061	6.9	0.52	1.02	7.6	14.9	0.61	0.03	-69	<0.8	-8.8	17	-6.5	25.6	0.721			
KFM01D	K01D-156	2006-08-06	2006-08-06	1410	26	684	85	106	3360	302	14.80	0.041	6.2			7.5				-76	2.4	-10.2							
KFM01D	K01D-212	2006-08-09	2006-08-09	1490	33	681	107	195	3570	352	14.90	0.044	5.5			7.5				-72	1.9	-9.3							
KFM01D	K01D-283	2006-08-08	2006-08-08	1530	31	751	106	154	3790	320	18.10	0.044	6.7			7.4				-72	1.7	-9.7							
KFM01D	K01D-294	2006-08-03	2006-08-03	1610	33	796	117	144	4070	288	21.10	0.043	6.8			7.5				-71	2.7	-9.7							
KFM01D	K01D-341	2006-06-26	2006-06-26	1630	9	1620	14	22	5160	79	37.90	0.028	18.1	1.36	0.17	7.5	1.9	0.10	0.03	-77	<0.8	-11.1			33.8	0.720			
KFM01D	K01D-446	2006-07-30	2006-07-30	1770	8	1830	15	20	5800	38	46.20	0.024	19.8	1.25	0.11	7.4	0.8	0.10	0.10	-65	1.3	-10.6			24.7	0.721			10
KFM02A	K02A-52	2002-11-29	2002-11-29	168	6	34	8	379	84	54	0.28	0.009	0.2			8.0				-82	11.2	-11.4	86	-6.6	13.9	0.720			
KFM02A	K02A-109	2003-11-18	2003-11-18	366	10	139	31	354	642	90	2.79	0.014	1.0	1.37	0.25	7.5	5.4	0.03	0.10	-81	<0.8	-11.2	65	-12.4	20.8	0.719			7
KFM02A	K02A-415	2004-02-23	2004-02-23	1820	21	1140	198	93	5380	434	25.80	0.057	11.2	0.74	1.81	7.4	13.9	0.10	0.43	-76	<0.8	-10.2	8	-5.9	26.0	0.717			
KFM02A	K02A-495	2005-11-07	2005-11-07	2160	36	890	244	126	5540	507	24.30	0.049	8.7	1.85	2.07	7.2	122.0	0.10	0.57	-66	0.9	-8.7	17	-4.9	21.9	0.718			1
KFM02A	K02A-504	2003-10-20	2003-10-20	2040	34	934	226	126	5410	498	23.80	0.051	8.0	1.70	2.16	7.2	88.6	0.10	0.18	-67	2.4	-8.8	17	-7.0	24.9	0.718			
KFM03A	K03A-380	2003-10-06	2003-10-06	2110	48	925	223	101	5450	495	22.77	0.050	8.3	0.74	1.13	7.3	3.5	0.10	0.18	-69	2.0	-9.1	20	-5.9	25.0	0.718			1
KFM03A	K03A-441	2003-10-24	2003-10-24	2070	27	985	202	92	5430	472	24.71	0.049	10.1	0.91	1.17	7.5	2.2	0.10	0.37	-71	<0.8	-9.4	19	-5.3	25.4	0.717			1
KFM03A	K03A-632	2004-02-23	2005-11-07	1755	18	1495	66	28	5535	214	39.50	0.031	17.9	0.61	0.41	7.5	45.7	0.10	0.32	-84	0.6	-11.5			26.5	0.717			1
KFM03A	K03A-970	2003-12-08	2005-11-07	2050	10	3830	9	9	10095	47	124.25	0.026	45.3	0.56	0.05	7.3	0.4	0.10	0.44	-98	<0.8	-13.7			29.4	0.718			10
KFM04A	K04A-185	2004-02-10	2004-02-10	1820	26	1340	224	111	5580	514	29.50	0.060	13.5	2.01	2.81		62.0	0.10	0.03	-84	<0.8	-9.0			24.5	0.718			
KFM05A	K05A-91	2004-02-17	2004-02-17	1710	47	862	197	127	4370	486	13.50	0.056	4.9			7.2				-64	1.5	-8.5	13	-5.7					3

IDCODE	Label	First	Last	Na	K	Ca	Mg	HCO3	Cl	SO_4	Br	Li	Sr	Fe	Mn	pH	U	Th	La	D	Tr	^{18}O	^{14}C	^{13}C	^{34}S	^{87}Sr	Ntot	Ptot	TOC
KFM06A	K06A-40	2003-12-08	2003-12-08	285	9	55	12	371	295	86	1.03	0.011	0.4			8.1				-84	9.3	-11.3	55	-11.6	19.1	0.719			13
KFM06A	K06A-302	2005-03-07	2005-03-07	1450	13	1300	71	46	4560	151	29.50	0.049	14.9	0.90	0.58		9.6	0.20	0.02	-86	<0.8	-11.9	29	-8.0	27.5	0.717			
KFM06A	K06A-646	2005-01-31	2005-01-31	1690	7	2500	4	6	7080	36	54.00	0.028	26.7	0.04	0.08	8.3				-82	<0.8	-11.5	37	-20.4	38.4	0.717			
KFM07A	K07A-760	2005-03-24	2005-03-24	2780	14	5740	22	7	14400	103	189.00	0.074	68.4	0.28	0.14		0.3	0.20	0.05	-87	<0.8	-12.9			22.8	0.718			
KFM08A	K08A-545	2005-10-31	2005-10-31	1560	11	2090	14	10	6100	92	44.50	0.021	23.3	0.68	0.19	7.8	6.4	0.10	0.01	-93	<0.8	-13.2			29.1	0.718			1
KFM09A	K09A-615	2006-04-27	2006-04-27	2620	13	6520	18	7	14800	118	143.00	0.074	73.7	0.13	0.11	8.2	0.1	0.10	0.03	-92	<0.8	-13.3			27.0	0.717			
PFM000001	PP01	2003-11-03	2004-10-19	43	32	159	32	620	50	114	0.30	0.026	0.5			7.0				-82	10.6	-11.9					3.490	0.006	7
PFM000007	PP07	2003-11-03	2004-10-12	6	8	186	7	513	5	89	0.15	0.002	0.3			6.9				-87	11.3	-12.6					0.942	0.064	11
PFM000008	PP08	2003-11-03	2004-10-19	392	17	191	52	358	824	180	3.67	0.016	0.5			6.9				-79	12.3	-11.1					0.820	0.008	6
PFM000009	PP09	2003-11-03	2004-10-18	1677	26	916	186	62	4660	296	25.17	0.044	8.2			7.0				-87	1.9	-11.7					1.515	0.003	1
PFM000038	PP38	2004-05-04	2004-05-04	70	8	75	11	386	20	44	0.10	0.007	0.3			7.4				-87	12.4	-12.3							
PFM000039	PP39	2003-11-03	2004-10-19	1373	27	729	160	156	3700	310	16.87	0.038	6.3			7.0				-75	7.1	-10.2					2.040	0.005	5
PFM000062	PO62S	2002-05-14	2006-08-14	1481	56	74	180	76	2716	387	9.16	0.025	1.1	0.02	0.01	7.9	0.7	0.12	0.02	-63	13.1	-8.2	108	-2.5	20.5	0.709	0.279	0.011	4
PFM000062	PO62B	2002-05-07	2004-04-06	1460	53	71	180	74	2665	367	9.15	0.024	1.0	0.01	0.00	8.0	0.6	0.05	0.01	-64	14.9	-8.1	109	-3.3	21.4	0.709	0.261	0.010	3
PFM000063	PO63S	2002-05-07	2004-06-14	1456	54	73	177	81	2666	378	8.76	0.025	1.1	0.03	0.01	7.9	0.7	0.07	0.02	-63	16.5	-8.3	109	-4.0	20.2	0.709	0.308	0.014	4
PFM000063	PO63B	2002-05-07	2004-04-04	1441	53	71	176	78	2649	369	8.91	0.027	1.0	0.05	0.02	7.8	0.6	0.05	0.01	-63	17.2	-8.2	108	-4.6	20.7	0.709	0.351	0.016	4
PFM000064	PO64S	2002-05-14	2004-06-14	1422	51	72	174	83	2584	356	8.62	0.025	1.0	0.10	0.01	8.0	0.7	0.06	0.03	-63	13.4	-7.9	109	-6.5	20.8	0.710	0.476	0.027	5
PFM000065	PO65S	2002-05-27	2003-11-12	1426	52	71	174	80	2596	361	8.40	0.025	1.0	0.04	0.00	8.0	0.7	0.08	0.02	-65	15.5	-8.1	109	-5.4	21.0	0.709	0.353	0.019	4
PFM000066	PW66	2002-03-20	2006-06-13	5	2	64	3	190	5	12	0.07	0.003	0.1	0.13	0.04	7.4	1.9	0.02	0.07	-80	11.6	-10.9	111	-12.7	5.9	0.723	0.772	0.010	16
PFM000067	PW67	2002-03-19	2004-06-15	39	3	44	7	133	71	18	0.24	0.003	0.1	0.11	0.02	7.9	2.5	0.02	0.11	-66	12.4	-7.8	111	-8.5	8.1	0.720	1.067	0.016	17
PFM000068	PW68	2002-03-18	2006-06-12	14	2	56	5	165	21	13	0.11	0.003	0.1	0.24	0.03	7.3	3.1	0.04	0.18	-78	11.5	-10.5	113	-13.1	3.8	0.723	0.977	0.015	20
PFM000069	PW69	2002-03-19	2006-06-12	17	2	62	5	184	30	14	0.14	0.003	0.1	0.21	0.02	7.3	2.9	0.01	0.12	-80	11.8	-11.0	115	-14.8	8.9	0.720	0.869	0.015	19
PFM000070	PW70	2002-03-18	2006-06-12	6	2	43	3	131	5	7	0.06	0.002	0.0	0.09	0.07	7.4	0.9	0.02	0.08	-69	11.9	-8.6	115	-10.3	4.6	0.723	1.132	0.010	18
PFM000071	PW71	2002-03-18	2004-06-14	4	2	75	4	239	3	8	0.05	0.002	0.1	0.20	0.02	7.6				-86	10.2	-11.8	97	-15.8			0.719	0.029	12
PFM000072	PW72	2002-03-18	2004-06-15	35	4	43	8	144	51	25	0.20	0.004	0.1	0.32	0.04	7.2	0.7	0.01	0.06	-67	12.0	-8.2	110	-15.2	1.9	0.721	1.272	0.046	17
PFM000073	PW73	2002-03-18	2004-06-01	10	8	120	14	388	8	58	0.09	0.011	0.2	0.07	0.01	7.9	26.5	0.01	0.02	-88	10.9	-12.1	101	-13.0	-10.3		2.429	0.081	8
PFM000074	PL074S	2002-06-09	2006-08-15	9	2	65	4	204	12	9	0.07	0.002	0.1	0.06	0.02	7.5	1.8	0.01	0.05	-78	12.0	-10.4	116	-10.0	7.4	0.722	0.816	0.009	17
PFM000087	PL087S	2002-04-17	2004-06-15	10	3	61	5	193	12	14	0.07	0.002	0.1	0.09	0.08	7.8	3.2	0.01	0.05	-78	12.4	-10.1	113	-11.0	3.7	0.723	0.793	0.010	16
PFM000087	PL087B	2002-04-17	2004-04-05	11	3	77	5	241	13	19	0.08	0.003	0.1	0.14	0.17	7.6	4.6	0.02	0.09	-75	12.6	-9.9	113	-11.5	4.0	0.723	1.009	0.012	18
PFM000097	PL097S	2002-04-17	2004-06-15	61	4	45	9	128	114	23	0.34	0.003	0.1	0.18	0.02	8.2	2.4	0.02	0.13	-70	12.1	-8.4	112	-10.0	7.6	0.722	1.043	0.014	19
PFM000107	PL107S	2002-04-01	2006-08-14	41	3	45	7	132	75	18	0.29	0.003	0.1	0.11	0.02	8.1	2.2	0.02	0.13	-67	11.7	-8.3	112	-8.0	8.0	0.721	0.989	0.012	17
PFM000107	PL107B	2002-04-01	2006-03-20	73	5	53	11	157	137	25	0.53	0.004	0.1	0.16	0.04	7.8	2.4	0.03	0.20	-67	12.7	-8.3	112	-8.3	6.2	0.720	1.105	0.012	18
PFM000117	PL117S	2002-04-01	2006-08-14	6	2	41	3	127	6	6	0.05	0.002	0.1	0.03	0.02	8.1	1.2	0.02	0.04	-64	12.0	-7.5	113	-6.6	4.2	0.724	1.243	0.009	18
PFM000117	PL117B	2002-04-01	2006-03-21	6	2	52	3	162	6	7	0.08	0.002	0.1	0.06	0.08	7.7	1.2	0.03	0.11	-69	12.5	-8.0	115	-6.4		0.723	1.536	0.009	19
PFM000127	PL127S	2002-05-27	2003-11-24	27	4	30	6	111	37	16	0.19	0.004	0.1	0.04	0.01	8.5				-51	9.9	-4.8	110	-7.4	1.9	0.720	1.637	0.022	18
PFM000127	PL127B	2002-05-27	2003-10-27	25	4	32	6	113	32	15	0.17	0.005	0.1	0.04	0.01	8.6	1.5	0.01	0.02	-52	10.4	-5.9	109	-7.6	5.2	0.720	1.536	0.022	18
PFM000135	PL135S	2002-03-19	2004-12-06	27	4	47	7	163	38	21	0.17	0.004	0.1	0.15	0.05	8.0	1.4	0.01	0.04	-66	11.7	-8.1	109	-1.6	1.3	0.721	1.737	0.018	19
PFM000135	PL135B	2004-02-09	2004-02-09	28	5	74	8	243	41	37	0.20	0.008	0.1			7.0											2.170	0.021	28
PFM002457	PN2457	2002-11-04	2003-09-15	1	0	0	0	1	1	2	0.00					5.2				-91	10.9	-12.7						0.005	
PFM002564	PN2564	2003-10-07	2005-11-22	1	0	0	0	1	1	1	0.03					5.2				-89	10.5	-12.5					0.250	0.039	

IDCODE	Label	First	Last	Na	K	Ca	Mg	HCO3	Cl	SO_4	Br	Li	Sr	Fe	Mn	pH	U	Th	La	D	Tr	^{18}O	^{14}C	^{13}C	^{34}S	^{87}Sr	Ntot	Ptot	TOC
SFM0001	S01-4	2002-07-18	2006-04-20	284	18	92	40	476	333	170	1.04	0.016	0.4	1.87	0.21	7.3	4.1	0.17	2.94	-80	11.4	-11.0	91	-13.9	5.0	0.721	1.198	0.043	26
SFM0002	S02-3	2002-09-20	2005-04-11	26	5	116	8	346	58	23	0.23	0.003	0.2	1.78	0.19	7.2	5.7	0.14	2.55	-85	11.5	-12.1	87	-14.0	6.5	0.722	0.496	0.050	15
SFM0003	S03-9	2002-09-20	2005-04-06	26	14	94	26	426	13	56	0.09	0.014	0.5	1.45	0.18	7.3	0.5	0.02	0.24	-75	13.5	-9.8	90	-12.6	-0.7	0.725	0.568	0.045	10
SFM0005	S05+4	2003-01-13	2005-04-08	7	2	108	5	337	10	14	0.08	0.003	0.1	0.07	0.11	7.0	4.5	0.05	3.58	-88	11.2	-12.3	95	-13.6	-0.2	0.723	0.559	0.010	11
SFM0006	S06+2	2003-05-07	2005-04-08	18	25	142	10	392	42	76	0.22	0.003	0.2	0.01	0.10	7.3	19.6	0.01	5.65	-91	10.2	-12.7	105	-14.3	-5.2	0.723	1.450	0.021	14
SFM0008	S08-2	2003-06-02	2005-04-07	29	7	167	16	387	122	79	0.28	0.010	0.2	0.50	0.12	7.1	11.1	0.01	0.52	-87	10.4	-12.3	97	-13.6	-7.1	0.727	0.311	0.008	6
SFM0009	S09+2	2003-03-31	2005-04-07	6	2	93	6	278	9	28	0.08	0.004	0.1	0.06	0.03	7.3	8.1	0.03	1.65	-85	11.8	-11.9	94	-13.1	-5.1	0.725	0.781	0.015	16
SFM0011	S11-2	2003-03-31	2003-03-31	1020	24	148	72	326	1778	219	7.03	0.026	1.1			7.6				-74	2.0	-9.5							
SFM0012	S12-3	2003-04-24	2005-04-05	1095	35	288	90	339	2223	215	10.56	0.034	2.0			7.2				-75	2.9	-9.7	53	-3.9	27.4	0.722	3.533	0.057	3
SFM0013	S13-1	2003-03-31	2003-03-31	794	31	250	96	242	1777	163	8.79	0.025	2.4			7.4				-81	7.0	-10.8							
SFM0014	S14+4	2003-02-18	2003-02-18	15	5	85	7	317	7	14	0.50	0.005	0.2			7.7				-88	13.5	-12.1							
SFM0015	S15-2	2003-02-26	2005-04-05	273	29	36	60	732	307	1	1.34	0.019	0.5			7.3	0.0	0.01	0.01	-67	4.2	-7.7	83	7.6		0.713	7.440	0.442	9
SFM0016	S16-2	2003-02-27	2003-02-27	23	4	90	8	335	26	15	0.08	0.002	0.2			7.6				-79	13.8	-10.1							
SFM0017	S17+2	2003-02-25	2003-02-25	153	9	44	11	536	18	7	0.07	0.007	0.2			7.7				-85	7.8	-11.5							
SFM0018	S18+1	2003-02-27	2003-02-27	129	6	29	4	429	12	20	0.05	0.002	0.1			8.1				-86	7.1	-11.9							
SFM0019	S19-1	2003-03-25	2003-03-25	7	6	98	10	348	5	30	0.10	0.005	0.3			7.6				-86	12.7	-11.9							
SFM0020	S20-2	2003-03-19	2003-03-19	8	5	116	8	366	11	43	0.06	0.005	0.2			7.3				-86	10.1	-11.9							
SFM0022	S22-5	2004-07-13	2004-10-15	628	31	216	62	370	1230	110	4.70	0.026	2.1			7.4				-75	1.3	-10.0	67	-8.1	18.5	0.717	2.435	0.008	5
SFM0023	S23-4	2003-07-16	2006-01-27	1577	66	521	171	130	3766	348	17.79	0.054	3.7		1.40	6.7	0.1	0.10	0.01	-69	4.1	-8.9	52	-3.3	24.5	0.725	2.877	0.007	4
SFM0024	S24-3	2003-03-26	2003-11-06	923	41	139	117	350	1712	269	6.33	0.028	1.0			7.5				-76	10.2	-9.9	89	-12.4	16.4	0.714	0.999	0.043	8
SFM0025	S25-6	2003-07-09	2005-04-13	738	19	431	78	242	1864	238	9.78	0.023	4.5			7.0	3.9	0.10	0.03	-87	7.9	-11.9	48	-9.8	15.2	0.719	1.352	0.014	2
SFM0027	S27-6	2003-04-25	2004-10-18	134	8	39	13	409	63	49	0.24	0.011	0.3	0.12	0.08	7.8	1.1	0.01	0.06	-87	10.6	-12.0	80	-13.7	1.7	0.738	0.809	0.067	6
SFM0029	S29-7	2003-07-08	2005-04-07	20	5	126	12	412	22	52	0.12	0.008	0.2	1.84	0.20	7.1	4.3	0.01	2.29	-86	11.9	-12.1	93	-12.6	-6.6	0.725	0.332	0.018	8
SFM0030	S30-2	2003-03-11	2003-03-11	111	13	67	19	406	69	105	0.27	0.011	0.4			7.9				-81	11.8	-10.2							
SFM0031	S31-2	2003-07-09	2005-04-06	20	10	145	19	440	9	120	0.14	0.011	0.4	0.53	0.24	7.2	7.8	0.01	1.87	-73	12.3	-10.3	95	-14.1	-11.7	0.727	0.381	0.016	8
SFM0032	S32-2	2003-03-04	2006-04-19	28	5	107	9	354	25	37	0.15	0.007	0.2	2.22	0.23	7.1	5.5	0.08	1.71	-84	11.3	-11.7	94	-11.1	0.1	0.727	0.671	0.014	18
SFM0034	S34-1	2003-03-11	2003-03-11	255	15	104	36	456	432	49	1.37	0.014	0.4			7.5				-81	12.9	-10.8							
SFM0036	S36-1	2003-03-12	2003-03-12	129	12	110	33	521	146	107	0.56	0.014	0.4			7.4				-81	11.5	-11.0							
SFM0037	S37-2	2003-07-10	2006-04-20	90	10	120	26	461	83	121	0.34	0.012	0.3	2.39	0.25	7.0	8.3	0.17	2.49	-78	12.1	-11.0	103	-14.5	-1.2	0.719	0.891	0.055	24
SFM0049	S49-1	2003-04-01	2006-04-19	12	3	63	5	208	16	2	0.07	0.003	0.1	1.21	0.13	6.8	0.2	0.12	1.72	-75	12.0	-10.1	111	-10.5	22.3	0.723	0.705	0.017	18
SFM0051	S51-3	2003-06-25	2006-07-25	16	5	121	8	352	40	18	0.14	0.007	0.2	8.28	0.27	7.4	1.2	0.44	1.44	-86	10.4	-12.2	88	-13.4		0.724			
SFM0053	S53-6	2003-06-26	2005-05-11	10	5	127	11	398	13	44	0.10	0.009	0.2	3.58	0.15	7.4	0.2	0.13	0.41	-86	9.2	-12.0	94	-11.4		0.725			
SFM0056	S56-3	2003-06-25	2005-05-09	431	9	65	19	449	443	222	1.48	0.017	0.4	0.71	0.08	7.9	0.1	0.05	0.16	-83	<0.8	-11.3				0.736			
SFM0057	S57+0	2003-11-04	2005-04-08	69	4	139	9	269	220	20	0.91	0.002	0.2	0.14	0.08	7.0	5.1	0.16	5.40	-87	10.7	-12.6	93	-13.0	15.0	0.719	0.624	0.010	15
SFM0059	S59-1	2003-12-02	2003-12-02	266	13	209	43	334	576	277	1.71	0.021	0.5			6.9				-82	9.0	-11.1							
SFM0060	S60-3	2004-01-21	2005-04-07	12	5	121	9	325	24	66	0.16	0.004	0.1	0.02	0.02	7.1	32.6	0.01	0.99	-87	9.9	-12.4	88	-11.3	-5.9	0.726	0.485	0.005	6
SFM0062	S62-3	2004-02-17	2004-05-28	25	6	92	8	290	28	38	0.13	0.007	0.2	4.62	0.14	7.3				-84	9.9	-11.9							
SFM0063	S63-3	2004-02-18	2004-05-11	61	7	75	12	199	145	40	0.47	0.009	0.3			7.4				-81	9.0	-11.3							
SFM0065	S65-4	2004-02-18	2004-02-18	217	14	83	38	313	370	87	1.20	0.013	0.4	0.01	0.63	7.5				-77		-11.2							
SFM0074	S74-3	2004-05-11	2004-05-24	40	5	106	10	352	52	44	0.21	0.007	0.2			7.4				-84	10.2	-11.7							

Appendix I

Time-series and mean values of major constituents in all sampling points

Visualisation of time series and mean values for all sampling points in surface water, shallow groundwater and groundwater in the bedrock (PFM, SFM, HFM and KFM).

Major constituents of groundwater, Na, K, Mg, Ca, Cl, SO_4, HCO_3.

Object **HFM01**

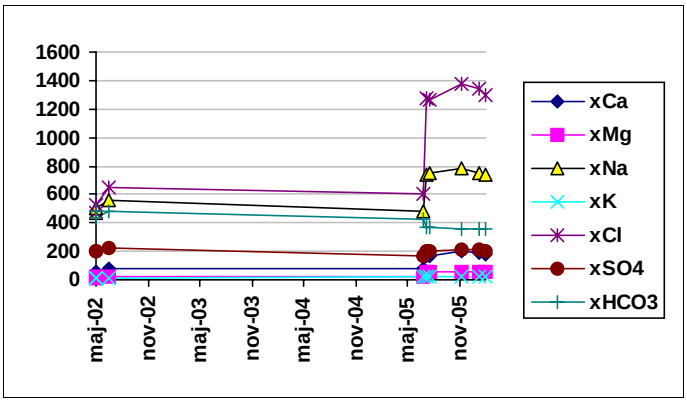

Sampling level (secmid -36.0 masl, RHB70

Mean concentration (mg/l)

Ca:	120
Mg:	35
Na:	619
K:	18
Cl:	892
SO4:	194
HCO3:	403

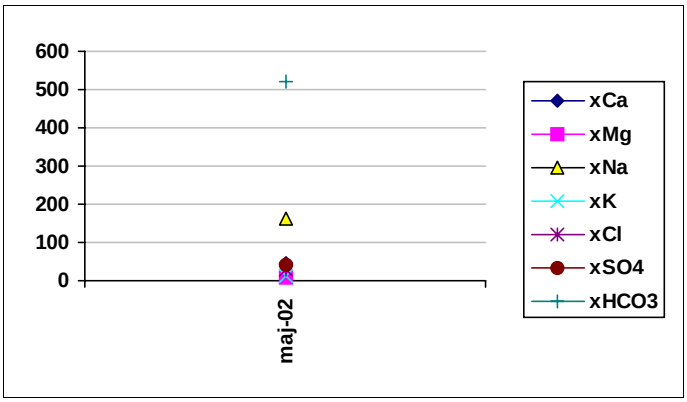

Sampling level (secmid -132.0 masl, RHB70

Mean concentration (mg/l)

Ca:	120
Mg:	35
Na:	619
K:	18
Cl:	892
SO4:	194
HCO3:	403

Object **HFM02**

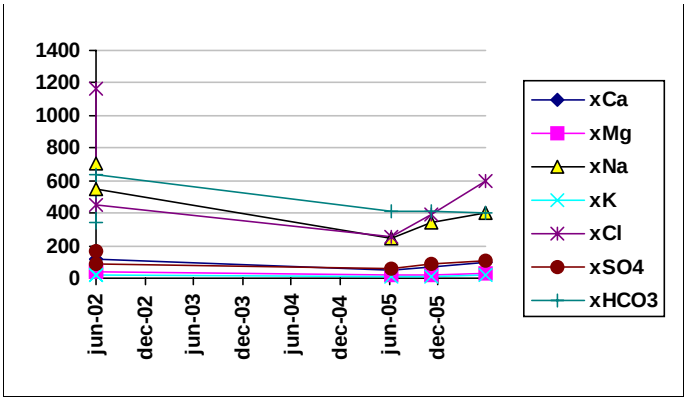

Sampling level (secmid -40.0 masl, RHB70

Mean concentration (mg/l)

Ca:	100
Mg:	29
Na:	448
K:	16
Cl:	572
SO4:	99
HCO3:	438

Object **HFM04**

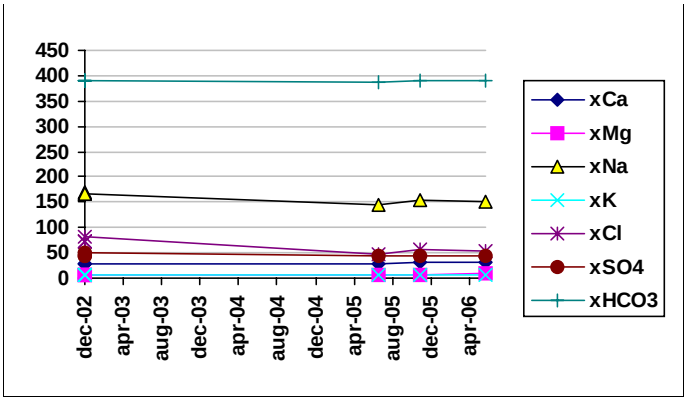

Sampling level (secmid -58.0 masl, RHB70

Mean concentration (mg/l)

Ca:	30
Mg:	7
Na:	158
K:	6
Cl:	64
SO4:	45
HCO3:	390

Object **HFM05**

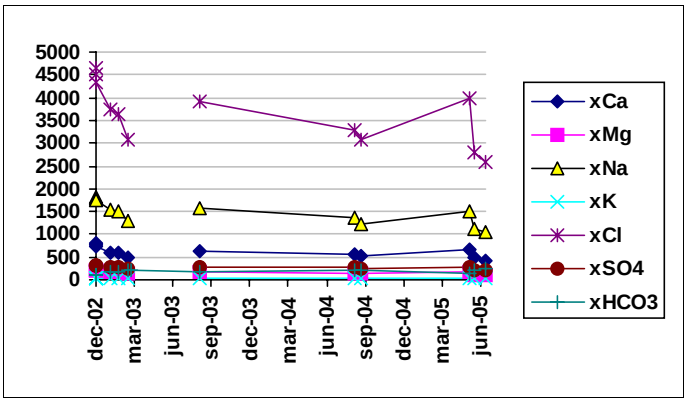

Sampling level (secmid -146.0 masl, RHB70

Mean concentration (mg/l)

Ca:	611
Mg:	161
Na:	1461
K:	36
Cl:	3632
SO4:	269
HCO3:	178

Object **HFM06**

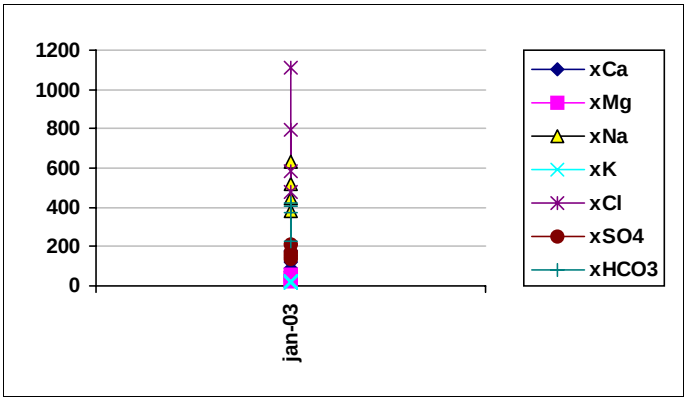

Sampling level (secmid -63.0 masl, RHB70

Mean concentration (mg/l)

Ca:	117
Mg:	35
Na:	495
K:	22
Cl:	742
SO4:	168
HCO3:	357

Object **HFM09**

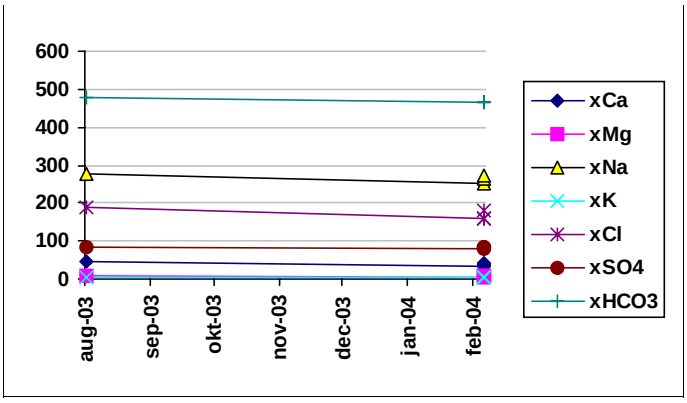

Sampling level (secmid -19.0 masl, RHB70

Mean concentration (mg/l)

Ca:	39
Mg:	7
Na:	268
K:	5
Cl:	172
SO4:	83
HCO3:	469

Object **HFM10**

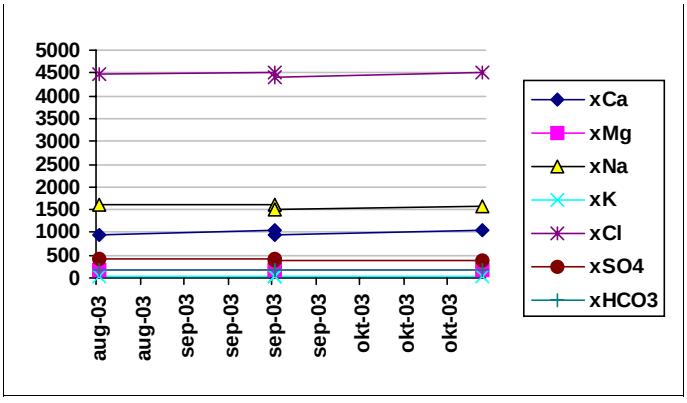

Sampling level (secmid -105.0 masl, RHB70

Mean concentration (mg/l)

Ca:	998
Mg:	183
Na:	1570
K:	21
Cl:	4471
SO4:	406
HCO3:	165

Object **HFM11**

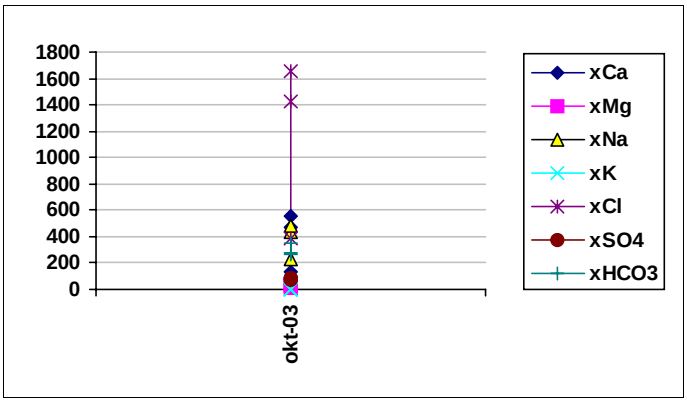

Sampling level (secmid -25.0 masl, RHB70

Mean concentration (mg/l)

Ca:	382
Mg:	25
Na:	382
K:	6
Cl:	1157
SO4:	81
HCO3:	298

Object **HFM12**

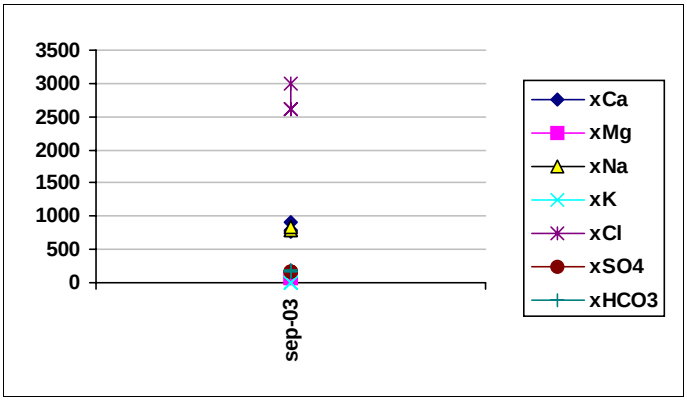

Sampling level (secmid -87.0 masl, RHB70

Mean concentration (mg/l)

Ca:	827
Mg:	66
Na:	803
K:	6
Cl:	2746
SO4:	172
HCO3:	175

Object **HFM13**

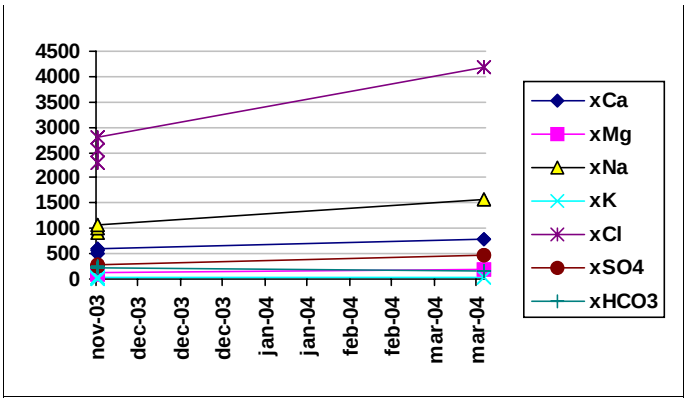

Sampling level (secmid -77.0 masl, RHB70

Mean concentration (mg/l)

Ca:	1190
Mg:	195
Na:	1687
K:	24
Cl:	4950
SO4:	460
HCO3:	126

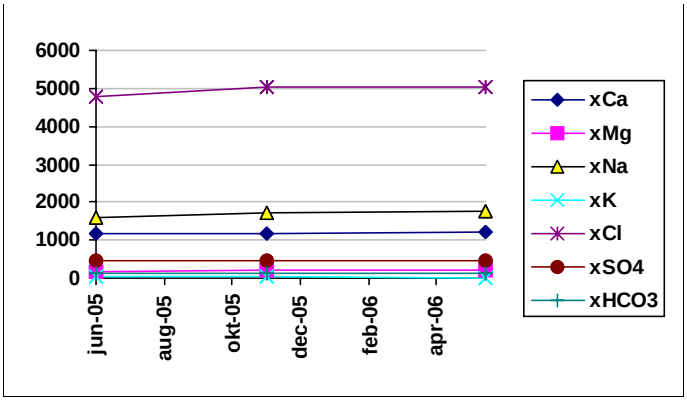

Sampling level (secmid -134.0 masl, RHB70

Mean concentration (mg/l)

Ca:	1190
Mg:	195
Na:	1687
K:	24
Cl:	4950
SO4:	460
HCO3:	126

Object **HFM14**

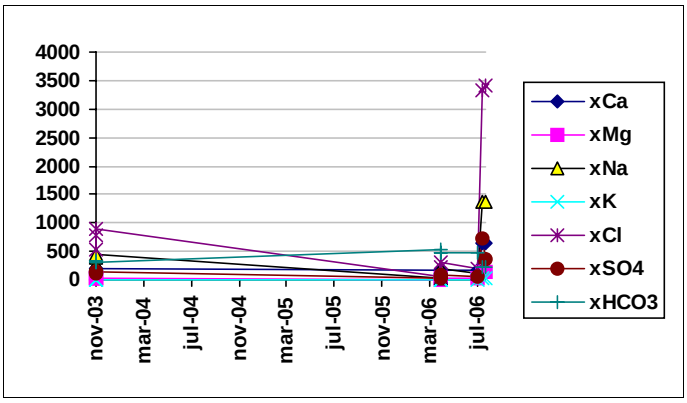

Sampling level (secmid -65.0 masl, RHB70

Mean concentration (mg/l)

Ca:	275
Mg:	49
Na:	479
K:	15
Cl:	1084
SO4:	192
HCO3:	372

Object **HFM15**

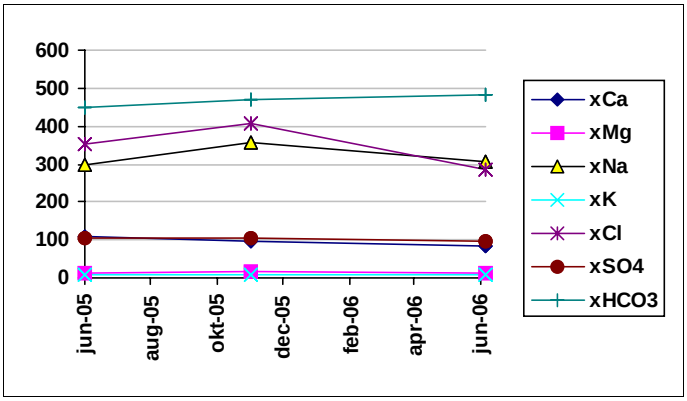

Sampling level (secmid -90.0 masl, RHB70

Mean concentration (mg/l)

Ca:	154
Mg:	23
Na:	306
K:	10
Cl:	537
SO4:	118
HCO3:	363

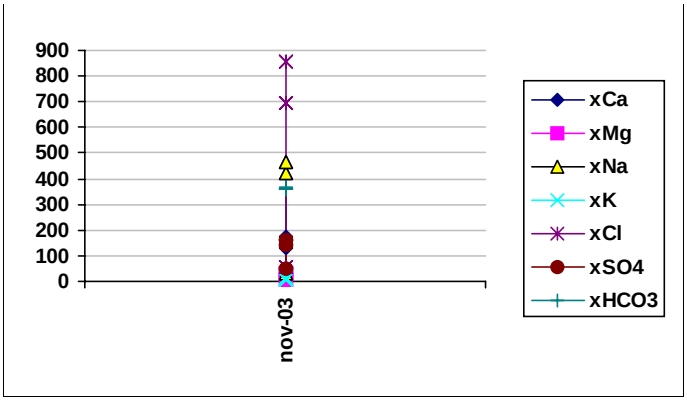

Sampling level (secmid -100.0 masl, RHB70

Mean concentration (mg/l)

Ca:	154
Mg:	23
Na:	306
K:	10
Cl:	537
SO4:	118
HCO3:	363

Object **HFM16**

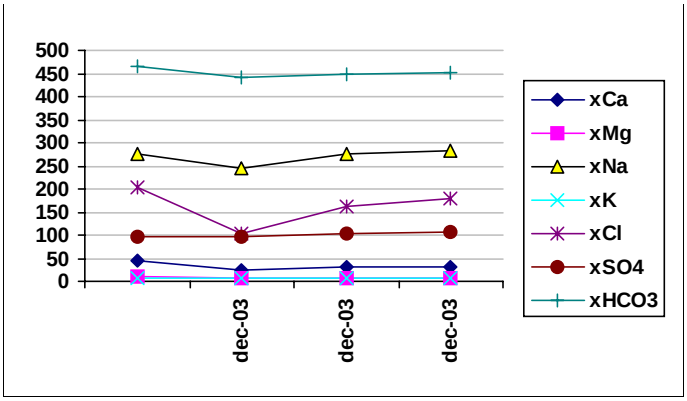

Sampling level (secmid -56.0 masl, RHB70

Mean concentration (mg/l)

Ca:	33
Mg:	8
Na:	269
K:	6
Cl:	162
SO4:	100
HCO3:	453

Object **HFM17**

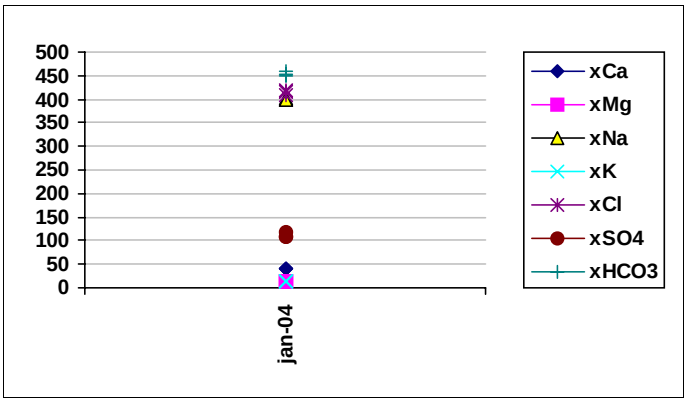

Sampling level (secmid -27.0 masl, RHB70

Mean concentration (mg/l)

Ca:	42
Mg:	13
Na:	400
K:	13
Cl:	414
SO4:	112
HCO3:	455

Object **HFM18**

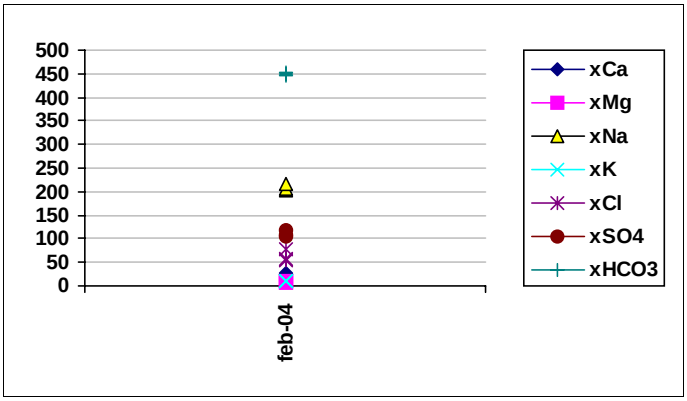

Sampling level (secmid -30.0 masl, RHB70

Mean concentration (mg/l)

Ca:	26
Mg:	9
Na:	209
K:	9
Cl:	62
SO4:	110
HCO3:	450

Object **HFM19**

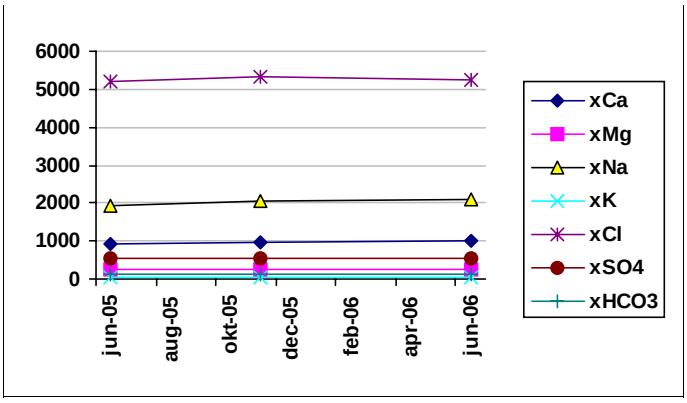

Sampling level (secmid -147.0 masl, RHB70

Mean concentration (mg/l)

Ca:	958
Mg:	254
Na:	2020
K:	56
Cl:	5260
SO4:	547
HCO3:	124

Object **HFM20**

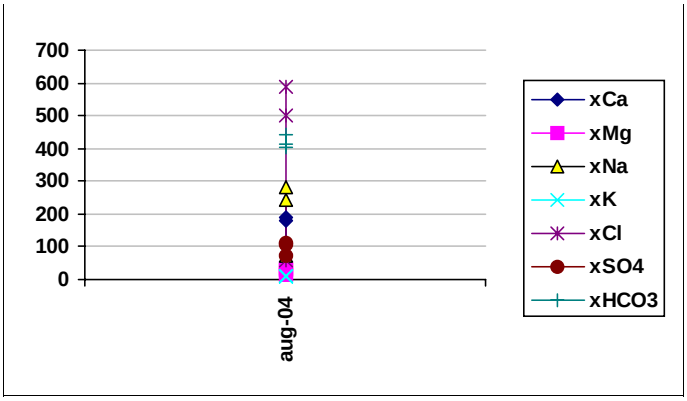

Sampling level (secmid -22.0 masl, RHB70

Mean concentration (mg/l)

Ca:	161
Mg:	25
Na:	200
K:	10
Cl:	383
SO4:	96
HCO3:	419

Object **HFM21**

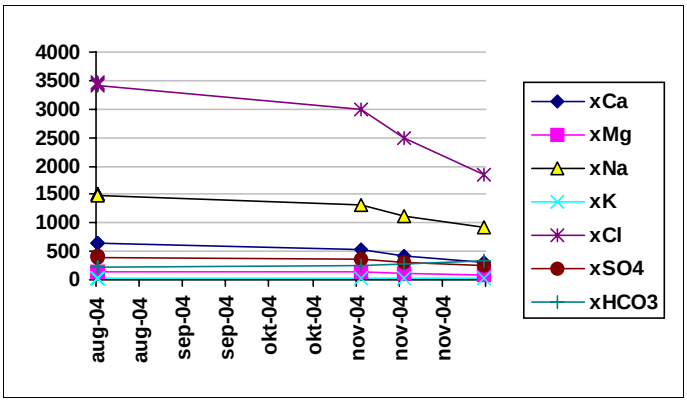

Sampling level (secmid -107.0 masl, RHB70

Mean concentration (mg/l)

Ca:	526
Mg:	126
Na:	1311
K:	30
Cl:	2938
SO4:	357
HCO3:	252

Object **HFM22**

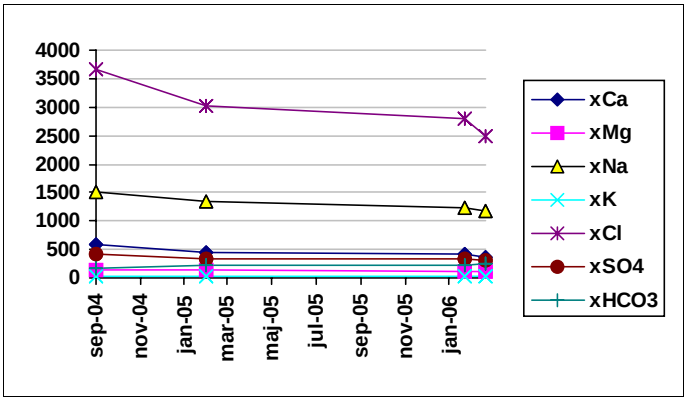

Sampling level (secmid -53.0 masl, RHB70

Mean concentration (mg/l)

Ca:	452
Mg:	122
Na:	1313
K:	36
Cl:	2993
SO4:	353
HCO3:	223

Object **HFM23**

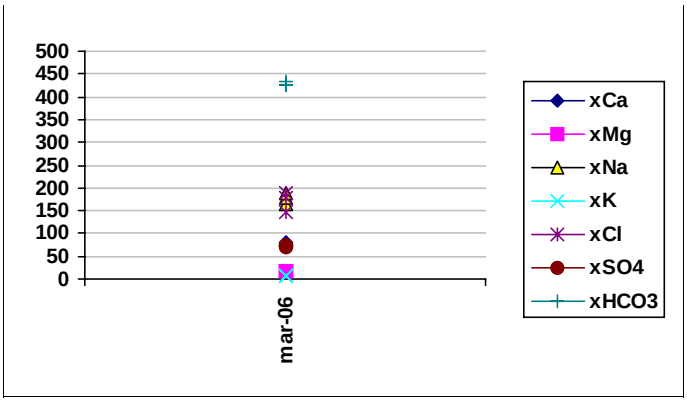

Sampling level (secmid -67.0 masl, RHB70

Mean concentration (mg/l)

Ca:	79
Mg:	17
Na:	178
K:	8
Cl:	171
SO4:	73
HCO3:	429

Object **HFM24**

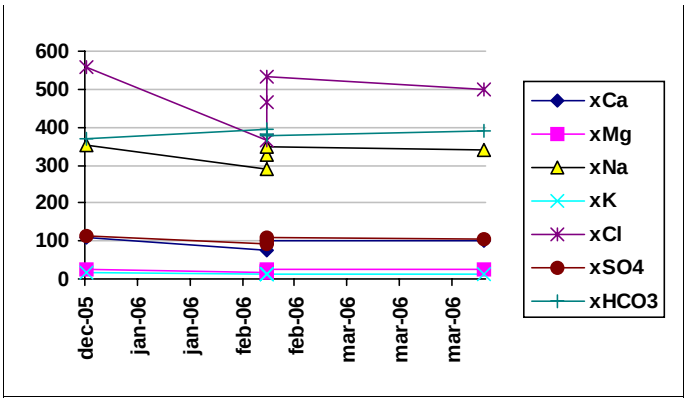

Sampling level (secmid -70.0 masl, RHB70

Mean concentration (mg/l)

Ca:	96
Mg:	22
Na:	332
K:	14
Cl:	484
SO4:	103
HCO3:	383

Object **HFM26**

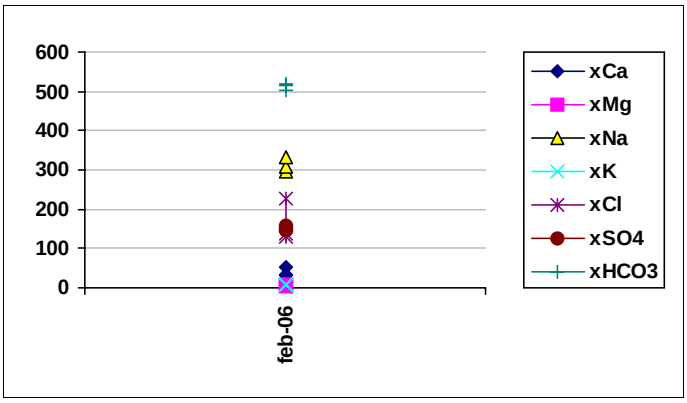

Sampling level (secmid -75.0 masl, RHB70

Mean concentration (mg/l)

Ca:	39
Mg:	7
Na:	311
K:	8
Cl:	165
SO4:	151
HCO3:	511

Object **HFM27**

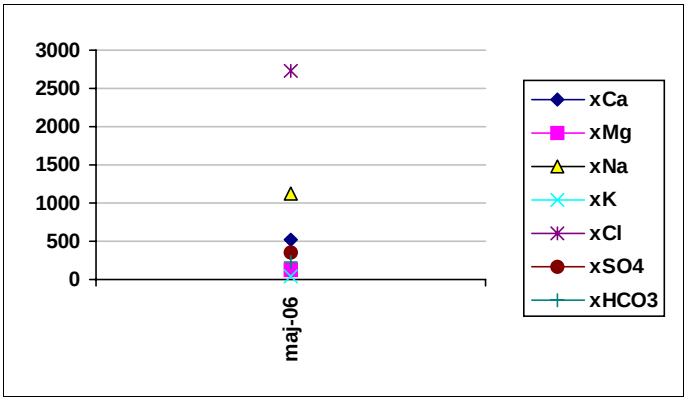

Sampling level (secmid -46.0 masl, RHB70

Mean concentration (mg/l)

Ca:	209
Mg:	39
Na:	535
K:	18
Cl:	1040
SO4:	133
HCO3:	346

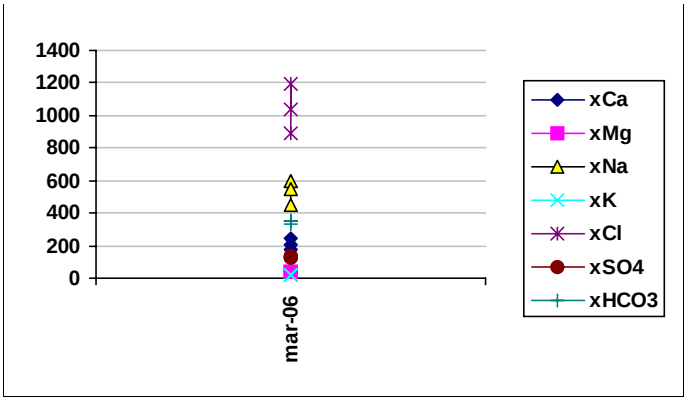

Sampling level (secmid -57.0 masl, RHB70

Mean concentration (mg/l)

Ca:	209
Mg:	39
Na:	535
K:	18
Cl:	1040
SO4:	133
HCO3:	346

Object **HFM28**

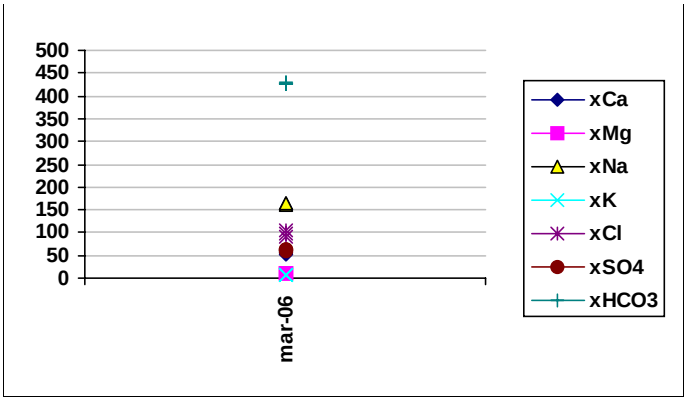

Sampling level (secmid -71.0 masl, RHB70

Mean concentration (mg/l)

Ca:	55
Mg:	10
Na:	163
K:	6
Cl:	99
SO4:	61
HCO3:	427

Object **HFM32**

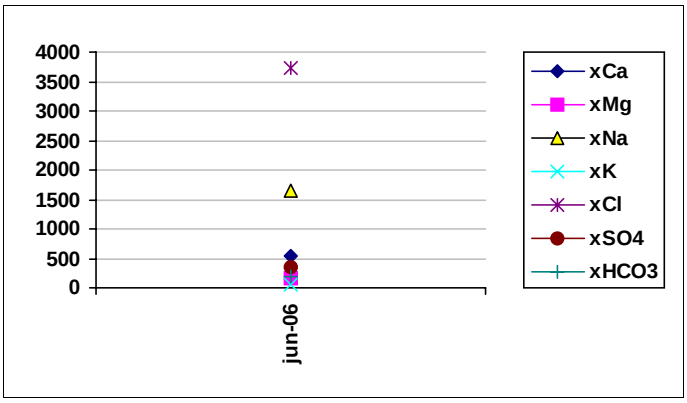

Sampling level (secmid -12.0 masl, RHB70

Mean concentration (mg/l)

Ca:	671
Mg:	180
Na:	1723
K:	50
Cl:	4205
SO4:	386
HCO3:	163

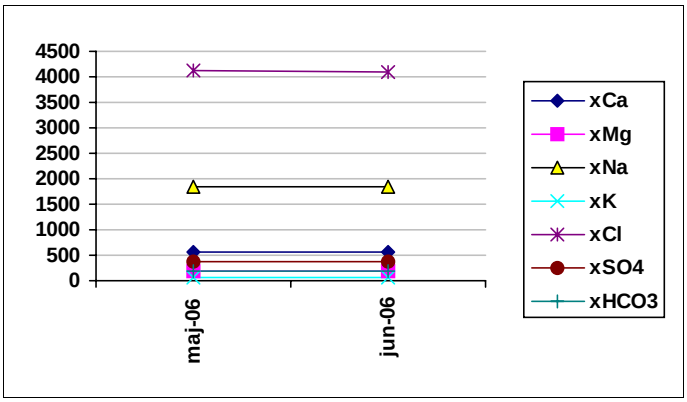

Sampling level (secmid -28.0 masl, RHB70

Mean concentration (mg/l)

Ca:	671
Mg:	180
Na:	1723
K:	50
Cl:	4205
SO4:	386
HCO3:	163

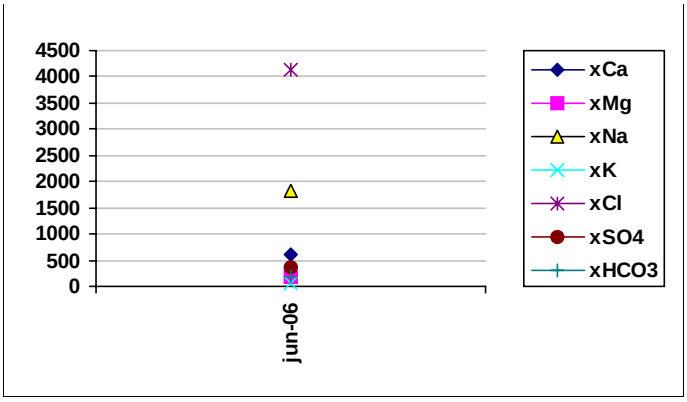

Sampling level (secmid -64.0 masl, RHB70

Mean concentration (mg/l)

Ca:	671
Mg:	180
Na:	1723
K:	50
Cl:	4205
SO4:	386
HCO3:	163

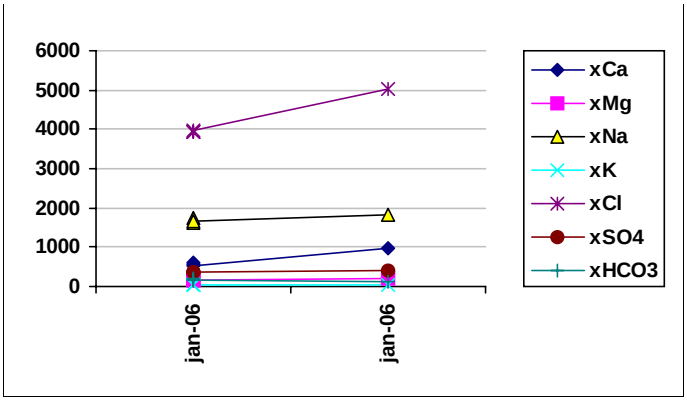

Sampling level (secmid -100.0 masl, RHB70

Mean concentration (mg/l)

Ca:	671
Mg:	180
Na:	1723
K:	50
Cl:	4205
SO4:	386
HCO3:	163

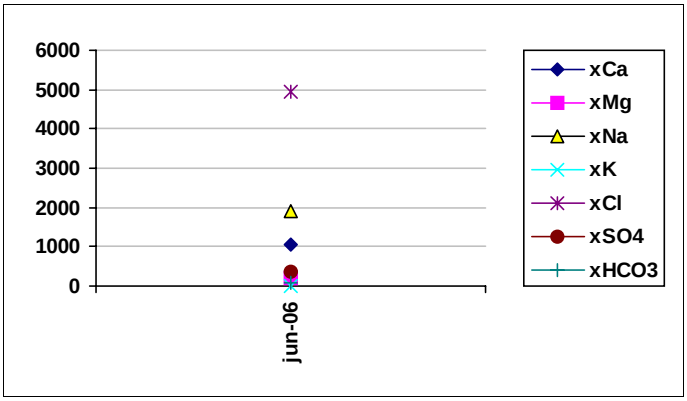

Sampling level (secmid -148.0 masl, RHB70

Mean concentration (mg/l)

Ca:	671
Mg:	180
Na:	1723
K:	50
Cl:	4205
SO4:	386
HCO3:	163

Object **HFM33**

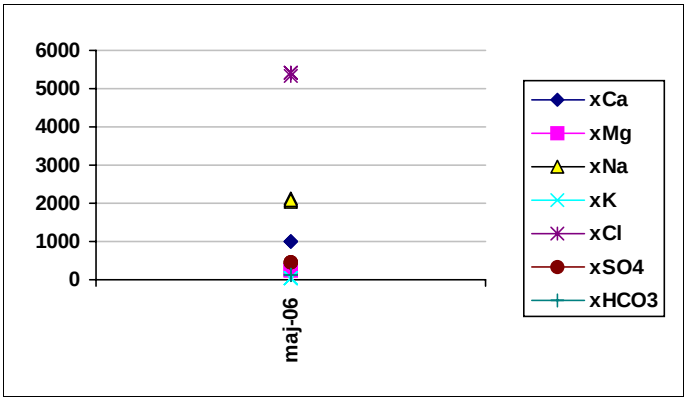

Sampling level (secmid -56.0 masl, RHB70

Mean concentration (mg/l)

Ca:	1007
Mg:	249
Na:	2087
K:	33
Cl:	5397
SO4:	449
HCO3:	122

Object **HFM34**

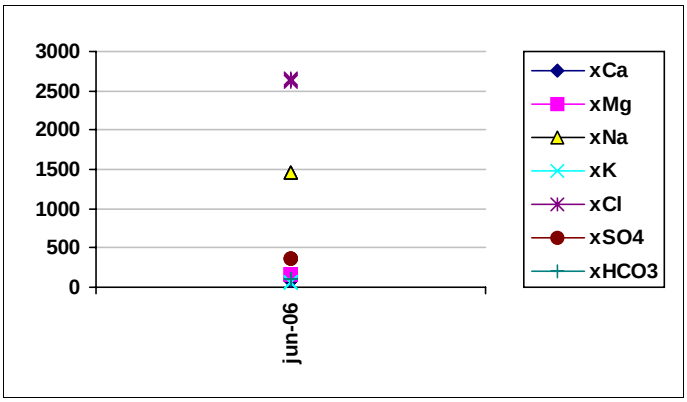

Sampling level (secmid -83.0 masl, RHB70

Mean concentration (mg/l)

Ca:	89
Mg:	170
Na:	1453
K:	59
Cl:	2630
SO4:	367
HCO3:	99

Object **KFM01A**

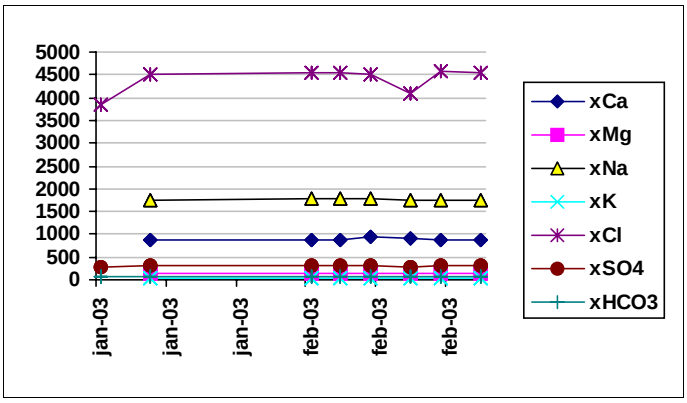

Sampling level (secmid -112.0 masl, RHB70

Mean concentration (mg/l)

Ca:	921
Mg:	199
Na:	2003
K:	32
Cl:	5180
SO4:	538
HCO3:	101

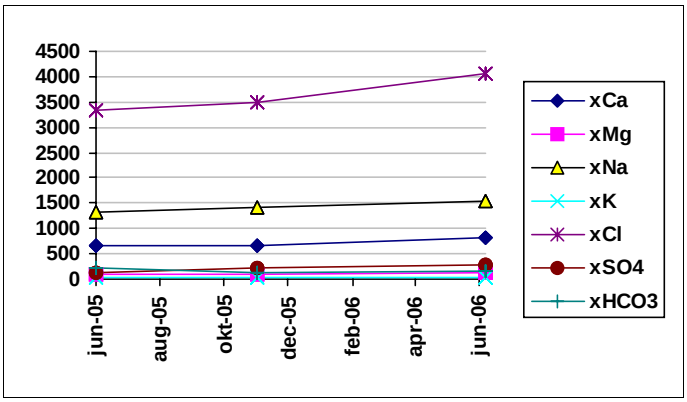

Sampling level (secmid -116.0 masl, RHB70

Mean concentration (mg/l)

Ca:	921
Mg:	199
Na:	2003
K:	32
Cl:	5180
SO4:	538
HCO3:	101

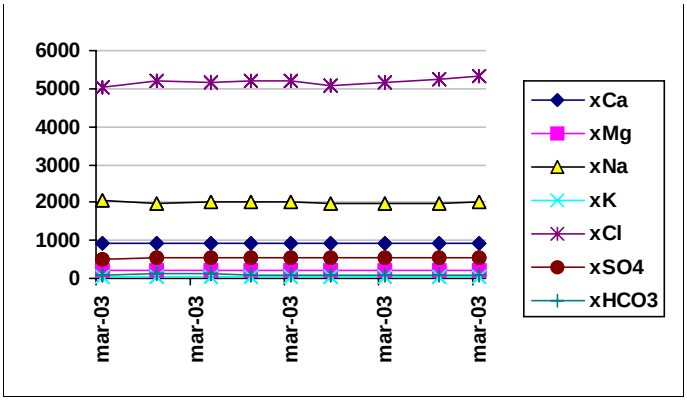

Sampling level (secmid -177.0 masl, RHB70

Mean concentration (mg/l)

Ca:	921
Mg:	199
Na:	2003
K:	32
Cl:	5180
SO4:	538
HCO3:	101

Object **KFM01D**

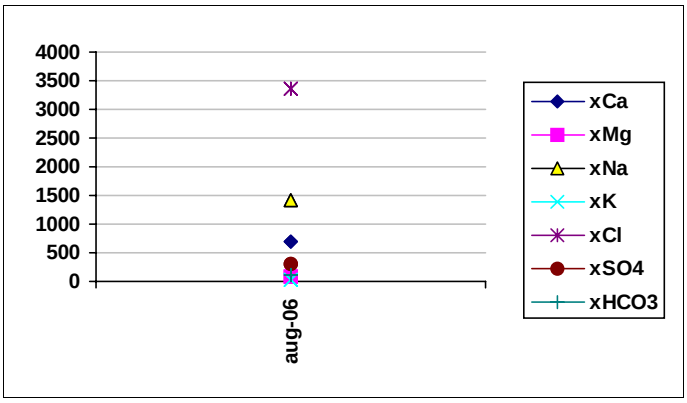

Sampling level (secmid -156.0 masl, RHB70

Mean concentration (mg/l)

Ca:	1828
Mg:	12
Na:	1765
K:	7
Cl:	5638
SO4:	32
HCO3:	17

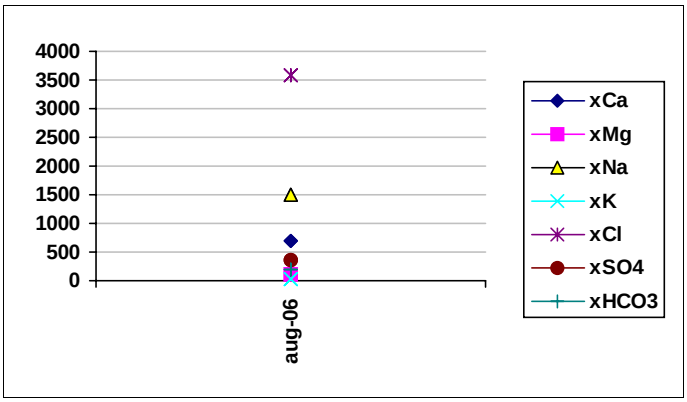

Sampling level (secmid -212.0 masl, RHB70

Mean concentration (mg/l)

Ca:	1828
Mg:	12
Na:	1765
K:	7
Cl:	5638
SO4:	32
HCO3:	17

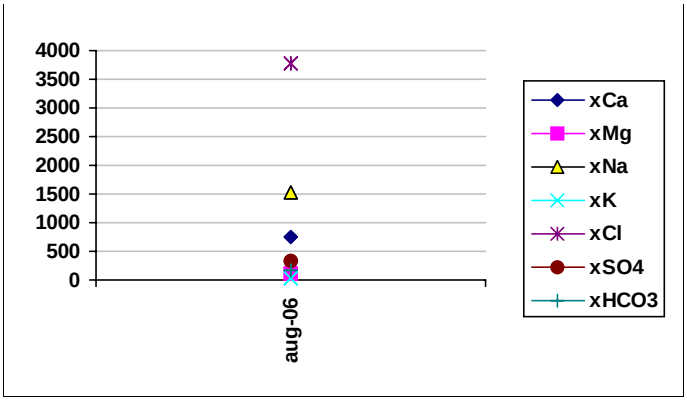

Sampling level (secmid -283.0 masl, RHB70

Mean concentration (mg/l)

Ca:	1828
Mg:	12
Na:	1765
K:	7
Cl:	5638
SO4:	32
HCO3:	17

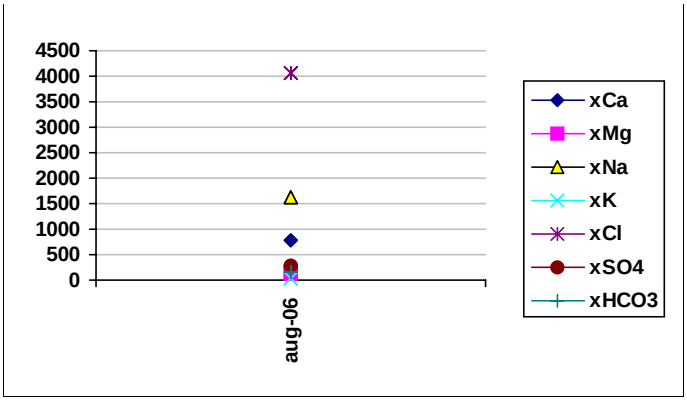

Sampling level (secmid -294.0 masl, RHB70

Mean concentration (mg/l)

Ca:	1828
Mg:	12
Na:	1765
K:	7
Cl:	5638
SO4:	32
HCO3:	17

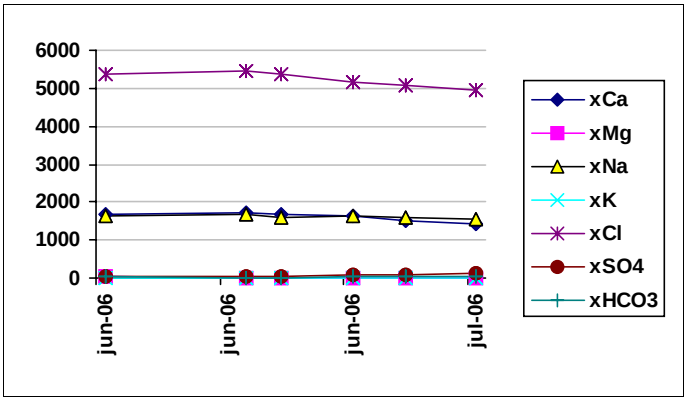

Sampling level (secmid -341.0 masl, RHB70

Mean concentration (mg/l)

Ca:	1828
Mg:	12
Na:	1765
K:	7
Cl:	5638
SO4:	32
HCO3:	17

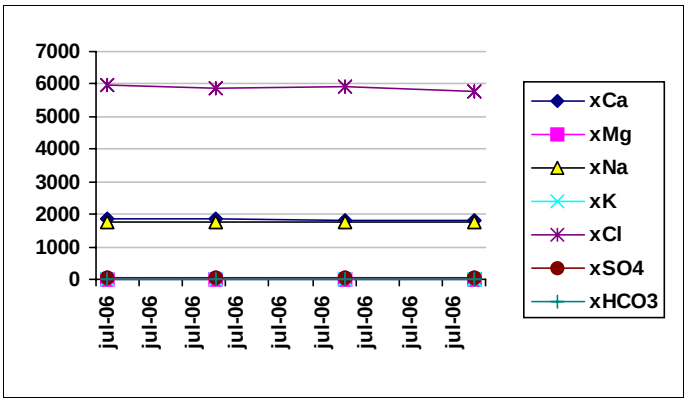

Sampling level (secmid -446.0 masl, RHB70

Mean concentration (mg/l)

Ca:	1828
Mg:	12
Na:	1765
K:	7
Cl:	5638
SO4:	32
HCO3:	17

Object **KFM02A**

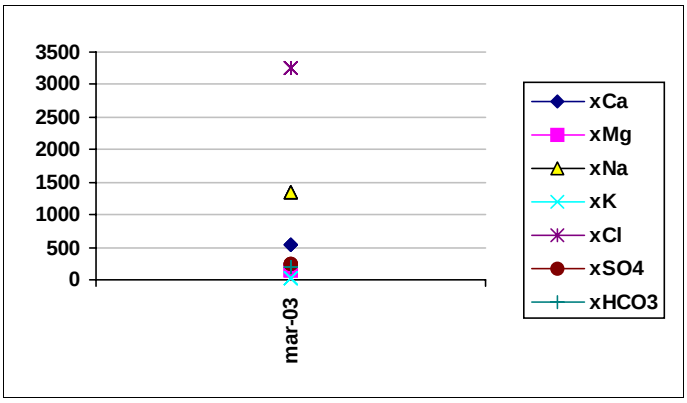

Sampling level (secmid -43.0 masl, RHB70

Mean concentration (mg/l)

Ca:	931
Mg:	232
Na:	2079
K:	34
Cl:	5431
SO4:	508
HCO3:	125

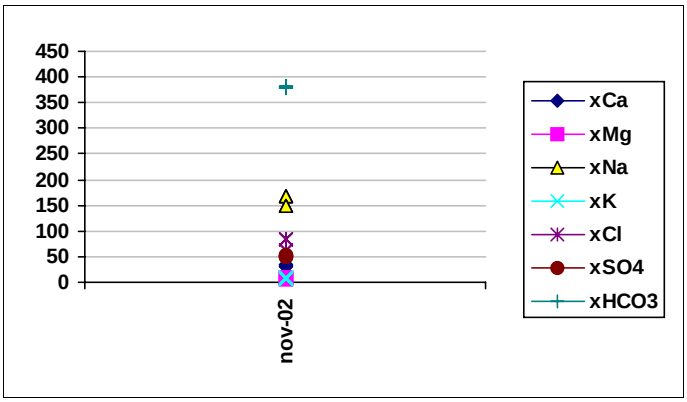

Sampling level (secmid -52.0 masl, RHB70

Mean concentration (mg/l)

Ca:	931
Mg:	232
Na:	2079
K:	34
Cl:	5431
SO4:	508
HCO3:	125

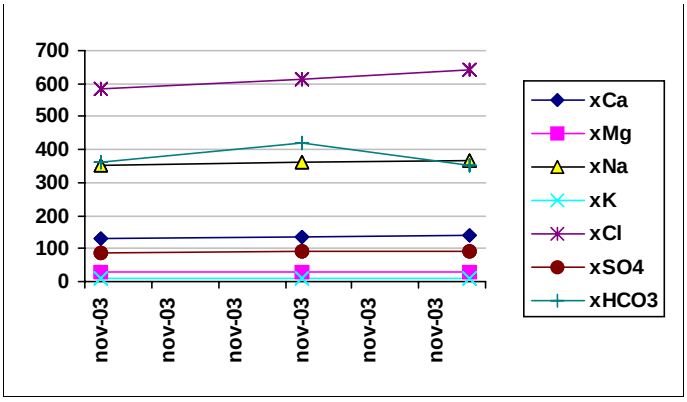

Sampling level (secmid -109.0 masl, RHB70

Mean concentration (mg/l)

Ca:	931
Mg:	232
Na:	2079
K:	34
Cl:	5431
SO4:	508
HCO3:	125

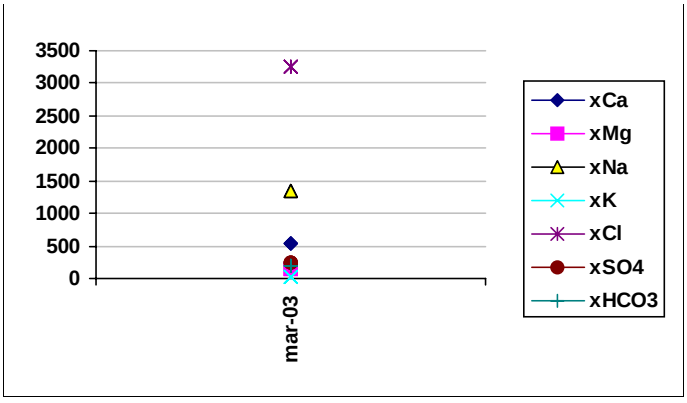

Sampling level (secmid -168.0 masl, RHB70

Mean concentration (mg/l)

Ca:	931
Mg:	232
Na:	2079
K:	34
Cl:	5431
SO4:	508
HCO3:	125

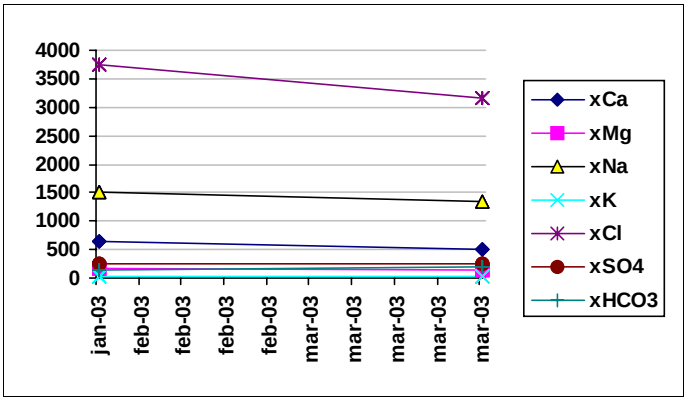

Sampling level (secmid -267.0 masl, RHB70

Mean concentration (mg/l)

Ca:	931
Mg:	232
Na:	2079
K:	34
Cl:	5431
SO4:	508
HCO3:	125

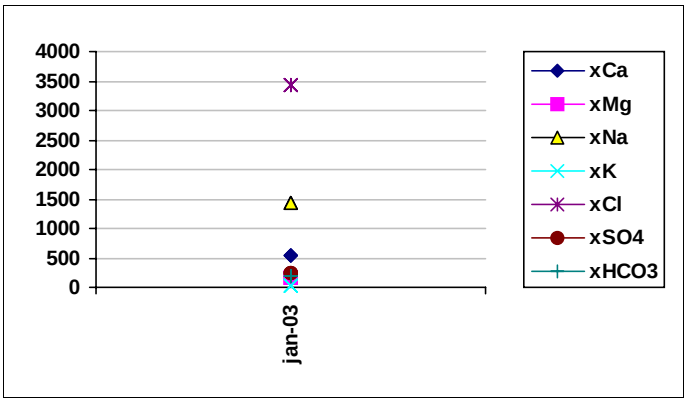

Sampling level (secmid -314.0 masl, RHB70

Mean concentration (mg/l)

Ca:	931
Mg:	232
Na:	2079
K:	34
Cl:	5431
SO4:	508
HCO3:	125

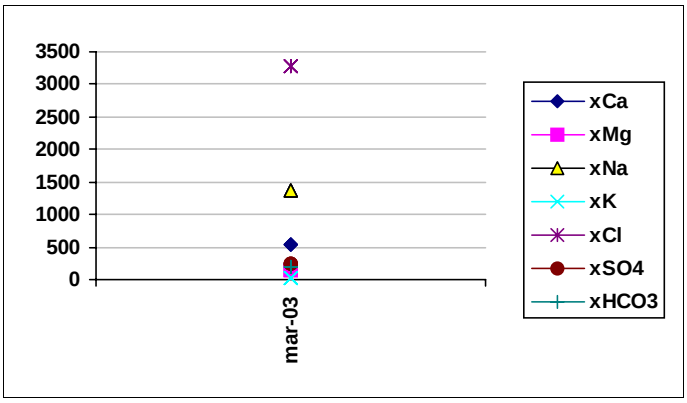

Sampling level (secmid -367.0 masl, RHB70

Mean concentration (mg/l)

Ca:	931
Mg:	232
Na:	2079
K:	34
Cl:	5431
SO4:	508
HCO3:	125

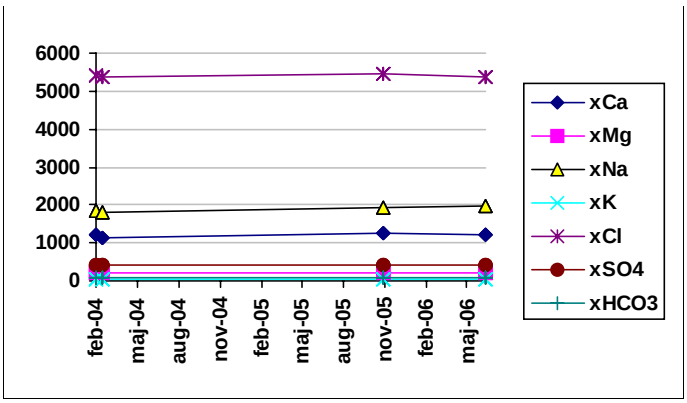

Sampling level (secmid -415.0 masl, RHB70

Mean concentration (mg/l)

Ca:	931
Mg:	232
Na:	2079
K:	34
Cl:	5431
SO4:	508
HCO3:	125

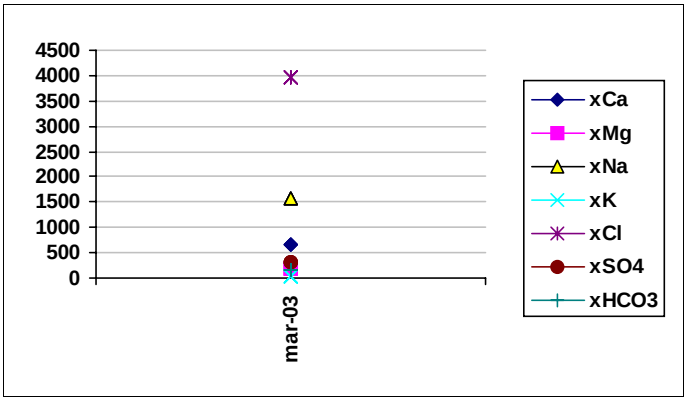

Sampling level (secmid -491.0 masl, RHB70

Mean concentration (mg/l)

Ca:	931
Mg:	232
Na:	2079
K:	34
Cl:	5431
SO4:	508
HCO3:	125

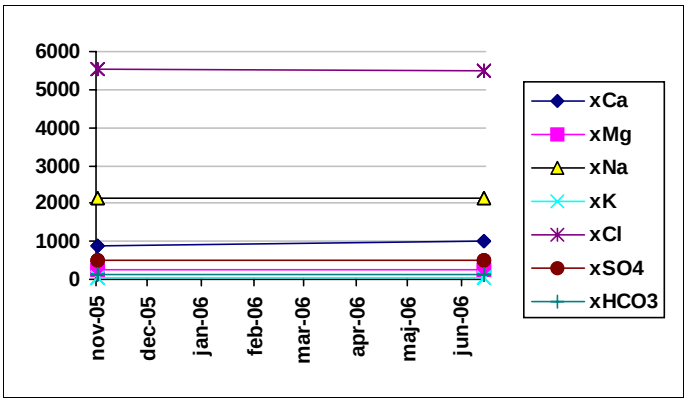

Sampling level (secmid -495.0 masl, RHB70

Mean concentration (mg/l)

Ca:	931
Mg:	232
Na:	2079
K:	34
Cl:	5431
SO4:	508
HCO3:	125

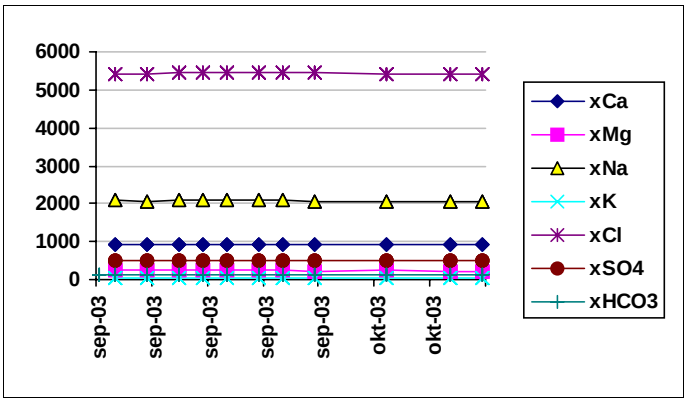

Sampling level (secmid -504.0 masl, RHB70

Mean concentration (mg/l)

Ca:	931
Mg:	232
Na:	2079
K:	34
Cl:	5431
SO4:	508
HCO3:	125

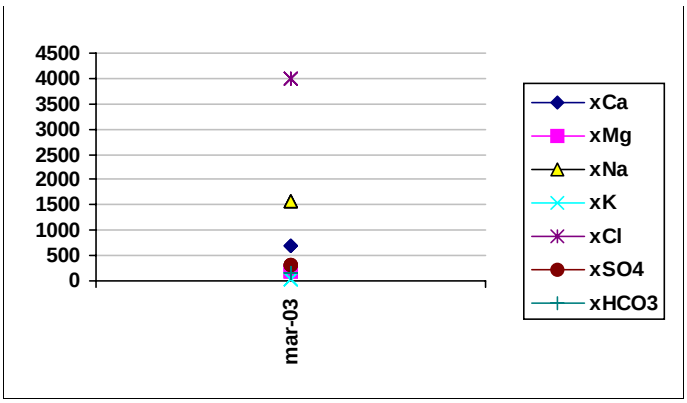

Sampling level (secmid -616.0 masl, RHB70

Mean concentration (mg/l)

Ca:	931
Mg:	232
Na:	2079
K:	34
Cl:	5431
SO4:	508
HCO3:	125

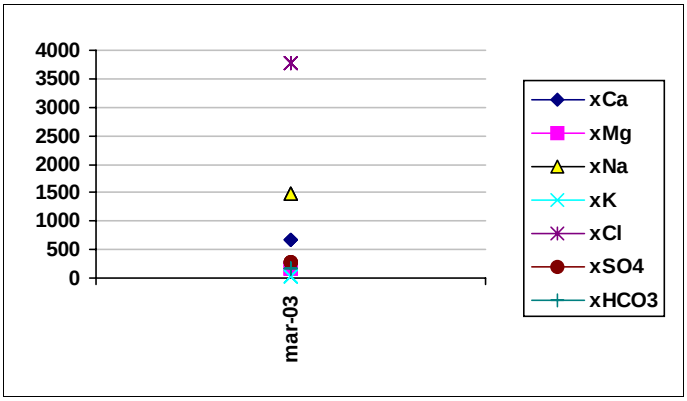

Sampling level (secmid -715.0 masl, RHB70

Mean concentration (mg/l)

Ca:	931
Mg:	232
Na:	2079
K:	34
Cl:	5431
SO4:	508
HCO3:	125

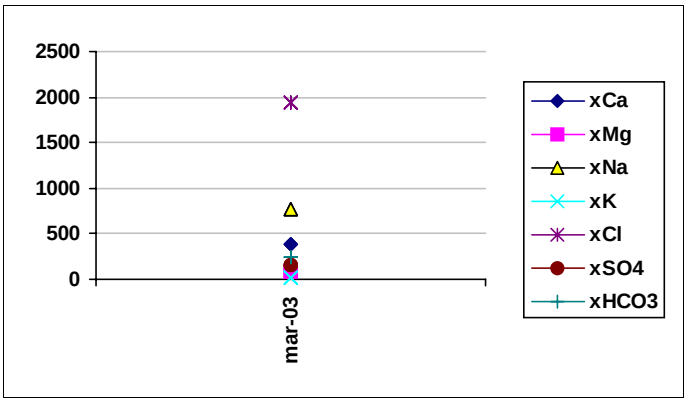

Sampling level (secmid -839.0 masl, RHB70

Mean concentration (mg/l)

Ca:	931
Mg:	232
Na:	2079
K:	34
Cl:	5431
SO4:	508
HCO3:	125

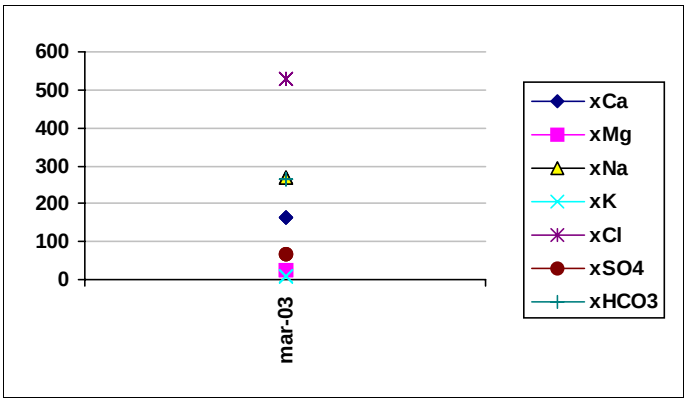

Sampling level (secmid -962.0 masl, RHB70

Mean concentration (mg/l)

Ca:	931
Mg:	232
Na:	2079
K:	34
Cl:	5431
SO4:	508
HCO3:	125

Object **KFM03A**

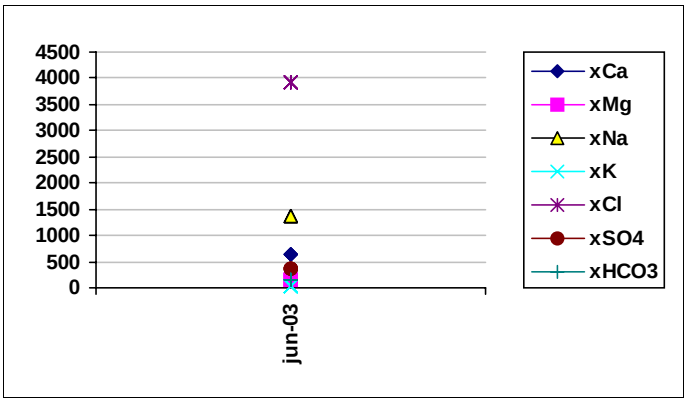

Sampling level (secmid -15.0 masl, RHB70

Mean concentration (mg/l)

Ca:	3766
Mg:	9
Na:	2031
K:	8
Cl:	10052
SO4:	46
HCO3:	8

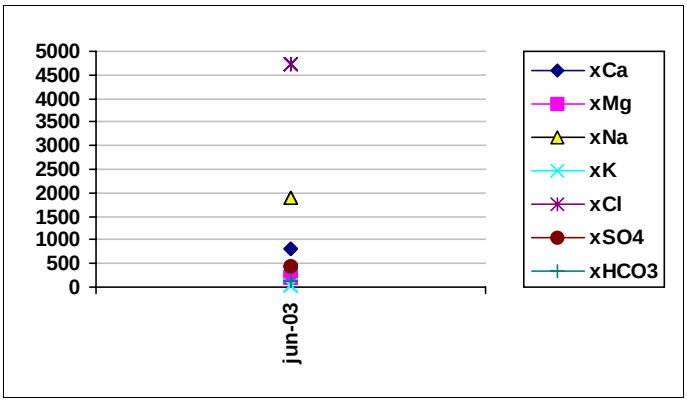

Sampling level (secmid -138.0 masl, RHB70

Mean concentration (mg/l)

Ca:	3766
Mg:	9
Na:	2031
K:	8
Cl:	10052
SO4:	46
HCO3:	8

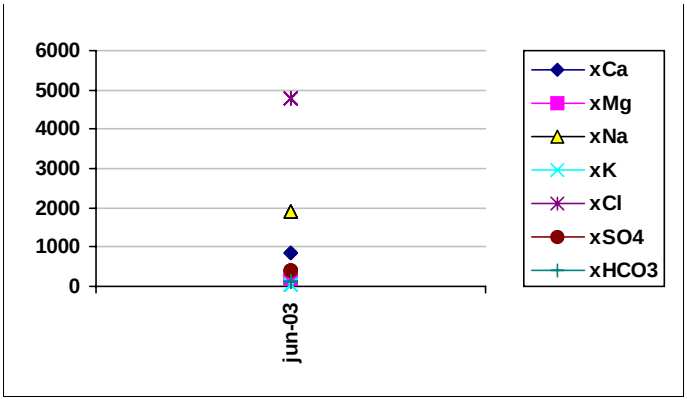

Sampling level (secmid -262.0 masl, RHB70

Mean concentration (mg/l)

Ca:	3766
Mg:	9
Na:	2031
K:	8
Cl:	10052
SO4:	46
HCO3:	8

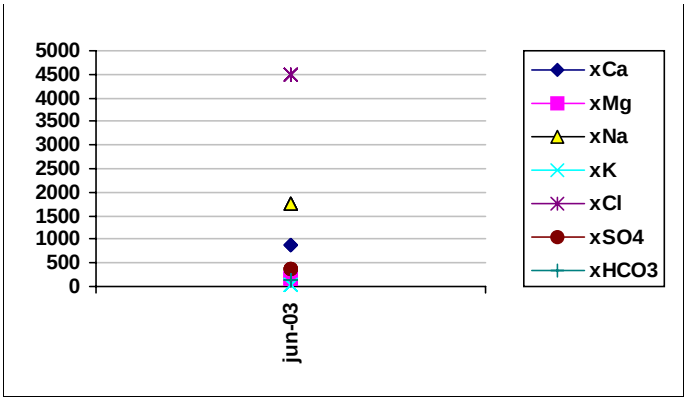

Sampling level (secmid -362.0 masl, RHB70

Mean concentration (mg/l)

Ca:	3766
Mg:	9
Na:	2031
K:	8
Cl:	10052
SO4:	46
HCO3:	8

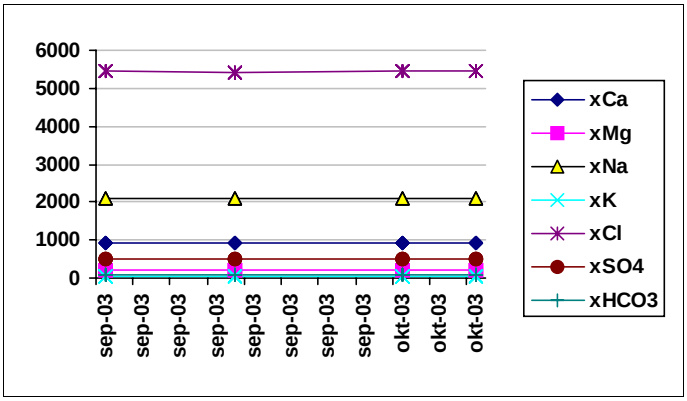

Sampling level (secmid -380.0 masl, RHB70

Mean concentration (mg/l)

Ca:	3766
Mg:	9
Na:	2031
K:	8
Cl:	10052
SO4:	46
HCO3:	8

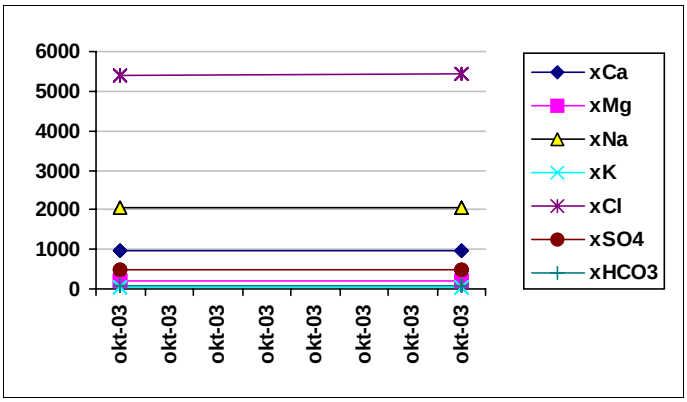

Sampling level (secmid -441.0 masl, RHB70

Mean concentration (mg/l)

Ca:	3766
Mg:	9
Na:	2031
K:	8
Cl:	10052
SO4:	46
HCO3:	8

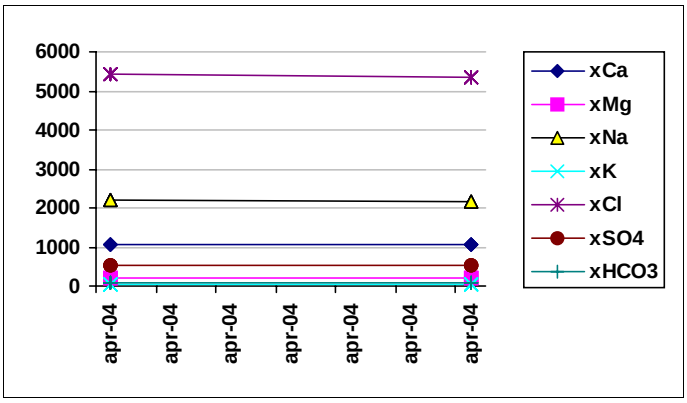

Sampling level (secmid -443.0 masl, RHB70

Mean concentration (mg/l)

Ca:	3766
Mg:	9
Na:	2031
K:	8
Cl:	10052
SO4:	46
HCO3:	8

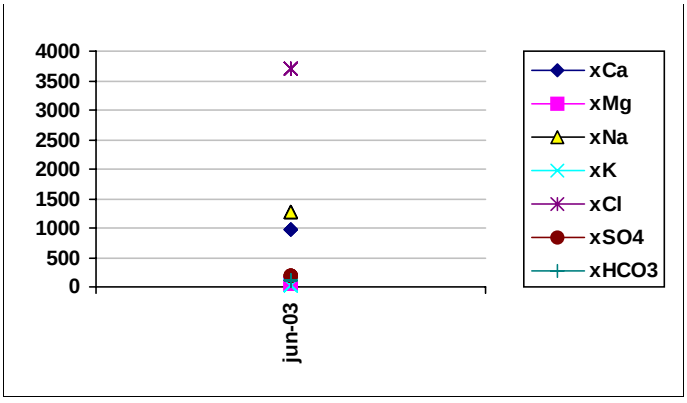

Sampling level (secmid -487.0 masl, RHB70

Mean concentration (mg/l)

Ca:	3766
Mg:	9
Na:	2031
K:	8
Cl:	10052
SO4:	46
HCO3:	8

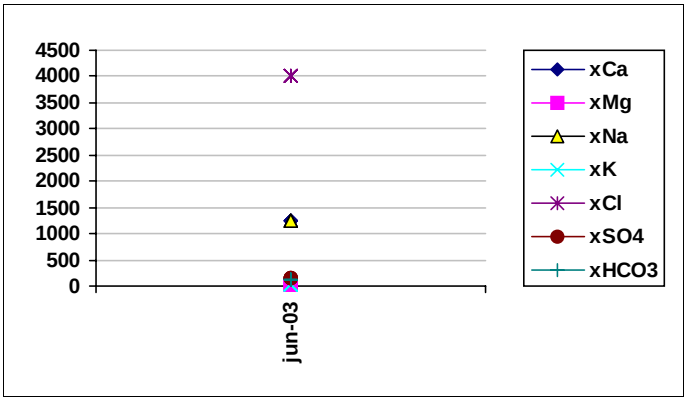

Sampling level (secmid -611.0 masl, RHB70

Mean concentration (mg/l)

Ca:	3766
Mg:	9
Na:	2031
K:	8
Cl:	10052
SO4:	46
HCO3:	8

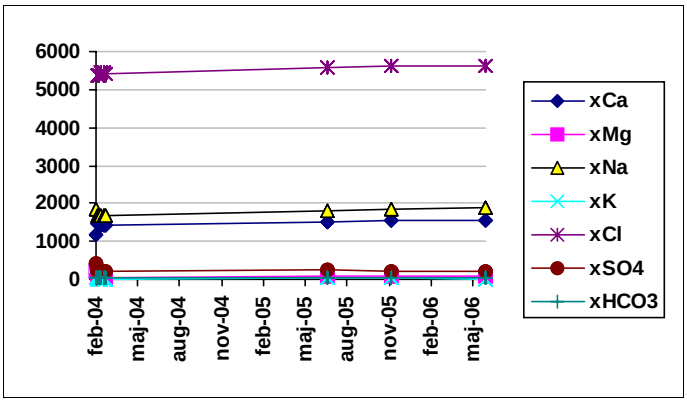

Sampling level (secmid -632.0 masl, RHB70

Mean concentration (mg/l)

Ca:	3766
Mg:	9
Na:	2031
K:	8
Cl:	10052
SO4:	46
HCO3:	8

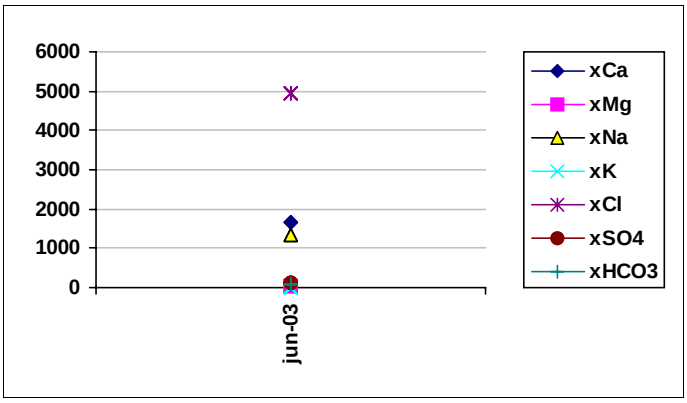

Sampling level (secmid -710.0 masl, RHB70

Mean concentration (mg/l)

Ca:	3766
Mg:	9
Na:	2031
K:	8
Cl:	10052
SO4:	46
HCO3:	8

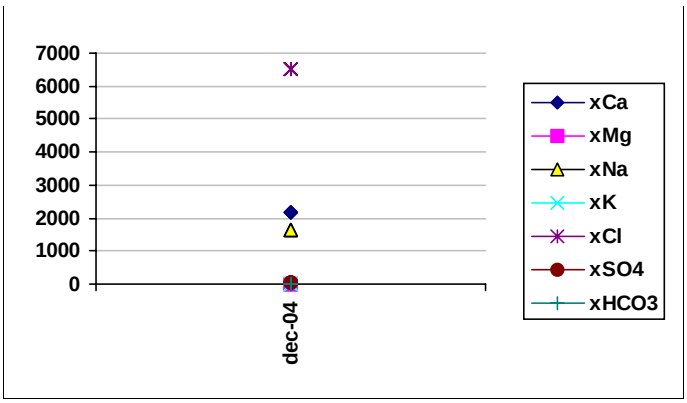

Sampling level (secmid -793.0 masl, RHB70

Mean concentration (mg/l)

Ca:	3766
Mg:	9
Na:	2031
K:	8
Cl:	10052
SO4:	46
HCO3:	8

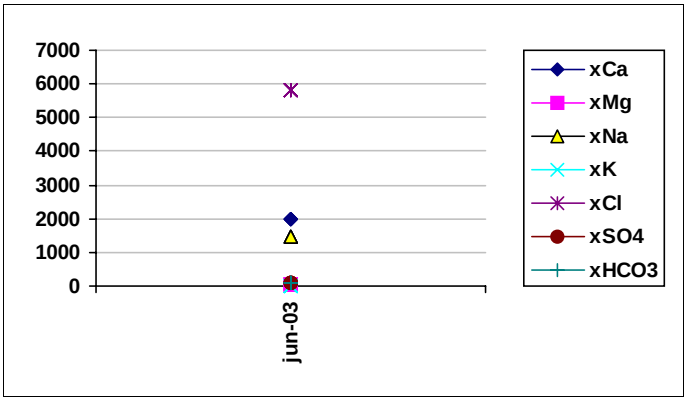

Sampling level (secmid -810.0 masl, RHB70

Mean concentration (mg/l)

Ca:	3766
Mg:	9
Na:	2031
K:	8
Cl:	10052
SO4:	46
HCO3:	8

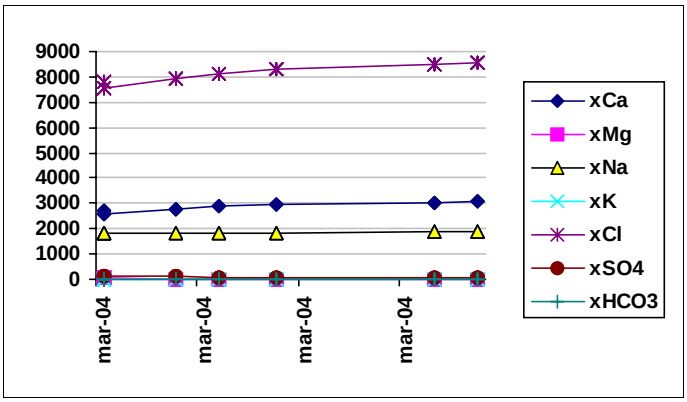

Sampling level (secmid -931.0 masl, RHB70

Mean concentration (mg/l)

Ca:	3766
Mg:	9
Na:	2031
K:	8
Cl:	10052
SO4:	46
HCO3:	8

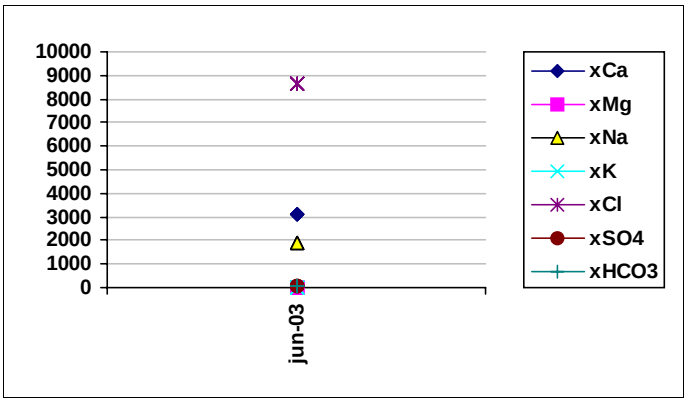

Sampling level (secmid -934.0 masl, RHB70

Mean concentration (mg/l)

Ca:	3766
Mg:	9
Na:	2031
K:	8
Cl:	10052
SO4:	46
HCO3:	8

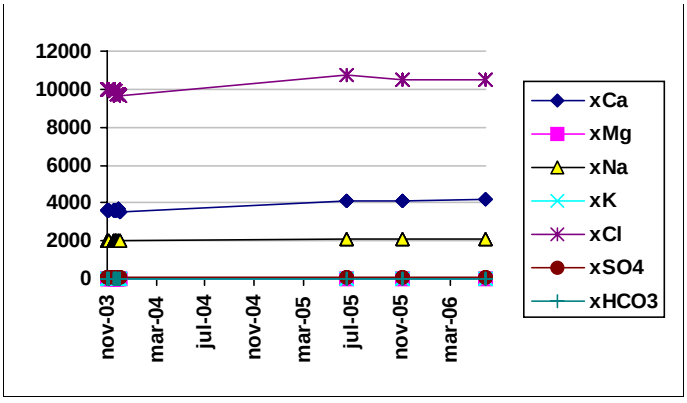

Sampling level (secmid -970.0 masl, RHB70

Mean concentration (mg/l)

Ca:	3766
Mg:	9
Na:	2031
K:	8
Cl:	10052
SO4:	46
HCO3:	8

Object **KFM04A**

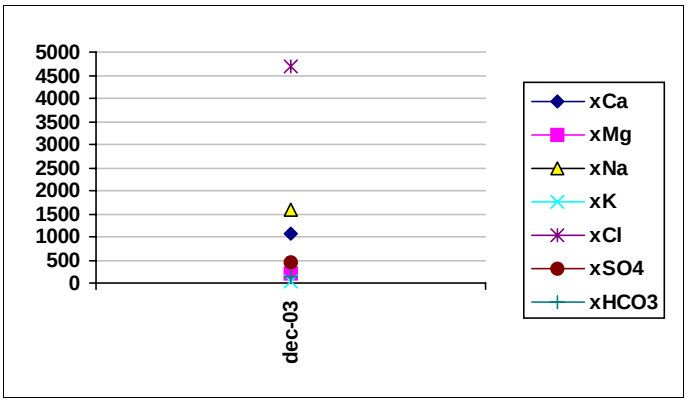

Sampling level (secmid -11.0 masl, RHB70

Mean concentration (mg/l)

Ca:	1332
Mg:	223
Na:	1803
K:	25
Cl:	5548
SO4:	516
HCO3:	105

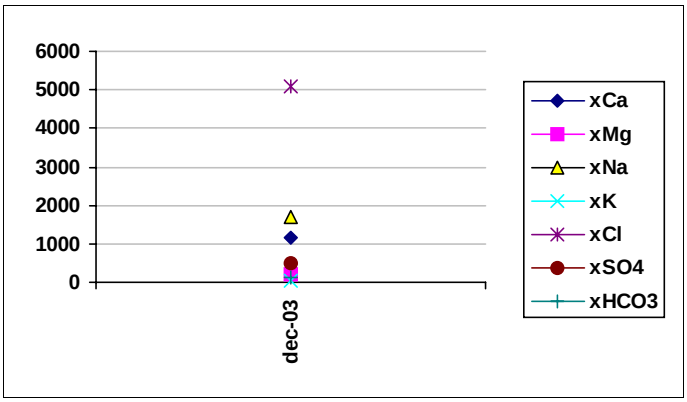

Sampling level (secmid -120.0 masl, RHB70

Mean concentration (mg/l)

Ca:	1332
Mg:	223
Na:	1803
K:	25
Cl:	5548
SO4:	516
HCO3:	105

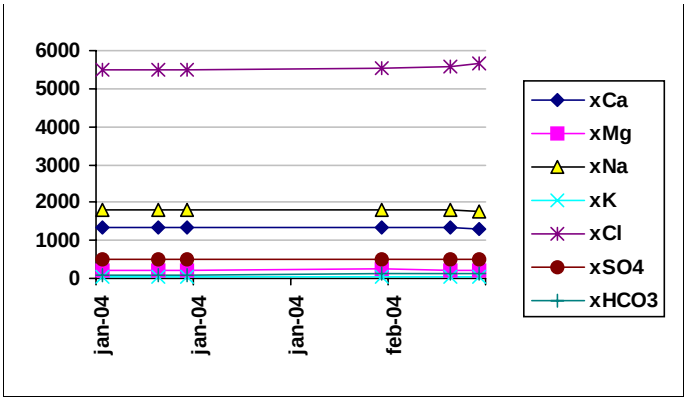

Sampling level (secmid -185.0 masl, RHB70

Mean concentration (mg/l)

Ca:	1332
Mg:	223
Na:	1803
K:	25
Cl:	5548
SO4:	516
HCO3:	105

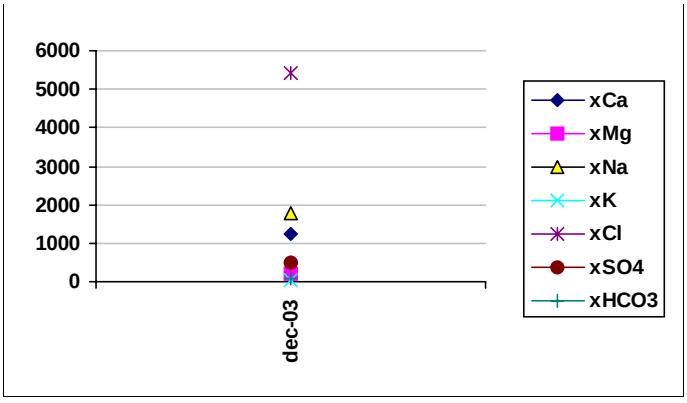

Sampling level (secmid -228.0 masl, RHB70

Mean concentration (mg/l)

Ca:	1332
Mg:	223
Na:	1803
K:	25
Cl:	5548
SO4:	516
HCO3:	105

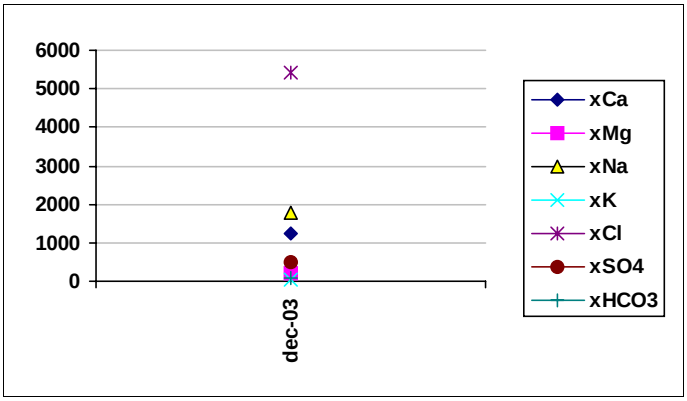

Sampling level (secmid -314.0 masl, RHB70

Mean concentration (mg/l)

Ca:	1332
Mg:	223
Na:	1803
K:	25
Cl:	5548
SO4:	516
HCO3:	105

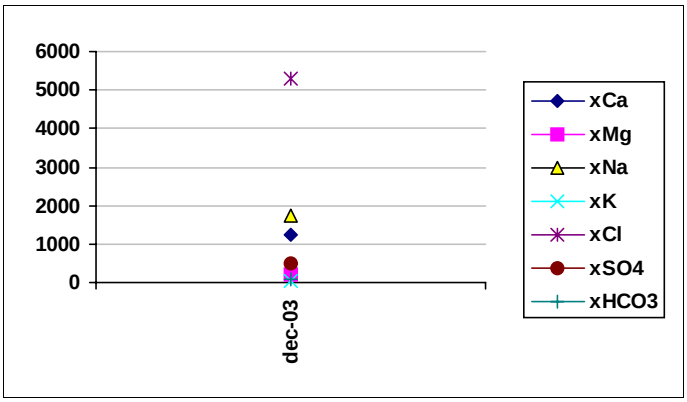

Sampling level (secmid -416.0 masl, RHB70

Mean concentration (mg/l)

Ca:	1332
Mg:	223
Na:	1803
K:	25
Cl:	5548
SO4:	516
HCO3:	105

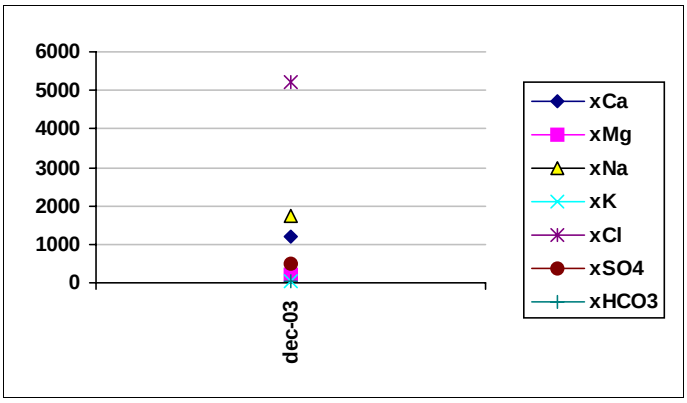

Sampling level (secmid -515.0 masl, RHB70

Mean concentration (mg/l)

Ca:	1332
Mg:	223
Na:	1803
K:	25
Cl:	5548
SO4:	516
HCO3:	105

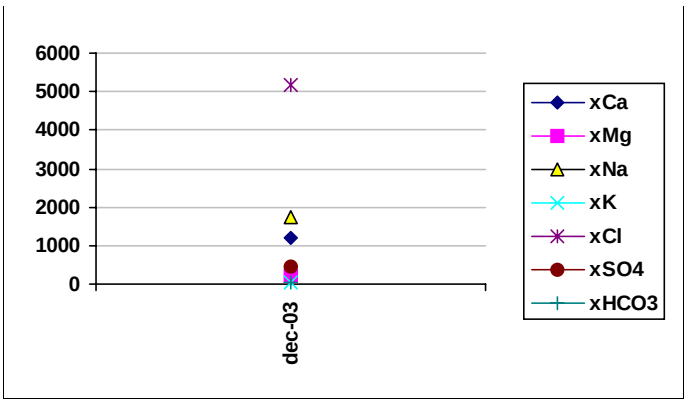

Sampling level (secmid -592.0 masl, RHB70

Mean concentration (mg/l)

Ca:	1332
Mg:	223
Na:	1803
K:	25
Cl:	5548
SO4:	516
HCO3:	105

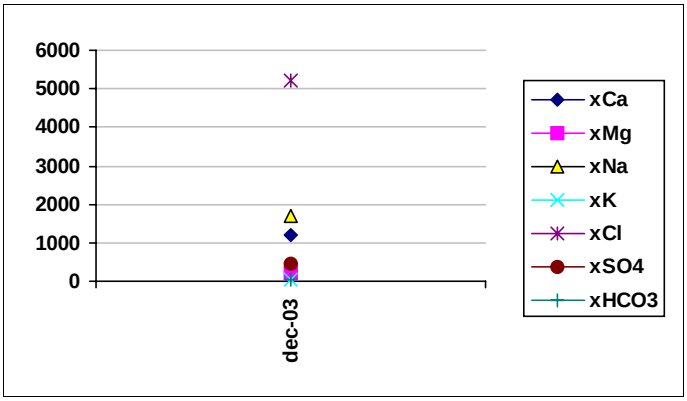

Sampling level (secmid -666.0 masl, RHB70

Mean concentration (mg/l)

Ca:	1332
Mg:	223
Na:	1803
K:	25
Cl:	5548
SO4:	516
HCO3:	105

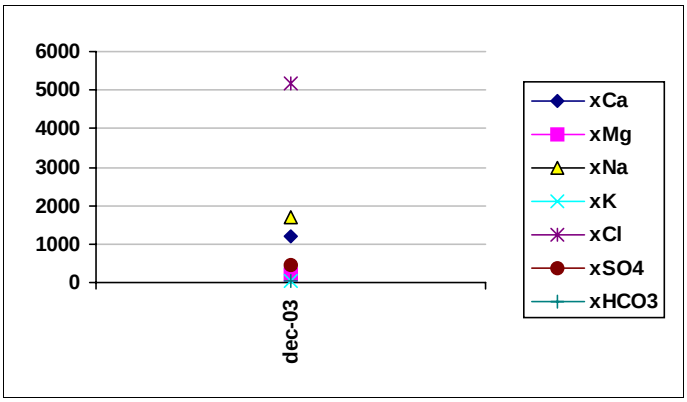

Sampling level (secmid -755.0 masl, RHB70

Mean concentration (mg/l)

Ca:	1332
Mg:	223
Na:	1803
K:	25
Cl:	5548
SO4:	516
HCO3:	105

Object **KFM06A**

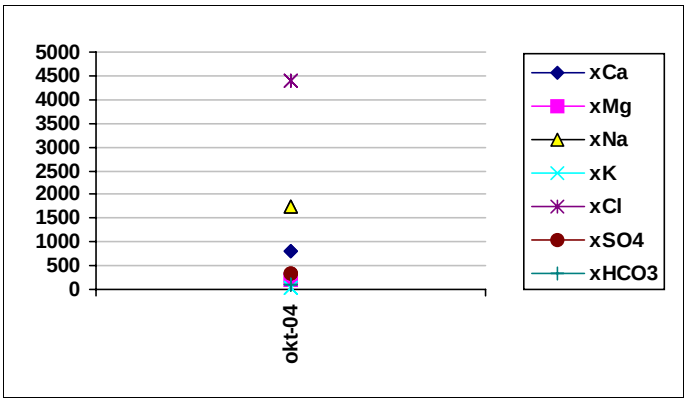

Sampling level (secmid -16.0 masl, RHB70

Mean concentration (mg/l)

Ca:	2440
Mg:	9
Na:	1752
K:	7
Cl:	6962
SO4:	47
HCO3:	9

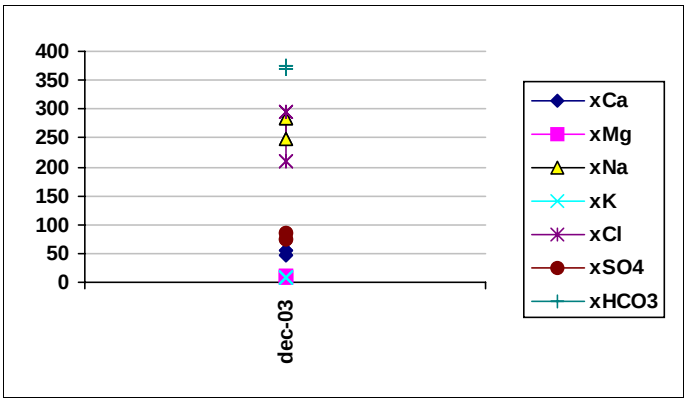

Sampling level (secmid -40.0 masl, RHB70

Mean concentration (mg/l)

Ca:	2440
Mg:	9
Na:	1752
K:	7
Cl:	6962
SO4:	47
HCO3:	9

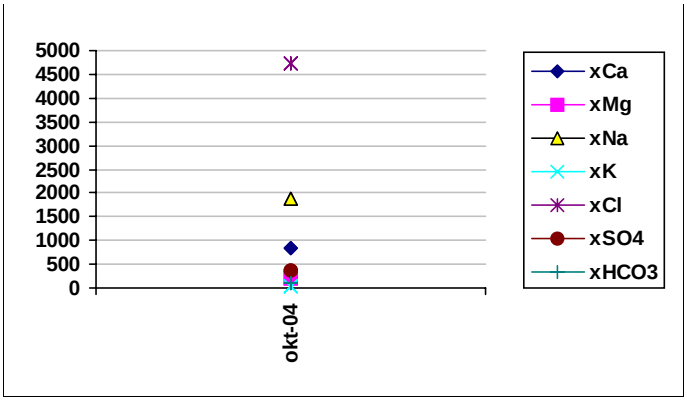

Sampling level (secmid -122.0 masl, RHB70

Mean concentration (mg/l)

Ca:	2440
Mg:	9
Na:	1752
K:	7
Cl:	6962
SO4:	47
HCO3:	9

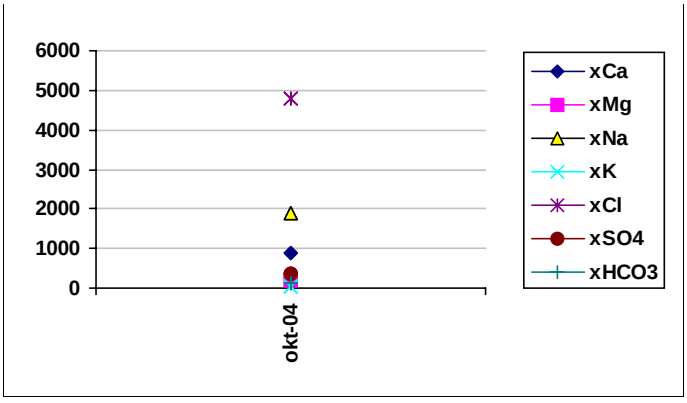

Sampling level (secmid -186.0 masl, RHB70

Mean concentration (mg/l)

Ca:	2440
Mg:	9
Na:	1752
K:	7
Cl:	6962
SO4:	47
HCO3:	9

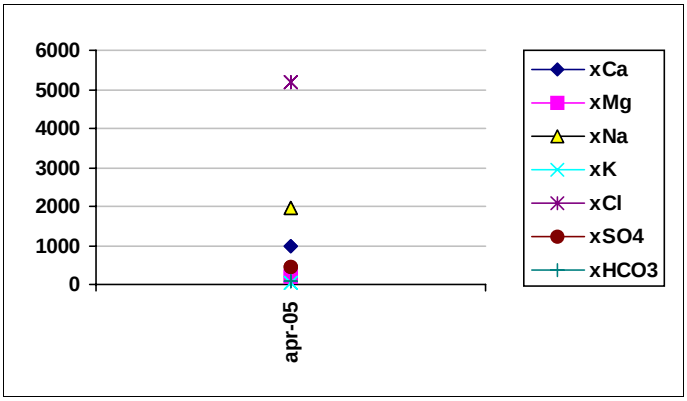

Sampling level (secmid -227.0 masl, RHB70

Mean concentration (mg/l)

Ca:	2440
Mg:	9
Na:	1752
K:	7
Cl:	6962
SO4:	47
HCO3:	9

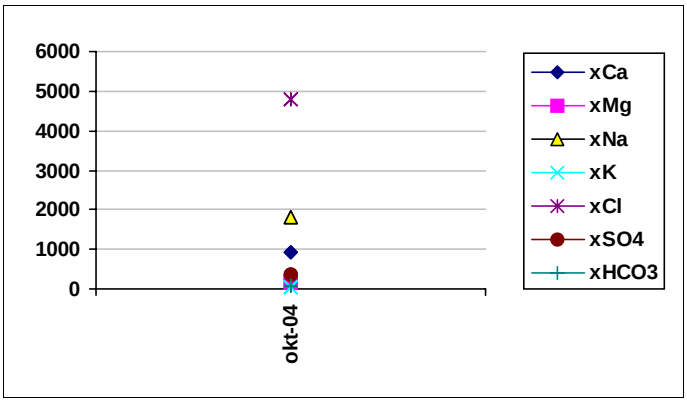

Sampling level (secmid -292.0 masl, RHB70

Mean concentration (mg/l)

Ca:	2440
Mg:	9
Na:	1752
K:	7
Cl:	6962
SO4:	47
HCO3:	9

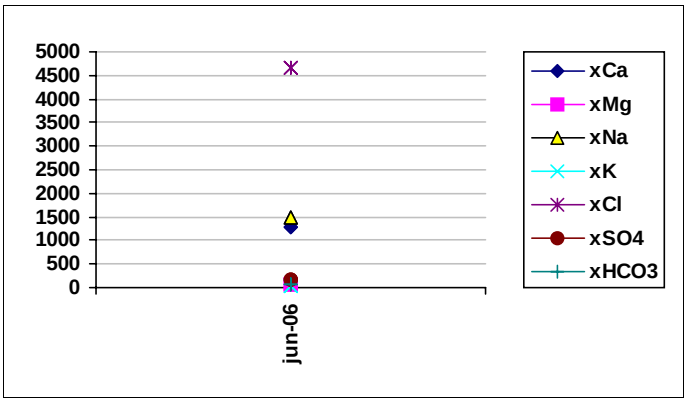

Sampling level (secmid -298.0 masl, RHB70

Mean concentration (mg/l)

Ca:	2440
Mg:	9
Na:	1752
K:	7
Cl:	6962
SO4:	47
HCO3:	9

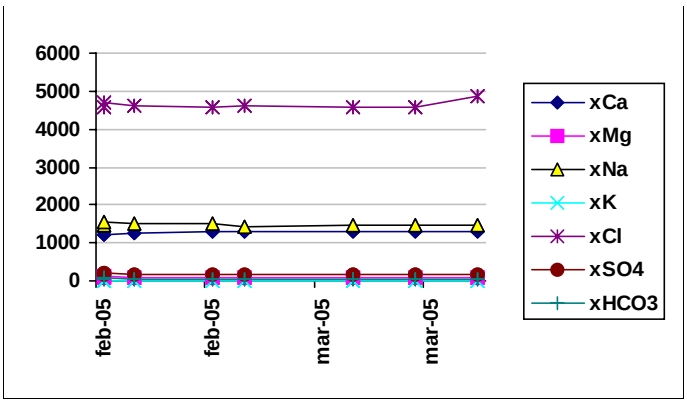

Sampling level (secmid -302.0 masl, RHB70

Mean concentration (mg/l)

Ca:	2440
Mg:	9
Na:	1752
K:	7
Cl:	6962
SO4:	47
HCO3:	9

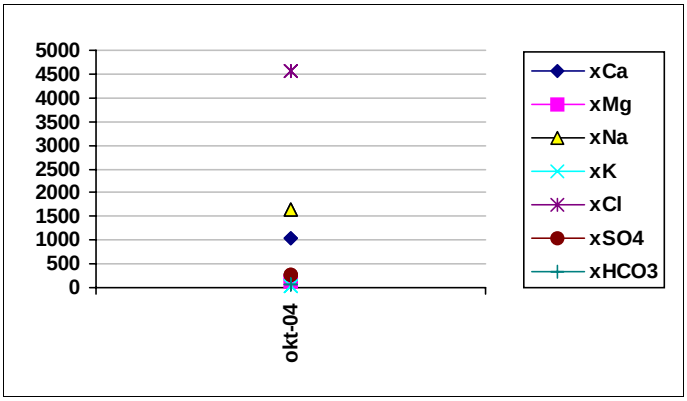

Sampling level (secmid -397.0 masl, RHB70

Mean concentration (mg/l)

Ca:	2440
Mg:	9
Na:	1752
K:	7
Cl:	6962
SO4:	47
HCO3:	9

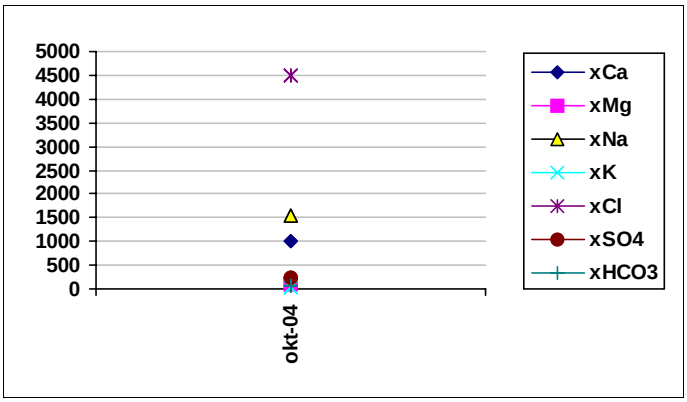

Sampling level (secmid -480.0 masl, RHB70

Mean concentration (mg/l)

Ca:	2440
Mg:	9
Na:	1752
K:	7
Cl:	6962
SO4:	47
HCO3:	9

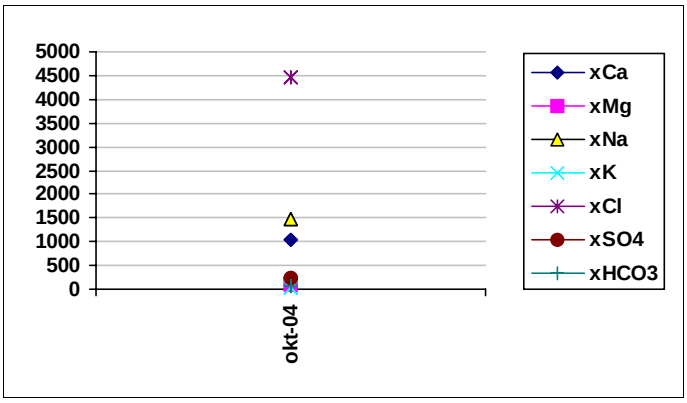

Sampling level (secmid -604.0 masl, RHB70

Mean concentration (mg/l)

Ca:	2440
Mg:	9
Na:	1752
K:	7
Cl:	6962
SO4:	47
HCO3:	9

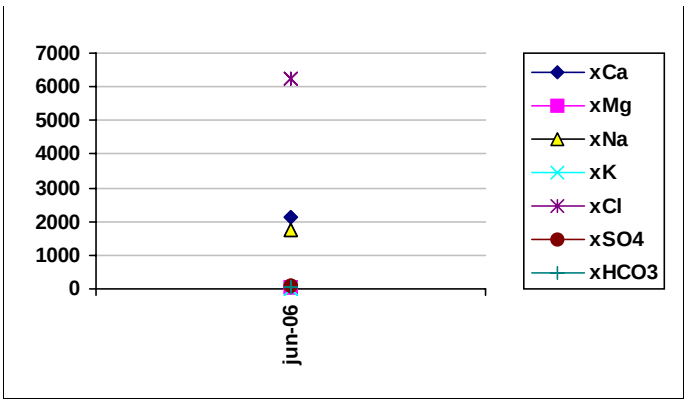

Sampling level (secmid -623.0 masl, RHB70

Mean concentration (mg/l)

Ca:	2440
Mg:	9
Na:	1752
K:	7
Cl:	6962
SO4:	47
HCO3:	9

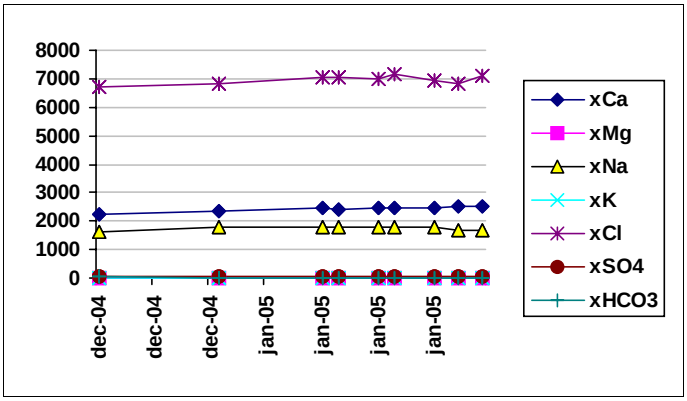

Sampling level (secmid -646.0 masl, RHB70

Mean concentration (mg/l)

Ca:	2440
Mg:	9
Na:	1752
K:	7
Cl:	6962
SO4:	47
HCO3:	9

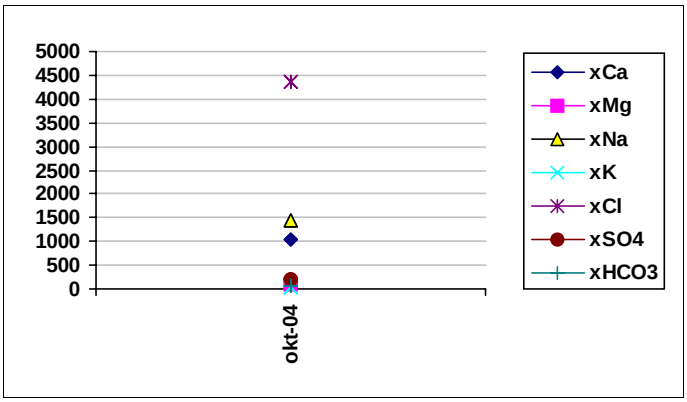

Sampling level (secmid -705.0 masl, RHB70

Mean concentration (mg/l)

Ca:	2440
Mg:	9
Na:	1752
K:	7
Cl:	6962
SO4:	47
HCO3:	9

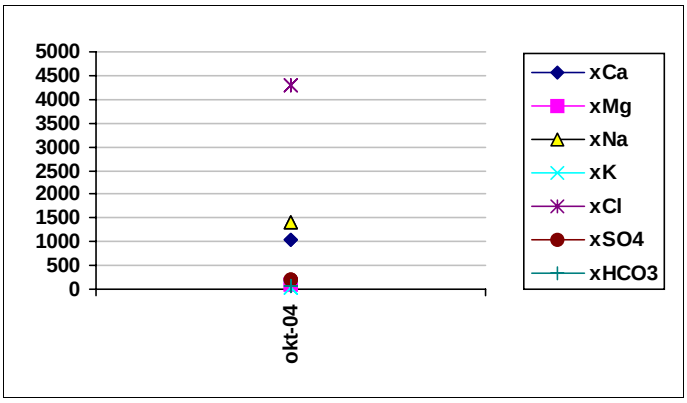

Sampling level (secmid -805.0 masl, RHB70

Mean concentration (mg/l)

Ca:	2440
Mg:	9
Na:	1752
K:	7
Cl:	6962
SO4:	47
HCO3:	9

Object **KFM07A**

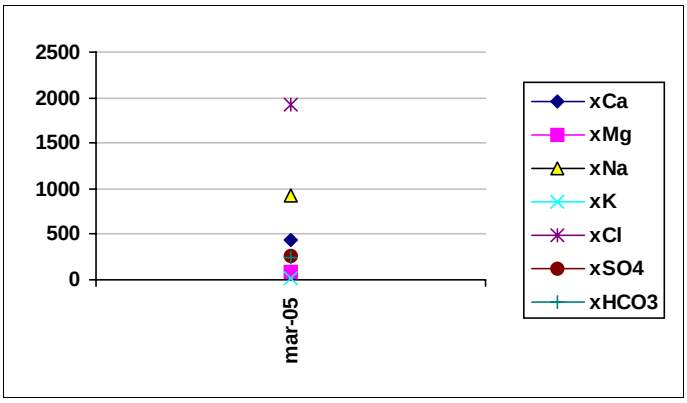

Sampling level (secmid -19.0 masl, RHB70

Mean concentration (mg/l)

Ca:	5785
Mg:	21
Na:	2828
K:	15
Cl:	14500
SO4:	99
HCO3:	7

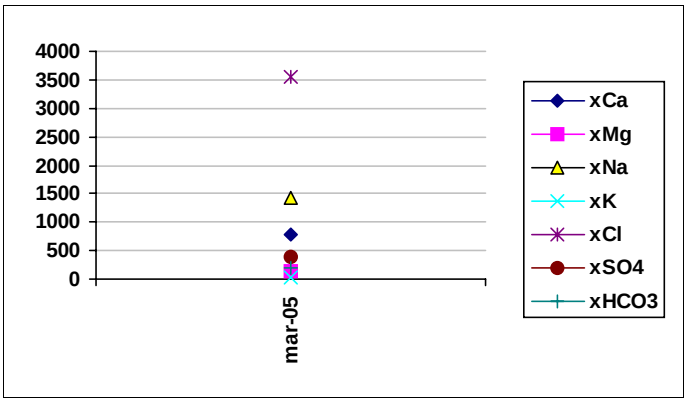

Sampling level (secmid -126.0 masl, RHB70

Mean concentration (mg/l)

Ca:	5785
Mg:	21
Na:	2828
K:	15
Cl:	14500
SO4:	99
HCO3:	7

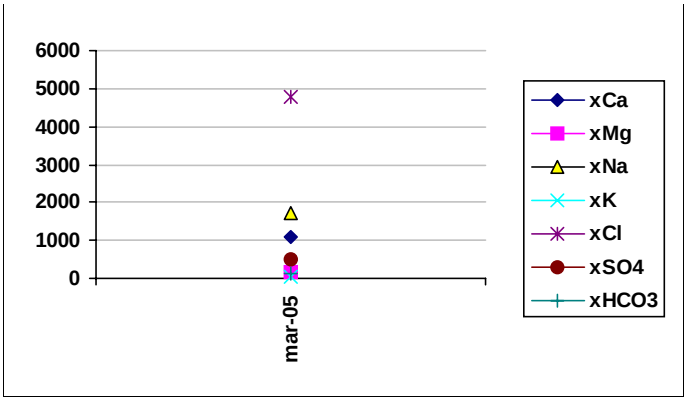

Sampling level (secmid -233.0 masl, RHB70

Mean concentration (mg/l)

Ca:	5785
Mg:	21
Na:	2828
K:	15
Cl:	14500
SO4:	99
HCO3:	7

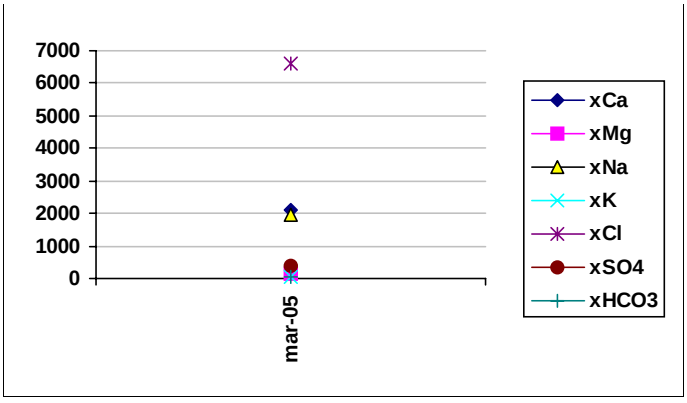

Sampling level (secmid -317.0 masl, RHB70

Mean concentration (mg/l)

Ca:	5785
Mg:	21
Na:	2828
K:	15
Cl:	14500
SO4:	99
HCO3:	7

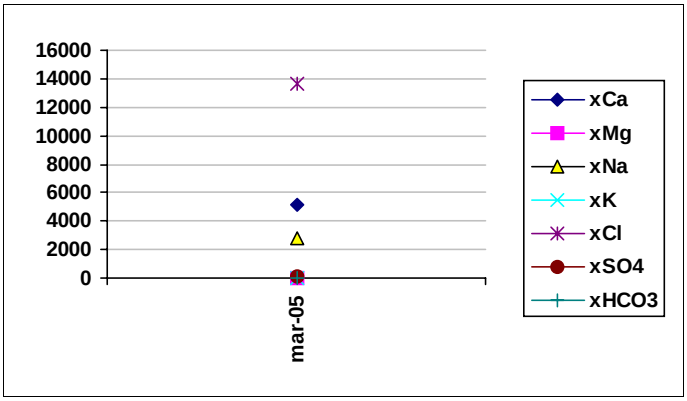

Sampling level (secmid -420.0 masl, RHB70

Mean concentration (mg/l)

Ca:	5785
Mg:	21
Na:	2828
K:	15
Cl:	14500
SO4:	99
HCO3:	7

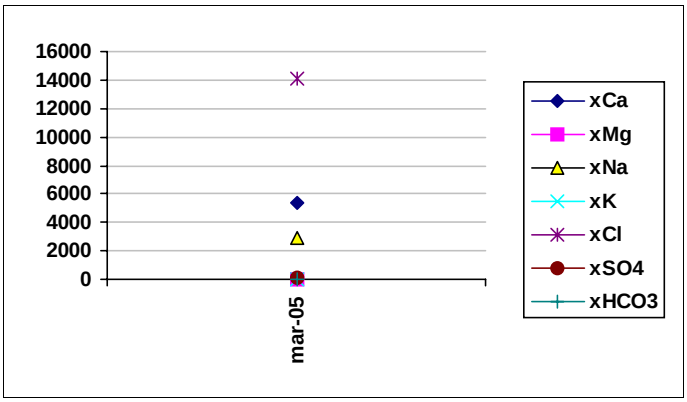

Sampling level (secmid -523.0 masl, RHB70

Mean concentration (mg/l)

Ca:	5785
Mg:	21
Na:	2828
K:	15
Cl:	14500
SO4:	99
HCO3:	7

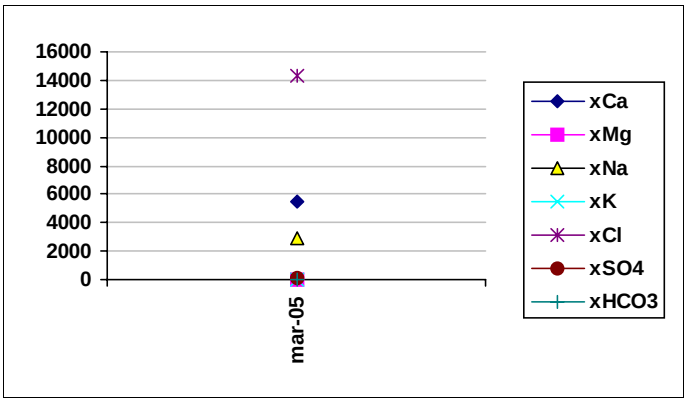

Sampling level (secmid -604.0 masl, RHB70

Mean concentration (mg/l)

Ca:	5785
Mg:	21
Na:	2828
K:	15
Cl:	14500
SO4:	99
HCO3:	7

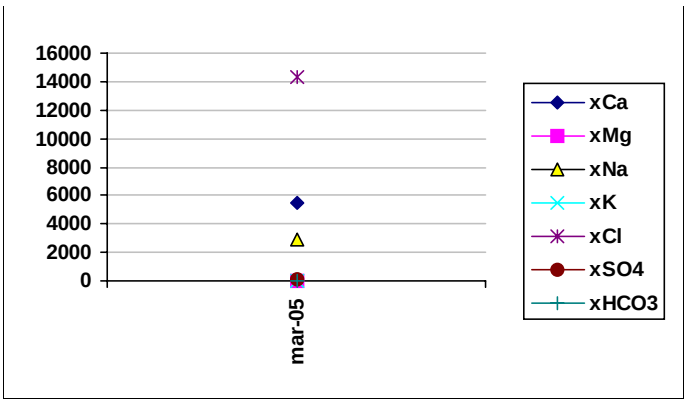

Sampling level (secmid -683.0 masl, RHB70

Mean concentration (mg/l)

Ca:	5785
Mg:	21
Na:	2828
K:	15
Cl:	14500
SO4:	99
HCO3:	7

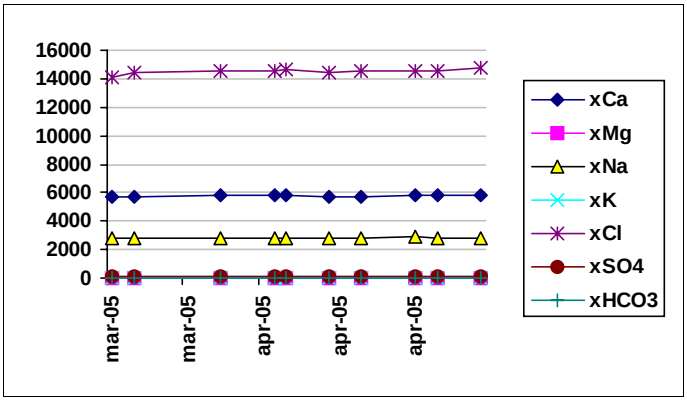

Sampling level (secmid -760.0 masl, RHB70

Mean concentration (mg/l)

Ca:	5785
Mg:	21
Na:	2828
K:	15
Cl:	14500
SO4:	99
HCO3:	7

Object **KFM08A**

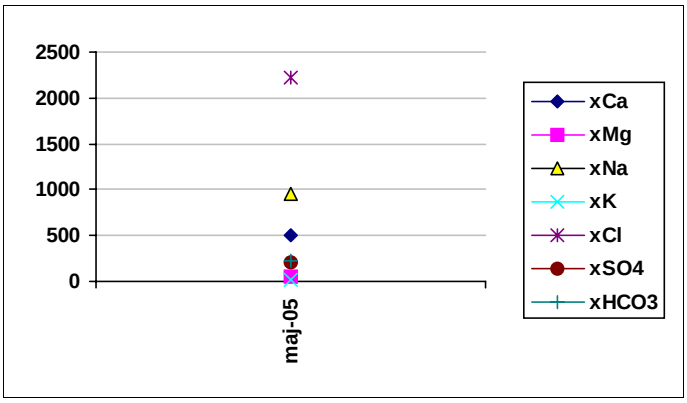

Sampling level (secmid -28.0 masl, RHB70

Mean concentration (mg/l)

Ca:	2145
Mg:	14
Na:	1514
K:	10
Cl:	6111
SO4:	91
HCO3:	11

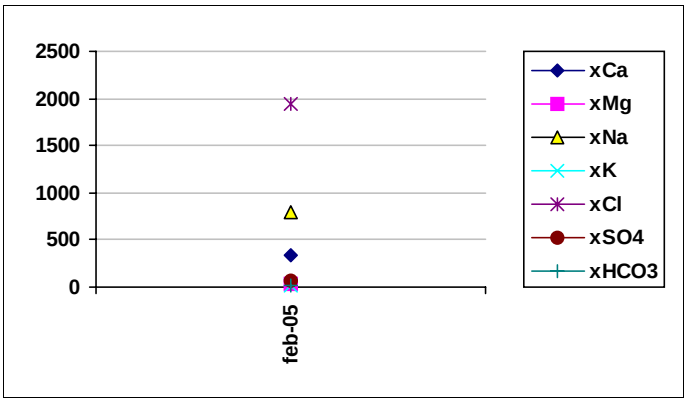

Sampling level (secmid -128.0 masl, RHB70

Mean concentration (mg/l)

Ca:	2145
Mg:	14
Na:	1514
K:	10
Cl:	6111
SO4:	91
HCO3:	11

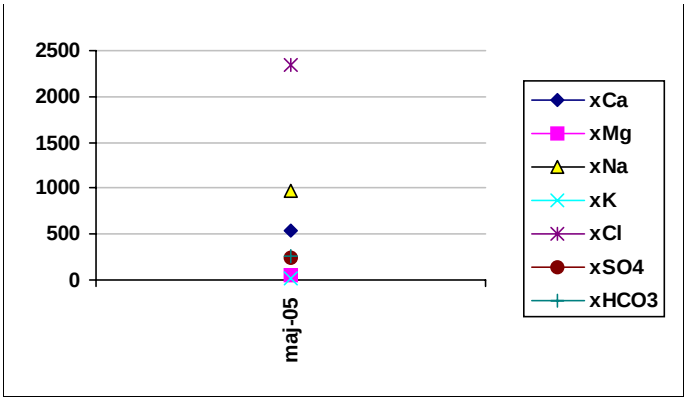

Sampling level (secmid -135.0 masl, RHB70

Mean concentration (mg/l)

Ca:	2145
Mg:	14
Na:	1514
K:	10
Cl:	6111
SO4:	91
HCO3:	11

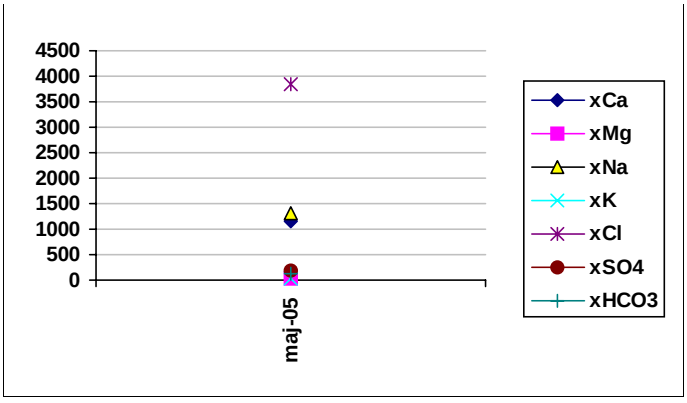

Sampling level (secmid -238.0 masl, RHB70

Mean concentration (mg/l)

Ca:	2145
Mg:	14
Na:	1514
K:	10
Cl:	6111
SO4:	91
HCO3:	11

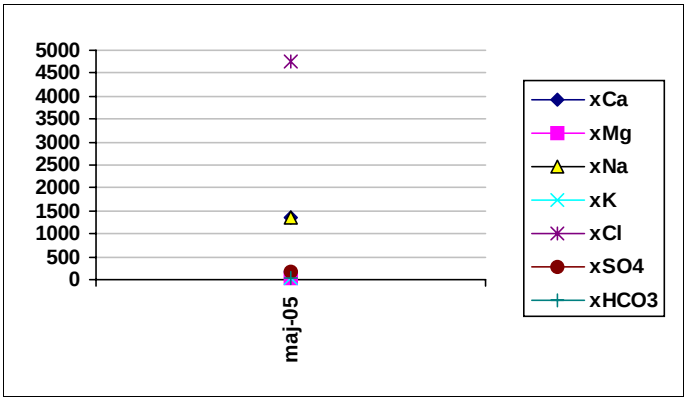

Sampling level (secmid -319.0 masl, RHB70

Mean concentration (mg/l)

Ca:	2145
Mg:	14
Na:	1514
K:	10
Cl:	6111
SO4:	91
HCO3:	11

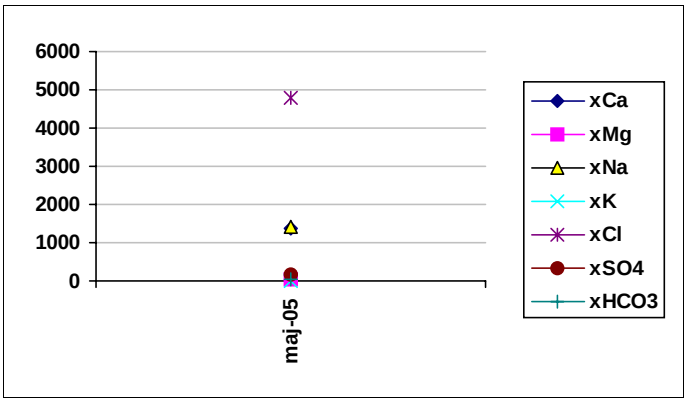

Sampling level (secmid -416.0 masl, RHB70

Mean concentration (mg/l)

Ca:	2145
Mg:	14
Na:	1514
K:	10
Cl:	6111
SO4:	91
HCO3:	11

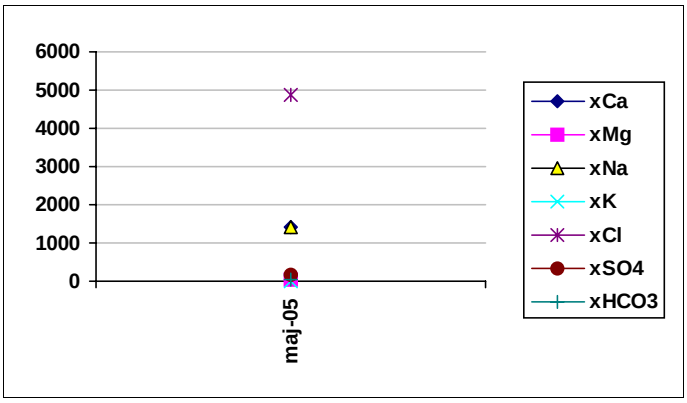

Sampling level (secmid -509.0 masl, RHB70

Mean concentration (mg/l)

Ca:	2145
Mg:	14
Na:	1514
K:	10
Cl:	6111
SO4:	91
HCO3:	11

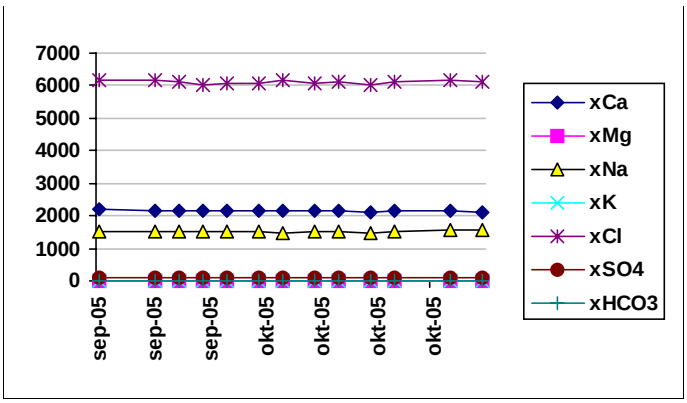

Sampling level (secmid -547.0 masl, RHB70

Mean concentration (mg/l)

Ca:	2145
Mg:	14
Na:	1514
K:	10
Cl:	6111
SO4:	91
HCO3:	11

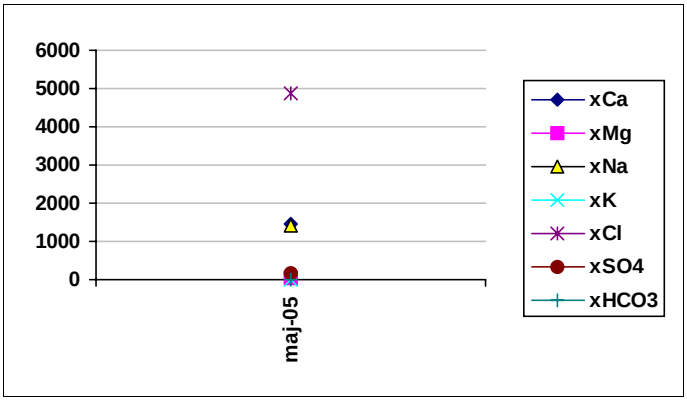

Sampling level (secmid -581.0 masl, RHB70

Mean concentration (mg/l)

Ca:	2145
Mg:	14
Na:	1514
K:	10
Cl:	6111
SO4:	91
HCO3:	11

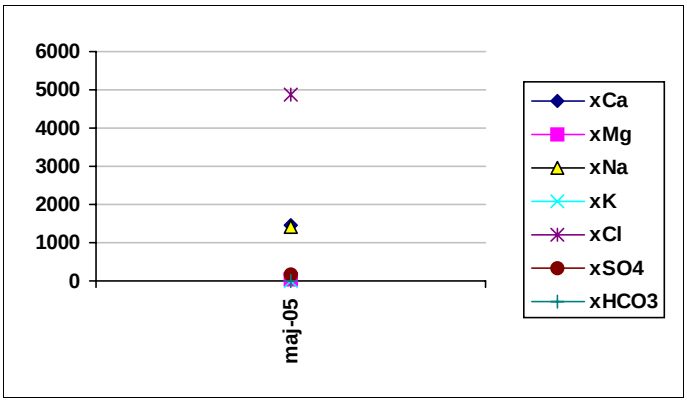

Sampling level (secmid -649.0 masl, RHB70

Mean concentration (mg/l)

Ca:	2145
Mg:	14
Na:	1514
K:	10
Cl:	6111
SO4:	91
HCO3:	11

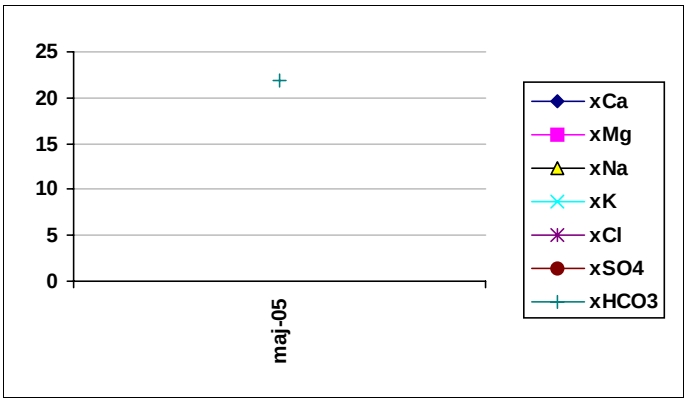

Sampling level (secmid -681.0 masl, RHB70

Mean concentration (mg/l)

Ca:	2145
Mg:	14
Na:	1514
K:	10
Cl:	6111
SO4:	91
HCO3:	11

Object **KFM09A**

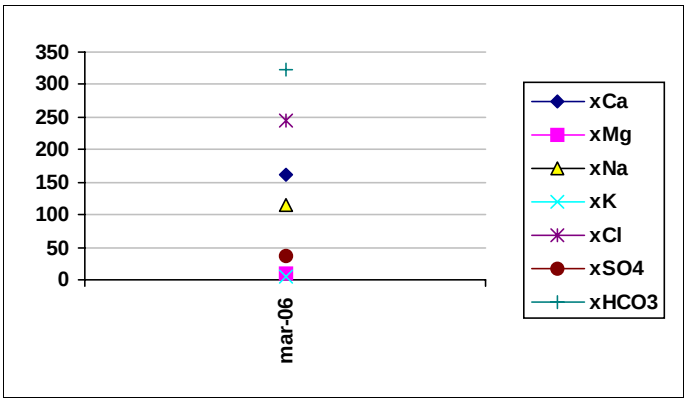

Sampling level (secmid -56.0 masl, RHB70

Mean concentration (mg/l)

Ca:	6513
Mg:	17
Na:	2620
K:	13
Cl:	14650
SO4:	118
HCO3:	7

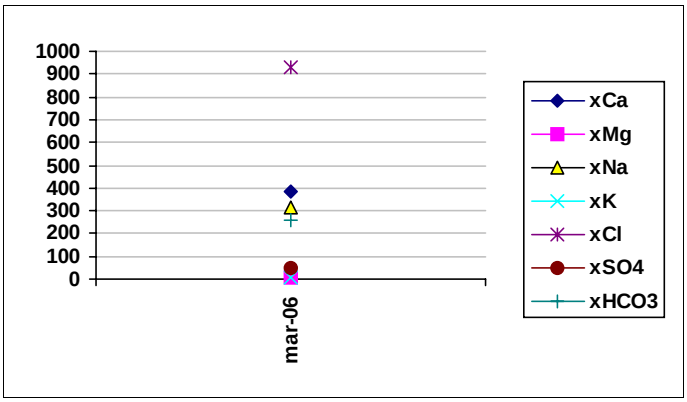

Sampling level (secmid -141.0 masl, RHB70

Mean concentration (mg/l)

Ca:	6513
Mg:	17
Na:	2620
K:	13
Cl:	14650
SO4:	118
HCO3:	7

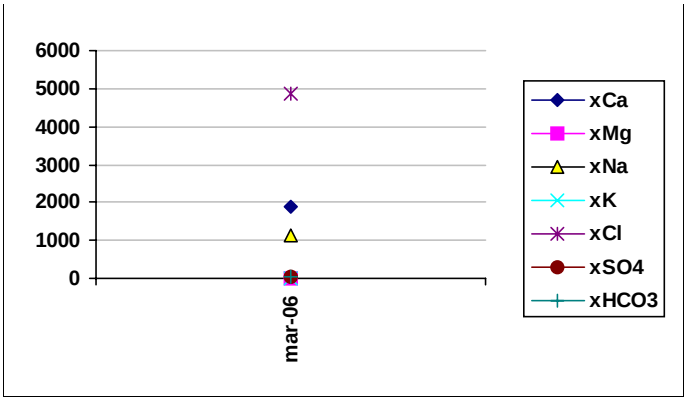

Sampling level (secmid -224.0 masl, RHB70

Mean concentration (mg/l)

Ca:	6513
Mg:	17
Na:	2620
K:	13
Cl:	14650
SO4:	118
HCO3:	7

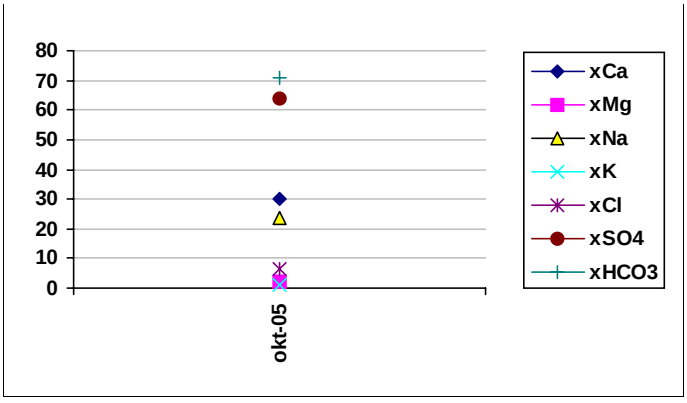

Sampling level (secmid -255.0 masl, RHB70

Mean concentration (mg/l)

Ca:	6513
Mg:	17
Na:	2620
K:	13
Cl:	14650
SO4:	118
HCO3:	7

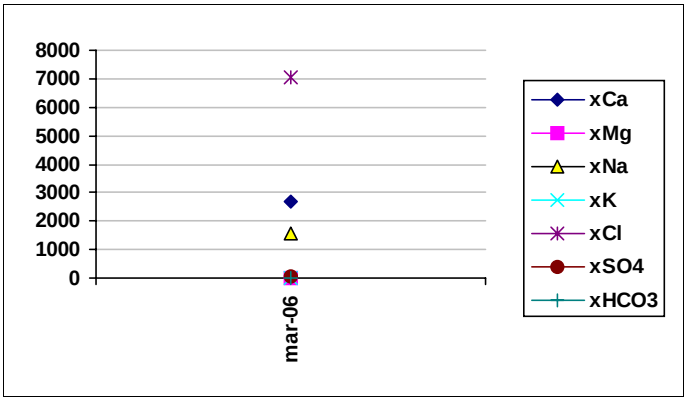

Sampling level (secmid -305.0 masl, RHB70

Mean concentration (mg/l)

Ca:	6513
Mg:	17
Na:	2620
K:	13
Cl:	14650
SO4:	118
HCO3:	7

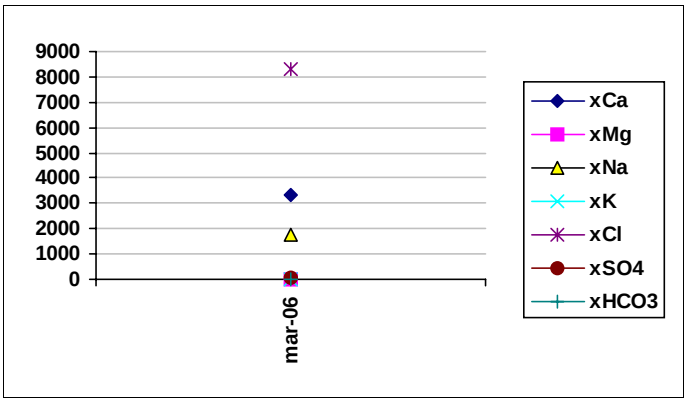

Sampling level (secmid -384.0 masl, RHB70

Mean concentration (mg/l)

Ca:	6513
Mg:	17
Na:	2620
K:	13
Cl:	14650
SO4:	118
HCO3:	7

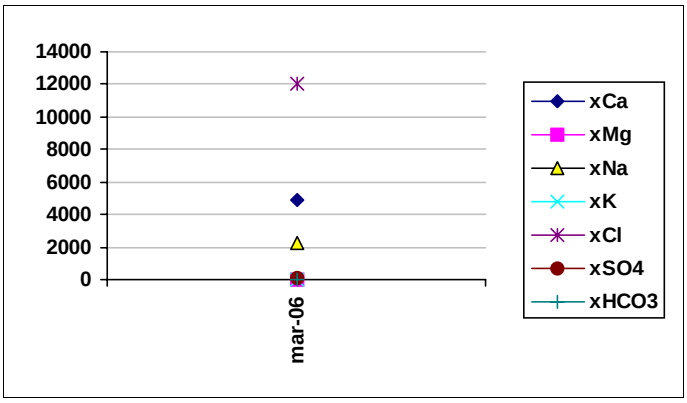

Sampling level (secmid -461.0 masl, RHB70

Mean concentration (mg/l)

Ca:	6513
Mg:	17
Na:	2620
K:	13
Cl:	14650
SO4:	118
HCO3:	7

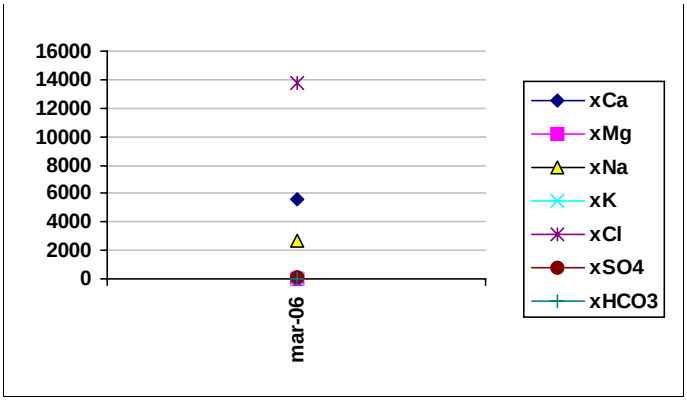

Sampling level (secmid -534.0 masl, RHB70

Mean concentration (mg/l)

Ca:	6513
Mg:	17
Na:	2620
K:	13
Cl:	14650
SO4:	118
HCO3:	7

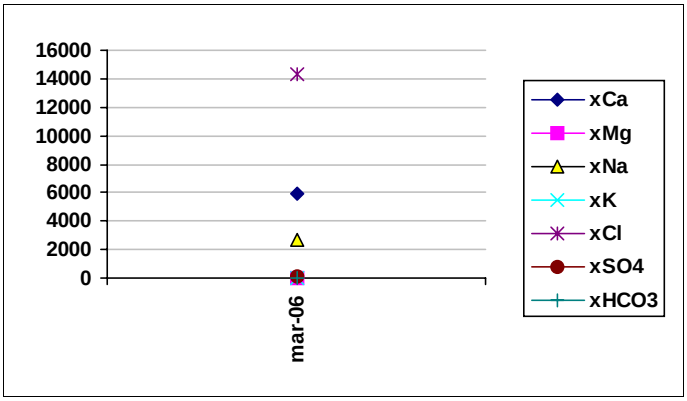

Sampling level (secmid -602.0 masl, RHB70

Mean concentration (mg/l)

Ca:	6513
Mg:	17
Na:	2620
K:	13
Cl:	14650
SO4:	118
HCO3:	7

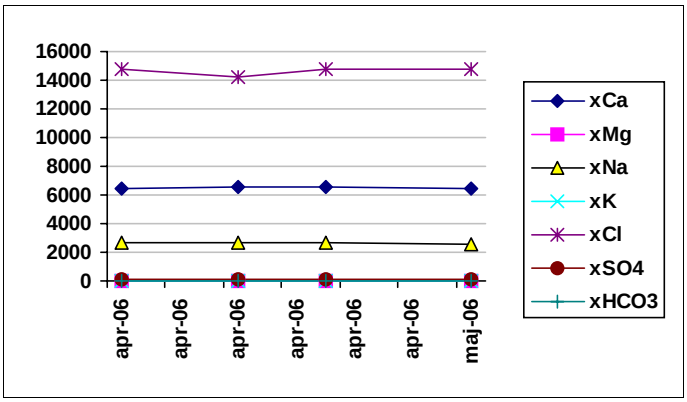

Sampling level (secmid -615.0 masl, RHB70

Mean concentration (mg/l)

Ca:	6513
Mg:	17
Na:	2620
K:	13
Cl:	14650
SO4:	118
HCO3:	7

Object **PFM000001**

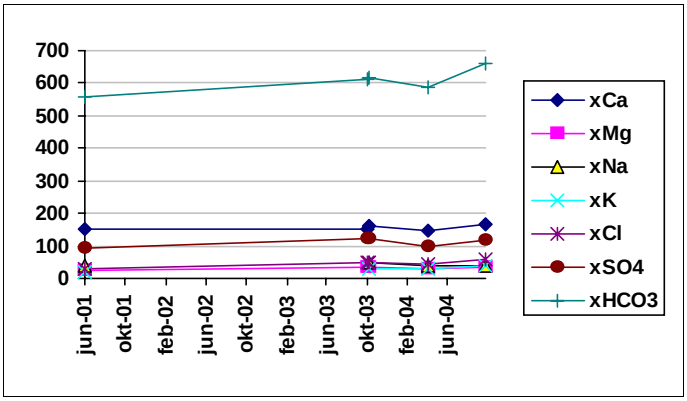

Sampling level (secmid -39.0 masl, RHB70

Mean concentration (mg/l)

Ca:	156
Mg:	31
Na:	41
K:	29
Cl:	46
SO4:	111
HCO3:	606

Object **PFM000007**

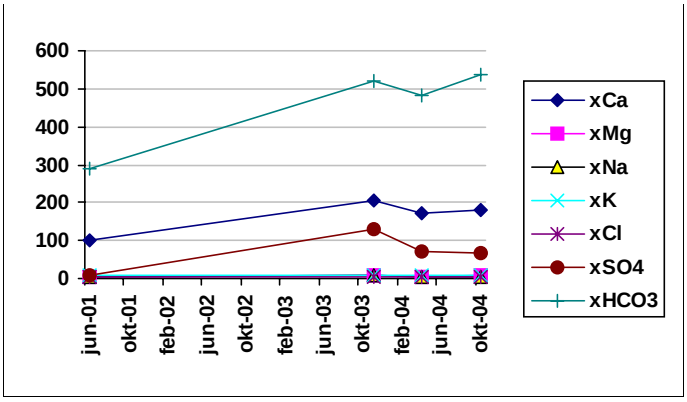

Sampling level (secmid -1.0 masl, RHB70

Mean concentration (mg/l)

Ca:	172
Mg:	6
Na:	5
K:	8
Cl:	5
SO4:	109
HCO3:	458

Object **PFM000008**

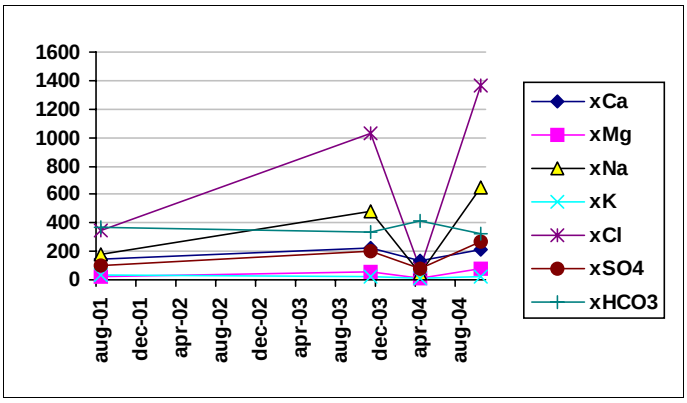

Sampling level (secmid -1.0 masl, RHB70

Mean concentration (mg/l)

Ca:	180
Mg:	55
Na:	338
K:	20
Cl:	945
SO4:	184
HCO3:	361

Object **PFM000009**

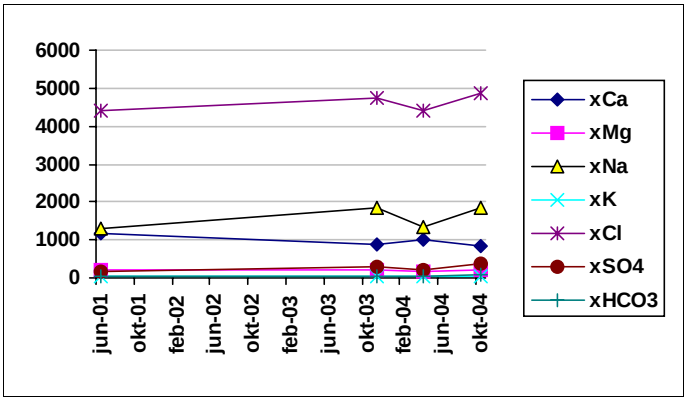

Sampling level (secmid -69.0 masl, RHB70

Mean concentration (mg/l)

Ca:	955
Mg:	188
Na:	1578
K:	25
Cl:	4796
SO4:	268
HCO3:	60

Object **PFM000010**

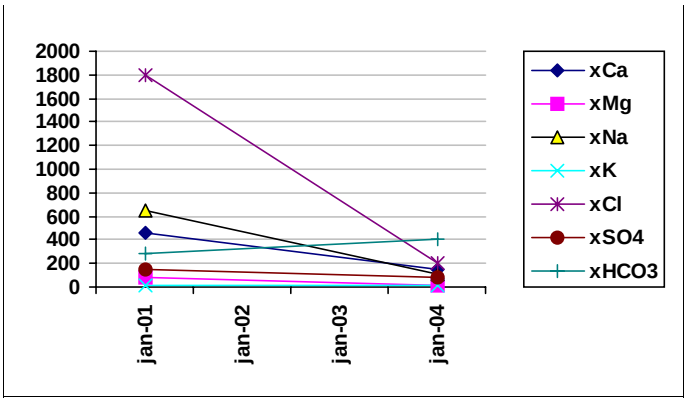

Sampling level (secmid -3.0 masl, RHB70

Mean concentration (mg/l)

Ca:	264
Mg:	43
Na:	330
K:	12
Cl:	847
SO4:	107
HCO3:	348

Object **PFM000039**

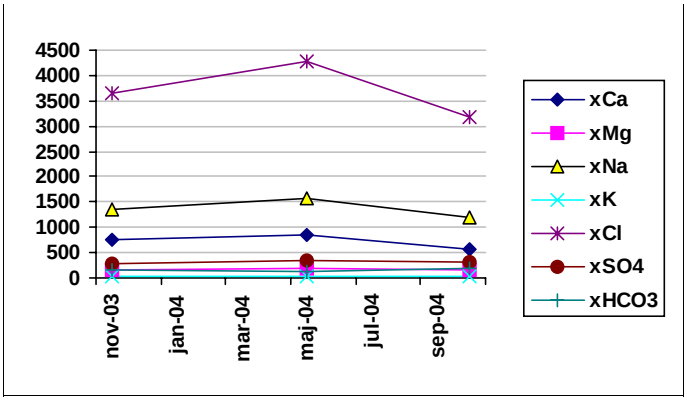

Sampling level (secmid -57.0 masl, RHB70

Mean concentration (mg/l)

Ca:	640
Mg:	140
Na:	1176
K:	24
Cl:	3282
SO4:	275
HCO3:	156

Object **PFM000062**

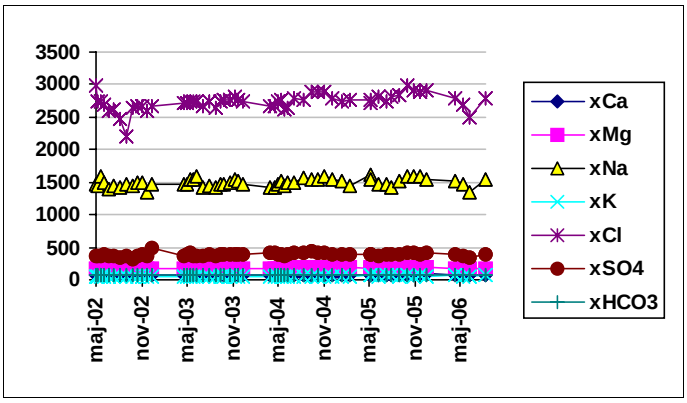

Sampling level (secmid -1.0 masl, RHB70

Mean concentration (mg/l)

Ca:	71
Mg:	179
Na:	1463
K:	53
Cl:	2648
SO4:	367
HCO3:	75

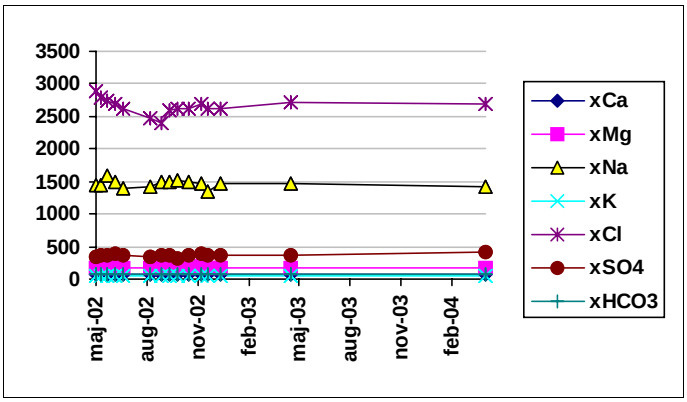

Sampling level (secmid -3.0 masl, RHB70

Mean concentration (mg/l)

Ca:	71
Mg:	179
Na:	1463
K:	53
Cl:	2648
SO4:	367
HCO3:	75

Object **PFM000063**

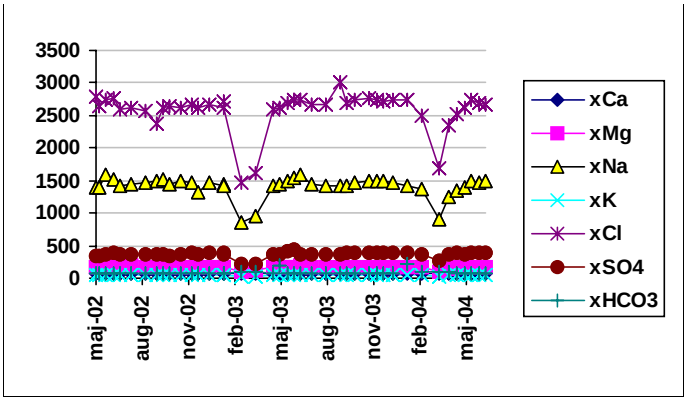

Sampling level (secmid -1.0 masl, RHB70

Mean concentration (mg/l)

Ca:	72
Mg:	176
Na:	1450
K:	53
Cl:	2641
SO4:	373
HCO3:	84

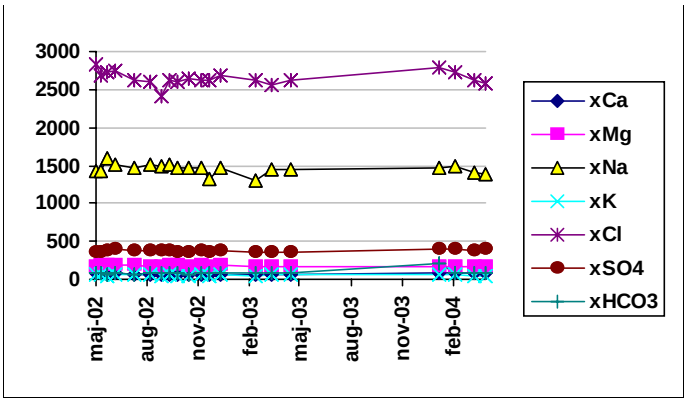

Sampling level (secmid -5.0 masl, RHB70

Mean concentration (mg/l)

Ca:	72
Mg:	176
Na:	1450
K:	53
Cl:	2641
SO4:	373
HCO3:	84

Object **PFM000064**

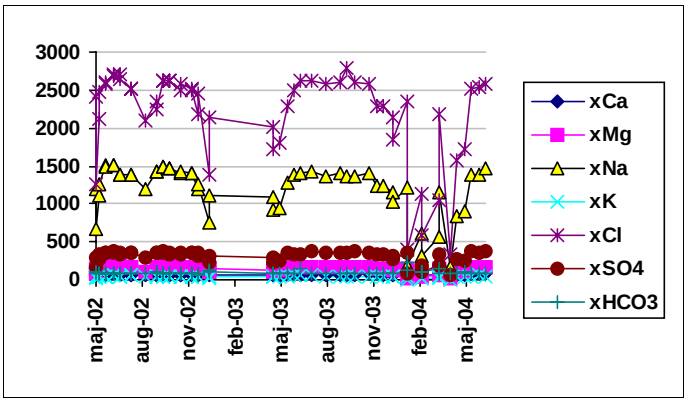

Sampling level (secmid -1.0 masl, RHB70

Mean concentration (mg/l)

Ca:	69
Mg:	146
Na:	1201
K:	44
Cl:	2197
SO4:	312
HCO3:	91

Object **PFM000065**

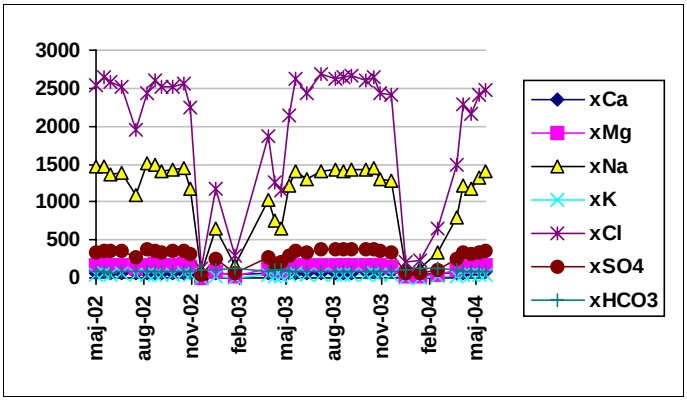

Sampling level (secmid -1.0 masl, RHB70

Mean concentration (mg/l)

Ca:	67
Mg:	135
Na:	1115
K:	41
Cl:	2022
SO4:	294
HCO3:	89

Object **PFM000066**

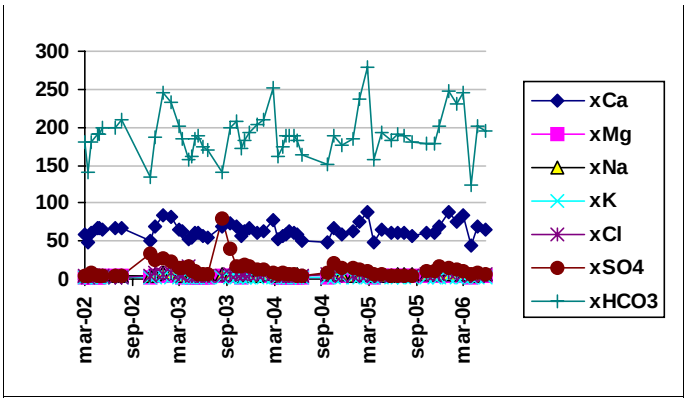

Sampling level (secmid 7.0 masl, RHB70

Mean concentration (mg/l)

Ca:	64
Mg:	3
Na:	5
K:	2
Cl:	5
SO4:	12
HCO3:	190

Object **PFM000067**

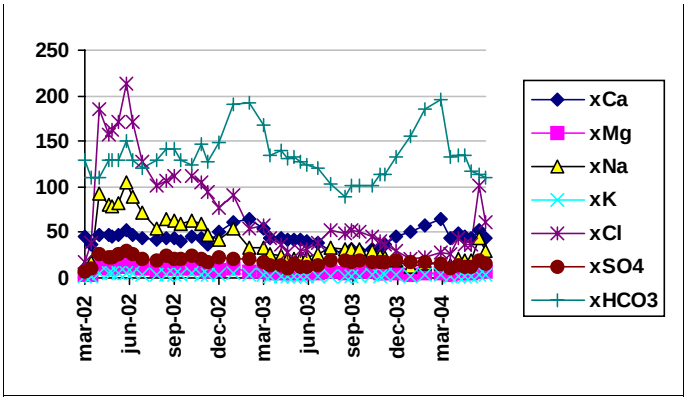

Sampling level (secmid 0.0 masl, RHB70

Mean concentration (mg/l)

Ca:	44
Mg:	7
Na:	41
K:	3
Cl:	74
SO4:	18
HCO3:	132

Object **PFM000068**

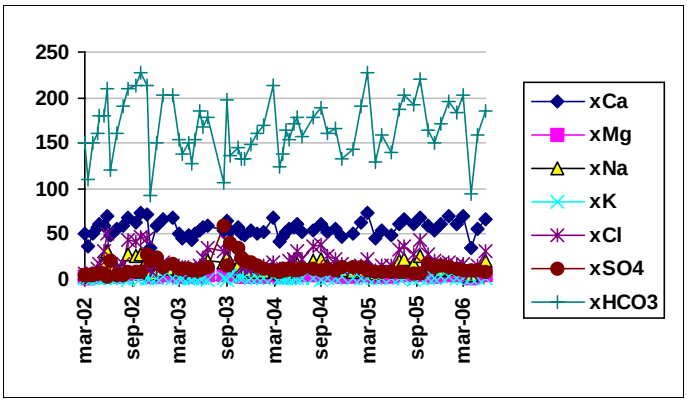

Sampling level (secmid 1.0 masl, RHB70

Mean concentration (mg/l)

Ca:	56
Mg:	5
Na:	14
K:	2
Cl:	22
SO4:	13
HCO3:	166

Object **PFM000069**

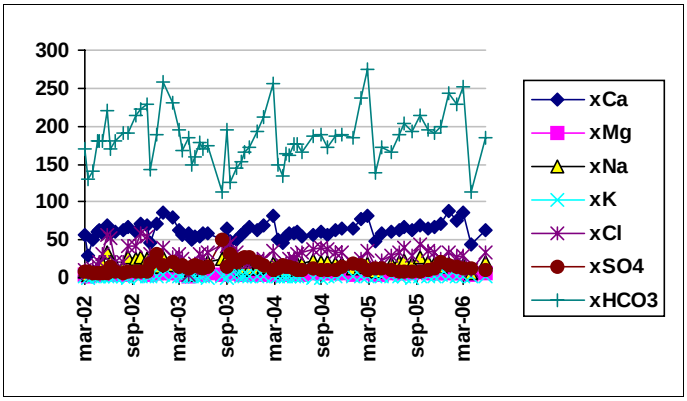

Sampling level (secmid 3.0 masl, RHB70

Mean concentration (mg/l)

Ca:	62
Mg:	5
Na:	17
K:	2
Cl:	29
SO4:	14
HCO3:	184

Object **PFM000070**

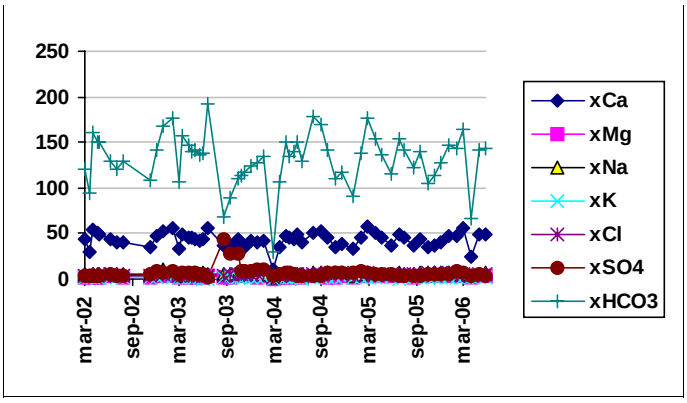

Sampling level (secmid 6.0 masl, RHB70

Mean concentration (mg/l)

Ca:	43
Mg:	3
Na:	6
K:	2
Cl:	5
SO4:	7
HCO3:	132

Object **PFM000071**

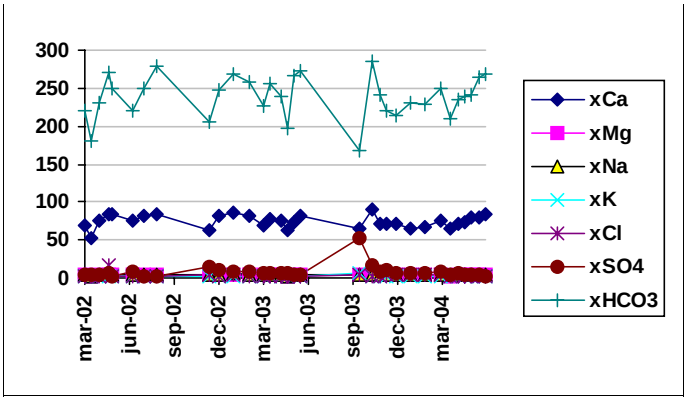

Sampling level (secmid 5.0 masl, RHB70

Mean concentration (mg/l)

Ca:	75
Mg:	4
Na:	4
K:	2
Cl:	3
SO4:	8
HCO3:	239

Object **PFM000072**

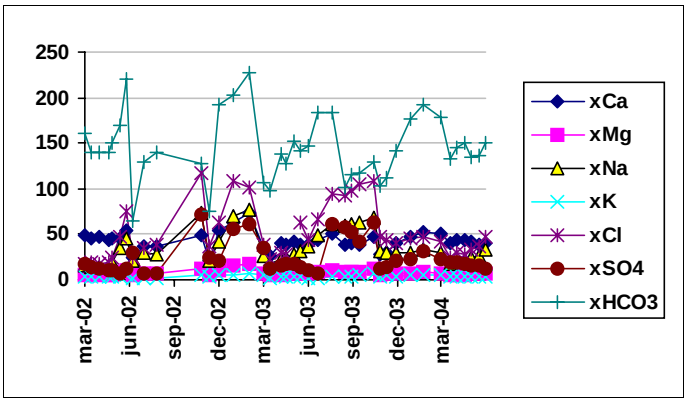

Sampling level (secmid
0.0 masl, RHB70

Mean concentration (mg/l)

Ca:	43
Mg:	8
Na:	35
K:	4
Cl:	51
SO4:	25
HCO3:	144

Object **PFM000073**

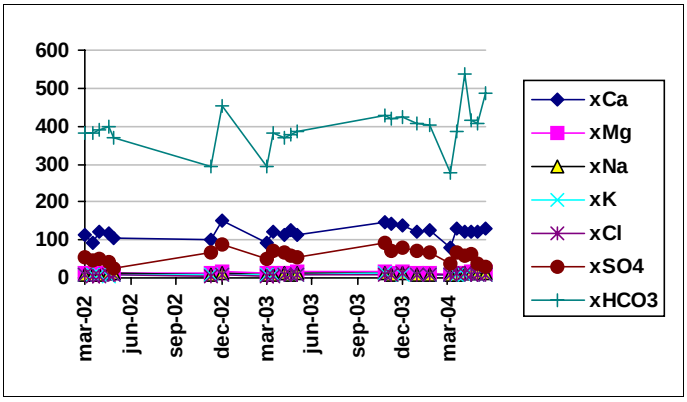

Sampling level (secmid
1.0 masl, RHB70

Mean concentration (mg/l)

Ca:	120
Mg:	14
Na:	10
K:	8
Cl:	8
SO4:	58
HCO3:	394

Object **PFM000074**

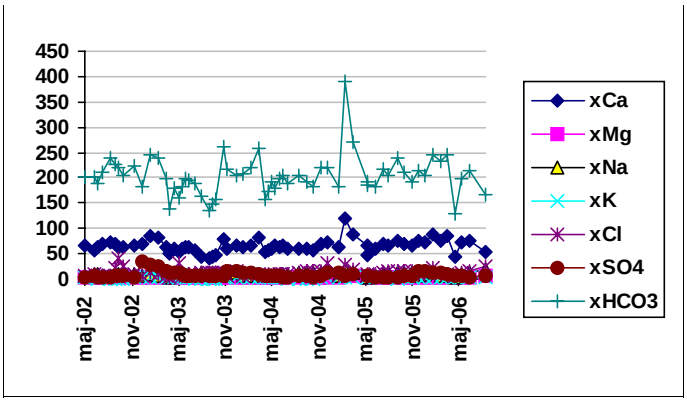

Sampling level (secmid
3.0 masl, RHB70

Mean concentration (mg/l)

Ca:	65
Mg:	4
Na:	9
K:	2
Cl:	12
SO4:	9
HCO3:	204

Object **PFM000082**

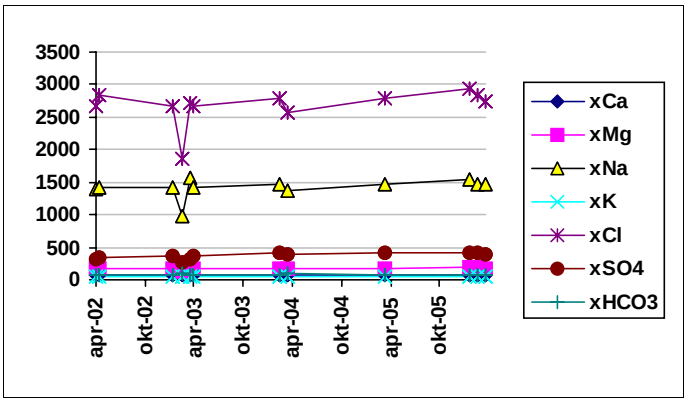

Sampling level (secmid -1.0 masl, RHB70

Mean concentration (mg/l)

Ca:	76
Mg:	179
Na:	1463
K:	55
Cl:	2774
SO4:	385
HCO3:	80

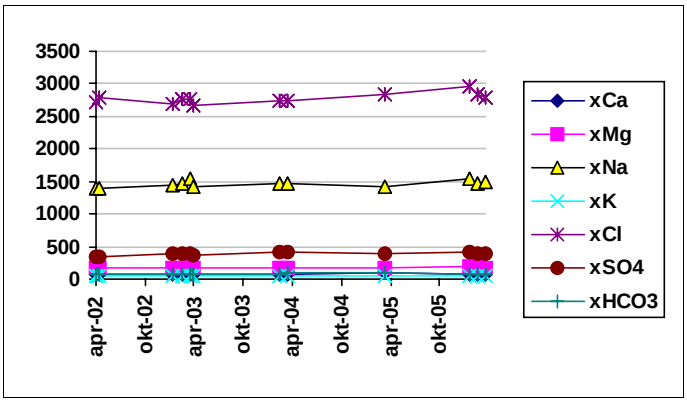

Sampling level (secmid -6.0 masl, RHB70

Mean concentration (mg/l)

Ca:	76
Mg:	179
Na:	1463
K:	55
Cl:	2774
SO4:	385
HCO3:	80

Object **PFM000083**

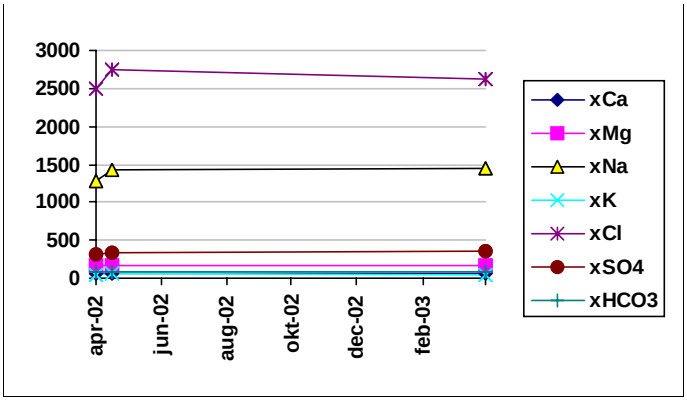

Sampling level (secmid -1.0 masl, RHB70

Mean concentration (mg/l)

Ca:	70
Mg:	173
Na:	1400
K:	52
Cl:	2677
SO4:	388
HCO3:	74

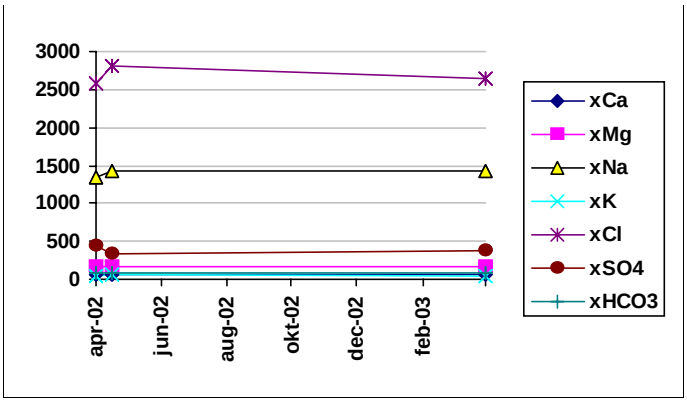

Sampling level (secmid -6.0 masl, RHB70

Mean concentration (mg/l)

Ca:	70
Mg:	173
Na:	1400
K:	52
Cl:	2677
SO4:	388
HCO3:	74

Object **PFM000084**

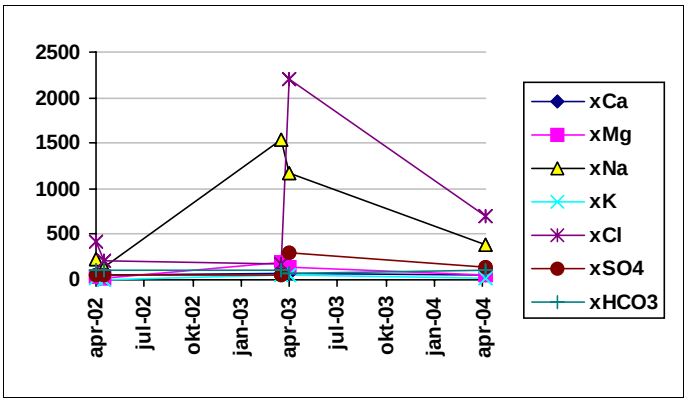

Sampling level (secmid -1.0 masl, RHB70

Mean concentration (mg/l)

Ca:	64
Mg:	125
Na:	1029
K:	39
Cl:	2021
SO4:	288
HCO3:	84

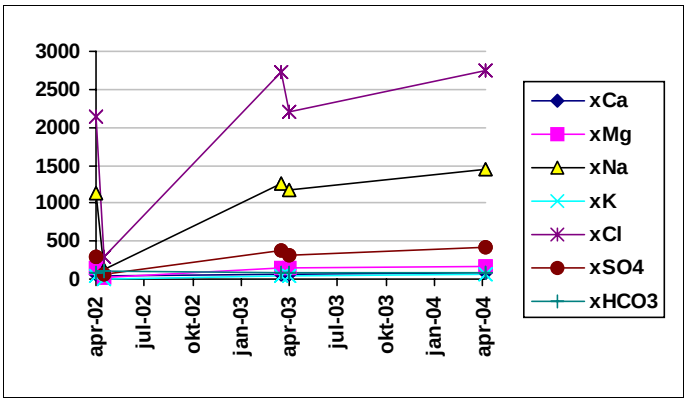

Sampling level (secmid -3.0 masl, RHB70

Mean concentration (mg/l)

Ca:	64
Mg:	125
Na:	1029
K:	39
Cl:	2021
SO4:	288
HCO3:	84

Object **PFM000087**

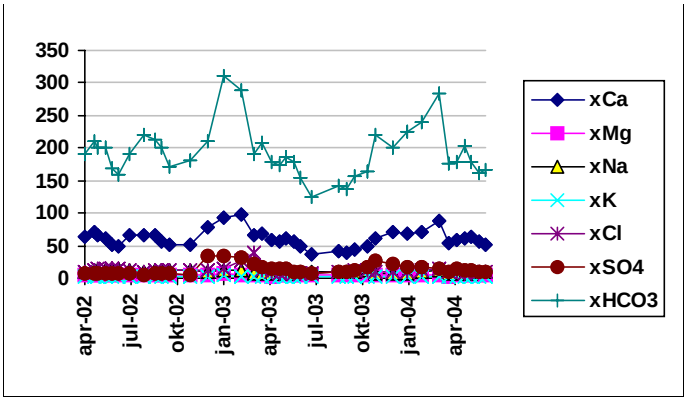

Sampling level (secmid 1.0 masl, RHB70

Mean concentration (mg/l)

Ca:	75
Mg:	5
Na:	11
K:	3
Cl:	12
SO4:	32
HCO3:	234

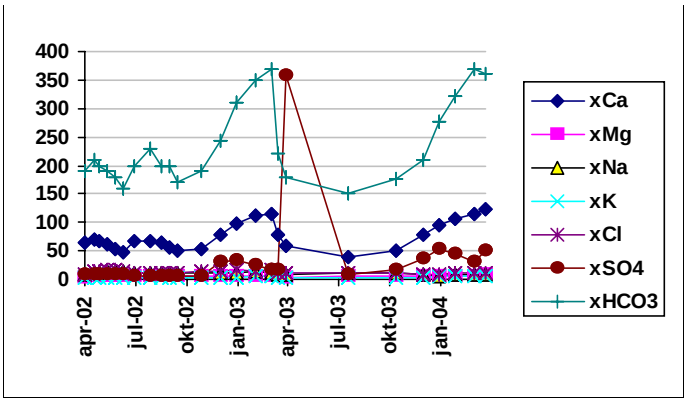

Sampling level (secmid 0.0 masl, RHB70

Mean concentration (mg/l)

Ca:	75
Mg:	5
Na:	11
K:	3
Cl:	12
SO4:	32
HCO3:	234

Object **PFM000097**

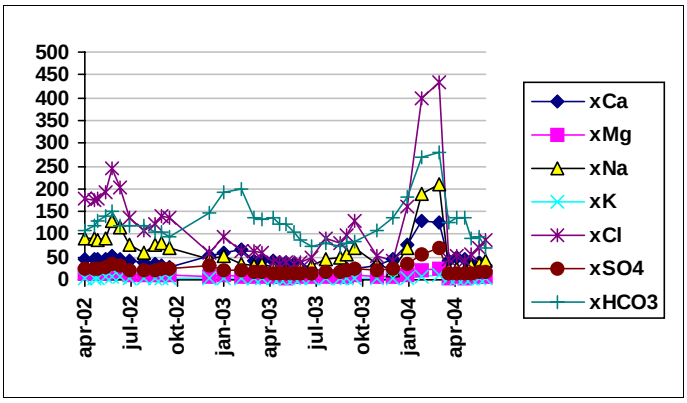

Sampling level (secmid 0.0 masl, RHB70

Mean concentration (mg/l)

Ca:	45
Mg:	9
Na:	61
K:	4
Cl:	114
SO4:	23
HCO3:	128

Object **PFM000107**

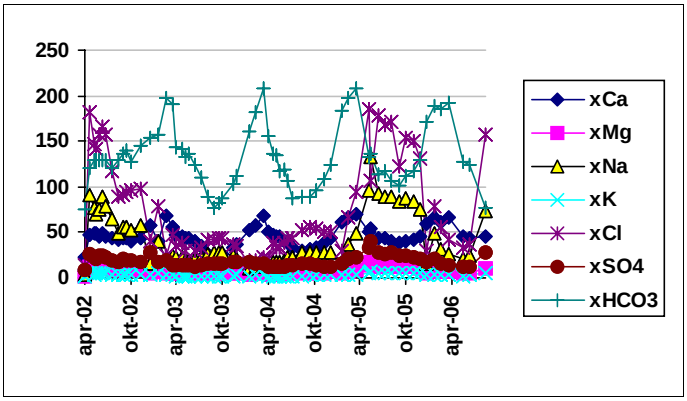

Sampling level (secmid 0.0 masl, RHB70

Mean concentration (mg/l)

Ca:	54
Mg:	13
Na:	90
K:	5
Cl:	151
SO4:	30
HCO3:	157

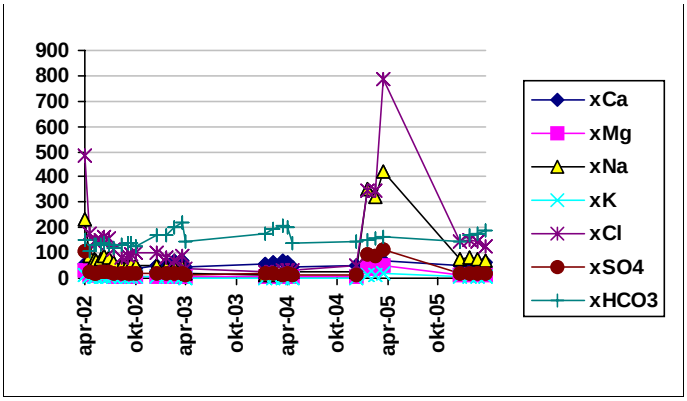

Sampling level (secmid -1.0 masl, RHB70

Mean concentration (mg/l)

Ca:	54
Mg:	13
Na:	90
K:	5
Cl:	151
SO4:	30
HCO3:	157

Object **PFM000117**

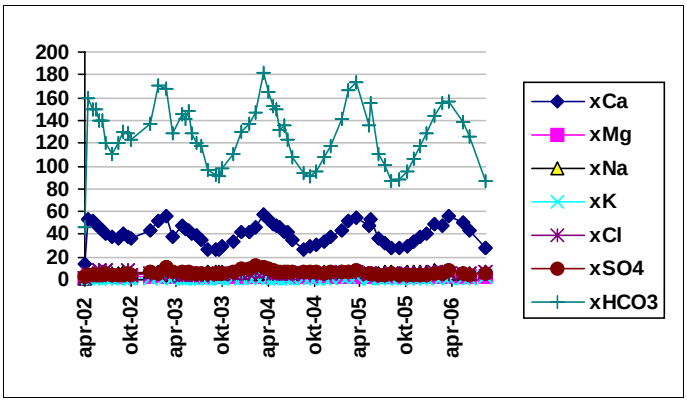

Sampling level (secmid 4.0 masl, RHB70

Mean concentration (mg/l)

Ca:	51
Mg:	3
Na:	6
K:	2
Cl:	6
SO4:	7
HCO3:	161

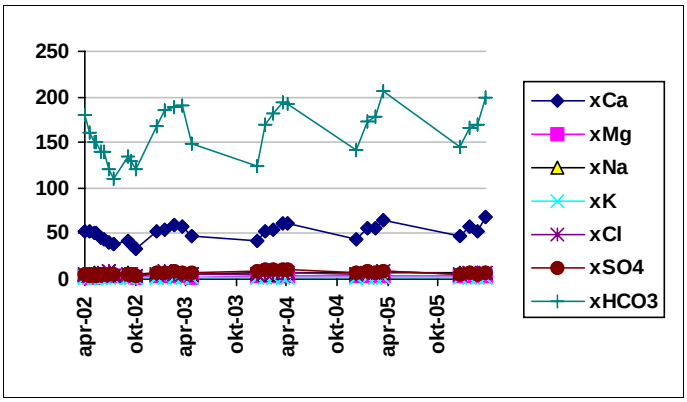

Sampling level (secmid 3.0 masl, RHB70

Mean concentration (mg/l)

Ca:	51
Mg:	3
Na:	6
K:	2
Cl:	6
SO4:	7
HCO3:	161

Object **PFM000127**

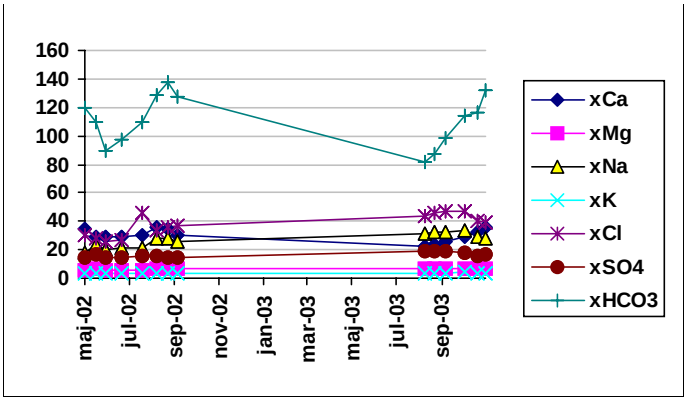

Sampling level (secmid 0.0 masl, RHB70

Mean concentration (mg/l)

Ca:	32
Mg:	6
Na:	25
K:	4
Cl:	32
SO4:	15
HCO3:	113

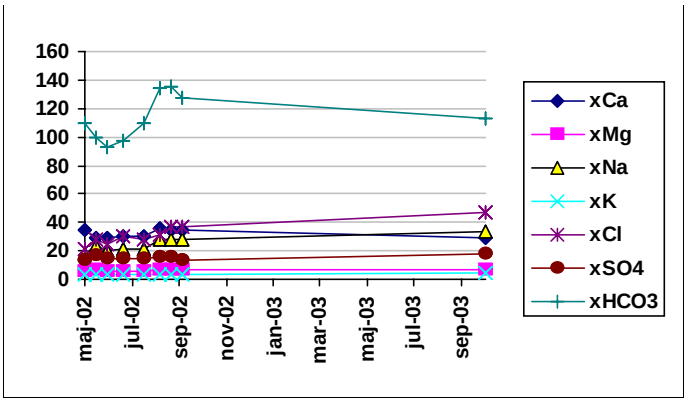

Sampling level (secmid -1.0 masl, RHB70

Mean concentration (mg/l)

Ca:	32
Mg:	6
Na:	25
K:	4
Cl:	32
SO4:	15
HCO3:	113

Object **PFM000135**

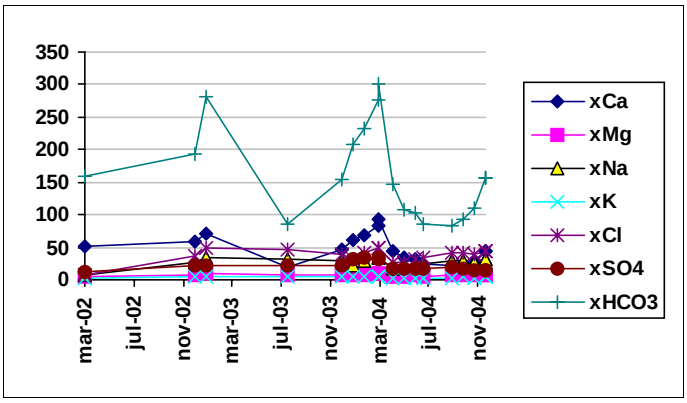

Sampling level (secmid 0.0 masl, RHB70

Mean concentration (mg/l)

Ca:	46
Mg:	7
Na:	27
K:	4
Cl:	38
SO4:	21
HCO3:	163

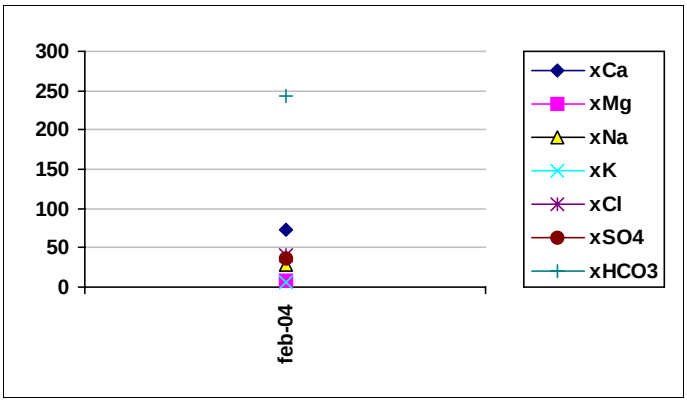

Sampling level (secmid -1.0 masl, RHB70

Mean concentration (mg/l)

Ca:	46
Mg:	7
Na:	27
K:	4
Cl:	38
SO4:	21
HCO3:	163

Object **PFM000151**

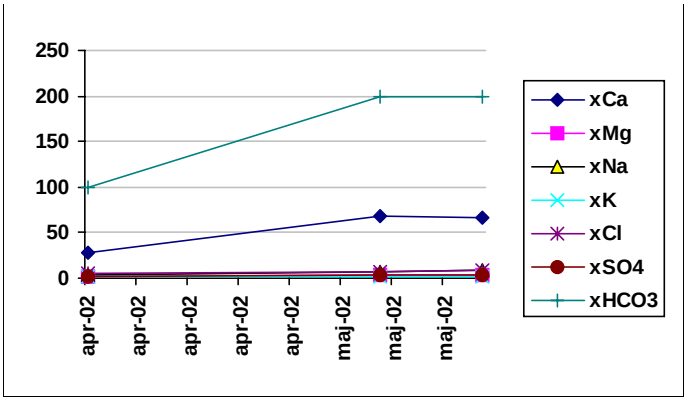

Sampling level (secmid 3.0 masl, RHB70

Mean concentration (mg/l)

Ca:	55
Mg:	3
Na:	6
K:	2
Cl:	6
SO4:	4
HCO3:	167

Object **PFM002457**

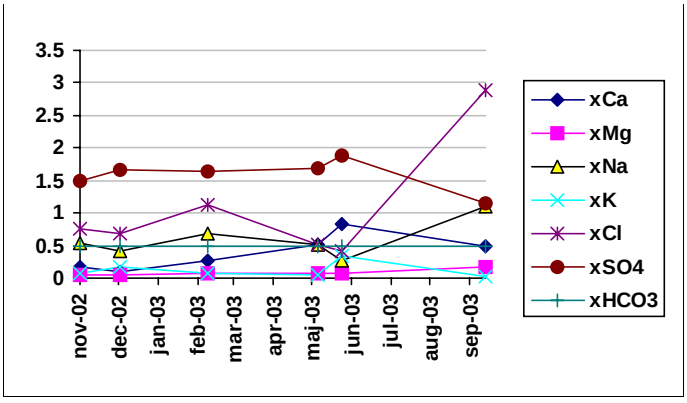

Sampling level (secmid 2.0 masl, RHB70

Mean concentration (mg/l)

Ca:	0
Mg:	0
Na:	1
K:	0
Cl:	1
SO4:	2
HCO3:	1

Object **PFM002564**

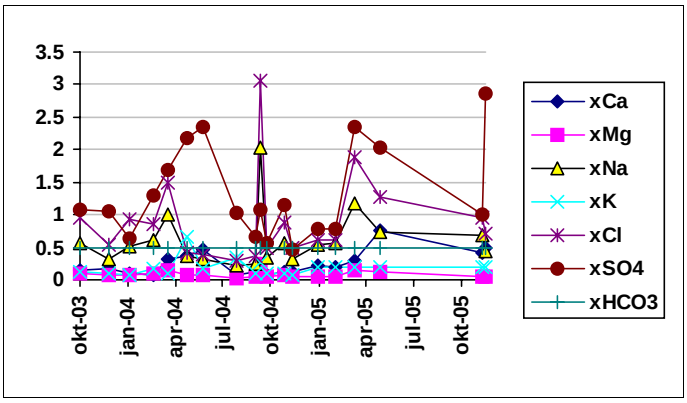

Sampling level (secmid 11.0 masl, RHB70

Mean concentration (mg/l)

Ca:	0
Mg:	0
Na:	1
K:	0
Cl:	1
SO4:	1
HCO3:	1

Object **PFM102269**

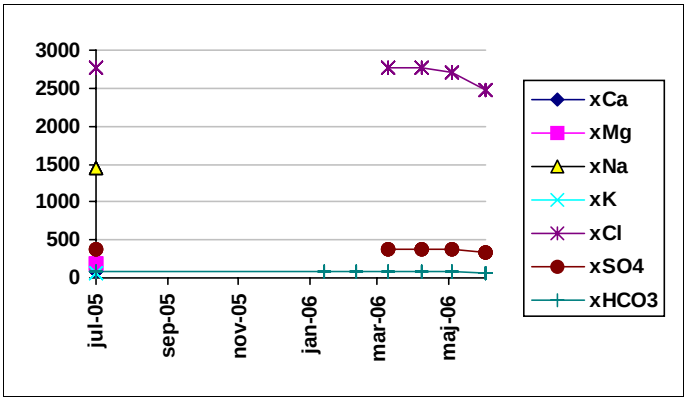

Sampling level (secmid 0.0 masl, RHB70

Mean concentration (mg/l)

Ca:	78
Mg:	189
Na:	1450
K:	60
Cl:	2694
SO4:	371
HCO3:	78

Object **SFM0001**

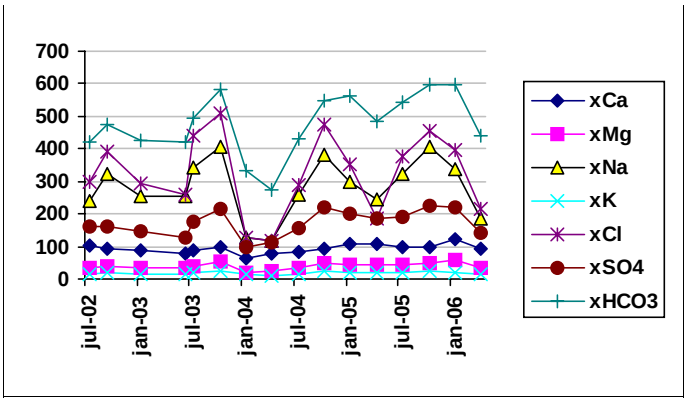

Sampling level (secmid -4.0 masl, RHB70

Mean concentration (mg/l)

Ca:	93
Mg:	40
Na:	282
K:	18
Cl:	324
SO4:	171
HCO3:	477

Object **SFM0002**

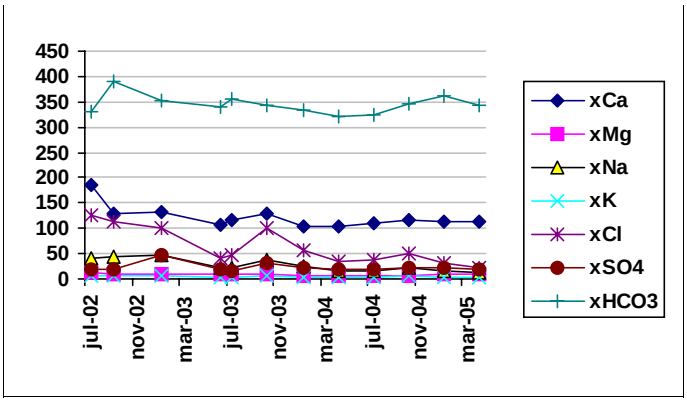

Sampling level (secmid -3.0 masl, RHB70

Mean concentration (mg/l)

Ca:	122
Mg:	9
Na:	27
K:	5
Cl:	64
SO4:	23
HCO3:	345

Object **SFM0003**

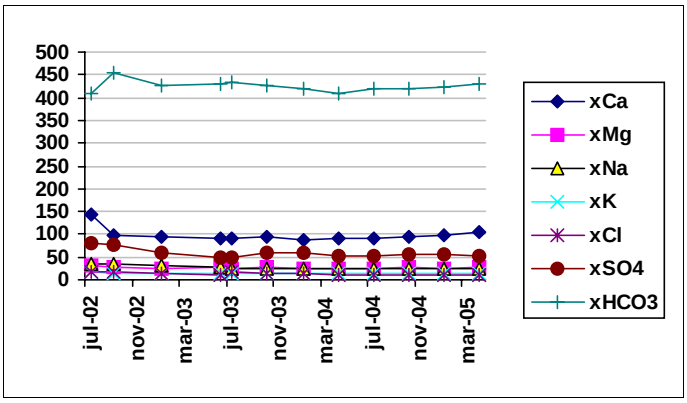

Sampling level (secmid -9.0 masl, RHB70

Mean concentration (mg/l)

Ca:	98
Mg:	27
Na:	27
K:	14
Cl:	13
SO4:	58
HCO3:	425

Object **SFM0005**

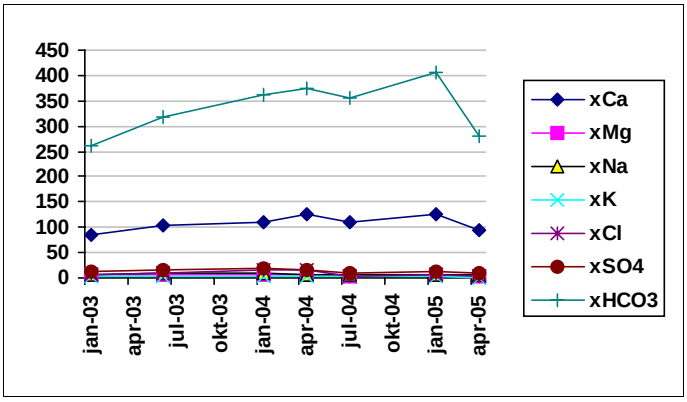

Sampling level (secmid 4.0 masl, RHB70

Mean concentration (mg/l)

Ca:	108
Mg:	5
Na:	7
K:	2
Cl:	10
SO4:	14
HCO3:	337

Object **SFM0006**

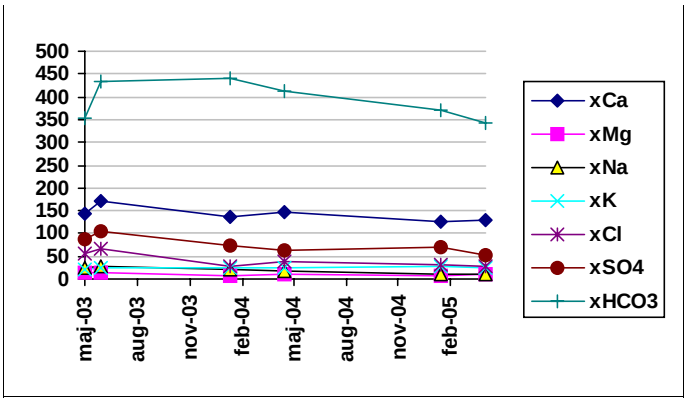

Sampling level (secmid 2.0 masl, RHB70

Mean concentration (mg/l)

Ca:	142
Mg:	10
Na:	18
K:	25
Cl:	42
SO4:	76
HCO3:	392

Object **SFM0008**

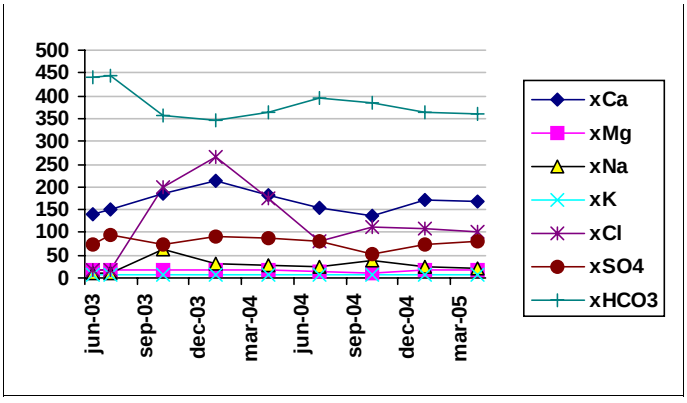

Sampling level (secmid -2.0 masl, RHB70

Mean concentration (mg/l)

Ca:	167
Mg:	17
Na:	28
K:	7
Cl:	120
SO4:	78
HCO3:	384

Object **SFM0009**

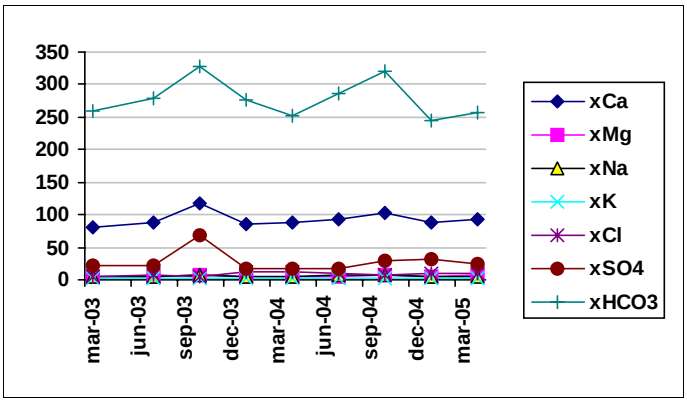

Sampling level (secmid 2.0 masl, RHB70

Mean concentration (mg/l)

Ca:	93
Mg:	6
Na:	6
K:	2
Cl:	9
SO4:	28
HCO3:	278

Object **SFM0012**

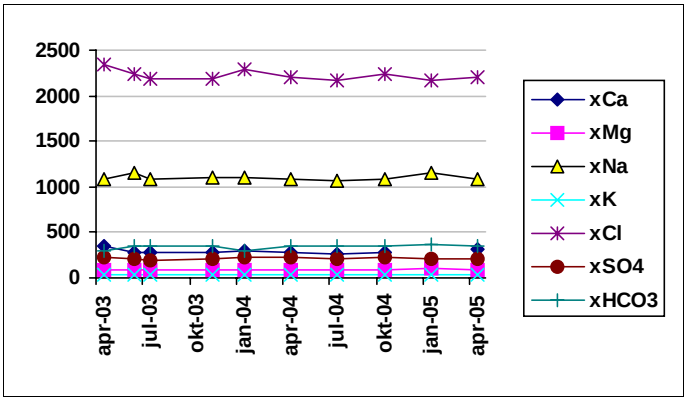

Sampling level (secmid -3.0 masl, RHB70

Mean concentration (mg/l)

Ca:	288
Mg:	91
Na:	1101
K:	35
Cl:	2223
SO4:	216
HCO3:	337

Object **SFM0015**

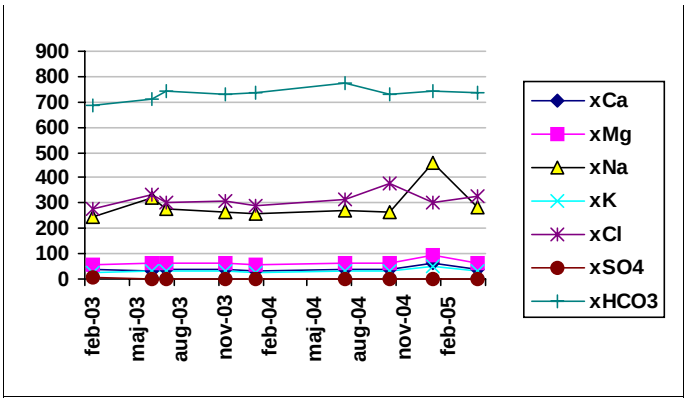

Sampling level (secmid -2.0 masl, RHB70

Mean concentration (mg/l)

Ca:	39
Mg:	64
Na:	293
K:	31
Cl:	314
SO4:	1
HCO3:	732

Object **SFM0022**

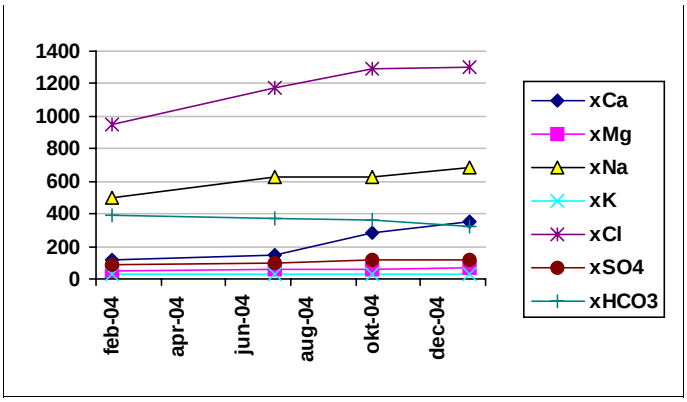

Sampling level (secmid -5.0 masl, RHB70

Mean concentration (mg/l)

Ca:	226
Mg:	60
Na:	610
K:	30
Cl:	1177
SO4:	105
HCO3:	362

Object **SFM0023**

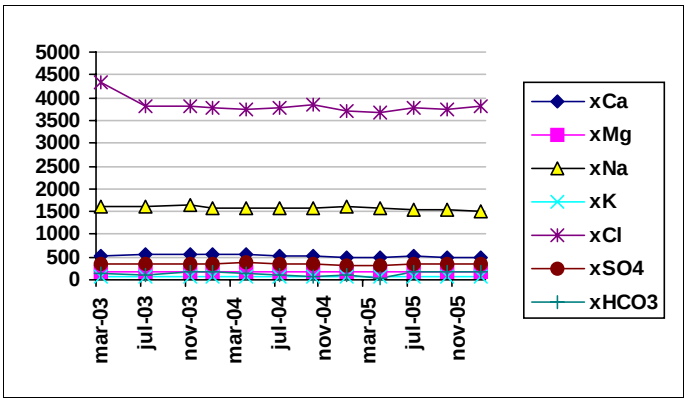

Sampling level (secmid -4.0 masl, RHB70

Mean concentration (mg/l)

Ca:	522
Mg:	172
Na:	1578
K:	66
Cl:	3815
SO4:	350
HCO3:	134

Object **SFM0024**

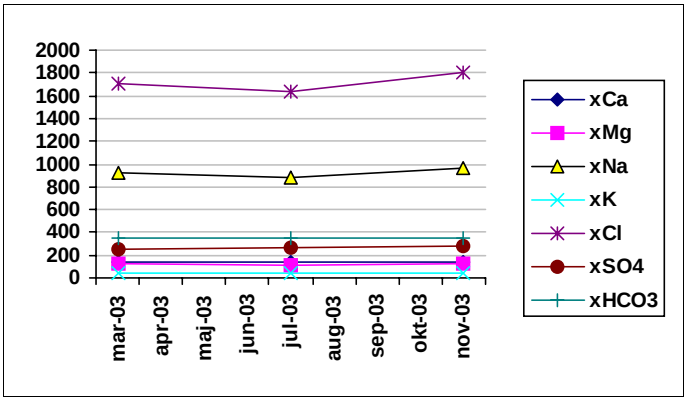

Sampling level (secmid -3.0 masl, RHB70

Mean concentration (mg/l)

Ca:	139
Mg:	117
Na:	923
K:	41
Cl:	1712
SO4:	269
HCO3:	350

Object **SFM0025**

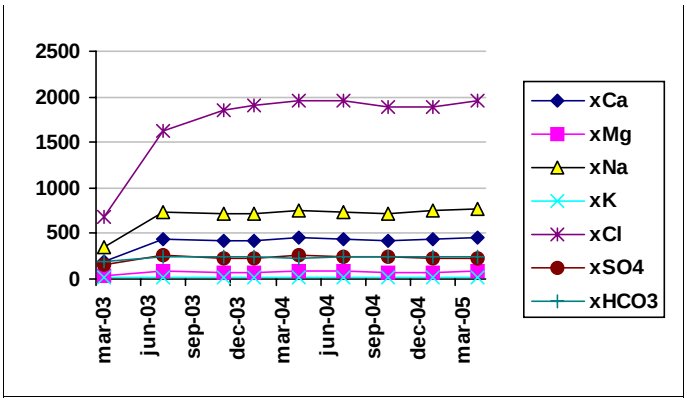

Sampling level (secmid -6.0 masl, RHB70

Mean concentration (mg/l)

Ca:	406
Mg:	74
Na:	695
K:	18
Cl:	1743
SO4:	229
HCO3:	237

Object **SFM0027**

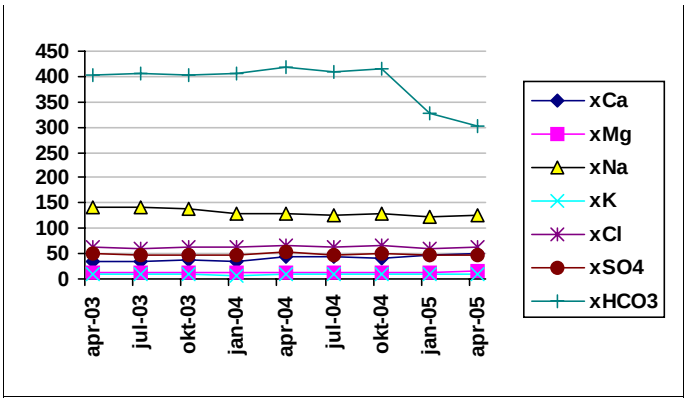

Sampling level (secmid -6.0 masl, RHB70

Mean concentration (mg/l)

Ca:	41
Mg:	13
Na:	131
K:	8
Cl:	62
SO4:	49
HCO3:	388

Object **SFM0029**

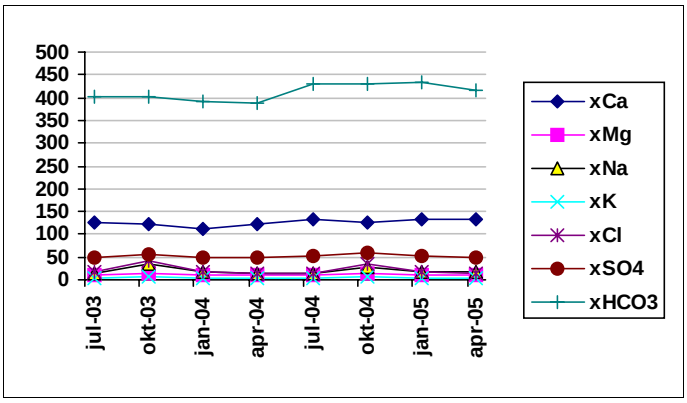

Sampling level (secmid -7.0 masl, RHB70

Mean concentration (mg/l)

Ca:	126
Mg:	12
Na:	20
K:	5
Cl:	22
SO4:	52
HCO3:	412

Object **SFM0031**

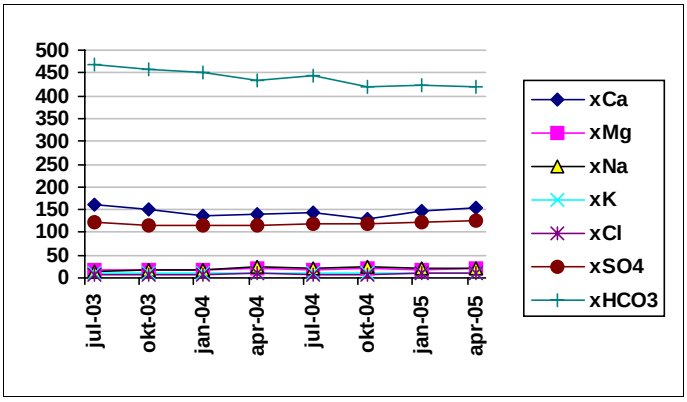

Sampling level (secmid -2.0 masl, RHB70

Mean concentration (mg/l)

Ca:	145
Mg:	19
Na:	20
K:	10
Cl:	9
SO4:	120
HCO3:	440

Object **SFM0032**

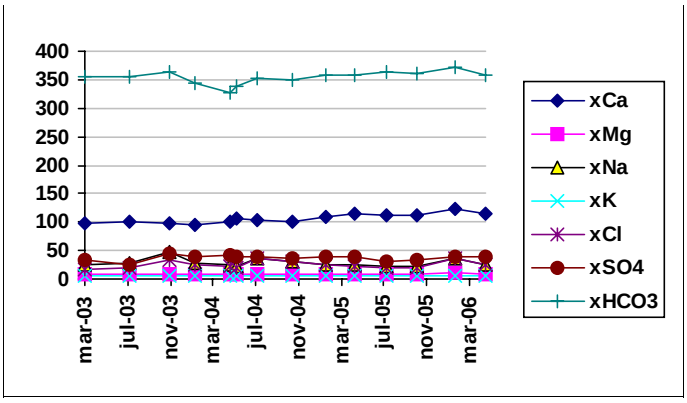

Sampling level (secmid -2.0 masl, RHB70

Mean concentration (mg/l)

Ca:	107
Mg:	9
Na:	28
K:	5
Cl:	25
SO4:	37
HCO3:	354

Object **SFM0037**

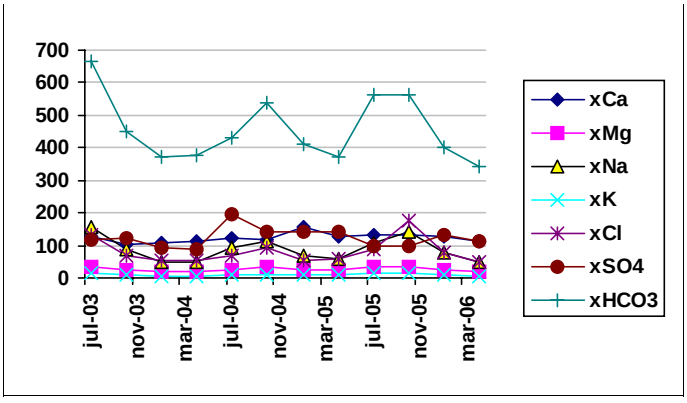

Sampling level (secmid -2.0 masl, RHB70

Mean concentration (mg/l)

Ca:	124
Mg:	26
Na:	88
K:	10
Cl:	81
SO4:	123
HCO3:	457

Object **SFM0049**

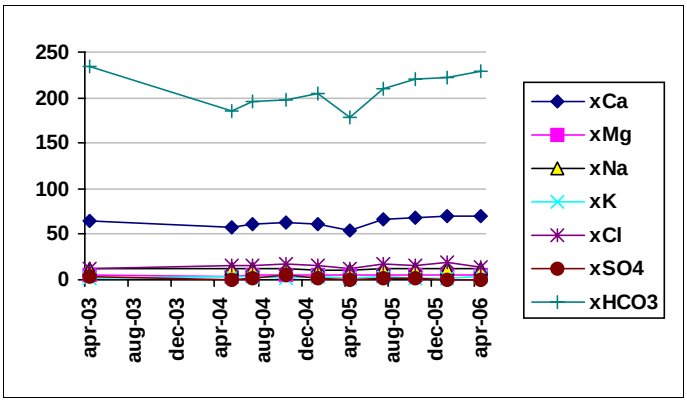

Sampling level (secmid -1.0 masl, RHB70

Mean concentration (mg/l)

Ca:	63
Mg:	5
Na:	12
K:	3
Cl:	16
SO4:	2
HCO3:	208

Object **SFM0051**

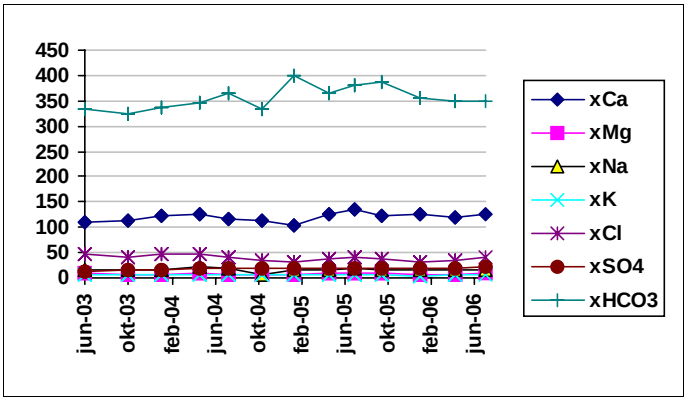

Sampling level (secmid -3.0 masl, RHB70

Mean concentration (mg/l)

Ca:	120
Mg:	8
Na:	16
K:	5
Cl:	40
SO4:	18
HCO3:	356

Object **SFM0053**

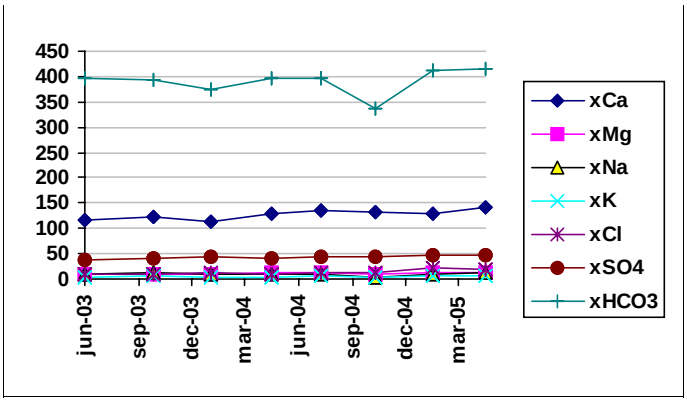

Sampling level (secmid -6.0 masl, RHB70

Mean concentration (mg/l)

Ca:	128
Mg:	11
Na:	10
K:	5
Cl:	13
SO4:	44
HCO3:	390

Object **SFM0056**

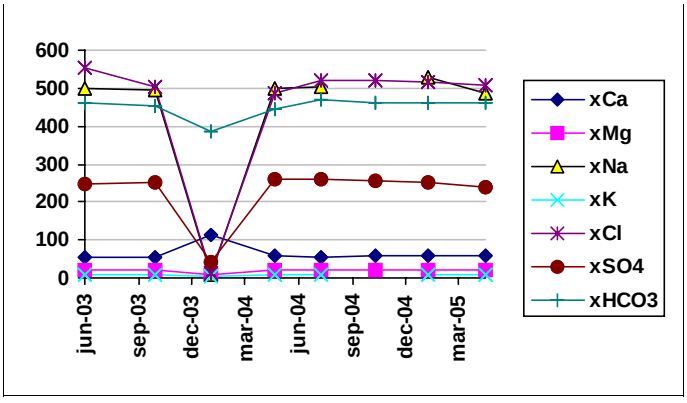

Sampling level (secmid -3.0 masl, RHB70

Mean concentration (mg/l)

Ca:	64
Mg:	19
Na:	431
K:	9
Cl:	452
SO4:	226
HCO3:	450

Object **SFM0057**

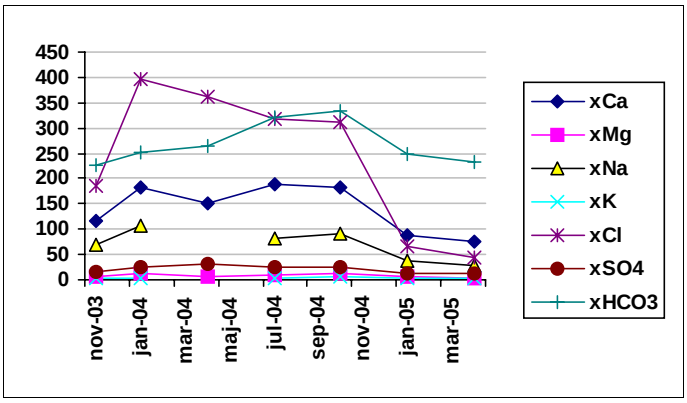

Sampling level (secmid
0.0 masl, RHB70

Mean concentration (mg/l)

Ca:	141
Mg:	9
Na:	69
K:	4
Cl:	241
SO4:	21
HCO3:	268

Object **SFM0060**

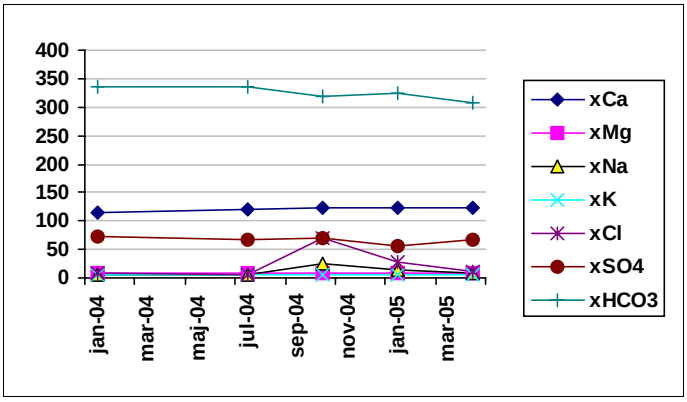

Sampling level (secmid
-3.0 masl, RHB70

Mean concentration (mg/l)

Ca:	121
Mg:	9
Na:	12
K:	5
Cl:	24
SO4:	66
HCO3:	325

Object **SFM0062**

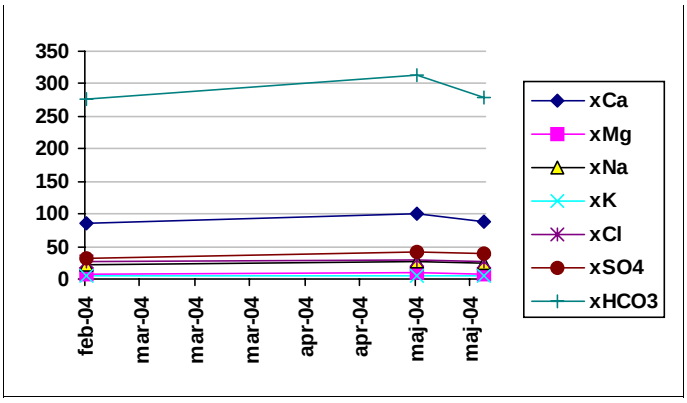

Sampling level (secmid
-3.0 masl, RHB70

Mean concentration (mg/l)

Ca:	92
Mg:	8
Na:	25
K:	6
Cl:	28
SO4:	38
HCO3:	290

Object **SFM0074**

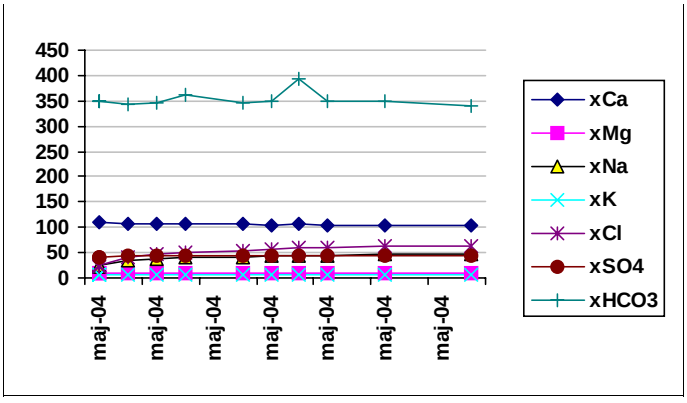

Sampling level (secmid
-3.0 masl, RHB70

Mean concentration (mg/l)

Ca:	106
Mg:	10
Na:	39
K:	5
Cl:	49
SO4:	44
HCO3:	352